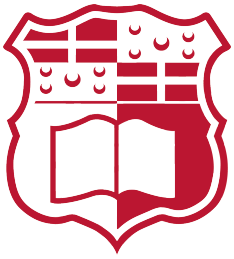

Cosmological Predictions of Physics beyond General Relativity

Maria Caruana

Supervised by Prof. Jackson Levi Said

Co-supervised by Prof. Joseph Sultana

Institute of Space Sciences and Astronomy

University of Malta

A dissertation submitted in partial fulfilment of the requirements for the degree of PhD in Space Sciences and Astronomy.

WWW.UM.EDU.MT

First edition, January 14, 2025

L-Università ta' Malta

FACULTY/INSTITUTE/CENTRE/SCHOOL Space Sciences and Astronomy
DECLARATION OF AUTHENTICITY FOR DOCTORAL STUDENTS

Student's Code mcar0143

Student's Name & Surname Maria Caruana

Course PhD in Space Sciences and Astronomy

Title of Dissertation/Thesis
Cosmological Predictions of Physics beyond General Relativity

(a) Authenticity of Thesis/Dissertation

I hereby declare that I am the legitimate author of this Thesis/Dissertation and that it is my original work.

No portion of this work has been submitted in support of an application for another degree or qualification of this or any other university or institution of higher education.

I hold the University of Malta harmless against any third party claims with regard to copyright violation, breach of confidentiality, defamation and any other third party right infringement.

(b) Research Code of Practice and Ethics Review Procedure

I declare that I have abided by the University's Research Ethics Review Procedures. Research Ethics & Data Protection form code SCI-2024-00031.

☑ As a Ph.D. student, as per Regulation 66 of the Doctor of Philosophy Regulations, I accept that my thesis be made publicly available on the University of Malta Institutional Repository.

□ As a Doctor of Sacred Theology student, as per Regulation 17 (3) of the Doctor of Sacred Theology Regulations, I accept that my thesis be made publicly available on the University of Malta Institutional Repository.

□ As a Doctor of Music student, as per Regulation 26 (2) of the Doctor of Music Regulations, I accept that my dissertation be made publicly available on the University of Malta Institutional Repository.

□ As a Professional Doctorate student, as per Regulation 54 of the Professional Doctorate Regulations, I accept that my dissertation be made publicly available on the University of Malta Institutional Repository.

[redacted]
Signature of Student

MARIA CARUANA
Name in Full (in Caps)

30/09/2024
Date

Acknowledgements

It's funny that after writing over two hundred pages, the hardest part is summing up my gratitude to everyone who helped me get here. Words feel inadequate to express how much I appreciate the support, guidance, and encouragement I have received.

First and foremost, I would like to start by thanking my supervisor Prof. Jackson Levi Said whose guidance, expertise, and insight have been instrumental throughout this process. I have often described you to people as a cheerleader, for always believing in me and your unwavering support. I want to thank my co-supervisor Prof. Joseph Sultana for always being quick and willing to help.

Throughout this journey, I have been fortunate enough to meet many people who, in their unique way, have made this experience not only enjoyable but memorable. A heartfelt thank you to Dr Gabriel Farrugia for being an inspiring example throughout both my undergraduate and doctoral studies. Your guidance, support, and dedication have left a lasting impact on my academic journey. Thanks goes to Dr Viktor Gakis for equipping me with the essential tools at the very start of this journey, laying a strong foundation for the success that followed. I would also like to thank Dr Konstantinos F. Dialektopoulos for especially making conferences a less scary experience.

Next, I would like to express my gratitude to the people in the research lab. To Rebecca Briffa with whom I have experienced ten years of my studies. I am grateful our paths crossed in sixth form and have someone to get lost with our horrible sense of direction. To Miguel Zammit for providing a world of suggestions for music, books, and films while enduring weekly roasts. To Xandru Mifsud for levelling out our craziness and always suggesting to get well-needed pints. And thanks to our 'elders' Dr Andrew Finch, Dr Denis Cutajar, and Dr Julian Bonello for always lending an ear. To Connor Sant Fournier, Jonathan Farrugia, and Federico Cilia for your encouragement and cheerful attitudes.

To my parents, Paul and Cettina, for instilling in me a love for learning from an early age. Your love and support have been the foundation for everything I have achieved. To my brothers, André and Keith, for making sure I don't take life too seriously and never miss the opportunity to drop an unemployment joke. To Nugget, who was a silent supporter and a source of comfort.

Thanks to Gianluca Baldacchino for being my rock, a shoulder to lean on, and for always believing in me. To Nadine Zammit, Keith George Ciantar, Martina Vassallo, Sara Ann Borg, Daphne Camilleri, and Dylan Zammit for your years of friendship and many laughs.

Abstract

The construction of the teleparallel analogue of Horndeski theory provides the most general second-order scalar-tensor framework within metric-teleparallel gravity for a single scalar field. This formalism opens up the possibility of reviving previously discarded Horndeski gravity models, as the inclusion of an additional teleparallel term allows for a wider range of cosmological solutions consistent with the constraints from gravitational wave event GW170817, particularly the excess speed of the tensor modes. The construction of such a generalised class of teleparallel gravity facilitates the theoretical work by compiling a list of constraints stemming from observational and mathematical limits which would hold for a large class of teleparallel models. In this work, teleparallel Horndeski is explored at both the background and perturbative level. The theory is applied to construct well-tempered models that use a dynamical scalar field to screen vacuum energy contributions, addressing the cosmological constant problem—the large discrepancy between its theoretical and observed values. Upon obtaining the linearised field equations through a scalar-vector-tensor decomposition, the gravitational wave polarisation structure can be realised: a maximum of seven propagating degrees of freedom and four polarisation modes of scalar and tensor nature across the massless and massive sectors for a Minkowski background. The dynamics of scalar-tensor theories provide insight into the physical evolution of cold dark matter, responsible for the formation of large structures such as galaxies and galaxy clusters. The solution of the Mészáros equation is used to derive cosmological parameters such as the growth factor, growth index, $f\sigma_8$, and S_8, highlighting any spatially dependent discrepancies in these models. When it comes to comparing models with observations, it becomes crucial that the choice is taken from healthy branches of teleparallel Horndeski. Ghost and Laplacian instabilities help identify these pathological sectors. Throughout this study, limits of well-established theories such as general relativity, Horndeski gravity, and $f(T)$ gravity are explored to emphasise the ability of generalised teleparallel Horndeski gravity to not only recover these familiar theories but also offer a richer structure of cosmologically viable models.

Publications

S. Bahamonde, M. Caruana, K. F. Dialektopoulos, V. Gakis, M. Hohmann, J. Levi Said, E. N. Saridakis, and J. Sultana. Gravitational-wave propagation and polarizations in the teleparallel analog of Horndeski gravity. *Phys. Rev. D*, 104(8):084082, 2021. * † ◊

R. C. Bernardo, J. Levi Said, M. Caruana, and S. Appleby. Well-tempered teleparallel Horndeski cosmology: a teleparallel variation to the cosmological constant problem. *JCAP*, 10:078, 2021. ‡ ◊

R. C. Bernardo, J. Levi Said, M. Caruana, and S. Appleby. Well-tempered Minkowski solutions in teleparallel Horndeski theory. *Class. Quant. Grav.*, 39(1):015013, 2022. ‡ ◊

S. Capozziello, M. Caruana, J. Levi Said, and J. Sultana. Ghost and Laplacian instabilities in teleparallel Horndeski gravity. *JCAP*, 03:060, 2023. * † ◊

S. Capozziello, M. Caruana, G. Farrugia, J. Levi Said, and J. Sultana. Cosmic growth in $f(T)$ teleparallel gravity. *Gen. Rel. Grav.*, 56(2):27, 2024. * † ◊

M. Caruana, G. Farrugia, J. Levi Said, and J. Sultana. Spatial dependence of the growth factor in scalar-tensor cosmology. *JCAP*, 06:053, 2024. * † ◊

Key: * corresponding author, † main author, ‡ co-author, ◊ calculations

Contents

List of Figures

List of Tables

List of Abbreviations

1

Introduction

Cosmology seeks to understand the Universe's formation, tracing its origins, and its evolution through distinct epochs that have shaped the large-scale structures observed today, and predicting its ultimate fate. What began as a philosophical curiosity about the cosmos has evolved into a rigorous scientific discipline, characterised by the interplay between theoretical models and observational evidence. Recent advancements in observational instrumentation have significantly enhanced our ability to probe the intricate details predicted by theoretical frameworks, effectively bridging the gap between abstract concepts and empirical data.

The philosopher Pythagoras was among the first to introduce geometry to explain the Universe, followed by the likes of the Aristotelian concept of celestial bodies governed by concentric spheres, giving the earliest idea of gravitation as these paths dictate the natural place to which objects fall towards [9]. Galileo provided the experimental groundwork to study the acceleration due to gravity [9]. Additionally, Euler and Hooke [10] proposed the existence of an aether as a medium through which electromagnetic and gravitational forces could propagate, and Lorentz [11] and Kelvin [12] explored the treatment of gravitation through the framework of electromagnetism.

The mathematical formulation describing the theory of gravity, developed by Newton [13] in the 17^{th} century, provided an understanding as to why objects fall towards Earth and how planets rotate around the Sun: any two objects are attracted to each other with a force proportional to the product of their masses and inversely proportional to their distance squared. Newtonian gravity became the foundation for classical mechanics and dominated for over 200 years, with applications to this day. By the 20^{th} century, as advancement in observations going beyond Earth occurred, the Newtonian formalism came into question. Primarily, the motion of Mercury predicted through Newtonian mechanics does not correspond to the one observed, as first noted by Le Verrier [14]. According to Newtonian physics, as an object orbits around a spherical mass, the latter mass becomes the focus of an elliptical path. In the case where the

Sun is the focus, the point of closest approach is referred to as the perihelion and predicted to be a fixed point. The influence of surrounding planets alters the predicted orbit, resulting in a perihelion precession [15]. In light of the discovery of Neptune through the perturbed orbit exhibited by Uranus [16], Le Verrier himself suggested that there exists another planet, dubbed Vulcan. Additionally, Newtonian physics did not correlate with calculations of the angular deviation of light from gravitational lensing observations [3] and the observation of gravitational redshift [17]. In reluctance to deviate from Newtonian formalism, many suggestions included slight modification from it, including reconsidering the existence of the aether [10, 11, 12]. The paradigm shift brought on by the formulation of GR accounted for the challenges that Newtonian mechanics was facing, wherein Einstein introduced a completely different treatment of gravitation.

GR, a geometric theory of gravity, states that the curvature of spacetime is related to the energy and momentum of matter. In the over 100 years since the development of GR, the theory has successfully passed the aforementioned classical tests along with additional tests stumbled upon throughout the years such as Shapiro time delay effect [18, 19], Lense-Thirring precession [20, 21], among others. While other theories of gravity have been developed, GR has always been a reference point as its limit has been shown to hold well within the solar system scales, despite inconsistencies on others. One issue is the lack of a link between GR and quantum mechanics, mainly due to the two mechanics governed by distinct, and somewhat contradicting, principles [22]: Strong Equivalence Principle (SEP) [23] and Heisenberg uncertainty [24] principle, respectively. Moreover, tracing back the evolution of the Universe, it results in a Big Bang singularity [25, 26, 27], where classical formalism breaks down. Additionally, GR does not resolve the horizon problem [28], flatness problem [29], and monopole problem [30, 31], for which an inflationary epoch is typically added onto the GR framework to resolve. The addition of inflation would require a particular set of initial conditions, some considering it to be a highly fine-tuned event.

The field equations stemming from GR were once altered by Einstein himself with the introduction of a cosmological constant Λ to describe what was once believed to be a static Universe [32]. The formalism was later retracted in light of Hubble's observation of an expanding Universe [33], but in recent years it has had a resurgence following observations of Type Ia supernovae indicating the Universe is experiencing an accelerated expansion [34]. An accelerated expansion suggests there exists a constituent within the Universe, referred to as *dark energy*, behaving as a repulsive force opposing gravity and dominating. The prefix *dark* is a befitting moniker as the nature of the dark energy is shrouded in mystery while also being difficult to obtain direct detection as it does not interact with the electromagnetic field [35]. This also applies to dark matter, used to describe the matter responsible for growth during the early Universe and maintaining large structures such as galaxies and galaxy clusters [36, 37, 38]. The Cosmological Constant (CC) is added to extend GR into a dark energy model with a vacuum

energy. Intuitively, the term vacuum, attributed to the absence of radiation and matter, suggests that an empty space would not have energy. While this holds at the classical level, quantum fluctuations arising from interactions between particle and antiparticle pairs result in a non-zero mean vacuum energy, as per the Heisenberg principle [24]. While vacuum is not null energy, it is the lowest energy level. CC is not short of its own issues. Comparison between theoretical and observational values of vacuum do not correlate. Merely calculating the contribution of proton-neutron interactions [39] results in a vacuum energy larger than what is observed by order of $\sim 10^{10}$. Approaches to resolving the CC problem include incorporation of different theoretical frameworks such as string theory [40] and supersymmetry [41, 42], self-tuning, well-tempering, among others. The classical approach of well-tempering formalism in scalar-tensor theories allows screening of the vacuum energy as it circumvents Weinberg's no-go theorem, which states that fields within the vacuum state have constant fields and are invariant under Poincaré [43] while being able to retain radiation and matter contributions which self-tuning fails to recover [44].

A complete departure from GR would be difficult to justify, especially following the recent success of Gravitational Wave (GW) detection. The prediction of GWs through the GR formalism marked its 100^{th} anniversary with the first detection of a GW as a product of binary blackhole merger by the Advanced Laser Interferometer Gravitational-wave Observatory (A-LIGO) and Virgo Collaboration using an Earth-based gravitational interferometer [45]. The first indirect evidence of the existence of GW occurred upon the discovery of binary pulsars by Taylor and Hulse [46], as following years of observation of energy losses coincided with GR predictions [47]. Such results further fuelled the interest in obtaining direct detection. After the detection of GW150914 [48], many other GW detections, with binary systems made up of blackholes, neutron stars and a combination of the two have been documented, all of which point towards two tensor polarisation modes given by GR. Additional mode detections can become possible as further sensitivity upgrades are implemented and upon operation of the Laser Interferometer Space Antenna (LISA) [49, 50] space-based mission which is designed to bypass the limitations of fixed orientation and eliminate interference from Earth-based noise. In particular, due to the template matching nature of interferometers [51, 52, 53, 54, 55, 56, 57], it becomes key to provide the foundation and theoretical background of modified theories of gravity to realise the detection of other propagating Degree of Freedoms (DoFs), apart from the tensor modes.

Modified theories of gravity have been developed to tackle a variety of tensions within cosmology. To name a few, there is Einstein-Cartan with the incorporation of torsion [58, 59, 60] and Brans-Dicke with the addition of scalar field [61] providing slight modifications to GR, $f(\mathring{R})$ [62, 63] and Tensor-Vector-Scalar Theory (TeVeS) [64] to tackle dark energy and dark matter, higher-dimensional theories such as string theory [40], quantum gravity [41, 65] aiming to unify with GR, scalar-tensor theories such as Horndeski gravity [66], and alternating the geometric background as done in Teleparallel Gravity (TG) [67] with nonmetric-based Symmetric

Teleparallel Gravity (STG) and torsion-based Metric Teleparallel Gravity (MTG)[1]. The latter formalism, where curvature and metricity are set to vanish, has gained prominence in recent years as Teleparallel Equivalent of General Relativity (TEGR) [1] can be obtained, providing an ode to Einstein-Cartan [58]. Here, while the TEGR action is distinct from the Einstein-Hilbert action, they are dynamically equivalent up to a boundary term B. The main distinction of this geometric formalism is that the fundamental dynamical object is no longer the metric but the tetrad which provides the foundation to construct the metric and describe the manifold, and spin connection to encompass inertial effects and counter the infinite choice of tetrads yielding the same metric [60, 68]. In the interest of having modified gravity, the torsion scalar T is upgraded to an arbitrary function $f(T)$ [69], which has been wildly studied due to its ability to study cosmology without dealing with fourth-order contributions. Naturally, other modified theories has been suggested such as New General Relativity (NGR) [70], $f(T, B)$ [71] which is able to replicate $f(\mathring{R})$ theories, and scalar-tensor theories [61, 72, 73], among others. The latter category is inspired by the possibility of relaxing Lovelock's theorem within four-dimensional geometry by introducing an additional scalar field ϕ and still being able to retrieve second-order field equations [74]. A scalar field offers an additional dynamical DoF to tackle inflation as it behaves as an inflaton, accounting for dark matter and drives dark energy [75, 76, 77]. While the $f(T)$ can be easily altered to $f(\phi, T)$, within the context of MTG, Bahamonde-Dialektopoulos-Levi Said (BDLS) provides the most generalised action in four-dimension based on the tetrad with a single scalar field [78].

BDLS can be described as a teleparallel analogue to Horndeski gravity. The curvature-based formalism of Horndeski gravity has recently gained traction[2] as it can provide the framework for cosmological tests for a large number of modified gravity candidates at the time, following the discovery of an accelerated expansion. Hence, from a theoretical standpoint, it became easier to study multiple branches of Horndeski theory. The observation of inspiral binary neutron star GW170817 [80] and its electromagnetic counterpart Gamma-Ray Burst (GRB)170817A [81] resulted in heavy constraints on the speed of propagation of tensor modes $c_{\rm T}$ to $\left|1 - \frac{c_{\rm T}}{c}\right| \lesssim 10^{-15}$ [82], where c is the speed of light. This outcome brought with it the elimination of large number of Horndeski models, specifically terms containing $g^{\mu\nu}\mathring{\nabla}_\mu\phi\mathring{\nabla}_\nu\phi$ which had already been implemented and studied into cosmological tests [83, 84]. By moving towards tetrad foundation, an additional teleparallel function along with the standard Horndeski action allows reviving previously discarded models while also being in line with observational data [78].

On a large scale, the Universe is considered to be spatially homogeneous and isotropic [85]; the Cosmological Principle. As done in GWs, exploring cosmological perturbations is vital to

[1] In literature, oftentimes the terms TG and MTG have been used interchangeably.

[2] In Ref. [79], to mark the $50^{\rm th}$ anniversary since the construction of Horndeski gravity, Horndeski details the revived interest in the theory.

study how small disturbances in the background of spacetime yield the ripple effects which result in the changes leading an initially hot, dense Universe into the current situation of a Universe with Cold Dark Matter (CDM) which formed galaxy and galaxy clusters [86, 87, 42]. Gravitational perturbations alter the behaviour of matter, hence dictating the structures present. Thus, a system of perturbations can be condensed down in terms of matter perturbations by obtaining the differential equation referred to as Mészáros equation, giving separate growth factor solutions at different horizon scales [88]. Taking into account the H_0 tension, an array of early Universe observations such as Planck [89, 2], Atacama Cosmology Telescope (ACT) [90], South Pole Telescope (SPT) [91] and local measurements such as H_0 Lenses in COSMOGRAIL's Wellspring (H0LiCOW) [92], Pantheon+ [93], Dark Energy Spectroscopic Instrument (DESI) [94], are currently being carried out and future data releases by Euclid [95] and LSST [8] to resolve such discrepancy in H_0 value. These data surveys could shed light on the growth structure of the Universe through the parameters $f\sigma_8$ and S_8, and determine deviations from the current standing ΛCDM model, a model where the Universe is mainly made up of dark energy represented by a CC, CDM and ordinary matter [9, 96]. This concordance model has had its long-standing issues such as the lithium problem [97, 98, 99, 100] and Cosmic Microwave Background (CMB) anomalies [101], topped with the current statistical cosmic tensions due to inconsistencies between direct measurements of expansion at late times [102, 103, 104] and the model dependent measurements provided by data from early Universe [2, 105, 106]. Many suggestions have been proposed, such as early dark energy models [107] and exotic neutrino models [108], which require altering the sound horizon to obtain a large Hubble constant given a fixed CMB angular scale, incompatible with the growth of large structures [109]. Again, this is where modified gravity may be able to reconcile issues with these modifications.

The introductory description of modified theories of gravity may have suggested that a new theory of gravity can be obtained by simply adding extra dependents to an arbitrary function in the action. Such theories could result in pathological branches as models within these subcases have ghost instabilities where the Hamiltonian is missing a lower bound [110], leading to the production of negative energy states [110, 111], and Laplacian instabilities which result in rapid and exponential growth of very small fluctuations [112]. Hence, it becomes important that modified theories of gravity are investigated to obtain the necessary constraints yielding viable cosmological models.

In this work, the topics aforementioned are explored through the lens of BDLS. The metric-teleparallel formalism and generalisation of BDLS provide the tools to study a plethora of subcases simultaneously. Restrictions obtained for BDLS also hold for branches such as $f(T)$ [69], $f(\phi, T)$ [113], NGR [70], generalised teleparallel dark energy [73], generalised teleparallel scalar tensor [72], tachyonic teleparallel gravity [114], among others. Thus, cosmological tests are simplified through a theoretical point of view, making a solid argument for the appeal of BDLS.

Not only can BDLS revive Horndeski models which have been previously eliminated through observational data [115, 116, 117, 118, 119], it offers an avenue to study other theories which have yet not been explored. The project is split into the following chapters.

Chapter 2 provides a theoretical overview of the construction of BDLS. Starting from GR and introducing the geometric formalism, while also highlighting the benefits and issues of the formalism. The most general second-order metric-based scalar-tensor theory of Horndeski gravity is fleshed out as a modified theory of gravity, where the scalar field opens up doors to implement inflation, dark matter and dark energy. To circumvent some issues persisting within the geometry of GR, the tetrad formalism is introduced with a focus on MTG. By combining Horndeski and MTG, additional scalar invariants yield the formation of BDLS.

Chapter 3 explores if BDLS gravity can obtain a well-tempering model in an attempt to resolve CC problem by screening the vacuum energy. Additionally, a well-tempering model is investigated to ensure that its behaviour yields a dynamically stable system through the implementation of phase-space diagrams, that it is consistent with a matter epoch through the evolution of the Hubble, scalar, matter and density parameters, and that during a phase transition, the scalar field continues to propagate to be in accordance with a dynamical cancellation.

A key interest lies in reviving previously discarded Horndeski functions [115, 116, 117, 119] as a result of GW170817 [80, 81] observations. Chapter 4 presents the foundations of perturbations and variational principles to obtain the equations of motion. To investigate the nature of modes, linearised field equations are expressed in terms of a Scalar-Vector-Tensor (SVT) decomposition. Moreover, gauge transformations are presented to express these field equations in terms of gauge-invariant variables. Such results can be easily adapted to theory limits and gauge choice convention favoured.

Chapter 5 investigates the propagating DoFs present in BDLS to indicate and realise the polarisation modes of GWs. This is done for the general full case of BDLS, while also considering subclasses which naturally arise from the principal polynomial representing the wave function. The constraints indicate which theories realise scalar, vector and tensor polarisation modes, setting up a baseline for template matching techniques used in GW interferometers.

Chapter 6 focuses on subcases of BDLS, $f(T)$ and modified GR, to explore the growth of CDM within the subhorizon epoch using scalar and matter perturbations. The behaviour of growth parameters such as growth factor, growth index, $f\sigma_8$ and S_8 illustrates the evolution of matter during a matter-dominated epoch, contributing to the formation of large structures, and providing an avenue to study discrepancies from the ΛCDM model. The focus is shifted towards studying spatial dependencies which may have been overlooked in literature due to previously implemented procedures.

Finally, Chapter 7 presents theoretical constraints on selecting gravitational models to prevent ghost and Laplacian instabilities across scalar, vector, and tensor modes. This ensures that

healthy branches of BDLS are possible, but also indicates which subclasses can realise them. Limits of theories already studied in literature are also presented to show the power and vastness of BDLS theory in aiding theoretical work for subclasses of the theory. The conclusion in Chapter 8 summarises the results obtained in the previous chapters and details proposals for future projects to further work within the teleparallel analogue of Horndeski gravity, to construct viable cosmologies corresponding to observational data.

2

Scalar-Tensor Cosmologies

The 16^{th} and 17^{th} centuries brought with them the scientific revolution; adopting scientific approaches fueled by empiricism, rationalism, and inductivism. Kepler's laws of planetary motion inspired Newton to take the behaviour between Moon and Earth and extend it to all objects surrounding us. Newton's law of gravitation states gravity is an attractive force between massive objects [13], which to this day elegantly explains phenomena on Earth. However, by the beginning of the 20^{th} century, the established framework provided by Newton had already encountered several obstacles when looking at the celestial surroundings beyond Earth: the perihelion of planets, notably that of Mercury [15]; the calculation of the angular deflection of light rays when compared to results obtained through gravitational lensing [3, 120]; and an explanation for the observed gravitational redshift [17]. This led to the consideration of a variety of amendments to keep in line with Newtonian gravity, such as the existence of a new planet influencing Mercury's precession. Beyond attempts to confirm such physical scenarios, alternative theories were also being considered. These ranged from treating gravitation as a wave emitted by bodies [10], a pulse produced by the bodies themselves [12], or a result of electromagnetic disturbances [11], all affecting the aether.

The formulation of GR through a geometric interpretation of gravity as a result of the curvature of spacetime, rather than a force, revolutionised cosmology. Soon after its construction, the theory was able to explain the perihelion of Mercury, gravitational lensing, and gravitational redshift. GR has shown be quite successful, predicting the existence of GW [121, 122] and holding up well within the solar system scale [123]. While still foundational within modern physics, GR has also been shown to not completely resolve issues that persist in the study of cosmology, such as accounting for dark matter and dark energy (even with the modification of ΛCDM), Big Bang singularity [25, 26, 27], Hubble tension [102, 104, 105], the lithium problem [97, 98, 100, 101] and growth tensions [124, 125, 126][1]. For this reason, modified theories of gravity became an

[1] Details of the success and issues of GR are delved into throughout the chapter.

appealing way to tackle these issues while retaining some of the benefits that GR can offer.

In this chapter, a geometric representation of gravity is illustrated to account for these classical inconsistencies with the Newtonian framework. This will start with the well-established theory of GR in Sec. 2.1, highlighting the success of the theory and the issues it still faces. In this work, the focus is on the modified gravity of scalar-tensor theories, as an alternative approach going beyond GR. Sec. 2.2 explores the theory of Horndeski gravity, as a generalised second-order scalar-tensor theory within the curvature framework. By switching the geometric foundation from curvature to torsion, Sec. 2.3 introduces the teleparallel framework, reaping the benefits of having a dynamical equivalence to GR while alleviating issues in GR due to the change in perspective. Thus, the combination of standard Horndeski gravity and TG offers an avenue to construct a teleparallel analogy to Horndeski theory, dubbed as BDLS, as presented in Sec. 2.4.

2.1 | General Relativity

The theory of *special relativity* by Einstein provided an understanding of the Universe from the perspective of a body travelling at a constant speed, with the exclusion of gravity [127]. The concept was later extended to include the idea of an object undergoing acceleration, hence generalising special relativity to obtain GR. In GR, gravity is the distortion which manifests through the curvature of spacetime rather than a force where interactions are presented in gauge theories [128, 129].

The geometric framework of gravity is based on the equivalence principle, where gravitational interactions are considered universal. The Weak Equivalence Principle (WEP) states that the gravitational m_g and inertial m_i masses are observed to be equal, such that the trajectory of a free-falling particle is independent of mass and composition [120]. This has been verified through the Eötvös experiment with a sensitivity of 2×10^{-9} [130], followed by more recent successors such as the MICROSCOPE minisatellite up to a sensitivity of 10^{-15} [131, 132]. The Einstein Equivalence Principle (EEP) further generalises the WEP by including the concepts of special relativity such that any local non-gravitational experiment in a free-falling laboratory is independent of the velocity of a frame and position in spacetime, provided small enough regions of spacetime are considered to allow for gravitational field gradients to be negligible [120]. Ultimately, the SEP further incorporates gravity, implying that the experiment performed in a free-falling laboratory is also independent of the gravitational effect [9].

Spacetime, first introduced by Minkowski to describe the flat spacetime of special relativity [133], represents a four-dimensional manifold wherein three-dimensional space and one-

dimensional time are combined and typically characterised by the coordinates

$$x^\mu = (x^0, x^1, x^2, x^3)\,, \tag{2.1}$$

where x^0 is the time component and the rest of the coordinates represent the spacial contributions, which in this work will represent the spatial Cartesian coordinates (x, y, z). When gravitation is treated as a manifestation of spacetime curvature, it is required to introduce the ingredients required to understand curvature. The metric tensor $g_{\mu\nu}$, a tensor of rank (0,2), provides the tool to describe geometric properties, such as distances and angles. In the four dimensions considered in Eq. (2.1), the metric tensor gives 16 independent components. The metric is symmetric

$$g_{\mu\nu} = g_{\nu\mu}\,, \tag{2.2}$$

to ensure that regardless of the frame of reference, the geometric properties between the same two points are consistent. Through the consideration of symmetry, the number of independent components reduces to 10. The metric gives the scalar product of two vectors, say u^α and v^α, such that

$$g(\mu, \nu) = g_{\mu\nu} u^\mu v^\nu\,. \tag{2.3}$$

Additionally, the metric is taken to be non-degenerate such that

$$g = \det(g) = 0\,, \qquad \text{or} \qquad g_{\mu\nu} u^\mu v^\nu = 0\,. \tag{2.4}$$

This property ensures that the rank corresponds to the dimensions expected for consistency throughout the framework since $g = 0$ would indicate that the rank value is less than the dimensions considered. Additionally, it ensures that the tangent space is properly defined, yielding the property that each metric tensor has a unique inverse associated with it. The inverse metric tensor $g^{\mu\nu}$ is defined such that

$$g_{\mu\alpha} g^{\alpha\nu} = \delta^\nu_\mu\,, \tag{2.5}$$

where δ^ν_μ is the four-dimensional Kronecker delta in the spacetime introduced by Eq. (2.1). Also, a Lorentzian signature, say $(-,+,+,+)$, is adopted to create a distinction between temporal and spatial contributions [9, 120].

Curvature can be described through the connection which links vectors in tangent space, making the affine connection another important tool. In the case of GR, this connection is given by the Levi-Civita connection $\mathring{\Gamma}^\lambda_{\mu\nu}$

$$\mathring{\Gamma}^\lambda_{\mu\nu} = \frac{1}{2} g^{\lambda\gamma} \left(\partial_\nu g_{\mu\gamma} + \partial_\mu g_{\gamma\nu} - \partial_\gamma g_{\mu\nu}\right)\,. \tag{2.6}$$

From this point forward, quantities stemming from the Levi Civita connection are represented with an overhead circle ($\mathring{}$). The partial derivative can be generalised through the covariant derivative $\mathring{\nabla}_\lambda$, which when applied to a tensor of the form $T_{\mu_1,\mu_2,\ldots,\mu_m}{}^{\nu_1,\nu_2,\ldots,\nu_n}$ is given by [120]

$$\begin{aligned}\mathring{\nabla}_\lambda T_{\mu_1\mu_2\ldots\mu_m}{}^{\nu_1\nu_2\ldots\nu_n} &= \partial_\lambda T_{\mu_1\mu_2\ldots\mu_m}{}^{\nu_1\nu_2\ldots\nu_n} \\ &\quad - \mathring{\Gamma}^{\gamma}_{\lambda\mu_1} T_{\gamma\mu_2\ldots\mu_m}{}^{\nu_1\nu_2\ldots\nu_n} - \mathring{\Gamma}^{\gamma}_{\lambda\mu_2} T_{\mu_1\gamma\ldots\mu_m}{}^{\nu_1\nu_2\ldots\nu_n} - \ldots \\ &\quad + \mathring{\Gamma}^{\nu_1}_{\lambda\gamma} T_{\mu_1\mu_2\ldots\mu_m}{}^{\gamma\nu_2\ldots\nu_n} + \mathring{\Gamma}^{\nu_2}_{\lambda\gamma} T_{\mu_1\mu_2\ldots\mu_m}{}^{\nu_1\gamma\ldots\nu_n} + \ldots\,. \end{aligned} \tag{2.7}$$

Hence, the curvature of spacetime can be understood as the geodesic deviation. A geodesic generalises the Euclidean straight line for a curved manifold. The geodesic equation

$$\frac{dx^\lambda}{ds^2} + \mathring{\Gamma}^{\lambda}_{\mu\nu}\frac{dx^\mu}{ds}\frac{dx^\nu}{ds} = 0 \tag{2.8}$$

considers the covariant derivative of a tangent vector to the path $x^\mu(s)$ where s is the affine parameter such that it describes the trajectory of an object in curved spacetime. Two objects starting off parallel to each other, being transported along a curved spacetime such that they moved along different geodesics, will end up with a separation between them [1]. This relative acceleration between two geodesics, referred to as geodesic deviation, manifests the effects of curvature [9]. Without going through the derivation, the Riemann curvature tensor $\mathring{R}^\lambda{}_{\mu\rho\nu}$ is given by

$$\mathring{R}^\lambda{}_{\mu\rho\nu} = \partial_\rho \mathring{\Gamma}^{\lambda}_{\mu\nu} - \partial_\nu \mathring{\Gamma}^{\lambda}_{\mu\rho} + \mathring{\Gamma}^{\lambda}_{\sigma\rho}\mathring{\Gamma}^{\sigma}_{\mu\nu} - \mathring{\Gamma}^{\lambda}_{\sigma\nu}\mathring{\Gamma}^{\sigma}_{\mu\rho}\,, \tag{2.9}$$

to represent the measure of curvature. Performing a contraction yields the Ricci tensor $\mathring{R}_{\mu\nu}$:

$$\mathring{R}_{\mu\nu} = \mathring{R}^\lambda{}_{\mu\lambda\nu} = g^{\lambda\gamma}\mathring{R}_{\lambda\mu\gamma\nu}\,, \tag{2.10}$$

with a further contraction which gives the Ricci scalar $\mathring{R}$

$$\mathring{R} = \mathring{R}^\lambda{}_\lambda = g^{\mu\nu}\mathring{R}_{\mu\nu}\,, \tag{2.11}$$

which represents the scalar curvature.

Another ingredient in GR is the energy-momentum tensor, encompassing the distribution of flow of energy, which for a perfect fluid is given by

$$\Theta^{\mu\nu} = (\rho + p)u^\mu u^\nu + p g^{\mu\nu}\,, \tag{2.12}$$

where ρ is the energy density, p is the pressure, and u^μ is the four-velocity. With the aid of the covariant derivative, the conservation of energy-momentum tensor can be extended to the curved geometry of GR [9]:

$$\mathring{\nabla}_\mu \Theta^{\mu\nu} = 0\,. \tag{2.13}$$

To obtain a relationship between curvature geometry and matter, the action containing both sectors in GR can be expressed through the Einstein-Hilbert (EH) action [134, 1, 120, 9]:

$$\mathcal{S}_{\rm EH} = \frac{1}{2\kappa^2}\int d^4x\sqrt{-g}\,\mathring{R} + \int d^4x\sqrt{-g}\,\mathcal{L}_m\,, \tag{2.14}$$

where $\mathcal{L}_m$ represents the matter Lagrangian and $\kappa^2 = 8\pi G$ is the Einstein gravitational constant for which G is the Newtonian gravitational constant. Taking variations with respect to the metric $g_{\mu\nu}$ yields the Einstein's field equation

$$\mathring{G}_{\mu\nu} = \mathring{R}_{\mu\nu} - \frac{1}{2}g_{\mu\nu}\mathring{R} = \kappa^2\Theta_{\mu\nu}\,, \tag{2.15}$$

where $\Theta_{\mu\nu} = -\frac{2}{\sqrt{-g}}\frac{\delta(\sqrt{-g}\mathcal{L}_m)}{\delta g^{\mu\nu}}$ is the variation of the matter contribution $\mathcal{L}_m$.

In the years following the construction of GR, the gravitational theory has undergone numerous tests; classic tests which brought into question the Newtonian formalism along with additional tests which came along as observational techniques improved. The perihelion shift observed can be well described through the geometry provided by GR as the precession of the orbit of a planet around the Sun due to curvature rather than treating these orbits as static, as done within Newtonian mechanics [135].

Despite the prediction of light bending around a massive object through Newtonian gravity [136], Einstein's prediction through GR [137] differed marginally from that obtained solely through the application of the equivalence principle [137] which had previously agreed with Soldner's result. The observation of a total solar eclipse in 1919 corroborated Einstein's GR results with a deflection angle of $\theta \simeq 1.75''$ [138], followed by various other measurements further confirming such a phenomenon with the Shapiro, David, Lebach and Gregory observations over 20 years yielding a result up to 3 orders of magnitude better than the original observation [19]. While the latter takes into account spatial deflection, its time counterpart has been provided through the Shapiro time delay effect [18]. The deflection in time when a photon passes through the gravitational field due to a massive object, as predicted by GR, has been verified through the radio links with the Cassini spacecraft up to 4 decimal places [139].

Moreover, in line with Mach's principle [140], the rotation of massive objects would result in a 'dragging' effect interpreted as a gravitational field. Lense and Thirring [20, 21], through the application of GR, were able to provide the theoretical correction to represent gravitomagnetism. This Lense-Thirring precession has been measured using the LAser GEOdynamics Satellite (LAGEOS) [141], Gravity Probe B mission [142] and LAser RElativity Satellite (LARES) [143, 144, 145].

In 1916, following the construction of GR, Einstein showed that the linearisation of the weak field equations concluded that GR predicts gravitational radiation propagating at the speed of light [122]; disturbances in spacetime. Following years of doubt surrounding this result, the

1974 discovery of binary pulsar PSR B1913+16 [46] along with a 30-year observation of orbital decay, provided indirect evidence of GW [146, 147]. A binary pulsar is a system consisting of a highly magnetised neutron star which emits electromagnetic radiation from its magnetic poles (referred to as pulsar) and a dense object such as a white dwarf or another neutron star. The orbital decay of the pulsar-neutron system provided by PSR B1913+16 was shown to correspond to the loss of energy due to a GW as predicted by GR with the ratio between observed and predicted value initially found to be 0.997 ± 0.002 [146]. This result has been further improved to 0.9986 ± 0.0016 [147]. The first observation of the GW signal GW150914 by Laser Interferometer Gravitational-wave Observatory (LIGO) and Virgo Collaboration [45] as a result of stellar binary blackhole merger. This was followed by numerous other mergers resulting from ones with two blackholes, two neutron stars, or a merger of a blackhole and a neutron star. Further details on GWs will be discussed in Sec. 5. Additionally, the double pulsar system PSR J0737-3039A/B [148] can provide multiple independent tests of relativistic gravity, which have been seen to fit well with the GR formalism [149].

Through these tests, GR has been shown to hold up well as a gravitational theory against classical and modern tests, within the strong field and at the cosmological scale. Hence, one may wonder why theories beyond GR are even considered nowadays.

One of the main issues with GR is that it fails to link to quantum mechanics. As stated by the Penrose-Hawking theorems [25, 26], there exists incomplete and inextendable geodesics yielding to singularities. Therefore, at the Big Bang singularity, where the Universe begins from an infinite density, the classical field equations fail [150, 151, 152]. At this stage, quantum effects would need to be considered, i.e. the quantisation of the gravitational field [27]. Despite the attempts through loop quantum cosmology [65, 41] and string theory [40], the main problem of unifying quantum and classical mechanics persists. This is because while GR is founded in the SEP, quantum mechanics relies on the Heisenberg uncertainty principle. While the former formalism explains test particle trajectories through the geodesic equation given by Eq. (2.8), in the latter scenario a test particle is allocated infinitely many trajectories, each assigned a probability [22]. Such a distinction in governing principles, i.e. locality vs. non-locality, makes it difficult to combine both frameworks, hence resulting in considering an alternative theory of gravity. One such possibility is using theories of gravity whose geometric structure does not arise from the equivalence principle.

The 1998 observations of standard candles Type Ia supernovae showed that not only was the Universe not static [33], but that it is undergoing an accelerated expansion [153, 34]. The driving force behind such accelerated expansion is hypothesised to be a constituent in the Universe dubbed as *dark energy*. One modification done to GR to account for dark energy was to include

the CC Λ [43] such that Einstein's field equation (2.15) changes to

$$\mathring{R}_{\mu\nu} - \frac{1}{2} g_{\mu\nu} \mathring{R} + \Lambda g_{\mu\nu} = \kappa^2 \Theta_{\mu\nu} \,. \tag{2.16}$$

The CC, originally introduced by Einstein as a means to achieve a static Universe, leads to accelerated expansion by dominating with negative pressure, which counteracts gravitational pull. Observations focused on measurements of CMB such as COsmic Background Explorer (COBE) [154], Planck satellite [155, 2] and Wilkinson Microwave Anisotropy Probe (WMAP) [156] have shown that dark energy is a dominant constituent in the Universe. These observations have shown to favour the Lambda Cold Dark Matter (ΛCDM), where apart from dark energy, baryonic matter and radiation, the Universe also includes CDM; non-relativistic matter which interacts gravitationally but does not interact with electromagnetic forces [86, 87, 42]. As a result, CDM plays a crucial role in explaining the current large-scale structures, as it allows for the gravitational collapse of slow-moving matter, leading to the formation of galaxies and galaxy clusters. However, the ΛCDM concordance model faces its own set of challenges: Hubble tension [2, 106, 105, 157, 102, 104, 158], growth tension [124, 125, 126], anomalies in CMB anisotropy such as significant angular fluctuations [101], lithium problem as measurements are less than what is predicted by Big Bang Nucleosynthesis (BBN) [97, 98, 99, 100], quasar Hubble diagram [159, 160, 161], age of the Universe as measured through Pop III stars [162, 163], among many other issues[2].

Given the range of issues, in recent years many different classes of modified gravity have been proposed [96, 165, 166, 167, 168, 169], including the consideration of scalar-tensor theories [170, 171] built around the ΛCDM model while being favoured to describe cosmic inflation with the aid of a dynamical scalar field during early Universe to account for horizon and flatness problems [76, 172]. Moreover, different approaches to tackling geometry have been considered [173, 22]. In the rest of the chapter, these different modifications are introduced, starting the with scalar-tensor Horndeski theory (Sec. 2.2), and introduction to teleparallel gravity (Sec. 2.3), finally presenting the construction of BDLS (Sec. 2.4) which combines both aspects of Horndeski and teleparallel gravity.

2.2 | Horndeski Theory

Following the motivations behind considering theories beyond GR, the procedure for the simplest modification is presented here. Lovelock's theorem states that the Einstein field equations are the only second-order field equations that can be obtained from a Lagrangian scalar density constructed from the metric in a four-dimensional geometry [74]. Therefore, for a scalar

[2]Ref. [164] provides a detailed review of challenges the ΛCDM model faces.

density of the form $\mathcal{L} = \mathcal{L}(g_{\mu\nu})$, not necessarily the Einstein-Hilbert action, yield the following Euler-Lagrange given by Eq. (2.16), such that that even for the most generalised action in four-dimensions and based on the metric would obtain the above solution as part of their field equations [96]. Hence, to modify the field equation obtained through Eq. (2.15), the following changes would need to be applied [96]:

- action includes other fields, instead of or apart from the metric tensor,
- includes higher order derivatives of the metric,
- consider higher dimensions of spacetime,
- alter properties that define the field equations, i.e. tensor rank, symmetry or divergencelessness,
- non-local theories of gravity.

To relax Lovelock's theorem, one approach would be to include a single scalar field along with the metric tensor. In general, multiple scalar fields can be considered. The extension adds another DoF such that the gravitational constant introduced in Eq. (2.16) becomes dynamical. Such theories are used to tackle issues in cosmology such as inflation, dark matter, and dark energy [174]. One of the first scalar-tensor theories was that of Brans-Dicke (BD) theory [61], which later was generalised a bit further in Generalised Brans-Dicke (GBD) [175]. In recent years, in particular, there has been a revived interest in Horndeski gravity [66] as the theory provides a generalised framework to explore a large number of scalar-tensor theories within the curvature-based formalism.

The aim behind the construction of Horndeski theory is to obtain the most general second-order Euler Lagrange equations obtained in a four-dimensional spacetime through a Lagrange scalar density of the form

$$\mathcal{L} = \mathcal{L}\left(g_{\mu\nu}, \partial_{\alpha_1} g_{\mu\nu}, \ldots, \partial_{\alpha_1} \ldots \partial_{\alpha_p} g_{\mu\nu}, \phi, \partial_{\alpha_1}\phi, \ldots, \partial_{\alpha_1} \ldots \partial_{\alpha_q}\phi\right) , \tag{2.17}$$

where $p, q \geq 2$. In general, the field equations obtained through the variation with respect to the metric and with respect to the scalar field, are respectively given by the relationships

$$W^{\mu\nu} = \frac{\partial \mathcal{L}}{\partial g_{\mu\nu}} - \partial_{\alpha_1}\left(\frac{\partial \mathcal{L}}{\partial(\partial_{\alpha_1} g_{\mu\nu})}\right) + \ldots + (-1)^p\, \partial_{\alpha_1}\partial_{\alpha_2}\ldots\partial_{\alpha_p}\left(\frac{\partial \mathcal{L}}{\partial(\partial_{\alpha_1}\partial_{\alpha_2}\ldots\partial_{\alpha_p} g_{\mu\nu})}\right) , \tag{2.18}$$

$$W = \frac{\partial \mathcal{L}}{\partial \phi} - \partial_{\alpha_1}\left(\frac{\partial \mathcal{L}}{\partial(\partial_{\alpha_1}\phi)}\right) + \ldots + (-1)^q\, \partial_{\alpha_1}\partial_{\alpha_2}\ldots\partial_{\alpha_q}\left(\frac{\partial \mathcal{L}}{\partial(\partial_{\alpha_1}\partial_{\alpha_2}\ldots\partial_{\alpha_q}\phi)}\right) . \tag{2.19}$$

A second-order theory can be obtained by allowing at most second-order derivatives of $g_{\mu\nu}$ and ϕ to appear in Eqs (2.18-2.19), ensuring that the field equations $W_{\mu\nu}$ are of a second order nature,

analogous to those obtained in GR, and further restricts $\mathring{\nabla}_\nu W^{\mu\nu}$ to also be of second order. Hence, it results in the action of the form given in Eq. (2.17) where $p = q = 2$.

To simplify the procedure to construct Horndeski theory functions, the starting point will be Galileon theory [176, 117, 112]; a theory where the scalar field is symmetric under the Galilean shift symmetry $\phi \to \phi + b_\mu x^\mu + c$, resulting in the Lagrangian [117]

$$\begin{aligned}\mathcal{L} = {} & c_1\phi + c_2\bar{X} + c_3\bar{X}\,\bar{\Box}\phi + \frac{c_4}{2}\Big[\bar{X}\left((\bar{\Box}\phi)^2 - \partial^\mu\partial^\nu\phi\,\partial_\mu\partial_\nu\phi\right) + \partial_\mu\phi\,\partial_\nu\phi\,\partial^\mu\partial^\nu\phi\,\bar{\Box}\phi - \partial_\mu X\,\partial^\mu X\Big] \\ & + \frac{c_5}{15}\Big[-2\bar{X}\,)(\bar{\Box}\phi)^3 - 3\,\partial_\mu\partial_\nu\phi\,\partial^\mu\partial^\nu\phi\,\bar{\Box}\phi + 2\,\partial_\mu\partial_\nu\phi\,\partial_\rho\partial^\nu\phi\,\partial^\mu\partial^\rho\phi\big) \\ & + 3\,\partial^\rho\phi\,\partial_\rho\bar{X}\left((\bar{\Box}\phi)^2 - \partial_\mu\partial_\nu\phi\,\partial^\mu\partial^\nu\phi\right) + 6\partial_\mu\bar{X}\left(\bar{\Box}\phi\,\partial^\mu\bar{X} - \partial^\mu\partial^\nu\phi\,\partial_\nu\bar{X}\right)\Big]\,, \end{aligned} \tag{2.20}$$

where $\bar{\Box} = \partial_\mu\partial^\mu$ is the Minkowski d'Alembert operator, $\bar{X} = -\frac{1}{2}\eta^{\mu\nu}\phi_{,\mu}\phi_{,\nu}$ and c_i are constants for $i \in [1, 5]$, such that the Lagrangian is described with a Minkowski background. When considering integration by parts, the Lagrangian reduces to

$$\begin{aligned}\mathcal{L} = {} & c_1\phi + c_2\bar{X} - c_3\bar{X}\bar{\Box}\phi + c_4\bar{X}\left((\bar{\Box}\phi)^2 - \partial_\mu\partial_\nu\phi\,\partial^\mu\partial^\nu\phi\right) \\ & - \frac{c_5}{3}\bar{X}\left((\bar{\Box}\phi)^3 - 3\,\partial_\mu\partial_\nu\phi\,\partial^\mu\partial^\nu\phi\,\bar{\Box}\phi + 2\,\partial_\mu\partial_\nu\phi\,\partial^\nu\partial^\lambda\phi\,\partial_\lambda\partial^\mu\phi\right)\,. \end{aligned} \tag{2.21}$$

As stated in Sec. 2.1, by the equivalence principle, all laws of physics holding in flat spacetime can be incorporated in curved spacetime. Hence, each Minkowski ingredient can be promoted to curvature spacetime, such that

$$\eta_{\mu\nu} \to g_{\mu\nu}\,, \qquad \text{and} \qquad \partial_\mu \to \mathring{\nabla}_\mu\,. \tag{2.22}$$

It should be noted that such a transformation is not as straightforward as simply replacing the quantities. In contrast with partial derivatives, the covariant derivative is not commutative. This results in undesired higher-order derivatives in the Lagrangian Eq. (2.21). Additional correction terms are introduced to cancel out these higher-order derivatives, thus ensuring that the theory remains a second-order gravitational theory. Moreover, for a further generalisation, constants c_i will be substituted with arbitrary functions $G_i(\phi, X)$ dependent on ϕ and

$$X = -\frac{1}{2}g^{\mu\nu}\partial_\mu\phi\partial_\nu\phi\,, \tag{2.23}$$

such that Horndeski theory is given by

$$\mathcal{L}_{\text{Horndeski}} = \sum_{i=2}^{5}\mathcal{L}_i\,, \tag{2.24}$$

where

$$\mathcal{L}_2 = G_2(\phi, X)\,, \tag{2.25}$$

$$\mathcal{L}_3 = -G_3(\phi, X)\,\mathring{\Box}\phi\,, \tag{2.26}$$

$$\mathcal{L}_4 = G_4(\phi, X)\,\mathring{R} + G_{4,X}\left[(\mathring{\Box}\phi)^2 - \mathring{\nabla}_\mu\mathring{\nabla}_\nu\phi\,\mathring{\nabla}^\mu\mathring{\nabla}^\nu\phi\right], \tag{2.27}$$

$$\begin{aligned}\mathcal{L}_5 = {} & G_5(\phi, X)\mathring{G}_{\mu\nu}\mathring{\nabla}^\mu\mathring{\nabla}^\nu\phi \\ & - \frac{1}{6}G_{5,X}(\phi, X)\Big[(\mathring{\Box}\phi)^3 + 2\mathring{\nabla}_\nu\mathring{\nabla}_\mu\phi\,\mathring{\nabla}^\nu\mathring{\nabla}^\lambda\phi\,\mathring{\nabla}_\lambda\mathring{\nabla}^\mu\phi - 3\mathring{\Box}\phi\,\mathring{\nabla}_\mu\mathring{\nabla}_\nu\phi\,\mathring{\nabla}^\mu\mathring{\nabla}^\nu\phi\Big]\,,\end{aligned} \tag{2.28}$$

where $G_i(\phi, X)$ are arbitrary functions for $i \in [2, 5]$, functions of the form $G_{i,j}(\phi, X) = \frac{\partial G(\phi,X)}{\partial j}$ for $j \in [\phi, X]$, $\mathring{\nabla}_\mu$ is the Levi-Civita based covariant derivative defined in Eq. (2.7), and $\mathring{\Box} = \mathring{\nabla}_\mu\mathring{\nabla}^\mu$ is the d'Alembert operator.

Such a theory encompasses other scalar-tensor theories, constructed with the same restrictions. These include, and are not limited to: Generalised Brans-Dicke (GBD) [175] which is a generalisation of the original Brans-Dicke (BD) theory [61], generalised Galileon [177] which is a further generalisation of covariant Galileon [176, 116], cubic Galileon [178], Kinetic Gravity Braiding (KGB) [179], quintessence models [180, 181], nonminimal coupling of the form $f(\phi)\mathring{R}$ [182] and of the form $\mathring{G}^{\mu\nu}\phi_{,\mu}\phi_{,\nu}$ [183], k-inflation [184] and k-essence [185] models, $f(\mathring{R})$ models recast in terms of scalar-tensor notation [186, 187], Fab Four model [118] which later was extended to Fab Five model [188], and importantly the Einstein-Hilbert action [134]. Such a list of diverse models within Horndeski gravity emphasises the richness of the theoretical foundation, making it possible to study subcases well-studied within the literature. The Lagrangians of some of the subcases have been detailed in Table 2.2.

Despite the recent interest in Horndeski theory, the multimessenger observations of GW170817 by A-LIGO and Virgo collaboration [80], along with the measurements of electromagnetic counterpart GRB170817A [81] showed that gravitational wave speed is almost equivalent to the speed of light in a homogeneous universe, with deviations within one part in 10^{15}, specifically

$$-3 \times 10^{-15} < c_{\rm GW} - 1 < 7 \times 10^{-16}\,, \tag{2.29}$$

where $c^2_{\rm GW}$ is the propagation speeds of the tensor modes where [112]

$$c^2_{\rm GW} = \frac{G_4 - X(\ddot{\phi}G_{5,X} + G_{5,\phi})}{G_4 - 2XG_{4X} - X(H\dot{\phi}G_{5,X} - G_{5,\phi})}\,. \tag{2.30}$$

As a consequence, such stringent constraints eliminate branches of Horndeski gravity [189, 190, 191] when imposing that Eq. (2.30) is equivalent to the speed of light. In particular, it is required that [112]

$$G_4(\phi, X) \to G_4(\phi)\,, \qquad \text{and} \qquad G_5(\phi, X) \to c\,, \tag{2.31}$$

where c is a constant. The mixing term $g^{\mu\nu}\mathring{\nabla}_\mu\phi\mathring{\nabla}_\nu\phi$ in Eqs (2.27-2.28) yield to alteration to the graviton speed, resulting in restrictions on quartic Galileon and quintic Galileon [116, 117] models, de-Sitter Horndeski [192], Fab Four [118], and purely kinetic coupled models [119]. These theories sum up some of the most interesting cases of Horndeski gravity. Therefore, inflation [189], blackhole solutions [193, 194, 195], and neutron star studies [193, 196, 197] investigated within Horndeski theory and its subclasses are severely restricted, calling into question whether or not the terms modified in Eq. (2.31) can be revived either by considering higher order derivatives or reconsidering geometric foundations, the latter suggesting moving away from curved spacetime.

2.3 | Teleparallel Gravity

The concept of considering a different geometrical framework is not a new idea. Weyl first attempted to unify gravitation and electromagnetism in 1918 [198], a framework which later became the foundation for the notation of gauge theory [199, 200]. Following studies on torsion by Weitzenböck [60] and Cartan [59], Einstein himself suggested the formalism of torsion through a TEGR approach in an attempt to unify the two realms [58] due to its gauge theory terms in which it is constructed. Despite the unsuccessful attempt at unification, in recent years it has provided an avenue to approach gravitational theories from an alternative geometric perspective. It would be interesting to have a look at the more generalised metric-affine geometry before exploring its subcase of MTG.

The generalised metric-affine formalism can be obtained through the metric $g_{\mu\nu}$ described in Sec. 2.1 along with an affine connection $\hat{\Gamma}^\lambda_{\mu\nu}$ [201], where $\hat{\nabla}$ is the associated covariant derivative. It should be noted that overhat ($\hat{}$) notation is reserved for quantities obtained through the affine connection $\hat{\Gamma}^\lambda_{\mu\nu}$, while an overring ($\mathring{}$) still represents objects constructed from the Levi-Civita connection $\mathring{\Gamma}^\lambda_{\mu\nu}$. With these two structures, different geometrical objects can be defined to classify geometries through three spacetime characteristics:

- *Non-metricity* is defined as the measure of length change of a vector as it is parallel transported. It can be defined as

$$\hat{Q}_{\lambda\mu\nu} := \hat{\nabla}_\lambda g_{\mu\nu}\,, \tag{2.32}$$

  where the connection is eliminated.

- *Torsion* is defined through the antisymmetry[3] of the affine connection as

$$T^\lambda{}_{\mu\nu} := -2\hat{\Gamma}^\lambda_{[\mu\nu]}\,, \tag{2.33}$$

[3]Square brackets represent antisymmetry operator for which $\hat{\Gamma}^\lambda_{[\mu\nu]} = \frac{1}{2}\left(\hat{\Gamma}^\lambda_{\mu\nu} - \hat{\Gamma}^\lambda_{\nu\mu}\right)$.

such that it represents the measure of non-closure when parallel transporting two infinitesimal vectors to form a parallelogram.

- The property of *curvature* previously described in the realm of curvature-based geometry given by Eq. (2.9) can be generalised for an affine connection as

$$\hat{R}^{\lambda}{}_{\mu\rho\nu} = \hat{\Gamma}^{\lambda}_{\mu\nu,\rho} - \hat{\Gamma}^{\lambda}_{\mu\rho,\nu} + \hat{\Gamma}^{\lambda}_{\sigma\rho}\hat{\Gamma}^{\sigma}_{\mu\nu} - \hat{\Gamma}^{\lambda}_{\sigma\nu}\hat{\Gamma}^{\sigma}_{\mu\rho}\,, \tag{2.34}$$

which interprets the measure of rotation of a vector at the original position after moving along a closed curve.

These individual properties can be illustrated through Fig. 2.1.

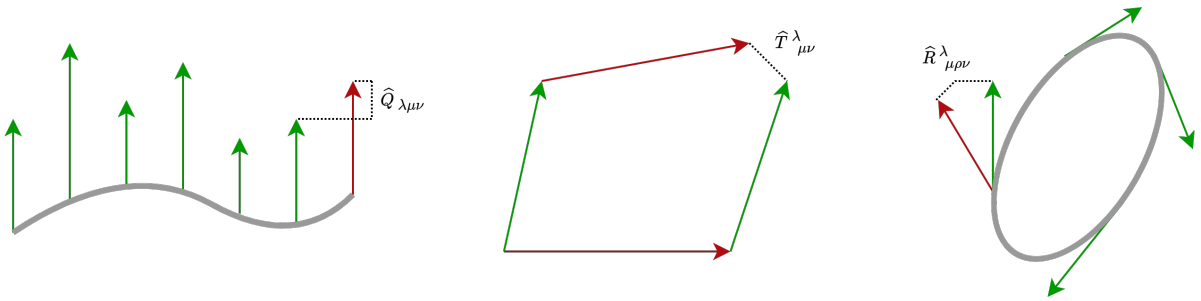

Figure 2.1: Illustration of the three characteristics of spacetime: non-metricity (2.32), torsion (2.33) and curvature (2.34). Figure adapted from Ref. [1].

The affine connection can be decomposed into

$$\hat{\Gamma}^{\lambda}_{\mu\nu} := \mathring{\Gamma}^{\lambda}_{\mu\nu} + \hat{K}^{\lambda}{}_{\mu\nu} + \hat{L}^{\lambda}{}_{\mu\nu}\,, \tag{2.35}$$

where $\mathring{\Gamma}^{\lambda}_{\mu\nu}$ is the Levi-Civita connection defined by Eq. (2.6), $\hat{K}^{\lambda}{}_{\mu\nu}$ is the contortion tensor

$$\hat{K}^{\lambda}{}_{\mu\nu} := \frac{1}{2}\left(\hat{T}_{\mu}{}^{\lambda}{}_{\nu} + \hat{T}_{\nu}{}^{\lambda}{}_{\mu} - \hat{T}^{\lambda}{}_{\mu\nu}\right)\,, \tag{2.36}$$

dependent on the torsion tensor and the disformation tensor

$$\hat{L}^{\lambda}{}_{\mu\nu} := \frac{1}{2}\left(\hat{Q}^{\lambda}{}_{\mu\nu} - \hat{Q}_{\mu}{}^{\lambda}{}_{\nu} - \hat{Q}_{\nu}{}^{\lambda}{}_{\mu}\right)\,, \tag{2.37}$$

expressed in terms of the non-metricity tensor. From metric-affine geometry, subclasses can be obtained by setting some of properties described by Eqs (2.32-2.34) [173], as summarised in Table. 2.1.

Subclass	**Connection**	**Geometry**
$\hat{Q}_{\lambda\mu\nu} = 0$	metric-compatible	Riemann-Cartan
$\hat{T}^{\lambda}{}_{\mu\nu} = 0$	symmetric	Weyl Gravity
$\hat{R}^{\lambda}{}_{\mu\rho\nu} = 0$	flat	General Teleparallel
$\hat{Q}_{\lambda\mu\nu} = 0$, $\hat{T}^{\lambda}{}_{\mu\nu} = 0$	Levi-Civita	GR and its extensions
$\hat{Q}_{\lambda\mu\nu} = 0$, $\hat{R}^{\lambda}{}_{\mu\rho\nu} = 0$	metric teleparallel	Metric Teleparallel / Torsional
$\hat{T}^{\lambda}{}_{\mu\nu} = 0$,$\hat{R}^{\lambda}{}_{\mu\rho\nu} = 0$	symmetric teleparallel	Symmetric Teleparallelism
$\hat{Q}_{\lambda\mu\nu} = 0$, $\hat{T}^{\lambda}{}_{\mu\nu} = 0$, $\hat{R}^{\lambda}{}_{\mu\rho\nu} = 0$	-	Minkowski Spacetime

Table 2.1: Subclasses of metric affine geometry by setting combination of Eqs (2.32-2.34) to vanish. For each subclass, the connection is listed along with the class of geometry in which these conditions are satisfied. TEGR action in Eq. (2.68) falls under the metric teleparallel class and STEGR action in Eq. (2.69) falls under the symmetric teleparallel class.

The trinity of gravity refers to the three major frameworks that describe gravity obtained by setting one of the characteristics in Fig. 2.1 to be non-zero: GR, metric teleparallel and symmetric teleparallel geometries [1]. In Sec. 2.1, it has already been shown that contraction of the Riemann tensor given by Eq. (2.9) after setting torsion and non-metricity tensors to vanish in Eq. (2.34), yield the Ricci scalar by which the Einstein-Hilbert action given by Eq. (2.14) is described. Similarly, contractions of torsion tensor (2.33) and non-metricity (2.32) separately, independent of the other spacetime characteristics, can obtain a dynamical equivalence to GR [1]. Here, the focus will be shifted to the metric teleparallel geometry in which we will obtain such equivalence.

As previously stated, the metric teleparallel geometry is curvatureless and satisfies the metricity condition:

$$R^{\lambda}{}_{\mu\rho\nu} = 0\,, \qquad \text{and} \qquad Q_{\lambda\mu\nu} = 0\,, \tag{2.38}$$

where the over-hat ($\hat{}$) notation has been dropped when referring to quantities using the torsionful connection $\Gamma^{\lambda}_{\mu\nu}$, with the latter being obtained through modifications of Eq. (2.35) yielding

$$\Gamma^{\lambda}_{\mu\nu} := \hat{\Gamma}^{\lambda}_{\mu\nu}(R^{\lambda}{}_{\mu\rho\nu} = 0\,, Q_{\lambda\mu\nu} = 0) = \mathring{\Gamma}^{\lambda}_{\mu\nu} + K^{\lambda}{}_{\mu\nu}\,, \tag{2.39}$$

such that the difference between a torsionful connection and a curvatureful connection is given by the contortion tensor. The disformation tensor vanishes as

$$L^{\lambda}{}_{\mu\nu} := \hat{L}^{\lambda}{}_{\mu\nu}(R^{\lambda}{}_{\mu\rho\nu} = 0\,, Q_{\lambda\mu\nu} = 0) = 0\,. \tag{2.40}$$

In contrast with the curvature-based theories such as GR and Horndeski gravity, the metric $g_{\mu\nu}$ is no longer the fundamental dynamical object of a torsionful theory, instead described through the tetrad ${e^A}_\mu$ and spin connection ${\omega^A}_{B\mu}$, where capital Latin indices $\{A, B, C, \ldots\}$ represent the local Minkowski spacetime, and Greek indices $\{\alpha, \beta, \gamma, \ldots\}$ represent the general manifold.

The foundation of gauge theories is to consider a general differentiable manifold where for each point x^μ of spacetime, there exists a tangent space represented by a basis of vector for the tetrad field given by

$$\{\mathbf{E}_A\} = \{\partial_A\}\,, \qquad \text{and} \qquad \{\mathbf{e}^A\} = \{dx^A\}\,, \tag{2.41}$$

such that the soldering between each point of the general spacetime and the Minkowski tangent space is given by

$$E_A = {E_A}^\mu \partial_\mu\,, \qquad \text{and} \qquad e^A = {e^A}_\mu dx^\mu\,, \tag{2.42}$$

where ${e^A}_\mu$ is the tetrad, and ${E_A}^\mu$ is the inverse tetrad which by definition of dual bases satisfies the orthogonality condition

$${e^A}_\mu {E_B}^\mu = \delta^A_B\,, \qquad \text{and} \qquad {e^A}_\mu {E_A}^\nu = \delta^\nu_\mu\,, \tag{2.43}$$

where δ^ν_μ is the four-dimensional Kronecker delta [22]. With the aid of the tetrad, the Minkowski spacetime η_{AB} can be linked to the general manifold $g_{\mu\nu}$ through the relationship

$$g_{\mu\nu} = \eta_{AB} {e^A}_\mu {e^B}_\nu\,, \qquad \text{and} \qquad \eta_{AB} = g_{\mu\nu} {E_A}^\mu {E_B}^\nu\,. \tag{2.44}$$

The commutator of the basis $\{\mathbf{E}_A\}$ gives the relationship [202, 129]

$$[\mathbf{E}_A, \mathbf{E}_B] = {f^C}_{AB} E_C\,, \tag{2.45}$$

where ${f^C}_{AB}$ represents the anholonomy of the frame such that

$${f^C}_{AB} = {E_A}^\mu {E_B}^\nu \left(\partial_\nu {e^C}_\mu - \partial_\mu {e^C}_\nu\right)\,, \tag{2.46}$$

and encapsulates both inertial and gravitational effects. In the case where ${f^C}_{AB} = 0$, this will result in a holonomic basis, such that they are locally integrable [22].

MTG, through the tetrad, naturally constructs a gauge theory of translations [203]. Gauge theory of rotation does not necessarily conserve the energy-momentum tensor covariantly [204]. Hence, by considering the gauge translation of [22]

$$\tilde{x}^A \to x^A + \xi^A\,, \tag{2.47}$$

where $\xi^A(x^\mu)$ represents the infinitesimal local transformation such that operators ∂_A generate these transformations and satisfy $[\partial_A, \partial_B] = 0$. When considering the infinitesimal transformation, denoted by δ_e, of a source field, $\Psi(\tilde{x}^A(x^\mu))$ is given by

$$\delta_e \tilde{\Psi} = \xi^A \partial_A \Psi \,, \tag{2.48}$$

while its derivative

$$\delta_e(\partial_\mu \tilde{\Psi}) = \xi^A \partial_A(\partial_\mu \Psi) + (\partial_\mu \xi^A)(\partial_A \Psi) \,, \tag{2.49}$$

where the second term on the left-hand side violates gauge invariance. Point-dependent transformations, such as gauge transformations, are said to be covariant under transformation but their derivatives are not necessarily covariant [23]. Therefore, it is required to introduce the gauge potential $B^A{}_\mu$, where, by definition,

$$\delta_e B^A{}_\mu = -\partial_\mu \xi^A \,. \tag{2.50}$$

This is obtained by defining the gauge derivative as

$$\mathbf{e}_\mu \Psi = e^A{}_\mu \partial_A \Psi := \partial_\mu \Psi + B^A{}_\mu \partial_A \Psi \,, \tag{2.51}$$

implying that the non-trivial tetrad is given by

$$e^A{}_\mu = \partial_\mu x^A + B^A{}_\mu \,, \tag{2.52}$$

such that gauge invariance is obtained and gives

$$\delta_e(\mathbf{e}_\mu \Psi) = \xi^A \partial_A(\partial_\mu \Psi) \,. \tag{2.53}$$

Apart from what $f^C{}_{AB}$ in Eq. (2.46) represents, up to this point, all relationships presented hold for both trivial and non-trivial frames. The inertial effects are introduced as the Lorentz transformation $\Lambda^A{}_B$ from Lorentz group $S0 = O(1,3)$ applicable to the local Minkowski spacetime such that

$$\tilde{x}^A = \Lambda^A{}_B x^B \,. \tag{2.54}$$

It should be noted that $B^A{}_\mu$ is classified as a Lorentz vector in tangent space, which by definition

$$\tilde{B}^A{}_\mu = \Lambda^A{}_B B^B{}_\mu \,. \tag{2.55}$$

Applying Local Lorentz Transformation (LLT) to the tetrad as defined in Eq. (2.52) and substituting Eqs (2.54-2.55) results in

$$\begin{aligned} \tilde{e}^A{}_\mu = \Lambda^A{}_B e^A{}_\mu &= \Lambda^A{}_B \partial_\mu x^A + \Lambda^A{}_B B^B{}_\mu \\ &= \partial_\mu x^A + B^A{}_\mu + \Lambda^A{}_B \partial_\mu \Lambda_C{}^B x^C \,. \end{aligned} \tag{2.56}$$

The last term is the flat spin connection

$$\omega^{A}{}_{C\mu} = \Lambda^{A}{}_{B}\partial_{\mu}\Lambda_{C}{}^{B} \tag{2.57}$$

showing that it is a pure gauge degree of freedom and is a fundamental component when dealing with metric teleparallelism [60, 68]. It is antisymmetric in the first two indices such that $\omega^{A}{}_{B\mu} = -\omega^{B}{}_{A\mu}$ and satisfies [173]

$$\partial_{[\mu}\omega^{A}{}_{|B|\nu} + \omega^{C[\mu]}\omega^{C}{}_{|B|\nu]} = 0\,. \tag{2.58}$$

The spin connection can counter the contributions of the tetrad, since an infinite number of tetrad choices yield the same metric tensor given in Eq. (2.44), ensuring it remains covariant [205]. In a pure tetrad MTG, the Weitzenböck gauge

$$\omega^{A}{}_{B\mu} = 0 \tag{2.59}$$

can be applied since there always exists a Lorentz frame wherein the spin connection experiences LLT invariance [60]. Additionally, the covariant derivative as a result of the spin connection is defined as

$$\mathcal{D}_{\mu}x^{A} = e^{A}{}_{\mu} = \partial_{\mu}x^{A} + B^{A}{}_{\mu} + \omega^{A}{}_{B\mu}x^{B}\,, \tag{2.60}$$

and commutating the gauge derivatives $e^{A}{}_{\mu}\partial_{A}$ defined in Eq. (2.60) gives

$$[e^{A}{}_{\mu}, e^{A}{}_{\nu}]\partial_{A} = T^{A}{}_{\mu\nu}\partial_{A} = 2(\partial_{[\mu}B^{A}{}_{\nu]} + \omega^{A}{}_{B[\mu}B^{B}{}_{\nu]})\partial_{A}\,.$$

By adding the vanishing term $[\mathcal{D}_{\mu}, \mathcal{D}_{\nu}] = 0$ to right-hand side [22] and substituting Eq. (2.60), followed by the spin connection condition in Eq. (2.58), an expression for the torsion tensor is obtained:

$$T^{A}{}_{\mu\nu} = \mathcal{D}_{\mu}e^{A}{}_{\nu} - \mathcal{D}_{\nu}e^{A}{}_{\mu}\,, \tag{2.61}$$

implying that since the tetrad is gauge invariant, then the torsion tensor is also gauge invariant [22, 173]. This makes the torsion tensor $T^{A}{}_{\mu\nu}$ the translation gauge field strength of TG which transforms covariantly under LLT and diffeomorphisms [205]. Therefore, the teleparallel connection defined in Eq. (2.39) can be expressed as [206, 207]

$$\Gamma^{\lambda}_{\nu\mu} := E_{A}{}^{\lambda}\mathcal{D}_{\mu}e^{A}{}_{\nu} = E_{A}{}^{\lambda}\left(\partial_{\mu}e^{A}{}_{\nu} + \omega^{A}{}_{B\mu}e^{B}{}_{\nu}\right)\,, \tag{2.62}$$

such that the torsion tensor expressed in terms of general coordinate indices is given by [23]

$$T^{\lambda}{}_{\mu\nu} = -2\Gamma^{\lambda}_{[\mu\nu]}\,. \tag{2.63}$$

It should be noted that through this work, the Weitzenböck gauge given in Eq. (2.59) has been applied. Next, the gauge current of the gravitational momentum tensor is given by the superpotential tensor [208, 23]

$$S_\lambda{}^{\mu\nu} = \frac{1}{2}K^{\mu\nu}{}_\lambda - \delta^\mu_\lambda T_\sigma{}^{\sigma\nu} + \delta^\nu_\lambda T_\sigma{}^{\sigma\mu}\,. \tag{2.64}$$

Contraction of the torsion tensor in Eq. (2.63) and the superpotential in Eq. (2.64) results in the torsion scalar

$$T = S_\lambda{}^{\mu\nu}T^\lambda{}_{\mu\nu}\,, \tag{2.65}$$

analogous to Ricci scalar $\mathring{R}$ given by Eq. (2.11) obtained in curvature-based theories using the Levi-Civita connection. In fact, comparing $\mathring{R}$ and T results in the relationship

$$\mathring{R} = -T + B\,. \tag{2.66}$$

The two quantities are seen to differ by a boundary term

$$B = 2\mathring{\nabla}_\mu T^\lambda{}_\lambda{}^\mu = \frac{2}{e}\partial_\mu\left(e\,T^\lambda{}_\lambda{}^\mu\right)\,. \tag{2.67}$$

While T accounts for second-order contributions, the total divergence term of B encapsulates fourth-order derivatives [209], leading to a dynamical equivalence between T and $\mathring{R}$. This implies that if one considers the action

$$\mathcal{S}_{\rm TEGR} = -\frac{1}{2\kappa^2}\int d^4x\,e\,T + \int d^4x\,e\,\mathcal{L}_{\rm m}\,, \tag{2.68}$$

and varying the action with respect to the tetrad, the Einstein field equation (2.15) is obtained. Hence, the action given by Eq. (2.68) is referred to as TEGR. A similar result can be obtained in the case of symmetric teleparallel gravity wherein Symmetric Teleparallel Equivalent of General Relativity (STEGR) action can be obtained by the action

$$\mathcal{S}_{\rm STEGR} = -\frac{1}{2\kappa^2}\int d^4x\,e\,\breve{Q} + \int d^4x\,e\,\mathcal{L}_{\rm m}\,, \tag{2.69}$$

where ($\breve{}$) symbolises quantities obtained solely through non-metricity property. Eq. (2.14), Eq. (2.68), and Eq. (2.69) together form the trinity of gravity [1].

TEGR, despite offering a different geometric foundation to represent gravity, still falls into the traps of GR, as discussed in Sec. 2.1. Thus, modified teleparallel theories are more appealing. Analogous to $f(\mathring{R})$ theory [186], the action can be extended to include functions dependent on the tetrad-based scalars such as $f(T)$ [69], NGR [70], $f(T,B)$ [71], Gauss-Bonnet theories [210, 211], non-minimally coupled matter [212], and scalar-tensor theories [61, 73, 72], some of which are summarised in Table 2.2. Such modifications have been explored to tackle inflation, dark matter, and dark energy [174]. Therefore, with the MTG formalism and the advantages of the Horndeski theory construction outlined in Sec. 2.2, a new avenue is provided to develop a broader class of scalar-tensor cosmologies.

2.4 | Teleparallel analog of Horndeski Theory

The most general second-order metric teleparallel theory of gravity with a single scalar field is obtained through BDLS [78]. This theory is considered to be the teleparallel analogue of Horndeski theory since it reaps the benefits of working within the metric teleparallel geometry while also allowing the introduction of a scalar field. While Horndeski theory became quite restricted following the observations of GW170817 [45, 81], as detailed in Sec. 2.2, BDLS has provided an avenue to revive previously discarded models by including teleparallel contributions [213].

In this section, the construction of BDLS is presented. The criteria for constructing BDLS theory are as follows [78]:

- field equations with respect to both tetrad and scalar are up to second order to avoid ghost instabilities that stem from higher-order theories,
- scalar invariants should not be parity violating to ensure they are in line with the observed isotropy and homogeneity of the Universe,
- consider up to quadratic contractions of torsion tensor.

The starting point of BDLS is the standard Horndeski Lagrangian given by Eq. (2.24), obtained through tetrad formalism. This means that all quantities expressed in terms of the metric are expanded by substituting the relationship in Eq. (2.44), and $\mathring{R}$ is expressed in terms of the equality given by Eq. (2.66). Next, the torsion tensor is considered, as it is the non-zero spacetime characteristic in MTG which transforms covariantly under diffeomorphisms and local Lorentz transformation, thus labelled as fully invariant [173]. The torsion tensor in Eq. (2.63) can be decomposed into irreducible parts with respect to the local Lorentz group [214]

$$T_{\lambda\mu\nu} = \frac{2}{3}\left(t_{\lambda\mu\nu} - t_{\lambda\nu\mu}\right) + \frac{1}{3}\left(g_{\lambda\mu}\, v_\nu - g_{\lambda\nu}\, v_\mu\right) + \epsilon_{\lambda\mu\nu\rho}\, a^\rho\,, \tag{2.70}$$

where

$$a_\mu = \frac{1}{6}\epsilon_{\mu\nu\lambda\rho}\, T^{\nu\lambda\rho}\,, \tag{2.71}$$

$$v_\mu = T^\lambda{}_{\lambda\mu}\,, \tag{2.72}$$

$$t_{\lambda\mu\nu} = \frac{1}{2}\left(T_{\lambda\mu\nu} + T_{\mu\lambda\nu}\right) + \frac{1}{6}\left(g_{\nu\lambda}\, v_\mu + g_{\nu\mu}\, v_\lambda\right) - \frac{1}{3} g_{\lambda\mu}\, v_\nu\,, \tag{2.73}$$

are the axial part associated with the complete antisymmetric portion of the torsion tensor related to spin and rotational effects, the vectorial part where the trace of the torsion tensor is related to its divergence, and the purely tensorial part stemming from the remaining traceless

portion, respectively [70]. Additionally, $\epsilon_{\mu\nu\lambda\rho}$ is the four-dimensional Levi-Civita tensor. The tensorial irreducible part has the following properties [70]:

$$t_{\lambda\mu\nu} = t_{\mu\lambda\nu}\,, \tag{2.74}$$

$$0 = t_{\lambda\mu}{}^{\mu} = t^{\mu}{}_{\mu\nu}\,, \tag{2.75}$$

$$0 = t_{\lambda\mu\nu} + t_{\mu\nu\lambda} + t_{\nu\lambda\mu}\,. \tag{2.76}$$

By considering the quadratic of each irreducible part, it results in three scalar invariants:

$$T_{\rm ax} = a_\mu a^\mu = -\frac{1}{18}\left(T_{\lambda\mu\nu}T^{\lambda\mu\nu} - 2T_{\lambda\mu\nu}T^{\mu\lambda\nu}\right)\,, \tag{2.77}$$

$$T_{\rm vec} = v_\mu v^\mu = T^{\lambda}{}_{\lambda\mu}T_{\rho}{}^{\rho\mu}\,, \tag{2.78}$$

$$T_{\rm ten} = t_{\lambda\mu\nu}t^{\lambda\mu\nu} = \frac{1}{2}\left(T_{\lambda\mu\nu}T^{\lambda\mu\nu} + T_{\lambda\mu\nu}T^{\mu\lambda\nu} - T^{\lambda}{}_{\lambda\mu}T_{\rho}{}^{\rho\mu}\right)\,. \tag{2.79}$$

Linear combination of these scalar invariants yields the torsion scalar

$$T = \frac{3}{2}T_{\rm ax} + \frac{2}{3}T_{\rm ten} - \frac{2}{3}T_{\rm vec}\,, \tag{2.80}$$

identical to the expression given by Eq. (2.64) constructed through the contraction of the torsion tensor and the superpotential tensor. It should be noted that these scalar invariants are also parity-preserving. This condition ensures that the laws of physics do not alter the behaviour of fields, matter, and spacetime when observing the Universe in different configurations. Additional tensorial contractions

$$P_1 = v^\mu a_\mu\,, \qquad \text{and} \qquad P_2 = \epsilon_{\mu\nu\sigma\rho}\,t^{\lambda\mu\nu}t_{\lambda}{}^{\rho\sigma}\,, \tag{2.81}$$

are in fact parity violating terms, thus omitted due to their non-physicality of the scalar. In general, the most general second-order Lagrangian formed through the quadratic contractions of torsion tensor with no parity violating terms is represented by

$$\mathcal{L}_{\rm NGR} = f(T_{\rm ax}, T_{\rm vec}, T_{\rm ten})\,, \tag{2.82}$$

dubbed as New General Relativity (NGR) [70, 214].

Up to this point, contributions from scalar and torsion tensor have been treated separately. Full construction of a generalised second-order Lagrangian requires considering the contractions between these distinct contributors. Starting with contractions between linear irreducible torsion tensor parts and first-order covariant derivatives of the scalar fields attain

$$I_1 = t^{\lambda\mu\nu}\,\mathring{\nabla}_\lambda\phi\,\mathring{\nabla}_\mu\phi\,\mathring{\nabla}_\nu\phi\,, \tag{2.83}$$

$$I_2 = v^\lambda\,\mathring{\nabla}_\lambda\phi\,, \tag{2.84}$$

$$I_3 = a^\lambda\,\mathring{\nabla}_\lambda\phi\,. \tag{2.85}$$

A combination of the conditions of the tensorial component given by Eqs (2.74-2.76) yield the condition $t_{(\lambda,\mu\nu)} = 0$, implying that scalar invariant I_1 in Eq. (2.83) naturally vanishes. I_3 in Eq. (2.85) contains an odd number of axial components, resulting in the scalar quantity being parity violating and thus excluded from the Lagrangian.

Additionally, contractions between quadratic torsion tensor parts with derivatives of the scalar field result in the following scalar quantities:

$$J_1 = a^\mu\, a^\nu\, \mathring{\nabla}_\mu\phi\, \mathring{\nabla}_\nu\phi\,, \tag{2.86}$$

$$J_2 = v^\mu\, v^\nu\, \mathring{\nabla}_\mu\phi\, \mathring{\nabla}_\nu\phi\,, \tag{2.87}$$

$$J_3 = v_\lambda\, t^{\lambda\mu\nu}\, \mathring{\nabla}_\mu\phi\, \mathring{\nabla}_\nu\phi\,, \tag{2.88}$$

$$J_4 = v_\mu\, t^{\lambda\mu\nu}\, \mathring{\nabla}_\lambda\phi\, \mathring{\nabla}_\nu\phi\,, \tag{2.89}$$

$$J_5 = t_\lambda{}^{\mu\nu}\, t^\lambda{}_{\bar{\mu}\nu}\, \mathring{\nabla}_\mu\phi\, \mathring{\nabla}^{\bar{\mu}}\phi\,, \tag{2.90}$$

$$J_6 = t^{\lambda\mu\nu}\, t_\lambda{}^{\bar{\mu}\bar{\nu}}\, \mathring{\nabla}_\mu\phi\, \mathring{\nabla}_\nu\phi\, \mathring{\nabla}_{\bar{\mu}}\phi\, \mathring{\nabla}_{\bar{\nu}}\phi\,, \tag{2.91}$$

$$J_7 = t^{\lambda\mu\nu}\, t^{\bar{\lambda}\bar{\mu}}{}_\lambda\, \mathring{\nabla}_\mu\phi\, \mathring{\nabla}_\nu\phi\, \mathring{\nabla}_{\bar{\lambda}}\phi\, \mathring{\nabla}_{\bar{\mu}}\phi\,, \tag{2.92}$$

$$J_8 = t^{\lambda\mu\nu}\, t_{\lambda\mu}{}^{\bar{\nu}}\, \mathring{\nabla}_\nu\phi\, \mathring{\nabla}_{\bar{\nu}}\phi\,, \tag{2.93}$$

$$J_9 = t^{\lambda\mu\nu}\, t^{\bar{\lambda}\bar{\mu}\bar{\nu}}\, \mathring{\nabla}_\lambda\phi\, \mathring{\nabla}_\mu\phi\, \mathring{\nabla}_\nu\phi\, \mathring{\nabla}_{\bar{\lambda}}\phi\, \mathring{\nabla}_{\bar{\mu}}\phi\, \mathring{\nabla}_{\bar{\nu}}\phi\,, \tag{2.94}$$

$$J_{10} = \epsilon^\mu{}_{\nu\rho\lambda}\, a^\nu t^{\sigma\rho\lambda}\, \mathring{\nabla}_\mu\phi\, \mathring{\nabla}_\sigma\phi\,. \tag{2.95}$$

Not all quantities are independent of each other, or other components previously defined. These relationships are summarised as

$$J_2 = I_2^2\,, \qquad J_4 = J_3\,, \qquad J_7 = -2J_6\,. \tag{2.96}$$

It suffices to include only $\{I_2, J_3, J_6\}$ instead of $\{I_2, J_2, J_3, J_4, J_6, J_7\}$. Additionally, total symmetry of tensorial component $t_{(\lambda\mu\nu)} = 0$ yields $J_9 = 0$.

Therefore, the full teleparallel Lagrangian is obtained by combining contributions from scalar field ϕ along with the kinetic term X, purely torsion tensor contributions given by Eqs (2.77-2.79), contractions between linear torsion tensor components and the derivative of the scalar field summarised in Eqs (2.83-2.85), and the contractions between quadratic torsion tensor components and scalar derivatives listed in Eqs (2.86-2.95):

$$\mathcal{L}_{\rm Tele} = G_{\rm Tele}(\phi, X, T, T_{\rm ax}, T_{\rm vec}, I_2, J_1, J_3, J_5, J_6, J_8, J_{10})\,, \tag{2.97}$$

where vanishing terms, parity-violating terms, and dependent terms are excluded in the arbitrary function. Note, that $T_{\rm ten}$ is not included in the function since it is being represented by T. This is done to easily see subcases of BDLS theory which are dependent on the torsion scalar, such as the commonly studied case of $f(T)$ [206, 69, 215, 216, 217, 218, 219, 220, 221]. The BDLS

action representing the most general second-order TG theory with one scalar field is given by

$$
\begin{aligned}
S_{\rm BDLS} = \frac{1}{2\kappa^2}\int d^4x\, e \Big\{ & G_2(\phi,X) - G_3(\phi,X)\,\mathring{\Box}\phi + G_4(\phi,X)\,(-T+B) \\
& + G_{4,X}(\phi,X)\left((\mathring{\Box}\phi)^2 - \mathring{\nabla}_\mu\mathring{\nabla}_\nu\phi\mathring{\nabla}^\mu\mathring{\nabla}^\nu\phi\right) + G_5(\phi,X)\,\mathring{G}_{\mu\nu}\,\mathring{\nabla}^\mu\mathring{\nabla}^\nu\phi \\
& - \frac{1}{6}G_{5,X}(\phi,X)\left((\mathring{\Box}\phi)^3 + 2\mathring{\nabla}_\nu\mathring{\nabla}_\mu\phi\mathring{\nabla}^\nu\mathring{\nabla}^\lambda\phi\mathring{\nabla}_\lambda\mathring{\nabla}^\mu\phi - 3\mathring{\Box}\phi\mathring{\nabla}_\mu\mathring{\nabla}_\nu\phi\mathring{\nabla}^\mu\mathring{\nabla}^\nu\phi\right) \\
& + G_{\rm Tele}\left(\phi,X,T,T_{\rm ax},T_{\rm vec},I_2,J_1,J_3,J_5,J_6,J_8,J_{10}\right)\Big\} + \int d^4x\, e\,\mathcal{L}_{\rm m}\,.
\end{aligned}
\tag{2.98}
$$

Here, the Ricci scalar $\mathring{R}$ previously included in the $\mathcal{L}_4$ Horndeski Lagrangian component in Eq. (2.27) has been replaced by the linear combination of $-T+B$ since they have been shown to be identical by Eq. (2.66). Additionally, this might raise the question as to why the boundary term B has been excluded in the teleparallel contribution of Eq. (2.97). B produces fourth order elements in the theory, and as such would violate the criterion listed in the beginning of the section.

2.5 | Summary

BDLS theory offers a richer framework with an abundance of possible viable cosmological models. The action given by Eq. (2.98) shows that casting Horndeski gravity into a metric-teleparallel framework can realise the Lagrangians listed in Eqs (2.25-2.28) with an additional teleparallel function. $G_{\rm Tele}$ in Eq. (3.29) is made up of twelve scalar invariants given by Eqs (2.23, 2.80, 2.77, 2.78, 2.84, 2.86, 2.88, 2.90, 2.91, 2.93, 2.95), constructed through tetrad-tetrad and tetrad-scalar combinations. One of the main interests in considering BDLS is that by taking appropriate limits a plethora of theories of gravity well-studied in literature can be obtained. Some of the subclasses are listed in Table 2.2. On the other hand, it provides an avenue to study other subcases not yet explored. In the subcases listed, it should be noted that if the G_4 contribution is omitted, it is counteracted by including a torsion dependency in $G_{\rm Tele}$. This is to the link between $\mathring{R}$ and T through Eq. (2.66) which signifies a dynamical equivalence as the two scalars differ by a boundary term. Hence, an equivalence to GR can be obtained for all theories listed provided appropriate limits are taken.

GR brought a revolution in our understanding of gravity, conceptualizing it as a phenomenon resulting from the curvature of spacetime caused by mass and energy in the Universe. Despite the many successes of GR, such as predicting GW [46, 223, 45] and explaining the perihelion precession of planets [135], it does not provide an explanation of dark matter which influences the structures of the Universe and dark energy which drive the observed accelerated expansion. While past observations have favoured the ΛCDM model to tackle these very issues, growing tensions

Theory	**Functions**					**References**
	$\boldsymbol{G_2}$	$\boldsymbol{G_3}$	$\boldsymbol{G_4}$	$\boldsymbol{G_5}$	$\boldsymbol{G_{\rm Tele}}$	
Horndeski	G_2	G_3	G_4	G_5	0	[66]
GBD	$f(\phi)X$	$2g(\phi)X$	$\frac{1}{2}h(\phi)$	0	0	[175]
BD	$2\omega_{\rm BD}\frac{X}{\phi}$	0	ϕ	0	0	[61]
Scalar $f(\mathring{R})$	$f(\phi)-\phi f'(\phi)$	0	$f'(\phi)$	0	0	[222]
KGB	$f(\phi,X)$	$g(\phi,X)$	1	0	0	[179]
GR	0	0	1	0	0	[134]
NGR	0	0	0	0	$f(T_{\rm ax},T_{\rm vec},T_{\rm ten})$	[70]
TEGR	0	0	0	0	$-T$	[58]
$f(T)$	0	0	0	0	$f(T)$	[69]
$f(\phi,X,T)$	0	0	0	0	$f(\phi,X,T)$	[114]
$f(\phi,T)+Xg(\phi)$	$Xf(\phi)$	0	0	0	$g(\phi,T)$	[113]
Generalised Teleparallel Dark Energy	$f(\phi)+X$	0	0	0	$-g(\phi)T$	[73]
Generalised Teleparallel Scalar Tensor	$f(\phi,X)$	$g(\phi,X)$	0	0	$h(\phi)T$	[72]

Table 2.2: Subclasses of BDLS theory given by the action in Eq. (2.98). Functions f, g, and h are arbitrary functions dependent on the components specified in each case. $\omega_{\rm BD}$ is the Brans-Dicke constant.

stemming from recent surveys [102, 89, 2, 224, 107, 225, 94] further drive the need to consider theories beyond GR. Horndeski gravity has provided the structure within a curvature-based geometry while including the additional scalar field. Additionally, shifting from curvature-based geometry and instead describing gravitational fields through torsion allows for a geometrical interpretation where it acts as a gauge theory for the translation group. Therefore, having a combination of Horndeski gravity and MTG would result in a higher number of DoFs and realise a local energy-momentum tensor which is linked to the superpotential given by Eq. (2.64); resulting in BDLS.

The generalised framework of BDLS is a broader theory than standard Horndeski gravity. While the number of possible cosmological models is larger, this does not imply that they are viable to explain the cosmic history of the Universe. Constraints for these models can be obtained through comparisons with observational data and mathematical restrictions, resulting in a list of conditions that would need to be satisfied. From a theoretical point of view, these restrictions would not only apply to the generalised BDLS systems but to the subcases of the theory. This implies that calculations would be facilitated, as derivations would not need to be carried out from scratch to study subcases of BDLS. The rest of the chapters will delve into a study of scalar-tensor theories through the lens of BDLS and its subclasses.

3

Well-Tempering Cosmology

The CC described through Λ has been introduced in Eq. (2.16) as a free parameter in addition to Einstein's original field equations in GR. Despite success and continual adoption of the ΛCDM model in recent studies, one of the main issues that has persisted is that of the CC problem: the observations of Baryon Acoustic Oscillations (BAO), CMB, supernova and the values of vacuum energy within the ΛCDM model do not coincide upon taking into consideration the entire selection of fundamental particles provided by the current standard model of particle physics [43]. Therefore, the CC problem can be summarised through the following statement: the theoretical predictions from particle physics predict a vacuum energy that is much larger than the one being observed nowadays. Further details will be fleshed out in the following pages of this section. Exploring the CC problem could shed light on the status of the dark energy, represented as a constant vacuum energy dominating the accelerated expansion of the Universe.

As already mentioned in the previous chapter, the CC is considered to behave as a repulsive force to counteract a Universe that otherwise would be experiencing a collapse as relativistic and non-relativistic matter contribute to a negative acceleration for the scale factor [43]. Initially, the CC modification was implemented to realise a static Universe, where Einstein found the formalism to be in concordance with Mach's principle that matter determined inertia [35]. The combination of de Sitter's cosmological model, which excludes matter from contributing to the production of inertia [226], its consistency with the observed redshifts of spiral nebulae [43, 227], and Hubble's discovery of the expanding Universe [33], rendered Einstein's CC unnecessary.

While Einstein retracted the CC, nowadays the term has adopted an altered meaning following the discovery that the Universe not only is expanding, but it is experiencing an accelerated expansion [153]. Supernovae Type Ia are classified as standard candles, as they have a relative peak intrinsic brightness, a property which is used as a tool to measure distances and determine the rate of expansion of the Universe [153]. From the discovery of accelerated expansion, the concept of *dark energy* became another ingredient within the Universe which comes into play

to drive the expansion. Here, the CC offered an avenue to describe dark energy as a constant net vacuum energy which is present throughout the history of the Universe in addition to other forms of energy. These other forms appear to be more prominent at earlier stages in cosmic history and die out with time, leaving dark energy to persist and become the dominant energy form. This can be seen through the following derivation. A vacuum can be described as a perfect fluid where

$$p_\Lambda = -\rho_\Lambda \,, \tag{3.1}$$

such that for a positive energy density, the pressure is negative to result in the accelerated expansion [228]. This result stems from the assumption of a constant energy density within GR applied to the Friedmann and fluid equations of motion. Provided a flat spacetime cosmology is considered, $k = 0$, the first Friedmann equation becomes

$$H^2 = \frac{8\pi}{3} G\rho \,. \tag{3.2}$$

When considering the energy densities of relativistic particles of the radiation epoch ρ_r and non-relativistic particles corresponding to the matter-dominated era ρ_m in addition to the vacuum energy, Eq. (3.2) can be expanded to

$$H^2 = \frac{8\pi}{3} G(\rho_\mathrm{m} + \rho_\mathrm{r} + \rho_\Lambda) \propto \frac{8\pi}{3} G \left(\frac{1}{a(t)^3} + \frac{1}{a(t)^4} + \rho_\Lambda \right) . \tag{3.3}$$

It can be seen as the Universe expands (as the scale factor value increases), the contributions from radiation and matter epoch diminish and the vacuum energy density, in this case a constant, persists.

It should be noted that in the above calculation, the assumption that vacuum energy density is positive has been taken. From a classical perspective, such a statement can be considered contradicting since a vacuum typically corresponds to a null energy density. But, this is not the case within particle physics. Eq. (2.16) illustrates the relationship between the geometry of spacetime and the energy and momentum of the Universe, which includes the contributions of radiation and matter sources as seen in Eq. (3.3) [35]. Heisenberg's principle states that quantum fluctuations occur as particle and antiparticle pairs are being created and annihilated [24] such that the summation of these processes of all fundamental particles, including the Higgs boson, as they interact with each other results in a non-zero vacuum energy density [35]. Thus, in quantum field theory, a vacuum is said to have the lowest energy density, which does not imply that it has a zero absolute value. Moreover, $\rho_\Lambda > 0$ corresponds to observations of Supernovae Type Ia [153], CMB studies performed by COBE satellite [154, 229] and Planck Collaboration [155, 2], investigations of matter density through gravitational lensing and temperature profiles of X-ray gas [230], provided CC model is assumed.

It is precisely this discrepancy between the theoretical and observational value of CC that yields a problem in our understanding of quantum field theory and GR. Provided quantum field theory holds up to Planck scale, the vacuum energy density is of orders of $\rho_\Lambda^{\text{Planck}} \sim \left(10^{18}\,\text{GeV}\right)^4$ while cosmological observations dictate that this value is of a much smaller order of magnitude of $|\rho_\Lambda^{\text{observations}}| \leq \left(10^{-12}\,\text{GeV}\right)^4$ [228]. Merely looking at the contributions of protons and neutrons, a calculation carried out by Zeldovich, still produced a significant contribution of $\rho_\Lambda^{\text{pn}} \sim 10^{-38}\,\text{GeV}^4$ [39]. Some of the attempts to resolve such an issue have been proposed through the consideration of supersymmetry [231], string theory [232, 233] and the anthropic principle [234] which considers a more philosophical approach to understand the fine-tuning of observed quantities necessary for the Universe to have observers [234], among other attempts [235, 236, 237, 238, 239, 240, 241, 242, 243, 244].

A classical approach to resolving the CC problem is the concept of self-tuning: using an evolving scalar field to dynamically cancel out the effects of the CC [118, 245, 246, 188, 247]. The mechanism is well-studied for the subclasses of Horndeski theory, dubbed as Fab Four [118, 245, 246], where in these scenarios the phase transitions are considered to be instantaneous such that ρ_Λ behaves as a piece-wise constant which discontinues at a point of transition by a constant change in value [118]. Weinberg's no-go theorem states that fields in a vacuum state are invariant under Poincaré and all fields are constant on-shell [43, 44]. Thus imposing a scalar field that is solely time-dependent circumvents this theorem as the phase transitions in the vacuum are attributed to the discontinuities of the scalar field derivatives [118]. On-shell refers to the conditions which satisfy the cosmological equations of motion. Specifically, in this context, the scalar field satisfies its equation of motion. Hence, a self-tuning mechanism is allowed through the partial break in the Poincaré invariance of the vacuum to allow screening of the vacuum energy through *degeneracy*. The Fab Four model has been extended to also include the kinetic term, referred to as the Fab Five model, wherein the cosmic acceleration is allowed to occur along with an asymptotic de Sitter behaviour [188]. Moreover, the same procedure can be extended to other subcases of Horndeski theory which includes a scalar field [248, 249].

The main issue with the self-tuning mechanism is that while the scalar field is intended to cancel ρ_Λ effects, it screens also the radiation and matter contributions [250, 247, 251]. For this reason, an alternative procedure to self-tuning has been proposed, called *well-tempering* [44]. Well-tempering mechanism retains the properties of the different epochs of the cosmic history of the Universe while also allowing the screening procedure to be applied solely for the vacuum energy density through self-tuning. This is done by dynamically cancelling out the vacuum energy density at each epoch, separately, to ensure that the fields entering the next epoch of cosmic history are accounted for appropriately [44]. Moreover, quantum radiative corrections need to be included. While classically the vacuum energy density is cancelled (at tree-level), in perturbative quantum field theory the picture might look different due to the inclusion of

quantum interactions [252]. This differs from the self-tuning mechanism, such that the well-tempering procedure employs shift symmetry: a constant shift of the scalar field $\phi \to \phi + c$ alters the Planckian mass scale and the vacuum energy density [253]. Further details of the procedure are included in Sec. 3.2.

In this chapter, different subcases of BDLS theory are investigated to obtain possible well-tempering models, focusing on models containing teleparallel contributions. Additionally, in line with the observed behaviour of the Universe, the dynamical stability, the behaviour during the matter-dominated era and the stability during phase transitions are also studied for these viable well-tempering models. The rest of the chapter is based on the published work [254, 255].

3.1 | Background Cosmology

Before delving into well-tempering models in the teleparallel analog of Horndeski gravity, it is important to look into the background cosmology of the theory. It should be noted that the following section applies to the general case of BDLS theory.

The flat Friedmann-Lemaître-Robertson-Walker (FLRW) metric

$$\mathrm{d}s^2 = -N(t)^2\mathrm{d}t^2 + a(t)^2(\mathrm{d}x^2 + \mathrm{d}y^2 + \mathrm{d}z^2)\,, \tag{3.4}$$

is used to describe the homogeneous and isotropic background cosmology. Here, N is the lapse function representing the change as proper time evolves and a is the scale factor that accounts for the expansion of the Universe. When considering symmetries of teleparallel gravity, it is important to ensure that these symmetries are satisfied by both the tetrad and the teleparallel connection [256, 257]. The geometrical objects are said to be invariant under the group action $\varphi : \mathrm{G} \times \mathcal{M} \to \mathcal{M}$, where $\mathcal{M}$ is the manifold. By taking the Lie derivative with respect to a vector $\chi_\xi \in \mathrm{Vect}\,\mathcal{M}$ on both the tetrad and the spin connection to obtain

$$\left(\mathcal{L}_{\chi_\xi} e\right)^A{}_\mu = \chi_\xi^\nu\, \partial_\nu e^A{}_\mu + \partial_\mu \chi_\xi^\nu\, e^A{}_\nu\,, \tag{3.5}$$

$$\left(\mathcal{L}_{\chi_\xi} \omega\right)^A{}_{B\mu} = \chi_\xi^\nu\, \partial_\nu \omega^A{}_{B\mu} + \partial_\mu \chi_\xi^\nu\, \omega^A{}_{B\nu}\,. \tag{3.6}$$

The metric is invariant under group G such that $\left(\mathcal{L}_{\chi_\xi} g\right)_{\mu\nu} = 0$, which implies that the Levi-Civita connection is also invariant, which is not necessarily the case for a teleparallel connection. To have

$$\left(\mathcal{L}_{\chi_\xi} g\right)_{\mu\nu} = 0\,, \qquad \left(\mathcal{L}_{\chi_\xi} \Gamma\right)^\rho_{\mu\nu} = 0\,, \tag{3.7}$$

then the tetrad and the spin connection need to be invariant[1], yielding

$$\left(\mathcal{L}_{\chi_\xi} e\right)^A{}_\mu = -\lambda_\xi{}^A{}_B\, e^B{}_\mu\,, \tag{3.8}$$

$$\left(\mathcal{L}_{\chi_\xi} \omega\right)^A{}_{B\mu} = \partial_\mu \lambda_\xi{}^A{}_B + \omega^A{}_{C\mu}\, \lambda_\xi{}^C{}_B - \omega^C{}_{B\mu}\, \lambda_\xi{}^A{}_C\,, \tag{3.9}$$

where λ_ξ is the local Lie homomorphism given by [258]

$$\lambda_\xi(x) = \frac{\mathrm{d}}{\mathrm{d}t}\Lambda_{\hat{\xi}}(x)\bigg|_{t=0}\,. \tag{3.10}$$

By imposing the Weitzenböck gauge given by Eq. (2.59) in Eq. (3.9) the conditions simplify greatly such that symmetric tetrads are defined by

$$\left(\mathcal{L}_{\chi_\xi} e\right)^A{}_\mu = -\lambda_\xi{}^A{}_B\, e^B{}_\mu\,, \qquad 0 \equiv \left(\mathcal{L}_{\chi_\xi} \omega\right)^A{}_{B\mu} = \partial_\mu \lambda_\xi{}^A{}_B\,. \tag{3.11}$$

Additionally, to ensure that the symmetric tetrad is compatible with the spin connection then it must either correspond to the Weitzenböck gauge (2.59) or satisfy Eq. (3.9), and solve the antisymmetric field equations. One such tetrad in the Weitzenböck gauge which obtains the result in Eq. (3.4) is given by the diagonal tetrad

$$e^a{}_\mu = \mathrm{diag}(N(t), a(t), a(t), a(t))\,. \tag{3.12}$$

Therefore, the determinant of the tetrad is given by

$$e = N(t)\, a(t)^3\,, \tag{3.13}$$

for which the relationship $\sqrt{-g} = e$ holds. In general, the background scalar field $\phi(t)$ is taken to be time dependent such that the kinetic term in Eq. (2.23) becomes

$$X = \frac{\dot{\phi}}{2N^2}\,, \tag{3.14}$$

where overdot represents time derivatives. The Hubble parameter, indicating the rate of change of the scale factor, becomes

$$H = \frac{\dot{a}}{aN}\,. \tag{3.15}$$

Next, the scalars that make up BDLS theory given in Eq. (2.98) are worked out. Starting with purely teleparallel quantities

$$T_{\mathrm{ax}} = 0\,, \qquad T_{\mathrm{vec}} = -\frac{9\dot{a}^2}{a^2 N^2}\,, \qquad T_{\mathrm{ten}} = 0\,, \tag{3.16}$$

[1] If the teleparallel connection is symmetric, i.e. $\left(\mathcal{L}_{\chi_\xi}\Gamma\right)^\rho_{\mu\nu} = 0$, then the torsion tensor satisfies symmetries by $\left(\mathcal{L}_{\chi_\xi} T\right)^\rho{}_{\mu\nu} = -2\left(\mathcal{L}_{\chi_\xi}\Gamma\right)^\rho_{[\mu\nu]} = 0$.

wherein only the vectorial component contributes to the torsion scalar through Eq. (2.80), giving

$$T = \frac{6\dot{a}^2}{a^2 N^2}\,. \tag{3.17}$$

As for the scalar resorting from the torsion tensor and derivative of scalars contractions, only I_2 given by Eq. (2.84) is non-zero

$$I_2 = \frac{3\dot{a}\dot{\phi}}{aN^2}\,, \tag{3.18}$$

while all J_i terms in Eqs (2.86-2.95) vanish.

The field equations are obtained through the variation of the action with respect to the lapse function, scale factor, and scalar field. By taking variations of BDLS action (2.98) with respect to N results in the first Friedmann equation, sometimes referred to as the Hamiltonian equation:

$$\mathcal{M}_{\rm Tele} + \sum_{i=2}^{5} \mathcal{M}_i = 0\,, \tag{3.19}$$

where

$$\mathcal{M}_{\rm Tele} = 6H\dot{\phi}G_{{\rm Tele},I_2} + 12H^2 G_{{\rm Tele},T} + 2XG_{{\rm Tele},X} - G_{\rm Tele} - 18H^2 G_{{\rm Tele},T_{\rm vec}}\,, \tag{3.20a}$$

$$\mathcal{M}_2 = 2XG_{2,X} - G_2\,, \tag{3.20b}$$

$$\mathcal{M}_3 = 6X\dot{\phi}HG_{3,X} - 2XG_{3,\phi}\,, \tag{3.20c}$$

$$\mathcal{M}_4 = -6H^2 G_4 + 24H^2 X(G_{4,X} + XG_{4,XX}) - 12HX\dot{\phi}G_{4,\phi X} - 6H\dot{\phi}G_{4,\phi}\,, \tag{3.20d}$$

$$\mathcal{M}_5 = 2H^3 X\dot{\phi}\,(5G_{5,X} + 2XG_{5,XX}) - 6H^2 X\,(3G_{5,\phi} + 2XG_{5,\phi X})\,, \tag{3.20e}$$

Next, variation with respect to a yields the second Friedmann equation, which will be referred to as the Hubble equation at times:

$$\mathcal{N}_{\rm Tele} + \sum_{i=2}^{5} \mathcal{N}_i = 0\,, \tag{3.21}$$

where

$$\begin{aligned}\mathcal{N}_{\rm Tele} = {} & -3H\dot{\phi}G_{{\rm Tele},I_2} - 12H^2 G_{{\rm Tele},T} - \frac{d}{dt}\Big(4HG_{{\rm Tele},T} + \dot{\phi}\,G_{{\rm Tele},I_2} - 6HG_{{\rm Tele},T_{\rm vec}}\Big) \\ & + G_{{\rm Tele},T_{\rm vec}} + 18H^2 G_{{\rm Tele},T_{\rm vec}} + G_{\rm Tele}\,,\end{aligned} \tag{3.22a}$$

$$\mathcal{N}_2 = G_2\,, \tag{3.22b}$$

$$\mathcal{N}_3 = -2X\left(G_{3,\phi} + \ddot{\phi}G_{3,X}\right)\,, \tag{3.22c}$$

$$\mathcal{N}_4 = 2\left(3H^2 + 2\dot{H}\right)G_4 - 12H^2 XG_{4,X} - 4H\dot{X}G_{4,X} - 8\dot{H}XG_{4,X}$$

$$- 8HX\dot{X}G_{4,XX} + 2\left(\ddot{\phi} + 2H\dot{\phi}\right)G_{4,\phi} + 4XG_{4,\phi\phi} + 4X\left(\ddot{\phi} - 2H\dot{\phi}\right)G_{4,\phi X}\,, \tag{3.22d}$$

$$\begin{aligned}\mathcal{N}_5 = &-2X\left(2H^3\dot{\phi} + 2H\dot{H}\dot{\phi} + 3H^2\ddot{\phi}\right)G_{5,X} - 4H^2X^2\ddot{\phi}G_{5,XX} \\ &+ 4HX\left(\dot{X} - HX\right)G_{5,\phi X} + 2\left(2\frac{d}{dt}(HX) + 3H^2X\right)G_{5,\phi} + 4HX\dot{\phi}G_{5,\phi\phi}\,.\end{aligned} \tag{3.22e}$$

The final result can be obtained through variation of the scalar field, expressed as a generalised Klein-Gordon equation:

$$\frac{1}{a^3}\frac{d}{dt}\left[a^3(\mathcal{P} + \mathcal{P}_{\rm Tele})\right] = \mathcal{Q}_\phi + \mathcal{Q}_{\rm Tele}\,, \tag{3.23}$$

for which

$$\begin{aligned}\mathcal{P}_\phi = &\dot{\phi}G_{2,X} + 6HXG_{3,X} - 2\dot{\phi}G_{3,\phi} + 6H^2\dot{\phi}\left(G_{4,X} + 2XG_{4,XX}\right) - 12HXG_{4,\phi X} \\ &+ 2H^3X\left(3G_{5,X} + 2XG_{5,XX}\right) - 6H^2\dot{\phi}\left(G_{5,\phi} + XG_{5,\phi X}\right)\,,\end{aligned} \tag{3.24a}$$

$$\mathcal{P}_{\rm Tele} = \dot{\phi}G_{{\rm Tele},X}\,, \tag{3.24b}$$

$$\begin{aligned}\mathcal{Q}_\phi = &G_{2,\phi} - 2X\left(G_{3,\phi\phi} + \ddot{\phi}G_{3,\phi X}\right) + 6\left(2H^2 + \dot{H}\right)G_{4,\phi} + 6H\left(\dot{X} + 2HX\right)G_{4,\phi X} \\ &- 6H^2XG_{5,\phi\phi} + 2H^3X\dot{\phi}G_{5,\phi X}\,,\end{aligned} \tag{3.24c}$$

$$\mathcal{Q}_{\rm Tele} = -9H^2G_{{\rm Tele},I_2} + G_{{\rm Tele},\phi} - 3\frac{d}{dt}\left(HG_{{\rm Tele},I_2}\right)\,. \tag{3.24d}$$

The lapse function has been set to unity for all background equations since this is sufficient when observing the spatial expansion of the Universe at a moment in time [259]. These results were first presented in Ref. [78] where the authors encapsulated the results depending on $T_{\rm vec}$ within the expression of T at a background level, since $T_{\rm vec} = -\frac{3}{2}T$. Here, the background portions depending on $T_{\rm vec}$ are written out separately to simplify the substitution in situations where perturbations about the background $T_{\rm vec}$ are considered. Additionally, matter is included in this system of equations in Chapter 6.

3.2 | Well-Tempering Cosmology Models

Equipped with the equations of motions within the BDLS gravity, the next step is to obtain models within this class of cosmologies that allow for well-tempering. First and foremost, the

arbitrary functions in the BDLS action in Eq. (2.98) are rewritten as follows:

$$G_2(\phi, X) = V(\phi, X) \,, \tag{3.25}$$

$$G_3(\phi, X) = G(\phi, X) \,, \tag{3.26}$$

$$G_4(\phi, X) = \kappa + \frac{A(\phi, X)}{2} \,, \tag{3.27}$$

$$G_5(\phi, X) = 0 \,, \tag{3.28}$$

$$G_{\rm Tele}(\phi, X, T, T_{\rm ax}, T_{\rm vec}, I_2, J_1, J_3, J_5, J_6, J_8, J_{10}) = \mathcal{G}(\phi, X, T, I_2) \,, \tag{3.29}$$

for simplification, such that G (3.25) and V (3.26) are the Horndeski potentials, A (3.27) is the conformal Horndeski potential that can attain the Einstein-Hilbert action in Eq. (2.14) upon a conformal transformation [260]. The kinetic mixing of ϕ and $g_{\mu\nu}$ provided by G_4 and G_5 terms alter the graviton speed [44] which in light of GW170817 observations, as mentioned in Sec. 2.2, requires restrictions in Refs. [44, 261, 248]. Since BDLS can revive some of the previously restricted models, A is kept a function of both ϕ and X [78, 261, 213]. On the other hand, to investigate the contribution of the teleparallel portion and its effect on X-dependent G_4 terms, G_5 (3.28) has been set to vanish. For a full analysis, G_5 contributions should not be eliminated. Finally, the teleparallel portion of BDLS gravity has been reduced to $\mathcal{G}$ (3.29) since at background the eliminated scalar invariants vanish while $T_{\rm vec} = -\frac{3}{2}T$.

The well-tempering mechanism allows for the violation of Weinberg's no-go theorem as the scalar field ϕ present in BDLS theory can evolve with time on a de Sitter vacuum. The dynamical screening of the vacuum energy density is obtained through the degeneracy of the field equations (3.19-3.23) for late-time cosmology on a de Sitter vacuum. The Hubble field equation given by Eq. (3.21) and the scalar equation in Eq. (3.23) are cast in the form

$$\dot{H} = \ddot{\phi}\mathcal{Z}\left(\phi, \dot{\phi}, H\right) + \mathcal{Y}\left(\phi, \dot{\phi}, H\right) \,, \tag{3.30}$$

$$0 = \ddot{\phi}\mathcal{D}\left(\phi, \dot{\phi}, H\right) + \mathcal{C}\left(\phi, \dot{\phi}, H, \dot{H}\right) \,, \tag{3.31}$$

where $\mathcal{Z}$, $\mathcal{Y}$, $\mathcal{D}$ and $\mathcal{C}$ are extracted from the theory. As per construction of BDLS, at most, second-order derivatives of metric and scalar fields are present. When considering a de Sitter vacuum case,

$$p_\Lambda = -\rho_\Lambda \,, \qquad \text{and} \qquad H(t) = h \,, \tag{3.32}$$

these functions are reduced to

$$\begin{aligned}
\mathcal{Y} &= 9h^2A_{XX}\dot{\phi}^4 + 9h^2A_X\dot{\phi}^2 - 15hA_{\phi X}\dot{\phi}^3 - 3hA_\phi\dot{\phi} + 3A_{\phi\phi}\dot{\phi}^2 + 9hG_X\dot{\phi}^3 + 3V_X\dot{\phi}^2 \\
&\quad - 6G_\phi\dot{\phi}^2 + 9h\mathcal{G}_{I_2}\dot{\phi} - 12h\mathcal{G}_{\phi T}\dot{\phi} + 3\mathcal{G}_X\dot{\phi}^2 - 3\mathcal{G}_{\phi I_2}\dot{\phi}^2\,, \qquad (3.33)\\
\mathcal{Z} &= -6hA_{XX}\dot{\phi}^3 - 6hA_X\dot{\phi} + 3A_{\phi X}\dot{\phi}^2 + 3A_\phi - 3G_X\dot{\phi}^2 - 3\mathcal{G}_{I_2} - 36h^2\mathcal{G}_{TI_2} - 3\mathcal{G}_{XI_2}\dot{\phi}^2 \\
&\quad - 9h\mathcal{G}_{I_2I_2}\dot{\phi} - 12h\mathcal{G}_{XT}\dot{\phi}\,, \qquad (3.34)\\
\mathcal{C} &= -9h^3A_{XX}\dot{\phi}^3 - 9h^3A_X\dot{\phi} - 3h^2A_{\phi XX}\dot{\phi}^4 + 9h^2A_{\phi X}\dot{\phi}^2 + 6h^2A_\phi - \mathcal{G}_{\phi X}\dot{\phi}^2 - V_{\phi X}\dot{\phi}^2 \\
&\quad + 3hA_{\phi\phi X}\dot{\phi}^3 - 9h^2G_X\dot{\phi}^2 - 3hG_{\phi X}\dot{\phi}^3 + 6hG_\phi\dot{\phi} + G_{\phi\phi}\dot{\phi}^2 + \mathcal{G}_\phi - 3hV_X\dot{\phi} + V_\phi \\
&\quad - 9h^2\mathcal{G}_{I_2} - 3h\mathcal{G}_X\dot{\phi} - 3h\mathcal{G}_{\phi I_2}\dot{\phi}\,, \qquad (3.35)\\
\mathcal{D} &= -3h^2A_{XXX}\dot{\phi}^4 - 12h^2A_{XX}\dot{\phi}^2 - 3h^2A_X + 3hA_{\phi XX}\dot{\phi}^3 + 9hA_{\phi X}\dot{\phi} - \mathcal{G}_{XX}\dot{\phi}^2 - V_X \\
&\quad - 3hG_{XX}\dot{\phi}^3 - 6hG_X\dot{\phi} + G_{\phi X}\dot{\phi}^2 + 2G_\phi - \mathcal{G}_X - 9h^2\mathcal{G}_{I_2I_2} - 6h\mathcal{G}_{XI_2}\dot{\phi} - V_{XX}\dot{\phi}^2\,. \qquad (3.36)
\end{aligned}$$

Within this system, it should be noted that the derivative with respect to the torsion scalar only crops up in conjunction with other scalar invariant derivatives. For this reason, theories such as $f(T)$ and NGR are quickly excluded from the system. This is a desired scenario as such theories do not consist of a scalar field which allows for dynamical screening. Drawing a comparison across these functions yields on-shell conditions

$$\mathcal{Z} \sim \mathcal{D}\,, \qquad \text{and} \qquad \mathcal{Y} \sim \mathcal{C}\,, \qquad (3.37)$$

which can be simplified to the on-shell *degeneracy equation*

$$\mathcal{Y}\mathcal{D} - \mathcal{C}\mathcal{Z} = 0\,. \qquad (3.38)$$

Also, functions coupled with $\ddot{\phi}$ are required to be non-vanishing on-shell to satisfy conditions arising from self-tuning. Hence, the *consistency conditions* are give by

$$\mathcal{Z} \neq 0\,, \qquad \text{and} \qquad \mathcal{D} \neq 0\,, \qquad (3.39)$$

allowing for a dynamic cancellation. Following these conditions, the Hamiltonian equation (3.19) and applying Eqs (3.25-3.29) at de Sitter vacuum, results in

$$3h^2 = \rho_\Lambda + F\left(\phi(t), \dot{\phi}(t)\right)\,, \qquad (3.40)$$

such that F is a function dependent solely on the scalar field which is still time dependent on-shell. It should be noted that having a dynamical scalar field ensures that the crux of the Weinberg no-go theorem is avoided. Therefore, Eqs (3.38-3.40) provide all the ingredients to dynamically cancel the vacuum energy within the well-tempering framework. The following subsections explore different possible well-tempered cosmologies within BDLS to exhibit such dynamical cancellation.

3.2.1 | Pure Teleparallel: Dependency on I_2

The first model considered is solely dependent on the teleparallel contribution by setting Horndeski potentials to vanish, specifically using a function of the form

$$\mathcal{G}\left(\phi, X, T, I_2\right) = \mathcal{I}\left(\frac{I_2^2}{2(3h^2)}\right) , \tag{3.41}$$

where this choice has been favoured due to the inclusion of a dynamical scalar within the definition of I_2 in Eq. (3.18). It is chosen as it is one of the simplest examples that includes teleparallel invariants. It is clear that at de Sitter

$$\frac{I_2^2}{2(3h^2)} = X\,, \tag{3.42}$$

which might suggest that the work should be performed for a function that is dependent on X instead of I_2 from the get-go. Because their contribution to the Friedmann and scalar equations is different, they are treated as separate parameters. Additionally, it was noted that the addition of T does not alter the results by much. It should be noted that without the assumption of de Sitter, where I_2^2 is simply being rescaled by a constant h, this is not necessarily the case. Therefore, throughout this chapter constraints given by Eqs (3.38-3.40) are performed for the general case presented, followed by substitution as an aftermath. The above model is substituted in the degeneracy equation (3.38)

$$X\mathcal{I}'(X)\left(4X\mathcal{I}''(X) + 3\mathcal{I}'(X)\right) = 0\,, \tag{3.43}$$

where Eq. (3.42) has been applied. By imposing that $X \neq 0$ for a non-trivial model, two possible solutions arise:

$$\mathcal{I}(X) = c_0\,, \qquad \text{and} \qquad \mathcal{I}(X) = 4c_1 X^{\frac{1}{4}} + c_2\,, \tag{3.44}$$

where c_0, c_1, c_2 are constants of integration. It should be noted that a non-trivial scenario is provided by the latter solution. Next, substituting the solution Eq. (3.44) in the consistency conditions of Eq. (3.39) yield

$$2X\mathcal{I}''(X) + \mathcal{I}'(X) = \frac{c_1}{2x^{\frac{3}{4}}} \neq 0\,, \tag{3.45}$$

$$\frac{\sqrt{X}\left(X\mathcal{I}''(X) + \mathcal{I}'(X)\right)}{h} = \frac{c_1}{hx^{\frac{1}{4}}} \neq 0\,, \tag{3.46}$$

which once again points out the importance of considering the non-trivial solution since $c_1 \neq 0$, and $|\dot{\phi}| < \infty$. The Hamiltonian equation (3.40) obtained by substituting function equation (3.41) and its solution (3.44) results in

$$3h^2 = \rho_\Lambda - c_2\,, \tag{3.47}$$

implying that there is no scalar field dependency and the model is not able to generate a well-tempered cosmology. Thus, this implies that dependency on X without any standard Horndeski models is not a viable ansatz model. Therefore, it would be interesting to still consider a purely teleparallel ansatz with additional dependent components.

3.2.2 | Pure Teleparallel: Dependency on ϕ and I_2

In this case, a *tadpole* term depending on the scalar field is included in addition to the function given in the previous case as seen in Eq. (3.41):

$$\mathcal{G}\left(\phi, X, T, I_2\right) = l\phi + \mathcal{I}\left(\frac{I_2^2}{2(3h)^2}\right) , \tag{3.48}$$

yielding a separable case, where l is a constant and I_2 is given by Eq. (3.42). Thus, the procedure presented in Sec. 3.2.1 is repeated. The degeneracy equation becomes

$$\mathcal{I}'(X)\left(12hX^2\mathcal{I}''(X) - \sqrt{2}l\sqrt{X}\right) + 9hX\mathcal{I}'(X)^2 - \sqrt{2}lX^{\frac{3}{2}}\mathcal{I}''(X) = 0\,, \tag{3.49}$$

once again solved and results in two solutions:

$$\begin{aligned}\mathcal{I}_{\mp}(X) = c_4 + \frac{1}{3\sqrt{2}hl\sqrt{X}}\Bigg[&l^2X \mp l\sqrt{72c_3h^2X^{\frac{3}{2}} + l^2X^2} \\ &\pm 18c_3h^2\sqrt{X}\left(\ln X - 2\ln\left(l\sqrt{72c_3h^2X^{\frac{3}{2}} + l^2X^2} + 36c_3h^2\sqrt{X} + l^2X\right)\right)\Bigg] ,\end{aligned} \tag{3.50}$$

where c_3, c_4 are integration constants. Additionally, it is important to have $c_3 \neq 0$ to ensure that there are $\ddot{\phi}$ contributions by the model. Therefore, the consistency conditions, in general, are given by

$$2X\mathcal{I}''(X) + \mathcal{I}'(X) \neq 0\,, \tag{3.51}$$

$$\frac{\sqrt{X}\left(X\mathcal{I}''(X) + \mathcal{I}'(X)\right)}{h} \neq 0\,, \tag{3.52}$$

which is identical to the general solution presented in Eqs (3.45-3.46). Finally, the solution given by Eq. (3.50) is substituted in the Hamiltonian constraint (3.40) to obtain the following result:

$$\begin{aligned}3h^2 = \rho_\Lambda - c_4 &\mp \frac{\sqrt{72c_3h^2X^{\frac{3}{2}} + l^2X^2}}{3\sqrt{2}h\sqrt{X}} + l\left(\frac{\sqrt{X}}{3\sqrt{2}h} - \phi\right) \\ &\mp \frac{3\sqrt{2}c_3h}{l}\left(\ln X - 2\ln\left(l\sqrt{72c_3h^2X^{\frac{3}{2}} + l^2X^2} + 36c_3h^2\sqrt{X} + l^2X\right)\right) .\end{aligned} \tag{3.53}$$

Hence, the time-dependent terms ϕ and X allow for the dynamical screening of ρ_Λ. Therefore, the model allows for well-tempering to occur thus illustrating the significance of having a tadpole

term, although it does not necessarily need to be included in this manner. In general, the teleparallel potential also includes a dependency on the torsion scalar T, apart from ϕ, X, and I_2. The calculations and results of functions with T dependency are not presented because the shape of the solution is not altered from the ansatz (3.48).

3.2.3 | Quartic Horndeski and Teleparallel: $A(\phi) + \mathcal{G}$

The next case will eliminate all standard Horndeski terms apart from A, specifically considering $A = A(\phi)$ since even within the standard Horndeski such dependency is in accordance to the GW170817 observations [45, 81]. Regardless, in Ref. [248], where $\mathcal{G} = 0$, it was shown that the model does not satisfy consistency conditions. Here, by including the teleparallel sector $\mathcal{G}$ this model can be revived as a well-tempering model. The $\mathcal{G}$ function is given by Eq. (3.41) and a simple conformal Horndeski potential A such that

$$A(\phi) = \alpha\phi\,, \qquad \text{and} \qquad \mathcal{G}(\phi, X, T, I_2) = \mathcal{I}\left(\frac{I_2^2}{2(3h)^2}\right)\,, \tag{3.54}$$

where α is a constant such that the tadpole term introduced in Eq. (3.48) is introduced within the A term and X is given by Eq. (3.42). The degeneracy equation (3.38) becomes

$$3\alpha h\left(\alpha h - \sqrt{2}X^{\frac{3}{2}}\mathcal{I}''(X)\right) + \mathcal{I}'(X)\left(4X^2\mathcal{I}''(X) - 4\sqrt{2}\alpha h\sqrt{X}\right) + 3x\mathcal{I}'(X)^2 = 0\,. \tag{3.55}$$

By rewriting this equation as a first-order, non-linear differential equation, its solution becomes

$$\begin{aligned}\mathcal{I}'(X) = {} & 2^{-\frac{5}{6}}3^{-\frac{2}{3}}\left(\sqrt{\frac{81\alpha^2 e^{c_5}h^2}{X^4} - \frac{12e^{\frac{3}{2}c_5}}{X^{\frac{9}{2}}}} + \frac{9\alpha e^{\frac{c_5}{2}}h}{X^2}\right)^{\frac{1}{3}} \\ & + \frac{e^{\frac{c_5}{2}}}{2^{\frac{1}{6}}3^{\frac{1}{3}}X^{\frac{3}{2}}}\left(\sqrt{\frac{81\alpha^2 e^{c_5}h^2}{X^4} - \frac{12e^{\frac{3}{2}c_5}}{X^{\frac{9}{2}}}} + \frac{9\alpha e^{\frac{c_5}{2}}h}{X^2}\right)^{-\frac{1}{3}} + \frac{3\alpha h}{\sqrt{2X}}\,,\end{aligned} \tag{3.56}$$

where c_5 is an integration constant. Next, the general forms of the consistency conditions are given by

$$2X\mathcal{I}''(X) + \mathcal{I}'(X) \neq 0\,, \tag{3.57}$$

$$3\alpha h - 2\sqrt{2X}\left(X\mathcal{I}''(X) + \mathcal{I}'(X)\right) \neq 0\,, \tag{3.58}$$

and are seen to hold when substituting solution (3.56). Due to the complexity of the exact solution to verify consistency, a numerical result is presented in Fig 3.1 where $X > 0$, c_5 is varied, and $h = 1$ and $\alpha = 1$ assumptions are applied. The different colour regions of the contour plots depict a range of solutions for each consistency equation. Albeit no exact values

are listed, the figure illustrates that there are no discontinuities or undefined regions for arbitrary values, concluding that the conditions are generally satisfied. Moving forward with analysing the Hamiltonian constraint (3.40), for this case it becomes

$$3h^2 = \rho_\Lambda - \mathcal{I}(X) - 3\alpha h^2\phi + 3\sqrt{2}\alpha h\sqrt{X} + \frac{2^{7/6}X}{3^{2/3}}\left(\sqrt{\frac{81\alpha^2 e^{c_1}h^2}{X^4} - \frac{12e^{3c_1/2}}{X^{9/2}}} + \frac{9\alpha e^{c_1/2}h}{X^2}\right)^{1/3} + \frac{2^{11/6}e^{c_1/2}}{3^{1/3}\sqrt{X}}\left(\sqrt{\frac{81\alpha^2 e^{c_1}h^2}{X^4} - \frac{12e^{3c_1/2}}{X^{9/2}}} + \frac{9\alpha e^{c_1/2}h}{X^2}\right)^{-1/3}, \tag{3.59}$$

showing the possibility of well-tempering dynamical cancellation of ρ_Λ.

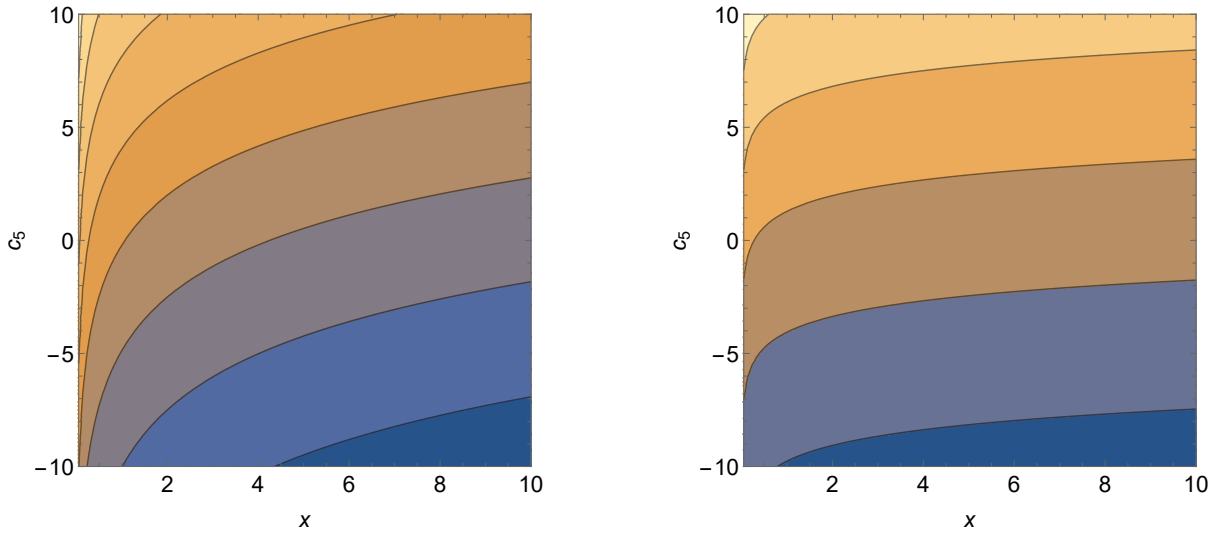

(a) $|\ln \mathcal{D}|$ (b) $|\ln \mathcal{Z}|$

Figure 3.1: Contour plots of the logarithmic consistency equations given by $\mathcal{D}$ in Eq. (3.57) and $\mathcal{Z}$ in Eq. (3.58) for the well-tempered solution of Eq. (3.56). These functions are plotted for the constant c_5 against X, without loss of generality, for $h = 1$ and $\alpha = 1$

3.2.4 | Revived Horndeski and Teleparallel: $A(X) + \mathcal{G}$

By adding to the models presented in Sec. (3.2.2-3.2.3), the previously ruled out case of $A = A(X)$ by GW170817 observations [45, 81] are now considered within the BDLS framework such that

$$A(\phi, X) = A(X)\,, \qquad \text{and} \qquad \mathcal{G}\,(\phi, X, T, I_2) = l\phi + g(X) + \mathcal{I}\left(\frac{I_2^2}{2(3h)^2}\right)\,, \tag{3.60}$$

where once again l is a constant, and g and $\mathcal{I}$ are arbitrary functions. The ϕ dependency is moved from the revived Horndeski potential A to the teleparallel sector $\mathcal{G}$. The degeneracy equation is

given by

$$0 = 2X\left(6h^2XA''(X) + 3h^2A'(X) + g'(X) + \mathcal{I}'(X)\right)\Big(12h^2X^2A^{(3)}(X) + 24h^2XA''(X) + 3h^2A'(X) + 2Xg''(X) + g'(X) + 2X\mathcal{I}''(X) + \mathcal{I}'(X)\Big) + \frac{2\sqrt{2X}}{3h}\Big(X(6h^2A''(X) + \mathcal{I}''(X)) + \mathcal{I}'(X) + 3h^2A'(X)\Big)\Big(18\sqrt{2}h^3X^{3/2}A''(X) + 9\sqrt{2}h^3\sqrt{X}A'(X) + 3\sqrt{2}h\sqrt{X}g'(X) + 3\sqrt{2}h\sqrt{X}\mathcal{I}'(X) - l\Big)\,, \tag{3.61}$$

with the consistency equations of

$$0 \neq -12h^2X^2A^{(3)}(X) - 24h^2XA''(X) - 3h^2A'(X) - 2Xg''(X) - g'(X) - 2X\mathcal{I}''(X) - \mathcal{I}'(X)\,, \tag{3.62}$$

$$0 \neq -\frac{2\sqrt{2}\sqrt{X}\left(X\left(6h^2A''(X) + \mathcal{I}''(X)\right) + 3h^2A'(X) + \mathcal{I}'(X)\right)}{3h}\,. \tag{3.63}$$

One ansatz that simplifies this analysis is given by

$$\mathcal{I}(X) = c_6 + 3h^2A(X) - 6h^2XA'(X) - g(X) + \xi(X)\,, \tag{3.64}$$

with c_6 an constant and ξ an arbitrary function to introduce additional function behaviour apart from the first four terms in Eq. (3.64). Rewriting the degeneracy equation (3.61) yields

$$0 = 2X\xi'(X)\left(2X\xi''(X) + \xi'(X)\right) - \frac{2\sqrt{2X}}{3h}\left(3\sqrt{2X}h\xi'(X) - l\right)\Big(g'(X) - \xi'(X) + X\left(6h^2XA^{(3)}(X) + 9h^2A''(X) + g''(X) - \xi''(X)\right)\Big)\,, \tag{3.65}$$

and allows for the integration of $A^{(3)}(X)$ to obtain

$$A''(X) = \frac{c_7}{X^{\frac{3}{2}}} + \frac{1}{X^{\frac{3}{2}}}\int^X \mathrm{d}u\left(\frac{3h\sqrt{u}\xi'(u)\left(2u\left(g''(u) - 2\xi''(u)\right) + 2g'(u) - 3\xi'(u)\right)}{6\left(\sqrt{2}h^2l\sqrt{u} - 6h^3u\xi'(u)\right)} + \frac{\sqrt{2}l\left(u\left(\xi''(u) - g''(u)\right) - g'(u) + \xi'(u)\right)}{6\left(\sqrt{2}h^2l\sqrt{u} - 6h^3u\xi'(u)\right)}\right)\,. \tag{3.66}$$

Additionally, Eqs. (3.62-3.63) simplify to

$$-2X\xi''(X) - \xi'(X) \neq 0\,, \tag{3.67}$$

$$-\frac{2\sqrt{2}\xi'(X)\left(2X\xi''(X) + \xi'(X)\right)}{\sqrt{2}l - 6h\sqrt{X}\xi'(X)} \neq 0\,, \tag{3.68}$$

provided that Eq. (3.67)

$$2x\xi''(X) + \xi'(X) \neq 0 \implies \xi(X) \neq 2\omega\sqrt{X} + \sigma\,, \tag{3.69}$$

where σ and ω are constants, and the denominator of Eq. (3.68) is not infinite. Therefore, the Hamiltonian constraint becomes

$$\begin{aligned}3h^2 = \rho_\Lambda - c_7 - 6h^2A(X) + X\left(6h^2A'(X) - 2g'(X) + 4\xi'(X)\right) - l\phi - \xi(x)\\ - 12c_7h^2\sqrt{X} - 12h^2\sqrt{X}\int^X du\Bigg(\frac{\sqrt{2}l\left(-ug''(u) - g'(u) + u\xi''(u) + \xi'(u)\right)}{6\left(\sqrt{2}h^2l\sqrt{u} - 6h^3u\xi'(u)\right)}\\ + \frac{3h\sqrt{u}\xi'(u)\left(2ug''(u) + 2g'(u) - 4u\xi''(u) - 3\xi'(u)\right)}{6\left(\sqrt{2}h^2l\sqrt{u} - 6h^3u\xi'(u)\right)}\Bigg),\end{aligned} \tag{3.70}$$

which, provided the function ansatz is chosen appropriately, the expression remains time-dependent and allows for the dynamical cancellation of ρ_Λ. The simplest ansatz by far is given by

$$g(X) = \beta X\,, \qquad \text{and} \qquad \xi(X) = \gamma X\,, \tag{3.71}$$

where the functions are of linear order, and β and γ are constants. Starting off with the degeneracy equation (3.65)

$$0 = 2X\gamma^2 - \frac{2\sqrt{2X}}{3h}\left(3\sqrt{2X}h\gamma - l\right)\left(\beta - \gamma + X\left(6h^2XA^{(3)}(X) + 9h^2A''(X)\right)\right), \tag{3.72}$$

for which the exact solution can be attained:

$$\begin{aligned}A(X) = c_8 + Xc_9 - \frac{1}{18h^3}\Big[-\sqrt{2X}l - 6hX\beta + 9hX\gamma + 72h^3\sqrt{X}c_9\\ + 6hX\left(\beta - \gamma\right)\ln X + \left(2\sqrt{2X}l - \frac{l^2}{3h\gamma} - 6hX\gamma\right)\ln\left(1 - 3\sqrt{2X}h\gamma\right)\Big],\end{aligned} \tag{3.73}$$

where c_7, c_8, c_9 are constants of integration. Substituting this solution within the consistency equations (3.67-3.68) gives

$$-\gamma \neq 0\,, \tag{3.74}$$

$$-\frac{2X\gamma^2\left(l^2 - 6\sqrt{2X}hl\gamma + 18h^2X\gamma^2\right)}{\left(l - 3\sqrt{2X}h\gamma\right)^3} \neq 0\,. \tag{3.75}$$

Provided both of the above conditions hold, the Hamiltonian constraint becomes

$$3h^2 = \rho_\Lambda - c_1 - 6c_2h^2 - \frac{l^2\ln\left(6\gamma h\sqrt{X} - \sqrt{2}l\right)}{9\gamma h^2} - \frac{\sqrt{2}l\sqrt{X}}{3h} - l\phi\,, \tag{3.76}$$

providing a model including the revived potential $A(X)$ in which vacuum energy can be dynamically screened.

3.2.5 | Shift Symmetric Sector

Up to this point, the number of functions considered has been limited. To investigate a broader subclass of BDLS, the following potentials are considered:

$$V(\phi, X) = l\phi + V(X)\,, \qquad G(\phi, X) = G(X)\,, \qquad A(\phi, X) = A(X)\,,$$
$$\mathcal{G}(\phi, X, T, I_2) = \mathcal{Q}(X)\,\mathcal{I}\left(\frac{I_2^2}{2\,(3h)^2}\right)\,. \tag{3.77}$$

Here, the shift symmetric sector is represented by the tadpole term coupled with the constant coefficient l. Additionally, V and G are considered to be dependent on X, and A is introduced to represent a revived model as seen in Sec. 3.2.4. Finally, $\mathcal{Q}$ and $\mathcal{I}$ are arbitrary functions that make up the BDLS potential. As seen in Sec. 3.2.4, adding more potentials does result in a complex system. For this reason, the approach to obtain a well-tempered solution adopted in Ref. [44] is implemented. Instead of evaluating the degeneracy equation (3.38), on-shell conditions (3.37) are extracted from the form

$$f\left(\dot{\phi}\right)\mathcal{Z} = \mathcal{D}\,, \qquad \text{and} \qquad f(\dot{\phi})\mathcal{Y} = \mathcal{C}\,, \tag{3.78}$$

where f is an arbitrary function. Since all functions in Eq. (3.77) can be expressed in terms of X (using Eq. (3.42)), then f is also reexpressed in terms of X using Eq. (2.23):

$$f(X) = \frac{1}{2}q\left(\frac{X^2}{2}\right)\,. \tag{3.79}$$

Substituting all functions into Eqs (3.78) gives two degeneracy equations

$$\begin{aligned} 0 = {} & 3h^2\left(4X^2A^{(3)}(X) + 8XA''(X) + A'(X)\right) + 2X\mathcal{K}'(X) + \mathcal{Q}(X)\mathcal{I}'(X) + 2X\mathcal{Q}(X)\mathcal{I}''(X) \\ & + \mathcal{K}(X) + 4X\mathcal{Q}'(X)\mathcal{I}'(X) + 2X\mathcal{I}(X)\mathcal{Q}''(X) + \mathcal{I}(X)\mathcal{Q}'(X) - \tfrac{q(X)}{3h}\big(3\sqrt{2}h\sqrt{X}G'(X) \\ & + 6h^2A'(X) + 2(6h^2XA''(X) + X\mathcal{Q}(X)\mathcal{I}''(X) + X\mathcal{Q}'(X)\mathcal{I}'(X) + \mathcal{Q}(X)\mathcal{I}'(X))\big)\,, \end{aligned} \tag{3.80}$$

$$l = \sqrt{2X}(3h + q(X))\left(6h^2XA''(X) + 3h^2A'(X) + \mathcal{K}(X) + \mathcal{Q}(X)\mathcal{I}'(X) + \mathcal{I}(x)\mathcal{Q}'(X)\right)\,, \tag{3.81}$$

where

$$\mathcal{K}(X) = V'(X) + 3h\sqrt{2X}G'(X)\,, \tag{3.82}$$

combines the Horndeski potentials. Restructuring Eq. (3.81) provides a solution for $\mathcal{K}$:

$$\mathcal{K}(X) = \frac{l}{\sqrt{2X}\,(3h + q(X))} - 6h^2XA''(X) - 3h^2A'(X) - \mathcal{Q}(X)\mathcal{I}'(X) - \mathcal{I}'(X)\mathcal{Q}'(X)\,, \tag{3.83}$$

which simplifies Eq. (3.80) such that

$$V'(X) = \frac{l\left(6hXq'(X) + 3hq(X) + q(X)^2\right)}{\sqrt{2X}q(X)(3h + q(X))^2} + 6h^2XA''(X) + 3h^2A'(X) + 2X\mathcal{Q}(X)\mathcal{I}''(X) + \left(2X\mathcal{Q}'(X) + \mathcal{Q}(X)\right)\mathcal{I}'(X) - \mathcal{I}(X)\mathcal{Q}'(X)\,, \tag{3.84}$$

$$G'(X) = -\frac{lq'(X)}{q(X)(3h + q(X))^2} - 2\sqrt{2}h\sqrt{X}A''(X) - \frac{\sqrt{2}hA'(X)}{\sqrt{X}} - \frac{\sqrt{2}\sqrt{X}\mathcal{Q}(X)\mathcal{I}''(X)}{3h} - \frac{\sqrt{2}\left(X\mathcal{Q}'(X) + \mathcal{Q}(X)\right)\mathcal{I}'(X)}{3h\sqrt{X}}\,, \tag{3.85}$$

upon comparison with Eq. (3.82). In this way, the five free functions $\{V,\, G,\, A,\, \mathcal{Q},\, \mathcal{I}\}$ reduce to the four arbitrary functions $\{q,\, A,\, \mathcal{Q},\, \mathcal{I}'\}$. Therefore, the on-shell Hamiltonian given by Eq. (3.40) becomes

$$3h^2 = \rho_\Lambda - l\phi + 2XV'(X) - V(X) + 6\sqrt{2}hX^{3/2}G'(X) + 12h^2X^2A''(X) + 12h^2XA'(X) - 3h^2A(X) + 4X\mathcal{Q}(X)\mathcal{I}'(X) + 2X\mathcal{I}(X)\mathcal{Q}'(X) - \mathcal{Q}(X)\mathcal{I}(X)\,, \tag{3.86}$$

thus able to provide a well-tempered model. Next, Hubble equation (3.30) and scalar field equation (3.31) both result in the same result:

$$\dot{X}q'(X) + 3hq(X) + q(X)^2 = 0\,, \tag{3.87}$$

resembling a Riccati equation of the form

$$\dot{y}(t) + y(t)[3h + y(t)] = 0\,, \tag{3.88}$$

which can be seen by setting $\dot{X} = \ddot{\phi}\dot{\phi}$ and $\dot{q} = \dot{X}q'(X)$. Therefore, the solution is given by

$$q\left(\frac{\dot{\phi}^2}{2}\right) = \frac{3h}{\exp\left(3h(t - c_{10})\right) - 1}\,, \tag{3.89}$$

where c_{10} is an integration constant. Due to the implicitly closed solution, it is required to choose $q(X)$ to obtain a solution for $\dot{\phi}$. If the Horndeski limit is taken, i.e. vanishing $\mathcal{Q}$ and $\mathcal{I}$, the result becomes similar to that obtained in Ref. [248].

3.2.6 | No Tempering Theorem

While the tadpole term has been seen to be an important feature in obtaining well-tempering models in cases explored in Sec. 3.2.2, Sec. 3.2.3 and Sec. 3.2.4, it might be the case that exploring

a more complex BDLS system, similar to that in Sec. 3.2.5 can be viable even without the tadpole term. By setting l to vanish in Eq. (3.77), the model is given by

$$V(\phi, X) = V(X)\,, \quad G(\phi, X) = G(X)\,, \quad A(\phi, X) = A(X)\,,$$
$$\mathcal{G}(\phi, X, T, I_2) = \mathcal{Q}(X)\,\mathcal{I}\left(\frac{I_2^2}{2\,(3h)^2}\right)\,. \tag{3.90}$$

The degeneracy equation (3.38) becomes

$$\begin{aligned} 0 = &\Big[\sqrt{2}(3h^2(2XA''(X) + A'(X)) + V'(X) + \mathcal{Q}(X)\mathcal{I}'(X) + \mathcal{I}(X)\mathcal{Q}'(X)) + 6h\sqrt{X}G'(X)\Big] \\ &\times \Big[3\sqrt{2}h^2(3A'(X) + 4X(XA^{(3)}(X) + 3A''(X))) + 6h\sqrt{X}(2XG''(X) + 3G'(X)) \\ &+ \sqrt{2}\Big(2X(V''(X) + 3\mathcal{Q}'(X)\mathcal{I}'(X) + \mathcal{I}(X)\mathcal{Q}''(X)) + \mathcal{Q}(X)\left(4X\mathcal{I}''(X) + 3\mathcal{I}'(X)\right) \\ &+ V'(X) + \mathcal{I}(X)\mathcal{Q}'(X)\Big)\Big]\,. \end{aligned} \tag{3.91}$$

The above equation results in two branches of the solution:

$$\mathcal{I}(X) = \frac{c_{11}}{\mathcal{Q}(X)} + \frac{1}{\mathcal{Q}(X)}\int^X du\left(-3h\left(2huA''(u) + hA'(u) + \sqrt{2}\sqrt{u}G'(u)\right) - V'(u)\right)\,, \tag{3.92}$$

$$\begin{aligned} \mathcal{I}(X) = \frac{X^{1/4}}{\sqrt{\mathcal{Q}(X)}}\Big[c_{12} + \int^x \frac{du}{4u^{5/4}\sqrt{2\mathcal{Q}(u)}}\Big(&3\sqrt{2}h^2\left(A(u) - 4u\left(uA''(u) + A'(u)\right)\right) \\ &+ c_{11} - 12hu^{3/2}G'(u) - 2\sqrt{2}uV'(u) + \sqrt{2}V(u)\Big)\Big]\,, \end{aligned} \tag{3.93}$$

where c_{11}, c_{12} are constants of integration. While the first solution, given by Eq. (3.92) violates the consistency condition as $\mathcal{D} = 0$, solution (3.93) aligns with consistency conditions and favoured to obtain a well-tempering model. A look at the on-shell Hamiltonian constraint gives

$$3h^2 = \rho_\Lambda + \frac{\sqrt{2}c_{11}}{2}\,, \tag{3.94}$$

where the model still does not well-tempering. Despite the added complexity to the BDLS model, the shift symmetric sector has been seen to be important to achieve well-tempering.

Hence, the models given by Eqs (3.48, 3.54, 3.60, 3.77) provide four examples of well-tempering models, satisfying the degeneracy condition (3.38), satisfying consistency conditions (3.39) and resulting in a scalar ϕ which can screen the vacuum energy density ρ_Λ. Table 3.1 summarises the models and their viability.

Case		Degeneracy Equations	Consistency Conditions	Hamiltonian Equation	Well-Tempering
Dependency on I_2	(3.41)	(3.43)	(3.45, 3.46)	(3.47)	×
Dependency on ϕ and I_2	(3.48)	(3.49)	(3.51, 3.51)	(3.53)	√
Quartic Horndeski and Teleparallel	(3.54)	(3.55)	(3.57, 3.58)	(3.59)	√
Revived Horndeski and Teleparallel	(3.60)	(3.61)	(3.62, 3.63)	(3.76)	√
Shift symmetric Sector	(3.77)	(3.80, 3.81)	–	(3.86)	√
No Tempering Theorem	(3.90)	(3.91)	–	(3.94)	×

Table 3.1: Summary of models in BDLS where the degeneracy equation (3.38) and consistency conditions (3.39) are evaluated to retrieve the Hamiltonian constraint (3.40). From this, the model can be classified as a viable well-tempering model. For the last two cases, a different approach was considered (detailed in Sec. 5.4.4), thus why no explicit expressions are listed for the consistency conditions.

3.3 | Dynamics in BDLS Well-Tempered Cosmology

In this section, the model presented in Sec. 3.2.5 will be further studied as it has been shown that it satisfies the well-tempering conditions while also featuring a large number of potentials from the BDLS cosmology. Before introducing the analysis of the dynamical stability of this well-tempering model, dynamical systems are introduced. Dynamical systems are a useful tool as models within a gravitational theory can be classified as viable cosmological solutions without obtaining exact form solutions of evolution equations. Dynamical systems are made up of a phase space and a rule describing the evolution of points in the phase space [262]. In general, a set of $x_i \in \mathbb{R}$ variables for $i \in [1, n]$ produce a dynamical system of the form

$$\dot{x}_i = f_i(x_1, x_2, \ldots, x_n)\,, \tag{3.95}$$

such that f_i are functions which describe how the system evolves and each variable has a corresponding function [263]. The trajectory of the phase space is determined by a solution of Eq. (3.95). Setting the function $f_i = 0$ yields the critical (fixed/equilibrium) points [262]. While there could be a scenario where the system stays within that state, our interest lies in the stability of these critical points. The system is linearised by taking a first-order Taylor expansion of the function f about a fixed point x_0:

$$f_i(\boldsymbol{x}) = f_i(x_0) + \sum_{j=1}^{n} \frac{\partial f_i}{\partial x_j}(x_0)\,(x_i - x_0) + \dots \,. \tag{3.96}$$

The derivative $J = \frac{\partial f_i}{\partial x_j}(x_0)$ corresponds to the Jacobian/stability matrix [262]. The eigenvalues of the stability matrix determine the behaviour of the stability [173]:

- *Hyperbolic*: All eigenvalues have nonzero real parts.
  - *Stable / Attractor*: All eigenvalues have negative real parts.
  - *Repeller*: All eigenvalues have positive real part.
  - *Saddle*: At least one eigenvalue has a positive real part.
- *Non-hyperbolic*: At least one eigenvalue has a zero real part.

Next, these procedures are adapted to the scenario of cosmological models which have been classified as viable well-tempering models. First and foremost, the system is expressed in terms of dimensionless quantities (see Sec. 3.3.1). The functions of the system are obtained through the Friedmann and scalar field equations, where the Hubble parameter and the scalar field correspond to the variable $x \in \mathbb{R}$. These equations are expanded up to first-order perturbation, and apply the necessary on-shell background equations and conditions to simplify. An equation associated with the Hubble parameter and scalar field of the form Eq. (3.95) is obtained. By implementing the system and using the `StreamPlot` in `Mathematica`, a two-dimensional phase portrait is obtained.

3.3.1 | $A(X) + V(X) + G(X) + \mathcal{G}$ Model

The potentials given by Eq. (3.77) can be reduced to the four functions, specifically of the form

$$q(X) = -\frac{3\gamma h}{\gamma - \sqrt{X}}\,, \qquad A(X) = \alpha x\,, \qquad \mathcal{Q}(X) = 1\,, \qquad \mathcal{I}(X) = \beta x\,, \tag{3.97}$$

such that α is the revived Horndeski potential, β is the BDLS parameter and γ will be referred to as the well-tempering parameter. Functions A and $\mathcal{I}$ are linearly dependent on X. While the function q appears slightly complicated, the choice is taken to simplify the constraints dictated

by the well-tempering formalism. The Hamiltonian equation (3.40), Hubble equation (3.30) and the scalar equation (3.31) for this case are given by

$$3H^2 = \rho_\Lambda + \rho + \tfrac{l}{3h^2}\left(\sqrt{2}H(\sqrt{X}-\gamma) - 3h^2\phi\right) + \tfrac{X}{h^2}(h-H)(h-3H)\left(3h^2\alpha+\beta\right)\,, \tag{3.98}$$

$$\begin{aligned} 0 = {} & \dot{H}\left(36h^2X - 12X^2\left(3h^2\alpha+\beta\right)\right) + \dot{X}\Big(12X(h-H)\left(3h^2\alpha+\beta\right) + \sqrt{2}l(\gamma-\sqrt{X})\Big) \\ & + 36X^2(h-H)^2\left(3h^2\alpha+\beta\right) + 6\sqrt{2}HlX(\sqrt{X}-\gamma) + 18h^2X(\rho+p)\,, \end{aligned} \tag{3.99}$$

$$\begin{aligned} 0 = {} & \dot{X}\left(3\sqrt{2}X(h-H)^2(3h^2\alpha+\beta) + \gamma Hl\right) + 18\sqrt{2}HX^2(h-H)^2(3h^2\alpha+\beta) \\ & + l\left(6X^{3/2}(H^2-h^2) - 6\gamma H^2X\right) + \dot{H}\left(-12\sqrt{2}X^2(h-H)(3h^2\alpha+\beta)\right. \\ & \left. +l(2X^{3/2}-2\gamma X)\right)\,, \end{aligned} \tag{3.100}$$

wherein vacuum energy density ρ_Λ and matter energy density ρ are treated separately. The same is done for pressure p, wherein $p_\Lambda = -\rho_\Lambda$ is seen to vanish in this system of equations. Matter fields obey the conservation law

$$\dot{\rho} + 3H\left(\rho + p\right) = 0\,. \tag{3.101}$$

Additionally, to simplify the notation, matter fields are expressed in the following terms:

$$\rho_\Lambda = 3h^2\lambda\,, \tag{3.102}$$

$$\rho(t) = 3H(t)^2\Omega(t)\,, \tag{3.103}$$

$$p(t) = \omega\rho(t)\,, \tag{3.104}$$

where λ is a constant, $\Omega(t)$ is the dimensionless counterpart of $\rho(t)$, and ω represents the equation of state constant whose value depends on the matter considered. Additionally, the constant h, representing the Hubble constant in a de Sitter vacuum, is set as the length scale such that

$$t = \frac{\tau}{h}\,, \tag{3.105}$$

where τ is the dimensionless counterpart of time t. Hence, the remaining gravitational components can be cast in their dimensionless notation through the definition of h and τ

$$H(t) = hy(\tau)\,, \qquad X(t) = h^2\chi(\tau)\,, \qquad \alpha = \frac{\overline{\alpha}}{h^2}\,, \qquad \gamma = h\overline{\gamma}\,, \qquad l = h^2\overline{l}\,. \tag{3.106}$$

Therefore, using Eqs (3.102-3.106) one can recast Eqs (3.98-3.100) into their dimensionless form:

$$0 = 3[\chi(3\,\overline{\alpha}+\beta)+3\lambda+3y^2\,(\chi(3\,\overline{\alpha}+\beta)+\Omega-1)]-3\bar{l}\phi-\sqrt{2}\,\bar{l}y(\overline{\gamma}-\sqrt{\chi}) \\ -12\chi y(3\,\overline{\alpha}+\beta)\,, \tag{3.107}$$

$$0 = 12\chi y'\,(3-\chi\,(3\alpha+\beta))+\chi'\Big[\sqrt{2}\,\bar{l}\,(\overline{\gamma}-\sqrt{\chi})-12\chi\,(y-1)\,(3\,\overline{\alpha}+\beta)\Big] \\ +6\sqrt{2}\,\bar{l}\chi y\,(\sqrt{\chi}-\overline{\gamma})+36\chi\Big[\frac{3}{2}\,(\omega+1)\,y^2\Omega+\chi\,(y-1)^2\,(3\,\overline{\alpha}+\beta)\Big]\,, \tag{3.108}$$

$$0 = \chi'\Big[\overline{\gamma}\,\bar{l}y+3\sqrt{2}\chi\,(y-1)^2\,(3\,\overline{\alpha}+\beta)\Big]+6\,\bar{l}\chi\,\big(\sqrt{\chi}(y^2-1)-\overline{\gamma}y^2\big) \\ +\bar{l}\,y'\left(2\chi^{\frac{3}{2}}-2\,\overline{\gamma}\,\chi\right)+18\sqrt{2}\chi^2\,(y-1)^2\,y\,(3\,\overline{\alpha}+\beta)+12\sqrt{2}\chi^2\,(y-1)\,(3\,\overline{\alpha}+\beta)\,, \tag{3.109}$$

and the matter equation (3.101) becomes

$$0 = 3\,(\omega+1)\,y^3\Omega+y^2\Omega'+2y\Omega y'\,, \tag{3.110}$$

where primes represent derivatives with respect to dimensionless time τ. Provided the system of equations is represented into dimensionless quantities, this model can be analysed for dynamical stability, its behaviour within the matter era which influences the cosmic structures and how well the model holds during phase transitions; these are all important components for a viable model to describe the cosmic evolution of our Universe.

3.3.2 | Dynamical Stability of Well-Tempered Vacuum

First and foremost, the background values for the system dependent on $\{y,\Omega,\chi\}$ need to be defined for the on-shell limit. Starting with

$$y(\tau)\to 1\,, \tag{3.111}$$

$$\Omega(\tau)\to 0\,, \tag{3.112}$$

as matter contributions die out, such that the Hamiltonian constraint (3.107) becomes

$$9\,(\lambda-1)+\bar{l}\left(\phi'-\sqrt{2}\,\overline{\gamma}\right)=3\bar{l}\phi\,. \tag{3.113}$$

The scalar field equation (3.109)

$$\phi''-3\phi'=0\,, \tag{3.114}$$

has the solution of

$$\phi(\tau)=\frac{C_1}{3}e^{3\tau}+C_2\,, \tag{3.115}$$

where C_1 and C_2 are constants of integration. Substituting the solution given by Eq. (3.115), the on-shell Hamiltonian result in Eq. (3.113) simplifies to

$$\bar{l}\,\left(3C_2+\sqrt{2}\,\overline{\gamma}\right)=9\,(\lambda-1)\,. \tag{3.116}$$

It should be noted that omitting all non-dynamical variables leaves the constant C_2 to take care of the dynamical self-tuning of the vacuum energy, and not well-temper.

Now, an on-shell perturbation is introduced by perturbing the Hubble (3.111) and scalar (3.115) field separately by

$$y(\tau)=1+\delta y(\tau)\,, \tag{3.117}$$

$$\phi(\tau)=\left(\frac{C_1}{3}e^{3\tau}+C_2\right)+\delta\phi(\tau)\,. \tag{3.118}$$

Perturbing the the Hamiltonian constraints (3.113) and the scalar field equation (3.114) result in dynamical equations

$$0=\delta y\Big[3C_1^2e^{6\tau}\,(3\,\overline{\alpha}+\beta)+\bar{l}\,\left(C_1e^{3\tau}-\sqrt{2}\,\overline{\gamma}\right)-18\Big]+\bar{l}\,\left(\delta\phi'-3\delta\phi\right) \tag{3.119}$$

$$0=C_1e^{3\tau}\left(\sqrt{2}C_1e^{3\tau}-2\overline{\gamma}\right)\delta y'+6C_1e^{3\tau}\delta y\left(\sqrt{2}C_1e^{3\tau}-\overline{\gamma}\right)+2\,\overline{\gamma}\left(\delta\phi''-3\delta\phi'\right)\,, \tag{3.120}$$

such that upon differentiation of Eq. (3.119), it can be equated to Eq. (3.120) to obtain a solution of δy by eliminating the $\delta\phi$ contribution:

$$\delta y(\tau)=-\frac{C_3}{C_1^2e^{6\tau}\left(\sqrt{2}\,\bar{l}-6\overline{\gamma}\,(3\,\overline{\alpha}+\beta)\right)-4C_1\overline{\gamma}\bar{l}e^{3\tau}+2\overline{\gamma}\left(18+\sqrt{2}\,\overline{\gamma}\,\bar{l}\right)}\,, \tag{3.121}$$

where C_3 is an integration constant. At the late times, where large values of τ are considered, the limit of Eq. (3.121) becomes

$$\delta y\to e^{-6\tau}\,, \tag{3.122}$$

an exponential behaviour. This relationship should be noted, as this solution will crop up in the remaining portion of the section. Therefore, as the case approaches the well-tempered vacuum, $\tau\to+\infty$, the Hubble perturbation $\delta y\to 0$. Additionally, by substituting Eq. (3.121) within the Hamiltonian constraints (3.113) results in an expression for ϕ and its derivatives:

$$\delta\phi'(\tau)-3\delta\phi(\tau)=\frac{C_3\left(3c_1^2e^{6\tau}\,(3\,\overline{\alpha}+\beta)+C_1\,\bar{l}\,e^{3\tau}-18-\sqrt{2}\,\overline{\gamma}\,\bar{l}\right)}{C_1^2e^{6\tau}\left(\sqrt{2}\,\bar{l}-6\overline{\gamma}\,(3\,\overline{\alpha}+\beta)\right)-4C_1\overline{\gamma}\bar{l}e^{3\tau}+2\overline{\gamma}\left(18+\sqrt{2}\,\overline{\gamma}\,\bar{l}\right)}\,. \tag{3.123}$$

The stability analysis is performed at late times, therefore it is sufficient to consider the asymptotic limit $\tau\to+\infty$. This simplifies Eq. (3.123) into

$$\delta\phi'(\tau)-3\delta\phi(\tau)\to\frac{3C_3\,(3\,\alpha+\beta)}{\bar{l}\,\left(\sqrt{2}\,\bar{l}-6\,\overline{\gamma}\,(3\,\overline{\alpha}+\beta)\right)}\,, \tag{3.124}$$

whose asymptotic solution is given by

$$\delta\phi(\tau) \to C_4 e^{3\tau} - \frac{C_3\,(3\,\overline{\alpha}+\beta)}{\bar{l}\left(\sqrt{2}\,\bar{l}-6\,\overline{\gamma}\,(3\,\overline{\alpha}+\beta)\right)}\,, \tag{3.125}$$

where C_4 is the integration constant. The leading order scalar perturbation has a behaviour similar to the on-shell solution, i.e.

$$\phi(\tau) \propto \delta\phi(\tau)\,, \tag{3.126}$$

implying that the perturbed portions of the scalar field eventually behave as the on-shell solution, allowing for the dynamical stability of a well-tempered vacuum.

Apart from the above perturbative analysis, summarised by the asymptotic solutions of δy in Eq. (3.122) and ϕ in Eq. (3.125), non-linear differential equations can be further represented as a two-dimensional dynamical system through phase portraits. By considering Eqs (3.107-3.109), where a pure vacuum system and Eq. (3.112) are applied, a framework for the vector field (χ, y) is given by

$$\begin{aligned}\chi' = -\frac{12}{\mathcal{K}[\chi,y]}\Big[&\sqrt{2}\,\bar{l}\,\chi^{\frac{3}{2}}(-\bar{l}\overline{\gamma}+\bar{l}\sqrt{\chi}+6\sqrt{2}\chi(y-1)(3\,\overline{\alpha}+\beta)) - \chi\Big(\sqrt{2}\,\bar{l}\,\overline{\gamma}-\sqrt{2}\,\bar{l}\sqrt{\chi}+18y\\ &+6\chi(2-3y)(3\,\overline{\alpha}+\beta)\Big)\Big(\bar{l}\left(\sqrt{\chi}(y^2-1)-\overline{\gamma}\,y^2\right)+3\sqrt{2}\chi y(y-1)^2(3\,\overline{\alpha}+\beta)\Big)\Big]\,, \qquad (3.127)\\ y' = \frac{3\sqrt{\chi}(y-1)}{\mathcal{H}[\chi,y]}\Big[&18\sqrt{2}\chi^{\frac{3}{2}}\,(3\,\overline{\alpha}+\beta)^2+\sqrt{2}\,\overline{\gamma}\,\bar{l}^2-\sqrt{2}\,\bar{l}^2\sqrt{\chi}+y\Big(-90\sqrt{2}\chi^{\frac{3}{2}}\,(3\,\overline{\alpha}+\beta)^2\\ &+\sqrt{2}\,\overline{\gamma}\,\bar{l}^2+12\,\bar{l}\chi\,(3\,\overline{\alpha}+\beta)-\bar{l}\sqrt{\chi}\left(6\,\overline{\gamma}(3\,\overline{\alpha}+\beta)+\sqrt{2}\,\bar{l}\right)\Big)-54\sqrt{2}\chi^{\frac{3}{2}}y^3\,(3\,\overline{\alpha}+\beta)^2\\ &+12\,\bar{l}\chi\,(3\,\overline{\alpha}+\beta)+6\sqrt{\chi}y^2\,(3\,\overline{\alpha}+\beta)\left(21\sqrt{2}\chi(3\,\overline{\alpha}+\beta)+3\,\overline{\gamma}\,\bar{l}-4\,\bar{l}\,\sqrt{\chi}\right)\Big]\,, \qquad (3.128)\end{aligned}$$

where χ is used instead of ϕ, as they are related through $\chi = \frac{\phi'^2}{2}$. This gives a possibility to transform a second-order differential equation into a first-order one. Functions $\mathcal{K}$ and $\mathcal{H}$ are given by

$$\begin{aligned}\mathcal{K}[\chi,y] = 2\,\bar{l}\,y\Big[&-\tfrac{54\sqrt{2}}{\bar{l}}\chi\,(y-1)^2\,(3\,\overline{\alpha}+\beta)\,(\chi(3\,\overline{\alpha}+\beta)+1)-\sqrt{2}\,\bar{l}\,(\overline{\gamma}-\sqrt{\chi})^2\\ &+6\left(\overline{\gamma}\chi(5y-4)(3\,\overline{\alpha}+\beta)-4\chi^{\frac{3}{2}}(y-1)(3\,\overline{\alpha}+\beta)-3\,\overline{\gamma}\,y\right)\Big]\,, \qquad (3.129)\\ \mathcal{H}[\chi,y] = -\frac{\mathcal{K}[\chi,y]}{2y}\,. \qquad (3.130)\end{aligned}$$

Through these equations, two points are inferred:

- **Independence of $\boldsymbol{\lambda}$**: λ is the dimensionless vacuum energy density given by Eq. (3.102). The independence of these equations from λ implies that the system applies, irrespective of the vacuum energy size.

- **Dependence on linear combination of $\bar{\alpha}$ and β:** Through the dynamical system described by Eqs (3.107-3.109), the constants $\bar{\alpha}$ and β always appear in the linear combination $3\bar{\alpha}+\beta$. The $\bar{\alpha}$ parameter arises from the revived Horndeski potential and β is related to the teleparallel extension of the model. This further indicates the additional cases arising from the introduction of the teleparallel sector allows through the consideration of BDLS action provided that $\bar{\alpha} \neq 0$, $\beta \neq 0$ and $3\bar{\alpha}+\beta \neq 0$.

Fig. 3.2 depicts phase portraits for different values of $3\bar{\alpha}+\beta$ for y and χ (where dimensionless quantities are expressed in Eq. (3.106)) given by Eqs (3.127-3.128) by fixing parameters

$$\bar{\gamma}=1 \implies \gamma \sim h\,, \qquad \text{and} \qquad \bar{l}=10 \implies l \sim 100h^2\,. \tag{3.131}$$

Through these plots, the following points can be concluded:

- **Approach of stability region:** The red-dashed line indicates the region of the self-tuning vacuum. For regions where $y=\frac{H}{h}>0$, as the solution approaches the stability region it results in an on-shell solution. The low-energy de Sitter state is an attractor from above with a smooth transition, verifying that the well-tempered model studied here is a viable representation of the dark energy sector. Additionally, there exists an attractor in the phase region $y=\frac{H}{h} \ll 0$ indicating that the well-tempering model does not result in the self-tuning vacuum as the only cosmological attractor of the system.

- **Critical curve:** The blue-solid line represents the critical curve where an undefined χ' and y' fields occur due to $\mathcal{K}=\mathcal{H}=0$. This undefined region is not necessarily a physical divergence, but it may be due to the coordinate choice of the phase space, requiring a better choice of coordinates.

- **$3\bar{\alpha}+\beta$ characteristic:** The different choices of values for $3\bar{\alpha}+\beta$ open up a large number of additional cosmological dynamics. The main distinction is between the cases where $3\bar{\alpha}+\beta>0$ where the critical curve appears well below the stability line (red-dashed) and that of $3\bar{\alpha}+\beta<0$ where the critical curve surrounds the well-tempered vacuum region.

Apart from being successful in obtaining a well-tempered model which exhibits regions of dynamical stability approaching the well-tempered vacuum, the model further stresses the importance of including the teleparallel sector which BDLS provides as a broader class of possibilities.

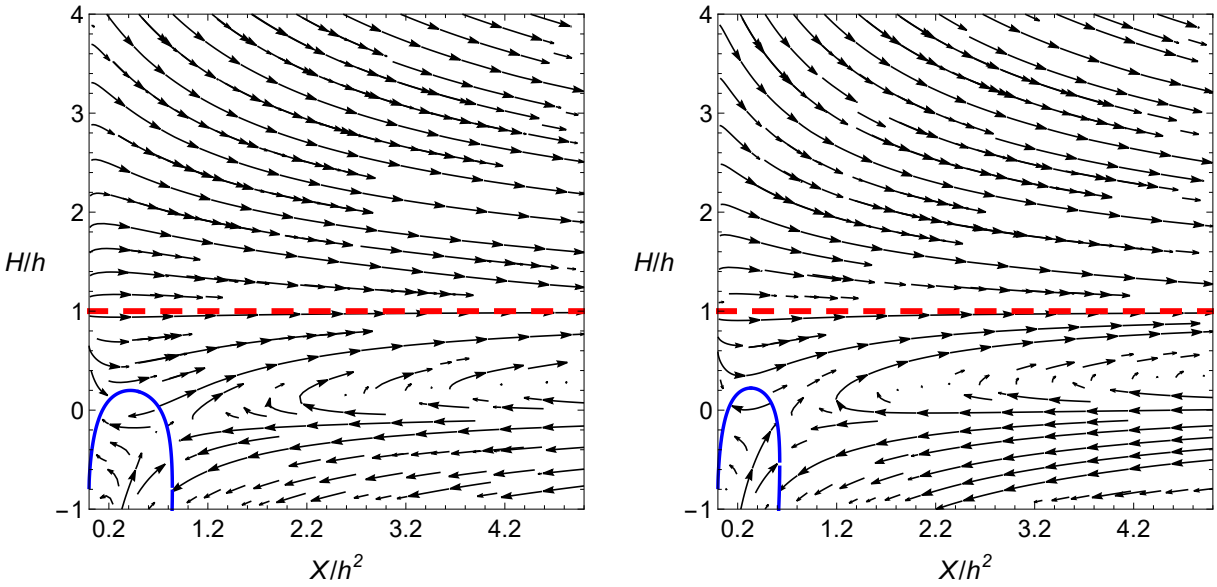

(a) $3\,\bar{\alpha} + \beta = -3$ (b) $3\,\bar{\alpha} + \beta = -2$

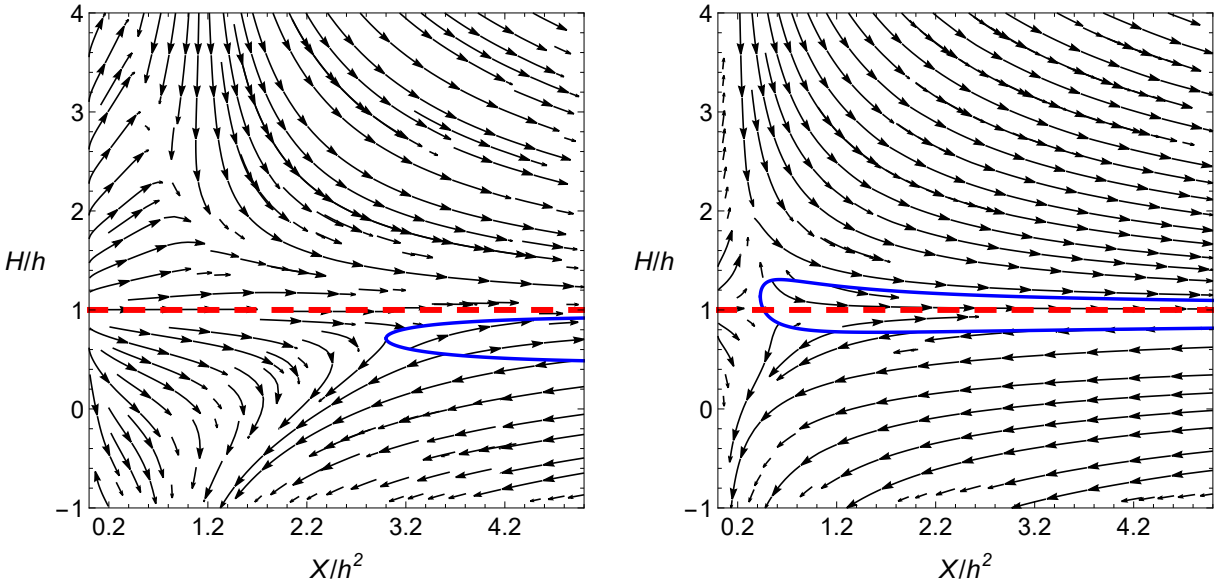

(c) $3\,\bar{\alpha} + \beta = 1$ (d) $3\,\bar{\alpha} + \beta = 7$

Figure 3.2: Phase portraits of the dynamical system given by Eq. (3.127) and Eq. (3.128) to depict the behaviour of the vector field (χ, y). The dependency on different values of $3\,\overline{\alpha} + \beta$ are considered with fixed parameters $\overline{\gamma} = 1$ and $\bar{l} = 10$. The red-dashed line represents the well-tempered vacuum and the blue-solid curve presents the critical curve occurring when $\mathcal{K}[\chi, y] = 0$ given by Eq. (3.129).

3.3.3 | Matter Dominated Era

The dark energy model introduced in this section requires consistent behaviour to describe a Universe experiencing a matter-dominated era before entering late-time cosmic acceleration. Since the well-tempering framework does not screen matter contributions, unlike self-tuning, it offers an avenue to check matter compatibility. Using the dimensionless versions of the Hubble (3.108), scalar (3.109) and matter (3.110) equations, their integration provides a solution for $a(\tau)$, $\phi(\tau)$ and $\Omega(\tau)$, provided that $y = \frac{a'(\tau)}{a(\tau)}$. Starting with the matter equation, the solution is easily calculated to be

$$\Omega(\tau) = \omega \frac{a(\tau)^{-(1+3\omega)}}{a'(\tau)^2}\,, \tag{3.132}$$

already reducing the number of dependent variables to a and ϕ. Moreover,

$$\Omega \sim 1\,, \qquad \omega = 1\,, \qquad a(\tau) \sim a_0 \tau^{\frac{2}{3}} \tag{3.133}$$

are set to represent the matter era, where $a_0 = a(\tau_0)$ at initial time τ_0. Similarly, ϕ_0 can be obtained from the Hamiltonian constraints given by Eq. (3.107). Setting the parameters to $\bar{\alpha} = -1$, $\beta = 1$ $\bar{\gamma} = 1$, $\bar{l} = 10$ and $\lambda = 10^{10}$, and considering different initial values for a_0 and ϕ_0' yields a variety of solutions for the Hubble parameter, scalar field, matter density parameter and dark energy density parameter. The numerical integration of these functions is illustrated in Fig. 3.3. It should be noted that the very large value of the vacuum energy dimensionless parameter λ in comparison to the other parameters is taken into consideration to show that, even for large vacuum energy density, there is no need for further fine-tuning.

Fig. 3.3a shows that the Hubble function follows an exponential drop towards the well-tempered vacuum solution established in Eq. (3.122) such that

$$\delta y \sim e^{-6\tau} \implies \ln \delta y = \ln \left| \frac{H}{h} - 1 \right| \sim -6\tau\,, \tag{3.134}$$

and the scalar is seen to continually evolve in Fig. 3.3b. The similar behaviour is noted across different initial conditions, with the case $(a_0, \phi_0') = (10, 10)$ evolution being slower. In the case of $(a_0, \phi_0') = (1, 1)$, the Hubble function gives an odd peak close to $\tau = 1$, suggesting that the value experiences a sudden decrease but immediately restores to its previous behaviour. For these choices of initial conditions, the difference between the initial and actual time becomes small enough to result in a spike as the plot reaches $\tau = 1$ in the exponential power of Eq. (3.134). Next, the density parameters can be split by looking at the coefficients of the Hamiltonian

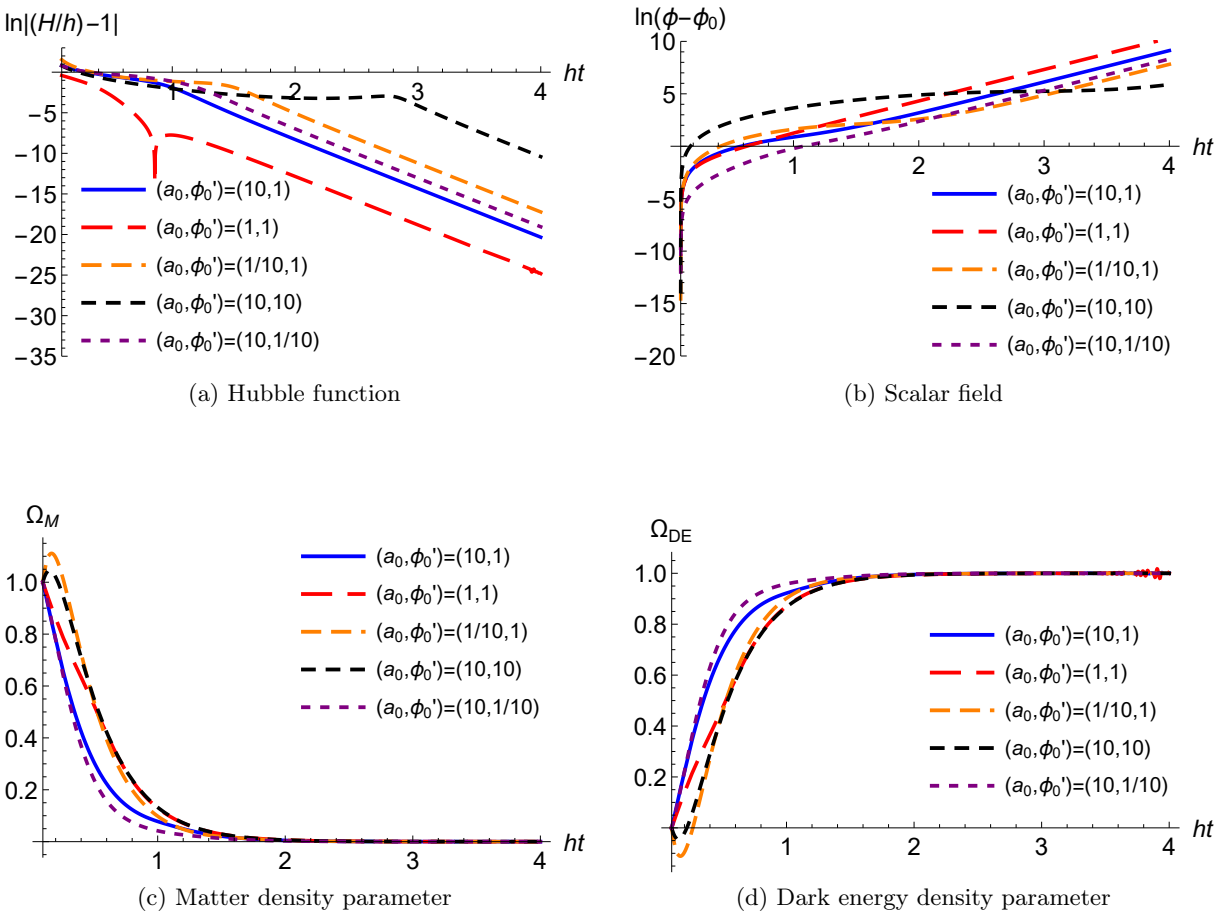

(a) Hubble function

(b) Scalar field

(c) Matter density parameter

(d) Dark energy density parameter

Figure 3.3: Numerical integration to obtain solutions for the (a) Hubble equation $y(\tau)$ given by Eq. (3.108), (b) scalar field $\phi(\tau)$ obtained through Eq. (3.109), (c) matter density parameter solution given by Eq. (3.132), and (d) dark energy density parameter obtain by Eq. (3.139). For these plots, the constant parameters $\lambda = 10^{10}$, $\bar{\alpha} = -1$, $\beta = 1$, $\bar{\gamma} = 1$ and $\bar{l} = 10$ are set, while different initial conditions for a_0 and ϕ_0' are considered.

constraints (3.107) as follows:

$$\Omega_{\rm M} = \frac{\omega}{a a'^2}\,, \tag{3.135}$$

$$\Omega_{\rm H}^{(\phi)} = -\frac{a\,\bar{l}\left(3a\phi + a'\left(\sqrt{2}\,\bar{\gamma} - \phi'\right)\right)}{9a'^2}\,, \tag{3.136}$$

$$\Omega_{\rm T}^{(\phi)} = \frac{\sigma\left(-4aa' + 3a'^2 + a^2\right)\phi'^{\,2}}{6a'^{\,2}}\,, \tag{3.137}$$

$$\Omega_{\Lambda} = \frac{\lambda a^2}{a'^{\,2}}\,, \tag{3.138}$$

where $\Omega_{\rm M}$ is the matter density parameter, $\Omega_{\rm H}^{(\phi)}$ is the density parameter for standard Horndeski, $\Omega_{\rm T}^{(\phi)}$ represents the revived Horndeski and teleparallel sector and Ω_Λ is the vacuum energy density parameter. Hence, the dark energy density parameter $\Omega_{\rm DE}$ can be expressed as a linear combination

$$\Omega_{\rm DE} = \Omega_\Lambda + \Omega_{\rm H}^{(\phi)} + \Omega_{\rm T}^{(\phi)} \,. \tag{3.139}$$

The plots for $\Omega_{\rm M}$ and $\Omega_{\rm DE}$ are shown in Fig. 3.3c and Fig. 3.3d, respectively. These two figures show that there is a smooth transition from one epoch to the next, whereas one of the values decreases, the other one gains value at the same rate to maintain the total $\Omega_{\rm M} + \Omega_{\rm DE} = 1$ throughout the matter-dominated epoch as current time is approached. The cases $(a_0, \phi_0') = (0.1, 1)$ and $(a_0, \phi_0') = (10, 10)$, while the summation of both density parameters remains unity, the dark energy density parameter begins with a negative value at early times implying that the matter density parameter exceeds the critical value. This issue is not tackled in this work but it would be of interest to see if such values at early times of the matter-dominated era arise due to a phase transition from the radiation era.

3.3.4 | Stability through Phase Transitions

The final check is the stability of the model when undergoing a phase transition. The analysis performed in Refs. [248] for well-tempered Horndeski cosmology has been extended to include the teleparallel sector. The phase transition is expressed through the effective energy density and effective pressure as follows:

$$\rho_{\rm eff} = \rho_\Lambda + \frac{\Delta\rho_\Lambda}{2} \arctan\left(\frac{t-\mathcal{T}}{\Delta\mathcal{T}}\right) , \tag{3.140}$$

$$p_{\rm eff} = -\rho_{\rm eff} - \frac{\dot{\rho}_{\rm eff}}{3H} , \tag{3.141}$$

where $\mathcal{T}$ and $\Delta\mathcal{T}$ are phase transition time scales such that there is a smooth transition of the vacuum energy density from $\rho_\Lambda - \frac{\Delta\rho_\Lambda}{2}$ at $t \ll \mathcal{T}$ to $\rho_\Lambda + \frac{\Delta\rho_\Lambda}{2}$ at $t \gg \mathcal{T}$. Fig. 3.4 illustrates Eqs. (3.140-3.141) where $\tau = ht$. The choice of values $h\mathcal{T} = 2$ and $h\Delta\mathcal{T} = 0.1$ is taken to obtain a phase transition of an energy scale with an order of magnitude $\frac{\Delta\rho_\Lambda}{3h^2} = 10^2$. The point of phase transition can be seen to occur at $\tau = 2$, where Fig. 3.4a reaches a maximum and plateaus after the phase transitions. Fig. 3.4b illustrates the behaviour of negative pressure, where a turning point occurs at the phase transition, to ensure that the fluid behaves as a vacuum where $\frac{p}{\rho} = -1$ before and after the transition.

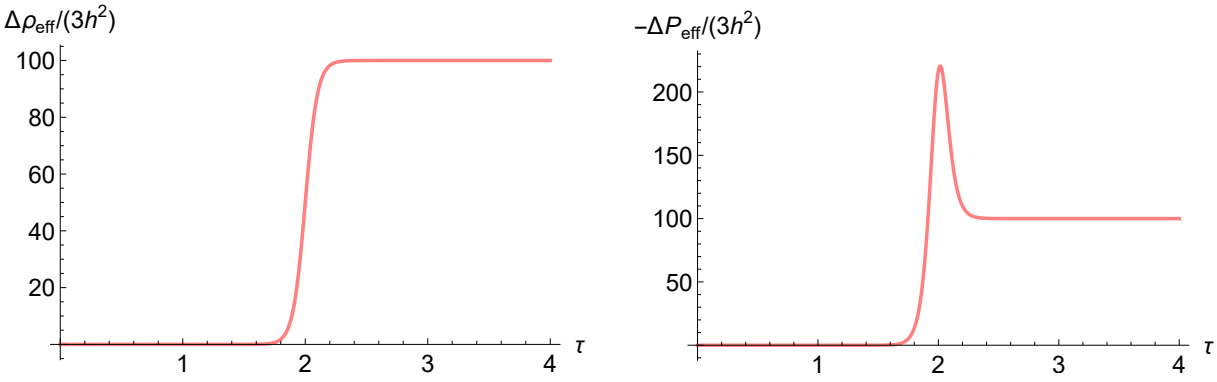

(a) Effective energy density

(b) Effective pressure

Figure 3.4: The behaviour of (a) effective energy density ρ_{eff} and (b) effective pressure p_{eff} for a system undergoing a phase transition at $\tau = 2$ for a duration of 0.1. The transition if of order of magnitude $\sim 10^2$ in the self-tuning vacuum energy scale.

The stability of the well-tempered vacuum, as it experiences phase transition, can be determined by substituting the effective energy density equation (3.140) and the effective pressure equation (3.141) within the field equations (3.107-3.109). By keeping the constants as those presented in Fig. 3.4, the Hubble and the scalar field solutions were obtained using numerical integration, and illustrated in Fig. 3.5. The Hubble function presented in Fig. 3.5a shows a change in the function upon experiencing a phase transition. The red-long-dashed line reflects the asymptotic solution $\delta y = \frac{\delta H}{h} \sim e^{-6ht}$, coinciding with the behaviour experienced before phase transition and corresponding to the matter sector solution obtained in Eq. (3.134). At the phase transition point $\tau = 2$, a disturbance occurs in the Hubble behaviour and as the negative pressure increases, but settles within the same asymptotic solution depicted by the pink-short-dashed line. Fig. 3.5b shows that the scalar field, despite the system undergoing a phase transition, exhibits a lack of discontinuity and continues to grow. This is an important feature when having a well-tempering model as a continually evolving dynamical field is required to screen the vacuum energy density to evade Weinberg's no-go theorem [43]. This is in line with the behaviour obtained in the matter sector shown in Fig. 3.3b.

3.4 | Summary

In summary, this chapter presented the construction of a well-tempering cosmology in BDLS gravity, with an emphasis on having a model that includes the teleparallel extension which sets apart BDLS from Horndeski gravity and additionally revived Horndeski potentials which had been previously discarded. It should be noted that, albeit the case explored in Sec. 3.3 does not

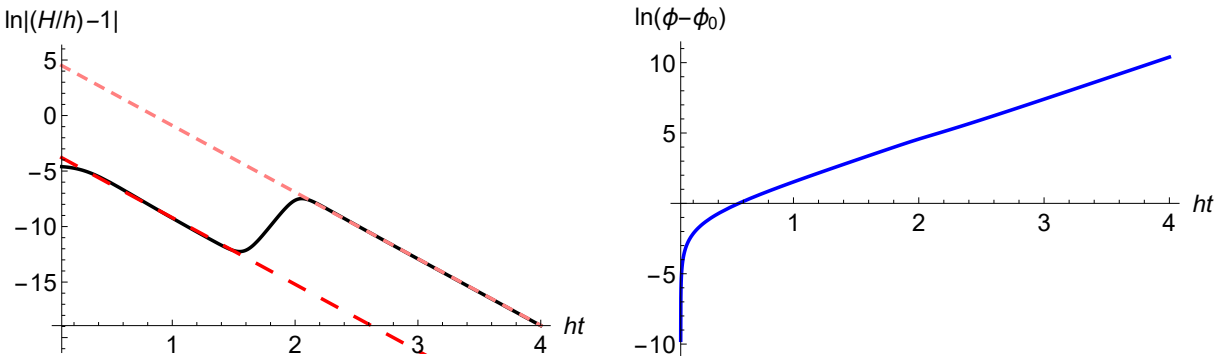

(a) Hubble function during phase transition

(b) Scalar field during phase transition

Figure 3.5: (a) The logarithmic Hubble function during phase transition, where the red-long-dashed line correlates to the solution $\delta H/h \propto e^{-6ht}$ before a disturbance, and the pink-short-dashed line illustrates the same solution after the disturbance. (b) The logarithmic behaviour of the scalar field during phase transition.

explore the full possibilities of the gravitational model, it does convey an array of examples of the interest by considering the potentials that BDLS has to offer.

Well-tempering [44, 248] has been implemented in place of the self-tuning mechanism typically applied in classical physics to tackle the CC problem. As BDLS contains the scalar field ϕ, either stemming from the Horndeski Lagrangian or the teleparallel section of the theory, it provides an avenue to break Weinberg's no-go theorem. A dynamical scalar field which evolves through the entire evolution of the Universe can be used to screen the vacuum energy arising from interactions between particles at different epochs. Hence, the discrepancy in the vacuum energy density between the theoretical prediction from the standard model of particle physics and that from observations can be minimised to result in a net cosmological constant which is attributed to the accelerated expansion of the Universe, making well-tempering a dark energy model.

The first step presented in Sec. 3.2 was to construct the viable well-tempering model. The no-tempering model presented in Sec. 3.2.6 further exemplifies the importance of having a scalar field in the Lagrangian, even if other teleparallel contributions are present. This is because the on-shell Hamiltonian constraint results in a case where no dynamical screening is possible. While certain models can be classified as well-tempered models, i.e. satisfy the degeneracy equations (3.38) and the consistency conditions (3.39), this does not necessarily make them viable cosmological models. Dynamical stabilities are a crucial check to ensure models can mimic the behaviour of our Universe. Phase portraits in Fig. 3.2 show that a large portion of the solutions approach the vacuum stability portion of the theory. Additionally, critical curves are also included to show the regions where the solutions are undefined due to zero value in the denominator in the vector field equations (3.127-3.128) representing the two-dimensional dynamical system. In the case

where $\mathcal{K}$ given by Eq. (3.129) vanishes, the evaluation would need to be done separately.

The large-scale structure of the Universe points to the importance of having dynamical stability in the matter-dominated era. For a range of initial values for the scale factor a_0 and the scalar field derivative ϕ_0' the Hubble function in Fig. 3.3a illustrates the $\delta y \sim e^{-6\tau}$ behaviour, similar to the expected late time behaviour for the model as given by Eq. (3.122). Moreover, the scalar field numerical solution, depicted in Fig. 3.3b shows that the scalar field continues to evolve at an increasing rate. It was of interest to consider the behaviour of the matter density parameter to ensure that as time passes the value depletes while the dark energy density parameter takes over. Figs (3.3c-3.3d) precisely illustrate the balance between the two quantities while preserving the total unity as one smoothly transitions to the other. The exception of two cases where the critical value of the $\Omega_{\rm M}$ is exceeded at the beginning of the matter-dominated epoch, albeit counterbalanced by a negative $\Omega_{\rm DE}$, points to a numerical issue caused, most likely, when the epoch experiences a phase transition from the radiation dominated era.

While the radiation epoch is not taken into account, studies of the phase transition are considered. Fig. 3.4 shows how the effective energy density and pressure behave before, during and after a phase transition. Evaluating the behaviour of the Hubble parameter in Fig. 3.5a shows that although a jump in value is experienced during the phase transition, numerical solution settles at the asymptotic result of $\delta y \sim e^{-6\tau}$. On the other hand, the scalar field solution shown in Fig. 3.5b drives home the fact that it continually evolves, without discontinuities, as required to perform vacuum screening at different epochs and phase transitions.

Note that during the matter epoch, and phase transition, would not be obtained if the self-tuning mechanism was implemented. This is because self-tuning, apart from not taking into consideration quantum radiative fluctuations, screens all energy densities and not just the vacuum energy density. The stability conditions are also met by standard Horndeski employing the well-tempering mechanism [248], but BDLS offers a broader framework with larger possibilities of well-tempering models. While the analysis with a cosmological background is presented in this chapter, the analysis was also carried out for a Minkowski spacetime where the vacuum is of Minkowski type. To avoid unnecessary repetition, the analysis has been omitted here but further details can be found in Ref. [254]. It was shown that the simplification of adopting a Minkowski background allows for the consideration of more complicated models. While it is known that the Universe experiences an accelerated expansion, looking at Minkowski solutions is still crucial to determining the behaviour where flat spacetime is considered an adequate limit. Additionally, the standard Horndeski limit of these solutions has been seen to corroborate with the results obtained in Ref. [249].

4

Cosmological Perturbations

The Cosmological principle, derived from the Copernican principle, has been adopted to describe the Universe [85, 264]. On a large scale, the small variations occurring at local points in the Universe can be averaged out such that the Universe can be interpreted as a single manifold, where there is no privileged position or direction within the Universe. More precisely, this manifold is described as both homogeneous and isotropic [3, 120, 9].

Homogeneity describes a Universe that is the same in all locations. Therefore, for any two points upon a manifold $\mathcal{M}$, there exists an isometry that maps one point onto the other. In terms of the cosmological notation presented in Chap. 2, the metric remains unchanged at different points on the manifold. Isotropy, assuming an observer is placed at a point in the Universe, will view the Universe to be the same irrespective of which direction they look at. Mathematically, consider a particular point $p \in \mathcal{M}$. Let vectors V and W be in the tangent space corresponding to a point p, denoted as $T_p\mathcal{M}$, such that the pushforward of W under isometry acts parallel with V [9]. It should be noted that both homogeneity and isotropy hold within the spatial portion of the manifold. Comparing the Universe at different time slices will show that the Universe has undergone an evolution as it experiences expansion. The FLRW metric presented in Eq. (3.4) is used to describe the standard model of hot big bang cosmology, where the Universe was initially hot, dense, and dominated by relativistic constituents, experienced cooling as it became dominated by non-relativistic matter and later started to experience dark energy domination.

While the Cosmological Principle suffices at the large scale of the Universe, the disruptions in spacetime caused by GWs and the formation of structures result in deviations from the assumption of spatial homogeneity and isotropy. Cosmological perturbations, representing small changes in the background, are an important mathematical tool as they realise insight into key physical phenomena. Cosmological perturbations at early times are the seeds that lead to the current large-scale structures and provide information about the nature of dark matter and dark energy. The temperature fluctuations observed in the CMB give insight into the

behaviour of the early Universe and constrain initial conditions through statistical properties and cosmological parameters by studying their evolution over time and understanding GWs. These small perturbations can affect the evolution of the underlying cosmology, and dictate the physical stability of the system. In this work, cosmological perturbations will be applied to investigate propagating degrees of freedom, polarisation of GWs, cosmic growth of CDM, ghost, and Laplacian instabilities presented in the later chapters.

4.1 | Introduction to Perturbations

Foreshadowing the following chapters, here the perturbations up to the second order are presented. Perturbations are taken about the cosmological background of FLRW given by Eq. (3.4). In GR, the metric is the fundamental dynamical object and is perturbed up to the first order to initialise a small perturbation such that

$$g_{\mu\nu} = \bar{g}_{\mu\nu} + \epsilon\, \delta g_{\mu\nu}\,, \qquad \text{and} \qquad |\delta g_{\mu\nu}| \ll 1\,, \tag{4.1}$$

where $\bar{g}_{\mu\nu}$ is the background metric and the order of ϵ indicates the order of perturbation. In the case of BDLS theory within the Weitzenböck gauge, the fundamental dynamical objects are the tetrad $e^A{}_\mu$ and the scalar field ϕ. Perturbing both these quantities up to the first order

$$\bar{e}^A{}_\mu = e^A{}_\mu + \epsilon\, \delta e^A{}_\mu\,, \tag{4.2}$$

$$\bar{\phi} = \phi(t) + \epsilon\delta\phi\,, \tag{4.3}$$

where an overhead bar ($\bar{}$) represents a quantity with background and perturbations, and $\phi(t)$ is the background scalar field that is taken to be solely a function of time. A spatial dependency in the background fields would violate the Cosmological Principle because background encompasses the large-scale behaviour of the Universe which is assumed to be homogeneous and isotropic.

In the background equations, the Weitzenböck gauge was applied to obtain a vanishing spin connection. The gauge can be extended to the first order, resulting in no additional contributions at the perturbative level as well [265, 266]. Consider an arbitrary function $G(\alpha, \beta)$ where α and β are perturbed constants such that

$$\bar{\alpha} = \alpha + \epsilon\, \delta\alpha + \epsilon^2\delta^2\alpha + \dots\,, \tag{4.4}$$

$$\bar{\beta} = \beta + \epsilon\, \delta\beta + \epsilon^2\delta^2\beta + \dots\,, \tag{4.5}$$

where δ and δ^2 represent first and second-order perturbations, respectively. Performing a Taylor

expansion on the function about the background quantities, yields

$$\begin{aligned}\bar{G}(\bar{\alpha},\bar{\beta}) &= G + G_{,\alpha}\left(\bar{\alpha}-\alpha\right) + G_{,\beta}\left(\bar{\beta}-\beta\right) + G_{,\alpha\beta}\left(\bar{\alpha}-\alpha\right)\left(\bar{\beta}-\beta\right) \\ &\quad + \frac{1}{2}\left[G_{,\alpha\alpha}\left(\bar{\alpha}-\alpha\right)^2 + G_{,\beta\beta}\left(\bar{\beta}-\beta\right)^2\right] + \dots, \qquad (4.6) \\ &= G + \epsilon\left(G_{,\alpha}\,\delta\alpha + G_{,\beta}\delta\beta\right) + \epsilon^2\left[G_{,\alpha}\delta^2\alpha + G_{,\beta}\,\delta^2\beta + G_{,\alpha\beta}\,\delta\alpha\delta\beta\right. \\ &\quad \left. + \frac{1}{2}\left(G_{,\alpha\alpha}\left(\delta\alpha\right)^2 + G_{,\beta\beta}\left(\delta\beta\right)^2\right)\right] + \mathcal{O}(\epsilon^3), \qquad (4.7)\end{aligned}$$

where $G = G(\alpha,\beta)$ is the background function. Applying this procedure to the functions in the BDLS action results in the following second-order perturbations:

$$\begin{aligned}&G_i(Y + \epsilon\delta Y + \epsilon^2\delta^2 Y) \\ &= G_i(0) + \epsilon\sum_Y \delta Y\, G_{i,Y}(0) \\ &\quad + \epsilon^2\left[\sum_Y\left(\delta^2 Y G_{i,Y}(0) + \frac{1}{2}\left(\delta Y\right)^2 G_{i,YY}(0)\right) + \sum_Y\sum_{Z,Z\neq Y}\delta Y\,\delta Z G_{i,YZ}(0)\right], \qquad (4.8)\end{aligned}$$

where $i \in \{2,3,4,5,\text{Tele}\}$, Y are the dependencies of the function, and the functions $G_i(0)$ following perturbations are expressed in terms of the background quantities of the dependent variables. Applying all the perturbations listed in this section yields a second order perturbation BDLS action given in Eq. (2.98) using the perturbative quantities of the fundamental objects in Eqs (4.2-4.3), as summarised in Tables 4.1, 4.2, and 4.3.

Table 4.2 lists the perturbations of the quantities making up the standard Horndeski portion of the action. Apart from the kinetic term X which is expressed in terms of scalar and tetrad perturbations, the remaining terms only rely on the metric perturbations, which in turn can be expressed through tetrad perturbations. It should be noted that within standard Horndeski the metric is perturbed up to first order only since it is the fundamental dynamical object of the formalism. Here, the metric is extended up to the second order to account for $\delta e^A{}_\mu \delta e^B{}_\nu$ combinations stemming from the linear order of the tetrad. Additionally, the perturbation of the inverse tetrad $E_A{}^\mu$ can be extracted in terms of the tetrad $e^A{}_\mu$. Starting from the orthogonality condition of the tetrad given by Eq. (2.43) and extending to perturbative levels yields

$$\begin{aligned}\bar{e}^A{}_\mu \bar{E}_A{}^\nu = \delta^\nu_\mu \implies &\left(e^A{}_\mu + \epsilon\delta e^A{}_\mu\right)\left(E_A{}^\nu + \epsilon\delta E_A{}^\nu + \dots\right) = \delta^\nu_\mu \\ \implies &\, e^A{}_\mu E_A{}^\nu + \epsilon\left(\delta e^A{}_\mu E_A{}^\nu + e^A{}_\mu \delta E_A{}^\nu\right) + \epsilon^2\left(\delta e^A{}_\mu \delta E_A{}^\nu + \dots\right) = \delta^\nu_\mu . \qquad (4.9)\end{aligned}$$

Comparing the left and right-hand side of the equation for the linear order, corresponding to coefficients of ϵ, results in

$$\delta e^A{}_\mu E_A{}^\nu + e^A{}_\mu \delta E_A{}^\nu = 0 \implies \delta E_B{}^\nu = -\delta e^A{}_\mu E_A{}^\nu E_B{}^\mu . \qquad (4.10)$$

Table 4.2 lists the perturbations of purely teleparallel contributions, such that all quantities can be expressed in terms of $\delta e^A{}_\mu$. Moreover, the scalar quantities of $\{T_{\rm ax}, T_{\rm vec}, T_{\rm ten}, T\}$ specifically rely on $\delta e^A{}_\mu$ and torsion tensor $T^\lambda{}_{\mu\nu}$, which in turn depend on $e^A{}_\mu$. Table 4.3 summarises the perturbations of quantities constructed through the mixing of tetrad and scalar fields. In the final column of the table, corresponding to the second-order perturbations of these quantities, there are no contributions stemming from purely scalar-dependent second-order perturbations or any quantities that are made up of only the scalar field. This is because the scalar field is the only quantity that is not mixed with the tetrad. Having said that, ϕ and $\delta\phi$ do appear in conjunctions with other perturbations.

4.2 | Equations of Motion in the Weitzenböck Gauge

In Sec. 3.1, the background equations of BDLS action, given by Eqs.(3.19-3.23), were found through the variation with respect to N, a and ϕ. Albeit being a viable approach when dealing with background equations only, it becomes difficult to perform perturbations on the equations of motion. While in Chapter 3, perturbations of the scalar field and Hubble parameter are taken, the behaviour of the gravitational perturbations modes within the fundamental dynamical object of the tetrad cannot be extracted. For this reason, a more generalised approach to obtaining the equations of motion is required. One approach is to perturb the action up to second order in terms of the scalar and tetrad field, then taking variation with respect to the first order perturbations of the dynamical fields, i.e. $\delta e^A{}_\mu$ and $\delta\phi$. Another approach, which will be fleshed out in this section, is to obtain the equations of motion in terms of tetrad and scalar field without performing perturbations, and then perturbing the equations of motion themselves.

For simplification, the notation for variations with respect to the tetrad and with respect to the scalar field are given by, respectively,

$$\delta_e := \frac{\delta}{\delta e^C{}_\gamma}\,, \qquad \delta_\phi := \frac{\delta}{\delta\phi}\,, \tag{4.11}$$

and

$$\bar{\delta} := \frac{\partial}{\partial\Phi}\,, \qquad \tilde{\delta} := \partial_\rho \frac{\partial}{\partial(\partial_\rho\Phi)} \qquad \hat{\delta} := \frac{\partial}{\partial(\partial_\omega\partial_\rho\Phi)} \tag{4.12}$$

such that

$$\delta_\Phi Y = \bar{\delta}Y - \partial_\rho\tilde{\delta}Y + \partial_\omega\partial_\rho\hat{\delta}Y\,, \tag{4.13}$$

where $\Phi = \{e^C{}_\gamma, \phi\}$ and Y is an object being varied.

Object Y	Y	δY	$\delta^2 Y$
ϕ	$\phi(t)$	$\delta\phi$	–
$\phi_{,\mu}$	$\phi_{,\mu}$	$\delta\phi_{,\mu}$	–
$\phi^{,\mu}$	$\phi_{,\nu}g^{\nu\mu}$	$\delta\phi_{,\nu}g^{\nu\mu}+\phi_{,\nu}\delta g^{\nu\mu}$	$\delta\phi_{,\nu}\delta g^{\nu\mu}+\phi_{,\nu}\delta^2 g^{\nu\mu}$
X	$-\frac{1}{2}\,\phi_{,\mu}\,\phi^{,\mu}$	$-\phi_{,\mu}\delta\phi^{,\mu}$	$-\frac{1}{2}(\delta\phi_{,\mu}\,\delta\phi^{,\mu}+\phi_{,\mu}\,\delta^2\phi^{,\mu})$
${e^A}_\mu$	${e^A}_\mu$	$\delta{e^A}_\mu$	–
${E_A}^\mu$	${E_A}^\mu$	$-\delta{e^B}_\nu{E_B}^\mu{E_A}^\nu$	$\delta^2{E_A}^\mu$
$g_{\mu\nu}$	$\eta_{AB}{e^A}_\mu{e^B}_\nu$	$\eta_{AB}\big(\delta{e^A}_\mu{e^B}_\nu+{e^A}_\mu\delta{e^B}_\nu\big)$	$\eta_{AB}\delta{e^A}_\mu\delta{e^B}_\nu$
$g^{\mu\nu}$	$\eta^{AB}{E_A}^\mu{E_B}^\nu$	$\eta^{AB}({E_A}^\mu\delta{E_B}^\nu+\delta{E_A}^\mu{E_B}^\nu)$	$\eta^{AB}(\delta{E_A}^\mu\delta{E_B}^\nu+\delta^2{E_A}^\mu{E_B}^\nu+{E_A}^\mu\delta^2{E_B}^\nu)$
$\mathring{\Gamma}^\lambda_{\mu\nu}$	$\frac{1}{2}g^{\lambda\gamma}(g_{\mu\gamma,\nu}+g_{\gamma\nu,\mu}-g_{\mu\nu,\gamma})$	$\frac{1}{2}\big[g^{\lambda\gamma}\big(\delta g_{\mu\gamma,\nu}+\delta g_{\gamma\nu,\mu}-\delta g_{\mu\nu,\gamma}\big)+\delta g^{\lambda\gamma}\big(g_{\mu\gamma,\nu}+g_{\gamma\nu,\mu}-g_{\mu\nu,\gamma}\big)\big]$	$\frac{1}{2}\big[g^{\lambda\gamma}\big(\delta^2 g_{\mu\gamma,\nu}+\delta^2 g_{\gamma\nu,\mu}-\delta^2 g_{\mu\nu,\gamma}\big)+\delta g^{\lambda\gamma}\big(\delta g_{\mu\gamma,\nu}+\delta g_{\gamma\nu,\mu}-\delta g_{\mu\nu,\gamma}\big)+\delta^2 g^{\lambda\gamma}\big(g_{\mu\gamma,\nu}+g_{\gamma\nu,\mu}-g_{\mu\nu,\gamma}\big)\big]$
$\mathring{R}^\lambda{}_{\mu\rho\nu}$	$2\Big(\mathring{\Gamma}^\lambda_{\mu[\nu,\rho]}+\mathring{\Gamma}^\sigma_{\mu[\nu|}\mathring{\Gamma}^\lambda_{\sigma|\rho]}\Big)$	$2\Big(\delta\mathring{\Gamma}^\lambda_{\mu[\nu,\rho]}+\mathring{\Gamma}^\sigma_{\mu[\nu|}\delta\mathring{\Gamma}^\lambda_{\sigma|\rho]}+\delta\mathring{\Gamma}^\sigma_{\mu[\nu|}\mathring{\Gamma}^\lambda_{\sigma|\rho]}\Big)$	$2\Big(\delta^2\mathring{\Gamma}^\lambda_{\mu[\nu,\rho]}+\mathring{\Gamma}^\sigma_{\mu[\nu|}\delta^2\mathring{\Gamma}^\lambda_{\sigma|\rho]}+\delta\mathring{\Gamma}^\sigma_{\mu[\nu|}\delta\mathring{\Gamma}^\lambda_{\sigma|\rho]}+\delta^2\mathring{\Gamma}^\sigma_{\mu[\nu|}\mathring{\Gamma}^\lambda_{\sigma|\rho]}\Big)$
$\mathring{R}_{\mu\nu}$	$\mathring{R}^\lambda{}_{\mu\lambda\nu}$	$\delta\mathring{R}^\lambda{}_{\mu\lambda\nu}$	$\delta^2\mathring{R}^\lambda{}_{\mu\lambda\nu}$
$\mathring{R}$	$g^{\mu\nu}\mathring{R}_{\mu\nu}$	$\delta g^{\mu\nu}\mathring{R}_{\mu\nu}+g^{\mu\nu}\delta\mathring{R}_{\mu\nu}$	$\delta^2 g^{\mu\nu}\mathring{R}_{\mu\nu}+\delta g^{\mu\nu}\delta\mathring{R}_{\mu\nu}+g^{\mu\nu}\delta^2\mathring{R}_{\mu\nu}$
$\mathring{G}_{\mu\nu}$	$\mathring{R}_{\mu\nu}-\frac{1}{2}g_{\mu\nu}\mathring{R}$	$\delta\mathring{R}_{\mu\nu}-\frac{1}{2}\big(\delta g_{\mu\nu}\mathring{R}+g_{\mu\nu}\delta\mathring{R}\big)$	$\delta^2\mathring{R}_{\mu\nu}-\frac{1}{2}\big(\delta^2 g_{\mu\nu}\mathring{R}+\delta g_{\mu\nu}\delta\mathring{R}+g_{\mu\nu}\delta^2\mathring{R}\big)$

Table 4.1: Perturbations of Horndeski quantities, listed in the first column, built from the tetrad and scalar field up to second order. The second column refers to the zeroth order of the perturbation, the third column contains first-order perturbations and the final column is the second-order perturbations. Note: $\delta^{(i)}$ refers to the i^{th} order of perturbation. A comma (,) represents the partial derivative to simplify the expressions within the table.

Object Y	Y	δY	$\delta^2 Y$
$\Gamma^{\lambda}_{\mu\nu}$	$E_A{}^{\lambda} e^A{}_{\mu,\nu}$	$\delta E_A{}^{\lambda} e^A{}_{\mu,\nu} + E_A{}^{\lambda} \delta e^A{}_{\mu,\nu}$	$\delta^2 E_A{}^{\lambda} e^A{}_{\mu\nu} + \delta E_A{}^{\lambda} \delta e^A{}_{\mu,\nu}$
$T^{\lambda}_{\mu\nu}$	$-2\Gamma^{\lambda}_{[\mu\nu]}$	$-2\delta\Gamma^{\lambda}_{[\mu\nu]}$	$-2\delta^2\Gamma^{\lambda}_{[\mu\nu]}$
a_μ	$\frac{1}{6}\epsilon_{\mu\nu\rho\sigma} g^{\rho\mu_1} g^{\sigma\nu_1} T^{\nu}{}_{\mu_1\nu_1}$	$\frac{1}{6}\epsilon_{\mu\nu\rho\sigma}[(g^{\rho\mu_1}\delta g^{\sigma\nu_1} + \delta g^{\rho\mu_1} g^{\sigma\nu_1}) T^{\nu}{}_{\mu_1\nu_1} + g^{\rho\mu_1} g^{\sigma\nu_1} \delta T^{\nu}{}_{\mu_1\nu_1}]$	$\frac{1}{6}\epsilon_{\mu\nu\rho\sigma}[(g^{\rho\mu_1}\delta^2 g^{\sigma\nu_1} + \delta g^{\rho\mu_1}\delta g^{\sigma\nu_1} + \delta^2 g^{\sigma\mu_1} g^{\sigma\nu_1}) T^{\nu}{}_{\mu_1\nu_1} + (g^{\rho\mu_1}\delta g^{\sigma\nu_1} + \delta g^{\rho\mu_1} g^{\sigma\nu_1})\delta T^{\nu}{}_{\mu_1\nu_1} + g^{\rho\mu_1} g^{\sigma\nu_1}\delta^2 T^{\nu}{}_{\mu_1\nu_1}]$
a^μ	$a_\nu g^{\nu\mu}$	$\delta a_\nu g^{\nu\mu} + a_\nu \delta g^{\nu\mu}$	$\delta^2 a_\nu g^{\nu\mu} + \delta a_\nu \delta g^{\nu\mu} + a_\nu \delta^2 g^{\nu\mu}$
v_μ	$T^{\lambda}{}_{\lambda\mu}$	$\delta T^{\lambda}{}_{\lambda\mu}$	$\delta^2 T^{\lambda}{}_{\lambda\mu}$
v^μ	$v_\nu g^{\nu\mu}$	$\delta v_\nu g^{\nu\mu} + v_\nu \delta g^{\nu\mu}$	$\delta^2 v_\nu g^{\nu\mu} + \delta v_\nu \delta g^{\nu\mu} + v_\nu \delta^2 g^{\nu\mu}$
$t_{\lambda\mu\nu}$	$g_{(\lambda\vert\rho} T^{\rho}{}_{\vert\mu)\nu} + \frac{1}{3}\big(g_{\nu(\lambda} v_{\mu)} - g_{\lambda\mu} v_\nu\big)$	$g_{(\lambda\vert\rho}\delta T^{\rho}{}_{\vert\mu)\nu} + \delta g_{(\lambda\vert\rho} T^{\rho}{}_{\vert\mu)\nu} + \frac{1}{3}\big(g_{\nu(\lambda}\delta v_{\mu)} + \delta g_{\nu(\lambda} v_{\mu)} - g_{\lambda\mu}\delta v_\nu - \delta g_{\lambda\mu} v_\nu\big)$	$\big(g_{(\lambda\vert\rho}\delta^2 T^{\rho}{}_{\vert\mu)\nu} + \delta g(\lambda\vert\rho\delta T^{\rho}{}_{\vert\mu)\nu} + \delta^2 g_{(\lambda\vert\rho} T^{\rho}{}_{\vert\mu)\nu}\big) + \frac{1}{3}\big(g_{\nu(\lambda}\delta^2 v_{\mu)} + \delta g_{\nu(\lambda}\delta v_{\mu)} + \delta^2 g_{\nu(\lambda} v_{\mu)} - g_{\lambda\mu}\delta^2 v_\nu - \delta g_{\lambda\mu}\delta v_\nu - \delta^2 g_{\lambda\mu} v_\nu\big)$
$t^{\lambda\mu\nu}$	$t_{\sigma\rho\omega} g^{\sigma\lambda} g^{\rho\mu} g^{\omega\nu}$	$g^{\rho\mu} g^{\omega\nu}(t_{\sigma\rho\omega}\delta g^{\sigma\lambda} + \delta t_{\sigma\rho\omega} g^{\sigma\lambda}) + t_{\sigma\rho\omega} g^{\sigma\lambda}(\delta g^{\rho\mu} g^{\omega\nu} + g^{\rho\mu}\delta g^{\omega\nu})$	$t_{\sigma\rho\omega}[g^{\omega\nu}(\delta g^{\sigma\lambda}\delta g^{\rho\mu} + g^{\sigma\lambda}\delta^2 g^{\rho\mu}) + g^{\sigma\lambda}(\delta g^{\rho\mu}\delta g^{\omega\nu} + g^{\rho\mu}\delta^2 g^{\omega\nu}) + g^{\rho\mu}(\delta g^{\sigma\lambda}\delta g^{\omega\nu} + g^{\omega\nu}\delta^2 g^{\sigma\lambda})] + \delta t_{\sigma\rho\omega}[g^{\sigma\lambda}(\delta g^{\rho\mu} g^{\omega\nu} + g^{\rho\mu}\delta g^{\omega\nu}) + \delta g^{\sigma\lambda} g^{\rho\mu} g^{\omega\nu}] + \delta^2 t_{\sigma\rho\omega} g^{\sigma\lambda} g^{\rho\mu} g^{\omega\nu}$
$T_{\rm ax}$	$a_\mu\, a^\mu$	$2\,\delta a_\mu\, a^\mu$	$\delta a_\mu\, \delta a^\mu + 2\,\delta^2 a_\mu\, a^\mu$
$T_{\rm vec}$	$v_\mu\, v^\mu$	$2\,\delta v_\mu\, v^\mu$	$\delta v_\mu\, \delta v^\mu + 2\,\delta^2 v_\mu\, v^\mu$
$T_{\rm ten}$	$t_{\lambda\mu\nu}\, t^{\lambda\mu\nu}$	$2\, t_{\lambda\mu\nu}\, \delta t^{\lambda\mu\nu}$	$\delta t_{\lambda\mu\nu}\, \delta t^{\lambda\mu\nu} + 2\,\delta^2 t_{\lambda\mu\nu}\, t^{\lambda\mu\nu}$
T	$\frac{3}{2}T_{\rm ax} + \frac{2}{3}T_{\rm ten} - \frac{2}{3}T_{\rm vec}$	$\frac{3}{2}\delta T_{\rm ax} + \frac{2}{3}\delta T_{\rm ten} - \frac{2}{3}\delta T_{\rm vec}$	$\frac{3}{2}\delta^2 T_{\rm ax} + \frac{2}{3}\delta^2 T_{\rm ten} - \frac{2}{3}\delta^2 T_{\rm vec}$

Table 4.2: Perturbations of teleparallel quantities, listed in the first column, built from the tetrad and scalar field up to second order. The second column refers to the zeroth order of the perturbation, the third column contains first-order perturbations and the final column is the second-order perturbations. Note: $\delta^{(i)}$ refers to the $i^{\rm th}$ order of perturbation. A comma (,) represents the partial derivative to simplify the expressions within the table.

Object Y	Y	δY	$\delta^2 Y$
I_2	$g^{\mu\nu}\, v_\nu\, \phi_{,\mu}$	$g^{\mu\nu}\, v_\nu\, \delta\phi_{,\mu} + (g^{\mu\nu}\, \delta v_\nu + \delta g^{\mu\nu}\, v_\nu)\phi_{,\mu}$	$(g^{\mu\nu}\, \delta v_\nu + \delta g^{\mu\nu}\, v_\nu)\delta\phi_{,\mu} + (g^{\mu\nu}\, \delta^2 v_\nu + \delta g^{\mu\nu}\, \delta v_\nu + \delta^2 g^{\mu\nu}\, v_\nu)\phi_{,\mu}$
J_1	$a^\mu\, a^\nu\, \phi_{,\mu}\, \phi_{,\nu}$	$2a^{(\mu}\, \delta a^{\nu)}\, \phi_{,\mu}\, \phi_{,\nu} + 2a^\nu\, a^\mu\, \phi_{,(\nu}\, \delta\phi_{,\mu)}$	$(\delta a^\mu\, \delta a^\nu + 2a^{(\nu}\, \delta^2 a^{\mu)})\phi_{,\mu}\, \phi_{,\nu} + 4a^{(\nu}\, \delta a^{\mu)}\, \delta\phi_{,(\mu}\, \phi_{,\nu)} + a^\nu\, a^\mu\, \delta\phi_{,\mu}\, \delta\phi_{,\nu}$
J_3	$\phi_{,\mu}\, \phi_{,\nu}\, t^{\lambda\mu\nu}\, v_\lambda$	$2\phi_{,(\nu}\, \delta\phi_{,\mu)}\, v_\lambda\, t^{\lambda\mu\nu} + \phi_{,\mu}\, \phi_{,\nu}(t^{\lambda\mu\nu}\, \delta v_\lambda + v_\lambda\, \delta t^{\lambda\mu\nu})$	$\delta\phi_{,\mu}\, \delta\phi_{,\nu}\, t^{\lambda\mu\nu}\, v_\lambda + 2\phi_{,(\mu}\, \delta\phi_{,\nu)}(\delta t^{\lambda\mu\nu}\, v_\lambda + t^{\lambda\mu\nu}\, \delta v_\lambda) + \phi_{,\mu}\, \phi_{,\nu}(\delta^2 t^{\lambda\mu\nu}\, v_\lambda + \delta t^{\lambda\mu\nu}\, \delta v_\lambda + t^{\lambda\mu\nu}\, \delta^2 v_\lambda)$
J_5	$g^{\sigma\rho}\, \phi_{,\mu}\, \phi_{,\rho}\, t_{\lambda\sigma\nu}\, t^{\lambda\mu\nu}$	$\phi_{,\mu}\, \phi_{,\rho}[g^{\sigma\rho}(t_{\lambda\sigma\nu}\, \delta t^{\lambda\mu\nu} + \delta t_{\lambda\sigma\nu}\, t^{\lambda\mu\nu}) + \delta g^{\sigma\rho}\, t_{\lambda\sigma\nu}\, t^{\lambda\mu\nu}] + 2g^{\sigma\rho}\, \phi_{,(\rho}\, \delta\phi_{,\mu)}\, t_{\lambda\sigma\nu}\, t^{\lambda\mu\nu}$	$\phi_{,\mu}\phi_{,\rho}[g^{\sigma\rho}(t_{\lambda\sigma\nu}\delta^2 t^{\lambda\mu\nu} + \delta^2 t_{\lambda\sigma\nu}t^{\lambda\mu\nu} + \delta t_{\lambda\sigma\nu}\delta t^{\lambda\mu\nu}) + \delta g^{\sigma\rho}(\delta t_{\lambda\sigma\nu}t^{\lambda\mu\nu} + t_{\lambda\sigma\nu}\delta t^{\lambda\mu\nu}) + \delta^2 g^{\sigma\rho}t_{\lambda\sigma\nu}t^{\lambda\mu\nu}] + g^{\sigma\rho}\delta\phi_{,\mu}\delta\phi_{,\rho}t_{\lambda\sigma\nu}t^{\lambda\mu\nu} + 2\phi_{,(\rho}\delta\phi_{,\mu)}[\delta g^{\sigma\rho}t_{\lambda\sigma\nu}t^{\lambda\mu\nu} + g^{\sigma\rho}(\delta t_{\lambda\sigma\nu}t^{\lambda\mu\nu} + t_{\lambda\sigma\nu}\delta t^{\lambda\mu\nu})]$
J_6	$\phi_{,\mu}\, \phi_{,\nu}\, \phi_{,\rho}\, \phi_{,\sigma}\, t_\lambda{}^{\mu\nu}\, t^{\lambda\sigma\rho}$	$\phi_{,\mu}\phi_{,\nu}\phi_{,\rho}\phi_{,\sigma}[\delta g_{\lambda\omega}t^{\lambda\mu\nu}t^{\omega\sigma\rho} + g_{\lambda\omega}\delta t^{\lambda\mu\nu}t^{\omega\sigma\rho} + g_{\lambda\omega}t^{\lambda\mu\nu}\delta t^{\omega\sigma\rho}] + 2[\phi_{,\mu}\phi_{,\rho}\phi_{,(\sigma}\delta\phi_{,\nu)} + \phi_{,\nu}\phi_{,\sigma}\phi_{,(\rho}\delta\phi_{,\mu)}]g_{\lambda\omega}t^{\lambda\mu\nu}t^{\omega\sigma\rho}$	$\phi_{,\mu}\phi_{,\nu}\phi_{,\rho}\phi_{,\sigma}[\delta g_{\lambda\omega}t^{\lambda\mu\nu}\delta t^{\omega\sigma\rho} + \delta g_{\lambda\omega}\delta t^{\lambda\mu\nu}t^{\omega\sigma\rho} + g_{\lambda\omega}\delta^2 t^{\lambda\mu\nu}t^{\omega\sigma\rho} + g_{\lambda\omega}\delta t^{\lambda\mu\nu}\delta t^{\omega\sigma\rho} + \delta^2 g_{\lambda\omega}t^{\lambda\mu\nu}t^{\omega\sigma\rho}] + 2(g_{\lambda\omega}\delta t^{\lambda\mu\nu}t^{\omega\sigma\rho} + g_{\lambda\omega}\delta t^{\omega\sigma\rho}t^{\lambda\mu\nu} + \delta g_{\lambda\omega}t^{\omega\sigma\rho}t^{\lambda\mu\nu})(\phi_{,\mu}\phi_{,\rho}\phi_{,(\nu}\delta\phi_{,\sigma)} + \phi_{,\nu}\phi_{,\sigma}\phi_{,(\rho}\delta\phi_{,\mu)}) + \big(\phi_{,\rho}\delta\phi_{,\mu}\delta\phi_{,\nu}\phi_{,\sigma} + \phi_{,\mu}\phi_{,\nu}\delta\phi_{,\rho}\delta\phi_{,\sigma} + 2\phi_{,\nu}\delta\phi_{,\mu}\delta\phi_{,(\rho}\phi_{,\sigma)} + 2\phi_{,\mu}\delta\phi_{,\nu}\delta\phi_{,(\rho}\phi_{,\sigma)}\big)\big(g_{\lambda\omega}t^{\lambda\mu\nu}t^{\omega\sigma\rho}\big)$
J_8	$g^{\sigma\rho}\phi_{,\nu}\phi_{,\sigma}t_{\lambda\mu\rho}t^{\lambda\mu\nu}$	$\phi_{,\nu}\phi_{,\sigma}[\delta g^{\sigma\rho}t_{\lambda\mu\rho}t^{\lambda\mu\nu} + g^{\sigma\rho}(\delta t_{\lambda\mu\rho}t^{\lambda\mu\nu} + t_{\lambda\mu\rho}\delta t^{\lambda\mu\nu})] + 2\phi_{,(\sigma}\delta\phi_{,\nu)}g^{\sigma\rho}t_{\lambda\mu\rho}t^{\lambda\mu\nu}$	$\phi_{,\nu}\phi_{,\sigma}[\delta^2 g^{\sigma\rho}t_{\lambda\mu\rho}t^{\lambda\mu\nu} + \delta g^{\sigma\rho}\delta t_{\lambda\mu\rho}t^{\lambda\mu\nu} + \delta g^{\sigma\rho}t_{\lambda\mu\rho}\delta t^{\lambda\mu\nu} + g^{\sigma\rho}t_{\lambda\mu\rho}\delta^2 t^{\lambda\mu\nu} + g^{\sigma\rho}\delta^2 t_{\lambda\mu\rho}t^{\lambda\mu\nu} + g^{\sigma\rho}\delta t\lambda\mu\rho\delta t^{\lambda\mu\nu}] + \delta\phi_{,\nu}\delta\phi_{,\sigma}g^{\sigma\rho}t_{\lambda\mu\rho}t^{\lambda\mu\nu} + 2\delta g^{\sigma\rho}t_{\lambda\mu\rho}\phi_{,(\sigma}\delta\phi_{,\nu)}t^{\lambda\mu\nu} + 2g^{\sigma\rho}\phi_{,(\sigma}\delta\phi_{,\nu)}(\delta t_{\lambda\mu\rho}t^{\lambda\mu\nu} + t_{\lambda\mu\rho}\delta t^{\lambda\mu\nu})$
J_{10}	$\epsilon_{\mu\nu\rho\lambda}a^\nu\phi^{,\mu}\phi_{,\sigma}t^{\sigma\rho\lambda}$	$\epsilon_{\omega\nu\rho\lambda}\big(\phi_{,\mu}\phi_{,\sigma}[\delta a^\nu g^{\mu\omega}t^{\sigma\rho\lambda} + a^\nu(\delta g^{\mu\omega}t^{\sigma\rho\lambda} + g^{\mu\omega}\delta t^{\sigma\rho\lambda})] + 2a^\nu g^{\mu\omega}\phi_{,(\sigma}\delta\phi_{,\mu)}t^{\sigma\rho\lambda}\big)$	$\epsilon_{\mu_1\nu\rho\lambda}\big[\delta^2 a^\nu g^{\mu\omega}\phi_{,\sigma}\phi_{,\mu}t^{\sigma\rho\lambda} + t^{\sigma\rho\lambda}[\phi_{,\sigma}\phi_{,\mu}(\delta a^\nu\delta g^{\mu\omega} + a^\nu\delta^2 g^{\mu\omega}) + 2\phi_{,(\mu}\delta\phi_{,\sigma)}(\delta a^\nu g^{\mu\omega} + a^\nu\delta g^{\mu\omega}) + a^\nu g^{\mu\omega}\delta\phi_{,\mu}\delta\phi_{,\sigma}] + \delta t^{\sigma\rho\lambda}[\phi_{,\mu}\phi_{,\sigma}(\delta a^\nu g^{\mu\omega} + a^\nu\delta g^{\mu\omega}) + 2a^\nu g^{\mu\omega}\phi_{,(\sigma}\delta\phi_{,\mu)}] + a^\nu g^{\mu\omega}\phi_{,\mu}\phi_{,\sigma}\delta^2 t^{\sigma\rho\lambda}\big]$

Table 4.3: Perturbations of teleparallel Horndeski quantities, listed in the first column, built from the tetrad and scalar field up to second order. The second column refers to the zeroth order of the perturbation, the third column contains first-order perturbations and the final column is the second-order perturbations. Note: $\delta^{(i)}$ refers to the i^{th} order of perturbation. A comma (,) represents the partial derivative to simplify the expressions within the table.

Hence, an arbitrary function G is varied by the following identity:

$$\begin{aligned}&\delta_\Phi G(Y,\dots)\\&\quad=\left(\frac{\partial G}{\partial Y}\frac{\partial Y}{\partial \Phi}+\dots\right)-\partial_\rho\left(\frac{\partial G}{\partial Y}\frac{\partial Y}{\partial(\partial_\rho\Phi)}+\dots\right)+\partial_\omega\partial_\rho\left(\frac{\partial G}{\partial Y}\frac{\partial Y}{\partial(\partial_\omega\partial_\rho\Phi)}+\dots\right).\end{aligned}\tag{4.14}$$

The rest of the components of the BDLS action are varied individually to obtain the equations of motion. The following subsections explore the variations with respect to the tetrad and scalar fields in more detail.

4.2.1 | Variation with respect to Tetrad

The first part is the variation with respect to the tetrad. It should be noted that throughout this section, C, γ, and ρ are reserved for the variation term. Taking the variation of the tetrad itself yields the relationship

$$\delta_e e^A{}_\mu = \delta^A_C \delta^\gamma_\mu\,.\tag{4.15}$$

Through the identity relation given by Eq. (2.43) obtained as a result of the orthogonality condition between the tetrad and inverse tetrad, the variation of the inverse tetrad can be obtained as follows:

$$e^A{}_\mu E_A{}^\nu = \delta^\nu_\mu \implies \delta_e(e^A{}_\mu E_A{}^\nu) = 0\,.\tag{4.16}$$

As shown in Table 4.4, the Euler-Lagrangian of the tetrad and inverse tetrad is equivalent to the first term only, such that

$$\delta_e e^A{}_\mu = \bar{\delta}_e e^A{}_\mu\,,\qquad\qquad \delta_e E_A{}^\mu = \bar{\delta}_e E_A{}^\mu\,.\tag{4.17}$$

By the Leibniz product rule, the above equation can be expressed as

$$\begin{aligned}\delta_e e^A{}_\mu E_A{}^\nu + e^A{}_\mu \delta_e E_A{}^\nu = 0 &\implies e^A{}_\mu \delta_e E_A{}^\nu = -\delta_e e^A{}_\mu E_A{}^\nu\\&\implies \delta_e E_B{}^\nu = -E_A{}^\nu E_B{}^\mu \delta_e e^A{}_\mu\,.\end{aligned}\tag{4.18}$$

The determinant can be expressed in terms of the tetrad by

$$e = \exp\left(\mathrm{tr}(\ln e^A{}_\mu)\right)\,,\tag{4.19}$$

such that its variation with respect to the tetrad yields

$$\delta_e e = e\,\delta_e\left(\mathrm{tr}(\ln e^A{}_\mu)\right) = e E_A{}^\mu \delta_e e^A{}_\mu\,.\tag{4.20}$$

Thus, the rest of the quantities can be built through Eq. (4.16), (4.18) and (4.20). In the case where ingredients/functions are present in the standard Horndeski action, their variation has been calculated with respect to the metric in Ref. [267] such that it can be expressed in terms of the tetrad variation by replacing the variation of the metric as follows [268]:

$$\delta_e g_{\mu\nu} = \eta_{AC}(\delta^\gamma_\mu e^A{}_\nu + \delta^\gamma_\nu e^A{}_\mu)\,, \qquad \text{and} \qquad \delta_e g^{\mu\nu} = -(E_C{}^\mu g^{\gamma\nu} + E_C{}^\nu g^{\mu\gamma})\,. \tag{4.21}$$

The variations of the basic quantities used throughout these derivations are summarised in Table 4.4. In hindsight, the variation of derivatives of the tetrad is included as these would be required to calculate the Horndeski quantities of $\mathring{R}$ and $\mathring{G}_{\mu\nu}$. It should be noted that quantities $\{e^A{}_\mu, \partial_\nu e^A{}_\mu, \partial_\lambda\partial_\nu e^A{}_\mu\}$ only give rise to a single term from the Euler-Langrangian relationship given by Eq. (4.13). This is not the case with the derivatives of the inverse tetrad due to the relationship given by Eq. (4.18). The results for quantities that appear in the standard Horndeski action are listed in Table 4.5. Covariant derivatives of the scalar field do not result in the last term of the Euler-Lagrangian expression given by Eq. (4.13), because the only second order derivative term is given by $\partial_\mu\partial_\nu\phi$, which independent of the tetrad. This would not be the case if a scalar variation is considered. Table 4.6 gives the evaluation of the quantities associated with purely teleparallel terms, while variations of scalar-tetrad quantities are listed in Table 4.7. All of these quantities can be expressed in terms of the tetrad and scalar field up to the first-order derivative. Therefore, the column associated with $\hat{\delta}_e$ is eliminated as they do not contribute to the variation.

Therefore, variation with respect to the tetrad of the Lagrangian densities in Eq. (2.98) yields

$$W_C{}^{\gamma\,(2)} = e\left(G_2 E_C{}^\gamma + G_{2,X}\bar{\delta}X\right)\,, \tag{4.22a}$$

$$W_C{}^{\gamma\,(3)} = -e\left(E_C{}^\gamma\, G_3\,\mathring{\Box}\phi + G_{3,X}\,\bar{\delta}X\,\mathring{\Box}\phi + G_3\,\bar{\delta}(\mathring{\Box}\phi)\right) + \partial_\rho\left(e\,G_3\,\tilde{\delta}(\mathring{\Box}\phi)\right)\,, \tag{4.22b}$$

$$\begin{aligned} W_C{}^{\gamma\,(4)} = e\Big(&E_C{}^\gamma\, G_4\mathring{R} + G_4\,\bar{\delta}\mathring{R} + \left(E_C{}^\gamma G_{4,X} + G_{4,XX}\,\bar{\delta}X\right)\left((\mathring{\Box}\phi)^2 - \mathcal{W}_1\right)\Big) \\ &+G_{4,X}\,\bar{\delta}X\,\mathring{R} + G_{4,X}\left(2\,\mathring{\Box}\phi\,\bar{\delta}(\mathring{\Box}\phi) - \bar{\delta}\mathcal{W}_1\right)\Big) - \partial_\rho\Big(e\,G_4\,\tilde{\delta}\mathring{R} \\ &+e\,G_{4,X}\,\left(2\,\mathring{\Box}\phi\,\tilde{\delta}(\mathring{\Box}\phi) - \tilde{\delta}\mathcal{W}_1\right)\Big) + \partial_\omega\partial_\rho\left(e\,G_4\,\hat{\delta}\mathring{R}\right)\,, \end{aligned} \tag{4.22c}$$

$$\begin{aligned} W_C{}^{\gamma\,(5)} = e\Big(&\left(E_C{}^\gamma G_5 + G_{5,X}\,\bar{\delta}X\right)\mathring{G}_{\mu\nu}\,\mathring{\nabla}^\mu\mathring{\nabla}^\nu\phi + G_5\left(\bar{\delta}\mathring{G}_{\mu\nu}\,\mathring{\nabla}^\mu\mathring{\nabla}^\nu\phi + \mathring{G}_{\mu\nu}\,\bar{\delta}(\mathring{\nabla}^\mu\mathring{\nabla}^\nu\phi)\right) \\ &-\frac{1}{6}\left(G_{5,X}E_C{}^\gamma + G_{5,XX}\,\bar{\delta}X\right)\left((\mathring{\Box}\phi)^3 + 2\mathcal{W}_2 - 3\mathring{\Box}\phi\,\mathcal{W}_1\right)\Big) \\ &\frac{1}{6}G_{5,X}\left(3(\mathring{\Box}\phi)^2\,\bar{\delta}(\mathring{\Box}\phi) + 2\bar{\delta}\mathcal{W}_2 - 3\left(\bar{\delta}(\mathring{\Box}\phi)\,\mathcal{W}_1 + \mathring{\Box}\phi\,\bar{\delta}\mathcal{W}_1\right)\right) \\ &-\partial_\rho\Big(e\,G_5\left(\tilde{\delta}\mathring{G}_{\mu\nu}\,\mathring{\nabla}^\mu\mathring{\nabla}^\nu\phi + \mathring{G}_{\mu\nu}\,\tilde{\delta}(\mathring{\nabla}^\mu\mathring{\nabla}^\nu\phi)\right) - \frac{1}{6}e\,G_{5,X}\left(3(\mathring{\Box}\phi)^2\,\tilde{\delta}(\mathring{\Box}\phi)\right. \end{aligned}$$

$$+2\tilde{\delta}\mathcal{W}_2 - 3\left(\tilde{\delta}(\mathring{\Box}\phi)\,\mathcal{W}_1 + \mathring{\Box}\phi\,\tilde{\delta}\mathcal{W}_1\right)\Big)\Big) + \partial_\omega\partial_\rho\left(e\,G_5\,\mathring{\nabla}^\mu\mathring{\nabla}^\nu\phi\,\hat{\delta}\mathring{G}_{\mu\nu}\right)\,, \tag{4.22d}$$

$$W_C{}^{\gamma\,(\text{Tele})} = e\left(E_C{}^\gamma G_{\text{Tele}} + \sum_Y G_{\text{Tele},Y}\bar{\delta}Y\right) - \partial_\rho\left(\sum_Y G_{\text{Tele},Y}\tilde{\delta}Y\right)$$
$$\text{for } Y \in \{\phi, X, T, T_{\text{ax}}, T_{\text{vec}}, I_2, J_1, J_3, J_5, J_6, J_8, J_{10}\}\,, \tag{4.22e}$$

where $\mathcal{W}_1 = \mathring{\nabla}_\mu\mathring{\nabla}_\nu\phi\,\mathring{\nabla}^\mu\mathring{\nabla}^\nu\phi$ and $\mathcal{W}_2 = \mathring{\nabla}_\mu\mathring{\nabla}^\nu\phi\,\mathring{\nabla}_\nu\mathring{\nabla}^\lambda\phi\,\mathring{\nabla}_\lambda\mathring{\nabla}^\mu\phi$. By contracting the equations of motion $W_C{}^{\gamma\,(i)}$ with the tetrad and metric, the expression $W_{\mu\nu} = g_{\gamma\nu}e^C{}_\mu W_C{}^\gamma$ is obtained [268]. The above results are not fully worked out due to the complexity of the system. This form of the results is easier to implement within `Mathematica`, as later components of the field equations will be calculated.

4.2.2 | Variation with respect to Scalar Field

Analogous to tetrad variations, the following portion contains variations with respect to the scalar field. While the objects that are purely teleparallel have a trivial variation result, all other terms are built on

$$\delta_\phi\phi = 1\,, \qquad \delta_\phi(\partial_\mu\phi) = -\partial_\rho(\delta^\rho_\mu) = 0\,, \qquad \text{and} \qquad \delta_\phi(\partial_\nu\partial_\mu\phi) = \partial_\nu\partial_\mu(\delta^\rho_\mu\delta^\omega_\nu) = 0\,, \tag{4.23}$$

as summarised in Table 4.8. The list is simpler than the ones with variations with respect to the tetrad. Only terms which have $\partial_\mu\partial_\nu\phi$ contributions result in the last term of Eq. (4.13). All terms, except for ϕ, have a scalar dependency stemming solely from derivatives of it. Thus, the second column of Table 4.8 is trivial for the most part. Additionally, $\{T, T_{\text{ax}}, T_{\text{vec}}\}$ are not included as these are pure tetrad-based quantities and their variation with respect to the scalar field yields trivial results.

Taking the Lagrangian densities presented in Eq. (2.98) and applying the results in Table. 4.8, results in the scalar field equation:

$$W^{(2)}_\phi = e\,G_{2,\phi} + \partial_\rho\{e\,\partial^\rho\phi\,G_{2,X}\}\,, \tag{4.24a}$$

$$W^{(3)}_\phi = e\,G_{3,\phi}\,\mathring{\Box}\phi - \partial_\rho\{e\,(g^{\mu\nu}\,\mathring{\Gamma}^\rho_{\mu\nu}\,G_3 + \partial^\rho\phi\,G_{3,X}\,\mathring{\Box}\phi)\} - \partial_\omega\partial_\rho\{e\,g^{\rho\omega}\,G_3\}\,, \tag{4.24b}$$

$$\begin{aligned} W^{(4)}_\phi = {} & e\,[\mathring{R}\,G_{4,\phi} + (\mathring{\Box}\phi^2 - \mathring{\nabla}_\mu\mathring{\nabla}_\nu\phi\,\mathring{\nabla}^\mu\mathring{\nabla}^\nu\phi)\,G_{4,\phi X}] - \partial_\rho\{e\,[2\,\mathring{\Gamma}^\rho_{\mu\nu}\,G_{4,X}\,(\mathring{\nabla}^\mu\mathring{\nabla}^\nu\phi \\ & - \mathring{\Box}\phi\,g^{\mu\nu}) - \partial^\rho\phi\,(\mathring{R}\,G_{4,X} + (\mathring{\Box}\phi^2 - \mathring{\nabla}_\mu\mathring{\nabla}_\nu\phi\,\mathring{\nabla}^\mu\mathring{\nabla}^\nu\phi)\,G_{4,XX})]\} \\ & - 2\,\partial_\omega\partial_\rho\{G_{4,X}\,(\mathring{\nabla}^\rho\mathring{\nabla}^\omega\phi - \mathring{\Box}\phi\,g^{\rho\omega})\}\,, \end{aligned} \tag{4.24c}$$

$$\begin{aligned} W^{(5)}_\phi = {} & e\,[\mathring{\nabla}^\mu\mathring{\nabla}^\nu\phi\,\mathring{G}_{\mu\nu}\,G_{5,\phi} - \frac{1}{6}\,G_{5,\phi X}\,(\mathring{\Box}\phi^3 + 2\,\mathring{\nabla}_\nu\mathring{\nabla}_\mu\phi\,\mathring{\nabla}_\lambda\mathring{\nabla}^\mu\phi\,\mathring{\nabla}^\nu\mathring{\nabla}^\lambda\phi \\ & - 3\,\mathring{\Box}\phi\,\mathring{\nabla}_\mu\mathring{\nabla}_\nu\phi\,\mathring{\nabla}^\mu\mathring{\nabla}^\nu\phi)] - \partial_\rho\{e\,[-\mathring{G}^{\mu\nu}\,\mathring{\Gamma}^\rho_{\mu\nu}\,G_5 + \frac{1}{6}\,G_{5,X}\,(-6\,\mathring{\nabla}^\mu\mathring{\nabla}^\nu\phi\,\partial^\rho\phi\,\mathring{G}_{\mu\nu} \\ & + [2\,\mathring{\nabla}_\nu\mathring{\nabla}^\lambda\phi\,\mathring{\nabla}^\nu\mathring{\nabla}^\sigma\phi + 2\mathring{\nabla}_\mu\mathring{\nabla}^\lambda\phi\,\mathring{\nabla}^\sigma\mathring{\nabla}^\mu\phi + 3\,(\mathring{\Box}\phi^2 - \mathring{\nabla}_\mu\mathring{\nabla}_\nu\phi\,\mathring{\nabla}^\mu\mathring{\nabla}^\nu\phi)\,g^{\sigma\lambda} \end{aligned}$$

$$
\begin{aligned}
&- 6\,\mathring{\Box}\phi\,\mathring{\nabla}^{\sigma}\mathring{\nabla}^{\lambda}\phi + 2\,\mathring{\nabla}_{\nu}\mathring{\nabla}_{\mu}\phi\,\mathring{\nabla}^{\lambda}\mathring{\nabla}^{\mu}\phi\,g^{\sigma\nu}\,\big]\,\mathring{\Gamma}^{\rho}_{\sigma\lambda}\big) + \frac{1}{6}\,\partial^{\rho}\phi\,G_{5,XX}\,\big(\mathring{\Box}\phi^{3} \\
&- 3\mathring{\Box}\phi\,\mathring{\nabla}_{\mu}\mathring{\nabla}_{\nu}\phi\,\mathring{\nabla}^{\mu}\mathring{\nabla}^{\nu}\phi + 2\mathring{\nabla}_{\nu}\mathring{\nabla}_{\mu}\phi\,\mathring{\nabla}_{\lambda}\mathring{\nabla}^{\mu}\phi\,\mathring{\nabla}^{\nu}\mathring{\nabla}^{\lambda}\phi)\big]\big\} + \partial_{\omega}\partial_{\rho}\big\{e\,\big[\mathring{G}^{\rho\omega}\,G_{5} \\
&- \frac{1}{6}\,G_{5,X}\,\big(2\,\mathring{\nabla}_{\nu}\mathring{\nabla}^{\omega}\phi\,\mathring{\nabla}^{\nu}\mathring{\nabla}^{\rho}\phi + 4\,\mathring{\nabla}_{(\lambda}\mathring{\nabla}_{\omega)}\phi\,\mathring{\nabla}^{\rho}\mathring{\nabla}^{\lambda}\phi - 6\,\mathring{\Box}\phi\,\mathring{\nabla}^{\rho}\mathring{\nabla}^{\omega}\phi + 3\,(\mathring{\Box}\phi^{2} \\
&- \mathring{\nabla}_{\mu}\mathring{\nabla}_{\nu}\phi\,\mathring{\nabla}^{\mu}\mathring{\nabla}^{\nu}\phi)\,g^{\rho\omega}\big)\big]\big\}\,, \qquad (4.24d)
\end{aligned}
$$

$$
\begin{aligned}
W^{(\mathrm{Tele})}_{\phi} &= e\,G_{\mathrm{Tele},\phi} - \partial_{\rho}\big\{e\,\big[-\partial^{\rho}\phi\,G_{\mathrm{Tele},X} + v^{\rho}\,G_{\mathrm{Tele},I_2} + 2\,a^{\rho}a^{\mu}\,\partial_{\mu}\phi\,G_{\mathrm{Tele},J_1} \\
&+ 2\partial_{\mu}v_{\nu}\,G_{\mathrm{Tele},J_3}\,t^{\nu(\mu\rho)} + 2\,\partial^{\mu}\phi\,t_{\lambda\mu\nu}\,t^{\lambda\rho\nu}\,G_{\mathrm{Tele},J_5} + 2\,\partial^{\sigma}\phi\,t_{\lambda\mu\sigma}\,t^{\lambda\mu\rho}\,G_{\mathrm{Tele},J_8} \\
&+ 4\,\partial_{\sigma}\phi\,\partial^{\mu}\phi\,\partial^{\nu}\phi\,t_{\lambda\mu\nu}\,t^{\lambda(\sigma\rho)}\,G_{\mathrm{Tele},J_6} - 2\,a^{\nu}\,\partial_{\mu}\phi\,\epsilon_{\omega\nu\lambda}{}^{(\mu}\,t^{\rho)\omega\lambda}\,G_{\mathrm{Tele},J_{10}}\big]\big\}\,, \qquad (4.24e)
\end{aligned}
$$

where $W^{(i)}$ for $i \in \{2,3,4,5,\mathrm{Tele}\}$ corresponds to terms which contain the function G_i. The background equations obtained from Eqs (4.24) correspond to those in Eq. (3.23) when cast in the form of the Klein-Gordon equation. Eqs (4.24a-4.24d) are identical to those obtained in standard Horndeski, while Eq. (4.24e) gives new contributions from the teleparallel sector. It should be noted that the derivatives ∂_ρ and $\partial_\omega\partial_\rho$ are not explicitly performed and presented here due to the complexity of the equations while also being easier to perform perturbations in this form.

4.3 | Linearised Field Equations

Eqs (4.22a-4.22e) and Eqs (4.24a-4.24e), along with the knowledge of the perturbations of quantities which are presented in Tables 4.1, 4.2, and 4.3, provide the tools to obtain the linearised field equations. Since the general form of these perturbations is cumbersome, here is presented the first-order perturbation of each sector when considering a SVT irreducible decomposition of the tetrad.

4.3.1 | Scalar-Vector-Tensor Decomposition

The scalar, vector, and tensor modes have different spins as a result of their transformation properties undergoing spatial rotations: scalar have spin-0, vectors have spin-1 and tensors have spin-2. In general, a metric within the four-dimensional spacetime considered thus far would have 16 DoFs. Only upon consideration of symmetric properties do these number of DoFs reduce to 10. Here, the fundamental dynamical object is no longer the metric, but the same decomposition is expected through the construction of a tetrad with 16 DoFs, containing both symmetric and

antisymmetric parts:

$$e^{A}{}_{\mu} = \begin{pmatrix} 1+\varphi & a\left(\partial_i\beta + \beta_i\right) \\ \delta^A_i\left(\partial^i b + b^i\right) & a\delta^{Aj}\left(\delta_{ij}(1+\psi) + \partial_i\partial_j h + 2\partial_{(i}h_{j)} + \frac{1}{2}h_{ij} + \epsilon_{ijk}(\partial^k\sigma + \sigma^k)\right) \end{pmatrix}, \quad (4.25)$$

where the tetrad perturbation has been split in scalars $\{\varphi, \beta, b, \psi, h\}$, pseudoscalar $\{\sigma\}$, vectors $\{\beta_i, b_i, h_i\}$, pseudovector $\{\sigma_i\}$ and tensor $\{h_{ij}\}$. The scalars and pseudoscalar have 1 DoF each, the vectors and pseudovector have 2 DoFs and are divergenceless such that $\partial^i\beta_i = \partial^i b_i = \partial^i h_i = \partial^i\sigma_i = 0$, and the tensor has 2 DoFs which are symmetric $h_{ij} = h_{ji}$, traceless $\delta^{ij}h_{ij} = 0$ and divergenceless $\partial^i h_{ij} = 0$. The divergenceless property of vector modes arises as these modes correspond to shear-like deformations of spacetime and as a pure rotational mode does not result in compressions and expansions, while the tensor modes are to ensure that shear deformations are realised to account for transverse distortions. Additionally, the traceless condition eliminates scalar behaviour to focus on shape distortion.

Constructing the metric through Eq. (2.44) up to first order results in

$$g_{\mu\nu} \to \begin{pmatrix} 1+2\varphi & a\left(\partial_i B + B_i\right) \\ a\left(\partial_i B + B_i\right) & -a^2\left((1+2\psi)\delta_{ij} + 2\partial_i\partial_j h + 4\partial_{(i}h_{j)} + h_{ij}\right) \end{pmatrix}, \quad (4.26)$$

where $B = -b + \beta$ and $B_i = -b_i + \beta_i$, for a total of 10 DoFs. Moreover, the pseudoscalar and pseudovector are seen to vanish in the metric perturbation up to first order, because they are associated with the antisymmetric part of the tetrad while the metric is completely symmetric. As shown in Table 4.1, the metric contains second-order perturbations when constructed through the tetrad. For this reason, only the fundamental dynamical objects are taken to have a small perturbation up to the first order, and in general, all other quantities are extended to the second order. In addition to the tetrad, the scalar field is also a fundamental quantity, to which the perturbation, classified under the scalar modes, is given by Eq. (3.120). Therefore, the linearised field equations for each sector mode can be obtained individually. The results for each mode are listed as functions of perturbation modes, with detailed equations included in Appendix A.

4.3.1.1 | Scalar Modes

Scalar perturbations are primarily linked to density fluctuations in matter and energy. They describe an important sector when dealing with structure formation. In the matter and radiation epochs of the Universe, scalar perturbations are associated with the fluctuations in matter and energy. During the matter-dominated era, scalar perturbations form gravitational wells where matter accumulates to eventually form clusters. In the early Universe, where radiation dominates, interactions between photons and baryons give rise to acoustic oscillations, which can be

observed in the CMB. Scalar perturbations leave an imprint on CMB observations, manifesting as temperature anisotropies due to their influence on gravitational potentials [269]. The scalar sector contains the modes $\{\varphi, \beta, b, h, \sigma\}$ in the tetrad

$$e^{A}{}_{\mu}^{\ \mathrm{S}} = \begin{pmatrix} 1+\varphi & a\,\partial_i\beta \\ \delta_i^A\,\partial^i b & a\delta^{Aj}\left(\delta_{ij}(1+\psi) + \partial_i\partial_j h + \epsilon_{ijk}\,\partial^k\sigma\right) \end{pmatrix}, \tag{4.27}$$

and

$$\phi^{\mathrm{S}} = \phi(t) + \delta\phi\,. \tag{4.28}$$

The mode σ is technically a pseudoscalar, as it changes sign under parity transformation, allowing the potential parity-violating interaction such as axions which have been used to model dark matter. The field equations become

$$\delta W_0{}^{0\ \mathrm{S}} = \mathcal{A}^{\mathrm{S}}\left(\delta\phi, \delta\dot\phi, \partial^2\delta\phi, \varphi, \partial^2\varphi, \partial^2\beta, \partial^2\dot\beta, \partial^2 b, \dot\psi, \partial^2\psi, \partial^2\dot h\right), \tag{4.29a}$$

$$\delta W_0{}^{i\ \mathrm{S}} = \mathcal{B}^{\mathrm{S}}\left(\partial^i\delta\phi, \partial^i\delta\dot\phi\partial^i\varphi, \partial^i\dot\varphi, \partial^i\dot\beta, \partial^i\ddot\beta, \partial^i\psi, \partial^i\dot\psi\right), \tag{4.29b}$$

$$\delta W_i{}^{0\ \mathrm{S}} = \mathcal{C}^{\mathrm{S}}\left(\partial_i\delta\phi, \partial_i\delta\dot\phi, \partial_i\varphi, \partial_i\partial^2 b, \partial_i\dot\psi, \partial_i\partial^2\dot h\right), \tag{4.29c}$$

$$\begin{aligned}\delta W_i{}^{j\ \mathrm{S}} = \mathcal{D}^{\mathrm{S}}\Big(&\partial_i\partial^j\delta\phi, \partial_i\partial^j\varphi, \partial_i\partial^j\beta, \partial_i\partial^j\dot\beta, \partial_i\partial^j b, \partial_i\partial^j\dot b, \partial_i\partial^j\psi, \partial_i\partial^j\dot h, \partial_i\partial^j\ddot h,\\ &\epsilon_i{}^{jk}\partial_k\sigma, \epsilon_i{}^{jk}\partial_k\dot\sigma, \epsilon_i{}^{jk}\partial_k\ddot\sigma, \epsilon_i{}^{jk}\partial_k\partial^2\sigma\Big),\end{aligned} \tag{4.29d}$$

$$\delta W_i{}^{i\ \mathrm{S}} = \mathcal{E}^{\mathrm{S}}\left(\delta\phi, \delta\dot\phi, \delta\ddot\phi, \partial^2\delta\phi, \varphi, \dot\varphi, \partial^2\varphi, \partial^2\beta, \partial^2\dot\beta, \partial^2 b, \partial^2\dot b, \dot\psi, \ddot\psi, \partial^2\psi, \partial^2\dot h, \partial^2\ddot h\right), \tag{4.29e}$$

$$\delta W_\phi^{\mathrm{S}} = \mathcal{F}^{\mathrm{S}}(\delta\phi, \delta\dot\phi, \delta\ddot\phi, \partial^2\delta\phi, \varphi, \dot\varphi, \partial^2\varphi, \partial^2\beta, \partial^2\dot\beta, \partial^2 b, \partial^2\dot b, \partial^2\psi, \dot\psi, \ddot\psi, \partial^2\dot h, \partial^2\ddot h)\,, \tag{4.29f}$$

where $\mathcal{Y}^{\mathrm{S}}$ for $\mathcal{Y} \in \{\mathcal{A}, \mathcal{B}, \mathcal{C}, \mathcal{D}, \mathcal{E}, \mathcal{F}\}$ are functions (see Appendix A for further details). The symmetric and antisymmetric portions of the field equations for the scalar fields are

$$W_{(0i)} = \mathcal{G}^{\mathrm{S}}\left(\partial_i\delta\phi, \partial_i\delta\dot\phi, \partial_i\varphi, \partial_i\dot\varphi, \partial_i\dot\beta, \partial_i\ddot\beta, \partial_i\partial^2 b, \partial_i\psi, \partial_i\dot\psi, \partial_i\partial^2\dot h\right), \tag{4.30}$$

$$W_{(ij)} = \mathcal{H}^{\mathrm{S}}\left(\partial_i\partial_j\delta\phi, \partial_i\partial_j\varphi, \partial_i\partial_j\beta, \partial_i\partial_j b, \partial_i\partial_j\dot b, \partial_i\partial_j\psi, \partial_i\partial_j\dot h, \partial_i\partial_j\ddot h\right), \tag{4.31}$$

$$W_{[0i]} = \mathcal{I}^{\mathrm{S}}\left(\partial_i\delta\phi, \partial_i\delta\dot\phi, \partial_i\varphi, \partial_i\dot\varphi, \partial_i\dot\beta, \partial_i\ddot\beta, \partial_i\partial^2 b, \partial_i\psi, \partial_i\dot\psi, \partial_i\partial^2\dot h\right), \tag{4.32}$$

$$W_{[ij]} = \mathcal{J}^{\mathrm{S}}(\epsilon_{ijk}\partial^k\sigma, \epsilon_{ijk}\partial^k\dot\sigma, \epsilon_{ijk}\partial^k\ddot\sigma, \epsilon_{ijk}\partial^k\partial^2\sigma)\,, \tag{4.33}$$

4.3.1.2 | Vector Modes

The physical characteristics of vector perturbations arise from their depiction of how different regions of the Universe move tangentially relative to one another. As the Universe expands, the shear modes are diluted resulting in a quick decay of the vector modes [269]. Regardless, their

remnants from the early Universe leave a mark on the polarisation of CMB, associated with B-mode polarisation. The vector sector contains the perturbation modes $\{\beta_i, b_i, h_i\}$, and σ_i in the tetrad

$$e^{A}{}_{\mu}^{\ \mathrm{V}} = \begin{pmatrix} 1 & a\,\beta_i \\ \delta^A_i\, b^i & a\delta^{Aj}\left(\delta_{ij} + 2\partial_{(i}h_{j)} + \epsilon_{ijk}\,\sigma^k\right) \end{pmatrix}, \tag{4.34}$$

which results in the following field equations:

$$\delta W_0{}^{i\ \mathrm{V}} = \mathcal{B}^{\mathrm{V}}\left(\dot{\beta}^i, \ddot{\beta}^i, \partial^2\beta^i, \partial^2 h^i, \partial^2\dot{h}^i, \epsilon^{ijk}\partial_j\sigma_k, \epsilon^{ijk}\partial_j\dot{\sigma}_k\right), \tag{4.35a}$$

$$\delta W_i{}^{0\ \mathrm{V}} = \mathcal{C}^{\mathrm{V}}\left(\partial^2\beta_i, \partial^2 b_i, \partial^2\dot{h}_i, \epsilon_{ijk}\partial^j\dot{\sigma}^k\right), \tag{4.35b}$$

$$\delta W_i{}^{j\ \mathrm{V}} = \mathcal{D}^{\mathrm{V}}\left(\partial^j\beta_i, \partial^j\dot{\beta}_i, \partial^j b_i, \partial^j\dot{b}_i, \partial^j\dot{h}_i, \partial^j\ddot{h}_i, \partial^j\partial^2 h_i, \epsilon_i{}^{jk}\dot{\sigma}_k, \epsilon_i{}^{jk}\ddot{\sigma}_k, \epsilon_i{}^{jk}\partial^2\sigma_k\right), \tag{4.35c}$$

$$\delta W^{\mathrm{V}}_{(0i)} = \mathcal{G}^{\mathrm{V}}\left(\dot{\beta}_i, \ddot{\beta}_i, \partial^2\beta_i, \partial^2 b_i, \partial^2 h_i, \partial^2\dot{h}_i, \epsilon_{ijk}\partial^j\sigma^k, \epsilon_{ijk}\partial^j\dot{\sigma}^k\right), \tag{4.35d}$$

$$\delta W^{\mathrm{V}}_{[0i]} = \mathcal{H}^{\mathrm{V}}\left(\dot{\beta}_i, \ddot{\beta}_i, \partial^2\beta_i, \partial^2 b_i, \partial^2 h_i, \partial^2\dot{h}_i, \epsilon_{ijk}\partial^j\sigma^k, \epsilon_{ijk}\partial^j\dot{\sigma}^k\right), \tag{4.35e}$$

$$\delta W^{\mathrm{V}}_{(ij)} = \mathcal{I}^{\mathrm{V}}\left(\partial_{(i}\beta_{j)}, \partial_{(i}\dot{\beta}_{j)}, \partial_{(i}b_{j)}, \partial_{(i}\dot{b}_{j)}, \partial_{(i}\dot{h}_{j)}, \partial_{(i}\ddot{h}_{j)}, \partial_{(i}\partial^2 h_{j)}, \partial_{(i}\partial^2\sigma_{j)}\right), \tag{4.35f}$$

$$\delta W^{\mathrm{V}}_{[ij]} = \mathcal{J}^{\mathrm{V}}\left(\partial_{[i}\beta_{j]}, \partial_{[i}\dot{\beta}_{j]}, \partial_{[i}b_{j]}, \partial_{[i}\dot{b}_{j]}, \partial_{[i}\partial^2 h_{j]}, \epsilon_{ijk}\dot{\sigma}^k, \epsilon_{ijk}\ddot{\sigma}^k, \epsilon_{ijk}\partial^2\sigma^k\right), \tag{4.35g}$$

while the remaining components and the scalar field equations are trivially zero (see Appendix A for further details). The mode σ_i is a pseudovector that does not change direction under parity transformation, unlike vector modes.

4.3.1.3 | Tensor Modes

Tensor perturbations are related to the geometrical effect stemming from GWs [270]. Their contribution to the CMB anisotropies is overshadowed by those of scalar perturbations [269]. Primordial GWs produced during the inflationary period give rise to B-mode polarisation in CMB. Hence, a spike in the BB power spectrum at large angular scales would indicate a key prediction of inflation [269]. Such direct evidence has not been observed, yet. The tensor sector contains solely the h_{ij} mode such that

$$e^{A}{}_{\mu}^{\ \mathrm{T}} = \begin{pmatrix} 1 & 0 \\ 0 & a\delta^{Aj}\left(\delta_{ij} + \frac{1}{2}h_{ij}\right) \end{pmatrix}, \tag{4.36}$$

resulting in the following field equations:

$$\delta W_i{}^{J\ \mathrm{T}} = \delta^{Jj}\mathcal{D}^{\mathrm{T}}\left(h_{ij}, \dot{h}_{ij}, \ddot{h}_{ij}, \partial^2 h_{ij},\right), \tag{4.37}$$

which is symmetric by nature of the tensor mode h_{ij} and the rest of the components vanish and once again the scalar field equation is trivial for the tensorial sector (see Appendix A).

4.3.2 | Gauge Invariance

The gauge transformation of the perturbed tetrad and scalar field under the linear coordinate transformation $\tilde{x}^\mu \to x^\mu + \xi^\mu$ [271, 272, 273] is described as the difference between two manifolds such that

$$\delta\tilde{\Phi} \to \delta\Phi + \mathcal{L}_\xi \Phi \,, \tag{4.38}$$

where $\Phi = \{\phi, e^A{}_\mu\}$, $\delta\Phi = \{\delta\phi, \delta e^A{}_\mu\}$, $\mathcal{L}$ is the Lie derivative along the vector change ξ^μ [9], which is further split into

$$\xi^\mu = \left[\xi^0, \frac{1}{a}(\xi^i + \delta^{ij}\partial_j \xi)\right] \tag{4.39}$$

where ξ^0 is the temporal component, ξ is the scalar spatial component, and ξ^i is the vectorial spatial component with the divergenceless condition $\partial_i \xi^i = 0$ [173]. The following identities are applied to transform the tetrad and the scalar field:

$$\tilde{\delta e}^A{}_\mu = \delta e^A{}_\mu + \xi^\nu \, \partial_\nu e^A{}_\mu + \partial_\mu \xi^\nu \, e^A{}_\nu \,, \tag{4.40}$$

$$\tilde{\delta\phi} = \delta\phi + \xi^\nu \partial_\nu \phi \,. \tag{4.41}$$

Evaluating all temporal, spatial, and temporal-spatial components, the transformation of each perturbation mode can be obtained:

$$\tilde{\sigma} = \sigma \,, \qquad \epsilon_{ijk}\tilde{\sigma}^k = \epsilon_{ijk}\sigma^k + \frac{1}{2a}\partial_i \xi_j \,, \tag{4.42a}$$

$$\tilde{\delta\phi} = \delta\phi + \dot{\phi}\xi^0 \,, \tag{4.42b}$$

$$\tilde{\varphi} = \varphi + \dot{\xi}^0 \,, \tag{4.42c}$$

$$\tilde{\psi} = \psi + H\xi^0 \,, \tag{4.42d}$$

$$\tilde{\beta} = \beta + \frac{1}{a}\xi^0 \,, \qquad \tilde{\beta}_i = \beta_i \,, \tag{4.42e}$$

$$\tilde{b} = b - H\xi + \dot{\xi} \,, \qquad \tilde{b}_i = b_i - H\xi_i + \dot{\xi}_i \,, \tag{4.42f}$$

$$\tilde{h} = h + \frac{1}{a}\xi \,, \qquad \tilde{h}_i = h_i + \frac{1}{2a}\xi_i \,, \qquad \tilde{h}_{ij} = h_{ij} \,, \tag{4.42g}$$

where σ, β_i and h_{ij} are gauge-invariant. The rest of the perturbations can be combined into the following groups:

$$\{\delta\phi, \varphi, \psi, \beta\} \,, \qquad \{b, h\} \,, \qquad \{\sigma_i, b_i, h_i\} \,. \tag{4.43}$$

It should be noted, that while the pseudoscalar can be treated as a separate mode from the scalar modes, calculations dealing with the vector fields always need to include the pseudovector as it

has a relationship with other vector modes unless the mode is ruled out through gauge fixing. The gauge fixing would require one from each group to be set to vanish. Moreover, the common gauges chosen for metric-based theories can be also replicated with the following restrictions in tetrad-based theories for the scalar sector:

$$\text{Flat Gauge :} \qquad \psi = 0\,, \qquad h = 0\,, \tag{4.44a}$$

$$\text{Unitary Gauge :} \qquad \delta\phi = 0\,, \qquad h = 0\,, \tag{4.44b}$$

$$\text{Newtonian/Longitudinal Gauge :} \qquad b = \beta\,, \qquad h = 0\,, \tag{4.44c}$$

$$\text{Synchronous Gauge :} \qquad \varphi = 0\,, \qquad b = \beta\,. \tag{4.44d}$$

In Ref. [274], the longitudinal gauge is implemented by adding the condition $\beta = 0$ to mimic an Arnowitt-Deser-Misner (ADM) decomposition with a gauge fix. In the context of SVT decomposition, such a condition could lead to an over-fixing of the gauge. As shown in Ref. [275], it is important not to eliminate the off-diagonals of the tetrad since technically β is present in the field equations. In metric-based theories, the vector sector is not evaluated as it is typically trivial. Another approach to gauge fixing is the consideration of combining the results given in Eq. (4.42) from which new gauge-invariant quantities are created:

$$\mathcal{X}_1 = \delta\phi - a\dot{\phi}\beta\,, \tag{4.45a}$$

$$\mathcal{X}_2 = \varphi - a(H\beta + \dot{\beta})\,, \tag{4.45b}$$

$$\mathcal{X}_3 = \psi - aH\beta\,, \tag{4.45c}$$

$$\mathcal{X}_4 = b - a\dot{h}\,, \tag{4.45d}$$

$$\mathcal{Y}_i = b_i - 2a\dot{h}_i\,, \tag{4.45e}$$

$$\mathcal{Z}_{ij} = \epsilon_{ijk}\sigma^k + \partial_j h_i\,. \tag{4.45f}$$

The scalar gauge-invariant quantities $\{\mathcal{X}_1, \mathcal{X}_2, \mathcal{X}_3, \mathcal{X}_4\}$ are not unique and other combinations exist. This choice is opted for simply because it facilitates the analysis when transformation equations in terms of gauge-invariant quantities. Changing equations to be in terms of gauge-invariant quantities and β allows an easier way to identify terms that rely on β to ensure that these contributions vanish. Therefore, the field equations can be cast in terms of these gauge-invariant quantities. The scalar sector is summarised by the following:

$$\delta W^{\rm S}_{00} = \mathcal{A}^{\rm S}\left(\mathcal{X}_1, \dot{\mathcal{X}}_1, \partial^2\mathcal{X}_1, \mathcal{X}_2, \partial^2\mathcal{X}_2, \mathcal{X}_3, \partial^2\mathcal{X}_3, \partial^2\mathcal{X}_4\right)\,, \tag{4.46a}$$

$$\delta W^{\rm S}_{0i} = \mathcal{B}^{\rm S}\left(\partial^i\mathcal{X}_1, \partial^i\dot{\mathcal{X}}_1, \partial^i\mathcal{X}_2, \partial^i\dot{\mathcal{X}}_2, \partial^i\mathcal{X}_3, \partial^i\dot{\mathcal{X}}_3, \partial^i\mathcal{X}_4\right)\,, \tag{4.46b}$$

$$\delta W^{\rm S}_{i0} = \mathcal{C}^{\rm S}\left(\partial_i\mathcal{X}_1, \partial_i\dot{\mathcal{X}}_i, \partial_i\mathcal{X}_2, \partial_i\dot{\mathcal{X}}_3, \partial_i\partial^2\mathcal{X}_4\right)\,, \tag{4.46c}$$

$$\delta W^{\rm S}_{ij} = \mathcal{D}^{\rm S}\left(\partial_i\partial_j\mathcal{X}_1, \partial_i\partial_j\mathcal{X}_2, \partial_i\partial_j\mathcal{X}_3, \partial_i\partial_j\mathcal{X}_4, \partial_i\partial_j\dot{\mathcal{X}}_4\right)\,, \tag{4.46d}$$

$$\delta W_i{}^{i\,\mathrm{S}} = \mathcal{E}^{\mathrm{S}}\left(\mathcal{X}_1, \dot{\mathcal{X}}_1, \ddot{\mathcal{X}}_1, \partial^2\mathcal{X}_1, \mathcal{X}_2, \dot{\mathcal{X}}_2, \partial^2\mathcal{X}_2, \mathcal{X}_3, \dot{\mathcal{X}}_3, \ddot{\mathcal{X}}_3, \partial^2\mathcal{X}_3, \partial^2\mathcal{X}_4, \partial^2\dot{\mathcal{X}}_4\right), \tag{4.46e}$$

$$W_\phi = \mathcal{F}^{\mathrm{S}}\left(\mathcal{X}_1, \dot{\mathcal{X}}_1, \ddot{\mathcal{X}}_1, \partial^2\mathcal{X}_1, \mathcal{X}_2, \dot{\mathcal{X}}_2, \partial^2\mathcal{X}_2, \mathcal{X}_3, \dot{\mathcal{X}}_3, \ddot{\mathcal{X}}_3, \partial^2\mathcal{X}_3, \partial^2\mathcal{X}_4, \partial^2\dot{\mathcal{X}}_4\right), \tag{4.46f}$$

$$W_{(0i)} = \mathcal{G}^{\mathrm{S}}\left(\partial_i\mathcal{X}_1, \partial_i\dot{\mathcal{X}}_1, \partial_i\mathcal{X}_2, \partial_i\dot{\mathcal{X}}_2, \partial_i\mathcal{X}_3, \partial_i\dot{\mathcal{X}}_3, \partial_i\mathcal{X}_4, \partial_i\partial^2\mathcal{X}_4\right), \tag{4.46g}$$

$$W_{(ij)} = \mathcal{H}^{\mathrm{S}}\left(\partial_i\partial_j\mathcal{X}_1, \partial_i\partial_j\mathcal{X}_2, \partial_i\partial_j\mathcal{X}_3, \partial_i\partial_j\mathcal{X}_4, \partial_i\partial_j\dot{\mathcal{X}}_4\right), \tag{4.46h}$$

$$W_{[0i]} = \mathcal{I}^{\mathrm{S}}\left(\partial_i\mathcal{X}_1, \partial_i\dot{\mathcal{X}}_1, \partial_i\mathcal{X}_2, \partial_i\dot{\mathcal{X}}_2, \partial_i\mathcal{X}_3, \partial_i\dot{\mathcal{X}}_3, \partial_i\partial^2\mathcal{X}_4\right), \tag{4.46i}$$

$$W_{[ij]} = \mathcal{J}^{\mathrm{S}}\left(\epsilon_{ijk}\partial^k\sigma, \epsilon_{ijk}\partial^k\dot{\sigma}, \epsilon_{ijk}\partial^k\ddot{\sigma}, \epsilon_{ijk}\partial^k\partial^2\sigma\right), \tag{4.46j}$$

and the vector sector transforms to

$$\delta W^{\mathrm{V}}_{0i} = \mathcal{B}^{\mathrm{V}}\left(\dot{\beta}_i, \ddot{\beta}_i, \partial^2\beta_i, \partial^2\mathcal{Y}_i, \partial^j\mathcal{Z}_{ij}, \partial^j\dot{\mathcal{Z}}_{ij}\right), \tag{4.47a}$$

$$\delta W^{\mathrm{V}}_{i0} = \mathcal{C}^{\mathrm{V}}\left(\partial^2\beta_i, \partial^2\mathcal{Y}_i, \partial^j\dot{\mathcal{Z}}_{ij}\right), \tag{4.47b}$$

$$\delta W^{\mathrm{V}}_{ij} = \mathcal{D}^{\mathrm{V}}\left(\partial_i\beta_j, \partial_i\dot{\beta}_j, \partial_i\mathcal{Y}_j, \partial_i\dot{\mathcal{Y}}_j, \partial^2\mathcal{Z}_{ij}, \dot{\mathcal{Z}}_{ij}, \ddot{\mathcal{Z}}_{ij}\right), \tag{4.47c}$$

$$\delta W^{\mathrm{V}}_{(0i)} = \mathcal{G}^{\mathrm{V}}\left(\dot{\beta}_i, \ddot{\beta}_i, \partial^2\beta_i, \partial^2\mathcal{Y}_i, \partial^j\mathcal{Z}_{ij}, \partial^j\dot{\mathcal{Z}}_{ij}\right), \tag{4.47d}$$

$$\delta W^{\mathrm{V}}_{[0i]} = \mathcal{H}^{\mathrm{V}}\left(\dot{\beta}_i, \ddot{\beta}_i, \partial^2\beta_i, \partial^2\mathcal{Y}_i, \partial^j\mathcal{Z}_{ij}, \partial^j\dot{\mathcal{Z}}_{ij}\right), \tag{4.47e}$$

$$\delta W^{\mathrm{V}}_{(ij)} = \mathcal{I}^{\mathrm{V}}\left(\partial_{(i}\beta_{j)}, \partial_{(i}\dot{\beta}_{j)}, \partial_{(i}\mathcal{Y}_{j)}, \partial_{(i}\dot{\mathcal{Y}}_{j)}, \partial_{(i}\partial^k\mathcal{Z}_{jk)}\right), \tag{4.47f}$$

$$\delta W^{\mathrm{V}}_{[ij]} = \mathcal{J}^{\mathrm{V}}\left(\partial_{[i}\beta_{j]}, \partial_{[i}\dot{\beta}_{j]}, \partial_{[i}\mathcal{Y}_{j]}, \partial_{[i}\dot{\mathcal{Y}}_{j]}, \partial_{[i}\partial^k h\mathcal{Z}_{jk]}\right), \tag{4.47g}$$

and the field equation of the tensor modes presented in Eq. (4.37) is already gauge-invariant.

4.4 | Summary

Cosmological perturbations play a crucial role in the study of cosmology. Small perturbations at the early stages of the Universe can evolve and interact with matter to result in the formation of large-scale structures observed nowadays. Perturbations of the tetrad in Eq. (4.2) and the scalar field in Eq. (4.3) provide the foundation to perturb the dependencies in the BDLS action when the Weitzenböck gauge is applied. These results have been tabulated in Tables 4.1-4.3 to summarise perturbations up to second order.

The gravitational modes perturbations governing the tetrad cannot be perturbed within the background equations in Eqs (3.19-3.23), hence it is more convenient to construct the equations of motion by taking variations of the action with respect to the tetrad and scalar field to yield Eq. (4.22) and Eq. (4.24), respectively. The SVT decomposition provides a system of linearised field equations for the scalar, vector, and tensor sectors, separately. These results would apply for all subclasses of BDLS, providing an avenue to apply a limit and obtain the results quickly

starting from Eqs (4.29, 4.35, 4.37). Moreover, the equations can be cast in terms of the gauge-invariant quantities. Applying a gauge transformation of each perturbation mode as done in Eq. (4.42) confirms once again that the SVT decomposition allows for the sector to decouple. The gauge-invariant quantities can be constructed as a linear combination of non-gauge-invariant ones.

The linearised field equations for different sectors of SVT decomposition are used to study the propagating DoFs and polarisation of GW in Chapter 5. By having such a generalised class of MTG, subclasses calculations are facilitated. Chapter 6 explores the growth structures through the effects of the scalar gravitational modes on CDM. The BDLS action can also be extended further up to second order, corresponding to the linearised field equations, to study the ghost and Laplacian instabilities to realise the model restrictions which do not give physically viable cosmologies as done in Chapter 7.

The details of the functions of the linearised field equations have not been included here due to the complicated nature of the expressions. Appendix A provides a link that summarises the results obtained through `Mathematica`. In comparison with the results in Ref. [112] for standard Horndeski gravity, an increasing number of terms are introduced by BDLS. The teleparallel sector can provide a richer structure of viable cosmological models able to revive discarded Horndeski cosmologies through an additional contribution and study theories beyond GR and beyond the curvature-based formalism.

Y	$\bar{\delta}Y = \frac{\partial}{\partial(e^C{}_\gamma)}Y$	$\tilde{\delta}Y = \frac{\partial}{\partial(\partial_\rho e^C{}_\gamma)}Y$	$\hat{\delta}Y = \frac{\partial}{\partial(\partial_\sigma\partial_\rho e^C{}_\gamma)}Y$
$e^A{}_\mu$	$\delta^A_C\delta^\nu_\mu$	0	0
$e^A{}_{\mu,\nu}$	0	$\delta^A_C\delta^\gamma_\mu\delta^\rho_\nu$	0
$e^A{}_{\mu,\nu\lambda}$	0	0	$\delta^A_C\delta^\gamma_\mu\delta^\rho_\nu\delta^\sigma_\lambda$
$E_A{}^\mu$	$-E_C{}^\mu E_A{}^\gamma$	0	0
$E_A{}^\mu{}_{,\nu}$	$-e^A{}_{\mu,\lambda}\left(\bar{\delta}E_A{}^\mu E_B{}^\mu + \bar{\delta}E_A{}^\mu E_A{}^\nu\right)$	$-E_A{}^\nu E_B{}^\mu\tilde{\delta}(e^A{}_{\mu,\lambda})$	0
e	$eE_C{}^\gamma$	0	0
$g_{\mu\nu}$	$\eta_{AC}(\delta^\gamma_\mu e^A{}_\nu + \delta^\gamma_\nu e^A{}_\mu)$	0	0
$g_{\mu\nu,\lambda}$	$2\eta_{AB}\bar{\delta}e^A{}_\mu e^B{}_{\nu,\lambda}$	$2\eta_{AB}e^A{}_\mu\tilde{\delta}(e^B{}_{\nu,\lambda})$	0
$g_{\mu\nu,\lambda\omega}$	$2\eta_{AB}e^A{}_{\mu,\lambda\omega}\,\bar{\delta}e^B{}_\nu$	$4\eta_{AB}e^A{}_{\mu,\lambda}\tilde{\delta}(e^B{}_{\nu,\omega})$	$2\hat{\delta}e^A{}_{\mu,\lambda\omega}e^B{}_\nu$
$g^{\mu\nu}$	$-(E_C{}^\mu g^{\gamma\nu} + E_C{}^\nu g^{\mu\gamma})$	0	0
$g^{\mu\nu}{}_\lambda$	$2\eta^{AB}\bar{\delta}E_A{}^\mu E_B{}^\nu$	$2\eta^{AB}E_A{}^\mu{}_{,\lambda}\,\tilde{\delta}(E_B{}^\nu{}_{,\lambda})$	0
X	$\phi_{,\mu}\phi^{,\gamma}E_C{}^\mu$	0	0

Table 4.4: Terms from the variation with respect to the tetrad for basic quantities. For each quantity Y, the result for $\bar{\delta}Y$, $\tilde{\delta}Y$ and $\hat{\delta}$ are tabulated. A comma (,) represents the partial derivative to simplify the expressions within the table.

Y	$\bar{\delta}Y = \frac{\partial}{\partial(e^C{}_\gamma)}Y$	$\tilde{\delta}Y = \frac{\partial}{\partial(\partial_\rho e^C{}_\gamma)}Y$	$\hat{\delta}Y = \frac{\partial}{\partial(\partial_\sigma\partial_\rho e^C{}_\gamma)}Y$
$\mathring{\Gamma}^\lambda_{\mu\nu}$	$\frac{1}{2}\,\bar{\delta}(g^{\lambda\alpha})\big(g_{\mu\alpha,\nu}+g_{\alpha\nu,\mu}-g_{\mu\nu,\alpha}\big)$	$\frac{1}{2}g^{\lambda\alpha}\big(\tilde{\delta}(g_{\mu\alpha,\nu})+\tilde{\delta}(g_{\alpha\nu,\mu})-\tilde{\delta}(g_{\mu\nu,\alpha})\big)$	0
$\mathring{\Gamma}^\lambda_{\mu\nu,\omega}$	$\frac{1}{2}\big[\bar{\delta}(g^{\lambda\alpha}{}_{,\omega})\big(g_{\mu\alpha,\nu}+g_{\alpha\nu,\mu}-g_{\mu\nu,\alpha}\big)+g^{\lambda\alpha}{}_{,\omega}\big(\bar{\delta}(g_{\mu\alpha,\nu})+\bar{\delta}(g_{\alpha\nu,\mu})-\bar{\delta}(g_{\mu\nu,\alpha})\big)+\bar{\delta}(g^{\lambda\alpha})\big(g_{\mu\alpha,\nu\omega}+g_{\alpha\nu,\mu\omega}-g_{\mu\nu,\alpha\omega}\big)+g^{\lambda\alpha}\big(\bar{\delta}(g_{\mu\alpha,\nu\omega})+\bar{\delta}(g_{\alpha\nu,\mu\omega})-\bar{\delta}(g_{\mu\nu,\alpha\omega})\big)\big]$	$\frac{1}{2}\big[g^{\lambda\alpha}{}_{,\omega}\big(g_{\mu\alpha,\nu}+g_{\alpha\nu,\mu}-g_{\mu\nu,\alpha}\big)+g^{\lambda\alpha}\big(g_{\mu\alpha,\nu\omega}+g_{\alpha\nu,\mu\omega}-g_{\mu\nu,\alpha\omega}\big)\big]$	$\frac{1}{2}\big[g^{\lambda\alpha}{}_{,\omega}\big(g_{\mu\alpha,\nu}+g_{\alpha\nu,\mu}-g_{\mu\nu,\alpha}\big)+g^{\lambda\alpha}\big(g_{\mu\alpha,\nu\omega}+g_{\alpha\nu,\mu\omega}-g_{\mu\nu,\alpha\omega}\big)\big]$
$\mathring{\nabla}_\mu\mathring{\nabla}_\nu\phi$	$-\bar{\delta}(\mathring{\Gamma}^\lambda_{\mu\nu})\phi_{,\lambda}$	$-\tilde{\delta}(\mathring{\Gamma}^\lambda_{\mu\nu})\,\phi_{,\lambda}$	0
$\mathring{\nabla}_\mu\mathring{\nabla}^\nu\phi$	$\bar{\delta}(g^{\nu\lambda})\mathring{\nabla}_\mu\mathring{\nabla}_\lambda\phi+g^{\nu\lambda}\bar{\delta}(\mathring{\nabla}_\mu\mathring{\nabla}_\lambda\phi)$	$g^{\nu\lambda}\tilde{\delta}(\mathring{\nabla}_\mu\mathring{\nabla}_\lambda\phi)$	0
$\mathring{\nabla}^\mu\mathring{\nabla}^\nu\phi$	$\bar{\delta}(g^{\mu\lambda})\,\mathring{\nabla}_\lambda\mathring{\nabla}^\nu\phi+g^{\mu\lambda}\bar{\delta}(\mathring{\nabla}_\lambda\mathring{\nabla}^\nu\phi)$	$g^{\mu\lambda}\tilde{\delta}(\mathring{\nabla}_\lambda\mathring{\nabla}^\nu\phi)$	0
$\mathring{\Box}\phi$	$\bar{\delta}(\mathring{\nabla}_\mu\mathring{\nabla}^\mu\phi)$	$\tilde{\delta}(\mathring{\nabla}_\mu\mathring{\nabla}^\mu\phi)$	0
$\mathring{R}^\lambda{}_{\mu\omega\nu}$	$\bar{\delta}(\mathring{\Gamma}^\lambda_{\mu\nu,\omega})-\bar{\delta}(\mathring{\Gamma}^\lambda_{\mu\omega,\nu})+\bar{\delta}(\mathring{\Gamma}^\lambda_{\sigma\omega})\,\mathring{\Gamma}^\sigma_{\mu\nu}+\mathring{\Gamma}^\lambda_{\sigma\omega}\,\bar{\delta}(\mathring{\Gamma}^\sigma_{\mu\nu})-\bar{\delta}(\mathring{\Gamma}^\lambda_{\sigma\nu})\,\mathring{\Gamma}^\sigma_{\mu\omega}-\mathring{\Gamma}^\lambda_{\sigma\nu}\,\bar{\delta}(\mathring{\Gamma}^\sigma_{\mu\omega})$	$\tilde{\delta}(\mathring{\Gamma}^\lambda_{\mu\nu,\omega})-\tilde{\delta}(\mathring{\Gamma}^\lambda_{\mu\omega,\nu})+\tilde{\delta}(\mathring{\Gamma}^\lambda_{\sigma\omega})\,\mathring{\Gamma}^\sigma_{\mu\nu}+\mathring{\Gamma}^\lambda_{\sigma\omega}\,\tilde{\delta}(\mathring{\Gamma}^\sigma_{\mu\nu})-\tilde{\delta}(\mathring{\Gamma}^\lambda_{\sigma\nu})\,\mathring{\Gamma}^\sigma_{\mu\omega}-\mathring{\Gamma}^\lambda_{\sigma\nu}\,\tilde{\delta}(\mathring{\Gamma}^\sigma_{\mu\omega})$	$\hat{\delta}(\mathring{\Gamma}^\lambda_{\mu\nu,\omega})-\hat{\delta}(\mathring{\Gamma}^\lambda_{\mu\omega,\nu})$
$\mathring{R}_{\mu\nu}$	$\bar{\delta}(\mathring{R}^\lambda{}_{\mu\lambda\nu})$	$\tilde{\delta}(\mathring{R}^\lambda{}_{\mu\lambda\nu})$	$\hat{\delta}(\mathring{R}^\lambda{}_{\mu\lambda\nu})$
$\mathring{R}$	$\bar{\delta}(g^{\mu\nu})\mathring{R}_{\mu\nu}+g^{\mu\nu}\bar{\delta}(\mathring{R}_{\mu\nu})$	$g^{\mu\nu}\tilde{\delta}(\mathring{R}_{\mu\nu})$	$g^{\mu\nu}\hat{\delta}(\mathring{R}_{\mu\nu})$
$\mathring{G}_{\mu\nu}$	$\bar{\delta}(\mathring{R}_{\mu\nu})-\frac{1}{2}\big(\bar{\delta}(g_{\mu\nu})\mathring{R}+g_{\mu\nu}\bar{\delta}(\mathring{R})\big)$	$\tilde{\delta}(\mathring{R}_{\mu\nu})-\frac{1}{2}g_{\mu\nu}\tilde{\delta}(\mathring{R})$	$\hat{\delta}(\mathring{R}_{\mu\nu})-\frac{1}{2}g_{\mu\nu}\hat{\delta}(\mathring{R})$

Table 4.5: Terms from the variation with respect to the tetrad for quantities present in standard Horndeski gravity. For each quantity Y, the result for $\bar{\delta}Y$, $\tilde{\delta}Y$ and $\hat{\delta}$ are tabulated. A comma (,) represents the partial derivative to simplify the expressions within the table.

Y	$\bar{\delta}Y = \frac{\partial}{\partial(e^{C}{}_{\gamma})}Y$	$\tilde{\delta}Y = \frac{\partial}{\partial(\partial_\rho e^{C}{}_{\gamma})}Y$
$T^{\lambda}{}_{\mu\nu}$	$\bar{\delta}(E_A{}^{\lambda})\left(e^{A}{}_{\mu,\nu} - e^{A}{}_{\nu,\mu}\right)$	$E_A{}^{\lambda}\left(\tilde{\delta}(e^{A}{}_{\mu,\nu}) - \tilde{\delta}(e^{A}{}_{\nu,\mu})\right)$
$T^{\lambda\mu\nu}$	$\bar{\delta}(g^{\mu\alpha})g^{\nu\beta}T^{\lambda}{}_{\alpha\beta} + g^{\mu\alpha}\bar{\delta}(g^{\nu\beta})T^{\lambda}{}_{\alpha\beta} + g^{\mu\alpha}g^{\nu\beta}\bar{\delta}(T^{\lambda}{}_{\alpha\beta})$	$g^{\mu\alpha}g^{\nu\beta}\tilde{\delta}(T^{\lambda}{}_{\alpha\beta})$
$T_{\lambda\mu\nu}$	$\bar{\delta}(g_{\lambda\alpha})T^{\alpha}{}_{\mu\nu} + g_{\lambda\alpha}\bar{\delta}(T^{\alpha}{}_{\mu\nu})$	$g_{\lambda\alpha}\tilde{\delta}(T^{\alpha}{}_{\mu\nu})$
a_μ	$\frac{1}{6}\epsilon_{\mu\lambda\alpha\beta}\bar{\delta}(T^{\lambda\alpha\beta})$	$\frac{1}{6}\epsilon_{\mu\lambda\alpha\beta}\tilde{\delta}(T^{\lambda\alpha\beta})$
a^μ	$\bar{\delta}(g^{\mu\alpha})a_\alpha + g^{\mu\alpha}\bar{\delta}(a_\alpha)$	$g^{\mu\alpha}\tilde{\delta}(a_\alpha)$
$T_{\rm ax}$	$\bar{\delta}(a_\mu)\, a^\mu + a_\mu\, \bar{\delta}(a^\mu)$	$\tilde{\delta}(a_\mu)\, a^\mu + a_\mu\, \tilde{\delta}(a^\mu)$
v_μ	$\bar{\delta}(T^{\lambda\lambda}{}_{\mu})$	$\tilde{\delta}(T^{\lambda\lambda}{}_{\mu})$
v^μ	$\bar{\delta}(g^{\mu\alpha})v_\alpha + g^{\mu\alpha}\bar{\delta}(v_\alpha)$	$g^{\mu\alpha}\tilde{\delta}(v_\alpha)$
$T_{\rm vec}$	$\bar{\delta}(v_\mu)\, v^\mu + v_\mu\, \bar{\delta}(v^\mu)$	$\tilde{\delta}(v_\mu)\, v^\mu + v_\mu\, \tilde{\delta}(v^\mu)$
$t_{\lambda\mu\nu}$	$\frac{1}{2}\big(\bar{\delta}(T_{\lambda\mu\nu}) + \bar{\delta}(T_{\mu\lambda\nu})\big) + \frac{1}{6}\big(\bar{\delta}(g_{\nu\lambda})\, v_\mu + g_{\nu\lambda}\, \bar{\delta}(v_\mu) + \bar{\delta}(g_{\nu\mu})\, v_\lambda + g_{\nu\mu}\, \bar{\delta}(v_\lambda)\big) - \frac{1}{3}\big(\bar{\delta}(g_{\lambda\mu})\, v_\nu + g_{\lambda\mu}\, \bar{\delta}(v_\nu)\big)$	$\frac{1}{2}\big(\tilde{\delta}(T_{\lambda\mu\nu}) + \tilde{\delta}(T_{\mu\lambda\nu})\big) + \frac{1}{6}\big(g_{\nu\lambda}\, \tilde{\delta}(v_\mu) + g_{\nu\mu}\, \tilde{\delta}(v_\lambda)\big) - \frac{1}{3}g_{\lambda\mu}\, \tilde{\delta}(v_\nu)$
$t^{\lambda\mu\nu}$	$\bar{\delta}(g^{\lambda\omega})g^{\mu\alpha}g^{\nu\beta}t_{\omega\alpha\beta} + g^{\lambda\omega}\bar{\delta}(g^{\mu\alpha})g^{\nu\beta}t_{\omega\alpha\beta} + g^{\lambda\omega}g^{\mu\alpha}\bar{\delta}(g^{\nu\beta})t_{\omega\alpha\beta} + g^{\lambda\omega}g^{\mu\alpha}g^{\nu\beta}\bar{\delta}(t_{\omega\alpha\beta})$	$g^{\lambda\omega}g^{\mu\alpha}g^{\nu\beta}\tilde{\delta}(t_{\omega\alpha\beta})$
$T_{\rm ten}$	$\bar{\delta}(t_{\lambda\mu\nu})\, t^{\lambda\mu\nu} + t_{\lambda\mu\nu}\, \bar{\delta}(t^{\lambda\mu\nu})$	$\tilde{\delta}(t_{\lambda\mu\nu})\, t^{\lambda\mu\nu} + t_{\lambda\mu\nu}\, \tilde{\delta}(t^{\lambda\mu\nu})$
T	$\frac{3}{2}\bar{\delta}(T_{\rm ax}) + \frac{2}{3}\bar{\delta}(T_{\rm ten}) - \frac{2}{3}\bar{\delta}(T_{\rm vec})$	$\frac{3}{2}\tilde{\delta}(T_{\rm ax}) + \frac{2}{3}\tilde{\delta}(T_{\rm ten}) - \frac{2}{3}\tilde{\delta}(T_{\rm vec})$

Table 4.6: Terms from the variation with respect to the tetrad for quantities present in the teleparallel portion of teleparallel Horndeski gravity. For each quantity Y, the result for $\bar{\delta}Y$, $\tilde{\delta}Y$ and $\hat{\delta}$ are tabulated. A comma (,) represents the partial derivative to simplify the expressions within the table.

Y	$\bar{\delta}Y = \frac{\partial}{\partial(e^C{}_\gamma)}Y$	$\tilde{\delta}Y = \frac{\partial}{\partial(\partial_\rho e^C{}_\gamma)}Y$
I_2	$\bar{\delta}(v^\lambda)\,\phi_{,\lambda}$	$\tilde{\delta}(v^\lambda)\,\phi_{,\lambda}$
J_1	$\big(\bar{\delta}(a^\mu)\,a^\nu + a^\mu\,\bar{\delta}(a^\nu)\big)\phi_{,\mu}\,\phi_{,\nu}$	$\big(\tilde{\delta}(a^\mu)\,a^\nu + a^\mu\,\tilde{\delta}(a^\nu)\big)\phi_{,\mu}\,\phi_{,\nu}$
J_3	$\big(\bar{\delta}(v_\lambda)\,t^{\lambda\mu\nu} + v_\lambda\,\bar{\delta}(t^{\lambda\mu\nu})\big)\phi_{,\mu}\,\phi_{,\nu}$	$\big(\tilde{\delta}(v_\lambda)\,t^{\lambda\mu\nu} + v_\lambda\,\tilde{\delta}(t^{\lambda\mu\nu})\big)\phi_{,\mu}\,\phi_{,\nu}$
J_5	$\big(\bar{\delta}(t^{\lambda\mu\nu})\,t_{\lambda\alpha\nu}\,\phi^{,\alpha} + t^{\lambda\mu\nu}\,\bar{\delta}(t_{\lambda\alpha\nu})\,\phi^{,\alpha} + t^{\lambda\mu\nu}\,t_{\lambda\alpha\nu}\,\bar{\delta}(\phi^{,\alpha})\big)\phi^{,\mu}$	$\big(\tilde{\delta}(t^{\lambda\mu\nu})\,t_{\lambda\alpha\nu}\,\phi^{,\alpha} + t^{\lambda\mu\nu}\,\tilde{\delta}(t_{\lambda\alpha\nu})\,\phi^{,\alpha}\big)\phi_{,\mu}$
J_6	$\big(\bar{\delta}(t^{\lambda\mu\nu})\,t_{\lambda\alpha\beta}\,\phi^{,\alpha}\,\phi^{,\beta} + t^{\lambda\mu\nu}\,\bar{\delta}(t_{\lambda\alpha\beta})\,\phi^{,\alpha}\,\phi^{,\beta} + t^{\lambda\mu\nu}\,t_{\lambda\alpha\beta}\,\bar{\delta}(\phi^{,\alpha})\,\phi^{,\beta} + t^{\lambda\mu\nu}\,t_{\lambda\alpha\beta}\,\phi^{,\alpha}\,\bar{\delta}(\phi^{,\beta})\big)\,\phi_{,\mu}\,\phi_{,\nu}$	$\big(\tilde{\delta}(t^{\lambda\mu\nu})\,t_{\lambda\alpha\beta}\,\phi^{,\alpha}\,\phi^{,\beta} + t^{\lambda\mu\nu}\,\tilde{\delta}(t_{\lambda\alpha\beta})\,\phi^{,\alpha}\,\phi^{,\beta}\big)\,\phi_{,\mu}\,\phi_{,\nu}$
J_8	$\big(\bar{\delta}(t^{\lambda\mu\nu})\,t_{\lambda\mu\alpha}\,\phi^{,\alpha} + t^{\lambda\mu\nu}\,\bar{\delta}(t_{\lambda\mu\alpha})\,\phi^{,\alpha} + t^{\lambda\mu\nu}\,t_{\lambda\mu\alpha}\,\bar{\delta}(\phi^{,\alpha})\big)\,\phi_{,\nu}$	$\big(\tilde{\delta}(t^{\lambda\mu\nu})\,t_{\lambda\mu\alpha}\,\phi^{,\alpha} + t^{\lambda\mu\nu}\,\tilde{\delta}(t_{\lambda\mu\alpha})\,\phi^{,\alpha}\big)\,\phi_{,\nu}$
J_{10}	$\epsilon_{\mu\nu\omega\lambda}\,\phi_{,\sigma}\,\big(\bar{\delta}(a^\nu)\,t^{\sigma\omega\lambda}\,\phi^{,\mu} + a^\nu\,\bar{\delta}(t^{\sigma\omega\lambda})\,\phi^{,\mu} + a^\nu\,t^{\sigma\omega\lambda}\,\bar{\delta}(\phi^{,\mu})\big)$	$\epsilon_{\mu\nu\omega\lambda}\,\phi_{,\sigma}\,\big(\tilde{\delta}(a^\nu)\,t^{\sigma\omega\lambda}\,\phi^{,\mu} + a^\nu\,\tilde{\delta}(t^{\sigma\omega\lambda})\,\phi^{,\mu}\big)\big)$

Table 4.7: Terms from the variation with respect to the tetrad for quantities present in the teleparallel portion of teleparallel Horndeski gravity. For each quantity Y, the result for $\bar{\delta}Y$, $\tilde{\delta}Y$ and $\hat{\delta}$ are tabulated. A comma (,) represents the partial derivative to simplify the expressions within the table.

Y	$\bar{\delta}Y = \frac{\partial}{\partial\phi}Y$	$\tilde{\delta}Y = \frac{\partial}{\partial(\partial_\rho\phi)}Y$	$\hat{\delta}Y = \frac{\partial}{\partial(\partial_\omega\partial_\rho\phi)}Y$
ϕ	1	0	0
$\phi_{,\mu}$	0	δ^ρ_μ	0
$\phi_{,\nu\mu}$	0	0	$\delta^\rho_\mu\delta^\omega_\nu$
X	0	$-\phi^{,\rho}$	0
$\mathring{\nabla}_\mu\mathring{\nabla}_\nu\phi$	0	$-\mathring{\Gamma}^\rho_{\mu\nu}$	$\delta^\rho_\mu\delta^\omega_\nu$
$\mathring{\nabla}_\mu\mathring{\nabla}^\nu\phi$	0	$-g^{\lambda\nu}\mathring{\Gamma}^\rho_{\mu\lambda}$	$g^{\omega\nu}\delta^\rho_\mu$
$\mathring{\nabla}^\mu\mathring{\nabla}^\nu\phi$	0	$-g^{\lambda\nu}g^{\sigma\mu}\mathring{\Gamma}^\rho_{\sigma\lambda}$	$g^{\rho\mu}g^{\omega\nu}$
$\mathring{\Box}\phi$	0	$-g^{\lambda\mu}\mathring{\Gamma}^\rho_{\mu\lambda}$	$g^{\omega\rho}$
I_2	0	v^ρ	0
J_1	0	$2\phi_{,\mu}a^\mu a^\rho$	0
J_3	0	$2\phi_{,\mu}v_\nu t^{\nu(\mu\rho)}$	0
J_5	0	$2\phi^{,\mu}t_{\lambda\mu\nu}t^{\lambda\rho\nu}$	0
J_6	0	$4\phi_{,\sigma}\phi^{,\mu}\phi^{,\nu}t_{\lambda\mu\nu}t^{\lambda(\rho\sigma)}$	0
J_8	0	$2\phi^{,\nu}t_{\lambda\mu\nu}t^{\lambda\mu\rho}$	0
J_{10}	0	$-2\phi_{,\mu}a^\nu\epsilon_{\omega\nu\lambda}{}^{(\rho}t^{\mu)\omega\lambda}$	0

Table 4.8: Terms from the variation of BDLS with respect to the scalar field ϕ. For each quantity Y, the result for $\bar{\delta}Y$, $\tilde{\delta}Y$ and $\hat{\delta}$ are tabulated. A comma (,) represents the partial derivative to simplify the expressions within the table.

5

Propagating Degrees of Freedom and Polarisation Modes of Gravitational Waves

GWs were predicted through the formulation of GR [128], manifesting as gravitational radiation when massive objects warp spacetime [121]. Recent observations of GWs [45, 80, 276, 55] have launched a series of theoretical and observational work for a better understanding of GWs as they provide a new window into the Universe to study theories of gravity, blackholes and neutron star mergers, the early Universe through primordial GWs, and dark energy. Future missions, such as LISA [277, 50] and Light satellite for the studies of B-mode polarization and Inflation from cosmic background Radiation Detection (LiteBIRD) [278], will operate from space, primarily focusing on GWs and primordial GWs.

The linearisation of weak field equations in GR represents a dynamical system for gravitational radiation, behaving as a transverse wave travelling at the speed of light [121, 122]. In 1936, Einstein and Rosen questioned the existence of GWs, concluding that polarised plane GWs would lead to a point of zero volume; a singularity [3]. The assumption that the coordinate system utilised was free of singularities led to the conclusion that there were physical singularities [279, 280]. The misunderstanding between coordinate and physical singularities led to a revisit of the calculations, this time changing to a cylindrical coordinate system for the metric [281], which confirmed that GWs could exist and carry energy [279].

The 1974 discovery of binary pulsar PSR B1913+16 by Taylor and Hulse provided direct evidence of gravitational propagation at the speed of light [46], with the later observation of energy loss as predicted by GR [47]. As the concept observed in the electromagnetic field came to hold also for the gravitational field [209], the existence of GW became a more likely possibility, hence propelling the search for the first GW observation.

Among the many attempts, the interferometric beam detector has become a favourable GW

detector [282]. The inspiration behind the interferometric GW detector is the 1800s Michelson interferometer initially designed to debunk the notion that there exists an aether around Earth [283]. The laser interferometer is equipped with a laser source which is split upon falling on a beam splitter, creating two separate beams travelling independently along perpendicular arms. Mirrors positioned at both ends of the arms allow the laser to reflect and intersect onto a photon detector. Here, phase differences can be recorded from the interference patterns generated [3]. The interferometer provides a system where two geodesics are generated, where one acts as the stationary field while the other represents the tidal forces created due to gravitational radiation [282], such that any change in displacement can be attributed to a GW [3].

LIGO is one such GW interferometer, having two separate interferometers at different locations (Hanford and Livingston Observatories in the United States) to account for local noise arising due to seismic activity, thermal variations, and electromagnetic interference [48]. The setup is placed within a vacuum to minimise light phase fluctuations arising due to air molecules [51]. Additionally, the 4 km arms increase the sensitivity [51] and are not responsive to electromagnetic waves induced by matter, primordial gases, stellar atmospheres, and interstellar media [283]. Following over 10 years of no GW detection, LIGO started to undergo a major upgrade to increase its sensitivity, resulting in A-LIGO [52]. The upgrades affected the majority of the interferometer, from an increase in laser power, larger and heavier test masses suspended by fused silica fibers instead of the previous steel wire, and the use of a seismic isolation system, to name a few. Shortly after its operation started in 2015, A-LIGO along with the Virgo Collaboration in Italy confirmed the first detection of a GW signal, dubbed GW150914, arising from inspiral binary blackhole merger [45]. The detection correlated with the theoretical prediction of GR [45, 122], adding to the number of tests which GR has passed.

The first detection was followed by numerous other binary system mergers but further improvements are still being worked on. A-LIGO is restricted to detect oscillations of frequencies over 10 Hz [48], as ground-based background disturbances create limitations along with the logistical problem of increasing the arms' length would require more land space. Hence, the next step is to move to a space-based GW detector. LISA, planned to launch in the mid-2030s, will be the first space-based interferometer operating at the low-frequency bandwidth of 10^{-4} and 10^{-1} Hz in the Sun's orbit with 20° behind Earth [49]. Apart from being able to generate arm lengths far greater than those achievable on Earth, the setup will be made up of three identical free-flying spacecraft forming an equilateral triangle to act as three pairs of Michelson interferometers. Also, in place of end mirrors, optical transponders will reflect signals [277, 49].

The current detections of GWs being done by A-LIGO [51, 52], Virgo collaboration [53, 54], Kamioka Gravitational Wave Detector (KAGRA)[55] and GEO600 [56, 57] rely on template matching, wherein data collected from the detector is compared with a large framework of theoretical predictions. It is important to have a large number of waveform templates represent-

ing a range of possible binary systems within astrophysically interesting regions containing the parameters of mass, spin, orbital phase, fiducial reference time, and amplitude of massive objects [284, 285]. Generating a template bank requires an underlying gravitational theory, making GR idyllic due to the vast work done, and continues to be explored, in this framework. Hence, while detection infers a correlation with GR where only tensor mode polarisations appear [48], it could be that GR is not the complete answer, especially with the numerous obstacles it faces[1]. The possibility of other polarisation modes is still open as current Earth-based observers, including the near-future operation of Indian Initiative in Gravitational-wave Observations (INDIGO), are restricted to a set orientation, making it more difficult to detect other modes. Additionally, the agreement between GR and detection only occurs at the lower end of the astrophysical energy scale such that any other hidden signals could induce deviations from GR [45]. Therefore, an increase in sensitivity, eliminating Earth-based interferences and tapping into frequency ranges from below 10 Hz, particularly < 1 mHz, will result in additional sources of GWs and deviations from GR might accumulate over long timescales. This makes the next generation of detectors, of the likes of LISA, Einstein Telescope, and Cosmic Explorer, more likely to observe GR deviations. For this reason, it has become increasingly appealing to develop well-posed frameworks that adopt theories beyond GR, supported by a range of well-studied cosmological models, to construct the necessary template bank.

In this chapter, the nature of GW polarisation modes in BDLS gravity is presented. Due to the vastness of the theory, here perturbations about a flat Minkowski background are considered to generate the linearised field equations representing the effects of gravitational radiation. Moreover, the propagating DoFs for the branches of cases stemming from BDLS are determined. The exhaustive cases arising from BDLS, with some corresponding to well-studied classes of gravity, show the rich approach and ease to reproduce the DoFs and polarisation modes of other gravitational theories, while circumventing issues of the GR framework. The work done in this section is based on the published work in Ref. [286]

5.1 | Modification to the System of Equations

Before commencing the analysis of DoFs and polarisation modes of gravitational waves, a presentation of the modification to the field equations is presented in Chapter 4. Here, the work is carried out in the signature $(+,-,-,-)$, implying a switch in sign whenever temporal and spatial derivatives are raised. Additionally, the scalar field is taken to be constant at the background level such that $\phi(t) \to \phi = \phi_0$ where ϕ_0 is a constant, with a Minkowski background

[1] Refer to Sec. 2.1 for further details regarding issues in GR.

$g_{\mu\nu} \to \eta_{\mu\nu}$. Hence, the gauge transformations given in Eq. (4.42) change to

$$\tilde{\sigma} = \sigma\,, \qquad \tilde{\sigma}_i = \sigma_i - \frac{1}{2}\epsilon_{ijk}\partial^j\xi^k\,, \tag{5.1a}$$

$$\tilde{\delta\phi} = \delta\phi\,, \tag{5.1b}$$

$$\tilde{\varphi} = \varphi - \dot{\xi}^0\,, \tag{5.1c}$$

$$\tilde{\psi} = \psi\,, \tag{5.1d}$$

$$\tilde{\beta} = \beta - \xi^0\,, \qquad \tilde{\beta}_i = \beta_i\,, \tag{5.1e}$$

$$\tilde{b} = b - \dot{\xi}\,, \qquad \tilde{b}_i = b_i + \dot{\xi}_i\,, \tag{5.1f}$$

$$\tilde{h} = h - \xi\,, \qquad \tilde{h}_i = h_i + \frac{1}{2}\xi_i\,, \qquad \tilde{h}_{ij} = h_{ij}\,, \tag{5.1g}$$

such that now the gauge invariant quantities increase $\{\sigma, \delta\phi, \psi, \beta_i, h_{ij}\}$ and the gauge invariant quantities presented in Eq. (4.45)[2] reduce to

$$\mathcal{X}_2 = \varphi - \dot{\beta}\,, \tag{5.2a}$$

$$\mathcal{X}_4 = b - \dot{h}\,, \tag{5.2b}$$

$$\mathcal{Y}_i = -b_i + 2\dot{h}_i\,, \tag{5.2c}$$

$$\mathcal{Z}_i = \sigma_i - \epsilon_{ijk}\partial^j h^k\,. \tag{5.2d}$$

Moreover, for simplification, the modification to Fourier space, in particular for the spatial components of the field equations, is adopted from this point forward. The Fourier space decomposition

$$f(x^\mu) \to f(k^\mu)e^{-i\omega t + ik_j x^j}\,, \tag{5.3}$$

yields the following identities:

$$\partial_j \to ik_j\,, \tag{5.4a}$$

$$\partial_j\partial^j = \eta^{jl}\partial_j\partial_l \to -\eta^{jl}k_j k_l\,, \tag{5.4b}$$

$$\Box = \partial_\mu\partial^\mu \to \partial_0^2 - \eta^{jl}k_j k_l =: \partial_0^2 + k^2\,. \tag{5.4c}$$

Following all the modifications listed here, the gauge invariant field equations (4.37,4.46,4.47) can be transformed to investigate the propagating DoFs and polarisation modes of GWs within the BDLS framework. The propagating DoFs in GWs sheds light on the fundamental nature of gravity. GR has two dynamical modes corresponding to the tensor sector: + and × modes. Modified theories of gravity could realise extra DoFs which may alter the speed at which a GW travels. The two propagating DoFs from GR are also the polarisation modes of GW within the

[2]Notation for $\mathcal{Z}_{ij}$ is altered to $\mathcal{Z}_i$ for convenience to simplify the equations.

theory, which reflect the behaviour of how spacetime is distorted. For + and × this corresponds to a contraction and elongation at different axes and the same behaviour at a diagonal between the axes, respectively. But these are not the only polarisation modes possible, theoretically. The following sections will delve into the details of both properties within BDLS, while also investigating interesting branches of the theory.

5.2 | Propagating Degrees of Freedom

The detection of GWs is realised by measuring the differences in arms' length of the GW interferometer as a GW propagates. Current interferometers, such as A-LIGO, Virgo Collaboration, KAGRA, and GEO600, are constrained by Earth-based limitations including a fixed orientation of the arms themselves with respect to the direction of the wave [287]. Thus, while current observations appear to be in line with GR predictions of two polarisation modes in weak gravitational radiation, + and × modes with helicity +2 and −2 respectively [3], other possible polarisation modes have not been completely ruled out.

A schematic derivation to calculate the formalism of GWs in GR is presented. Additionally, its modifications to adapt it to BDLS theory are provided as well. Consider a locally free-falling observer. The test particle at spatial coordinates x^j experiences a relative acceleration towards its spatial origin such that

$$\ddot{x}_i = -\mathring{R}_{0i0j}x^j \,, \tag{5.5}$$

where $\mathring{R}_{0i0j}$ are the electric components of the Riemann tensor which the GW detector detects. The six possible components of $\mathring{R}_{0i0j}$ in Eq. (5.5) are used to describe the propagation of GWs [288].

The linearised field equations presented in Sec 4.3.1 provide an avenue to explore the effects of the weak gravitational field. While the GR limit results in the Einstein field equations with two DoFs which all contribute as polarisation modes of GW, this might not be the case for BDLS. This section explores all the possible propagating that could occur, of which some or all can be detected as polarisation modes. Eqs. (4.37,4.46,4.47) are modified and listed separately, according to mode.

Scalar and Pseudoscalar Modes: The scalar sector is made up of five linearly independent equations, corresponding to each of the five scalar gauge invariant scalars $\{\delta\phi, \psi, \mathcal{X}_2, \mathcal{X}_4, \sigma\}$[3]:

$$\begin{aligned}
\tfrac{1}{k^2}W_{00} &= (G_{\mathrm{Tele},I_2} - 2G_{4,\phi})\delta\phi + 4(G_4 - G_{\mathrm{Tele},T} + G_{\mathrm{Tele},T_{\mathrm{vec}}})\psi + 2G_{\mathrm{Tele},T_{\mathrm{vec}}}\mathcal{X}_2\,, && \text{(5.6a)}\\
-\tfrac{i}{k^2}k^j W_{j0} &= (G_{\mathrm{Tele},I_2} - 2G_{4,\phi})\delta\dot{\phi} + 2\left(2(G_4 - G_{\mathrm{Tele},T}) + 3G_{\mathrm{Tele},T_{\mathrm{vec}}}\right)\dot{\psi}\\
&\quad + 2k^2 G_{\mathrm{Tele},T_{\mathrm{vec}}}\mathcal{X}_4\,, && \text{(5.6b)}\\
\eta_{jl}W^{jl} &= 3(G_{\mathrm{Tele},I_2} - 2G_{4,\phi})\delta\ddot{\phi} + 6\left(2(G_4 - G_{\mathrm{Tele},T}) + 3G_{\mathrm{Tele},T_{\mathrm{vec}}}\right)\ddot{\psi}\\
&\quad + 2k^2\Big[(2(G_4 - G_{\mathrm{Tele},T}) + 3G_{\mathrm{Tele},T_{\mathrm{vec}}})\dot{\mathcal{X}}_4 + (G_{\mathrm{Tele},I_2} - 2G_{4,\phi})\delta\phi\\
&\quad + 2(G_4 - G_{\mathrm{Tele},T} + G_{\mathrm{Tele},T_{\mathrm{vec}}})\mathcal{X}_2 + 2\left(G_4 - G_{\mathrm{Tele},T} + 2G_{\mathrm{Tele},T_{\mathrm{vec}}}\right)\psi\Big]\,, && \text{(5.6c)}\\
k_l\,\epsilon^{ljk}\,W_{jk} &= -\frac{8}{3}i\,G_{\mathrm{Tele},T_{\mathrm{ax}}}k^2(\ddot{\sigma} + k^2\sigma)\,, && \text{(5.6d)}\\
W_\phi &= \left(G_{\mathrm{Tele},\phi\phi} + G_{2,\phi\phi} + (G_{\mathrm{Tele},X} + G_{2,X} - 2G_{3,\phi})k^2\right)\delta\phi + (G_{\mathrm{Tele},X} + G_{2,X}\\
&\quad - 2G_{3,\phi})\delta\ddot{\phi} - (G_{\mathrm{Tele},I_2} - 2G_{4,\phi})\left(k^2(\dot{\mathcal{X}}_4 + \mathcal{X}_2 + 2\psi) + 3\ddot{\psi}\right)\,. && \text{(5.6e)}
\end{aligned}$$

The pseudoscalar is only present provided $G_{\mathrm{Tele},T_{\mathrm{ax}}} = 0$. $\mathcal{X}_2$ is the only mode that is not dynamic in the system. Only the scalar field equation indicates a dependency on G_2 and G_3 functions, while G_5 never appears in the scalar mode equations. It must be emphasised that this only holds for a Minkowski background and a constant background scalar field. A more general system, with cosmological perturbations and a time-dependent scalar field, would result in a more intricate setup.

The system is further simplified through the temporal Fourier transformation

$$\begin{aligned}
\partial_0 &\to -i\omega\,, && \text{(5.7a)}\\
\partial_0\partial^0 = \partial_0^2 &\to -\omega^2\,, && \text{(5.7b)}
\end{aligned}$$

yielding a matrix of linearly independent equations

$$\begin{pmatrix}
M_{\mathrm{S}11} & M_{\mathrm{S}12} & M_{\mathrm{S}13} & 0 & 0\\
M_{\mathrm{S}21} & M_{\mathrm{S}22} & 0 & M_{\mathrm{S}24} & 0\\
M_{\mathrm{S}31} & M_{\mathrm{S}32} & M_{\mathrm{S}33} & M_{\mathrm{S}34} & 0\\
0 & 0 & 0 & 0 & M_{\mathrm{S}45}\\
M_{\mathrm{S}51} & M_{\mathrm{S}52} & M_{\mathrm{S}53} & M_{\mathrm{S}54} & 0
\end{pmatrix}
\begin{pmatrix}
\delta\phi\\ \psi\\ \mathcal{X}_2\\ \sigma\\ \mathcal{X}_4
\end{pmatrix}
=: M_{\mathrm{S}}Y_{\mathrm{S}} = 0\,, \qquad \text{(5.8)}$$

[3]Technically, four equations correspond to four gauge invariant quantities $\{\delta\phi, \psi, \mathcal{X}_2, \mathcal{X}_4\}$ and another equation which corresponds to the gauge-invariant pseudoscalar $\{\sigma\}$.

where

$$
\begin{aligned}
M_{\mathrm{S}11} &= \left(G_{\mathrm{Tele},I_2} - 2G_{4,\phi}\right)k^2\,, & M_{\mathrm{S}13} &= M_{\mathrm{S}12} - \frac{M_{\mathrm{S}22}}{\omega}\,,\\
M_{\mathrm{S}12} &= -4k^2\left(G_4 - G_{\mathrm{Tele},T} + G_{\mathrm{Tele},T_{\mathrm{vec}}}\right)\,, & M_{\mathrm{S}21} &= \omega M_{\mathrm{S}11}\,,\\
M_{\mathrm{S}22} &= -2k^2\omega\left[2\left(G_4 - G_{\mathrm{Tele},T}\right) + 3G_{\mathrm{Tele},T_{\mathrm{vec}}}\right]\,, & M_{\mathrm{S}34} &= iM_{\mathrm{S}22}\,,\\
M_{\mathrm{S}31} &= \left(2 - \frac{3\omega^2}{k^2}\right)M_{\mathrm{S}11}\,, & M_{\mathrm{S}33} &= -M_{\mathrm{S}12}\,,\\
M_{\mathrm{S}32} &= -M_{\mathrm{S}12} + \frac{M_{\mathrm{S}22}}{\omega}\left(2 - \frac{3\omega^2}{k^2}\right)\,, & M_{\mathrm{S}24} &= \frac{ik^2}{\omega}\left(\omega M_{\mathrm{S}12} - M_{\mathrm{S}22}\right)\,,\\
M_{\mathrm{S}45} &= \frac{8}{3}i\,G_{\mathrm{Tele},T_{\mathrm{ax}}}k^2\left(\omega^2 - k^2\right)\,, & M_{\mathrm{S}54} &= i\omega M_{\mathrm{S}11}\,,\\
M_{\mathrm{S}52} &= M_{\mathrm{S}31}\,, & M_{\mathrm{S}53} &= -M_{\mathrm{S}11}\,,\\
M_{\mathrm{S}51} &= G_{\mathrm{Tele},\phi\phi} + G_{2,\phi\phi} - \left(G_{\mathrm{Tele},X} + G_{2,X} - 2G_{3,\phi}\right)\left(\omega^2 - k^2\right)\,.
\end{aligned}
$$

The same procedure is applied to the vectorial and tensorial sectors. The imaginary contributions in the above equation may suggest that the system is complex. In reality, these would counter the imaginary portion of the field equations as presented in Eq. (5.6) to ultimately obtain real coefficients.

Vector Modes: The vector sector can be expressed with a system of three linearly independent field equations, each one corresponding to a gauge-invariant variable from $\{\beta_i, \mathcal{Y}_i, \mathcal{Z}_i\}$:

$$
\begin{aligned}
9W_{0j} &= -18G_{\mathrm{Tele},T_{\mathrm{vec}}}\ddot{\beta}_j - 2\left(9G_{\mathrm{Tele},T_{\mathrm{vec}}} + 2G_{\mathrm{Tele},T_{\mathrm{ax}}}\right)\dot{\mathcal{Z}}_j\\
&\quad + k^2\left[-\left(2G_{\mathrm{Tele},T_{\mathrm{ax}}} - 9\left(G_4 - G_{\mathrm{Tele},T}\right)\right)\mathcal{Y}_j + \left(9\left(G_4 - G_{\mathrm{Tele},T}\right) + 2G_{\mathrm{Tele},T_{\mathrm{ax}}}\right)\beta_j\right]\,, \qquad (5.9)\\
9W_{j0} &= 4G_{\mathrm{Tele},T_{\mathrm{ax}}}\dot{\mathcal{Z}}_j\\
&\quad + k^2\left[-(2G_{\mathrm{Tele},T_{\mathrm{ax}}} - 9(G_4 - G_{\mathrm{Tele},T}))\beta_j + (9(G_4 - G_{\mathrm{Tele},T}) + 2G_{\mathrm{Tele},T_{\mathrm{ax}}})\mathcal{Y}_j\right]\,, \qquad (5.10)\\
9ik^lW_{lj} &= k^2\Big[-\left(9\left(G_4 - G_{\mathrm{Tele},T}\right) + 2\left(9G_{\mathrm{Tele},T_{\mathrm{vec}}} + G_{\mathrm{Tele},T_{\mathrm{ax}}}\right)\right)\dot{\beta}_j\\
&\quad - \left(9\left(G_4 - G_{\mathrm{Tele},T}\right) - 2G_{\mathrm{Tele},T_{\mathrm{ax}}}\right)\dot{\mathcal{Y}}_j - 18G_{\mathrm{Tele},T_{\mathrm{vec}}}\mathcal{Z}_j\Big] + 4G_{\mathrm{Tele},T_{\mathrm{ax}}}\ddot{\mathcal{Z}}_j\,. \qquad (5.11)
\end{aligned}
$$

While all of $\{\beta_i, \mathcal{Y}_i, \mathcal{Z}_i\}$ have a time derivative, only $\{\beta_i, \mathcal{Z}_i\}$ have a second-order time derivative. This indicates that $\mathcal{Y}_i$ is not a dynamical DoF because it is not actively evolving in the action. The temporal Fourier transformation, given by Eq. (5.7), is applied to the linearly independent vectorial field equations:

$$
\begin{pmatrix}
M_{\mathrm{V}11} & M_{\mathrm{V}12} & M_{\mathrm{V}13}\\
M_{\mathrm{V}21} & M_{\mathrm{V}22} & M_{\mathrm{V}23}\\
M_{\mathrm{V}31} & M_{\mathrm{V}32} & M_{\mathrm{V}33}
\end{pmatrix}
\begin{pmatrix}
\beta_j\\
\mathcal{Z}_j\\
\mathcal{Y}_j
\end{pmatrix}
=: M_{\mathrm{V}}Y_{\mathrm{V}} = 0\,, \qquad (5.12)
$$

where matrix $M_{\rm V}$ components are

$$
\begin{aligned}
M_{\rm V11} &= 2\omega^2 G_{\mathrm{Tele},T_{\rm vec}} + \frac{1}{9}k^2\left(9G_4 - G_{\mathrm{Tele},T} + 2G_{\mathrm{Tele},T_{\rm ax}}\right), & M_{\rm V12} &= \frac{i\left(\omega M_{\rm V13} - M_{\rm V31}\right)}{k^2}, \\
M_{V13} &= \frac{1}{9}k^2(9G_4 + G_{\mathrm{Tele},T} - 2G_{\mathrm{Tele},T_{\rm ax}}), & M_{\rm V21} &= M_{\rm V13}, \\
M_{\rm V22} &= \frac{-i\omega\left[-k^2 M_{\rm V11} - \left(\omega^2 - k^2\right) M_{V13} + \omega M_{\rm V31}\right]}{k^2\left(\omega^2 - k^2\right)}, & M_{\rm V23} &= \frac{\left(k^2 M_{\rm V11} - \omega M_{\rm V31}\right)}{\omega^2 - k^2}, \\
M_{\rm V31} &= \frac{1}{9}\omega k^2\left[9G_4 - G_{\mathrm{Tele},T} + 2\left(9G_{\mathrm{Tele},T_{\rm vec}} + G_{\mathrm{Tele},T_{\rm ax}}\right)\right], & M_{\rm V33} &= \omega M_{\rm V13}, \\
M_{\rm V32} &= -\frac{i}{k^2}\left[\left(-k^2 M_{\rm V11} - \omega^2 M_{\rm V13}\right) + \frac{\left(\omega^2 + k^2\right)}{\omega} M_{\rm V31}\right].
\end{aligned}
$$

The matrix components have been expressed in terms of the components $M_{\rm V11}$, $M_{\rm V13}$ and $M_{\rm V31}$ whenever possible. The gauge invariant mode $\mathcal{Z}_i$, where the pseudovector σ_i is present within the definition of $\mathcal{Z}_i$ given by Eq. (5.2a), appears only coupled with coefficients $G_{\mathrm{Tele},T_{\rm ax}}$ and/or $G_{\mathrm{Tele},T_{\rm vec}}$. This aligns with the fact that pseudovectors are absent in metric-based theories like Horndeski gravity, as the symmetry of the metric tensor excludes contributions from the Levi-Civita tensor. Therefore, only within the teleparallel formalism can the pseudovector mode be realised. Moreover, if $G_{\rm Tele} = 0$ is applied to generate the standard Horndeski theory, the system boils down to a single mode by combining $\beta_i + \mathcal{Y}_i$ as a single gauge invariant quantity. This quantity would be coupled with G_4 such that to obtain a solution corresponding to a theory with a $\mathring{R}$ contribution, $G_4 \neq 0$ must be imposed. This would result in a case where $\beta_i + \mathcal{Y}_i = 0$ to solve the field equation; the vector sector becomes trivial.

Tensor Modes: The tensor field results in a single equation corresponding to the only transverse-traceless mode h_{ij}. Eq. (4.37) is expressed for a Minkowski background with signature $(+,-,-,-)$ to obtain

$$
W_{ij} = \left(G_4 - G_{\mathrm{Tele},T}\right)\left(\ddot{h}_{ij} + k^2 h_{ij}\right), \tag{5.13}
$$

which in matrix form is given by

$$
-\left(G_4 - G_{\mathrm{Tele},T}\right)\left(\omega^2 - k^2\right) h_{ij} =: M_{\rm T} Y_{\rm T} = 0, \tag{5.14}
$$

where matrix $M_{\rm T} \coloneqq -\left(G_4 - G_{\mathrm{Tele},T}\right)\left(\omega^2 - k^2\right)$ and $Y_{\rm T} \coloneqq h_{ij}$ is the tensorial gauge invariant variable. Following the success of tensor mode GW detection, it is crucial to ensure that any gravitational theory considered could realise this result. Specifically, this is done by stating

$$
G_4 - G_{\mathrm{Tele},T} \neq 0. \tag{5.15}
$$

Later in the dissertation, it will be shown that this result is given, in particular, by $G_4 - G_{\mathrm{Tele},T} > 0$ to circumvent ghost and Laplacian instabilities. More details about the stability of the theory will be explored in Chapter 7.

The effect of teleparallel gravity can be seen through a characteristic plot for the propagation of tensor modes in comparison to its GR and ΛCDM counterparts since these modes always appear in these models. In particular, in the context of Minkowski background, the propagation of the tensor modes changes for a model which is dependent on T, such as $f(T)$ gravity. Fig. 5.1 illustrates different solutions corresponding to these models. The power law model, which will be explored later in more detail in Sec. 6.4.1, is considered since the model has been well-studied in literature [216, 217, 218, 275, 289]. The initial value of $z = z_i = 10^4$ is taken to explore a GW solution starting well within the radiation-dominated epoch. Therefore, $h(z_i) = 1$ and $h'(z_i) = -\frac{h(z_i)}{H(z_i)(1+z_i)}$ are the initial set of conditions for all models. Fig. 5.1 depicts only the ranges from $z = 0$ and $z = 1$ to show the behaviour of the model during matter and late-time eras; the current detectable ranges. The $f(T)$ model remains with a higher amplitude across all redshifts. The change in $h(z)$ is highlighted with the plot for $h'(z)$ such that the GR model can be seen to have an amplitude lower than $f(T)$ at early times but exceeds it at later times. This shows that GR tensor modes diminish quicker than ΛCDM and $f(T)$ models. It should be emphasised that this holds only for the tensor modes. An extra scalar or vector mode provided by modified theories of gravity may result in more energy losses, and the propagation of GWs is altered due to additional ingredients mixed in with the tensor modes. Further details regarding additional polarisation modes are explored in Sec. 5.3.

Detection prospects of tensor polarisation deviations depend on the capabilities of the GW detectors. Currently, A-LIGO operates in a high-frequency range and is sensitive to GR predictions for binary blackhole and binary neutron star mergers [290]. Modified theories of gravity would result in a deviation from GR through changes in amplitude and phase. In the case of A-LIGO, this would require operations in conjunction with other detectors, such as Virgo and KAGRA, to provide a network to break degeneracies between additional polarisation modes that might be mixing with tensor modes which result in outcomes similar to GR. A-LIGO, Virgo, and KAGRA are limited in sensitivity, due to their specific orientation and restriction of the detector's arms length. The proposal of the Einstein Telescope [291] could shed light on GWs in modified theories of gravity due to its increased sensitivity through longer arms, triangular setup (where each pair can be treated as an interferometer), and lower noise floor [292]. The future mission carried out by LISA will result in higher sensitivity, explore lower frequencies (aiming to reach $1\,\mu$m), and have arms lengths much larger than those possible for ground-based detectors [293]. LISA would observe GWs stemming from supermassive blackholes and extreme mass ratio inspirals, providing additional sources that are more sensitive to GR deviations. Further details on polarisation modes will be explored in Sec. 5.3.

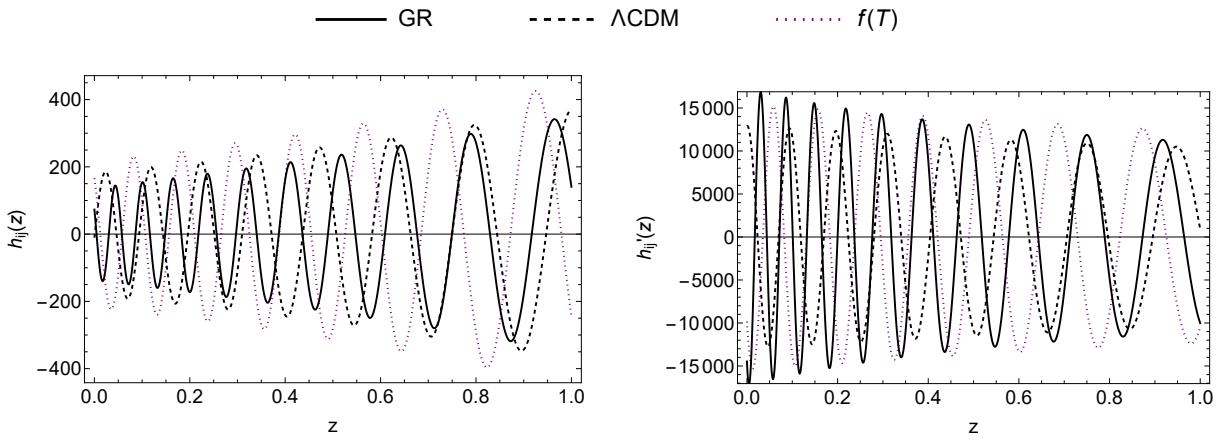

Figure 5.1: Characteristic plots for the propagation of tensor modes to redshift, where $z = 0$ is the Universe currently. The plot compares the results for GR, ΛCDM models ($H_0 = 67.4$ km s^{-1} Mpc^{-1}, $\Omega_{m0} = 0.315$, $\Omega_{r0} = 8.4 \times 10^{-5}$) using Planck collaboration data [2], and $f(T)$ power law model introduced in Eq. (6.78) ($H_0 = 68.5$ km s^{-1} Mpc^{-1}, $\Omega_{m0} = 0.35$, $\Omega_{r0} = 8.4 \times 10^{-5}$, $\beta_1 = -0.22$) using data summarised in Table 6.1. The solution assumed $k = 100H_0$. Eq. (5.14) is solved with initial conditions at $z = z_i = 10^4$ such that $h(z_i) = 1$ and $h'(z_i) = -\frac{h(z_i)}{H(z_i)(1+z_i)}$. The figure illustrates the solution for tensor modes $h_{ij}(z)$ and the change in solution through the derivative $h'_{ij}(z)$.

In the meantime, astrophysical electromagnetic counterparts of GW are an important tool to independently measure source properties. The observations of GRB170817A, counterpart to A-LIGO's GW detection, provided a limit on the GW's propagation speed to be almost at the speed of light: $|c_{\rm GW} - 1| \lesssim 10^{-15}$ [81]. Additionally, electromagnetic counterparts can offer independent luminosity distance measurements that lead to breaking degeneracies in GW observations, time delays, phase shifts, and identifying dampening effects, potentially giving insight into deviations from GR [294].

The scalar, vector and tensorial systems given by Eqs (5.8,5.12,5.14) can be combined to form a block matrix:

$$\begin{pmatrix} M_{\rm S} & 0 & 0 \\ 0 & M_{\rm V} & 0 \\ 0 & 0 & M_{\rm T} \end{pmatrix} \begin{pmatrix} Y_{\rm S} \\ Y_{\rm V} \\ Y_{\rm T} \end{pmatrix} =: MY = 0\,, \tag{5.16}$$

where, since vectors and tensors have 2 DoFs for each mode, the system is slightly modified to have

$$M_V \to M_V \otimes \mathbf{I}_2\,, \qquad \text{and} \qquad M_T \to M_T \otimes \mathbf{I}_2\,. \tag{5.17}$$

Here, $\mathbf{I}_2$ is the two-dimensional identity matrix such that a vector or tensor, say β_i, is expressed as $\beta_i = \{\beta_{i,1}, \beta_{i,2}\}$. Hence, in Eq. (5.16), there is a maximally independent system M with the basis set $\{Y_{\rm S}, Y_{\rm V}, Y_{\rm T}\}$.

The characteristics of propagating GWs can be determined through the principal polynomial of the block matrix [295, 296, 297], to realise the relationship for the wave whose propagation is expressed through differential equations provided by the field equations [296, 297]. The spatial Fourier principal polynomial is set to vanish, i.e., the diagonal matrix's determinant is equal to zero. The result, expressed in terms of the wave covector k, determines the nature of the propagation velocity; whether it corresponds to the speed of light or behaves as a massive object [298]. The principal polynomial in the case of BDLS is given by

$$\begin{aligned} P(k) &:= \det(M) = \det(M_{\rm S})\det(M_{\rm V})\det(M_{\rm T}) \\ &= -2^{14}3^{-5}\left(G_4 - G_{{\rm Tele},T}\right)^5 G^3_{{\rm Tele},T_{\rm vec}} G^3_{{\rm Tele},T_{\rm ax}} k^{12}\left(\omega^2 - k^2\right)^8 \left[\tilde{c}_1 + \tilde{c}_2\left(\omega^2 - k^2\right)\right] , \end{aligned} \tag{5.18}$$

where constants $\tilde{c}_1$ and $\tilde{c}_2$ are given by

$$\tilde{c}_1 := 2\left(G_{{\rm Tele},\phi\phi} + G_{2,\phi\phi}\right)\left(2\left(G_4 - G_{{\rm Tele},T}\right) + 3G_{{\rm Tele},T_{\rm vec}}\right) , \tag{5.19a}$$

$$\begin{aligned} \tilde{c}_2 :=& -3\left(G_{{\rm Tele},I_2} - 2G_{4,\phi}\right)^2 \\ & - 2\left(G_{{\rm Tele},X} + G_{2,X} - 2G_{3,\phi}\right)\left(2\left(G_4 - G_{{\rm Tele},T}\right) + 3G_{{\rm Tele},T_{\rm vec}}\right) . \end{aligned} \tag{5.19b}$$

Thus, apart from the trivial solution of $k = 0$, $P(k) = 0$ provides two nontrivial solutions: massless $k = \pm\omega$ or massive $k^2 = \omega^2 - m^2$, where m is the effective mass. Thus, the full BDLS framework with a Minkowski background realises a maximum of 7 propagating DoFs.

The general case provided here shows that taking certain limits in Eq. (5.18), such as $0 = G_4 - G_{{\rm Tele},T}$, $0 = G_{{\rm Tele},T_{\rm vec}}$, $0 = G_{{\rm Tele},T_{\rm ax}}$, $0 = \tilde{c}_1 + \tilde{c}_2(\omega^2 - k^2)$, or a combination of these conditions would result in a trivial solution. Thus, some subcases of BDLS cannot be analysed through Eq. (5.18). These scenarios require a separate analysis, starting at the block matrix level. This iterative process is not included in this section but can be found in Sec. 5.4 and results summarised in Table 5.1. As examples, the cases of GR and standard Horndeski are included to ensure that the expected results are realised through BDLS.

5.2.1 | General Relativity

The GR limit can be obtained from Eq. (2.98) by setting $G_4 = 1$ and all other coefficients are set to vanish. This limit increases the number of linearly dependent equations. Thus, the block

matrix in Eq. (5.16) reduces to

$$M_{\rm GR}Y_{\rm GR} = \begin{pmatrix} 4k^2 & 0 & 0 & 0 \\ 4\left(3\omega^2 - k^2\right) & 4k^2 & 0 & 0 \\ 0 & 0 & -k^2 & 0 \\ 0 & 0 & 0 & -\omega^2 + k^2 \end{pmatrix} \begin{pmatrix} \psi \\ \mathcal{X}_2 \\ \beta_i \\ h_{ij} \end{pmatrix}, \tag{5.20}$$

where $\beta_i = \{\beta_{i,1}, \beta_{i,2}\}$ and $h_{ij} = \{h_{ij,1}, h_{ij,2}\}$ to account for two DoFs of vector and tensor modes. The principal polynomial becomes

$$P_{\rm GR}(k) = -16k^8 \left(\omega^2 - k^2\right)^2 , \tag{5.21}$$

wherein the only non-trivial solution for $P_{\rm GR}(k)$ is given by $\omega^2 - k^2 = 0$, implying the dispersion relation for massless, speed of light propagation. Thus, for the case $\omega = \pm k$, substituting back in Eq. (5.20) yields

$$M_{\rm GR}Y_{\rm GR}(\omega \to |k|) = \begin{pmatrix} 4k^2 & 0 & 0 & 0 \\ 8k^2 & -4k^2 & 0 & 0 \\ 0 & 0 & k^2 & 0 \\ 0 & 0 & 0 & 0 \end{pmatrix} \begin{pmatrix} \psi \\ \mathcal{X}_2 \\ \beta_i \\ h_{ij} \end{pmatrix}. \tag{5.22}$$

The nullspace of the linear transformation $M_{\rm GR}$ provides a set of solutions for the invariants of $M_{\rm GR}Y_{\rm GR} = 0$ [299]:

$$Y_{\rm GR}(\omega) = \{\psi, \mathcal{X}_2, \beta_{i_1}, \beta_{i_2}, h_{ij_1}, h_{ij_2}\}^T \implies Y_{\rm GR}(|k|) = \{0, 0, 0, 0, A_1, A_2\}^T , \tag{5.23}$$

where $A_i \in \mathbb{C}$ are elements of the nullspace generated by $M_{\rm GR}$. This procedure aims to obtain the propagating DoFs and classify them according to their nature. Hence, the actual A_i value is unimportant. As expected, two propagating DoFs corresponding to the tensor modes give nontrivial solutions. Therefore, despite $\{\psi, \mathcal{X}_2, \beta_i\}$ modes are present in the field equations, they are not necessarily propagating DoFs.

5.2.2 | Horndeski Gravity

BDLS, as a teleparallel analogue to Horndeski theory, provides a natural avenue to study standard Horndeski by setting $G_{\rm Tele} = 0$ and the rest of the arbitrary functions remain in the same form.

This implies that terms associated with the pseudoscalar and pseudovector modes, which appear in σ_i and $\mathcal{Z}_i$ modes, vanish and the block matrix is given by

$$M_{\rm H}Y_{\rm H} = \begin{pmatrix} M_{\rm H1} & M_{\rm H2} & 0 & 0 & 0 \\ M_{\rm H3} & M_{\rm H4} & M_{\rm H2} & 0 & 0 \\ M_{\rm H5} & M_{\rm H3} & -M_{\rm H1} & 0 & 0 \\ 0 & 0 & 0 & -\frac{1}{4}M_{\rm H2} & 0 \\ 0 & 0 & 0 & 0 & M_{\rm H6} \end{pmatrix} \begin{pmatrix} \delta\phi \\ \psi \\ \mathcal{X}_2 \\ \beta_i \\ h_{ij} \end{pmatrix}, \tag{5.24}$$

where

$$\begin{aligned} M_{\rm H1} &= -2G_{4,\phi}k^2\,, & M_{\rm H2} &= -4G_4k^2\,, \\ M_{\rm H3} &= -2M_{\rm H1} - 6G_{4,\phi}\omega^2\,, & M_{\rm H4} &= -M_{\rm H2} - 12G_4\omega^2\,, \\ M_{\rm H5} &= G_{2,\phi\phi} + (G_{2,X} - 2G_{3,\phi})\left(-\omega^2 + k^2\right)\,, & M_{\rm H6} &= -\frac{1}{4}M_{\rm H2} - G_4\omega^2\,, \end{aligned}$$

such that β_i and h_{ij} are still considered to represent two DoFs each. Thus, the principal polynomial simplifies to

$$P_{\rm H}(k) = -16G_4^5\,k^8\,\left(\omega^2 - k^2\right)^2\left[G_4G_{2,\phi\phi} + \left(-3G_{4,\phi}^2 + G_4\left(2G_{3,\phi} - G_{2,X}\right)\right)\left(\omega^2 - k^2\right)\right]. \tag{5.25}$$

In line with the full BDLS principal polynomial given by Eq. (5.18), and in contrast with the GR case of Eq. (5.21), a massive sector is realised in addition to the massless one. This is because now there are two possible solutions for $P_{\rm H}(k) = 0$:

Case H.I:	$G_4 \neq 0, G_{2,\phi\phi} \neq 0, -3G_{4,\phi}^2 + G_4(2G_{3,\phi} - G_{2,X}) \neq 0$
Case H.II:	$G_4 \neq 0, G_{2,\phi\phi} = 0, -3G_{4,\phi}^2 + G_4(2G_{3,\phi} - G_{2,X}) = 0$

Case H.I does not alter the general principal polynomial presented in Eq. (5.25), generating a massless and massive solution. For the massless case, substituting $\omega = \pm k$ obtains the nullspace

$$Y_{\rm H.I}(\omega) = \{\delta\phi, \psi, \mathcal{X}_2, \beta_{i_1}, \beta_{i,2}, h_{ij_1}, h_{ij_2}\}^T \implies Y_{\rm H.I}(|k|) = \{0,0,0,0,0,B_1,B_2\}^T\,, \tag{5.26}$$

where $B_i \in \mathbb{C}$ for the nullspace of $M_{\rm H}$ for which two tensor modes can be seen to be propagating DoFs. As for the massive case, substitution of $\omega = \pm\sqrt{m^2 + k^2}$ for which m is the effective mass

$$m^2 = -\frac{G_4G_{2,\phi\phi}}{-3G_{4,\phi}^2 + G_4\left(2G_{3,\phi} - G_{2,X}\right)}\,, \tag{5.27}$$

which gives a nullspace solution of the form

$$Y_{\mathrm{H.I}}(\omega) = \{\delta\phi, \psi, \mathcal{X}_2, \beta_{i_1}, \beta_{i,2}, h_{ij_1}, h_{ij_2}\}^T \\ \implies Y_{\mathrm{H.I}}(|m|) = \{2G_4C_1, -G_{4,\phi}C_1, G_{4,\phi}C_1, 0, 0, 0, 0\}^T\,, \tag{5.28}$$

where $C_1 \in \mathbb{C}$ is also an element of nullspace of M_{H}.

Case H.II is obtained by substituting

$$G_{2,X} = -\frac{3G_{4,\phi}^2}{G_4} + 2G_{3,\phi}\,. \tag{5.29}$$

The expressions obtained through this particular choice of substitution may differ in appearance throughout the derivation, but the same result and solutions would be produced. The principal polynomial reduces to

$$P_{\mathrm{H.II}}(k) = -8G_4^5G_{4,\phi}k^8\left(\omega^2 - k^2\right)^2\,, \tag{5.30}$$

giving a massless solution when $\omega = \pm k$, and a scenario that is independent of the functions G_2 and G_3. In the case of $G_{4,\phi} \neq 0$ the solutions are of the form

$$Y_{\mathrm{H.II}}(\omega, G_{4,\phi} \neq 0) = \{\delta\phi, \psi, \beta_{i_1}, \beta_{i_2}, h_{ij_1}, h_{ij_2}\}^T \\ \implies Y_{\mathrm{H.II}}(|k|, G_{4,\phi} \neq 0) = \{0, 0, 0, 0, D_1, D_2\}^T\,, \tag{5.31}$$

for $D_i \in \mathbb{C}$, while for $G_{4,\phi} = 0$, the solution reduces to

$$Y_{\mathrm{H.II}}(|k|, G_{4,\phi} = 0) = \{\psi, \beta_{i_1}, \beta_{i_2}, h_{ij_1}, h_{ij_2}\}^T \implies Y_{\mathrm{H_B}}(G_{4,\phi} = 0) = \{0, 0, 0, E_1, E_2\}^T\,, \tag{5.32}$$

where $E_i \in \mathbb{C}$. Both cases show that only tensor modes propagate. In Ref. [300], the procedure adopted to analyse GW propagation in Horndeski theory omits the latter subcase.

The branches of BDLS presented in Sec. 5.4 are obtained by taking all possible combinations arising through the BDLS principal polynomial in Eq. (5.18). While these scenarios do not explicitly result in the GR and Horndeski gravity cases depicted in this section, they can be classified within the cases realised provided appropriate limits are taken. While the propagating DoFs of the theory are identified, they do not necessarily act as a polarisation mode. The next section will explore the procedure to show the nature of the polarisation modes.

5.3 | Polarisation Modes

For a weak, plane and nearly null GW propagating in the $+z$ direction within a local Lorentz frame with the delayed time $u = t - z$ and the wave is travelling in the opposite direction

described by the function of advanced time $v = t + z$. These time functions are defined through the Newman-Penrose (NP) formalism [301] where the gauge freedom depends on the choice of tetrad based on a null basis rather than an orthonormal basis [302]. Therefore,

$$l_\mu \coloneqq -u_{,\mu}\,, \qquad n_\mu \coloneqq \frac{1}{2} v_{,\mu}\,, \tag{5.33}$$

to obtain the four-vector fields

$$l^\mu = (1,0,0,1)\ , \quad n^\mu = \frac{1}{2}(1,0,0,-1)\ , \quad m^\mu = \frac{1}{\sqrt{2}}(0,1,i,0)\ , \quad \bar{m}^\mu = \frac{1}{\sqrt{2}}(0,1,-i,0)\ , \tag{5.34}$$

with overbar $\bar{m}$ denoting the complex conjugate of m. The four-vector fields are classified as null, thus satisfying the orthogonality condition [3]

$$l^\mu l^\nu \eta_{\mu\nu} = n^\mu n^\nu \eta_{\mu\nu} = m^\mu m^\nu \eta_{\mu\nu} = \bar{m}^\mu \bar{m}^\nu \eta_{\mu\nu} = 0\,, \tag{5.35}$$

and satisfy the normalisation conditions

$$l^\mu n^\nu \eta_{\mu\nu} = -m^\mu \bar{m}^\nu \eta_{\mu\nu} = 1\,. \tag{5.36}$$

A linear combination of these null tetrads basis constructs an additional GW vector

$$\tilde{l}^\mu = l^\mu - \epsilon_n \left(\frac{1}{2} l^\mu - n^\mu\right)\,, \qquad \text{and} \qquad \epsilon_n = \frac{c}{v_g} - 1\,, \tag{5.37}$$

where ϵ_n accounts for the discrepancy between the speed of light c and the speed of the GW propagation v_g [3], which vanishes in null scenarios. Thus, $\tilde{l}$ represents an observer oriented on a spatial basis such that the null wave is acting in the same direction as the propagation.

The Riemann tensor in Eq. (2.9)[4] can be reexpressed as follows:

$$\mathring{R}_{\lambda\mu\rho\nu} = \mathring{C}_{\lambda\mu\rho\nu} - \frac{1}{2}\left(\eta_{\lambda\rho}\mathring{R}_{\mu\nu} - \eta_{\mu\rho}\mathring{R}_{\lambda\nu} - \eta_{\lambda\nu}\mathring{R}_{\mu\rho} + \eta_{\mu\nu}\mathring{R}_{\lambda\rho}\right) + \frac{1}{6}\left(\eta_{\lambda\rho}\eta_{\mu\nu} - \eta_{\lambda\nu}\eta_{\mu\rho}\right)\mathring{R}\,, \tag{5.38}$$

where $\mathring{C}_{\lambda\mu\rho\nu}$ is the Weyl tensor which represents the trace-free part of the Riemann tensor. Ten independent components can be constructed from the five complex Weyl scalar [302]

$$\begin{aligned}
&\Psi_0 = -\mathring{C}_{\lambda\mu\rho\nu} l^\lambda m^\mu l^\rho m^\nu\,, \qquad \Psi_1 = -\mathring{C}_{\lambda\mu\rho\nu} l^\lambda n^\mu l^\rho m^\nu\,, \qquad \Psi_2 = -\mathring{C}_{\lambda\mu\rho\nu} l^\lambda m^\mu \bar{m}^\rho n^\nu\,,\\
&\Psi_3 = -\mathring{C}_{\lambda\mu\rho\nu} l^\lambda n^\mu \bar{m}^\rho n^\nu\,, \qquad \Psi_4 = -\mathring{C}_{\lambda\mu\rho\nu} n^\lambda \bar{m}^\mu n^\rho \bar{m}^\nu\,,
\end{aligned} \tag{5.39}$$

along with the ten components from the Ricci tensor which are expressed in terms of the real scalars $\{\Phi_{00}, \Phi_{11}, \Phi_{22}, \Lambda\}$[5] and complex scalars $\{\Phi_{02}, \Phi_{20}, \Phi_{01}, \Phi_{10}, \Phi_{12}, \Phi_{21}\}$. The twelve spin coefficients which describe rotational effects in the NP formalism [301] have been omitted in

[4] Eq. (2.9) has been modified to for a Minkowski background and for a signature $(+,-,-,-)$

[5] The Λ scalar representing the Ricci tensor should not be confused with the cosmological constant.

this work as their application is more within blackhole studies [302]. This is because GWs are studied at regions far away from the source, and spacetime can be assumed to be flat, while for blackholes studied in strong gravitational fields these coefficients help to describe the rotations and twists stemming from warped spacetime . Thus, the electrical components of the Riemann tensor can be expressed in terms of the NP formalism [301]:

$$\Psi_2 \coloneqq -\frac{1}{6}\mathring{R}_{nlnl} + \mathcal{O}(\epsilon_n R) \qquad (s=0)\,, \tag{5.40a}$$

$$\Phi_{22} \coloneqq -\mathring{R}_{nmn\bar{m}} + \mathcal{O}(\epsilon_n R) \qquad (s=0)\,, \tag{5.40b}$$

$$\Psi_3 \coloneqq -\frac{1}{2}\mathring{R}_{nln\bar{m}} \qquad (s=-1)\,, \tag{5.40c}$$

$$\bar{\Psi}_3 = -\frac{1}{2}\mathring{R}_{\overline{nln\bar{m}}} \qquad (s=1)\,, \tag{5.40d}$$

$$\Psi_4 \coloneqq -\mathring{R}_{n\bar{m}n\bar{m}} \qquad (s=-2)\,, \tag{5.40e}$$

$$\bar{\Psi}_4 \coloneqq -\mathring{R}_{\overline{n\bar{m}n\bar{m}}} \qquad (s=2)\,, \tag{5.40f}$$

where s represents the helicity state. When $\epsilon_n = 0$, these amplitudes become invariant and form a subgroup of the Lorentz group $E(2)$ [3] and result in the following classification:

$$\begin{aligned}
&\mathrm{II}_6 : \Psi_2 \neq 0\,, && \mathrm{III}_5 : \Psi_2 = 0, \Psi_3 \neq 0\,,\\
&N_3 : \Psi_2 = \Psi_3 = 0, \Psi_4 \neq 0, \Phi_{22} \neq 0\,, && N_2 : \Psi_2 = \Psi_3 = \Phi_{22} = 0, \Psi_4 \neq 0\,,\\
&O_1 : \Psi_2 = \Psi_3 = \Psi_4 = 0, \Phi_{22} \neq 0\,, && O_0 : \Psi_2 = \Psi_3 = \Psi_4 = \Phi_{22} = 0\,,
\end{aligned} \tag{5.41}$$

such that the omission of an amplitude indicates there is an observer dependency [3, 288]. The six possible polarisation modes of GWs travelling in the $+z$ direction are given by the variables $\{\Psi_2, \Phi_{22}, \Re\Psi_3, \Im\Psi_3, \Re\Psi_4, \Im\Psi_4\}$ and illustrated in Fig. 5.2. Mode classification can be deduced by comparing the helicity of the electrical components of the Riemann tensor: Ψ_2 and Φ_{22} are scalar DoFs, Ψ_3 and its complex conjugate are related to the vectorial DoFs, and Ψ_4 and its complex conjugate is the tensorial DoFs. The breathing mode Φ_{22} results in a circular pattern signifying an isotropic expansion/contraction as particles move outwards/inwards while remaining perpendicular to the wave. The longitudinal mode given by Ψ_2 represents the compression/stretching along the direction of the wave. x and y modes, respectively introduced by the appearance of $\Re\Psi_3$ and $\Im\Psi_3$, represent transverse shearing through a stretch along one axis while moving sideways along another axis. $\Re\Psi_4$ corresponds to the h_+ tensor mode that elongates spacetime along an axis and compressed from another. $\Im\Psi_4$ represents the $h_\times$ tensor mode, whose effects are similar to those of h_+ but at a rotation of 45° such that the stretching and compression

occurs diagonally. Thus,

$$\mathring{R}_{0i0j} = \begin{pmatrix} \frac{1}{2}(\Re\Psi_4 + \Phi_{22}) & \frac{1}{2}\Im\Psi_4 & -2\Re\Psi_3 \\ \frac{1}{2}\Im\Psi_4 & -\frac{1}{2}(\Re\Psi_4 - \Phi_{22}) & 2\Im\Psi_3 \\ -2\Re\Psi_3 & 2\Im\Psi_3 & -6\Psi_2 \end{pmatrix}, \tag{5.42}$$

is expressed in terms of NP variables.

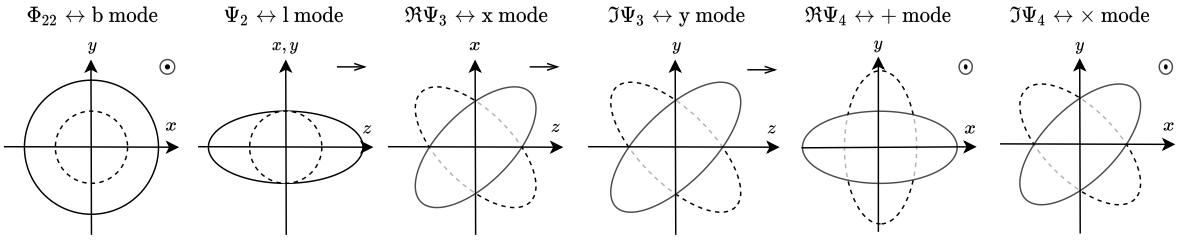

Figure 5.2: Sphere deformation from a free-falling test particle depicting polarisation modes of a GW travelling in the $+z$ direction: scalar modes given by breathing b and longitudinal l, vector modes given by x and y, and tensor modes given by $+$ and $\times$. Illustration based on figure in Ref. [3].

The SVT decomposition implemented in Sec. 5.2 can also be applied to the electric components of the Riemann tensor through Eq. (2.9):

$$\begin{aligned} \mathring{R}_{0i0j} &= \frac{1}{2}\left(\partial_0\partial_i\delta g_{0j} - \partial_0\partial_0\delta g_{ij} + \partial_i\partial_j\delta g_{00} + \partial_j\partial_0\delta g_{0i}\right) \\ &= \begin{pmatrix} \ddot{\psi} - \frac{1}{2}\ddot{h}_+ & -\frac{1}{2}\ddot{h}_\times & -\frac{1}{2}ik(\dot{\beta}_1 + \dot{\Lambda}_1) \\ -\frac{1}{2}\ddot{h}_\times & \ddot{\psi} + \frac{1}{2}\ddot{h}_+ & -\frac{1}{2}ik(\dot{\beta}_2 + \dot{\Lambda}_2) \\ -\frac{1}{2}ik(\dot{\beta}_1 + \dot{\Lambda}_1) & -\frac{1}{2}ik(\dot{\beta}_2 + \dot{\Lambda}_2) & \ddot{\psi} - k^2(\dot{\chi} + \Phi) \end{pmatrix}, \end{aligned} \tag{5.43}$$

where $h_+ = h_{11} = h_{22}$ and $h_\times = h_{12} = h_{21}$, and $\mathring{R}_{0i0j}$ is expressed solely in terms of invariant variables. The result holds for both massless and massive sectors, in contrast with the NP formalism that only holds in the null scenarios of massless cases. Here, the GR and Horndeski subcases are explored in this section. The analysis for other branches of BDLS have been fleshed out in Sec. 5.4 and summarised in Table 5.2.

Before exploring branches of BDLS theory, it is important to note the phenomenological implications of additional GW polarisation modes. In the discussion around Fig. 5.1 in Sec. 5.2, the tensor modes stemming from the modified theory of gravity of $f(T)$ were shown to have higher amplitudes than their GR counterparts. The presence of additional modes, either scalar

or vector modes, is expected to result in more GW energy losses from the entire system as more channels are available to carry away energy. Signals containing a combination of modes may result in degeneracies with the GR predictions, therefore it becomes crucial for GW detectors to distinguish between the different modes.

Currently, ground-based GW interferometers are classified as second-generation detectors, reaching redshift of $z \sim 0.05$ for binary neutron stars and $z \sim 0.5$ for binary blackhole mergers [303]. While waveforms used in A-LIGO, Virgo, and KAGRA have shown to realise only tensor polarisation modes, the detection of additional polarisation modes has not been ruled out. Long duration GW sources, in particular the stochastic background, have been used to search for possible deviations from GR. Ref. [304] showed that at least three detectors are required to separate the mixture of polarisation mode that the detector picks up. A-LIGO, using its first three runs in collaboration with Virgo and KAGRA, albeit not able to detect the presence of background for any polarisation modes, has been able to provide an upper limit for the energy density of different components of the SVT sectors: $\Omega^{\rm T}_{\rm GW} < 6.4 \times 10^{-9}$, $\Omega^{\rm V}_{\rm GW} < 7.9 \times 10^{-9}$, and $\Omega^{\rm S}_{\rm GW} < 2.1 \times 10^{-8}$ [305].

The upcoming third-generation of GW detectors are expected to improve the sensitivity of over a factor of 10, reaching redshifts of $z \sim 2$ for binary neutron star mergers and $z \sim 15$ for binary blackhole mergers [303]. The Einstein Telescope and Cosmic Explorer have been proposed as such interferometers. Despite the triangulation topology of the Einstein telescope, the orientation of the ground-based interferometer is still proven to be limited. Ref. [306] considers different possible orientations and locations of the Earth, providing the analysis for tests of scalar-tensor and vector-tensor theories. Moreover, space-based operations such as LISA have been theoretically shown to provide a smaller upper limit for the detectable energy density: $\Omega^{\rm V}_{\rm GW} \sim 10^{-12}$ and $\Omega^{\rm S}_{\rm GW} \sim 10^{-12}$ [307].

Branches of BDLS can predict additional polarisation modes. Identifying their nature is crucial to map out how their signal will alter the waveform template. Here, the GW and Horndeski subcases are explored in this section. The analysis for other branches of BDLS has been fleshed out in Sec. 5.4 and summarised in Table 5.2.

5.3.1 | General Relativity

The propagating DoFs in the GR limit of BDLS in Eq. (5.23) are solely the two tensor modes: h_+ and $h_\times$. Both DoFs survive when analysing the electric components of the Riemann tensor:

$$\mathring{R}_{0i0j}\left(Y_{\mathrm{GR}}(|k|)\right) = \begin{pmatrix} -\frac{1}{2}\ddot{h}_+ & -\frac{1}{2}\ddot{h}_\times & 0 \\ -\frac{1}{2}\ddot{h}_\times & \frac{1}{2}\ddot{h}_+ & 0 \\ 0 & 0 & 0 \end{pmatrix} = \frac{k^2}{2}\begin{pmatrix} A_1 & A_2 & 0 \\ A_2 & -A_1 & 0 \\ 0 & 0 & 0 \end{pmatrix}. \tag{5.44}$$

5.3.2 | Horndeski Gravity

The Horndeski branch in Sec. 5.2.2 realised two major subcases. Case H.I has two tensor modes $\{h_+, h_\times\}$ as propagating DoFs in the massless sector and three scalars DoFs in the massive sector $\{\delta\phi, \psi, \mathcal{X}_2\}$. Evaluation of $\mathring{R}_{0i0j}$ yields

$$\mathring{R}_{0i0j}\left(Y_{\mathrm{H_I}}(|k|)\right) = \begin{pmatrix} -\frac{1}{2}\ddot{h}_+ & -\frac{1}{2}\ddot{h}_\times & 0 \\ -\frac{1}{2}\ddot{h}_\times & \frac{1}{2}\ddot{h}_+ & 0 \\ 0 & 0 & 0 \end{pmatrix} = -\frac{k^2}{2}\begin{pmatrix} B_1 & B_2 & 0 \\ B_2 & -B_1 & 0 \\ 0 & 0 & 0 \end{pmatrix}, \tag{5.45}$$

and

$$\begin{aligned} \mathring{R}_{0i0j}\left(Y_{\mathrm{H_I}}(|m|)\right) &= \begin{pmatrix} \ddot{\psi} & 0 & 0 \\ 0 & \ddot{\psi} & 0 \\ 0 & 0 & \ddot{\psi} - k^2\mathcal{X}_2 \end{pmatrix} \\ &= G_{4,\phi}\begin{pmatrix} \left(m^2+k^2\right)C_1 & 0 & 0 \\ 0 & \left(m^2+k^2\right)C_1 & 0 \\ 0 & 0 & m^2 C_1 \end{pmatrix}, \end{aligned} \tag{5.46}$$

respectively. Thus, the massive sector has an additional entry in the longitudinal and breathing modes along with the tensorial modes in the massless sector, totalling to 3 polarisation modes; in agreement with the results obtained in Ref. [300].

In case H.II, the solutions given by Eq. (5.31) and Eq. (5.32) both lead to the same electric

Riemann tensor:

$$\mathring{R}_{0i0j}\left(Y_{\mathrm{H_{II}}}(|k|)\right) = \begin{pmatrix} -\frac{1}{2}\ddot{h}_+ & -\frac{1}{2}\ddot{h}_\times & 0 \\ -\frac{1}{2}\ddot{h}_\times & \frac{1}{2}\ddot{h}_+ & 0 \\ 0 & 0 & 0 \end{pmatrix} = -\frac{k^2}{2}\begin{pmatrix} D_1 & D_2 & 0 \\ D_2 & -D_1 & 0 \\ 0 & 0 & 0 \end{pmatrix}, \tag{5.47}$$

where $D_i = E_i$, with two tensorial polarisation modes. Note, that this result is not realised in the Horndeski analysis in Ref. [300] due to the limitations of the technique applied.

In Ref. [300], the polarisation modes were obtained through the investigation of the transverse-traceless gauge method in Horndeski gravity, while in Ref. [295] the principal symbol method was adopted in NGR. These methods have been performed in BDLS but omitted in this work as the transverse-traceless method was seen to be limiting and fails when subcases of the theory are considered which do not utilise the full extent of the theory. Additionally, the principal symbol method employed through the principal polynomial under a different tensor decomposition resulted in an extra DoF in comparison to the results obtained in the literature. The latter procedure would require a Hamiltonian analysis to provide the necessary constraints due to differences between linearised and non-linear portions in the theory, as done in Ref. [308] for NGR.

5.4 | Branches of BDLS

One of the interests in BDLS is the ability to obtain several subcases corresponding to theories of gravity explored in literature, such as those of GR and Horndeski analysed in Secs (5.2-5.3). Additionally, many subclasses naturally arise within BDLS, each with a variety of propagating DoFs and polarisation modes. All subcases are determined by initially considering the general form of the principal polynomial given by Eq. (5.18) while also imposing $G_4 - G_{\mathrm{Tele},T} > 0$ to ensure that the two tensor modes favoured by A-LIGO observations [45] are present. The eight major subclasses of BDLS can be obtained through a combination of the terms $G_{\mathrm{Tele},T_{\mathrm{ax}}}$, $G_{\mathrm{Tele},T_{\mathrm{vec}}}$, $\tilde{c}_1$ given by Eq. (5.19a) and $\tilde{c}_2$ given by Eq. (5.19b). The procedure displayed in Secs 5.2-5.3 for the GR and Horndeski cases is replicated to obtain all possible combinations of the principal polynomial, in some cases producing their own subcases. All the results presented in this section are summarised in Tables 5.1-5.2. Preemptively, some constants will be defined here and used in later portions of the analysis:

$$Z_2 := \frac{3(G_{\mathrm{Tele},I_2} - 2G_{4,\phi})^2 + 2(2(G_4 - G_{\mathrm{Tele},T}) + 3G_{\mathrm{Tele},T_{\mathrm{vec}}})(G_{\mathrm{Tele},X} + G_{2,X})}{4\left(2(G_4 - G_{\mathrm{Tele},T}) + 3(G_{\mathrm{Tele},T_{\mathrm{vec}}})\right)}, \tag{5.48}$$

$$\tilde{c}_3 := -G_{\mathrm{Tele},\phi\phi} - G_{2,\phi\phi}\,, \tag{5.49}$$

$$\tilde{c}_4 := G_{\mathrm{Tele},X} + G_{2,X} - 2G_{3,\phi}\,, \tag{5.50}$$

while $\tilde{c}_1$ and $\tilde{c}_2$ are given by Eq. (5.19a) and Eq. (5.19b), respectively. Throughout these cases, the massless solutions are presented with $A_i \in \mathbb{C}$ and massive solutions are presented with $B_i \in \mathbb{C}$, where $i \in \mathbb{Z}^+$. In the following subsections, the notation A_i and B_i will be used across different cases. While this does not imply that the solutions are identical for each case, A_i and B_i serve as placeholders to indicate the existence of a solution. The explicit forms of these solutions are not crucial at this stage, as the focus is on identifying the propagating modes and determining the polarisation states.

5.4.1 | Case 1: $G_{\text{Tele},T_{\text{vec}}} \neq 0\,, G_{\text{Tele},T_{\text{ax}}} \neq 0\,, \tilde{c}_1 \neq 0\,, \tilde{c}_2 \neq 0$

Case 1 represents the full BDLS theory, meaning that no assumptions leading to vanishing terms are applied, such that

$$G_{\text{Tele},T_{\text{vec}}} \neq 0\,, \qquad G_{\text{Tele},T_{\text{ax}}} \neq 0\,. \qquad \tilde{c}_1 \neq 0\,, \qquad \tilde{c}_2 \neq 0\,. \tag{5.51}$$

This case showcases the full extent of the theory in Minkowski background, where J_i terms from action (2.98) do not play a role. The principal polynomial corresponds to the one presented in Eq. (5.18), i.e.

$$P_1(k) = -\tfrac{16384}{243}(G_4 - G_{\text{Tele},T})^5 (G_{\text{Tele},T_{\text{vec}}})^3 (G_{\text{Tele},T_{\text{ax}}})^3 k^{12} (\omega^2 - k^2)^8 (\tilde{c}_1 + \tilde{c}_2(\omega^2 - k^2))\,, \tag{5.52}$$

giving the non-trivial and non-degenerate solutions for the massless sector $\omega^2 - k^2 = 0$ and the massive sector $\tilde{c}_1 + \tilde{c}_2\left(\omega^2 - k^2\right) = 0$ where the effective mass $m^2 = -\frac{\tilde{c}_1}{\tilde{c}_2} > 0$. Thus, the propagating DoFs are given by:

$$Y_1(\omega) = \{\delta\phi, \psi, \mathcal{X}_2, \mathcal{X}_4, \sigma, \beta_{j_1}, \beta_{j_2}\mathcal{Z}_{j_1}, \mathcal{Z}_{j_2}, \mathcal{Y}_{j_1}, \mathcal{Y}_{j_2}, h_{ij_1}, h_{ij_2}\}^T\,, \tag{5.53}$$

$$\begin{aligned} Y_1(|k|) = \Big\{0, -\tfrac{1}{k^2}A_1, -\tfrac{2(G_4 - G_{\text{Tele},T} + G_{\text{Tele},T_{\text{vec}}})}{G_{\text{Tele},T_{\text{vec}}} k^2}A_1, \tfrac{i(2(G_4 - G_{\text{Tele},T}) + 3G_{\text{Tele},T_{\text{vec}}})}{G_{\text{Tele},T_{\text{vec}}}|k|^3}A_1, \\ A_2, -A_3, -A_4, i|k|A_3, i|k|A_4, A_3, A_4, \tfrac{2}{k^2}A_5, \tfrac{2}{k^2}A_6\Big\}^T\,, \end{aligned} \tag{5.54}$$

$$\begin{aligned} Y_1(|m|) = \{-2(2(G_4 - G_{\text{Tele},T}) + 3G_{\text{Tele},T_{\text{vec}}})B_1, -(G_{\text{Tele},I_2} - 2G_{4,\phi})B_1, \\ (G_{\text{Tele},I_2} - 2G_{4,\phi})B_1, 0, 0, 0, 0, 0, 0, 0, 0, 0, 0\}^T\,, \end{aligned} \tag{5.55}$$

totaling to 7 DoFs, a maximum number generated through BDLS theory: 6 stemming from the massless sector $\{A_1, \ldots, A_6\}$ of which $\{A_1, A_2\}$ are from two scalars, $\{A_3, A_4\}$ from one vector, $\{A_5, A_6\}$ from one tensor, and 1 massive scalar B_1. The massless case given by Eq. (5.54) further emphasises that $G_{\text{Tele},T_{\text{vec}}}$. These solutions are employed to calculate the electric components of

the Riemann tensor for each respective sector:

$$\mathring{R}_{0i0j}\left(Y_1(|k|)\right) = \begin{pmatrix} A_1 + A_5 & A_6 & 0 \\ A_6 & A_1 - A_5 & 0 \\ 0 & 0 & 0 \end{pmatrix}, \tag{5.56}$$

$$\mathring{R}_{0i0j}\left(Y_1(|m|)\right) = \left(G_{\text{Tele},I_2} - 2G_{4,\phi}\right) \begin{pmatrix} \left(m^2 + k^2\right) B_1 & 0 & 0 \\ 0 & \left(m^2 + k^2\right) B_1 & 0 \\ 0 & 0 & m^2 B_1 \end{pmatrix}. \tag{5.57}$$

As $(G_{\text{Tele},I_2} - 2G_{4,\phi}) \to 0$, the massive scalar mode in Eq. (5.57) becomes undetectable by the detector despite continuing to propagate. The massive sector indicates that the GW can exhibit both breathing and longitudinal modes, which reflect the presence of a graviton with mass. The breathing mode corresponds to a dilation of space perpendicular to the wave's propagation, while the longitudinal mode describes distortions along the direction of propagation of the GW. The massless result of Eq. (5.56) realises the tensor modes through A_5 and A_6, and A_1 specifically comes from the ψ mode. Therefore, in addition to the tensor modes that appear in GR, a breathing mode propagates at a relativistic speed.

5.4.2 | Case 2: $G_{\text{Tele},T_{\text{vec}}} \neq 0\,, G_{\text{Tele},T_{\text{ax}}} \neq 0\,, \tilde{c}_1 = 0\,, \tilde{c}_2 = 0$

By looking again at Eq. (5.18), a trivial solution can be obtained when setting

$$G_{\text{Tele},T_{\text{vec}}} \neq 0, \qquad G_{\text{Tele},T_{\text{ax}}} \neq 0, \qquad \tilde{c}_1 = 0, \qquad \tilde{c}_2 = 0\,. \tag{5.58}$$

Merely applying these limits to the final result presented in Sec. 5.4.1 would result in an incorrect or undefined solution. Starting from the block matrix of Eq. (5.16) and applying the conditions of Eq. (5.58), the vanishing principal polynomial gives rise to two additional branches: subcases 2.I and 2.II.

5.4.2.1 | Case 2.I

The equations of $\tilde{c}_1 = 0$ and $\tilde{c}_2 = 0$ can be solved for different constants. For the choice of substitution

$$G_{\text{Tele},T_{\text{vec}}} = -\tfrac{2}{3}(G_4 - G_{\text{Tele},T})\,, \qquad \text{and} \qquad G_{4,\phi} = \tfrac{1}{2} G_{\text{Tele},I_2}\,, \tag{5.59}$$

the determinant of the system corresponding to the principal polynomial is given by

$$P_{2.\mathrm{I}}(k) = 2^{17}3^{-9}(G_4 - G_{\mathrm{Tele},T})^8(G_{\mathrm{Tele},T_{\mathrm{ax}}})^3 k^{12}\big(\omega^2 - k^2\big)^7\Big(\tilde{c}_3 + \tilde{c}_4\big(\omega^2 - k^2\big)\Big)\,, \tag{5.60}$$

where $\tilde{c}_3$ and $\tilde{c}_4$ are given by Eq. (5.49) and Eq. (5.50), respectively. Once again, two additional subcases emerge: $\tilde{c}_3 \neq 0$, $\tilde{c}_4 \neq 0$ and $\tilde{c}_3 = \tilde{c}_4 = 0$.

Case 2.I.a The first subcase for $\tilde{c}_3 \neq 0$ and $\tilde{c}_4 \neq 0$ does not alter the principal polynomial presented in Eq. (5.60), hence the propagating DoFs arise in the massless and massive sectors:

$$Y_{2.\mathrm{I.a}}(\omega) = \{\delta\phi, \mathcal{X}_2, \mathcal{X}_4, \sigma, \beta_{i_1}, \beta_{i_2}, \mathcal{Z}_{i_1}, \mathcal{Z}_{i_2}, \mathcal{Y}_{i_1}, \mathcal{Y}_{i_2}, h_{ij_1}, h_{ij_2}\}^T\,, \tag{5.61}$$

$$Y_{2.\mathrm{I.a}}(|k|) = \big\{0, 0, 0, A_1, -A_2, -A_3, i|k|A_2, i|k|A_3, A_2, A_3, \tfrac{2}{k^2}A_4, \tfrac{2}{k^2}A_5\big\}^T\,, \tag{5.62}$$

$$Y_{2.\mathrm{I.a}}(|m|) = \{B_1, 0, 0, 0, 0, 0, 0, 0, 0, 0, 0, 0\}^T\,, \tag{5.63}$$

The remaining DoFs are $\{\sigma, \beta_i, \mathcal{Z}_i, \mathcal{Y}_i, h_{ij}\}$ in the massless sector and $\{\delta\phi\}$ in the massive sector. The electric components of the Riemann tensor for the respective cases are given by

$$\mathring{R}_{0i0j}\left(Y_{2.\mathrm{I.a}}(|k|)\right) = \begin{pmatrix} A_4 & A_5 & 0 \\ A_5 & -A_4 & 0 \\ 0 & 0 & 0 \end{pmatrix}, \qquad \mathring{R}_{0i0j}\left(Y_{2.\mathrm{I.a}}(|m|)\right) = \begin{pmatrix} 0 & 0 & 0 \\ 0 & 0 & 0 \\ 0 & 0 & 0 \end{pmatrix}. \tag{5.64}$$

Hence, while the scalar σ in the massless sector and the scalar $\delta\phi$ in the massive sector are said to be propagating DoFs, they do not contribute to the polarisation modes. Moreover, the massive sector shows that no polarisation modes are detected in Eq. (5.64). Although their influence may not be directly observable by GW interferometers, σ and $\delta\phi$ could still impact the cosmological growth of structures, the overall expansion of the Universe, and the strong-field regime. This result can mimic the behaviour of GR, although the amplitudes at which the tensor modes are observed would not necessarily be identical.

Case 2.I.b The other scenario arises when $\tilde{c}_3 = 0$ and $\tilde{c}_4 = 0$, which reduces the determinant to

$$P_{2.\mathrm{I.b}}(k) = \tfrac{131072}{19683}(G_4 - G_{\mathrm{Tele},T})^8\,(G_{\mathrm{Tele},T_{\mathrm{ax}}})^3\,k^{12}\big(\omega^2 - k^2\big)^7\,, \tag{5.65}$$

where only a massless solution can be obtained with a nullspace solution given by

$$Y_{2.\mathrm{I.b}}(\omega) = \{\mathcal{X}_2, \mathcal{X}_4, \sigma, \beta_{i_1}, \beta_{i_2}, \mathcal{Z}_{i_1}, \mathcal{Z}_{i_2}, \mathcal{Y}_{i_1}, \mathcal{Y}_{i_2}, h_{ij_1}, h_{ij_2}\}^T\,, \tag{5.66}$$

$$Y_{2.\mathrm{I.b}}(|k|) = \big\{0, 0, A_1, -A_2, -A_3, i\,|k|\,A_2, i|k|A_3, A_2, A_3, , \tfrac{2}{k^2}A_4, \tfrac{2}{k^2}A_5\big\}^T\,. \tag{5.67}$$

The only DoF which drops out from the system is $\delta\phi$ but the massless sector appears identical to Case 2.I.a explored in Sec. 5.4.2.1. While other DoFs are seen to propagate, only the tensor modes leave an imprint on the polarisation of the system with the electrical component of the Riemann tensor being

$$\mathring{R}_{0i0j}\left(Y_{\text{2.I.b}}(|k|)\right) = \begin{pmatrix} A_4 & A_5 & 0 \\ A_5 & -A_4 & 0 \\ 0 & 0 & 0 \end{pmatrix} . \tag{5.68}$$

Therefore, the main distinction between Case 2.I.a and Case 2.I.b is that the former has an additional DoF. In the field of GW studies, such a difference can manifest only when examining the intricacies of the inspiral merger of two massive objects such as blackholes, neutron stars, and pulsars. Both subclasses indicate no polarisation mode in the massive sector.

5.4.2.2 | Case 2.II

The other solutions $\tilde{c}_1 = \tilde{c}_2 = 0$ are given by

$$G_{3,\phi} = Z_2 \qquad \text{and} \qquad G_{2,\phi\phi} = -G_{\text{Tele},\phi\phi}\,, \tag{5.69}$$

which allow for $2(G_4 - G_{\text{Tele},T}) + 3G_{\text{Tele},T_{\text{vec}}} \neq 0$ and $G_{\text{Tele},I_2} - 2G_{4,\phi} \neq 0$, although not necessarily, giving rise to two scenarios.

Case 2.II.a The first scenario is the Case 2.II without any further modifications such that $2(G_4 - G_{\text{Tele},T}) + 3G_{\text{Tele},T_{\text{vec}}} \neq 0$. The determinant becomes

$$P(k) = \tfrac{16384}{243}(G_4 - G_{\text{Tele},T})^5 \left(G_{\text{Tele},T_{\text{vec}}}\right)^3 \left(G_{\text{Tele},T_{\text{ax}}}\right)^3 (G_{\text{Tele},I_2} - 2G_{4,\phi})k^{12} \left(\omega^2 - k^2\right)^8 , \tag{5.70}$$

which, when set to zero, results only in a massless case of $\omega = \pm k$ such that the nullspace solutions are

$$Y_{\text{2.II.a}}(\omega) = \{\delta\phi, \psi, \mathcal{X}_4, \sigma, \beta_{i_1}, \beta_{i_2}, \mathcal{Z}_{i_1}, \mathcal{Z}_{i_2}, \mathcal{Y}_{i_1}, \mathcal{Y}_{i_2}, h_{ij_1}, h_{ij_2}\}^T , \tag{5.71}$$

$$Y_{\text{2.II.a}}(|k|) = \Big\{ -\tfrac{4(G_4 - G_{\text{Tele},T} + G_{\text{Tele},T_{\text{vec}}})}{(G_{\text{Tele},I_2} - 2G_{4,\phi})k^2} A_1, -\tfrac{1}{k^2}A_1, \tfrac{i}{k^3}A_1, A_2, \\ -A_3, -A_4, ikA_3, ikA_4, A_3, A_4, \tfrac{2}{k^2}A_5, \tfrac{2}{k^2}A_6 \Big\}^T . \tag{5.72}$$

All modes available in the theory are DoFs. The denominator of $G_{\text{Tele},I_2} - 2G_{4,\phi}$ should not vanish as it would result in an undefined region. The polarisation modes which can be detected

are

$$\mathring{R}_{0i0j}\left(Y_{2.\mathrm{II.a}}(|k|)\right) = \begin{pmatrix} A_1 + A_5 & A_6 & 0 \\ A_6 & A_1 - A_5 & 0 \\ 0 & 0 & 0 \end{pmatrix}, \tag{5.73}$$

corresponding to the scalar ψ and the tensor modes h_+ and $h_\times$. In this case, a propagating GW would cause matter to stretch and squeeze in orthogonal directions, as described by the tensor modes, while the additional scalar mode manifests as an isotropic expansion or contraction. Unlike Case 1, the breathing mode in this scenario arises solely from a relativistic mode.

Case 2.II.b On the other hand, if $G_{\mathrm{Tele},I_2} - 2G_{4,\phi} = 0$, the determinant is altered. Provided $G_4 - G_{\mathrm{Tele},T} + G_{\mathrm{Tele},T_{\mathrm{vec}}} \neq 0$, the principal polynomial and massless solution are given by

$$\begin{aligned} P_{2.\mathrm{II.b.1}}(k) &= -\tfrac{16384}{243}(G_4 - G_{\mathrm{Tele},T})^4 \\ &\quad \times (G_{\mathrm{Tele},T_{\mathrm{vec}}} G_{\mathrm{Tele},T_{\mathrm{ax}}})^3 (G_4 - G_{\mathrm{Tele},T} + G_{\mathrm{Tele},T_{\mathrm{vec}}}) k^{12} (\omega^2 - k^2)^7 , \qquad (5.74) \\ Y_{2.\mathrm{II.b.1}}(\omega) &= \{\mathcal{X}_2, \mathcal{X}_4, \sigma, \beta_{i_1}, \beta_{i_2}, \mathcal{Z}_{i_1}, \mathcal{Z}_{i_2}, \mathcal{Y}_{i_1}, \mathcal{Y}_{i_2}, h_{ij_1}, h_{ij_2}\}^T , \qquad (5.75) \\ Y_{2.\mathrm{II.b.1}}(|k|) &= \left\{0, 0, A_1, -A_2, -A_3, i|k|A_2, i|k|A_3, A_2, A_3, \tfrac{2}{k^2}A_4, \tfrac{2}{k^2}A_5\right\}^T . \qquad (5.76) \end{aligned}$$

$\mathcal{X}_2$ and $\mathcal{X}_4$ drop from the list of propagating DoFs, and only pseudoscalar, vector and tensor modes contribute. If $G_4 - G_{\mathrm{Tele},T} + G_{\mathrm{Tele},T_{\mathrm{vec}}} = 0$, the determinant further simplifies to

$$\begin{aligned} P_{2.\mathrm{II.b.2}}(k) &= -\tfrac{4096}{243} i (G_4 - G_{\mathrm{Tele},T})^7 (G_{\mathrm{Tele},T_{\mathrm{ax}}})^3 \omega k^8 (\omega^2 - k^2)^7 , \qquad (5.77) \\ Y_{2.\mathrm{II.b.2}}(\omega) &= \{\mathcal{X}_2, \sigma, \beta_{i_1}, \beta_{i_2}, \mathcal{Z}_{i_1}, \mathcal{Z}_{i_2}, \mathcal{Y}_{i_1}, \mathcal{Y}_{i_2}, h_{ij_1}, h_{ij_2}\}^T , \qquad (5.78) \\ Y_{2.\mathrm{II.b.2}}(|k|) &= \left\{0, A_1, -A_2, -A_3, i|k|A_2, i|k|A_3, A_2, A_3, \tfrac{2}{k^2}A_4, \tfrac{2}{k^2}A_5\right\}^T . \qquad (5.79) \end{aligned}$$

When comparing to the latter two cases, the same propagating DoFs are present despite the models being different. Moreover, both solutions $Y_{2.II.b.1}$ and $Y_{2.II.b.2}$ result in polarisation modes similar in nature. The electric components of the Riemann tensor are given by

$$\mathring{R}_{0i0j}\left(Y_{2.\mathrm{II.b}}(|k|)\right) = \begin{pmatrix} A_4 & A_5 & 0 \\ A_5 & -A_4 & 0 \\ 0 & 0 & 0 \end{pmatrix}, \tag{5.80}$$

with only tensor modes being detectable.

5.4.3 | Case 3: $G_{\text{Tele},T_{\text{vec}}} \neq 0\,, G_{\text{Tele},T_{\text{ax}}} = 0\,, \tilde{c}_1 \neq 0\,, \tilde{c}_2 \neq 0$

The next branch sets the axial portion of the torsion tensor to vanish such that the model has

$$G_{\text{Tele},T_{\text{vec}}} \neq 0\,, \qquad G_{\text{Tele},T_{\text{ax}}} = 0\,, \qquad \tilde{c}_1 \neq 0\,, \qquad \tilde{c}_2 \neq 0\,. \tag{5.81}$$

Only σ mode is eliminated from the block matrix in Eq. (5.16) while the rest of the coefficients simplify slightly such that the resulting determinant is given by

$$P_3(k) = -32i(G_4 - G_{\text{Tele},T})^5 \left(G_{\text{Tele},T_{\text{vec}}}\right)^3 \omega^2 k^{10} \left(\omega^2 - k^2\right)^3 \left(\tilde{c}_1 + \tilde{c}_2 \left(\omega^2 - k^2\right)\right)\,, \tag{5.82}$$

and when it is set to zero, attains a massless and a massive sector. Hence, the nullspace solutions become

$$Y_3(\omega) = \{\delta\phi, \psi, \mathcal{X}_2, \mathcal{X}_4, \beta_{i_1}, \beta_{i_2}, \mathcal{Z}_{i_1}, \mathcal{Z}_{i_2}, h_{ij_1}, h_{ij_2}\}\,, \tag{5.83}$$

$$\begin{aligned} Y_3(|k|) = \Big\{0, -\tfrac{A_1}{k^2}, -\tfrac{2(G_4 - G_{\text{Tele},T} + G_{\text{Tele},T_{\text{vec}}})}{(G_{\text{Tele},T_{\text{vec}}})k^2} A_1, \\ \tfrac{i(2(G_4 - G_{\text{Tele},T}) + 3G_{\text{Tele},T_{\text{vec}}})}{(G_{\text{Tele},T_{\text{vec}}})|k|^3} A_1, 0, 0, 0, 0, \tfrac{2}{k^2} A_2, \tfrac{2}{k^2} A_3 \Big\}^T\,, \end{aligned} \tag{5.84}$$

$$\begin{aligned} Y_3(|m|) = \{-2(2(G_4 - G_{\text{Tele},T}) + 3G_{\text{Tele},T_{\text{vec}}})B_1, \\ -(G_{\text{Tele},I_2} - 2G_{4,\phi})B_1, (G_{\text{Tele},I_2} - 2G_{4,\phi})B_1, 0, 0, 0, 0, 0, 0, 0\}^T\,, \end{aligned} \tag{5.85}$$

emphasising $G_{\text{Tele},T_{\text{vec}}} \neq 0$ as it appears in the denominator in the nullspace solution for the massless sector. The electric components of the Riemann tensor, respectively, are given by

$$\mathring{R}_{0i0j}\left(Y_3(|k|)\right) = \begin{pmatrix} A_1 + A_2 & A_3 & 0 \\ A_3 & A_1 - A_2 & 0 \\ 0 & 0 & 0 \end{pmatrix}\,, \tag{5.86}$$

$$\mathring{R}_{0i0j}\left(Y_3(|m|)\right) = (G_{\text{Tele},I_2} - 2G_{4,\phi}) \begin{pmatrix} \left(m^2 + k^2\right)B_1 & 0 & 0 \\ 0 & \left(m^2 + k^2\right)B_1 & 0 \\ 0 & 0 & m^2 B_1 \end{pmatrix}\,. \tag{5.87}$$

The massive sector has contributions from the scalar modes $\{\delta\phi, \psi, \mathcal{X}_2\}$ whose combination boils down to a solution proportional to B_1. Both sectors appear to have an identical form as that of Case 1 shown in Eqs (5.56-5.57), including the same condition $(G_{\text{Tele},I_2} - 2G_{4,\phi}) = 0$ to produce a hidden massive scalar polarisation. Albeit similar, the number of propagating DoFs is less in Case 3 as this case contains fewer propagating DoFs.

5.4.4 | Case 4: $G_{\text{Tele},T_{\text{vec}}} \neq 0\,, G_{\text{Tele},T_{\text{ax}}} = 0\,, \tilde{c}_1 = 0\,, \tilde{c}_2 = 0$

Case 4 resembles the Case 2 branch discussed in Sec. 5.4.2, except for the addition of the extra condition $T_{\text{ax}} = 0$, such that

$$G_{\text{Tele},T_{\text{vec}}} \neq 0\,, \qquad G_{\text{Tele},T_{\text{ax}}} = 0\,, \qquad \tilde{c}_1 = 0\,, \qquad \tilde{c}_2 = 0\,. \tag{5.88}$$

The omission of T_{ax} creates a great distinction in the number of DoFs contributing to the polarisation modes. Analogous to Case 2, further subcases arise, and a similar procedure is applied.

5.4.4.1 | Case 4.I

Without imposing any further conditions, hence corresponding to the general scenario that Case 4 by Eq. (5.88) provides, constants $\tilde{c}_1 = 0$ and $\tilde{c}_2 = 0$ are rearranged to obtain the limits

$$G_{\text{Tele},T_{\text{vec}}} = -\tfrac{2}{3}(G_4 - G_{\text{Tele},T}) \qquad \text{and} \qquad G_{4,\phi} = \tfrac{1}{2}G_{\text{Tele},I_2}\,, \tag{5.89}$$

yielding a principal polynomial of the form

$$P_{4.\text{I}}(k) = \tfrac{256}{81} i (G_4 - G_{\text{Tele},T})^8 \omega^2 k^{10} \left(\omega^2 - k^2\right)^2 \left(\tilde{c}_3 + \tilde{c}_4 \left(\omega^2 - k^2\right)\right)\,, \tag{5.90}$$

resulting in another branch of solutions surrounding the behaviour of the constants $\tilde{c}_3$ and $\tilde{c}_4$. The general solution of $P_{4.\text{I}}(k) = 0$ provides both massless and massive sectors, but if $\tilde{c}_3 = \tilde{c}_4 = 0$ the entire system is transformed and the analysis would need to be done separately.

Case 4.I.a Given $\tilde{c}_3 \neq 0$ and $\tilde{c}_4 \neq 0$, the principal polynomial in Eq. (5.90) becomes

$$P_{4.\text{I.a}}(k) = P_{4.\text{I}}(k)\,. \tag{5.91}$$

The propagating DoFs are identified for both the massless and massive sectors:

$$Y_{4.\text{I.a}}(\omega) = \{\delta\phi, \psi, \mathcal{X}_4, \beta_{i_1}, \beta_{i_2}, \mathcal{Z}_{i_1}, \mathcal{Z}_{i_2}, h_{ij_1}, h_{ij_2}\}^T\,, \tag{5.92}$$

$$Y_{4.\text{I.a}}(|k|) = \{0, 0, 0, 0, 0, 0, 0, \tfrac{2}{k^2}A_1, \tfrac{2}{k^2}A_2\}^T\,, \tag{5.93}$$

$$Y_{4.\text{I.a}}(|m|) = \{B_1, 0, 0, 0, 0, 0, 0, 0, 0\}^T\,. \tag{5.94}$$

In the massless sector, only the tensor modes h_{ij} are seen to propagate even though scalar and vector modes are present in the field equations. On the other hand, the massive sector is dictated

by $\delta\phi$ which stems from the scalar inclusion of scalar-tensor theories. Eq. (5.43) gives

$$\mathring{R}_{0i0j}\left(Y_{4.\mathrm{I.a}}(|k|)\right) = \begin{pmatrix} A_1 & A_2 & 0 \\ A_2 & -A_1 & 0 \\ 0 & 0 & 0 \end{pmatrix}, \qquad \mathring{R}_{0i0j}\left(Y_{4.\mathrm{I.a}}(|m|)\right) = \begin{pmatrix} 0 & 0 & 0 \\ 0 & 0 & 0 \\ 0 & 0 & 0 \end{pmatrix}, \tag{5.95}$$

for both sectors. While the massive sectors contain propagating DoFs, the electric components of the Ricci scalar show that none of them contribute to the polarisation of GWs.

Case 4.I.b Next, consider the subcase when $\tilde{c}_3 = 0$ and $\tilde{c}_4 = 0$. These two equations are rearranged to obtain $G_{3,\phi} = \frac{1}{2}(G_{\mathrm{Tele},X} + G_{2,X})$ and $G_{2,\phi\phi} = -G_{\mathrm{Tele},\phi\phi}$, for which the principal polynomial becomes

$$P_{4.\mathrm{I.b}}(k) = \tfrac{256}{81} i (G_4 - G_{\mathrm{Tele},T})^8 \omega^2 k^{10} \left(\omega^2 - k^2\right)^2 , \tag{5.96}$$

providing a solution for the massless sector only, such that

$$Y_{4.\mathrm{I.b}}(\omega) = \{\psi, \mathcal{X}_5, \beta_{i_1}, \beta_{i_2}, \mathcal{Z}_{i_1}, \mathcal{Z}_{i_2}, h_{ij_1}, h_{ij_2}\}^T , \tag{5.97}$$

$$Y_{4.\mathrm{I.b}}(|k|) = \left\{0, 0, 0, 0, 0, 0, \tfrac{2}{k^2} A_1, \tfrac{2}{k^2} A_2\right\}^T , \tag{5.98}$$

since $\delta\phi$ contribution drops from the field equations. The polarisation modes, determined from $\mathring{R}_{0i0j}$ in Eq. (5.43) shows a result similar in nature to Case 4.I.a on page 112 such that $\mathring{R}_{0i0j}\left(Y_{4.\mathrm{I.b}}(|k|)\right) = \mathring{R}_{0i0j}\left(Y_{4.\mathrm{I.a}}(|k|)\right)$.

5.4.4.2 | Case 4.II

Along with the conditions presented in Eq. (5.88), additional constraints are considered which stem from the solution of $\tilde{c}_1 = 0$ and $\tilde{c}_2 = 0$ not considered in Case 4.I in Sec. 5.4.4.1:

$$G_{3,\phi} = Z_2 , \qquad G_{2,\phi\phi} = -G_{\mathrm{Tele},\phi\phi} , \qquad 2(G_4 - G_{\mathrm{Tele},T}) + 3G_{\mathrm{Tele},T_{\mathrm{vec}}} \neq 0 . \tag{5.99}$$

The determinant alters to

$$P_{4.\mathrm{II}}(k) = -32 i (G_4 - G_{\mathrm{Tele},T})^5 \left(G_{\mathrm{Tele},T_{\mathrm{vec}}}\right)^3 (G_{\mathrm{Tele},I_2} - 2G_{4,\phi}) \omega^2 k^{10} \left(\omega^2 - k^2\right)^3 , \tag{5.100}$$

immediately eliminating the possibility of having a massive sector. Now, only the conditions for $G_{\mathrm{Tele},I_2} - 2G_{4,\phi}$ would dictate the subcases of Case 4.II by further specifying constraints.

Case 4.II.a Provided $G_{\text{Tele},I_2} - 2G_{4,\phi} \neq 0$, the principal polynomial remains the same, i.e.

$$P_{4.\text{II.a}}(k) = P_{4.\text{II}}(k)\,, \tag{5.101}$$

for which the nullspace solution can be obtained only for the massless sector:

$$Y_{4.\text{II.a}}(\omega) = \{\delta\phi, \psi, \mathcal{X}_4, \beta_{i_1}, \beta_{i_2}, \mathcal{Z}_{i_1}, \mathcal{Z}_{i_2}, h_{ij_1}, h_{ij_2}\}\,, \tag{5.102}$$

$$Y_{4.\text{II.a}}(|k|) = \left\{-\tfrac{4(G_4 - G_{\text{Tele},T} + G_{\text{Tele},T\text{vec}})}{(G_{\text{Tele},I_2} - 2G_{4,\phi})k^2}A_1, -\tfrac{1}{k^2}A_1, \tfrac{i}{|k|^3}A_1, 0, 0, 0, 0, \tfrac{2}{k^2}A_2, \tfrac{2}{k^2}A_3\right\}^T\,. \tag{5.103}$$

The form of this branch is very distinct from Case 4.I.a in Sec. 5.4.4.1 as both scalar and tensor modes are propagating DoFs. Specifically, all scalar modes $\{\delta\phi, \psi, \mathcal{X}_4\}$ present in field equations contribute. The polarisation modes which persist are

$$\mathring{R}_{0i0j}\left(Y_{4.\text{II.a}}(|k|)\right) = \begin{pmatrix} A_1 + A_2 & A_3 & 0 \\ A_3 & A_1 - A_2 & 0 \\ 0 & 0 & 0 \end{pmatrix}\,. \tag{5.104}$$

such that in addition to the tensor modes, there is a scalar mode propagating which sets it apart from other subcases obtained through Case 4 (Sec. 5.4.4). Only the print of scalar ψ appears in the system, as it cancels out the contributions of $\mathcal{X}_4$ in the longitudinal contribution which corresponds to the last entry of the matrix.

Case 4.II.b Adding the condition $G_{\text{Tele},I_2} - 2G_{4,\phi} = 0$ while $G_4 - G_{\text{Tele},T} + G_{\text{Tele},T_{\text{vec}}} \neq 0$ leads to

$$\begin{aligned} P_{4.\text{II.b.1}}(k) &= 32i\omega^2 k^{10}(\omega^2 - k^2)^2 \\ &\quad \times (G_4 - G_{\text{Tele},T})^4 (G_{\text{Tele},T_{\text{vec}}})^3 (G_4 - G_{\text{Tele},T} + G_{\text{Tele},T_{\text{vec}}})\,, \end{aligned} \tag{5.105}$$

$$Y_{4.\text{II.b.1}}(\omega) = \{\psi, \mathcal{X}_5, \beta_{i_1}, \beta_{i_2}, \mathcal{Z}_{i_1}, \mathcal{Z}_{i_2}, h_{ij_1}, h_{ij_2}\}^T\,, \tag{5.106}$$

But, if $G_4 - G_{\text{Tele},T} + G_{\text{Tele},T_{\text{vec}}} = 0$, the invariant $\mathcal{X}_4$ is eliminated from the possible solution as given by

$$P_{4.\text{II.b.2}}(k) = -8(G_4 - G_{\text{Tele},T})^7 \omega^3 k^6 \left(\omega^2 - k^2\right)^2\,, \tag{5.107}$$

$$Y_{4.\text{II.b.2}}(\omega) = \{\psi, \beta_{i_1}, \beta_{i_2}, \mathcal{Z}_{i_1}, \mathcal{Z}_{i_1}, h_{ij_1}, h_{ij_2}\}^T\,. \tag{5.108}$$

While the setups of these two scenarios appear different, both realise the same nature of propagating DoFs:

$$Y_{4.\text{II.b}}(|k|) = \left\{0, 0, 0, 0, 0, \tfrac{2}{k^2}A_1, \tfrac{2}{k^2}A_2\right\}^T\,, \tag{5.109}$$

and the polarisation modes

$$\mathring{R}_{0i0j}\left(Y_{4.\mathrm{II.b}}(|k|)\right) = \begin{pmatrix} A_1 & A_2 & 0 \\ A_2 & -A_1 & 0 \\ 0 & 0 & 0 \end{pmatrix}, \tag{5.110}$$

replicating the behaviour similar to Case 4.I.b in Sec. 5.4.4.1

5.4.5 | Case 5: $G_{\mathrm{Tele},T_{\mathrm{vec}}} = 0\,, G_{\mathrm{Tele},T_{\mathrm{ax}}} \neq 0\,, \tilde{c}_1 \neq 0\,, \tilde{c}_2 \neq 0$

The following cases will be carried out with the omission of the vectorial torsion tensor contribution. The first of such cases is given by the conditions

$$G_{\mathrm{Tele},T_{\mathrm{vec}}} = 0\,, \qquad G_{\mathrm{Tele},T_{\mathrm{ax}}} \neq 0\,, \qquad \tilde{c}_1 \neq 0\,, \qquad \tilde{c}_2 \neq 0\,, \tag{5.111}$$

where the determinant from the respective block matrix is given by

$$P(k) = -\tfrac{2048}{243} i (G_4 - G_{\mathrm{Tele},T})^5 \left(G_{\mathrm{Tele},T_{\mathrm{ax}}}\right)^3 \omega^2 k^{10} \left(\omega^2 - k^2\right)^3 \left(\tilde{c}_1 + \tilde{c}_2 \left(\omega^2 - k^2\right)\right)\,, \tag{5.112}$$

The massless sector for $\omega^2 - k^2 = 0$ and massive sector for $\tilde{c}_1 + \tilde{c}_2 \left(\omega^2 - k^2\right) = 0$ provide possible solutions of the nullspace to determine the propagating DoFs:

$$Y_5(\omega) = \{\delta\phi, \psi, \mathcal{X}_2, \sigma, \beta_{i_1}, \beta_{i_2}, \mathcal{Z}_{i_1}, \mathcal{Z}_{i_2}, h_{ij_1}, h_{ij_2}\}^T\,, \tag{5.113}$$

$$Y_5(|k|) = \left\{0, 0, 0, A_1, 0, 0, 0, 0, \tfrac{2}{k^2} A_2, \tfrac{2}{k^2} A_3\right\}^T\,, \tag{5.114}$$

$$Y_5(|m|) = -(G_{\mathrm{Tele},I_2} - 2G_{4,\phi}) \left\{\tfrac{4(G_4 - G_{\mathrm{Tele},T})}{(G_{\mathrm{Tele},I_2} - 2G_{4,\phi})} B_1, B_1, -B_1, 0, 0, 0, 0, 0, 0, 0\right\}^T\,. \tag{5.115}$$

The denominator present in the massive sector for mode $\delta\phi$ is balanced out by the common factor of $G_{\mathrm{Tele},I_2} - 2G_{4,\phi}$, allowing to have cases where this expression is zero. The electric components of the Riemann tensor are given by

$$\mathring{R}_{0i0j}\left(Y_5(|k|)\right) = \begin{pmatrix} A_2 & A_3 & 0 \\ A_3 & -A_2 & 0 \\ 0 & 0 & 0 \end{pmatrix} \tag{5.116}$$

for the massless sector. This shows that $\mathcal{X}_2$, the only propagating DoF, does not contribute to the polarisation imprint. For the massive sector, the result changes to

$$\mathring{R}_{0i0j}\left(Y_5(|k|)\right) = (G_{\mathrm{Tele},I_2} - 2G_{4,\phi}) \begin{pmatrix} \left(m^2 + k^2\right) B_1 & 0 & 0 \\ 0 & \left(m^2 + k^2\right) B_1 & 0 \\ 0 & 0 & m^2 B_1 \end{pmatrix}, \tag{5.117}$$

implying that now there is a dependency on the condition $G_{\text{Tele},I_2} - 2G_{4,\phi} \neq 0$ to realise polarisation modes. Unlike Case 1 and Case 3, the breathing mode appears alongside the longitudinal mode in the massive sector only, meaning a non-relativistic graviton is responsible for the isotropic expansion/contraction.

5.4.6 | Case 6: $G_{\text{Tele},T_{\text{vec}}} = 0\,, G_{\text{Tele},T_{\text{ax}}} \neq 0\,, \tilde{c}_1 = 0\,, \tilde{c}_2 = 0$

Similar to other cases which include the vanishing $\tilde{c}_1$ and $\tilde{c}_2$, explored in Case 2 in Sec. 5.4.2 and in Case 4 in Sec.5.4.4, numerous subcases emerge. Case 6 starts with the conditions of

$$G_{\text{Tele},T_{\text{vec}}} = 0\,, \qquad G_{\text{Tele},T_{\text{ax}}} \neq 0\,, \qquad \tilde{c}_1 = 0\,, \qquad \tilde{c}_2 = 0\,, \tag{5.118}$$

where the latter equations are chosen to be recast in the following equations

$$G_{3,\phi} = \frac{3(G_{\text{Tele},I_2} - 2G_{4,\phi})^2}{8(G_4 - G_{\text{Tele},T})} + \frac{1}{2}(G_{\text{Tele},X} + G_{2,X})\,, \qquad G_{2,\phi\phi} = -G_{\text{Tele},\phi\phi}\,. \tag{5.119}$$

The subject of the formula does alter the appearance of the results but ultimately attains the same nature of results, which is the interest of the analysis. Regardless, the substitutions suggested here are favoured as the relationship $G_4 - G_{\text{Tele},T} \neq 0$ has already been imposed to attain tensor modes, ensuring the equations do not result in undefined scenarios. The principal polynomial becomes

$$P_6(k) = -\frac{2048}{243} i (G_4 - G_{\text{Tele},T})^5 \left(G_{\text{Tele},T_{\text{ax}}}\right)^3 (G_{\text{Tele},I_2} - 2G_{4,\phi}) \omega^2 k^{10} \left(\omega^2 - k^2\right)^3\,, \tag{5.120}$$

leading to several solely massless solutions corresponding to a variety of limits.

5.4.6.1 | Case 6.I

By imposing $G_{\text{Tele},I_2} - 2G_{4,\phi} \neq 0$, the generalised solution for Case 6 can be determined such that

$$P_{6.\text{I}}(k) = P_6(k)\,. \tag{5.121}$$

The nullspace solution obtained by setting the determinant to zero is given by

$$Y_{6.\text{I}}(\omega) = \{\delta\phi, \psi, \sigma, \beta_{i_1}, \beta_{i_2}, \mathcal{Z}i_1, \mathcal{Z}_{i_2}, h_{ij_1}, h_{ij_2}\}^T\,, \tag{5.122}$$

$$Y_{6.\text{I}}(|k|) = \left\{0, 0, A_1, 0, 0, 0, 0, \tfrac{2}{k^2}A_2, \tfrac{2}{k^2}A_3\right\}^T\,, \tag{5.123}$$

which holds for the massless case. Apart from the two tensor modes, the only other propagating DoF is contributed by the pseudoscalar σ. The Riemann tensor is given by

$$\mathring{R}_{0i0j}\left(Y_{6.\mathrm{I}}(|k|)\right) = \begin{pmatrix} A_2 & A_3 & 0 \\ A_3 & -A_2 & 0 \\ 0 & 0 & 0 \end{pmatrix} , \tag{5.124}$$

such that only the tensor polarisation modes remain. As expected, due to the Riemann tensor being constructed through the perturbation of the metric $\delta g_{\mu\nu}$ in Eq. (4.26), the pseudoscalar σ stemming from the antisymmetry of the tetrad, does not contribute to the electric components of the Riemann tensor since by definition it is symmetric.

5.4.6.2 | Case 6.II

The next subcase is for $G_{\mathrm{Tele},I_2} - 2G_{4,\phi} = 0$, modifying the principal polynomial to

$$P_{6.\mathrm{II}}(k) = \tfrac{2048}{243} i (G_4 - G_{\mathrm{Tele},T})^5 \left(G_{\mathrm{Tele},T_{\mathrm{ax}}}\right)^3 \omega^2 k^8 \left(\omega^2 - k^2\right)^3 . \tag{5.125}$$

From this polynomial, no further subcases can be obtained unless a different branch is considered where $T_{\mathrm{ax}} = 0$. This case eliminates the $\delta\phi$ scalar as a possible contributing factor as shown in the nullspace analysis given by

$$Y_{6.\mathrm{II}}(\omega) = \{\psi, \sigma, \beta_{i_1}, \beta_{i_2}, \mathcal{Z}_{i_1}, \mathcal{Z}_{i_2}, h_{ij_1}, h_{ij_2}\}^T , \tag{5.126}$$

$$Y_{6.\mathrm{II}}(|k|) = \left\{0, A_1, 0, 0, 0, 0, \tfrac{2}{k^2} A_2, \tfrac{2}{k^2} A_3\right\}^T . \tag{5.127}$$

This omission does not contribute to any additional polarisation modes, thus the $\mathring{R}_{0i0j}$ remains the same as Case 6.I:

$$\mathring{R}_{0i0j}\left(Y_{6.\mathrm{II}}(|k|)\right) = \mathring{R}_{0i0j}\left(Y_{6.\mathrm{I}}(|k|)\right) . \tag{5.128}$$

It should be noted that the equivalence between the two results only holds for the nature of the polarisation modes, and the actual expressions for these modes will change according to the expressions of the gravitational theory being represented by the particular subcase.

5.4.7 | Case 7: $G_{\mathrm{Tele},T_{\mathrm{vec}}} = 0\,, G_{\mathrm{Tele},T_{\mathrm{ax}}} = 0\,, \tilde{c}_1 \neq 0\,, \tilde{c}_2 \neq 0$

The remaining cases investigate the cases for gravitational theories independent of T_{ax} and T_{vec}, starting with the particular case

$$G_{\mathrm{Tele},T_{\mathrm{vec}}} = 0\,, \qquad G_{\mathrm{Tele},T_{\mathrm{ax}}} = 0\,, \qquad \tilde{c}_1 \neq 0\,, \qquad \tilde{c}_2 \neq 0\,, \tag{5.129}$$

giving the principal polynomial of the form

$$P_7(k) = -4(G_4 - G_{\text{Tele},T})^5(\omega^2 - k^2)^2 k^8 \left(\tilde{c}_1 + \tilde{c}_2\left(\omega^2 - k^2\right)\right) , \tag{5.130}$$

where separate solutions are attained for the massless sector when $\omega = \pm k$ and massive sector with mass $m = -\frac{\tilde{c}_1}{\tilde{c}_2}$.

$$Y_7(\omega) = \{\delta\phi, \psi, \mathcal{X}_2, \beta_{i_1}, \beta_{i_2}, h_{ij_1}, h_{ij_2}\}^T , \tag{5.131}$$

$$Y_7(|k|) = \left\{0, 0, 0, 0, 0, \tfrac{2}{k^2}A_1, \tfrac{2}{k^2}A_2\right\}^T , \tag{5.132}$$

$$Y_7(|m|) = -(G_{\text{Tele},I_2} - 2G_{4,\phi}) \left\{\tfrac{4(G_4 - G_{\text{Tele},T})}{G_{\text{Tele},I_2} - 2G_{4,\phi}} B_1, B_1, -B_1, 0, 0, 0, 0\right\}^T , \tag{5.133}$$

where the massless sector provides the two tensor modes as propagating DoFs, and the massive sector produces one DoF appearing for the scalars $\delta\phi, \psi, \mathcal{X}_2$ scalars. The respective Riemann tensor components are

$$\mathring{R}_{0i0j}\left(Y_7(|k|)\right) = \begin{pmatrix} A_1 & A_2 & 0 \\ A_2 & -A_1 & 0 \\ 0 & 0 & 0 \end{pmatrix} , \tag{5.134}$$

$$\mathring{R}_{0i0j}\left(Y_7(|m|)\right) = (G_{\text{Tele},I_2} - 2G_{4,\phi}) \begin{pmatrix} \left(m^2 + k^2\right) B_1 & 0 & 0 \\ 0 & \left(m^2 + k^2\right) B_1 & 0 \\ 0 & 0 & m^2 B_1 \end{pmatrix} . \tag{5.135}$$

In this case, all the propagating DoFs realised from the theory also appear as contributing polarisation modes of a GW. In the previous cases explored, the symmetric properties of the Riemann tensor have eliminated at least one of the DoFs. This is largely because the majority of constants have been set to vanish, corresponding to the terms that appear in the antisymmetry of the field equations such as $G_{\text{Tele},T_{\text{ax}}}$ and $G_{\text{Tele}_{T_{\text{vec}}}}$.

5.4.8 | Case 8: $G_{\text{Tele},T_{\text{vec}}} = 0\,, G_{\text{Tele},T_{\text{ax}}} = 0\,, \tilde{c}_1 = 0\,, \tilde{c}_2 = 0$

The final case is given by the combination

$$G_{\text{Tele},T_{\text{vec}}} = 0\,, \qquad G_{\text{Tele},T_{\text{ax}}} = 0\,, \qquad \tilde{c}_1 = 0\,, \qquad \tilde{c}_2 = 0\,. \tag{5.136}$$

The solutions of $\tilde{c}_1 = 0$ and $\tilde{c}_2 = 0$ are written as

$$G_{3,\phi} = \frac{3(G_{\text{Tele},I_2} - 2G_{4,\phi})^2}{8(G_4 - G_{\text{Tele},T})} + \tfrac{1}{2}(G_{\text{Tele},X} + G_{2,X})\,, \qquad G_{2,\phi\phi} = -G_{\text{Tele},\phi\phi}\,. \tag{5.137}$$

For these solutions, the principal polynomial expression (5.18) simplifies to

$$P_8(k) = 4(G_4 - G_{\text{Tele},T})^5(G_{\text{Tele},I_2} - 2G_{4,\phi})k^8\left(\omega^2 - k^2\right)^2 . \tag{5.138}$$

Setting the determinant to zero results in two additional subcases dictated by the expression $G_{\text{Tele},I_2} - 2G_{4,\phi}$.

5.4.8.1 | Case 8.I

The first of these cases leaves the principal polynomial unaltered

$$P_{8.\text{I}}(k) = P_8(k)\,, \tag{5.139}$$

by imposing that $G_{\text{Tele},I_2} - 2G_{4,\phi} \neq 0$. The nullspace solution of the block matrix containing a large number of vanishing terms is given by

$$Y_{8.\text{I}}(\omega) = \{\delta\phi, \psi, \beta_{i_1}, \beta_{i_2}, h_{ij_1}, h_{ij_2}\}^T\,, \tag{5.140}$$

$$Y_{8.\text{I}}(|k|) = \left\{0, 0, 0, 0, \tfrac{2}{k^2}A_1, \tfrac{2}{k^2}A_2\right\}^T\,, \tag{5.141}$$

generating only a massless solution with tensor propagating DoFs, and present themselves as the only polarisation modes:

$$\mathring{R}_{0i0j}\left(Y_{8.\text{I}}(|k|)\right) = \begin{pmatrix} A_1 & A_2 & 0 \\ A_2 & -A_1 & 0 \\ 0 & 0 & 0 \end{pmatrix} . \tag{5.142}$$

Once again, a large number of vanishing terms result in the omission of antisymmetric contributions, thus all propagating DoFs correspond to the polarisation modes.

5.4.8.2 | Case 8.II

Finally, when $G_{\text{Tele},I_2} - 2G_{4,\phi} = 0$, the principal polynomial becomes

$$P_{8.\text{II}}(k) = -4(G_4 - G_{\text{Tele},T})^5 k^6\left(\omega^2 - k^2\right)^2, \tag{5.143}$$

whose solution is solely dependent on the terms $G_4 - G_{\text{Tele},T}$. In contrast to the previous cases, the subcase of $G_4 - G_{\text{Tele},T} = 0$ is not considered as this would result in a system without tensor mode DoFs, thus contradicting the observations obtained in GR and the tensor mode natures

detected in the A-LIGO experiments detailed in Ref. [45]. Hence, $G_4 - G_{\text{Tele},T} \neq 0$ results in the nullspace solution of

$$Y_{8.\text{II}}(\omega) = \{\psi, \beta_{i_1}, \beta_{i_2}, h_{ij_1}, h_{ij_2}\}^T \ , \tag{5.144}$$

$$Y_{8.\text{II}}(|k|) = \left\{0, 0, 0, \tfrac{2A_1}{k^2}, \tfrac{2A_2}{k^2}\right\}^T \ , \tag{5.145}$$

where $\delta\phi$ is omitted from the system by nature of the limits from even being a possible DoF in comparison with Case 8.I evaluated in page 119 but results in similar electric components of the Riemann tensor:

$$\mathring{R}_{0i0j}\left(Y_{8.\text{II}}(|k|)\right) = \mathring{R}_{0i0j}\left(Y_{8.\text{I}}(|k|)\right) \ . \tag{5.146}$$

The results for the different branches of BDLS presented here have been obtained by checking the mathematical restrictions when solving the principal polynomial (5.18) which is set to vanish. While these branches may not directly correspond to theories of gravity that have been studied in the literature, they can be obtained by taking appropriate limits within the best-fit result. Table 5.3 offers a short list of gravitational theories and their corresponding BDLS cases as classified by the procedure in this chapter. These results only apply to a Minkowski background and constant background scalar field. Here, GR and $f(T)$ can both be described by Case 8 where only the tensor modes propagate. This is a good example to point out that if an FLRW background is considered the two theories would not have the same results. In Chapter 7 it will be shown that $f(T)$ can realise an additional scalar propagating DoF when considering a cosmological perturbation. The Horndeski case falls within category 7, with a total of 3 DoFs. While subcases of Horndeski gravity can be adequately placed in this category, like BD and GBD, others would be better suited within a different part of the branches, such as GR. Additionally, noting the drop in the number of DoFs when comparing Horndeski gravity to a case where G_{Tele} is the only function, shows how much the teleparallel portion of BDLS contributes. While not subclasses of Horndeski gravity, the likes of Generalised Teleparallel dark energy, Generalised Teleparallel Scalar Tensor, and Tachyonic Teleparallel Gravity share the same category.

Cases	**Conditions**	**Sectors**					**DoF**
		Massless			Massive		
		S	V	T	S	m^2	
1	$G_{\mathrm{Tele},T_{\mathrm{vec}}} \neq 0,\, G_{\mathrm{Tele},T_{\mathrm{ax}}} \neq 0, \tilde{c}_1 \neq 0, \tilde{c}_2 \neq 0$	2	1	1	1	$-\frac{\tilde{c}_1}{\tilde{c}_2}$	7
2	$G_{\mathrm{Tele},T_{\mathrm{vec}}} \neq 0,\, G_{\mathrm{Tele},T_{\mathrm{ax}}} \neq 0, \tilde{c}_1 = 0, \tilde{c}_2 = 0$						
2.I	$G_{\mathrm{Tele},T_{\mathrm{ax}}} \neq 0, \tilde{c}_3 \neq 0, \tilde{c}_4 \neq 0$						
2.I.a	$G_{\mathrm{Tele},T_{\mathrm{ax}}} \neq 0, \tilde{c}_3 \neq 0, \tilde{c}_4 \neq 0$	1	1	1	1	$-\frac{\tilde{c}_3}{\tilde{c}_4}$	6
2.I.b	$G_{\mathrm{Tele},T_{\mathrm{ax}}} \neq 0, \tilde{c}_3 = 0, \tilde{c}_4 = 0$	1	1	1	-	-	5
2.II	$G_{3,\phi} = Z_2,\, G_{2,\phi\phi} = -G_{\mathrm{Tele},\phi\phi}$						
2.II.a	$G_{\mathrm{Tele},I_2} - 2G_{4,\phi} \neq 0$	2	1	1	-	-	6
2.II.b	$G_{\mathrm{Tele},I_2} - 2G_{4,\phi} = 0$	1	1	1	-	-	5
3	$G_{\mathrm{Tele},T_{\mathrm{vec}}} \neq 0,\, G_{\mathrm{Tele},T_{\mathrm{ax}}} = 0, \tilde{c}_1 \neq 0, \tilde{c}_2 \neq 0$	1	-	1	1	$-\frac{\tilde{c}_1}{\tilde{c}_2}$	4
4	$G_{\mathrm{Tele},T_{\mathrm{vec}}} \neq 0,\, G_{\mathrm{Tele},T_{\mathrm{ax}}} = 0, \tilde{c}_1 = 0, \tilde{c}_2 = 0$						
4.I	$G_{\mathrm{Tele},T_{\mathrm{vec}}} = -\frac{2}{3}(G_4 - G_{\mathrm{Tele},T}),\, G_{4,\phi} = \frac{1}{2}G_{\mathrm{Tele},I_2}$						
4.I.a	$\tilde{c}_3 \neq 0, \tilde{c}_4 \neq 0$	-	-	1	1	$-\frac{\tilde{c}_3}{\tilde{c}_4}$	3
4.I.b	$\tilde{c}_3 = 0, \tilde{c}_4 = 0$	-	-	1	-	-	2
4.II	$G_{3,\phi} = Z_2,\, G_{2,\phi\phi} = -G_{\mathrm{Tele},\phi\phi}$						
4.II.a	$G_{\mathrm{Tele},I_2} - 2G_{4,\phi} \neq 0$	1	-	1	-	-	3
4.II.b	$G_{\mathrm{Tele},I_2} - 2G_{4,\phi} = 0$	-	-	1	-	-	2
5	$G_{\mathrm{Tele},T_{\mathrm{vec}}} = 0,\, G_{\mathrm{Tele},T_{\mathrm{ax}}} \neq 0, \tilde{c}_1 \neq 0, \tilde{c}_2 \neq 0$	1	-	1	1	$-\frac{\tilde{c}_1}{\tilde{c}_2}$	4
6	$G_{\mathrm{Tele},T_{\mathrm{vec}}} = 0, G_{\mathrm{Tele},T_{\mathrm{ax}}} \neq 0, \tilde{c}_1 = 0, \tilde{c}_2 = 0$	1	-	1	-	-	3
7	$G_{\mathrm{Tele},T_{\mathrm{vec}}} = 0,\, G_{\mathrm{Tele},T_{\mathrm{ax}}} = 0,\, \tilde{c}_1 \neq 0, \tilde{c}_2 \neq 0$	-	-	1	1	$-\frac{\tilde{c}_1}{\tilde{c}_2}$	3
8	$G_{\mathrm{Tele},T_{\mathrm{vec}}} = 0,\, G_{\mathrm{Tele},T_{\mathrm{ax}}} = 0, \tilde{c}_1 = 0, \tilde{c}_2 = 0$	-	-	1	-	-	2

Table 5.1: Branches of teleparallel analogue of Horndeski theory with their respective propagating DoFs. Each scalar represents 1 DoF, each vector represents 2 DoFs, and each tensor represents 2 DoFs. Quantities $\tilde{c}_1$, $\tilde{c}_2$, $\tilde{c}_3$, $\tilde{c}_4$ are defined respectively in Eqs (5.19a), (5.19b), (5.49), (5.50) and Z_2 defined in Eq. (5.48).

		Polarisations							
Cases	**Conditions**	Massless						Massive	
		S		V		T		S	
		b	l	x	y	+	×	b	l
1	$G_{\text{Tele},T_{\text{vec}}} \neq 0,\ G_{\text{Tele},T_{\text{ax}}} \neq 0,\ \tilde{c}_1 \neq 0,\ \tilde{c}_2 \neq 0$	√	-	-	-	√	√	√	√
2	$G_{\text{Tele},T_{\text{vec}}} \neq 0,\ G_{\text{Tele},T_{\text{ax}}} \neq 0,\ \tilde{c}_1 = 0,\ \tilde{c}_2 = 0$								
2.I	$G_{\text{Tele},T_{\text{ax}}} \neq 0, \tilde{c}_3 \neq 0, \tilde{c}_4 \neq 0$								
2.I.a	$G_{\text{Tele},T_{\text{ax}}} \neq 0,\ \tilde{c}_3 \neq 0,\ \tilde{c}_4 \neq 0$	-	-	-	-	√	√	-	-
2.I.b	$c \neq 0,\ \tilde{c}_3 = 0,\ \tilde{c}_4 = 0$	-	-	-	-	√	√	-	-
2.II	$G_{3,\phi} = Z_2,\ G_{2,\phi\phi} = -G_{\text{Tele},\phi\phi}$								
2.II.a	$G_{\text{Tele},I_2} - 2G_{4,\phi} \neq 0$	√	-	-	-	√	√	-	-
2.II.b	$G_{\text{Tele},I_2} - 2G_{4,\phi} = 0$	-	-	-	-	√	√	-	-
3	$G_{\text{Tele},T_{\text{vec}}} \neq 0,\ G_{\text{Tele},T_{\text{ax}}} = 0,\ \tilde{c}_1 \neq 0,\ \tilde{c}_2 \neq 0$	√	-	-	-	√	√	√	√
4	$G_{\text{Tele},T_{\text{vec}}} \neq 0,\ G_{\text{Tele},T_{\text{ax}}} = 0,\ \tilde{c}_1 = 0,\ \tilde{c}_2 = 0$								
4.I	$G_{\text{Tele},T_{\text{vec}}} = -\frac{2}{3}(G_4 - G_{\text{Tele},T}),\ G_{4,\phi} = \frac{1}{2}G_{\text{Tele},I_2}$								
4.I.a	$\tilde{c}_3 \neq 0, \tilde{c}_4 \neq 0$	-	-	-	-	√	√	-	-
4.I.b	$\tilde{c}_3 = 0, \tilde{c}_4 = 0$	-	-	-	-	√	√	-	-
4.II	$G_{3,\phi} = Z_2,\ G_{2,\phi\phi} = -G_{\text{Tele},\phi\phi}$								
4.II.a	$G_{\text{Tele},I_2} - 2G_{4,\phi} \neq 0$	√	-	-	-	√	√	-	-
4.II.b	$G_{\text{Tele},I_2} - 2G_{4,\phi} = 0$	-	-	-	-	√	√	-	-
5	$G_{\text{Tele},T_{\text{vec}}} = 0,\ G_{\text{Tele},T_{\text{ax}}} \neq 0,\ \tilde{c}_1 \neq 0,\ \tilde{c}_2 \neq 0$	-	-	-	-	√	√	√	√
6	$G_{\text{Tele},T_{\text{vec}}} = 0,\ G_{\text{Tele},T_{\text{ax}}} \neq 0,\ \tilde{c}_1 = 0,\ \tilde{c}_2 = 0$	-	-	-	-	√	√	-	-
7	$G_{\text{Tele},T_{\text{vec}}} = 0,\ G_{\text{Tele},T_{\text{ax}}} = 0,\ \tilde{c}_1 \neq 0,\ \tilde{c}_2 \neq 0$	-	-	-	-	√	√	√	√
8	$G_{\text{Tele},T_{\text{vec}}} = 0,\ G_{\text{Tele},T_{\text{ax}}} = 0,\ \tilde{c}_1 = 0,\ \tilde{c}_2 = 0$	-	-	-	-	√	√	-	-

Table 5.2: Branches of teleparallel analog of Horndeski theory with their corresponding polarisations. Quantities $\tilde{c}_1$, $\tilde{c}_2$, $\tilde{c}_3$, $\tilde{c}_4$ are defined respectively in Eqs (5.19a), (5.19b), (5.49), (5.50) and Z_2 defined in Eq. (5.48).

Theory	**Case**	**DoF**	**Lagrangian Density $\mathcal{L}_i$ $\left(S_i = \frac{1}{2\kappa^2}\int d^4x\, e\, \mathcal{L}_i\right)$**
GR or $f(T)$	8	2	$\mathring{R}$ or $f(T)$
Horndeski	7	3	Eq. (2.24)
$G_{\rm Tele}$	1	7	$G_{\rm Tele}\left(\phi, X, T, T_{\rm ax}, T_{\rm vec}, I_2, J_1, J_3, J_5, J_6, J_8, J_{10}\right)$
Generalized NGR	2.I.b	5	$f(T, T_{\rm ax}, T_{\rm vec})$
Generalized Teleparallel Dark Energy	7	3	$-A(\phi)T - \frac{1}{2}\partial_\mu\phi\partial^\mu\phi - V(\phi)$
Generalized Teleparallel Scalar Tensor	7	3	$F(\phi)T + P(\phi, X) - G_3(\phi, X)\Box\phi$
Tachyonic Teleparallel Gravity	7	3	$f(T, X, \phi)$

Table 5.3: Categorisation of literature models within the branches of Teledeski found in Table 5.1. The models are a particular scenario that falls within the case indicated. Additionally, standard Horndeski includes Brans-Dicke and $f(R)$ theories.

5.5 | Summary

Considering the full BDLS cases, where no terms of the action (2.98) are omitted, the maximum number of propagating DoFs is 7: 2 scalar modes, 1 vector mode, and 1 tensor mode in the massless sector, and an additional scalar mode arising from the massive sector. This result has been fleshed out in Sec. 5.4.1. Across the branches stemming from BDLS the tensor modes h_+ and $h_\times$ always appear as per the imposition of the condition $G_4 - G_{\rm Tele},_T \neq 0$. Within the massive sector, provided that ψ and $\mathcal{X}_2$ are nontrivial DoFs, realises a scalar propagating DoF. Two distinct categories can be established from the analysis carried out in Sec. 5.4: propagating DoFs in the massless sector only containing a combination of scalar-vector-tensor modes or an amalgamation of massless and massive sectors. The propagating DoFs subcases obtained from the generalised BDLS model have been summarised in Table 5.1.

By calculating the electric components of the Riemann tensor one can determine which of the propagating DoFs appear as a polarisation mode to describe the nature of GW propagating. While the tensor polarisation modes consistently appear in the massless sector, four subcases (Cases 1, 2.II.a,3, 4.II.a) also include an additional breathing scalar mode. As for the massive sector, scalar polarisation modes appear in four cases (Cases 1,3, 5, 7) contributing to the breathing and longitudinal portions. Polarisation modes have been summarised in Table 5.2.

While additional scenarios can be explored, the nature of the results presented in Tables 5.1-5.2 remains unaltered. Thus, theories of gravity explored in the literature that fall under the

BDLS formalism, can be classified under these subcases. In fact, GR can be categorised within Case 8 (Sec. 5.4.8) and Horndeski within Case 7 (Sec. 5.4.7). Hence, the gravitational theory of BDLS, and the methodology of determining the propagating DoFs and polarisation modes presented in this chapter can retrieve results for other established theories, some of which have been listed in Table 5.3, while also providing results for other subclasses that fall under the standard Horndeski model and second order tetrad-based theories.

6

Growth of Structures in Teleparallel Gravity

The current structures in the Universe have originated from gravitational instabilities, responsible for matter accumulation which has led to the large-scale structure formation including clusters of galaxies. The expansion rate of the Universe affects how the growth of structure behaves. Slow growth is experienced during the radiation epoch in comparison to the matter-dominated era, and growth slows down again as dark energy takes over and the Universe undergoes an accelerated expansion. Additionally, baryons and photons exert pressure, thus as gas migrates to lower pressure areas, baryons are unable to accumulate as much as the pressureless counterpart of dark matter [88].

Cosmological evolution of perturbations can be split into three parts [88, 309]:

- **Superhorizon:** The large scales, where long wavelength modes are initially outside the horizon such that $k \ll aH$, contribute to the conditions that shape the large-scale structures of the early Universe.
- **Horizon entry:** Wavelengths start to enter the horizon and the Universe shifts from a radiation epoch where $a \ll a_{\rm eq}$ to a matter-dominated one where $a \gg a_{\rm eq}$, given $a_{\rm eq}$ represents the point when radiation and matter densities are equivalent; linking the large and small scale regions.
- **Subhorizon:** Deep within the matter-dominated era, the growth of matter perturbations overtakes that of radiation density, such that dark matter continues to evolve and the radiation becomes negligible. Here, small-scale modes are represented by the relationship $k \gg aH$.

In this chapter, the main focus is the growth of CDM but it should be noted that other constituents of the Universe play a role, somewhat small, which results in the small structures

observed today. Within the horizon, baryon densities are suppressed as they are still tightly bound to photons at early times. Post decoupling, the now free-moving baryons fall within the gravitational wells that dark matter had time to create, ultimately also contributing to structure formation [36, 37, 38]. Additionally, BAOs influence the transfer function and can be detected, despite them being a small portion of the total matter [310]. Massive neutrinos, still retaining a relatively high velocity, smooth out density perturbations, hence resulting in a dampening of the growth of small structures [311, 312]. As the Universe enters a dark energy-dominated epoch, the growth of perturbations is directly affected by the Hubble rate. Thus, the growth factor behaviour is altered in accordance to the dark energy model used [313, 86, 269].

The chapter is split up as follows: Sec. 6.1 elaborates on the matter sector; Sec. 6.2 provides a general overview of obtaining the Mészáros equations; Sec. 6.3 introduces the growth factor, growth index, $f\sigma_8$, and S_8 parameters; Sec. 6.4 provides the cosmic growth structures of gravitational models of $f(T)$ and modified GR; and all results summarised in Sec. 6.5. The following work is based on the published work in Refs [314, 315]. In this chapter, the signature is changed to $(+,-,-,-)$ since data values are obtained from literature where this signature is utilised.

6.1 | Matter Perturbations

In the BDLS action given by Eq. (2.98), the matter has been introduced but not thoroughly explored, as up to this point the systems were considered to be in a vacuum. As gravity interacts with matter, it becomes important to understand the dynamics of gravitational theory to ensure consistency with a viable Universe. It becomes crucial to make predictions and comparison with observations such as gravitational lensing [316, 317, 318, 126], CMB [319], large scale structures and BAO [310, 320, 321], and GWs [45, 80, 276]. The energy-momentum tensor $\Theta^{\mu\nu}$ for a perfect fluid can be written in terms of the fluid four-velocity u^μ [9][1]:

$$\Theta^{\mu\nu} := (\rho + p)u^\mu u^\nu - pg^{\mu\nu} - \Pi^{\mu\nu}\,, \tag{6.1}$$

where ρ is the energy density and p is the pressure which are solely time-dependent, and $\Pi^{\mu\nu}$ is the anisotropic stress tensor with the properties

$$\Pi^{00} = \Pi^{0i} = u^\mu \Pi_{\mu\nu} = 0\,, \tag{6.2}$$

where u^μ is given by

$$u^\mu = (1, 0, 0, 0)\,, \tag{6.3}$$

[1]This relationship has been introduced in Eq. (2.12). The minus sign in the second term arises due to the opposite sign convention. Additionally, the anisotropic stress is included.

which yields the property

$$u^\mu u_\mu = g_{\mu\nu} u^\mu u^\nu = 1\,. \tag{6.4}$$

Note, under gauge transformation the background values of ρ and p maintain their functional forms. The energy-momentum tensor $\Theta^{\mu\nu}$ is symmetric and can be obtained from the action (2.98) through the variation with respect to the tetrad of the matter sector $\mathcal{L}_m$:

$$\Theta_C{}^\gamma = e^{-1} \frac{\partial(e\,\mathcal{L}_m)}{\partial e^C{}_\gamma}\,, \tag{6.5}$$

which can be contracted with the tetrad and inverse metric to obtain Eq. (6.1). The conservation of the energy-momentum tensor implies [9]

$$\mathring{\nabla}_\mu \Theta^{\mu\nu} = \partial_\mu \Theta^{\mu\nu} + \mathring{\Gamma}^\mu_{\mu\alpha}\Theta^{\alpha\nu} + \mathring{\Gamma}^\nu_{\mu\alpha}\Theta^{\mu\alpha} = 0\,, \tag{6.6}$$

which at the background level results in the continuity equation

$$\mathring{\nabla}_\mu \Theta^{\mu 0} = \dot{\rho} + 3H(\rho + p) = 0\,, \tag{6.7}$$

while the component $\mathring{\nabla}_\mu \Theta^{\mu i}$, corresponding to the Euler/velocity equation, gives a trivial result at the background level.

The perturbation of the energy-momentum tensor up to the first order in the scalar sector is given by

$$\Theta_\mu{}^\nu = \begin{pmatrix} \rho + \delta\rho & (\rho + p)\partial^i v \\ -a^2(\rho + p)\partial_i v & -((p + \delta p)\,\delta^j_i + \partial_i \partial^j \pi^{\mathrm{s}}) \end{pmatrix}\,, \tag{6.8}$$

where $\delta\rho$ is the perturbation of the energy density, δp is the pressure perturbation, v is the scalar component of the velocity vector

$$v^i = \frac{u^i}{u^0}\,, \tag{6.9}$$

and π^{s} is the scalar component of the anisotropic stress [322]. The perturbations are taken to be of both temporal and spatial coordinates. The gauge transformations of these additional matter scalar perturbations are checked through the Lie derivative notation

$$\tilde{\Theta}_\mu{}^\nu = \Theta_\mu{}^\nu + \partial_\alpha \Theta_\mu{}^\nu\,\xi^\alpha + \partial_\mu \xi^\alpha \Theta_\alpha{}^\nu - \partial_\alpha \xi^\nu \Theta_\mu{}^\alpha\,, \tag{6.10}$$

where $\xi^\mu = \{\xi^0, \frac{1}{a}\partial^i \xi\}$ for the scalar transformation, analogous to the procedure presented in Eq. (4.40) and Eq. (4.41) for tetrad and scalar, respectively. Hence, the transformations are [271]

$$\tilde{\delta\rho} = \delta\rho + \dot{\rho}\xi^0\,, \tag{6.11a}$$

$$\tilde{\delta p} = \delta p + \dot{p}\xi^0 \,, \tag{6.11b}$$

$$\tilde{\pi}^{\rm s} = \pi^{\rm s} \,, \tag{6.11c}$$

$$\tilde{v} = v - \frac{1}{a^2}\xi^0 \,, \tag{6.11d}$$

where $\pi^{\rm s}$ is the only gauge-invariant quantity. The remaining variables can be combined to construct other gauge-invariant quantities:

$$\Gamma = \delta p - \frac{\dot{p}}{\dot{\rho}}\delta\rho \,, \tag{6.12a}$$

$$\delta_m = \frac{\delta\rho + a^2\dot{\rho}v}{\rho} \,, \tag{6.12b}$$

$$\Delta_m = \frac{\delta p + a^2\dot{p}v}{\rho} = \frac{\Gamma}{\rho} + \frac{\dot{p}\delta_m}{\dot{\rho}} \,, \tag{6.12c}$$

where Γ is the entropy perturbation for which $\frac{\delta p}{\delta\rho}$ is referred to as the effective speed of sound and $\frac{\dot{p}}{\dot{\rho}}$ is the adiabatic speed of sound, δ_m is the comoving gauge density perturbation, and Δ_m is the pressure perturbation. The conservation of energy-momentum relationship given by Eq. (6.6) can be extended to the perturbative level to obtain the continuity and velocity equations, respectively:

$$0 = \dot{\delta\rho} + (\rho + p)\left(-\partial^2 v + 3\dot{\psi} - \partial^2\dot{h}\right) + 3H\left(\delta\rho + \delta p - \frac{\partial^2\pi^{\rm s}}{3}\right) \,, \tag{6.13}$$

$$0 = \delta p - \partial^2\pi^{\rm s} + a^2[(2H(\rho + p) + \dot{p})v + (\rho + p)\dot{v}] + (\rho + p)[\varphi + aH(b - \beta)] \,. \tag{6.14}$$

The addition of Eq. (6.8) to Eqs (3.19-3.21) and Eq. (4.29) extends the scalar sector to include matter contributions for a perfect fluid, such that

$$W_0{}^0 = 2\kappa^2\rho \,, \tag{6.15}$$

$$W^i_{\ i} = -2\kappa^2 p \,, \tag{6.16}$$

where the background equations $W_0{}^0$ and $W_i{}^i$ are given by Eq. (3.19) and Eq. (3.21), respectively, and

$$\delta W_0{}^{0\,\rm S} = 2\kappa^2\delta\rho \,, \tag{6.17a}$$

$$\delta W_0{}^{i\,\rm S} = 2\kappa^2(\rho + p)\partial_i v \,, \tag{6.17b}$$

$$\delta W_i{}^{0\,\rm S} = 2\kappa^2(\rho + p)\partial_i v \,, \tag{6.17c}$$

$$\delta W_i{}^{i\,\rm S} = -2\kappa^2\delta p \,, \tag{6.17d}$$

$$\delta W_i{}^{j\,\rm S} = 0 \,, \tag{6.17e}$$

wherein the background equations have already been applied. The gravitational portion of the field equations ($\delta W_0{}^{0\,\rm S}$, $\delta W_0{}^{i\,\rm S}$, $\delta W_i{}^{0\,\rm S}$, $\delta W_i{}^{i\,\rm S}$, $\delta W_i{}^{j\,\rm S}$) is given by Eq. (4.29). Thus, along

with the conservation of momentum equations (6.7, 6.13-6.14), provide the tools to construct the Mészáros equation.

6.2 | Mészáros Equation

The Mészáros equation can describe the growth of density perturbations originating in the early Universe as they evolve during the matter-dominated eras. Through the lens of linear perturbation theories, it combines the gravitational equations of motion with the dynamics of fluids to understand small homogeneities grow at later stages due to gravitational instabilities. First, the tools used throughout this section are introduced. The effective equation of state is given by

$$\omega_{\text{eff}} := \frac{p}{\rho}\,, \tag{6.18}$$

such that upon substitution of Eq. (6.15) for ρ and Eq. (6.16) for p, one retrieves an expression in terms of the modified part of the theory. A similar relationship can be obtained for the perturbative portions $\delta\rho$ and δp, in which Eqs. (6.17a,6.17d) are utilised to define the effective sound speed as

$$c_s^2 := \frac{\delta p}{\delta \rho}\,. \tag{6.19}$$

The entropy perturbation given by Eq. (6.12a) is set to zero; it is said that there is adiabaticity i.e.

$$\Gamma = 0 \implies \frac{\delta p}{\delta \rho} = \frac{\dot{p}}{\dot{\rho}}\,. \tag{6.20}$$

By using the continuity equation (6.13), velocity equation (6.14) and the gauge-invariant variables δ_m and Γ given by Eq. (6.12b) and Eq. (6.12a), respectively, the variables v, $\delta\rho$ and δp can be eliminated and replaced by gauge-invariant variables.

When studying the subhorizon epoch, it is assumed that the evaluation is being applied within a deep matter era, such that only CDM is considered. Hence,

$$p = \delta p = 0\,, \tag{6.21}$$

such that $\omega_{\text{eff}} = 0$, $c_s^2 \to 0$, and subscript m is now associated with CDM only. The anisotropic stress is excluded as it is associated with quadrupole contributions whose role is mainly within the radiation epoch and are negligible when considering CDM in the matter epoch. Additionally, longitudinal gauge[2] is applied such that

$$b = \beta\,, \qquad \text{and} \qquad h = 0\,. \tag{6.22}$$

[2]Refer to Eq. (4.44) for a summary of different gauge choices which can be applied instead of the longitudinal gauge.

The gauge choice removes any residual freedoms, resulting in gauge-invariant field equations. This implies that physical quantities are independent of arbitrary choices of coordinates or internal symmetries, reflecting only the underlying physics.

Due to the linear relationship between the perturbations, the field equations can be rewritten to express gravitational perturbations as functions of matter perturbations. Given that the antisymmetric $W_{[ij]}$ given by Eq. (4.33) corresponds to the $\{\sigma, \dot{\sigma}, \ddot{\sigma}\}$ terms in the W_{ij} expression in Eq. (4.29d), the σ mode can be eliminated. The remaining field equations are

$$\delta W_0{}^0: \quad \mathcal{F}_1(\delta\phi, \delta\dot{\phi}, \varphi, \beta, \dot{\beta}, \psi, \dot{\psi}) = \mathcal{G}_1(\delta_m, \dot{\delta}_m)\,, \tag{6.23}$$

$$\delta W_0{}^i: \quad \mathcal{F}_2(\delta\phi, \delta\dot{\phi}, \varphi, \dot{\varphi}, \dot{\beta}, \ddot{\beta}, \psi, \dot{\psi}) = \mathcal{G}_2(\dot{\delta}_m)\,, \tag{6.24}$$

$$\delta W_i{}^0: \quad \mathcal{F}_3(\delta\phi, \delta\dot{\phi}, \varphi, \beta, \dot{\psi}) = \mathcal{G}_3(\dot{\delta}_m)\,, \tag{6.25}$$

$$\delta W_i{}^j: \quad \mathcal{F}_4(\delta\phi, \varphi, \beta, \dot{\beta}, \psi) = 0\,, \tag{6.26}$$

$$\delta W_i{}^i: \quad \mathcal{F}_5(\delta\phi, \delta\dot{\phi}, \delta\ddot{\phi}, \varphi, \dot{\varphi}, \beta, \dot{\beta}, \psi, \dot{\psi}, \ddot{\psi}) = 0\,, \tag{6.27}$$

$$\delta \dot{W}_0{}^0: \quad \mathcal{F}_6(\delta\phi, \delta\dot{\phi}, \delta\ddot{\phi}, \varphi, \dot{\varphi}, \beta, \dot{\beta}, \ddot{\beta}, \psi, \dot{\psi}, \ddot{\psi}) = \mathcal{G}_6(\delta_m, \dot{\delta}_m, \ddot{\delta}_m)\,, \tag{6.28}$$

$$\delta \dot{W}_0{}^i: \quad \mathcal{F}_7(\delta\phi, \delta\dot{\phi}, \delta\ddot{\phi}, \varphi, \dot{\varphi}, \ddot{\varphi}, \beta, \dot{\beta}, \ddot{\beta}, \dddot{\beta}, \psi, \dot{\psi}, \ddot{\psi}) = \mathcal{G}_7(\dot{\delta}_m, \ddot{\delta}_m)\,, \tag{6.29}$$

$$\delta \dot{W}_i{}^0: \quad \mathcal{F}_8(\delta\phi, \delta\dot{\phi}, \delta\ddot{\phi}, \varphi, \dot{\varphi}, \beta, \dot{\beta}, \dot{\psi}, \ddot{\psi}) = \mathcal{G}_8(\dot{\delta}_m, \ddot{\delta}_m)\,, \tag{6.30}$$

$$\delta \dot{W}_i{}^j: \quad \mathcal{F}_9(\delta\phi, \delta\dot{\phi}, \varphi, \dot{\varphi}, \beta, \dot{\beta}, \ddot{\beta}, \psi, \dot{\psi}) = 0\,, \tag{6.31}$$

$$\delta W_\phi: \quad \mathcal{F}_{10}(\delta\phi, \varphi, \beta, \psi, \delta\dot{\phi}, \dot{\varphi}, \dot{\beta}, \dot{\psi}, \delta\ddot{\phi}, \ddot{\psi}) = 0\,, \tag{6.32}$$

$$\delta W_{(0i)}: \quad \mathcal{F}_{11}\left(\delta\phi, \delta\dot{\phi}, \varphi, \dot{\varphi}, \beta, \dot{\beta}, \ddot{\beta}, \psi, \dot{\psi}\right) = \mathcal{G}_{11}\left(\dot{\delta}_m\right)\,, \tag{6.33}$$

$$\delta W_{[0i]}: \quad \mathcal{F}_{12}\left(\delta\phi, \delta\dot{\phi}, \varphi, \dot{\varphi}, \beta, \dot{\beta}, \ddot{\beta}, \psi, \dot{\psi}\right) = 0 \tag{6.34}$$

$$\delta W_{(ij)}: \quad \mathcal{F}_{13}\left(\delta\phi, \varphi, \beta, \dot{\beta}, \psi\right) = 0\,, \tag{6.35}$$

$$\delta \dot{W}_{(ij)}: \quad \mathcal{F}_{14}\left(\delta\phi, \delta\dot{\phi}, \varphi, \dot{\varphi}, \beta, \dot{\beta}, \ddot{\beta}, \psi, \dot{\psi}\right) = 0\,, \tag{6.36}$$

cast in matrix form

$$\mathcal{F}\chi = \mathcal{G}\,, \tag{6.37}$$

where $\mathcal{F}$ is a matrix of coefficients arising from functions $[\mathcal{F}_1, \mathcal{F}_{14}]$ corresponding to the gravitational perturbations given by $\chi = \{\delta\phi, \delta\dot{\phi}\, \delta\ddot{\phi}, \varphi, \dot{\varphi}, \beta, \dot{\beta}, \ddot{\beta}, \dddot{\beta}, \psi, \dot{\psi}, \ddot{\psi}\}$, while each row of matrix $\mathcal{G}$ is given by a linear combination of matter contributions $\{\delta_m, \dot{\delta}_m, \ddot{\delta}_m\}$ corresponding to functions $\{\mathcal{G}_1, \mathcal{G}_2, \mathcal{G}_3, \mathcal{G}_6, \mathcal{G}_7, \mathcal{G}_8, \mathcal{G}_{11}\}$. The number of equations in the system is larger than the number of modes for which a solution is required. In the general case of BDLS, it is ideal to eliminate $\delta\dot{W}_0{}^i$ in Eq. (6.29) to avoid introducing higher order derivatives. It may be that the expression comes in useful when dealing with subcases of BDLS where $9G_{\mathrm{Tele},T_{\mathrm{vec}}} + 2X(-2G_{\mathrm{Tele},J_8} - 5G_{\mathrm{Tele},J_5} + 3G_{\mathrm{Tele},J_3} + 2XG_{\mathrm{Tele},J_6}) = 0$ since these higher order derivatives are not present. Additionally, the

choice of eliminating equations relies upon ensuring that the matrix $\mathcal{F}$ is constructed completely with linearly independent equations, such that $\det(\mathcal{F}) \neq 0$ and is invertible. By obtaining the inverse of matrix $\mathcal{F}$, the solution for χ is obtained:

$$\chi = \mathcal{F}^{-1}\mathcal{G}\,, \tag{6.38}$$

giving a solution for each gravitational quantity.

Next, the initial form of the Mészáros equation can be obtained through the continuity and velocity equations (6.13-6.14). These equations simplify upon applying Eq. (6.21), Eq. (6.12b) and longitudinal gauge, yielding

$$0 = \dot{\delta}_m + 3\dot{H}\tilde{v} + 3H\dot{\tilde{v}} - \frac{k^2}{a^2}\tilde{v} + 3\dot{\psi}\,, \tag{6.39}$$

$$0 = \dot{\tilde{v}} + \varphi\,. \tag{6.40}$$

where $\tilde{v} = a^2 v$, and expressed with a spatial Fourier transformation. Substituting Eq. (6.40) in Eq. (6.39), an expression for v can be obtained from

$$0 = \dot{\delta}_m - 3H\varphi + 3\dot{\psi}\left(\frac{k^2}{a^2} - 3\dot{H}\right)\tilde{v}\,. \tag{6.41}$$

Taking a time derivative, and substituting Eq.(6.41) and Eq. (6.40) results in the following:

$$0 = \ddot{\delta}_m + 3\left(\ddot{H}\tilde{v} + \dot{H}\dot{\tilde{v}}\right) - 3\left(\dot{H}\varphi + H\dot{\varphi}\right) + \frac{k^2}{a^2}\left(2aH\tilde{v} - \dot{\tilde{v}}\right) + 3\ddot{\psi}\,. \tag{6.42}$$

All gravitational potentials present in Eq. (6.42) can be substituted by the solution χ in Eq. (6.38) where all modes are solved and expressed solely in terms of matter perturbation δ_m and its derivative. Therefore, the Mészáros equation can be written in the form

$$0 = \ddot{\delta}_m + 2H\nu(t)\dot{\delta}_m - \frac{1}{2}\kappa^2\rho\mu(t)\delta_m\,, \tag{6.43}$$

where ν and μ are time-dependent functions on the gravitational theory considered. Through this equation, the evolution of CDM can be obtained when considering the matter-dominated era by solving the second-order differential equation. This solution provides an avenue to study growth parameters: growth factor D, growth index γ, $f\sigma_8$, and S_8. Eq. (6.43) resembles the form of the Mészáros equation for the ΛCDM model. All the effective contributions from gravitational potentials are encapsulated in the μ and ν coefficients.

6.3 | Cosmic Growth Parameters

Solving the second order differential equation given by the Mészáros equation (6.43) results in the solution of the matter perturbation δ_m. By switching the equation to be dependent on the

evolution scale of the scale factor a or redshift z, one can obtain an understanding of growth structures assisted by observable data. The former notation has been adopted in this project. The Mészáros equation is constructed under the assumption that the system is within the matter-dominated era, hence the energy density is given by

$$\rho(t) = \frac{3H_0^2\Omega_{m0}}{\kappa^2}a^{-3}\,, \tag{6.44}$$

where Ω_{m0} is the current matter density parameter. Additionally, the matter density parameter can be derived to be

$$\Omega_m(a) = \frac{\Omega_{m0}a^{-3}}{h(a)^2}\,, \tag{6.45}$$

where h is the normalised Hubble parameter

$$h(a) = \frac{H(a)}{H_0}\,. \tag{6.46}$$

The evolution of the Hubble parameter can be obtained through the Friedmann equations (3.19-3.21), provided a gravitational theory is supplied to substitute for the arbitrary functions G_i for $i \in [2,5]$ and G_{Tele}. At a later point, the relationship

$$\Omega_m'(a) = -\frac{3\Omega_m(a)}{a}\left(1 + \frac{2ah'(a)}{3h(a)}\right)\,, \tag{6.47}$$

becomes useful. Casting Eq. (6.43) in terms of a results in

$$0 = -\frac{3}{2}\Omega_m(a)\mu(a)\delta_m(a) + a\left(2\nu(a) + 1 + a\frac{h'(a)}{h(a)}\right)\delta_m'(a) + a^2\delta_m''(a)\,, \tag{6.48}$$

where ν and μ are now dependent on a, and primes ($'$) derivatives with represent to scale factor. Next, derivations of the growth factor solution, growth index relationship, $f\sigma_8$ and S_8 parameters using Eq. (6.48) are presented.

6.3.1 | Growth Factor

Growth is defined as a ratio of the matter perturbation amplitude at a scale factor a against its value at scale factor a_i when the deep-matter era begins [275]:

$$D(a) = \frac{\delta_m(a)}{\delta_m(a_i)}\,. \tag{6.49}$$

The solution of δ_m is obtained by solving Eq. (6.48), which requires setting some initial conditions. To ensure that $a \gg a_{\text{eq}}$ and in the matter-dominated era, the range $0.1 \leq a \leq 1$ is considered where $a_i = 0.1$. The following initial conditions are imposed throughout the analysis [88]:

$$\delta_m(a_i) = 1\,, \qquad \delta_m'(a_i) = 10\,, \tag{6.50}$$

which implies that $D(a) = \delta_m(a)$ since the denominator is unitary.

6.3.2 | Growth Index

The growth factor equation in Eq. (6.49) can also be expressed in terms of the variable growth index $\gamma(a)$ through the equation [313]

$$D(a) = \exp\left(\int_1^a \frac{\Omega_m(\tilde{a})^{\gamma(\tilde{a})}}{\tilde{a}}\, d\tilde{a}\right), \tag{6.51}$$

where the limit $\tilde{a} = 1$ is included to represent the current time in the evolution of the Universe. Therefore, the growth rate clustering [323]

$$g(a) = \frac{d\ln\delta_m}{d\ln a} \simeq \Omega_m(a)^{\gamma(a)}\,. \tag{6.52}$$

This relationship can quantify the growth of structure g as it shows that a small fluctuation in the matter distribution influences the growth, linking the growth of matter to the expansion of the Universe. As the solution for the function g arises from the solution of the Mészáros equation, the growth index is useful to differentiate between different modified theories of gravity. Eq. (6.52) yielding a restructuring of Eq. (6.48) as

$$\begin{aligned} 0 = -\frac{3}{2}\mu(a)\Omega_m(a) + \Omega_m(a)^{\gamma(a)} \\ + \Omega_m(a)\left(a(1-2\gamma(a))\frac{h'(a)}{h(a)} + 2\nu(a) - 3\gamma(a) + a\gamma'(a)\ln\Omega_m(a)\right). \end{aligned} \tag{6.53}$$

The growth index is considered to be a constant value, hence making it sufficient to analyse Eq. (6.53) at current time $a = 1$ only. Regardless, the linear parametrisation of a dynamical growth index [313, 323, 324, 325]

$$\gamma(a) = \gamma_0 + (1-a)\gamma_1\,, \tag{6.54}$$

is applied to be able to replicate the expected ΛCDM result by adjusting the γ_1 value. Therefore, Eq. (6.53) at $a = 1$ is given by:

$$0 = -\frac{3}{2}\mu(1)\Omega_{m0} + \Omega_{m0}^{2\gamma_0} + \Omega_{m0}^{\gamma_0}\left(-3\gamma_0 + 2\nu(1) - \gamma_1\ln\Omega_{m0} + (1-2\gamma_0)h'(1)\right), \tag{6.55}$$

where $h(1) = 1$ as per definition in Eq. (6.46). This equation can be solved for γ_1 in terms of γ_0. The constant growth index value depending on the gravitational theory can be determined when $\gamma_1 = 0$.

6.3.3 | $f\sigma_8$

The growth factor encapsulates the evolution of matter density perturbations and the growth index provides a good picture linking the evolution of matter to the formation of cosmic structures,

but $f\sigma_8$ provides a link with observable quantities as a measurable quantity. The parameter $f\sigma_8$ is obtained through the combination of the growth clustering function given by Eq. (6.52) and

$$\sigma_8(a) := \sigma_{8,0}\frac{\delta_m(a)}{\delta_m(1)}\,, \tag{6.56}$$

where $\sigma_{8,0}$ is the current value of $\sigma_8(a)$ yielding [326]

$$f\sigma_8(a) := g(a)\sigma_8(a) = a\,\sigma_{8,0}\frac{\delta_m'(a)}{\delta_m(a=1)}\,. \tag{6.57}$$

The σ_8 parameter is the root mean square fluctuations of matter density at the scale of 8 Mpc; a scale at which the internal structures of galaxies can be averaged out but still small enough to study galaxy clustering [327]. Apart from moving due to the expansion of the Universe, galaxies experience motion due to peculiar velocities giving rise to distortions in the redshift observed [328]. Measurements of Redshift Space Distortions (RSDs) provide direct observation to these peculiar velocities which are linked to $f\sigma_8$ [329].

6.3.4 | S_8

An alternative to describe the amplitude of matter fluctuations is given by parameter S_8, given by

$$S_8(a) := \sigma_8(a)\left(\frac{\Omega_m(a)}{0.3}\right)^{0.5}\,. \tag{6.58}$$

This parameter takes into account both σ_8 and Ω_m quantities; a middle-ground between the growth index relation given by Eq. (6.55) and that of $f\sigma_8$ in Eq. (6.57). S_8 tackles the degeneracy that can arise when using σ_8 and Ω_m, as several combinations of these values yield observational effects which appear identical [317]. Additionally, it is closely related to weak lensing measurements of the distortion of light from distant galaxies, providing a direct observation [317, 318].

6.4 | Cosmic Growth in Teleparallel Gravity

The procedure introduced in the previous sections differs slightly from the method typically adopted to analyse cosmological growth structures. Typically, when considering only the growth of CDM, subhorizon limit $k \gg aH$ is applied at first principle when deriving the Mészáros equation within a theory of gravity. Within the teleparallel framework, this is exactly the procedure taken in Refs [275, 322]. In the case of $f(\mathring{R})$ gravity, it was noted that the two approaches (the method where the subhorizon limit is assumed throughout the calculations and the other

method with a generalised approach as the one presented in Sec. 6.2) may result in inconsistencies, yielding a different final result. Application of the subhorizon limit in the field equations, as done in Ref. [330, 222], results in ignoring the time derivatives of potentials present in the theory, providing a simplified system of equations to work with. Albeit being more appealing to work with, especially when dealing with more complicated gravitational theories, it may result in an oversimplification, in contrast to the quasi-static result obtained in Ref. [331]. To avoid running into these issues, the generalised approach presented in Sec. 6.2 is favoured, allowing an investigation of k-scales.

An important feature when determining viable k values is to ensure that they fall within the expected values of the matter-dominated era. Hence, the k value at the radiation-matter equality is determined as a comparative value. This is done by considering the energy densities of radiation $\rho_{\rm r} \propto a^{-4}$ and matter $\rho_{\rm m} \propto a^{-3}$, and equating them to obtain

$$a_{\rm eq} = \frac{\rho_{r0}}{\rho_{m0}} = \frac{\Omega_{r0}}{\Omega_{m0}} \tag{6.59}$$

and expressed in terms of current density parameters, where $\Omega_{r0} = \Omega_r(a=1) = 8.4 \times 10^{-5}$. By determining $H_{\rm eq}$ from the Friedmann equation (6.15), it is used to determine k using

$$k \sim a_{\rm eq} H_{\rm eq}\,, \tag{6.60}$$

at radiation-matter equality.

Along with the comparison between different k values and the subhorizon limit, the deviations from the ΛCDM are also taken into account. This is obtained by taking a Lagrangian of the form $f = -T + c$, where c is a constant. The Planck collaboration results are given by

$$\Omega_{m0} = 0.315\,, \qquad H_0 = 67.4 \text{ km s}^{-1} \text{ Mpc}^{-1}\,, \qquad \sigma_{8,0} = 0.811\,, \tag{6.61}$$

yielding the growth index value of

$$\gamma_{\Lambda\rm CDM} = 0.5595\,, \tag{6.62}$$

up to 4 d.p.

6.4.1 | $f(T)$ Gravity

The study of growth factor in $f(T)$ gravity has already been performed in Refs. [275] through the application of the subhorizon limit throughout the analysis. In this section, the main focus is to verify that such a procedure is sufficient within the realm of $f(T)$ by ensuring that there are no spatial dependencies when considering growth structure studies.

The action is of the form

$$\mathcal{S}_{f(T)} = \frac{1}{2\kappa^2}\int d^4x\, e\, f(T) + \int d^4x e\, \mathcal{L}_m\,, \tag{6.63}$$

yielding the background Friedmann equations from Eqs (3.19-3.21) for the case $G_{\rm Tele} = f(T)$ and the remaining terms vanish:

$$2\kappa^2\rho = f + 12H^2 f_T\,, \tag{6.64}$$

$$-2\kappa^2 p = f + 4(3H^2 + \dot{H})f_T - 48H^2\dot{H}f_{TT}\,, \tag{6.65}$$

from which the GR limit can be obtained for the case when $f(T) = -T$, such that additional terms stem from the modified theory and contribute to the effective dark energy density and pressure. The effective portions are given by

$$2\kappa^2\rho_{\rm eff} = -2\kappa^2\rho - 6H^2\,, \tag{6.66}$$

$$-2\kappa^2 p_{\rm eff} = 2\kappa^2 p - 2(3H^2 + 2\dot{H})\,, \tag{6.67}$$

such that the effective equation of state is

$$\omega_{\rm eff} = -1 + \frac{-4(\dot{H}f_T - 12H^2\dot{H}f_{TT} + \dot{H})}{f + 12H^2 f_T + 6H^2}\,. \tag{6.68}$$

The linearised field equations (6.23)[3] simplify to

$$\delta W_{00}: \quad \mathcal{F}_1(\varphi,\beta,\psi,\dot{\psi}) = \mathcal{G}_1(\delta_m,\dot{\delta}_m)\,, \tag{6.69a}$$

$$\delta W_{0i}: \quad \mathcal{F}_2(\varphi,\psi,\dot{\psi}) = \mathcal{G}_2(\dot{\delta}_m)\,, \tag{6.69b}$$

$$\delta W_{i0}: \quad \mathcal{F}_3(\varphi,\beta,\psi,\dot{\psi}) = \mathcal{G}_3(\dot{\delta}_m)\,, \tag{6.69c}$$

$$\delta W_{ij}: \quad \mathcal{F}_4(\varphi,\beta,\psi) = 0\,, \tag{6.69d}$$

$$\delta W_i{}^i: \quad \mathcal{F}_5(\varphi,\dot{\varphi},\beta,\dot{\beta},\psi,\dot{\psi},\ddot{\psi}) = 0\,, \tag{6.69e}$$

$$\delta \dot{W}_{00}: \quad \mathcal{F}_6(\varphi,\dot{\varphi},\beta,\dot{\beta},\psi,\dot{\psi},\dot{\psi}) = \mathcal{G}_6(\delta_m,\dot{\delta}_m,\ddot{\delta}_m)\,, \tag{6.69f}$$

$$\delta \dot{W}_{0i}: \quad \mathcal{F}_7(\varphi,\dot{\varphi},\psi,\dot{\psi},\ddot{\psi}) = \mathcal{G}_7(\dot{\delta}_m,\ddot{\delta}_m)\,, \tag{6.69g}$$

$$\delta \dot{W}_{i0}: \quad \mathcal{F}_8(\varphi,\dot{\varphi},\beta,\dot{\beta},\psi,\dot{\psi},\ddot{\psi}) = \mathcal{G}_8(\dot{\delta}_m,\ddot{\delta}_m)\,, \tag{6.69h}$$

$$\delta W_{ij}: \quad \mathcal{F}_9(\varphi,\dot{\varphi},\beta,\dot{\beta},\psi,\dot{\psi}) = 0\,. \tag{6.69i}$$

The expressions obtained for $W_i{}^i$ in Eq. (6.69e) and $\delta\dot{W}_{i0}$ in Eq. (6.69h) are omitted as they are linearly dependent on other equations in the system, totalling to 7 linearly independent equations corresponding to the variables $\{\varphi,\dot{\varphi},\beta,\dot{\beta},\psi,\dot{\psi},\ddot{\psi}\}$. Additionally, the scalar field equation naturally vanishes since there is no dependency on the scalar field ϕ. Since functions $\mathcal{F}_i$ and $\mathcal{G}_i$ are

[3]The detailed expressions of these functions have been omitted. Only the portions relevant to the derivation are expressed at a later point.

a linear combination of the variables associated with the function, a matrix can be constructed as follows:

$$\overbrace{\begin{pmatrix} \mathcal{F}_{11} & 0 & \mathcal{F}_{13} & 0 & \mathcal{F}_{15} & \mathcal{F}_{16} & 0 \\ \mathcal{F}_{21} & 0 & 0 & 0 & \mathcal{F}_{25} & \mathcal{F}_{26} & 0 \\ \mathcal{F}_{31} & 0 & \mathcal{F}_{33} & 0 & 0 & \mathcal{F}_{36} & 0 \\ \mathcal{F}_{41} & 0 & \mathcal{F}_{43} & 0 & \mathcal{F}_{45} & 0 & 0 \\ \dot{\mathcal{F}}_{11} & \mathcal{F}_{11} & \dot{\mathcal{F}}_{13} & \mathcal{F}_{13} & \dot{\mathcal{F}}_{15}\,, & \mathcal{F}_{15}+\dot{\mathcal{F}}_{16} & \mathcal{F}_{16} \\ \dot{\mathcal{F}}_{21} & \mathcal{F}_{21} & 0 & 0 & \dot{\mathcal{F}}_{25} & \mathcal{F}_{25}+\dot{\mathcal{F}}_{26} & \mathcal{F}_{26} \\ \dot{\mathcal{F}}_{41} & \mathcal{F}_{41} & \dot{\mathcal{F}}_{43} & \mathcal{F}_{43} & \dot{\mathcal{F}}_{45} & \mathcal{F}_{45} & 0 \end{pmatrix}}^{\mathcal{F}} \overbrace{\begin{pmatrix} \varphi \\ \dot{\varphi} \\ \beta \\ \dot{\beta} \\ \psi \\ \dot{\psi} \\ \ddot{\psi} \end{pmatrix}}^{\chi} = \overbrace{\begin{pmatrix} \mathcal{G}_1 \\ \mathcal{G}_2 \\ \mathcal{G}_2 \\ 0 \\ \dot{\mathcal{G}}_1 \\ \dot{\mathcal{G}}_2 \\ 0 \end{pmatrix}}^{\mathcal{G}} \tag{6.70}$$

where

$$\mathcal{F}_{11} = 3H^2\left(\mathcal{F}_{26} + 12H^2 f_{TT}\right)\,, \quad \mathcal{F}_{13} = 12\frac{k^2}{a}H^3 f_{TT}\,, \quad \mathcal{F}_{15} = \frac{k^2}{a^2}f_T\,,$$
$$\mathcal{F}_{16} = -\frac{1}{H}\mathcal{F}_{11}\,, \quad \mathcal{F}_{21} = -H\mathcal{F}_{26}\,, \quad \mathcal{F}_{25} = 12H\dot{H}f_{TT}\,,$$
$$\mathcal{F}_{26} = -f_T - \frac{\frac{3}{2}\kappa^2\rho}{\frac{k^2}{a^2}-3\dot{H}}\,, \quad \mathcal{F}_{31} = -\frac{1}{3H}\mathcal{F}_{11}\,, \quad \mathcal{F}_{33} = -\frac{1}{3H}\mathcal{F}_{13}\,,$$
$$\mathcal{F}_{36} = -\frac{1}{3H}\mathcal{F}_{16}\,, \quad \mathcal{F}_{41} = -f_T\,, \quad \mathcal{F}_{43} = -a\mathcal{F}_{25}\,,$$
$$\mathcal{F}_{45} = \mathcal{F}_{41}\,, \quad \mathcal{G}_1 = -\frac{1}{2}\kappa^2\rho\left(\delta_m + \frac{3H}{\frac{k^2}{a^2}-3\dot{H}}\dot{\delta}_m\right)\,, \quad \mathcal{G}_2 = -\frac{\kappa^2\rho}{\frac{k^2}{a^2}-3\dot{H}}\dot{\delta}_m\,.$$

Solving for matrix χ results in the Mészáros equation being solely dependent on the matter perturbations δ_m:

$$0 = \ddot{\delta}_m + 2H\nu(t)\dot{\delta}_m - \frac{\kappa^2\rho}{2}\mu(t)\delta_m\,, \tag{6.71}$$

where

$$\nu = 1 + \left(\frac{18\frac{a^2}{k^2}\left((2\dot{H}^2 + H\ddot{H} + 2H^2\dot{H})f_T f_{TT} - 12H^2\dot{H}^2 f_T f_{TTT} + 6H^2\dot{H}^2 f_{TT}^2\right)}{f_T\left(f_T - 36\frac{a^2}{k^2}H^2\dot{H}f_{TT}\right)}\right)\,, \tag{6.72a}$$

$$\mu = \frac{1}{f_T - 36\frac{a^2}{k^2}H^2\dot{H}f_{TT}} - \frac{36\frac{a^2}{k^2}}{f_T(f_T - 36\frac{a^2}{k^2}H^2\dot{H}f_{TT})}\Bigg(f_{TT}(3H^2\dot{H} + 2\dot{H}^2 + H\ddot{H})$$
$$12H^2\dot{H}^2\left(-f_{TTT} + \frac{f_{TT}^2}{f_T}\right)\Bigg)\,. \tag{6.72b}$$

The subhorizon limit is set in the matter-dominated era where

$$a(t) \propto t^{\frac{2}{3}} \implies \begin{cases} \dot{H} &= \kappa_1 H^2 \,, \\ \ddot{H} &= \kappa_2 H^3 \,, \end{cases} \tag{6.73}$$

where $\kappa_1 = -\frac{3}{2}$ and $\kappa_2 = \frac{9}{2}$. By rewriting Eq. (6.71) in terms of the variable $\xi = \frac{aH}{k}$

$$\nu = 1 + \left(\frac{18\xi^2 H^2}{f_T - 36\xi^2 \kappa_1 H^2 f_{TT}} \right) \left((2\kappa_1^2 + \kappa_2 + 2\kappa_1) f_{TT} - 12\kappa_1^2 H^2 f_{TTT} + \frac{6\kappa_1^2 H^2 f_{TT}^2}{f_T} \right) \tag{6.74}$$

$$\mu = \frac{1}{f_T - 36\xi\kappa_1 H^2 f_{TT}} - \frac{36\xi^2 H^2}{f_T (f_T - 36\xi^2 \kappa_1 H^2 f_{TT})} \Bigg(f_{TT}(3\kappa_1 + 2\kappa_1^2 + \kappa_2) \\ 12\kappa_1^2 H^2 \left(-f_{TTT} + \frac{f_{TT}^2}{f_T} \right) \Bigg) \,, \tag{6.75}$$

and performing a Taylor expansion of ξ about 0 up to the first order, the possibly oversimplified subhorizon limit is obtained such that

$$\nu^{\text{sub}} = 1 \,, \qquad\qquad \mu^{\text{sub}} = \frac{1}{f_T} \,, \tag{6.76}$$

corresponding to the result obtained in Ref. [275]. As the Universe enters into a dark energy-dominated era, it is of interest to ensure that these results hold up when considering a de Sitter phase where

$$a(t) \propto e^{H_{\text{ds}} t} \,, \tag{6.77}$$

given H_{ds} is a positive constant. Substitution within Eq. (6.72a-6.72b) gives the same result as the subhorizon limit. The subhorizon and de Sitter results will be used to compare the results obtained when considering the generalised Eq. (6.71) for different k values.

The Mészáros equation (6.71) along with the expressions (6.72a-6.72b) are recast in terms of a to obtain a result in the form of Eq. (6.48). The growth factor given in Eq. (6.49) and growth index result given in Eq. (6.55) are utilised to illustrate possible k-dependencies that arise within $f(T)$ gravity. The models considered here have been chosen to ensure that the dependency on torsion scalar T is recovered at late times while GR limits can be attained at early times to be in accordance with CMB constraints and primordial nucleosynthesis observations. $f(T)$ offers a plethora of viable models, but here are presented five models which have been thoroughly studied in the literature: Power Law (6.4.1.1), Linder (6.4.1.2), Exponential (6.4.1.3), Logarithmic (6.4.1.4) and Hyperbolic Tangent (6.4.1.5). For each model, the parameters H_0, Ω_{m0} and β_i constant ($i \in [1, 5]$ where the value of i corresponds to the different models) have been obtained from different combination of observational data sets [289] based on the following assumptions:

- **Cosmic Chronometers (CC)[4]:** Massive passively evolving galaxies, which rapidly accumulate their mass at high redshift and deplete their gas reservoirs early on, can serve as cosmic chronometers. By examining two such galaxies with a slight redshift difference, the age difference can be calculated [332]. The compilation of data sets [333, 334, 335, 336, 337, 338, 339] covers various redshift ranges up to $z \lesssim 2$; some use the differential age method, while others employ the differential D4000 technique, which necessitates stellar population synthesis models for calibration.

- **Supernovae Type Ia (SN)[5]:** These supernovae, distinguished by the absence of hydrogen lines in their spectra, exhibit exceptional brightness and a consistent peak luminosity, making them ideal standard candles for measuring distances in the Universe. Notably, the Pantheon compilation of Type Ia supernovae (SNeIa), which combines data from multiple surveys measuring relative luminosity distances in the redshift range of $0.01 < z < 2.26$ [93], is utilized.

- **Baryon Acoustic Oscillations (BAO):** Remnants of sound waves that travelled through the early Universe leave a distinctive imprint on the large-scale structure, creating characteristic peaks in galaxy clustering at the sound horizon scale. BAO data sets utilise several sources: the Sloan Digital Sky Survey (SDSS) Data Set 7 [340], the Six-degree Field Galaxy Survey (6dFGS) [320], Lyα-forest flux transmission from the complete SDSS-III [341], the Baryon Oscillation Spectroscopic Survey (BOSS) [321], and the extended BOSS Data Release 14 quasar (DR14Q) survey [342].

The H_0 priors are obtained from

- **Supernova H_0 for the Equation of State (SH0ES):** Estimates of H_0 (R19) are derived from observing 70 long-period Cepheids in the Large Magellanic Cloud (LMC) using the Hubble Space Telescope (HST) [102].

- **H_0 Lenses in COSMOGRAIL's Wellspring (H0LiCOW):** Measurements of H_0 using gravitational lensing are conducted by determining the time-delay distance $D_{\Delta t}$, which is sensitive to H_0 [104].

- **Tip of the Red Giant Branch (TRGB):** The TRGB occurs when stars on the red giant branch reach maximum luminosity, just before they transition to helium core burning. At the TRGB point, stars are bright and red, offering an independent method to determine H_0 [343].

[4]The acronym CC is reserved for Cosmic Chronometers throughout this chapter, not to be confused with the acronym previously used for Cosmological Constant.

[5]Typically, acronym for Supernovae Type Ia is SNeIa. Since these are the only type of supernovae used, the acronym has been shortened to SN.

The remaining parameters introduced for each model can be obtained through the background equations and the different constant values from the data sets provided. Note, future analysis should also consider results stemming from weak gravitational lensing: slight distortion of light from distant galaxies as it passes through the gravitational field of matter. These distortions are affected by the large-scale distribution of matter, allowing for the mapping of matter and testing modified theories of gravity on a cosmological scale. While HST [344] and Dark Energy Survey (DES) [124, 345] have provided weak lensing maps to constrain dark matter and dark energy, the upcoming Euclid [95] and LSST [8] will have higher precision. Modified theories of gravity alter the matter power spectrum, which is closely linked to the shear power spectrum, and higher-precision observations from missions like Euclid and LSST will be able to detect these deviations from ΛCDM. Additionally, recent observations of BAO by DESI [94] have pointed towards a time-varying equation of state which is supplied by some modified theories of gravity [346].

6.4.1.1 | $f_1(T)$: Power Law Model

The first model considered is the Power Law model [216], able to produce the elements of late-time accelerated cosmic expansion through the function

$$f_1(T) = -T + \alpha_1(-T)^{\beta_1}\,, \tag{6.78}$$

where α_1 and β_1 are constants. This is the torsionful analogy to the modified Einstein-Hilbert Lagrangian $f(\mathring{R}) = -\alpha_0\mathring{R}^{\beta_0}$ where α_0 and β_0 are constants. The power law model in $f(\mathring{R})$ provides one of the simplest forms of models to study fourth-order field equations but does not recover a matter-dominated era before the Universe reaches the status of an accelerated expansion [347], diverging from the known cosmic history. Eq. (6.78) within the torsion framework, can provide a linear relationship of matter density contrast provided α_1 and β_1 parameter are suitable [275]. In addition to this, the power law model in $f(T)$ gravity has been well-studied, retrieving promising results with solar system regime [348, 349, 350, 351], galactic realms [352] and on a cosmological scale [353, 354]. The ΛCDM limit can be obtained directly from the function by setting $\beta_1 = 0$ and mimicking GR at early times. The case of $\beta_1 = \frac{1}{2}$ result in function corresponding to the higher dimensional theory of Dvali-Gabadadze-Porrati (DGP) gravity [355]. The parameter α_1, being itself a constant throughout time, can be obtained by evaluating the first Friedmann equation (6.64) at current time t_0 such that $a(t_0) = 1$, which gives

$$\alpha_1 = \frac{(6H_0^2)^{1-\beta_1}(1-\Omega_{m0})}{2\beta_1 - 1}\,, \tag{6.79}$$

and Eq. (6.64) can be rewritten using the relationship of Eq. (6.79) and Eq. (6.46) to obtain

$$h(a)^2 = \Omega_{m0}a^{-3} + (1-\Omega_{m0})h(a)^{2\beta_1}\,. \tag{6.80}$$

The restrictions on the β_1 parameter are determined through observations at the current time, which show that the power law model fits for $\beta_1 \ll 1$, implying that $f_{1,T} \ll 1$ during the matter era [217] and further derivatives of the f_1 function are even smaller.

In Ref. [275], the growth factor was considered to be k independent. Next, it will be demonstrated that only for high growth index precision, of order 10^{-4} and lower, do k dependencies come into play. Assuming a constant γ value by setting $\gamma_1 = 0$ in Eq. (6.55) and substituting the solution of h through Eq. (6.80), the growth index value $\gamma = \gamma_0$ can be obtained for different Ω_{m0} and H_0 values provided by different data set, tabulated in Table 6.1. These results tabulate the k values at which the γ value matches with that expected from the subhorzion limit up to 4 d.p. For the Power Law model, it is crucial to identify where the subhorizon condition $k \gg aH$ starts to apply, as not all k values larger than the matter-radiation equality $k_{\rm eq}$ necessarily fall within the subhorizon regime. The highest γ value is given by the CC+SN-BAO set at 0.5718, while the lowest value is for CC+SN at 0.5284. At face value, there seems to be a correlation between the growth index value and β_1 value, as smaller model indices yield a smaller γ constant. Additionally, the CC+SN+R19 case has the highest k value for which the subhorizon results match up to four d.p.

Power Law Model						
Data Set	β_1	H_0	Ω_{m0}	$k_{\rm eq}/H_0$	k/H_0	γ
CC + SN	-0.22	68.5	0.35	54.0062	> 411.89	0.5284
CC + SN + R19	-0.13	71.3	0.326	50.3029	> 1130.40	0.5398
CC + SN + HW	-0.16	71.0	0.329	50.7658	> 1422.26	0.5361
CC + SN + TRGB	-0.20	69.1	0.344	53.0803	> 327.57	0.5308
CC + SN + BAO	0.06	67.1	0.294	45.3652	> 204.17	0.5718
CC + SN + BAO + R19	-0.14	69.9	0.305	47.0625	> 176.48	0.5400
CC + SN + BAO + HW	-0.12	67.7	0.304	46.9082	> 565.63	0.5424
CC + SN + BAO + TRGB	-0.01	68.1	0.298	45.9824	> 123.77	0.5585

Table 6.1: Power Law model results for different data sets constraints. The first column gives the data set combination considered, the second column corresponds to the β_1 parameter value, the third and fourth columns give the result of H_0 and Ω_{m0}, respectively. For each set, the fifth column gives the $k_{\rm eq}$ value, and the sixth column shows the minimum value of k for the Mészáros equation to behave like the subhorizon limit as determined by the constant value of γ obtained up to 4 d.p. given by the sixth column.

The variations with k are further illustrated in Fig. 1 when solving for the growth factor $D(a)$. In all cases, the values of $k_{\rm eq}$ and $k = 100H_0$ are further from the subhorizon limit as they fall below the required regime. However, the value given in the sixth column of Table 6.1, denoted as $k_{\rm limit}$, approaches the subhorizon limit. Any value above $k_{\rm limit}$ coincides with the subhorizon curve and hence is not visible. Discrepancies are mainly observed when considering changes to five significant figures (in the last 10^{-4} of the scale factor range). When considering growth at $0.1 \leq a \leq 1$, the subhorizon limit from Ref. [275] suffices, as shown in Fig. 6.1a. For most of the sets considered, the growth factor increases with the k value, as illustrated by the specific case of CC+SN in Fig. 6.1b. The only exception to this pattern is the case of CC+SN+BAO in Fig. 6.1c, primarily due to the positive nature of β_1 in the CC+SN+BAO constraints.

6.4.1.2 | $f_2(T)$: Linder Model

The Linder model [217] given by the function

$$f_2(T) = -T + \alpha_2 T_0 \left(1 - \exp\left(-\beta_2 \sqrt{\frac{T}{T_0}}\right)\right) , \tag{6.81}$$

where $T_0 = -6H_0^2$, and α_2 and β_2 are constants, was originally constructed in the context of late time cosmological issues but has shown to be more broadly applicable. The model was motivated by the $f(\mathring{R})$ model with an exponential dependency on $\mathring{R}$ to allow for small variations in gravitational coupling [217]. The ΛCDM limit of function (6.81) can be obtained when $\beta_2 \to +\infty$. When looking at the equation from $\omega_{\rm eff}$ given by Eq. (6.68), β_2 determined the amplitude deviation from equation of state around $\omega_{\rm eff} = -1$, specifically allowing for values satisfying $\omega_{\rm eff} > -1$ [217]. The α_2 parameter is obtained from the current expression of the first Friedmann equation (6.64) and normalised to obtain

$$\alpha_2 = \frac{e^{\beta_2}(1 - \Omega_{m0})}{e^{\beta_2} - 1 - \beta_2} , \tag{6.82}$$

resulting in

$$h(a)^2 = \Omega_{m0} a^{-3} + (1 - \Omega_{m0}) \frac{1 - e^{-\beta_2 h(a)}(1 + \beta_2 h(a))}{1 - e^{-\beta_2}(1 + \beta_2)} . \tag{6.83}$$

where the solution of h is obtained numerically. The results associated with the Linder model are shown in Table 6.2 and Fig. 6.2. Across the data sets, the growth index ranges from $0.5601 \leq \gamma \leq 0.5659$, with the CC+SN+BAO model contributing to the upper end of this range when considering up to 4 d.p. For the k values where the subhorizon limit applies, most are below the radiation-matter equality value $k_{\rm eq}$, except for the CC+SN+BAO model. These results correspond to the growth factor behaviour where, in many cases, the growth factor at $k_{\rm eq}$ is not

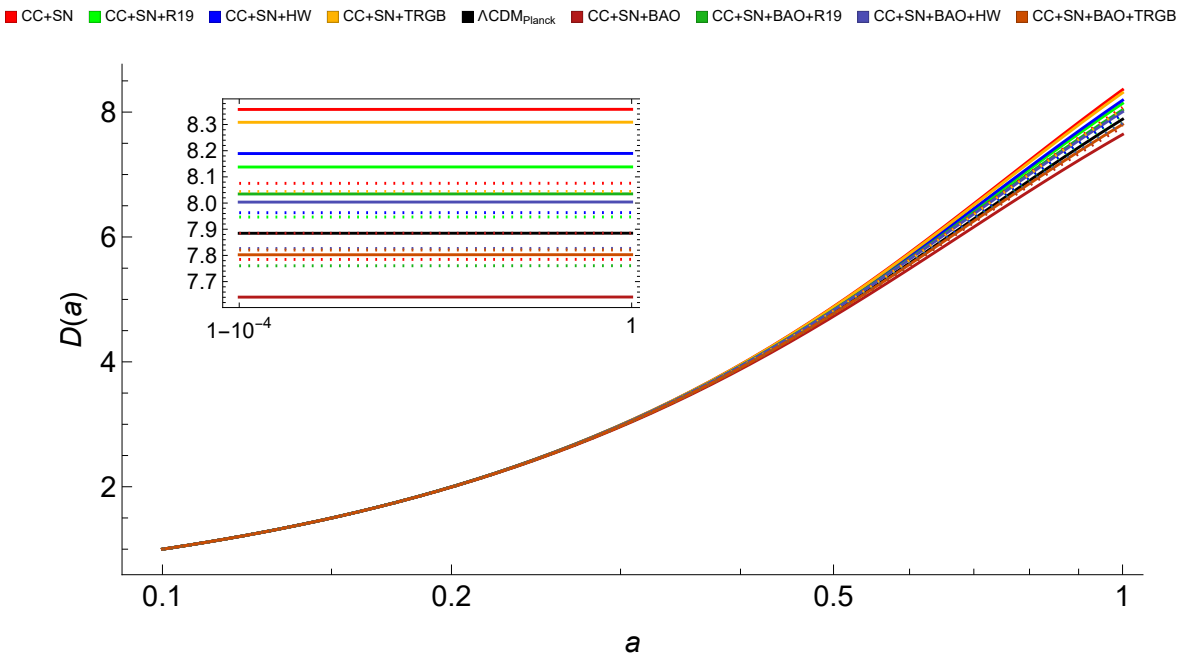

(a) Growth factor plots for all models at the subhorizon (solid line), the ΛCDM limits at $\beta_1 \to 0$ (dotted line), and the result obtained in the Planck collaboration ($\Lambda\text{CDM}_{\text{Planck}}$) [2].

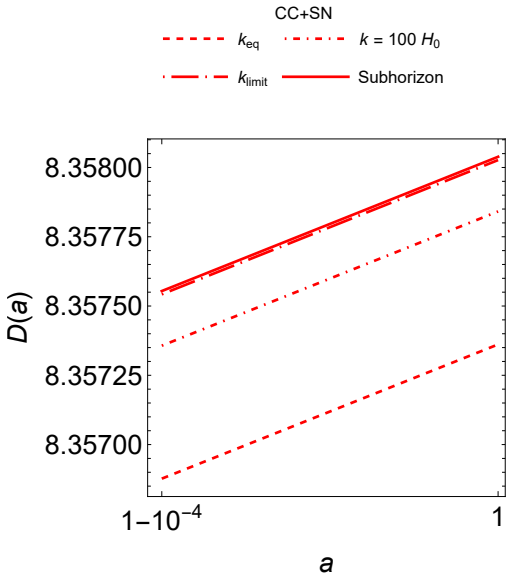

(b) CC + SN growth factor solution at radiation-matter equality k_{eq} (. . . .), at $k = 100H_0$ (. – . –), just before the subhorizon limit k_{limit} (. — . —), and the subhorizon solution (——).

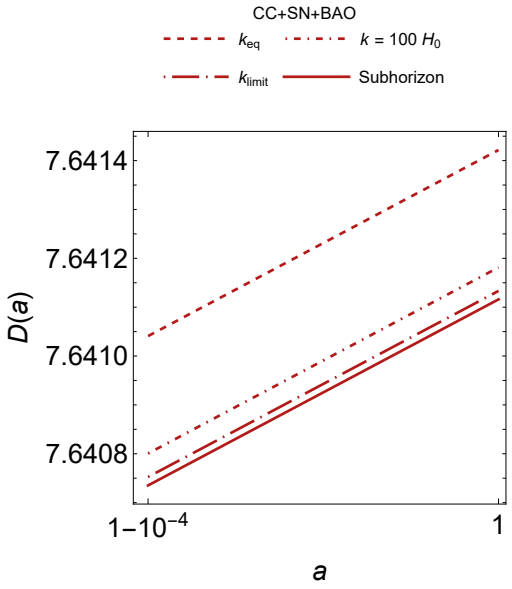

(c) CC + SN + BAO growth factor solution at radiation-matter equality k_{eq} (. . . .), at $k = 100H_0$ (. – . –), just before the subhorizon limit k_{limit} (. — . —), and the subhorizon solution (——).

Figure 6.1: Growth factor solution of the Power Law model.

visible in the plot as these values are well within the subhorizon regime given by Eq. (6.76). In Fig. 6.2b, all values satisfying $k \leq 119.26H_0$ exhibit a slight deviation from the subhorizon limit. Values larger than k_{limit} are encapsulated within the subhorizon plot. Additionally, the model results are lower than the ΛCDM Planck collaboration result, as seen in Fig. 6.2a.

Linder Model						
Data Set	$\frac{1}{\beta_2}$	H_0	Ω_{m0}	k_{eq}/H_0	k/H_0	γ
CC + SN	0.101	68.7	0.298	45.9824	> 15.79	0.5603
CC + SN + R19	0.088	71.4	0.283	43.6679	> 15.05	0.5609
CC + SN + HW	0.096	71.0	0.285	43.9764	> 16.82	0.5608
CC + SN + TRGB	0.088	69.2	0.296	45.6738	> 24.25	0.5603
CC + SN + BAO	0.220	66.9	0.294	45.3652	> 119.26	0.5659
CC + SN + BAO + R19	0.079	68.71	0.300	46.2910	> 6.64	0.5601
CC + SN + BAO + HW	0.076	68.58	0.300	46.2910	> 5.61	0.5601
CC + SN + BAO + TRGB	0.128	67.7	0.297	45.8281	> 45.00	0.5606

Table 6.2: Linder model results for different data sets constraints. The first column gives the data set combination considered, the second column corresponds to β_1 parameter value, the third and fourth columns give the result of H_0 and Ω_{m0}, respectively. For each set, the fifth column gives the k_{eq} value, and the sixth column shows the minimum value of k for the Mészáros equation to behave like the subhorizon limit as determined by the constant value of γ obtained up to 4 d.p. given by the sixth column.

For the remaining datasets, the subhorizon limit can be considered to be appropriate given $k > k_{\text{eq}}$, as the growth index listed in Table 6.2 can be attained for these values. The growth factor solution for the radiation-matter equality can be described by the subhorizon limit where $\frac{G_{\text{eff}}}{G} = \frac{1}{f_T}$, as shown in Eq.(6.76). Due to the large values of β_2, its exponential behaviour yields a solution closer to the ΛCDM limit. This can be seen in the absence of deviation in the growth factor on a larger scale, in contrast with the CC+SN+BAO model in Fig. 6.2b. For the data of CC+SN+BAO+TRGB in Fig. 6.2c, $k_{\text{subhorizon}} \approx k_{\text{eq}}$, making it difficult to differentiate the different k modes from the subhorizon plot without considering very small orders of magnitude.

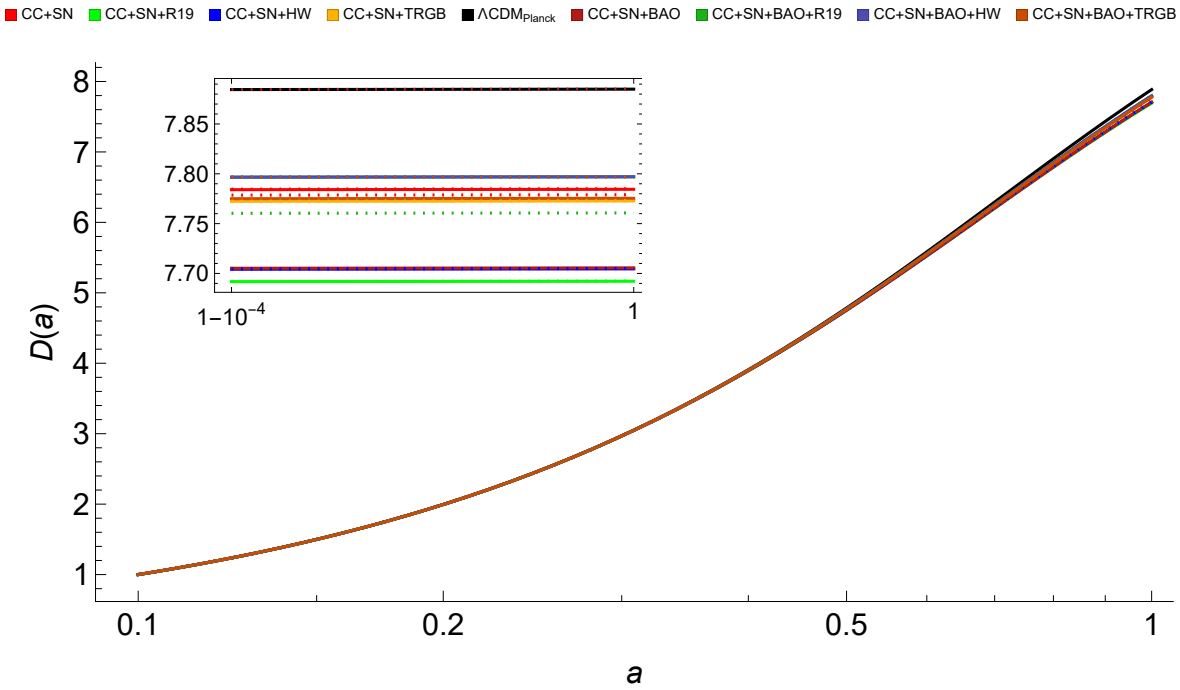

(a) Growth factor plots for all models at the subhorizon (solid line), their corresponding ΛCDM limits at $\beta_2 \to +\infty$ (dotted line), and the result obtained in the Planck collaboration ($\Lambda\text{CDM}_{\text{Planck}}$) [2].

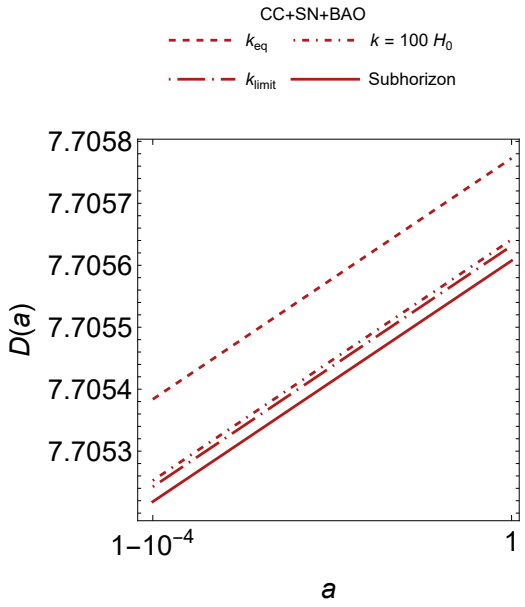

(b) CC + SN + BAO growth factor solution at k_{eq} (. . . .), at $k = 100H_0$ (. _ . _), just before the subhorizon limit k_{limit} (. — . —), and the subhorizon solution (—).

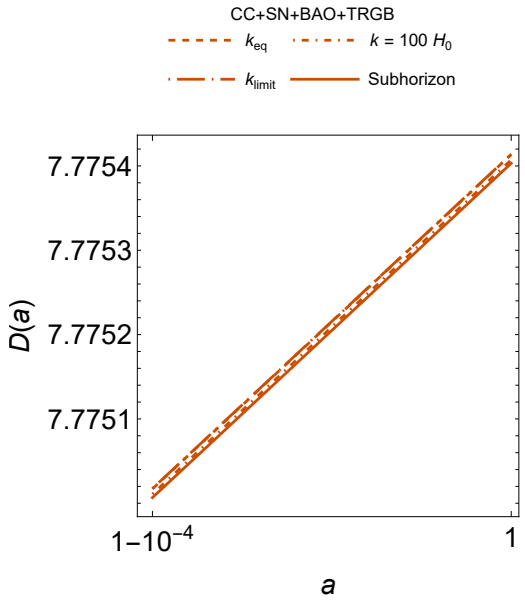

(c) CC + SN + BAO + TRGB growth factor solution at k_{eq} (. . . .), at $k = 100H_0$ (. _ . _), just before the subhorizon limit k_{limit} (. — . —), and the subhorizon solution (—).

Figure 6.2: Growth factor solutions for the Linder model.

6.4.1.3 | $f_3(T)$: Exponential Model

Building on the exponential nature of the Linder model, the Exponential model is given by

$$f_3(T) = -T + \alpha_3 T_0 \left(1 - \exp\left(-\beta_3 \frac{T}{T_0}\right)\right) , \tag{6.84}$$

where α_3 and β_3 are constants. The absence of the square root on the torsion scalar provides a distinct cosmic evolution while keeping the important features that the exponential form provided in the Linder model. Additionally, the form given by Eq. (6.84) is analogous to the exponential model in $f(\mathring{R})$ gravity [217]. The Friedmann equation (6.64) at current time gives

$$\alpha_3 = \frac{e^{\beta_3}(1 - \Omega_{m0})}{e^{\beta_3} - 1 - 2\beta_3} , \tag{6.85}$$

yielding

$$h(a)^2 = \Omega_{m0} a^{-3} + (1 - \Omega_{m0}) \frac{\left(1 - e^{-\beta_3 h(a)^2}(1 + 2\beta_3 h(a)^2)\right)}{1 - e^{-\beta_3}(1 + 2\beta_3)} . \tag{6.86}$$

The ΛCDM model is approached as $\beta_3 \to +\infty$.

For the results obtained from the data set combinations, the subhorizon limits given in Eq. (6.76) are appropriate for any value $k \geq k_{\rm eq}$. This is evident from the low k values in the sixth column of Table 6.3, which yield γ values accurate up to 4 d.p. Consequently, the k dependencies are only noticeable at very low orders of magnitude. Additionally, the growth index values fall within the range $0.5603 \leq \gamma \leq 0.5613$.

In Fig. 6.3, the subhorizon limits of different data sets presented in Table 6.3 are compared. The distinction in the growth factor for various data set combinations is amplified by the inclusion of the different β_3 constant parameter. This amplification can be seen in the differences between the subhorizon plots and their corresponding ΛCDM plots. Notably, the greatest deviation from the ΛCDM model is shown by the CN+SN+BAO+HW model, particularly when compared to its respective model without the BAO result.

6.4.1.4 | $f_4(T)$: Logarithmic Model

The Logarithmic model [356] has similarities with self-accelerating cosmologies in DGP braneworld models [355], and is given by

$$f_4(T) = -T + \alpha_4 T_0 \sqrt{\frac{T}{\beta_4 T_0}} \ln\left(\frac{\beta_4 T_0}{T}\right) , \tag{6.87}$$

with constants α_4 and β_4. The former constant is given by

$$\alpha_4 = \frac{\sqrt{\beta_4}(1 - \Omega_{m0})}{2} , \tag{6.88}$$

Exponential Model						
Data Set	$\frac{1}{\beta_3}$	H_0	Ω_{m0}	$k_{\rm eq}/H_0$	k/H_0	γ
CC + SN	0.067	69.6	0.286	44.1308	> 0.66	0.5607
CC + SN + R19	0.042	72.0	0.273	42.1248	> 0.06	0.5613
CC + SN + HW	0.070	71.5	0.275	42.4334	> 1.31	0.5613
CC + SN + TRGB	0.048	69.7	0.285	43.9764	> 0.30	0.5608
CC + SN + BAO	0.043	67.35	0.289	44.5937	> 0.35	0.5606
CC + SN + BAO + R19	0.059	68.7	0.293	45.2109	> 1.19	0.5604
CC + SN + BAO + HW	0.034	68.52	0.295	45.5195	> 0.01	0.5603
CC + SN + BAO + TRGB	0.074	67.79	0.292	45.0566	> 2.34	0.5605

Table 6.3: Exponential model results for different data sets constraints. The first column gives the data set combination considered, the second column corresponds to β_1 parameter value, the third and fourth columns give the result of H_0 and Ω_{m0}, respectively. For each set, the fifth column gives the $k_{\rm eq}$ value, and the sixth column shows the minimum value of k for the Mészáros equation to behave like the subhorizon limit as determined by the constant value of γ obtained up to 4 d.p. given by the sixth column.

through the Friedmann equation (6.64) which becomes

$$h(a)^2 = \Omega_{m0} a^{-3} + (1 - \Omega_{m0}) h(a)\,. \tag{6.89}$$

It should be noted that the model does not retrieve ΛCDM cosmology but corresponds to the DGP at a background level [355, 357], while this correspondence does not necessarily hold at a perturbative level because the $G_{\rm eff}$ value is expected to evolve differently on a subhorizon level [353]. For this reason, it would be interesting to see whether tension in the data is realised when performing the analysis throughout the deep matter-dominated era, despite having stable perturbations, and whether the model can describe the cosmic history, as observed in Ref. [353].

In the logarithmic case, a different approach will be taken as no constraint was obtained for the β_4 parameter in Ref. [289], given its lack of influence on the Friedmann background equation (6.89). However, the investigation of the growth factor and growth index still relies on this value. Regardless of the β_4 value, the background equation of state remains within the non-phantom phase $\omega_{\rm eff} > -1$ until it approaches the phantom divide line $\omega_{\rm eff} = -1$ [358]. Some constraints on the β_4 value can be determined from the model and definitions of the growth factor and growth index themselves. From Eq. (6.87), the logarithm must be positive definite. Given the positve nature of $\frac{T_0}{T}$, it is necessary to impose that $\beta_4 > 0$. Next, consider the

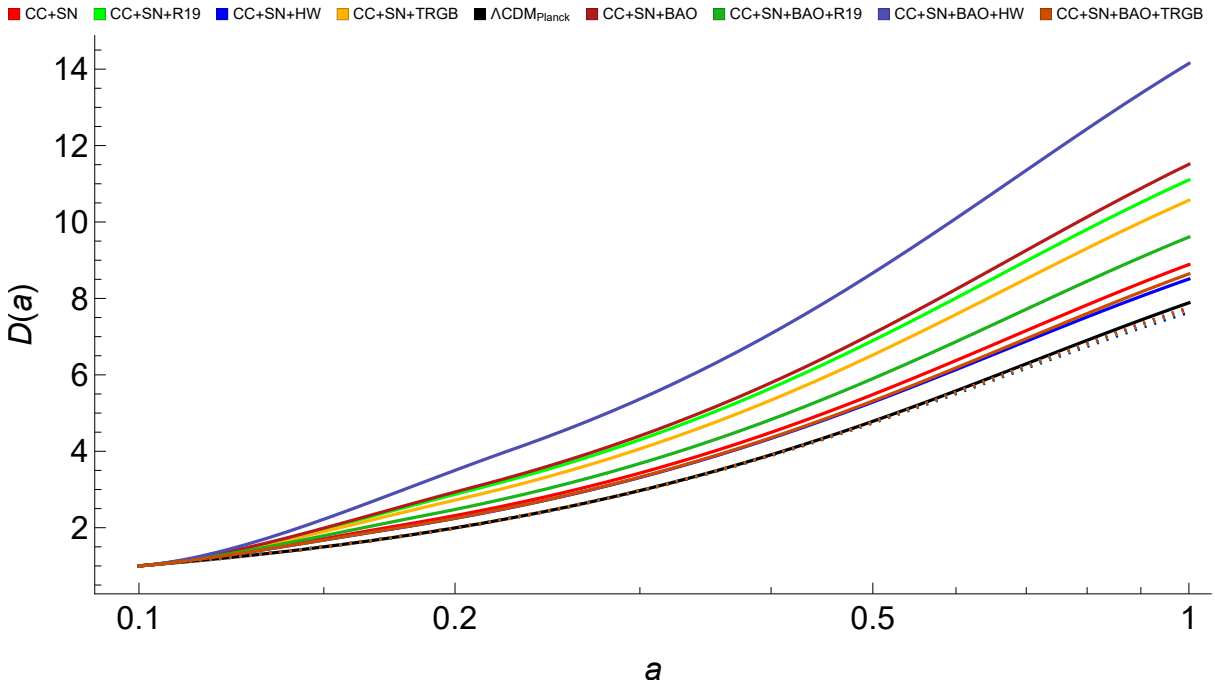

Figure 6.3: Growth factor solutions for the Exponential model at the subhorizon (solid line), their corresponding ΛCDM limits at $\beta_3 \to +\infty$ (dotted line), and the result obtained in the Planck collaboration ($\Lambda\text{CDM}_{\text{Planck}}$) [2].

Mészáros equation (6.71), where both its general (6.72a-6.72b) and subhorizon limit (6.76) forms are undefined at $f_T = 0$. Thus, an undetermined result is obtained, holding for when

$$\beta_4 \neq h(a)^2 \exp\left(2 - \frac{4h(a)}{1-\Omega_{m0}}\right), \tag{6.90}$$

when the condition $1 - \Omega_{m0} \neq 0$ is consistent with the data set values listed in Table 6.4. The dependency on a indicates that this β_4 value is undefined for a range of values as the Universe evolves during $0.1 \leq a \leq 1$. The solution of h and the value of Ω_{m0} depend on the data set considered. Thus, the constraints for H_0 and Ω_{m0} listed in Table 6.4 can be applied. It should be noted that the range of β_4 values is undefined when Eq. (6.90) does not hold, as such values correspond to negative constant growth index γ values in Eq. (6.55).

Logarithmic Model			
Data Set	H_0	Ω_{m0}	$\beta_4^{a=0.1} \leq \beta_4 \leq \beta_4^{a=1}$
CC + SN	68.8	0.207	$6.45814 \times 10^{-30} \leq \beta_4 \leq 0.0476374$
CC + SN + R19	71.4	0.194	$1.90723 \times 10^{-28} \leq \beta_4 \leq 0.0516751$
CC + SN + HW	71.0	0.195	$1.47207 \times 10^{-28} \leq \beta_4 \leq 0.0513575$
CC + SN + TRGB	69.2	0.205	$1.09022 \times 10^{-29} \leq \beta_4 \leq 0.0482458$
CC + SN + BAO	60.89	0.252	$3.50098 \times 10^{-35} \leq \beta_4 \leq 0.0351689$
CC + SN + BAO + R19	62.77	0.261	$2.81590 \times 10^{-36} \leq \beta_4 \leq 0.0329515$
CC + SN + BAO + HW	62.77	0.260	$3.37274 \times 10^{-36} \leq \beta_4 \leq 0.0331934$
CC + SN + BAO + TRGB	62.02	0.257	$8.67071 \times 10^{-36} \leq \beta_4 \leq 0.0339258$

Table 6.4: Undefined regions of β_4 values determined through Eq. (6.90) which do not hold in the Mészáros equation (6.71) in the general form (6.72a-6.72b) and in its subhorizon limit (6.76).

When taking into account the constraint $f_T \ll 1$, small deviations from the ΛCDM model are expected. Additionally, this scenario works if the coupling condition $G_{\text{eff}} \to G$ is viable. Therefore, the constraint in Eq. (6.90) is restricted further through the requirement of

$$\beta_4 \ll h(a)^2 \exp\left(2 + \frac{4h(a)}{1-\Omega_{m0}}\right). \tag{6.91}$$

The results, deep in the matter era (e.g. $a = 0.1$), correspond to β_4 values of a large order of magnitude, which exponentially decrease as the current time is approached ($a = 1$). To ensure that the same β_4 value remains adequate as the Universe evolves, the minimum value obtained for current times, where β_4 is much smaller, is listed in Table 6.5. Eliminating the $\ll$ symbol yields to γ values using Eq. (6.55). Hence, the result obtained through Eq. (6.91) is required to be smaller than that listed in Table 6.5.

Logarithmic Model				
Data Set	H_0	Ω_{m0}	β_4	γ
CC + SN	68.8	0.207	$\ll 1146.12$	< 0.6908
CC + SN + R19	71.4	0.194	$\ll 1056.57$	< 0.6860
CC + SN + HW	71.0	0.195	$\ll 1063.10$	< 0.6863
CC + SN + TRGB	69.2	0.205	$\ll 1131.67$	< 0.6900
CC + SN + BAO	60.89	0.252	$\ll 1552.46$	< 0.7089
CC + SN + BAO + R19	62.77	0.261	$\ll 1656.93$	< 0.7127
CC + SN + BAO + HW	62.77	0.260	$\ll 1644.85$	< 0.7123
CC + SN + BAO + TRGB	62.02	0.257	$\ll 1609.34$	< 0.7110

Table 6.5: Restrictions arising from the constraint $f_T \ll 1$. The fourth column gives the β_4 values obtained through Eq. (6.91). The fifth column contains the γ values given the exact value of the fourth column utilised (inequality ignored). The inequality symbol in Eq. (6.91) indicates that significantly smaller values of β_4 result in smaller γ values. Thus, the inequality symbol $<$ is introduced in the fifth column.

The growth index equation (6.55) in its subhorizon form for the logarithmic model is given by

$$0 = \Omega_{m0}^{2\gamma} - \frac{6\Omega_{m0}}{2(1+\Omega_{m0}) + (1-\Omega_{m0})\ln\beta_4} + \Omega_{m0}^{\gamma}\left[2 + h'(1) - \gamma(3+2h'(1))\right] , \tag{6.92}$$

where $\gamma = \gamma_0$ is a constant and is undefined if $2(1+\Omega_{m0}) + (1-\Omega_{m0})\ln\beta_4 = 0$. Since Eq. (6.92) is considered at $a = 1$, following the restriction given by Eq. (6.90), the β_4 values at which the growth index is undefined in the differential equation is given by the upper bound of the fourth column in Table. 6.4. Solving Eq. (6.92) for β_4 gives:

$$\beta_4 = \exp\left[\frac{-6\Omega_{m0} + 2\Omega_{m0}^{2\gamma}(1+\Omega_{m0}) - 2\Omega_{m0}^{\gamma}(1+\Omega_{m0})\left[-2+3\gamma+(-1+2\gamma)h'(1)\right]}{\Omega_{m0}^{\gamma}(-1+\Omega_{m0})\left[2+\Omega_{m0}^{\gamma}+h'(1)-\gamma(3+2h'(1))\right]}\right] , \tag{6.93}$$

where $h(1) = 1$ has already been substituted. Another undefined region is obtained as the exponent in Eq. (6.91) approaches $+\infty$, i.e.

$$2 + \Omega_{m0}^{\gamma} + h'(1) - \gamma(3+2h'(1)) = 0 , \tag{6.94}$$

where the value of $h'(1)$ changes with different data sets upon solving the Friedmann equations. Hence, the constant γ also varies depending on the data sets. Solving Eq. (6.94) for γ gives the

values for which the logarithmic model does not hold, as summarised in Table 6.6. Next, γ is taken to be within the range $0 < \gamma < 1$, consistent with studies carried out in $f(\mathring{R})$ [359, 360], running vacuum models [361], DGP gravity [362, 363, 364, 365], Finsler-Randers type cosmologies [366] and the GR result of $\gamma = \frac{6}{11}$. β_4 values at $\gamma = 0$ are given in Table 6.6. β_4 is noted to increase to large orders of magnitude as γ increases, until they reach the undefined range given by $\gamma^{\text{undefined}}$ obtained when solving Eq. (6.94). Immediately after $\gamma^{\text{undefined}}$, β_4 values drop to zero. Hence, the spike in value and sudden drop corresponds to discontinuities due to the undefined expressions. Once again, as the γ value continues to increase beyond $\gamma^{\text{undefined}}$, β_4 increases. While the range $\beta_4^{\gamma=0} \leq \beta_4 \leq \beta_4^{\gamma=1}$ coincide with the condition given by Eq. (6.91), the $\gamma = 1$ results are not viable as per growth index values given by Table 6.5.

Logarithmic Model					
Data Set	H_0	Ω_{m0}	$\gamma^{\text{undefined}}$	$\beta_4^{\gamma=0}$	$\beta_4^{\gamma=1}$
CC + SN	68.8	0.207	0.880459	0.0894568	7.57215×10^{-14}
CC + SN + R19	71.4	0.194	0.866199	0.0918131	3.67027×10^{-12}
CC + SN + HW	71.0	0.195	0.867282	0.0916297	2.81499×10^{-12}
CC + SN + TRGB	69.2	0.205	0.878239	0.0898153	1.47126×10^{-13}
CC + SN + BAO	60.89	0.252	0.933138	00817573	2.4102×10^{-26}
CC + SN + BAO + R19	62.77	0.261	0.944366	0.0802988	4.48921×10^{-32}
CC + SN + BAO + HW	62.77	0.260	0.943106	0.0804596	2.55792×10^{-31}
CC + SN + BAO + TRGB	62.02	0.257	0.939345	0.0809438	2.99871×10^{-29}

Table 6.6: The first column gives the data set considered, the second and third columns give the corresponding H_0 and Ω_{m0} values, the fourth column contains the γ value obtained when solving Eq. (6.94) and giving an undefined value for β_4 determined by Eq. (6.93). The fifth column gives the β_4 value when $\gamma = 0$: $\beta_4^{\gamma=0}$. As γ increases, β_4 increases to large orders of magnitude until it reaches undefined values corresponding to $\gamma^{\text{undefined}}$. Beyond this value, β_4 drops to zero and increases once again to the value of $\beta_4^{\gamma=1}$ listed in the sixth column.

All the constraints for β_4 have been summarised in Table 6.7. Next, a more restricted range of γ is considered: $0.5 \leq \gamma \leq 0.6$ as it is a significant range presented in the literature for different models and gravitational theories. The β_4 value is determined for both ends of the range, tabulated in Fig. 6.4, along with the k values at which the subhorizon limit is replicated. The $\gamma = 0.5$ case results in the range $1.74 \leq \beta_4 \leq 1.99$, while $\gamma = 0.6$ gives higher values with a range of $15.51 \leq \beta_4 \leq 16.31$. Any k value well above k_{eq} can recover the subhorizon limit;

$k < 2.2k_{\rm eq}$ is the minimum value to recover the subhorizon limit with the assumption of $\gamma = 0.5$, in the case of CC+SN+BAO+R19. Irrespective of the growth index value within the range $0.5 \leq \gamma \leq 0.6$ it is sufficient to consider $k > 34.78k_{\rm eq}$ across all data sets considered in Table 6.4.

Logarithmic Data Set	β_4 Range	γ Range
CC + SN	$0.0476374 < \beta_4 \ll 1146.12$	$\gamma < 0.6908$
CC + SN + R19	$0.0516751 < \beta_4 \ll 1056.57$	$\gamma < 0.6860$
CC + SN + HW	$0.0513575 < \beta_4 \ll 1063.10$	$\gamma < 0.6863$
CC + SN + TRGB	$0.0482458 < \beta_4 \ll 1131.67$	$\gamma < 0.6900$
CC + SN + BAO	$0.0351689 < \beta_4 \ll 1552.46$	$\gamma < 0.7089$
CC + SN + BAO + R19	$0.0329515 < \beta_4 \ll 1656.93$	$\gamma < 0.7127$
CC + SN + BAO + HW	$0.0331934 < \beta_4 \ll 1644.85$	$\gamma < 0.7123$
CC + SN + BAO + TRGB	$0.0339258 < \beta_4 \ll 1609.34$	$\gamma < 0.7110$

Table 6.7: β_4 parameter and growth index γ constraints obtained from restrictions of Eqs (6.90), (6.91) and (6.94). The minimum growth index constraint is either negative or undefined.

Fig. 6.4 illustrates the growth factor solution for the logarithmic model for different data sets. Fig. 6.4a shows the subhorizon limit when $\gamma = 0.5$, for which all data sets result in curves above the ΛCDM$_{\rm Model}$ (obtained through the values of the respective data set for a constant function for $f(T)$). As for the $\gamma = 0.6$ results seen in Fig. 6.4b, they yield slower growth curves in comparison with ΛCDM$_{\rm Planck}$ (value corresponding to the Planck collaboration data [2]). The models without BAO data sets give a slower growth than the ΛCDM$_{\rm Planck}$ case. When the BAO data is considered, an overall faster growth is noted in comparison to the other plots.

6.4.1.5 | $f_5(T)$: Hyperbolic-Tangent Model

The last $f(T)$ model examined here is the Hyperbolic Tangent model [367], characterised by asymptotes that align with the expansion profiles inferred from measurements of the Universe:

$$f_5(T) = -T + \alpha_5(-T)^{\beta_5} \tanh\left(\frac{T_0}{T}\right), \tag{6.95}$$

where α_5 and β_5 are constants. The background Friedmann equation at current time provides an expression for α_5:

$$\alpha_5 = \frac{(6H_0^2)^{1-\beta_5}(1-\Omega_0)}{\tanh(1)(2\beta_5 - 1) - 2\,\mathrm{sech}^2(1)}, \tag{6.96}$$

Logarithmic Model							
Data Set	H_0	Ω_{m0}	$k_{\rm eq}/H_0$	$\beta_4^{\gamma=0.5}$	$k^{\gamma=0.5}/H_0$	$\beta_4^{\gamma=0.6}$	$k^{\gamma=0.6}/H_0$
CC + SN	68.8	0.207	31.9410	1.75	> 119.20	16.16	> 921.40
CC + SN + R19	71.4	0.194	29.9350	1.69	> 107.44	16.31	> 1041.72
CC + SN + HW	71.0	0.195	30.0893	1.69	> 82.62	16.30	> 808.05
CC + SN + TRGB	69.2	0.205	31.6324	1.74	> 107.14	16.18	> 569.75
CC + SN + BAO	60.89	0.252	38.8846	1.96	> 98.93	15.62	> 785.53
CC + SN + BAO + R19	62.77	0.261	40.2733	1.99	> 88.75	15.51	> 628.97
CC + SN + BAO + HW	62.77	0.260	40.1190	1.99	> 266.85	15.53	> 645.22
CC + SN + BAO + TRGB	62.02	0.257	39.6561	1.98	> 128.87	15.56	> 848.85

Table 6.8: Logarithmic model results for different data sets constraints. The type of data set combination is listed in the first column, with the second and third columns listing the H_0 and Ω_{m0} values, respectively. For each set, the k cutoff value is listed in the fourth column to show the k value at which radiation-matter densities are equal. The fifth and sixth columns give the β_4 and minimum k value required to obtain subhorizon limit results at $\gamma = 0.5$, and the seventh and eighth columns represent the same quantities but for $\gamma = 0.6$.

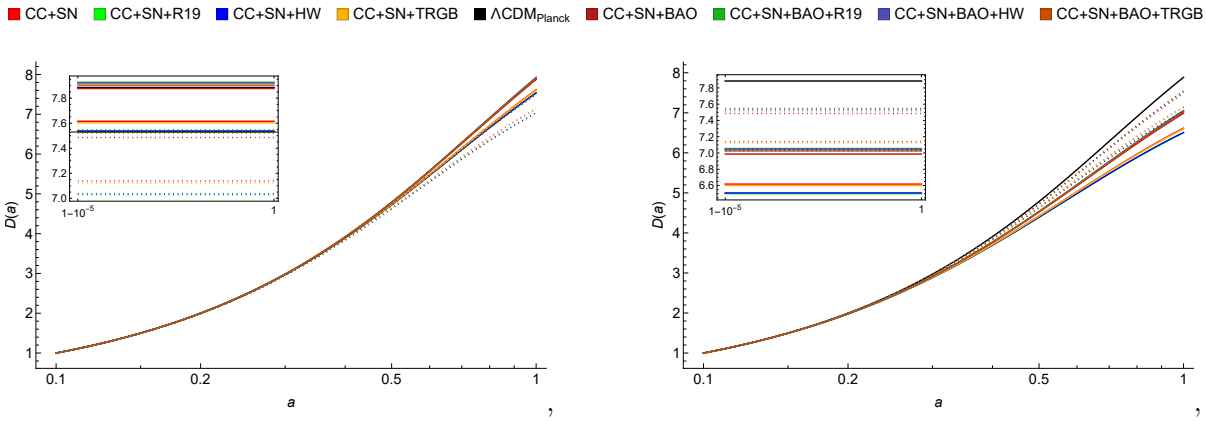

(a) Subhorizon solution at $\gamma = 0.5$

(b) Subhorizon solution at $\gamma = 0.6$

Figure 6.4: Growth factor solutions for the Logarithmic model at the subhorizon (solid line), their corresponding ΛCDM case, and the result obtained in the Planck collaboration ($\Lambda\text{CDM}_{\text{Planck}}$) [2]. Fig. 6.4a corresponds to the solution when the growth index $\gamma = 0.5$, while Fig. 6.4b illustrates the result for $\gamma = 0.6$.

such that Eq. (6.64) becomes

$$h(a)^2 = \Omega_{m0}a^{-3} + \frac{(1-\Omega_{m0})h(a)^{2(-1+\beta_5)}\left(-2\,\mathrm{sech}^2(h(a)^{-2}) + (-1+2\beta_5)h(a)^2\tanh(h(a)^{-2})\right)}{\tanh(1)(2\beta_5-1) - 2\,\mathrm{sech}^2(1)}\,. \quad (6.97)$$

The ΛCDM limit is not attained by the hyperbolic tangent model. Regardless, it provides a model behaving as a possible phantom divide line crossing the $f(T)$ model [367]. While, in line with the logarithmic model, the lack of ΛCDM limit is expected to be in tension with observational data as per results in Ref. [353]. Through the study of growth factor and growth index behaviour, the tensions might materialise when considering the data set explored in Ref. [289]. The ΛCDM limit is considered by setting $f(T) = -T + c$, where c is a constant, for different data sets. Analogous to the power law model explored in Sec. 6.4.1.1, the k values at which the subhorizon limit is resolved when considering γ value up to 4 d.p., are always larger than the radiation-matter equality value $k_{\rm eq}$. In Table 6.9, subhorizon limit plays a role when $k > 3.7k_{\rm eq}$ at a minimum for the CC+SN+BAO case and $k > 8.39k_{\rm eq}$ at a maximum for CC+SN+HW. The subhorizon growth index when taken to be a constant, appears in a lower range when compared with the rest of the models: $0.4905 \leq \gamma \leq 0.5193$. The sets containing BAO data result in negative β_5 values resulting with values $\gamma < 0.5$. On the other hand, the rest of the data sets have a positive β_5 value with corresponding γ values at $\gamma > 0.5$.

The distinction within the model when considering BAO values is also highlighted in the growth factor solution plots in Fig. 6.5. Case CC+SN in Fig. 6.5b has faster growth than the BAO counterpart of CC+SN+BAO in Fig. 6.5c. Additionally, when the BAO results are considered, the ΛCDM limit given by $f(T) = -T + c$ is close to the result obtained by the Planck collaboration [2].

From the $f(T)$ cases considered here, it suffices to conclude that the application of the subhorizon limit at first principle provides an adequate result when considering precision up to 2 d.p. for the growth index value. Higher index precision can come into play as future surveys realise improved analysis of the growth index, possibly becoming sensitive to k dependencies. Table 6.10 shows the k requirement to produce the subhorizon γ value up to 2 d.p., all of which correspond to scales smaller than those considered to evaluate the growth evolution of CDM. Only four cases are listed, as for the rest of the models and data sets any value above $k_{\rm eq}$ holds; lower values of k would not yield an adequate range to consider in the first place.

While $f(T)$ gravity does not result in a significant discrepancy among k values and the subhorizon limit, this is not necessarily the case when considering broader classes of teleparallel theories. One such class is that of scalar-tensor theories, in which the effects of a scalar field ϕ can contribute to a richer phenomenology towards more physically viable models.

Hyperbolic Tangent Model						
Data Set	β_5	H_0	Ω_{m0}	k_{eq}/H_0	k/H_0	γ
CC + SN	-0.36	69.2	0.369	56.9379	> 327.98	0.4905
CC + SN + R19	-0.28	71.8	0.349	53.8519	> 403.54	0.4946
CC + SN + HW	-0.29	71.3	0.353	54.4691	> 456.95	0.4939
CC + SN + TRGB	-0.35	69.5	0.366	56.4750	> 383.85	0.4911
CC + SN + BAO	0.144	68.4	0.302	46.5996	> 172.47	0.5193
CC + SN + BAO + R19	0.079	70.6	0.308	47.5254	> 217.63	0.5142
CC + SN + BAO + HW	0.039	70.2	0.308	47.5254	> 293.25	0.5118
CC + SN + BAO + TRGB	0.115	68.9	0.304	46.9082	> 275.94	0.5170

Table 6.9: Hyperbolic Tangent model results for different data sets constraints. The first column gives the data set combination considered, the second column corresponds to β_1 parameter value, the third and fourth columns give the result of H_0 and Ω_{m0}, respectively. For each set, the fifth column gives the k_{eq} value, and the sixth column shows the minimum value of k for the Mészáros equation to behave like the subhorizon limit as determined by the constant value of γ obtained up to 4 d.p. given by the sixth column.

Model	Data Set	γ (2 d.p.)	k/H_0
Power Law	CC + SN + R19	0.54	> 79.9281
Power Law	CC + SN + R19	0.54	> 49.1356
Hyperbolic Tangent	CC + SN	0.49	> 94.5143
Hyperbolic Tangent	CC + SN + TRGB	0.49	> 66.8440

Table 6.10: Models which attain the subhorizon growth index γ match up to 2 d.p. at $k > k_{\text{eq}}$. The remaining cases reach 2 d.p. precision of all values above k_{eq}.

6.4.2 | Modified GR

An easy introduction of the scalar field is through the consideration of modified GR, given by the action

$$\mathcal{S}_{\text{Mod GR}} = \frac{1}{2\kappa^2}\int d^4x e(-T + V(\phi) + P(\phi)X) + \int d^4x\, e\, \mathcal{L}_m\,, \tag{6.98}$$

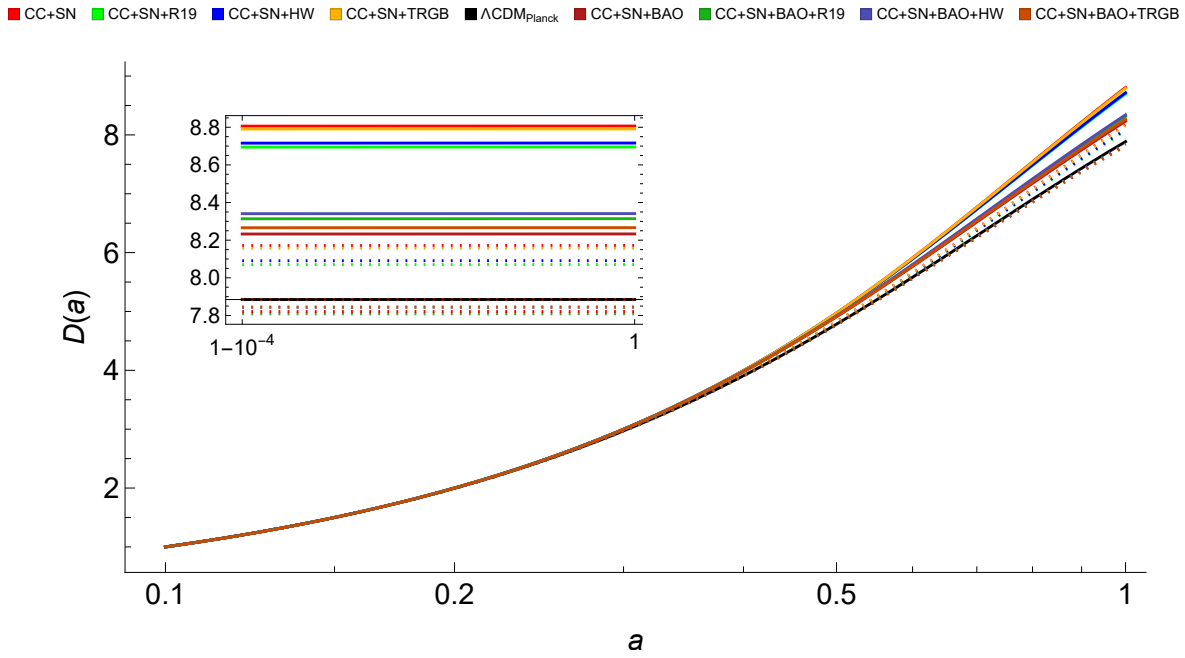

(a) Growth factor plots for all models at the subhorizon (solid line), their corresponding ΛCDM limits when $f(T) = -T+c$ (dotted line), and the result obtained in the Planck collaboration ($\Lambda\text{CDM}_{\text{Planck}}$) [2].

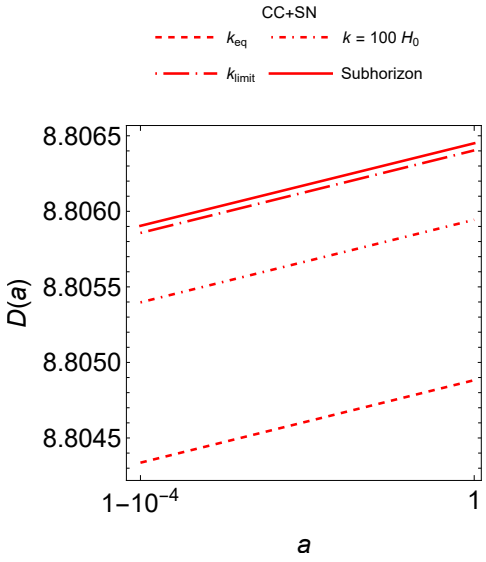

(b) CC + SN growth factor solution analyzed at radiation-matter equality k_{eq} (. . . .), at the case $k = 100H_0$ (. _ . _), at the point just before the subhorizon limit applies k_{limit} (. — . —), and the subhorizon solution (——).

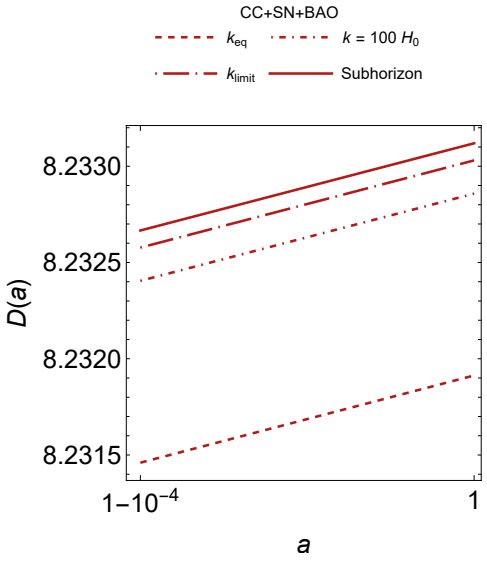

(c) CC + SN + BAO growth factor solution at k_{eq} (. . . .), at $k = 100H_0$ (. _ . _), just before the subhorizon limit k_{limit} (. — . —), and the subhorizon solution (——).

Figure 6.5: Growth factor solutions for the Hyperbolic Tangent model.

where V and P are arbitrary functions of the scalar field ϕ. Such theories have been typically used to explore inflationary models [368, 369], where the scalar field drives the expansion at very early stages of the Universe to smoothen out spacetime, yielding a homogeneous and isotropic Universe. Alternatively, the scalar field can be attributed to the effective portion of the theory, driving the accelerated expansion at late times of the Universe.[6] Through the BDLS action (2.98), this can be attained for $G_2 = V + PX$, $G_{\rm Tele} = -T$ and the rest of the terms vanish. While the action is expressed in terms of tetrad notation, it can be modified to the curvature-based formalism with the changes $e \to \sqrt{-g}$ and $-T \to \mathring{R}$. Now, limits from the BDLS action are attained for $G_2 = V + PX$, $G_4 = 1$, and the rest of the terms vanish. While at the action level, there are distinctions, on a dynamical level the two actions are considered to be identical up to a boundary term, as noted in Eq. (2.66).

The appropriate limits to the Friedmann equation (3.19-3.23) result in the background equations

$$2\kappa^2\rho = 6H^2 - V + PX\,, \tag{6.99}$$

$$-2\kappa^2 p = 6H^2 + 4\dot{H} - V - PX\,, \tag{6.100}$$

$$0 = V_\phi - XP_\phi + 3HP\dot{\phi} + P\ddot{\phi}\,, \tag{6.101}$$

such that the effective energy density $\rho_{\rm eff}$ and the effective pressure $p_{\rm eff}$ are defined by Eqs (6.66-6.67) modified for the system in Eqs (6.99-6.100). The effective portions $\rho_{\rm eff}$ and $p_{\rm eff}$ stem from the additional contributions of V and P, such that

$$\omega_{\rm eff} = \frac{p_{\rm eff}}{\rho_{\rm eff}} = -1 - \frac{2PX}{V - PX}\,, \tag{6.102}$$

where the ΛCDM limit $\omega_{\rm eff} = -1$ is obtained by elimination of P or X. The linearised field equations (6.17) are given in the form presented in Eq. (6.23)

$$\delta W_{00}: \qquad \mathcal{F}_1(\delta\phi, \delta\dot{\phi}, \varphi, \psi, \dot{\psi}) = \mathcal{G}_1(\delta_m, \dot{\delta}_m)\,, \tag{6.103a}$$

$$\delta W_{0i}: \qquad \mathcal{F}_2(\delta\phi, \varphi, \dot{\psi}) = \mathcal{G}_2(\dot{\delta}_m)\,, \tag{6.103b}$$

$$\delta W_{i0}: \qquad \mathcal{F}_3(\delta\phi, \varphi, \dot{\psi}) = \mathcal{G}_3(\dot{\delta}_m)\,, \tag{6.103c}$$

$$\delta W_{ij}: \qquad \mathcal{F}_4(\varphi, \psi) = 0\,, \tag{6.103d}$$

$$\delta W_i{}^i: \qquad \mathcal{F}_5(\delta\phi, \delta\dot{\phi}, \varphi, \dot{\varphi}, \psi, \dot{\psi}, \ddot{\psi}) = 0\,, \tag{6.103e}$$

$$\delta \dot{W}_{00}: \qquad \mathcal{F}_6(\delta\phi, \delta\dot{\phi}, \delta\ddot{\phi}, \varphi, \dot{\varphi}, \psi, \dot{\psi}, \ddot{\psi}) = \mathcal{G}_6(\delta_m, \dot{\delta}_m, \ddot{\delta}_m)\,, \tag{6.103f}$$

$$\delta \dot{W}_{0i}: \qquad \mathcal{F}_7(\delta\phi, \delta\dot{\phi}, \varphi, \dot{\varphi}, \dot{\psi}, \ddot{\psi}) = \mathcal{G}_7(\dot{\delta}_m, \ddot{\delta}_m)\,, \tag{6.103g}$$

[6] It is worth noting that the same scalar field can be associated with both the inflationary and accelerated expansion periods, though its behavior varies across different epochs. Alternatively, two distinct scalar fields can be introduced to independently account for each phenomenon.

$$\delta\dot{W}_{i0}: \qquad \mathcal{F}_8(\delta\phi, \delta\dot{\phi}, \varphi, \dot{\varphi}, \dot{\psi}, \ddot{\psi}) = \mathcal{G}_8(\dot{\delta}_m, \ddot{\delta}_m)\,, \tag{6.103h}$$

$$\delta\dot{W}_{ij}: \qquad \mathcal{F}_9(\varphi, \dot{\varphi}, \psi, \dot{\psi}) = 0\,, \tag{6.103i}$$

$$\delta W_{\phi}: \qquad \mathcal{F}_{10}(\delta\phi, \delta\dot{\phi}, \delta\ddot{\phi}, \varphi, \dot{\varphi}, \dot{\psi}) = 0\,, \tag{6.103j}$$

of which 8 equations are linearly independent. By omitting δW_{i0} given by Eq. (6.103c) and $\delta\dot{W}_{i0}$ given by Eq. (6.103h), the remaining equations can be used to solve for the eight gravitational perturbation modes $\{\delta\phi, \delta\dot{\phi}, \delta\ddot{\phi}, \varphi, \dot{\varphi}, \psi, \dot{\psi}, \ddot{\psi}\}$. These equations can be expressed as a matrix system of the form Eq. (6.37)

$$\overbrace{\begin{pmatrix}
\mathcal{F}_{11} & \mathcal{F}_{12} & 0 & \mathcal{F}_{14} & 0 & \mathcal{F}_{16} & \mathcal{F}_{17} & 0 \\
\mathcal{F}_{21} & 0 & 0 & \mathcal{F}_{24} & 0 & 0 & \mathcal{F}_{27} & 0 \\
0 & 0 & 0 & 1 & 0 & -1 & 0 & 0 \\
\mathcal{F}_{51} & -\frac{1}{2}P\dot{\phi} & 0 & \mathcal{F}_{54} & 24H & \mathcal{F}_{56} & 72H & 24 \\
\dot{\mathcal{F}}_{11} & \mathcal{F}_{11}+\dot{\mathcal{F}}_{12} & \mathcal{F}_{12} & \dot{\mathcal{F}}_{14} & \mathcal{F}_{14} & \dot{\mathcal{F}}_{16} & \mathcal{F}_{16}+\dot{\mathcal{F}}_{17} & \mathcal{F}_{17} \\
\dot{\mathcal{F}}_{21} & \mathcal{F}_{21} & 0 & \dot{\mathcal{F}}_{24} & \mathcal{F}_{24} & 0 & \dot{\mathcal{F}}_{27} & \mathcal{F}_{27} \\
0 & 0 & 0 & 0 & 1 & 0 & -1 & 0 \\
\mathcal{F}_{101} & \mathcal{F}_{102} & P & 2V_{\phi} & -P\dot{\phi} & -3P\dot{\phi} & \mathcal{F}_{107} & \mathcal{F}_{108}
\end{pmatrix}}^{\mathcal{F}}
\overbrace{\begin{pmatrix}
\delta\phi \\ \delta\dot{\phi} \\ \delta\ddot{\phi} \\ \varphi \\ \dot{\varphi} \\ \psi \\ \dot{\psi} \\ \ddot{\psi}
\end{pmatrix}}^{\chi}
=
\overbrace{\begin{pmatrix}
\mathcal{C}_1 \\ \mathcal{C}_2 \\ 0 \\ 0 \\ 0 \\ \dot{\mathcal{C}}_1 \\ \dot{\mathcal{C}}_2 \\ 0
\end{pmatrix}}^{\mathcal{G}}\,, \tag{6.104}$$

where

$$\begin{aligned}
\mathcal{F}_{11} &= \tfrac{1}{4}(2V_{\phi} + P_{\phi}\dot{\phi}^2)\,, & -6\mathcal{F}_{12} &= 3\mathcal{F}_{21} = -3P\dot{\phi}\,, \\
\mathcal{F}_{14} &= -H\mathcal{F}_{17} + \dot{\phi}\mathcal{F}_{12}\,, & 4\mathcal{F}_{16} &= \mathcal{F}_{56} = 8\tfrac{k^2}{a^2}\,, \\
-\tfrac{3}{2}H\mathcal{F}_{17} &= H\mathcal{F}_{24} = \mathcal{F}_{27}\,, & \mathcal{F}_{27} &= 4 - \tfrac{6\kappa^2\rho}{\frac{k^2}{a^2}-3\dot{H}}\,, \\
\mathcal{B}_{54} &= -8\tfrac{k^2}{a^2} + 6(12H^2 + 8\dot{H} + P\dot{\phi}^2)\,, & \mathcal{B}_{51} &= 3(2V_{\phi} - P_{\phi}\dot{\phi}^2)\,, \\
\mathcal{B}_{102} &= (3HP + P_{\phi}\dot{\phi})\,, & \mathcal{B}_{101} &= \tfrac{1}{2}\left(2\tfrac{k^2}{a^2} - 4\tfrac{P_{\phi}}{P}\mathcal{F}_{11} + 2V_{\phi\phi} + P_{\phi\phi}\dot{\phi}^2\right)\,, \\
\mathcal{C}_1 &= -\kappa^2\rho\delta_m - \tfrac{3H}{\frac{k^2}{a^2}-3\dot{H}}\dot{\delta}_m\,, & \mathcal{C}_2 &= -\tfrac{2\kappa^2\rho}{\frac{k^2}{a^2}-3\dot{H}}\dot{\delta}_m\,.
\end{aligned}$$

Solution of χ, and its substitution in the Mészáros equation (6.43) gives

$$0 = \ddot{\delta}_m + 2H\nu(t)\dot{\delta}_m - \frac{1}{2}\kappa^2\mu(t)\rho\delta_m\,, \tag{6.105}$$

where

$$\nu = 1 + \frac{36\dot{H} + 3HP\dot{\phi}^2 + 12\ddot{H}}{2H(4\frac{k^2}{a^2} + 3P\dot{\phi}^2)}\,, \tag{6.106}$$

$$\mu = 1 + \frac{4P\dot{\phi}^2}{4\frac{k^2}{a^2} - P\dot{\phi}^2}\,, \tag{6.107}$$

implying that the growth of CDM is not explicitly dependent on the potential $V(\phi)$, but the solution for the Hubble parameter H through the Friedmann equation (6.99) is. The conditions of matter dominated era given by Eq. (6.73) simplify Eq. (6.106) to $\nu = 1 + \frac{3P\dot{\phi}^2}{2(4\frac{k^2}{a^2}+3P\dot{\phi}^2)}$. The magnitude of the scalar field ϕ in comparison to the k contribution is unknown, hence application of the subhorizon limit at the field equation level would yield a superficial result. To contrast with the solutions obtained for different values of ϕ, this superficial subhorizon estimate is still included, which is given by

$$\nu^{\rm sub} = 1\,, \qquad\qquad \mu^{\rm sub} = 1\,, \tag{6.108}$$

corresponding to the GR limit. The Mészáros equation (6.105) and Eqs (6.106-6.107) are expressed in terms of the scale factor to obtain the form in Eq. (6.48). The growth factor in Eq. (6.49), growth index in Eq. (6.55), $f\sigma_8$ in Eq. (6.57) and S_8 in Eq. (6.58) are used to investigate the k dependencies for the modified GR model. The three cases considered have $P = 1$, with different potentials: Quadratic in Sec. 6.4.2.1, Quartic in Sec. 6.4.2.2, and Exponential in Sec. 6.4.2.3.

Next, it will be shown how the growth index result is independent of the potential function. Eq. (6.55) is an evaluation at current time, where $\nu(1)$ and $\mu(1)$ are independent of the potential V. Additionally, $h(1) = 1$ as per definition in Eq. (6.46), and $\phi(1)$ and $\phi'(1)$ are set constraints. The first Friedmann equation evaluated at the current time gives an equation for the current value of the potential:

$$V(1) = 6H_0^2(1 - \Omega_{m0}) - \frac{1}{2}H_0^2\phi'(1)\,, \tag{6.109}$$

which when substituted into the equation of state (6.102) at current time results in

$$\omega_{\rm eff}(1) = -1 + \frac{\phi'(1)^2}{6(1 - \Omega_{m0})}\,. \tag{6.110}$$

By imposing that the current equation of state value recovers the result $\omega_{\rm eff} = -1$, then

$$\phi'(1) = 0 \tag{6.111}$$

is the nontrivial solution and leaves only the choice of $\phi(1)$. In these cases considered, the P function is given by the same constant, making only $h'(1)$ a case-dependent constant. Regardless

of the different background equations provided by different potentials, no alterations to the main result are obtained. Fig. 6.6 illustrates the behaviour of a dynamical growth index at $a = 1$, illustrating the balance between the γ_0 and γ_1 constants of Eq. (6.54) to obtain the ΛCDM value, $\gamma_{\Lambda\text{CDM}}$. As k increases, the results move towards the subhorizon solution, previously noted to be obtained through an overlook of the magnitude of ϕ and ϕ'. In the $f(T)$ case, the majority of the cases were seen to behave well into the subhorizon limit for modes $k > 100H_0$ at a precision of 4 d.p. The result presented here, hence, implies k dependency. Table 6.11 gives a summary of coordinates (γ_0, γ_1) for different k values and at the subhorizon limit to obtain the ΛCDM limit, $\gamma_0 = 0.55$ and $\gamma_0 = 0.56$, as it is the main range of interest.

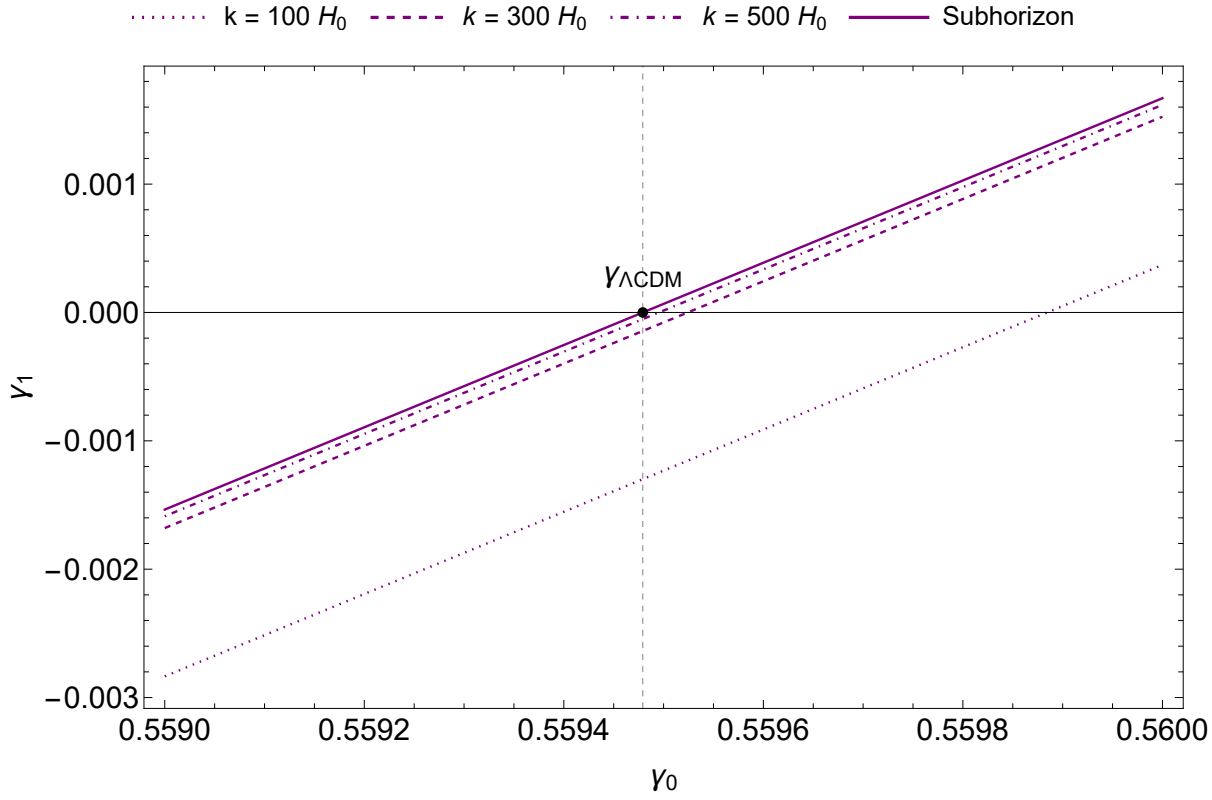

Figure 6.6: Growth index plots for cases of the form $-T + V(\phi) + X$ comparing γ_1 to γ_0. The ΛCDM limit $\gamma_{\Lambda\text{CDM}} = 0.5594792$ can be obtained using different k values, depicted by a vertical dashed line.

Up to this point, the value of $\phi_0 = \phi(1)$ has not been used. The value becomes crucial when solving the background equations, which are substituted in the matter perturbation solutions. The goal is to illustrate k dependencies that arise from the inclusion of a scalar field, but the choice of ϕ_0 has been determined through constraints on background equations, and detailed for each case separately in the respective sections.

	(γ_0, γ_1)			
	$\gamma = \gamma_0$	ΛCDM solution at $\gamma = \gamma_0$	$\gamma_0 = 0.55$	$\gamma_0 = 0.56$
$k = 100H_0$	$(0.559884, 0)$	$(0.5594792, -0.001299)$	$(0.55, -0.031657)$	$(0.56, 0.000370)$
$k = 300H_0$	$(0.559524, 0)$	$(0.5594792, -0.000144)$	$(0.55, -0.030503)$	$(0.56, 0.001525)$
$k = 500H_0$	$(0.559495, 0)$	$(0.5594792, -0.000052)$	$(0.55, -0.03041)$	$(0.56, 0.001617)$
Subhorizon	$(0.559479, 0)$	$(0.5594792, 2.8 \times 10^{-16})$	$(0.55, -0.030358)$	$(0.56, 0.001669)$

Table 6.11: Growth index with the dynamical relationship $\gamma = \gamma_0 + (1 - a)\gamma_1$ at different k values and at subhorizon limit for models of the form $-T + V(\phi) + X$ depicted in Fig. 6.6. The second column gives the result at which the growth index is taken to be a constant such that $\gamma_1 = 0$. The third column corresponds to a γ value at which the growth index is constant at the ΛCDM limit. The fourth column and fifth column give the coordinates to obtain $\gamma_0 = 0.55$ and $\gamma_0 = 0.56$, respectively.

6.4.2.1 | Quadratic

The first case in modified GR considered is for a quadratic potential [368] given by

$$V_1(\phi) = V_0\phi(a)^2\,, \qquad P_1 = 1\,, \tag{6.112}$$

mimicking a simple harmonic oscillator potential where V_0 is a constant. Evaluation of the first Friedmann equation (6.99) with functions in Eq. (6.112)

$$h(a)^2 = \frac{2(6H_0^2\Omega_{m0} + V_0a^3\phi(a)^2)}{a^3H_0^2(12 - a^2\phi'(a)^2)}\,, \tag{6.113}$$

where V_0 is determined by setting the above equation to current time along with the equation of case constraint of Eq. (6.111):

$$V_0 = \frac{4H_0^2(1 - \Omega_{m0})}{\phi_0^2}\,, \tag{6.114}$$

where $\phi_0 = \phi(1)$ is an unknown constant. The scalar field equation (6.101) is given by

$$0 = 12(1 - \Omega_{m0})\frac{\phi(a)}{\phi_0^2} + ah(a)((4h(a) + ah'(a))\phi'(a) + ah(a)\phi''(a))\,. \tag{6.115}$$

Given a choice of ϕ_0 and using Eq. (6.111) as the initial condition for $\phi'(1)$, Eq. (6.113) and Eq. (6.115) are numerically solved simultaneously for h and ϕ. Fig. 6.7 illustrates the changes

in the equation of state ω_{eff} when changing the value of ϕ_0. But, the field equation itself provides some constraints on the constant. The scalar field equation (6.115) resembles a damped harmonic oscillator with a linear restoring force. Imposing an overdamped scenario by setting the discriminant for real roots yields the constraint at $a = 1$:

$$\phi_0^2 > \frac{192(1-\Omega_{m0})}{(8-3\Omega_{m0})^2} \sim 1\,. \tag{6.116}$$

Values $\phi_0 = 0.1$ and $\phi_0 = 1$ result in an underdamped scenario, and are still considered throughout the analysis to see the behaviour reflected within the Mészáros equation. In Fig. 6.7, the $\phi_0 = 0.1$ case gives an equation of state which oscillates with a decreasing period at late times are approached. The oscillatory nature for ω_{eff} is not a favoured behaviour as it implies that the matter-dominated era experiences periods of accelerated and decelerated expansion, which would otherwise result in different large-scale structures observed today. $\phi_0 = 1$ exhibits a stiff behaviour such that $p_{\text{eff}} \sim \rho_{\text{eff}}$ before setting the path the reach $\omega_{\text{eff}} = -1$, as imposed. These evolutions show the interplay between different components. Setting $\omega_{\text{eff}} = -1$ at the final stage of the scale factor's evolution ensures a transition in the model from a matter-dominated era to a dark energy-dominated era. The damped oscillator solution results in $\omega_{\text{eff}} \sim 1$ at $a = 0.1$, implying a high pressure-density state and deviating from the expected radiation or matter epochs. Hence, it can be attributed to the kinetic energy of the scalar field dominating over its potential term.[7] The cases for $\phi_0 = 10$ and $\phi_0 = 100$ give a dynamical behaviour, thus favoured over the oscillatory and stiff plots, in accordance to the constraint given by Eq. (6.116).

Fig. 6.8 illustrates the growth factor for the quadratic model. Each quadrant depicts the results for different ϕ_0 values, in which the deviations of the growth factor solutions for different k values and subhorizon from the ΛCDM limit are considered. For large values of ϕ_0, such as $\phi_0 = 100$ in Fig. 6.8d, the k solutions are closer to the subhorizon and ΛCDM solutions, in comparison with the other ϕ_0 values. For $\phi_0 = 0.1$, shown in Fig. 6.8a, the deviations from the ΛCDM solutions are more significant while for $k > 100H_0$ results almost replicate the subhorizon limit.

$f\sigma_8$ given by Eq. (6.57) and S_8 in Eq. (6.58) provide another avenue to observe how k dependencies manifest in growth parameters. The cases satisfying the condition in Eq. (6.116) are evaluated further, i.e. cases $\phi_0 = 10$ and $\phi_0 = 100$. In Fig. 6.9 for $\phi_0 = 10$, the difference between k values and ΛCDM are presented for both parameters. In comparison with the ΛCDM result, the solutions for $f\sigma_8$ grow faster as point $a = 1$ is approached, while S_8 solutions are observed to be smaller throughout the matter-dominated era. For both cases, the subhorizon results give the largest deviation. The results for $\phi_0 = 100$ were noted to be of deviations at the order of 10^{-4}, and not presented here as the plots appear to behave identical to ΛCDM. As ϕ_0

[7] This point holds for all models considered in this section, as seen in Figs 6.10, 6.13, and 6.16.

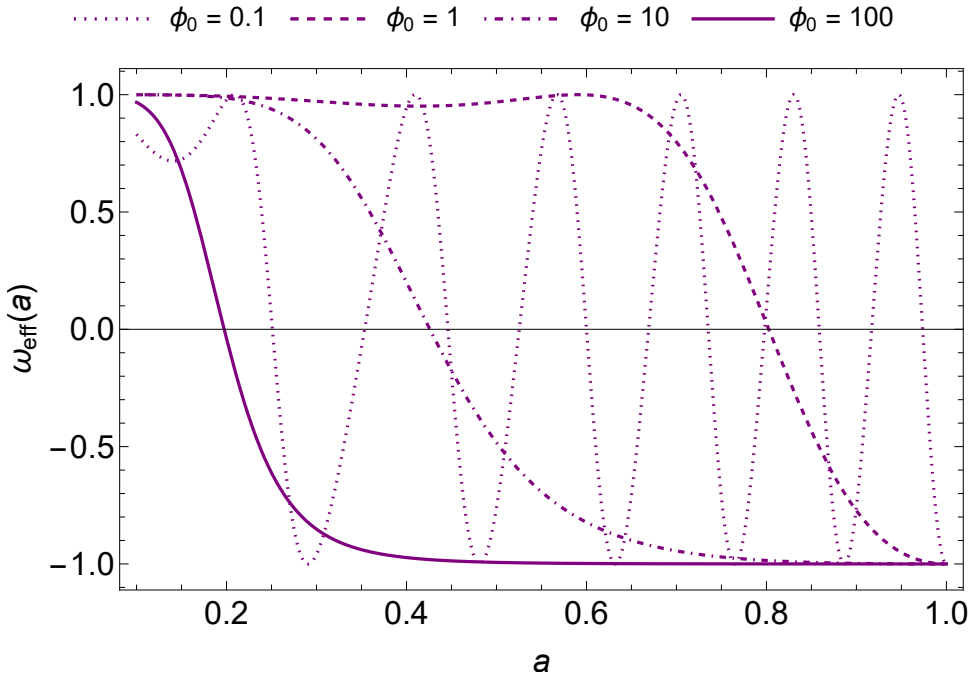

Figure 6.7: Effective equation of state ω_{eff} for different values of ϕ_0 for $V(\phi) = V_0\phi^2$. $\omega_{\text{eff}} \sim 1$ implies that the kinetic energy of the scalar field dominated at earlier stages of the Universe.

values increase, the results appear closer to ΛCDM values along with less significant distinction between the different k values.

6.4.2.2 | Quartic

Adjacent to the quadratic potential considered in Sec. 6.4.2.1, is the quartic potential, previously studied as an inflationary model wherein the expansion of the Universe initiates at earlier times:

$$V_2(\phi) = V_0\phi^4\,, \qquad P_2 = 1\,. \tag{6.117}$$

The Friedmann equation (6.99) alters to

$$h(a)^2 = \frac{2(6H_0^2\Omega_{m0} + a^3V_0\phi(a)^4)}{a^3H_0^2(12 - a^2\phi'(a)^2)}\,. \tag{6.118}$$

for which

$$V_0 = \frac{6H_0^2(1-\Omega_{m0})}{\phi_0^4}\,, \tag{6.119}$$

is obtained when Eq. (6.118) is set to $a = 1$. For this case, the scalar field equation (6.101) becomes

$$0 = -12(\Omega_{m0} - 1)\frac{\phi(a)^3}{\phi_0^4} + ah(a)((4h(a) + ah'(a))\phi'(a) + ah(a)\phi''(a))\,. \tag{6.120}$$

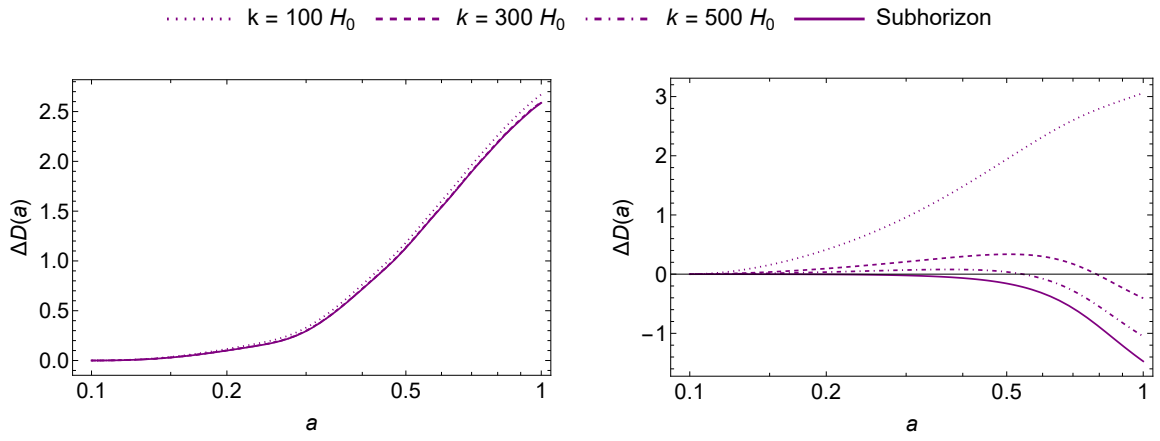

(a) $\phi_0 = 0.1$

(b) $\phi_0 = 1$

(c) $\phi_0 = 10$

(d) $\phi_0 = 100$

Figure 6.8: Difference in growth factor from the ΛCDM solution for the case $V(\phi) = V_0\phi^2$. Each quadrant presents the solution for the set boundary condition of ϕ_0. Each plot compares k values and the subhorizon limit result obtained through the immediate assumption of $k \gg aH$. Plot (b) requires a very large value of k to approach the subhorizon limit. The subhorizon limit can be obtained, within an order of 10^{-2}: (a) at $k > 300$, (c) at $k > 400H_0$, and (d) at $k > 30H_0$.

Again, solutions for h and ϕ are obtained through Eq. (6.118) and Eq. (6.120) when a ϕ_0 value is assumed.

Fig. 6.10 illustrates the behaviour of the effective equations of state ω_{eff} for a range of ϕ_0 values. ϕ_0 gives an oscillatory pattern, with a shorter period in comparison with the quadratic counterpart in Fig. 6.7. This is because the potential has a higher-order index. In fact, for the quartic potential, the case $\phi_0 = 1$ exhibits a stiff behaviour, whereas $\phi_0 = 10$ and $\phi_0 = 100$ display dynamical behaviour. Consequently, the latter two boundary conditions are more viable.

For a small ϕ value, the scalar field equation (6.115) can be expanded up to first order to obtain

$$2(11 - 12\Omega_{m0})(3\phi(a) - 2\phi_0) + a\phi_0^2 h(a)[(4h(a) + ah'(a))\phi'(a) + ah(a)\phi''(a)] = 0\,, \qquad (6.121)$$

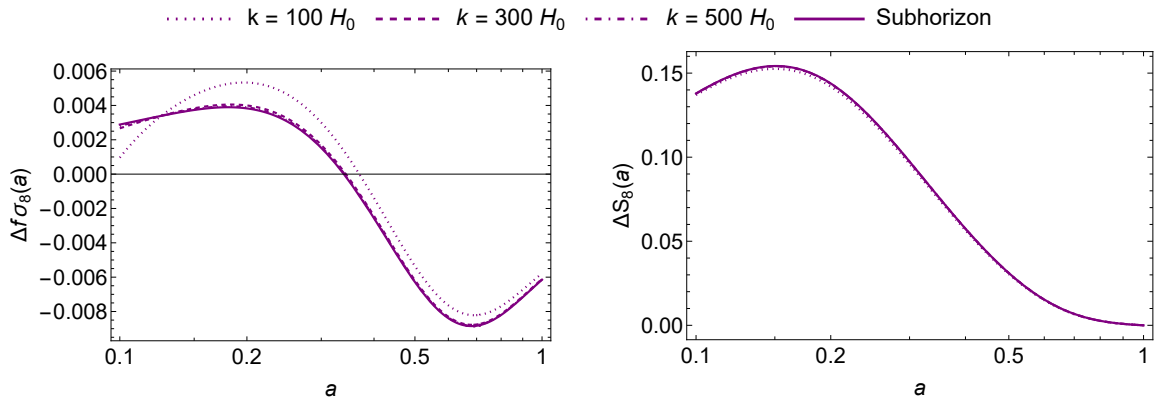

Figure 6.9: $\Delta f\sigma_8 = (f\sigma_8)_{\Lambda\text{CDM}} - f\sigma_8$ and $\Delta S_8 = (S_8)_{\Lambda\text{CDM}} - S_8$ solutions for the case $V(\phi) = V_0\phi^2$ when $\phi_0 = 10$.

giving a result mimicking a linear harmonic oscillator analogous to the form obtained in Sec. 6.4.2.1 with an additional constant driving force. The discriminant for an overdamped system still holds as the additional constant term would only affect the particular solution of the differential equation. The discriminant now becomes

$$\phi_0^2 > \frac{96(11 - 12\Omega_{m0})}{(8 - 3\Omega_{m0})^2} \sim 10\,. \tag{6.122}$$

While $\phi_0 > 100$ values are not excluded through the discriminant, the equations of state illustrated in Fig. 6.10 indicates that these cases would give a sudden drop to ω_{eff} while still in the matter-dominated era. Hence, $10 \leq \phi_0 \leq 100$ is still the most relevant range.

Evaluation of the Mészáros equation (6.105) for different values of ϕ_0, considering a range of k values, gives the solutions illustrated in Fig. 6.11. The results are similar to those obtained in Fig. 6.8 with the exception of $\phi_0 = 10$ in Fig. 6.11c. Overall, quartic potential cases yield slower growth than their quadratic potential counterparts in Fig. 6.8. Fig. 6.12 illustrates the faster growth for $\phi_0 = 10$ in comparison to the rest of the quadrants within the quartic case through the deviations of $f\sigma_8$ and S_8 results. Additionally, the discrepancies between the different k values become more prominent. Once again, as the values of ϕ_0 increase, the deviations become significantly smaller across all the solutions.

6.4.2.3 | Exponential

The final model within modified GR is given by the exponential potential for which the scalar field drives the inflationary expansion at early Universe [369]:

$$V_3 = V_0 e^{\lambda\phi}\,, \qquad\qquad P_3 = 1\,, \tag{6.123}$$

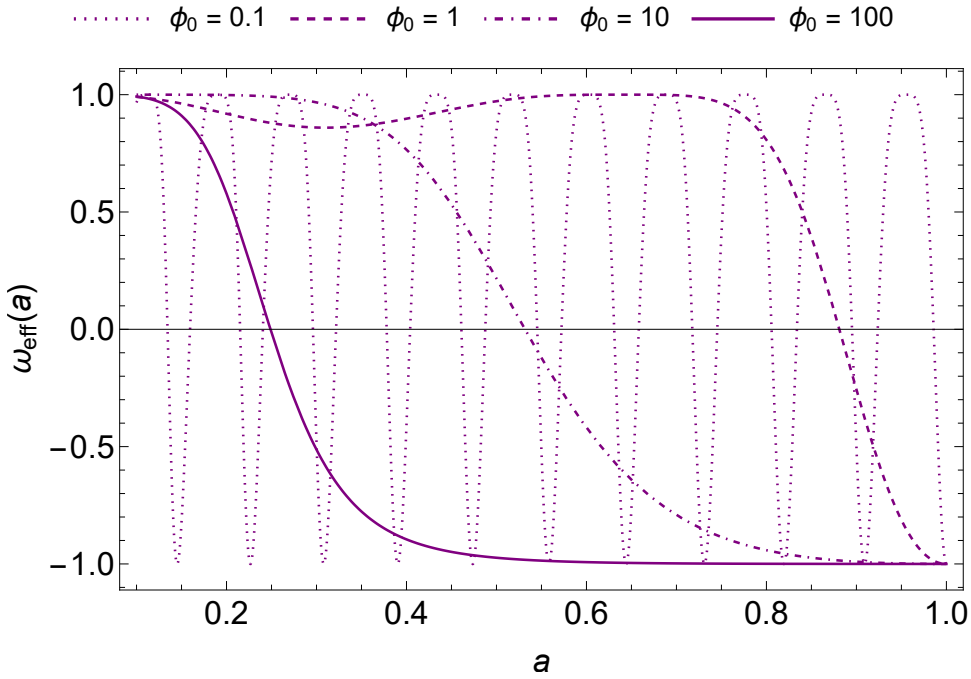

Figure 6.10: Effective equation of state ω_{eff} for different values of ϕ_0 for the case $V(\phi) = V_0\phi^4$. $\omega_{\text{eff}} \sim 1$ implies that the kinetic energy of the scalar field dominated at earlier stages of the Universe.

where V_0 and λ are constants. The background equations given by the first Friedmann equation (6.99) and Klein-Gordon scalar field equation (6.101) for this model are given by

$$h(a)^2 = \frac{2(V_0 a^3 e^{\lambda\phi(a)} + 6H_0^2\Omega_{m0})}{a^3 H_0^2(12 - a^2\phi'(a)^2)}\,, \tag{6.124}$$

$$0 = V_0\lambda e^{\lambda\phi(a)} + aH_0^2 h(a)((4h(a) + ah'(a))\phi'(a) + ah(a)\phi''(a))\,. \tag{6.125}$$

The constant V_0 is determined by solving Eq. (6.124) at $a = 1$ to obtain

$$V_0 = 6H_0^2 e^{-\lambda\phi_0}(1 - \Omega_{m0})\,, \tag{6.126}$$

where the condition in Eq. (6.111) has been applied, and ϕ_0 is an unknown constant.

Consider $\lambda = 1$ to focus on the growth factor evolution at different k values. The numerical solutions for h and ϕ are determined simultaneously by Eqs (6.124-6.125), such that the effective equation of state (6.102) is illustrated in Fig. 6.13. All the ϕ_0 values seemingly give identical results. It should be noted that there are in fact differences but are of a small order of magnitude ($\lesssim |10^{-8}|$) for the scale considered.

Difference in growth factor solutions, between particular k values and ΛCDM solution is shown in Fig. 6.14. The plots appear to have identical behaviour. $k = 100H_0$ gives slower

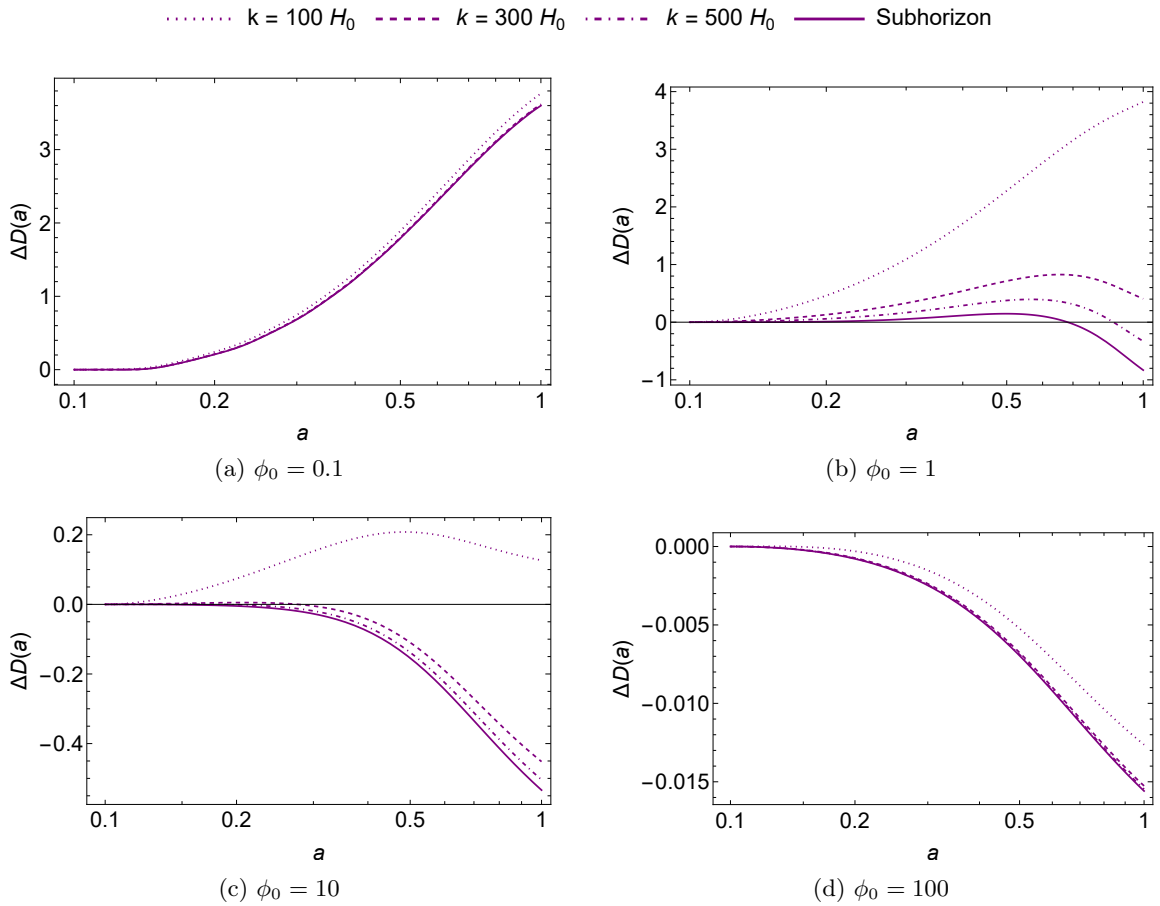

(a) $\phi_0 = 0.1$ (b) $\phi_0 = 1$

(c) $\phi_0 = 10$ (d) $\phi_0 = 100$

Figure 6.11: Difference in growth factor from the ΛCDM solution for the case $V(\phi) = V_0\phi^4$. Each quadrant presents the solutions for a set of boundary conditions of ϕ_0. Each plot compares k values and the subhorizon limit result obtained through the immediate assumption of $k \gg aH$. Plot (b) requires a very large value of k to approach the subhorizon limit. The subhorizon limit can be obtained, within an order of 10^{-2}: (a) at $k > 430$, (c) at $k > 870H_0$, and (d) at $k > 60H_0$.

growth than the ΛCDM limit. Higher values, such as $k = 300H_0$ and $k = 500H_0$, give a higher result than ΛCDM, with the subhorizon being the fastest growth within each subcase. Since the ϕ dependency appears in the exponential portion of the function, the difference among the quadrants appears in the last 10^{-6} of the scale. When comparing the results with the quadratic and quartic case, shown in Sec. 6.4.2.1 and Sec. 6.4.2.2, the $f\sigma_8$ and S_8 result in larger deviations from ΛCDM for the exponential case. This is illustrated in Fig. 6.15 for the same boundary condition of $\phi_0 = 10$.

As the different ϕ_0 values alter the system slightly, it would be interesting to see how the growth function behaves for different λ values in the exponent. To obtain an estimate of the

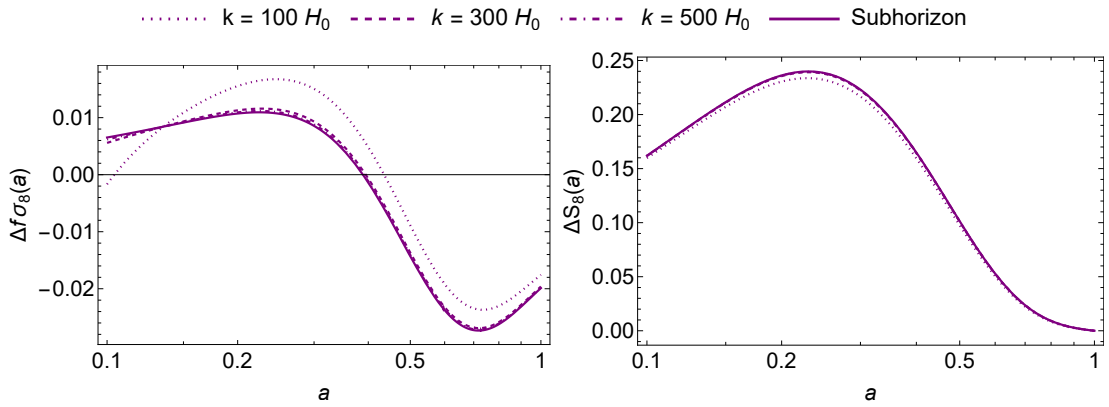

Figure 6.12: $\Delta f\sigma_8 = (f\sigma_8)_{\Lambda\text{CDM}} - f\sigma_8$ and $\Delta S_8 = (S_8)_{\Lambda\text{CDM}} - S_8$ solutions for the case $V(\phi) = V_0\phi^4$ when $\phi_0 = 10$.

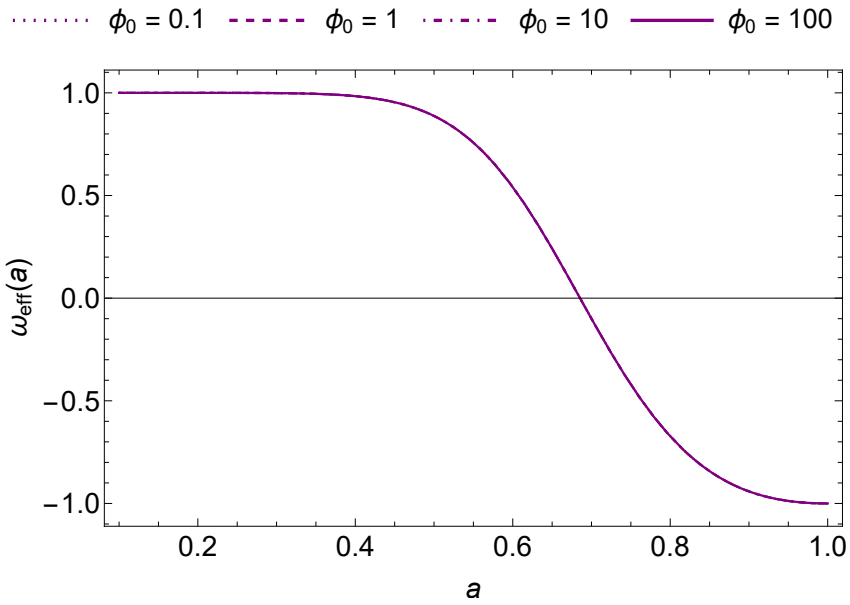

Figure 6.13: Effective equation of state ω_{eff} for different values of ϕ_0 for the case $V(\phi) = V_0 e^{\lambda\phi}$ when $\lambda = 1$. All cases of ϕ_0 considered overlap. $\omega_{\text{eff}} \sim 1$ implies that the kinetic energy of the scalar field dominated at earlier stages of the Universe.

viable λ value, the scalar field equation (6.125) is expanded to

$$0 = 6\lambda(1-\Omega_{m0})[1+\lambda(\phi(a)-\phi_0)] + a^2h(a)^2\left[\left(\frac{4}{a}+\frac{h'(a)}{h(a)}\right)\phi'(a)+\phi''(a)\right] , \tag{6.127}$$

to obtain a harmonic oscillator form, provided ϕ is small. The discriminant at current time gives

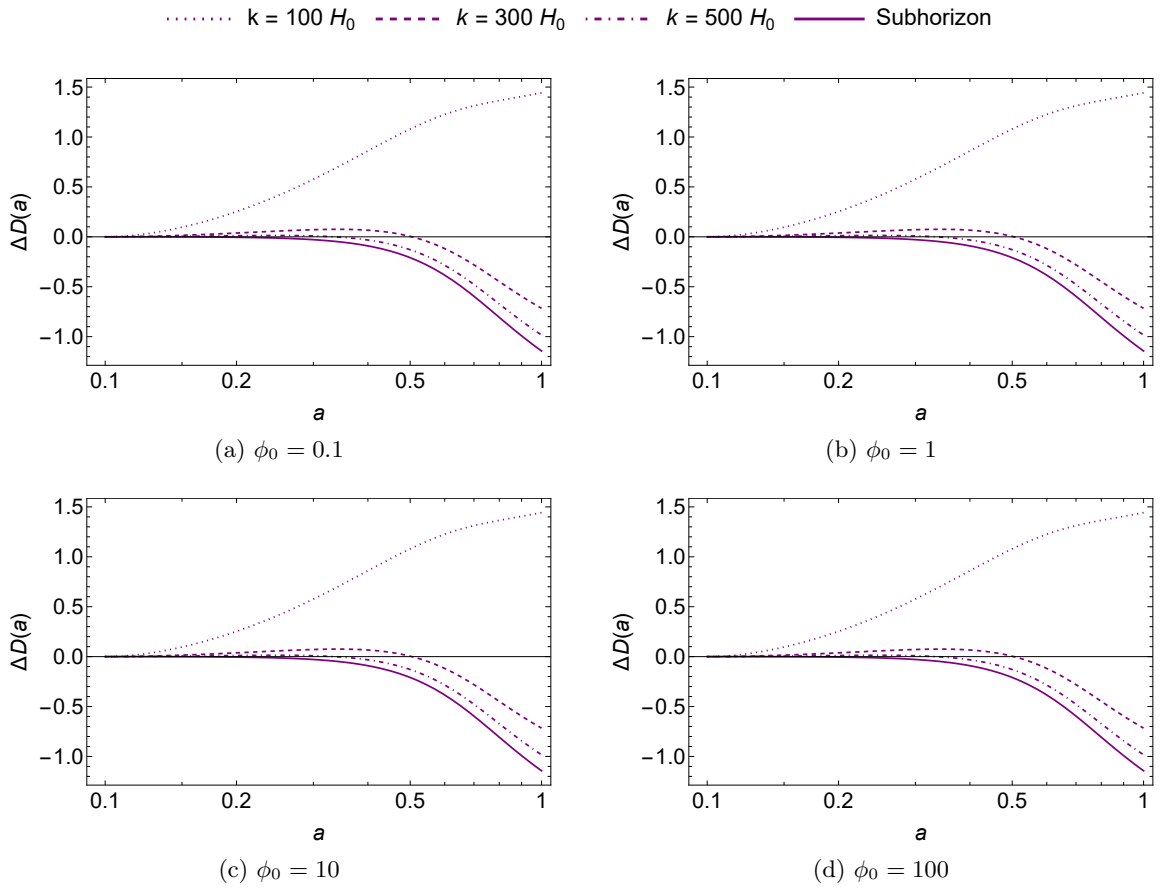

(a) $\phi_0 = 0.1$ (b) $\phi_0 = 1$

(c) $\phi_0 = 10$ (d) $\phi_0 = 100$

Figure 6.14: Difference in growth factor from the ΛCDM solution for the case $V(\phi) = V_0 e^{\lambda\phi}$ when $\lambda = 1$. Each quadrant presents the solutions for a set of boundary conditions of ϕ_0. Each plot compares k values and the subhorizon limit result obtained through the immediate assumption of $k \gg aH$. The subhorizon limit corresponds to values of $k > 2000H_0$.

a restriction on λ of

$$\lambda^2 < \frac{(-31 + 12\Omega_{m0})^2}{384H_0^2(\Omega_{m0} - 1)} \sim 1\,, \tag{6.128}$$

indicating that negative values yield the same results. The sign changes in Eq (6.124-6.125) are accounted for by the constant V_0 in Eq. (6.126). Additionally, $\phi_0 = 1$ is set as per the minute differences noted in Fig. 6.13. ω_{eff} for different λ values is given in Fig. 6.16. $\lambda = 0$ gives a constant value of $\omega_{\text{eff}} = -1$. Albeit the result appears to be identical to that of GR, the Lagrangian would be given by $-T + V_0 + X$ and also distinguishable from ΛCDM. Additionally, breaking the constraint given by Eq. (6.128) would result in an effective equation of state with stiff-like behaviour.

The growth factor solutions for different λ values are illustrated in Fig. 6.17, each quadrant

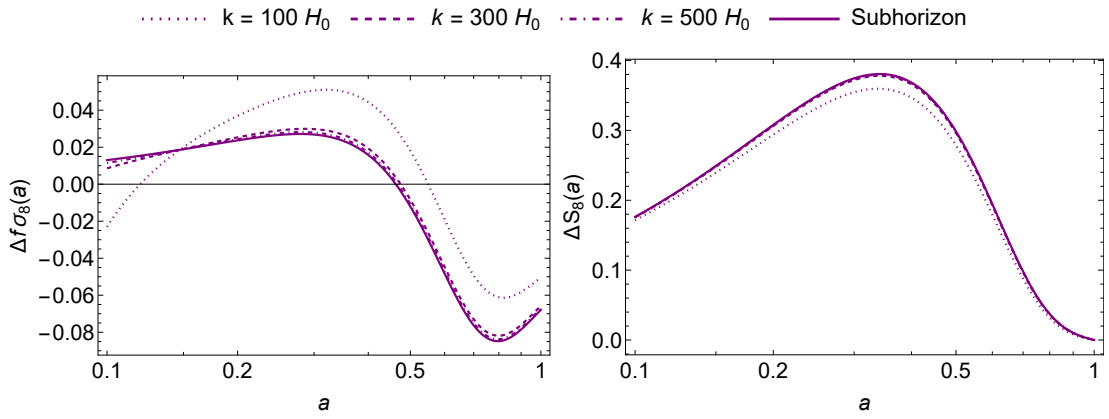

Figure 6.15: $\Delta f\sigma_8 = (f\sigma_8)_{\Lambda\text{CDM}} - f\sigma_8$ and $\Delta S_8 = (S_8)_{\Lambda\text{CDM}} - S_8$ solutions for the case $V(\phi) = V_0 e^{\lambda\phi}$ when $\lambda = 1$ and $\phi_0 = 10$.

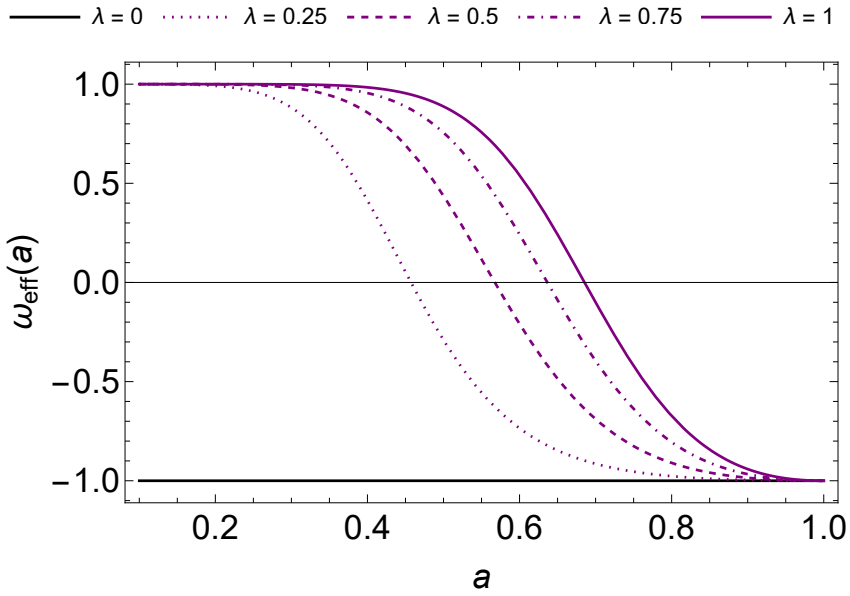

Figure 6.16: Effective equation of state ω_{eff} for different values of λ for the case $V(\phi) = V_0 e^{\lambda\phi}$ when $\phi_0 = 1$ and $\phi'(1) = 0$. $\omega_{\text{eff}} \sim 1$ implies that the kinetic energy of the scalar field dominated at earlier stages of the Universe.

corresponding to a different k value. For $\lambda = 0$, the result is consistently replicating the ΛCDM limit. Figure 6.17a illustrates that in the case $k = 100H_0$, the growth factor increases with λ. This is in contrast with the rest of the k and subhorizon results in Figs 6.17b-6.17d, where an increasing λ gives a slower growth. Additionally, the latter cases result in solutions closer to each other for different λ values.

While the $f(T)$ models have shown k independency, the additional scalar mode indicates

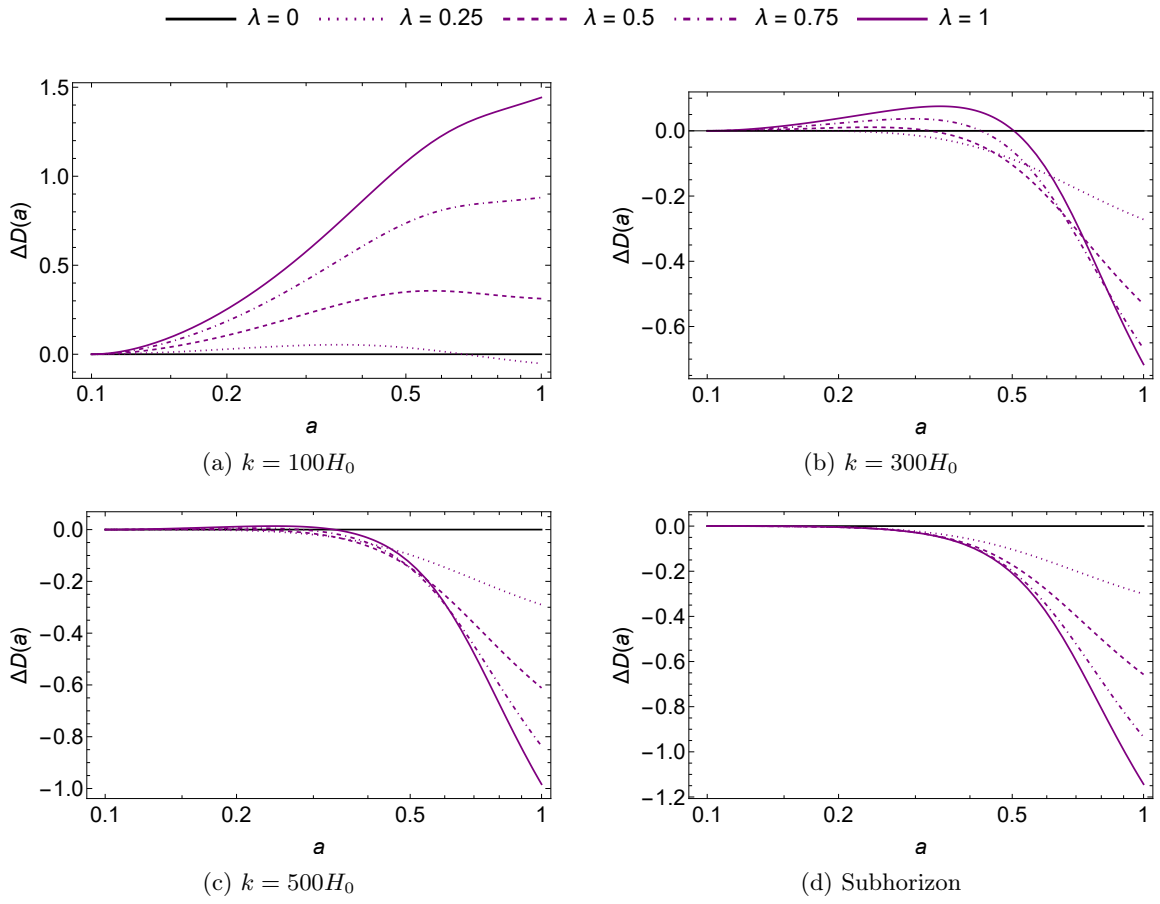

(a) $k = 100H_0$ (b) $k = 300H_0$

(c) $k = 500H_0$ (d) Subhorizon

Figure 6.17: Difference in growth factor from the ΛCDM solution for the case $V(\phi) = V_0 e^{\lambda\phi}$ for varying λ values when $\phi_0 = 1$. Each quadrant corresponds to different k values, including the subhorizon limit result where $k \gg aH$ is assumed. The subhorizon corresponds to different k values for different λ values; within order of 10^{-2}: $k > 520H_0$ for $\lambda = 0.25$, $k > 1080H_0$ for $\lambda = 0.5$, $k > 1590H_0$ for $\lambda = 0.75$, and $k > 2000H_0$ for $\lambda = 1$. $\lambda = 0$ corresponds to the ΛCDM model.

possible significant deviations that are detectable through observations of large-scale structures. The current work by DESI aims to map the three-dimensional dark matter distribution, covering larger volumes than previous missions. Among other scientific goals, DESI can be used to detect deviations from the ΛCDM model. In the recent results summarised in Ref. [94], it has been shown that a dynamical equation of state is favoured over a constant dark energy constant. Additionally, the mission has the capabilities of detecting k-dependencies through precision measurements of the matter power spectrum, BAO features in clusters of galaxies, and RSD; all measurements which would be appearing for different k values at redshifts $z < 2$ [370]. The upcoming missions by Euclid and LSST aim to achieve similar goals, focusing on redshift

Model	Deviation from ΛCDM			k Dependency Deviations		
	γ	$f\sigma_8$	S_8	γ	$f\sigma_8$	S_8
Instruments	10^{-2}	10^{-2}	10^{-2}	10^{-2}	10^{-2}	10^{-2}
Quadratic	10^{-3}	10^{-3}	10^{-3}	10^{-3}	10^{-4}	10^{-4}
Quartic	10^{-3}	10^{-2}	10^{-3}	10^{-3}	10^{-3}	10^{-3}
Exponential	10^{-3}	10^{-2}	10^{-1}	10^{-3}	10^{-2}	10^{-2}

Table 6.12: Order of magnitudes at which deviations from ΛCDM and from different k values can be observed. The first row of results lists the limitations of the instruments for γ, $f\sigma_8$, and S_8. The instruments considered are DESI ($z < 2$) [4, 5], Euclid ($0.5 < z < 1.5$) [6, 7] and LSST ($z \sim 1$) [8]. The rest of the results are estimates from the models presented in Figs 6.6, 6.9, 6.12, and 6.15, with a focus around $0 < z < 1$ ($0.5 < a < 1$). The k dependency deviations listed take into consideration the largest deviations. Ideal instruments should operate within smaller orders of magnitude.

ranges $0.5 < z < 1.5$ [371] and $z \sim 1$ [372], respectively. The current instruments' precisions are around $(\gamma, \sigma_8, f\sigma_8, S_8) = (10^{-2}, 10^{-3} - 10^{-2}, 10^{-2}, 10^{-2})$ [6, 7, 4, 5, 8], where the lower range of 10^{-3} order of magnitude for σ_8 measurements is provided only by Euclid mission proposal [7].

Table 6.12 is a list of orders of magnitude at which deviations from ΛCDM model and deviation between different values of k can be detected. The estimates from the quadratic, quartic, and exponential models are considered for initial conditions $\phi(1) = 10$ and $\phi'(1) = 0$, corresponding to the plots given by Figs 6.6, 6.9, 6.12, and 6.15. Only the range $0.5 < a < 1$ are considered, since these are the common redshifts that DESI, Euclid and LSST will operate. The current proposed instruments would not be able to detect such deviations, except for the Exponential model when measuring the S_8 value. Ideally, the instruments used would also have precision at a lower magnitude than those presented in the table. This is because only the largest deviations are provided within the model. Smaller deviations would require better precision.

6.5 | Summary

The Mészáros equation (6.43) summarises the behaviour of matter perturbations governed through gravitational perturbations, whose solution gives an understanding of the growth profile of structures. The subhorizon realm $k \gg aH$, specifically, gives an insight into the behaviour of CDM. In this chapter, a generalised approach to obtaining the solution of δ_m is presented. Matter

is treated as non-relativistic, consistent with the conditions under which the subhorizon regime occurs. The derivatives of potentials and k dependencies are not ignored, as they may contribute significantly to certain gravitational theories. This allows the opportunity to construct an entire system without any oversimplifications while providing an avenue to study spatial dependencies and at which order of magnitude these come into play.

In Sec. 6.1, the matter sector is introduced in further detail, modifying the field equations (6.17), with the additional continuity (6.7-6.13) and velocity (Euler) (6.14) equations stemming from the conservation of the energy-momentum tensor given by Eq. (6.6).

Sec. 6.2 provides an overview of obtaining the Mészáros equation. Assuming that subhorizon limit applies deep within the matter-dominated era where relativistic matter is attributed mainly to CDM, such that Eq. (6.21) applies. Moreover, the Newtonian (longitudinal) gauge (6.22) provides a gauge choice, while matter perturbations are reduced to the comoving gauge density perturbation δ_m (6.12b), such that the entire system removes redundant DoFs. Expressing gravitation perturbations χ in terms of the matter perturbations given by Eq. (6.37), provides a system to solve for χ. Hence, the CDM Mészáros equation (6.43) results in a second order ordinary differential equation of δ_m. With the solution of δ_m, a variety of parameters/functions correlating to growth structures can be explored, as introduced in Sec. 6.3: growth factor D (6.49), growth index (6.55), $f\sigma_8$ (6.57) and S_8 (6.58).

While gravitational theories such as $f(\mathring{R})$ [330, 222], $f(T)$ [275] and $f(T, \mathcal{T})$ [322] have been studied with the application of the subhorizon limit at each step of the Mészáros equation, Ref. [331] showed that in the case of $f(\mathring{R})$, a generalised approach to obtaining the Mészáros equation followed by the application of the subhorizon limit results in discrepancies in the result often quoted from Refs [330, 222]. Hence, the question becomes whether or not the procedure previously adopted to study the growth of CDM suffices, and if the subhorizon limit holds at certain scales during the matter-dominated epoch. Within the realm of teleparallel gravity, $f(T)$ has been studied in Sec. 6.4.1 to compare with the established result in Ref. [275] and in modified GR in Sec. 6.4.2 as a subcase of $f(\phi, T)$ to explore how introducing a scalar field modifies this behaviour, both theories explored through a variety of models. While the case of $f(T)$ concluded that the result in Ref. [275] suffices, it is not the case when introducing ϕ, mainly due to the fact the choice of boundary conditions of ϕ and ϕ' do result in k dependencies, with some cases pointing towards slight deviations from the subhorizon limit result.

7

Ghost and Laplacian Instabilities

When considering modified theories of gravity, it is crucial to ensure that the models falling within the formalism can realise physical viability. In the previous chapters, BDLS and its subcases have been analysed as possible resolutions to the CC problem (Chapter 3), obtaining the number of propagating DoFs and the polarisation modes of GW (Chapter 5), and the growth structures of simpler models (Chapter 6). Another check is that the gravity theory is stable, as understanding these instabilities limits pathological branches, in particular ghost and Laplacian (gradient) instabilities.

Typically, *ghost instabilities* emerge when considering higher order derivatives gravitational theories, where Ostrogradsky instabilities occur [222]. The Ostrogradsky theorem states that non-degenerate higher-order derivative Lagrangians have a Hamiltonian without a lower bound [110]. Hamiltonian, which encapsulates the total energy, requires a lower bound as this correlates with the ground state. As a result, certain DoFs may have a kinetic energy term associated with them, implying that a system can produce a nonphysical negative energy [110, 111]. The construction of BDLS (see Chapter 2) is by design free of higher order derivatives [78]. Even so, some subcases of BDLS can be eliminated by studying the limits imposed by ghost stability. *Laplacian instabilities* occur when the square of the propagating speed c^2 is negative. This value has been introduced in Sec. 6.2 as it is linked to the growth of perturbations when dealing with scalar and matter perturbations. Thus, gradient instabilities influence the dynamics of perturbation at early times in the Universe, as a negative value implies that small fluctuations result in rapid and uncontrolled growth [112].

In this chapter, ghost, and Laplacian instabilities are investigated within BDLS gravity. Sec. 7.1 illustrates the construction of an action expanded up to the second order. The action is split into scalar, pseudoscalar, vector, and tensor sectors, and each sector can be expressed in terms of gauge-invariant quantities. In Sec. 7.2, the ghost and Laplacian stability conditions are obtained and summarised in Sec. 7.4. This work is based on an extension of Ref. [373].

7.1 | Gauge-Invariant Action in BDLS

Up to this point, only first-order perturbations have been utilised. Preemptively, Chapter 4 presented the perturbations of each BDLS ingredient up to second order, with a summary given by Tables 4.1, 4.2 and 4.3. The extension of the BDLS action given in Eq. (2.98) up to second-order perturbations correlates with the linearised field equations listed in Sec. 4.3 and utilised in Chapters 5 and 6. By compiling all these perturbations, the action becomes of the form

$$
\begin{aligned}
\delta^2\mathcal{S} = \frac{1}{2\kappa^2}\int d^4x\Big\{&\delta^2 e\Big[G_2 - \mathring{\phi}\,G_3 + G_4\,\mathring{R} + G_{4,X}\big((\mathring{\Box}\phi)^2 - \mathcal{U}\big) + G_5\,\mathring{G}_{\mu\nu}\,\mathring{\nabla}^\mu\mathring{\nabla}^\nu\phi \\
&- \frac{1}{6}\,G_{5,X}\big((\mathring{\Box}\phi)^2 - 2\mathcal{V} - 3\mathcal{W}\big)\Big]\Big\} + \delta e\Big[\delta G_2 - G_3\,\delta(\mathring{\Box}\phi) - \delta G_3\,\mathring{\Box}\phi + G_4\,\delta\mathring{R} \\
&+ \delta G_4\,\mathring{R} + G_{4,X}\big(2\,\mathring{\Box}\phi\,\delta(\mathring{\Box}\phi) - \delta\mathcal{U}\big) + \delta G_{4,X}\big((\mathring{\Box}\phi)^2 - \mathcal{U}\big) + G_5\big(\mathring{G}_{\mu\nu}\,\delta(\mathring{\nabla}^\mu\mathring{\nabla}^\nu\phi) \\
&+ \delta\mathring{G}_{\mu\nu}\,\mathring{\nabla}^\mu\mathring{\nabla}^\nu\phi\big) + \delta G_5\,\mathring{G}_{\mu\nu}\,\mathring{\nabla}^\mu\mathring{\nabla}^\nu\phi - \frac{1}{6}\,G_{5,X}\big(3(\mathring{\Box}\phi)^2\delta(\mathring{\Box}\phi) + 2\delta\mathcal{V} - 3\delta\mathcal{W}\big) \\
&- \frac{1}{6}\,\delta G_{5,X}\big((\mathring{\Box}\phi)^2 + 2\mathcal{V} - 3\mathcal{W}\big) + \delta G_{\text{Tele}}\Big] + e\Big[\delta^2 G_2 - G_3\,\delta^2(\mathring{\Box}\phi) - \delta G_{3,X}\,\delta\big((\mathring{\Box}\phi)^2\big) \\
&- \delta^2 G_3\,\mathring{\Box}\phi + G_4\,\delta^2\mathring{R} + \delta G_4\,\delta\mathring{R}\delta^2 G_4\,\mathring{R} + G_{4,X}\,\big(\delta(\mathring{\Box}\phi)^2 + 2\mathring{\Box}\phi\,\delta^2(\mathring{\Box}\phi) - \delta^2\mathcal{U}\big) \\
&+ \delta G_{4,X}\big(2\,\mathring{\Box}\phi\,\delta(\mathring{\Box}\phi) - \delta\mathcal{U}\big) + \delta^2 G_{4,X}\big((\mathring{\Box}\phi)^2 - \mathcal{U}\big) + G_5\big(\mathring{G}_{\mu\nu}\,\delta^2(\mathring{\nabla}^\mu\mathring{\nabla}^\nu\phi) \\
&+ \delta\mathring{G}_{\mu\nu}\,\delta(\mathring{\nabla}^\mu\mathring{\nabla}^\nu\phi) + \delta^2\mathring{G}_{\mu\nu}\,\mathring{\nabla}^\mu\mathring{\nabla}^\nu\phi\big) + \delta G_5\big(\mathring{G}_{\mu\nu}\,\delta(\mathring{\nabla}^\mu\mathring{\nabla}^\nu\phi) + \delta\mathring{G}_{\mu\nu}\,\mathring{\nabla}^\mu\mathring{\nabla}^\nu\phi\big) \\
&+ \delta^2 G_5\mathring{G}_{\mu\nu}\,\mathring{\nabla}^\mu\mathring{\nabla}^\nu\phi - \frac{1}{6}\big[3G_{5,X}\,\mathring{\Box}\phi\,\big((\delta(\mathring{\Box}\phi))^2 + \mathring{\Box}\phi\,\delta^2(\mathring{\Box}\phi)\big) + 2G_{5,X}\,\delta^2\mathcal{V} - 3G_{5,X}\,\delta^2\mathcal{W} \\
&+ \delta G_{5,X}\big(3(\mathring{\Box}\phi)^2\,\delta(\mathring{\Box}\phi) + 2\delta\mathcal{V} - 3\delta\mathcal{W}\big) + \delta^2 G_{5,X}\big((\mathring{\Box}\phi)^3 + 2\mathcal{V} - 3\mathcal{W}\big)\big] + \delta^2 G_{\text{Tele}}\Big]\Big\}\,,
\end{aligned}
\tag{7.1}
$$

where the superscript of δ determines the perturbative order to the quantity attached to it: δ is first order and δ^2 is second order. This action holds in a vacuum and

$$\mathcal{U} = \mathring{\nabla}_\mu\mathring{\nabla}_\nu\phi\,\mathring{\nabla}^\mu\mathring{\nabla}^\nu\phi\,, \tag{7.2a}$$

$$\delta\mathcal{U} = \delta(\mathring{\nabla}_\mu\mathring{\nabla}_\nu\phi)\,\mathring{\nabla}^\mu\mathring{\nabla}^\nu\phi + \mathring{\nabla}_\mu\mathring{\nabla}_\nu\phi\,\delta(\mathring{\nabla}^\mu\mathring{\nabla}^\nu\phi)\,, \tag{7.2b}$$

$$\delta^2\mathcal{U} = \delta^2(\mathring{\nabla}_\mu\mathring{\nabla}_\nu\phi)\,\mathring{\nabla}^\mu\mathring{\nabla}^\nu\phi + \delta(\mathring{\nabla}_\mu\mathring{\nabla}_\nu\phi)\,\delta(\mathring{\nabla}^\mu\mathring{\nabla}^\nu\phi) + \mathring{\nabla}_\mu\mathring{\nabla}_\nu\phi\,\delta^2(\mathring{\nabla}^\mu\mathring{\nabla}^\nu\phi)\,, \tag{7.2c}$$

$$\mathcal{V} = \mathring{\nabla}_\mu\mathring{\nabla}^\nu\phi\,\mathring{\nabla}_\nu\mathring{\nabla}^\lambda\phi\,\mathring{\nabla}_\lambda\mathring{\nabla}^\mu\phi\,, \tag{7.2d}$$

$$\delta\mathcal{V} = 3\,\delta(\mathring{\nabla}_\mu\mathring{\nabla}^\nu\phi)\,\mathring{\nabla}_\nu\mathring{\nabla}^\lambda\phi\,\mathring{\nabla}_\lambda\mathring{\nabla}^\mu\phi\,, \tag{7.2e}$$

$$\delta^2\mathcal{V} = 3\,\delta^2(\mathring{\nabla}_\mu\mathring{\nabla}^\nu\phi)\,\mathring{\nabla}_\nu\mathring{\nabla}^\lambda\phi\,\mathring{\nabla}_\lambda\mathring{\nabla}^\mu\phi + 3\,\delta(\mathring{\nabla}_\mu\mathring{\nabla}^\nu\phi)\,\delta(\mathring{\nabla}_\nu\mathring{\nabla}^\lambda\phi)\,\mathring{\nabla}_\lambda\mathring{\nabla}^\mu\phi\,, \tag{7.2f}$$

$$\mathcal{W} = \mathring{\Box}\phi\,\mathcal{U}\,, \tag{7.2g}$$

$$\delta\mathcal{W} = \mathring{\Box}\phi\,\delta\mathcal{U} + \delta(\mathring{\Box}\phi)\,\mathcal{U}\,, \tag{7.2h}$$

$$\delta^2\mathcal{W} = \mathring{\Box}\phi\,\delta^2\mathcal{U} + \delta(\mathring{\Box}\phi)\,\delta\mathcal{U} + \delta^2(\mathring{\Box}\phi)\,\mathcal{U}\,. \tag{7.2i}$$

SVT decomposition can be applied to this action, allowing sectors of scalars, vector, and tensor modes to be treated separately as they do not interact with each other. Moreover, from the gauge transformations given in Eq. (4.42), the pseudoscalar σ is gauge-invariant and can be detached from the rest of the scalar quantities. This cannot be said for the pseudovector σ_i as it can be expressed as a linear combination of b_i and h_i perturbations. The following explores the perturbations of these actions for different sectors in their simplest form. Additionally, whenever required, the action is transformed in terms of gauge-invariant quantities obtained in Eq. (4.45). The results are presented in spatial Fourier transformation form as shown in Appendix B while maintaining time derivatives unless stated otherwise.

Scalar: The scalar action governed by the scalar modes $\{\delta\phi, \varphi, \beta, b, \psi, h\}$ presented in Eq. (4.27) and the additional scalar field in Eq. (4.3) while excluding pseudoscalar σ, is given by

$$\begin{aligned}\delta^2\mathcal{S}_{\rm S} = \frac{1}{2\kappa^2}\int \mathrm{d}t\,\frac{\mathrm{d}^3k}{(2\pi)^{\frac{3}{2}}}\,a^3\Bigg[&\frac{k^2}{a^2}\left(\frac{k^2}{a^2}\mathcal{A}_1\left(b-a\dot{h}\right)^2-\left(b-a\dot{h}\right)\left(\mathcal{A}_2\varphi+\mathcal{A}_3\dot{\psi}+\mathcal{A}_4\delta\phi+\mathcal{A}_5\dot{\delta\phi}\right)\right.\\&\left.-\beta\left(\mathcal{A}_6\varphi+\mathcal{A}_8\delta\phi+\mathcal{A}_9\dot{\delta\phi}+\mathcal{A}_{10}\psi+\mathcal{A}_{12}\dot{\psi}\right)+\mathcal{A}_{13}\dot{\beta}^2\right)+\frac{k^2}{a^2}\dot{\beta}\left(\mathcal{A}_7\varphi+\mathcal{A}_{11}\psi\right)\\&+\varphi\left(-\frac{k^2}{a^2}\mathcal{A}_{14}\psi+\mathcal{A}_{15}\dot{\psi}+\mathcal{A}_{16}\delta\phi-\frac{k^2}{a^2}\mathcal{A}_{17}\delta\phi+\mathcal{A}_{18}\dot{\delta\phi}\right)+\left(\frac{k^2}{a^2}\mathcal{A}_{19}+\mathcal{A}_{20}\right)\varphi^2\\&+\frac{k^2}{a^2}\mathcal{A}_{21}\psi^2+\mathcal{A}_{22}\dot{\psi}^2+\frac{k^2}{a^2}\mathcal{A}_{23}\psi\,\delta\phi+\mathcal{A}_{24}\delta\phi\dot{\psi}+\mathcal{A}_{25}\dot{\delta\phi}\dot{\psi}+\left(\frac{k^2}{a^2}\mathcal{A}_{26}+\mathcal{A}_{27}\right)\delta\phi^2\\&+\mathcal{A}_{28}\dot{\delta\phi}^2\Bigg]\,,\end{aligned}\tag{7.3}$$

where coefficients $\mathcal{A}_i$ for $i \in [1, 28]$ are listed in Appendix C. The $\{\mathcal{A}_1, \mathcal{A}_7, \mathcal{A}_{10}, \mathcal{A}_{11}, \mathcal{A}_{13}, \mathcal{A}_{19}\}$ coefficients are purely due to the teleparallel contribution, and all coefficients are of linear order of BDLS contribution. All coefficients do not realise quantities with derivatives higher than two, in line with the construction of BDLS presented in Sec. 2.4. The coefficients reduce significantly when standard Horndeski gravity is considered, as obtained in Ref. [112]. This limit is discussed further in Sec. 7.3. A gauge choice can be applied at this stage. For the scalar sector, the choice is between the flat gauge, unitary gauge, longitudinal gauge, and synchronous gauge, whose conditions are listed in Eq. (4.44). Depending on the choice, different coefficients are no longer contributing, with the flat gauge and unitary gauges providing simpler actions upon application, thus one of the reasons why the latter is favoured to perform theoretical calculations. The gauge

choice actions are given by

$$\delta^2\mathcal{S}_{\rm S}^{\rm Flat} = \frac{1}{2\kappa^2}\int \mathrm{d}t\,\frac{\mathrm{d}^3k}{(2\pi)^{\frac{3}{2}}}\,a^3\left[\frac{k^2}{a^2}\left(\frac{k^2}{a^2}\mathcal{A}_1 b^2 - b\left(\mathcal{A}_2\varphi + \mathcal{A}_4\delta\phi + \mathcal{A}_5\dot{\delta\phi}\right) - \beta\left(\mathcal{A}_6\varphi + \mathcal{A}_8\delta\phi + \mathcal{A}_9\dot{\delta\phi}\right) + \mathcal{A}_{13}\dot{\beta}^2 - \mathcal{A}_7\dot{\beta}\varphi\right) + \varphi\left(\mathcal{A}_{16}\delta\phi - \frac{k^2}{a^2}\mathcal{A}_{17}\delta\phi + \mathcal{A}_{18}\dot{\delta\phi}\right) + \left(\frac{k^2}{a^2}\mathcal{A}_{19} + \mathcal{A}_{20}\right)\varphi^2 + \left(\frac{k^2}{a^2}\mathcal{A}_{26} + \mathcal{A}_{27}\right)\delta\phi^2 + \mathcal{A}_{28}\dot{\delta\phi}^2\right], \tag{7.4}$$

$$\delta^2\mathcal{S}_{\rm S}^{\rm Unitary} = \frac{1}{2\kappa^2}\int \mathrm{d}t\,\frac{\mathrm{d}^3k}{(2\pi)^{\frac{3}{2}}}\,a^3\left[\frac{k^2}{a^2}\left(\frac{k^2}{a^2}\mathcal{A}_1 b^2 - b\left(\mathcal{A}_2\varphi + \mathcal{A}_3\dot{\psi}\right) - \beta\left(\mathcal{A}_6\varphi + \mathcal{A}_{10}\psi + \mathcal{A}_{12}\dot{\psi}\right) + \mathcal{A}_{13}\dot{\beta}^2\right) + \frac{k^2}{a^2}\dot{\beta}\left(\mathcal{A}_7\varphi + \mathcal{A}_{11}\psi\right) + \varphi\left(-\frac{k^2}{a^2}\mathcal{A}_{14}\psi + \mathcal{A}_{15}\dot{\psi}\right) + \left(\frac{k^2}{a^2}\mathcal{A}_{19} + \mathcal{A}_{20}\right)\varphi^2 + \frac{k^2}{a^2}\mathcal{A}_{21}\psi^2 + \mathcal{A}_{22}\dot{\psi}^2\right], \tag{7.5}$$

$$\begin{aligned}\delta^2\mathcal{S}_{\rm S}^{\rm Longitudinal} = \frac{1}{2\kappa^2}\int \mathrm{d}t\,\frac{\mathrm{d}^3k}{(2\pi)^{\frac{3}{2}}}\,a^3\Bigg[&\frac{k^2}{a^2}\Bigg(\frac{k^2}{a^2}\mathcal{A}_1\beta^2 - \beta\left(\mathcal{A}_2\varphi + \mathcal{A}_3\dot{\psi} + \mathcal{A}_4\delta\phi + \mathcal{A}_5\dot{\delta\phi}\right) \\ &-\beta\left(\mathcal{A}_6\varphi + \mathcal{A}_8\delta\phi + \mathcal{A}_9\dot{\delta\phi} + \mathcal{A}_{10}\psi + \mathcal{A}_{12}\dot{\psi}\right) + \mathcal{A}_{13}\dot{\beta}^2\Bigg) + \dot{\beta}\frac{k^2}{a^2}\left(\mathcal{A}_7\varphi + \mathcal{A}_{11}\psi\right) + \varphi\left(-\frac{k^2}{a^2}\mathcal{A}_{14}\psi + \mathcal{A}_{15}\dot{\psi} + \mathcal{A}_{16}\delta\phi - \frac{k^2}{a^2}\mathcal{A}_{17}\delta\phi + \mathcal{A}_{18}\dot{\delta\phi}\right) \\ &+\left(\frac{k^2}{a^2}\mathcal{A}_{19} + \mathcal{A}_{20}\right)\varphi^2 + \frac{k^2}{a^2}\mathcal{A}_{21}\psi^2 + \mathcal{A}_{22}\dot{\psi}^2 + \frac{k^2}{a^2}\mathcal{A}_{23}\psi\,\delta\phi + \mathcal{A}_{24}\delta\phi\dot{\psi} \\ &+\mathcal{A}_{25}\dot{\delta\phi}\dot{\psi} + \left(\frac{k^2}{a^2}\mathcal{A}_{26} + \mathcal{A}_{27}\right)\delta\phi^2 + \mathcal{A}_{28}\dot{\delta\phi}^2\Bigg],\end{aligned} \tag{7.6}$$

$$\begin{aligned}\delta^2\mathcal{S}_{\rm S}^{\rm Synchronous} = \frac{1}{2\kappa^2}\int \mathrm{d}t\,\frac{\mathrm{d}^3k}{(2\pi)^{\frac{3}{2}}}\,a^3\Bigg[&\frac{k^2}{a^2}\Bigg(\frac{k^2}{a^2}\mathcal{A}_1(\beta - a\dot{h})^2 - \left(\beta - a\dot{h}\right)\left(\mathcal{A}_3\dot{\psi} + \mathcal{A}_4\delta\phi + \mathcal{A}_5\dot{\delta\phi}\right) - \beta\left(\mathcal{A}_8\delta\phi + \mathcal{A}_9\dot{\delta\phi} + \mathcal{A}_{10}\psi + \mathcal{A}_{12}\dot{\psi}\right) + \mathcal{A}_{13}\dot{\beta}^2\Bigg) + \frac{k^2}{a^2}\mathcal{A}_{11}\,\dot{\beta}\,\psi \\ &+\frac{k^2}{a^2}\mathcal{A}_{21}\psi^2 + \mathcal{A}_{22}\dot{\psi}^2 + \frac{k^2}{a^2}\mathcal{A}_{23}\,\psi\,\delta\phi + \mathcal{A}_{24}\delta\phi\dot{\psi} + \mathcal{A}_{25}\dot{\delta\phi}\dot{\psi} \\ &+\left(\frac{k^2}{a^2}\mathcal{A}_{26} + \mathcal{A}_{27}\right)\delta\phi^2 + \mathcal{A}_{28}\dot{\delta\phi}^2\Bigg].\end{aligned} \tag{7.7}$$

Not only can the linearised field equation be expressed in terms of the gauge-invariant quantities, but so can the action. This is done by applying the gauge-invariant variable definitions given in Eq. (4.45) and substituting in Eq. (7.3) to express the action in terms of the variables

$\{\mathcal{X}_1, \mathcal{X}_2, \mathcal{X}_3, \mathcal{X}_4\}$:

$$\delta^2\mathcal{S}_{\rm S} = \frac{1}{2\kappa^2}\int \mathrm{d}t\,\frac{\mathrm{d}^3k}{(2\pi)^{\frac{3}{2}}}\,a^3\left\{\tilde{\mathcal{A}}_1\,\mathcal{X}_2^2 + \frac{k^2}{a^2}\left(\tilde{\mathcal{A}}_2\,\mathcal{X}_2 + \tilde{\mathcal{A}}_3\,\mathcal{X}_3^2\right) + \tilde{\mathcal{A}}_4\dot{\mathcal{X}}_3^2 + \tilde{\mathcal{A}}_5\,\mathcal{X}_1^2 + \tilde{\mathcal{A}}_6\,\dot{\mathcal{X}}_1^2\right.$$
$$+\frac{k^2}{a^2}\left(\tilde{\mathcal{A}}_7\,\mathcal{X}_1^2 + \tilde{\mathcal{A}}_8\,\frac{k^2}{a^2}\mathcal{X}_4^2\right) + \tilde{\mathcal{A}}_9\mathcal{X}_2\dot{\mathcal{X}}_3 + \frac{k^2}{a^2}\tilde{\mathcal{A}}_{10}\,\mathcal{X}_2\,\mathcal{X}_3 a^2 + \tilde{\mathcal{A}}_{11}\,\mathcal{X}_2\mathcal{X}_1 + \tilde{\mathcal{A}}_{12}\,\mathcal{X}_2\dot{\mathcal{X}}_1$$
$$+\frac{k^2}{a^2}\left(\tilde{\mathcal{A}}_{13}\,\mathcal{X}_2\,\mathcal{X}_1 - \tilde{\mathcal{A}}_{14}\,\mathcal{X}_2\mathcal{X}_4\right) + \tilde{\mathcal{A}}_{15}\,\dot{\mathcal{X}}_3\mathcal{X}_1 + \tilde{\mathcal{A}}_{16}\,\dot{\mathcal{X}}_3\dot{\mathcal{X}}_1 + \frac{k^2}{a^2}\tilde{\mathcal{A}}_{17}\,\mathcal{X}_3\,\mathcal{X}_1$$
$$\left.-\frac{k^2}{a^2}\mathcal{X}_4\left(\tilde{\mathcal{A}}_{18}\,\dot{\mathcal{X}}_3 + \tilde{\mathcal{A}}_{19}\,\mathcal{X}_1 + \tilde{\mathcal{A}}_{20}\,\dot{\mathcal{X}}_1\right)\right\}\,, \tag{7.8}$$

where coefficients $\tilde{\mathcal{A}}_i$ for $i \in [1, 20]$ are listed in Appendix C. The spurious DoFs are $\{\mathcal{X}_2, \mathcal{X}_4\}$ and the expressions remain as a linear combination of functions in BDLS. The non-dynamical modes are removed by minimising the action with respect to them. This is done to obtain an action that is only expressed in terms of dynamical modes. Taking variations with respect to $\mathcal{X}_2$ and $\mathcal{X}_4$, respectively, yields the constraints

$$0 = 2\tilde{\mathcal{A}}_1\mathcal{X}_2 + \tilde{\mathcal{A}}_{11}\mathcal{X}_1 + \tilde{\mathcal{A}}_9\dot{\mathcal{X}}_3 + \tilde{\mathcal{A}}_{12}\dot{\mathcal{X}}_1 + \frac{k^2}{a^2}\left(\tilde{\mathcal{A}}_{13}\mathcal{X}_1 + 2\tilde{\mathcal{A}}_2\mathcal{X}_2 + \tilde{\mathcal{A}}_{10}\mathcal{X}_3 - \tilde{\mathcal{A}}_{14}\mathcal{X}_4\right)\,, \tag{7.9}$$

$$0 = 2\frac{k^2}{a^2}\tilde{\mathcal{A}}_8\mathcal{X}_4 - \tilde{\mathcal{A}}_{19}\mathcal{X}_1 - \tilde{\mathcal{A}}_{14}\mathcal{X}_2 + \tilde{\mathcal{A}}_{20}\dot{\mathcal{X}}_1 - \tilde{\mathcal{A}}_{18}\dot{\mathcal{X}}_3\,. \tag{7.10}$$

Substituting Eqs (7.9-7.10) back into Eq. (7.8) gives an action expressed in only the dynamical gauge-invariant modes:

$$\delta^2\mathcal{S}_{\rm S} = \frac{1}{2\kappa^2}\int \mathrm{d}t\,\frac{\mathrm{d}^3k}{(2\pi)^{\frac{3}{2}}}\,a^3\left[\hat{\mathcal{A}}_1\mathcal{X}_1^2 + \hat{\mathcal{A}}_2\mathcal{X}_1\dot{\mathcal{X}}_1 + \hat{\mathcal{A}}_3\dot{\mathcal{X}}_1^2 + \hat{\mathcal{A}}_4\mathcal{X}_3^2 + \hat{\mathcal{A}}_5\mathcal{X}_3\dot{\mathcal{X}}_3 + \hat{\mathcal{A}}_6\dot{\mathcal{X}}_3^2\right.$$
$$\left.+\hat{\mathcal{A}}_7\mathcal{X}_1\mathcal{X}_3 + \hat{\mathcal{A}}_8\dot{\mathcal{X}}_1\mathcal{X}_3 + \hat{\mathcal{A}}_9\mathcal{X}_1\dot{\mathcal{X}}_3 + \hat{\mathcal{A}}_{10}\dot{\mathcal{X}}_1\dot{\mathcal{X}}_3\right]\,, \tag{7.11}$$

where coefficients $\hat{\mathcal{A}}_i$ for $i \in [1, 10]$ can be found in Appendix C. These coefficients highlight the k dependencies within the action which become important when evaluating the Laplacian instabilities. k dependencies appear in both the numerator and the denominator and their influence is dictated by the coefficients stemming from the gravitational theory, hence cannot be eliminated without imposing some sort of limits, be it on the scale of k or from the theory. After performing integration by parts, the action is simplified to

$$\delta^2\mathcal{S}_{\rm S} = \frac{1}{2\kappa^2}\int \mathrm{d}t\,\frac{\mathrm{d}^3k}{(2\pi)^{\frac{3}{2}}}\,a^3\left[\left(\hat{\mathcal{A}}_1 - \frac{1}{2a^3}\frac{\mathrm{d}}{\mathrm{d}t}\left(a^3\hat{\mathcal{A}}_2\right)\right)\mathcal{X}_1^2 + \hat{\mathcal{A}}_3\dot{\mathcal{X}}_1^2 + \left(\hat{\mathcal{A}}_4 - \frac{1}{2a^3}\frac{\mathrm{d}}{\mathrm{d}t}\left(a^3\hat{\mathcal{A}}_5\right)\right)\mathcal{X}_3^2\right.$$
$$\left.+\hat{\mathcal{A}}_6\dot{\mathcal{X}}_3^2 + \left(\hat{\mathcal{A}}_7 - \frac{1}{a^3}\frac{\mathrm{d}}{\mathrm{d}t}\left(a^3\hat{\mathcal{A}}_8\right)\right)\mathcal{X}_1\mathcal{X}_3 + \left(\hat{\mathcal{A}}_9 - \hat{\mathcal{A}}_8\right)\mathcal{X}_1\dot{\mathcal{X}}_3 + \hat{\mathcal{A}}_{10}\dot{\mathcal{X}}_1\dot{\mathcal{X}}_3\right]\,. \tag{7.12}$$

The action has two interesting terms which could require further investigation. The first term is given by $(\hat{\mathcal{A}}_9 - \hat{\mathcal{A}}_8)\mathcal{X}_1\dot{\mathcal{X}}_3$, which can have a complex value upon introducing temporal Fourier

transformation. The other term is that of $\hat{\mathcal{A}}_{10}\dot{\mathcal{X}}_1\dot{\mathcal{X}}_3$ which indicates that there is a mix kinetic term contribution, making it ideal to diagonalise the kinetic portion of the action to obtain the ghost stability conditions. This portion of the analysis will be delved into in Sec. 7.2.

The result in Eq. (7.12) holds provided $\tilde{a} \neq 0$, where equation for $\tilde{a}$ is given by Eq. (C.3). If this is not the case, the result would need to be reevaluated, starting from Eq. (7.8) and applying the substitution of

$$\frac{k^2}{a^2}\tilde{\mathcal{A}}_2 = \frac{\tilde{\mathcal{A}}_{14}^2}{4\tilde{\mathcal{A}}_8} - \tilde{\mathcal{A}}_1 \,. \tag{7.13}$$

The procedure is quite repetitive and the entire derivation is not shown here, but the key points are highlighted. While the variation with respect to $\mathcal{X}_4$ provides a solution for it, variation with respect to $\mathcal{X}_2$ gives a relationship in terms of $\mathcal{X}_1$ and $\mathcal{X}_3$ and their derivatives. Whether the variation is solved for $\dot{\mathcal{X}}_1$ or $\dot{\mathcal{X}}_3$, the number of DoFs reduces to a single dynamical mode, and an additional undefined region is identified, represented by $\tilde{\mathcal{A}}_{14}\tilde{\mathcal{A}}_{20} + 2\tilde{\mathcal{A}}_8\tilde{\mathcal{A}}_{12} = 0$ when eliminating $\dot{\mathcal{X}}_1$ and $\tilde{\mathcal{A}}_{14}\tilde{\mathcal{A}}_{18} - 2\tilde{\mathcal{A}}_8\tilde{\mathcal{A}}_9 = 0$ when eliminating $\dot{\mathcal{X}}_3$. The dynamical part of the mode eliminated through this step requires performing an additional variation with respect to it as now it is a superfluous mode, and eliminated from the action.

Pseudoscalar: Since the pseudoscalar in Eq. (4.27) is gauge-invariant (see Eq. (4.42)), it can be treated separately from the rest of scalar modes. The expansion of Eq. (7.1) results in

$$\delta^2 S_{\rm PS} = \frac{1}{2\kappa^2}\int \mathrm{d}t \frac{\mathrm{d}^3k}{(2\pi)^{\frac{3}{2}}}\frac{a^3}{9}k^2\left[\mathcal{B}_1\dot{\sigma}^2 - \frac{k^2}{a^2}\mathcal{B}_2\sigma^2\right] , \tag{7.14}$$

where

$$\begin{aligned}\mathcal{B}_1 &= 4G_{\mathrm{Tele},T_{\rm ax}} + 9XG_{\mathrm{Tele},J_5} - 12XG_{\mathrm{Tele},J_{10}} \,,\\ \mathcal{B}_2 &= 4\left(G_{\mathrm{Tele},T_{\rm ax}} - 2XG_{\mathrm{Tele},J_1}\right) \,.\end{aligned}$$

Fourth-order derivatives appear, as indicated by k^4, as per the definition of the pseudoscalar in the tetrad. All coefficients appearing in this action are purely teleparallel. This shows that the pseudoscalar does not contribute in subcases of standard Horndeski, in line with the fact that such theories are constructed by a symmetric metric tensor. Specifically, σ comes into play for gravitational theories with non-vanishing terms $\{T_{\rm ax}, J_1, J_5, J_{10}\}$ with the exception of the case $\mathcal{B}_1 = 0$.

Vector: The vector sector governed by modes $\{\beta_i, b_i, h_i, \sigma_i\}$ in Eq. (4.34), this time including the pseudovector mode, is given by the action

$$\begin{aligned}\delta^2\mathcal{S}_{\rm V} = \frac{1}{2\kappa^2}\int \mathrm{d}t\,\frac{\mathrm{d}^3k}{(2\pi)^{\frac{3}{2}}}\,a^3\Bigg[&\frac{k^2}{a^2}\mathcal{C}_1\,b_i\,b^i + \frac{k^4}{a^2}\mathcal{C}_2\,h_i\,h^i + k^2\mathcal{C}_3\,\dot{h}_i\,\dot{h}^j + \frac{k^2}{a^2}\mathcal{C}_4\,\sigma^i\,\sigma_i + \mathcal{C}_5\,\dot{\sigma}^i\,\dot{\sigma}_i \\ &+ \mathcal{C}_6\,\dot{\beta}_i\,\dot{\beta}^i + \frac{k^2}{a^2}\mathcal{C}_7\,\beta_i\,\beta^i + \frac{k^2}{a}\mathcal{C}_8\,b_i\,\dot{h}^i + \frac{k^2}{a^2}\mathcal{C}_9\,b_i\,\beta^i + \frac{k^2}{a}\mathcal{C}_{10}\,\beta_i\,h^i + \frac{k^2}{a}\mathcal{C}_{11}\dot{\beta}_i\,h^i \\ &+ \epsilon^{ijk}\frac{ik_j}{a}\left(\mathcal{C}_{12}\,b_k\,\dot{\sigma}_i + \mathcal{C}_{13}\beta_k\,\sigma_i + \mathcal{C}_{14}\,\sigma_i\,\dot{\beta}_k + \mathcal{C}_{15}\,\dot{\sigma}_i\,\beta_k\right) - i\epsilon^{ijk}k_k\frac{k^2}{a^2}\mathcal{C}_{16}\,\sigma_j\,h_i\Bigg], \end{aligned} \tag{7.15}$$

where coefficients $\mathcal{C}_i$ for $i \in [1, 16]$ are listed in Appendix C. Due to common coefficients, the action can be simplified further to

$$\begin{aligned}\delta^2\mathcal{S}_{\rm V} = \frac{1}{2\kappa^2}\int \mathrm{d}t\,\frac{\mathrm{d}^3k}{(2\pi)^{\frac{3}{2}}}\,a^3\Bigg[&\frac{k^2}{a^2}\left(\mathcal{C}_1\,b_i\,b^i + \mathcal{C}_2\left(k^2h_i\,h^i + \sigma^i\,\sigma_i - 2i\epsilon^{ijk}k_k\,\sigma_j\,h_i\right)\right) + \mathcal{C}_6\,\dot{\beta}_i\,\dot{\beta}^i \\ &+ k^2\mathcal{C}_3\dot{h}^i\left(\dot{h}_i - \frac{1}{a}\,b_i\right) + \mathcal{C}_5\,\dot{\sigma}_i\left(\dot{\sigma}^i + i\epsilon^{ijk}\frac{k_j}{a}\,b_k\right) + \frac{k^2}{a^2}\left(\mathcal{C}_7\,\beta_i + \mathcal{C}_9\,b_i\right)\beta^i + \frac{k^2}{a}\mathcal{C}_{11}\dot{\beta}_i\,h^i \\ &+ \mathcal{C}_{10}\left(\frac{k^2}{a}\,\beta_i\,h^i + 4i\epsilon^{ijk}\frac{k_j}{a}\beta_k\,\sigma_i\right) + i\epsilon^{ijk}\frac{k_j}{a}\left(4\mathcal{C}_{12}\,\sigma_i\,\dot{\beta}_k + \mathcal{C}_{15}\,\dot{\sigma}_i\,\beta_k\right)\Bigg], \end{aligned} \tag{7.16}$$

and only coefficients $\{\mathcal{C}_2, \mathcal{C}_5, \mathcal{C}_6, \mathcal{C}_7, \mathcal{C}_{15}\}$ contain purely teleparallel terms. At this stage, while some terms contain standard Horndeski theory contributions, it does not necessarily mean that vector modes propagate in Horndeski gravity. Investigating these particular cases would require performing further analysis with the appropriate limits, as explored in Sec. 7.3.

While β_i is gauge-invariant, the vector modes $\{b_i, h_i, \sigma_i\}$ can be expressed as a linear combination to form other gauge-invariant quantities. Therefore, by setting any one of the non-gauge-invariant quantities to zero, the action is gauge fixed, which reduces the number of redundant DoFs that can be altered without affecting the physical content of the system. In the case of tetrad-based theories, where antisymmetries of the tetrad result in the pseudovector contributions, dealing with the Levi-Civita tensor ϵ_{ijk} may lead to cumbersome calculations due to having additional indices to deal with. For this reason, the gauge $\sigma_i = 0$ is favoured, where

$$\begin{aligned}\delta^2\mathcal{S}_{\rm V}^{\sigma_i=0} = \frac{1}{2\kappa^2}\int \mathrm{d}t\,\frac{\mathrm{d}^3k}{(2\pi)^{\frac{3}{2}}}\,a^3\Bigg[&\frac{k^2}{a^2}\mathcal{C}_1\,b_i\,b^i + \frac{k^4}{a^2}\mathcal{C}_2 h_i\,h^i + k^2\mathcal{C}_3\dot{h}^i\left(\dot{h}_i - \frac{1}{a}\,b_i\right) + \mathcal{C}_6\,\dot{\beta}_i\,\dot{\beta}^i \\ &+ \frac{k^2}{a^2}\left(\mathcal{C}_7\,\beta_i\,\beta^i + \mathcal{C}_9\,b_i\,\beta^i + a\mathcal{C}_{10}\beta_i\,h^i + a\mathcal{C}_{11}\dot{\beta}_i\,h^i\right)\Bigg]. \end{aligned} \tag{7.17}$$

Moreover, in the metric-based theories, the vector sector is not included in the calculations and

is regarded as trivially zero. Moreover, the remaining possible gauge choices are presented here:

$$\delta^2\mathcal{S}_{\rm V}^{b_i=0} = \frac{1}{2\kappa^2}\int \mathrm{d}t\,\frac{\mathrm{d}^3k}{(2\pi)^{\frac{3}{2}}}\,a^3\Bigg[\frac{k^2}{a^2}\mathcal{C}_2\left(k^2 h_i\,h^i + \sigma^i\,\sigma_i - 2i\epsilon^{ijk}k_k\,\sigma_j\,h_i\right) + k^2\mathcal{C}_3\dot{h}^i\dot{h}_i + \mathcal{C}_5\,\dot{\sigma}_i\dot{\sigma}^i$$
$$+ \mathcal{C}_6\,\dot{\beta}_i\,\dot{\beta}^i + \frac{k^2}{a^2}\mathcal{C}_7\,\beta_i\,\beta^i + \mathcal{C}_{10}\left(\frac{k^2}{a}\,\beta_i\,h^i + 4i\epsilon^{ijk}\frac{k_j}{a}\beta_k\,\sigma_i\right) + \frac{k^2}{a}\mathcal{C}_{11}\dot{\beta}_i\,h^i$$
$$+ i\epsilon^{ijk}\frac{k_j}{a}\left(4\mathcal{C}_{12}\,\sigma_i\,\dot{\beta}_k + \mathcal{C}_{15}\,\dot{\sigma}_i\,\beta_k\right)\Bigg], \tag{7.18}$$

$$\delta^2\mathcal{S}_{\rm V}^{h_i=0} = \frac{1}{2\kappa^2}\int \mathrm{d}t\,\frac{\mathrm{d}^3k}{(2\pi)^{\frac{3}{2}}}\,a^3\Bigg[\frac{k^2}{a^2}\left(\mathcal{C}_1\,b_i\,b^i + \mathcal{C}_2\sigma^i\,\sigma_i\right) + \mathcal{C}_5\,\dot{\sigma}_i\left(\dot{\sigma}^i + i\epsilon^{ijk}\frac{k_j}{a}\,b_k\right) + \mathcal{C}_6\,\dot{\beta}_i\,\dot{\beta}^i$$
$$+ \frac{k^2}{a^2}\left(\mathcal{C}_7\,\beta_i\,\beta^i + \mathcal{C}_9\,b_i\,\beta^i\right) + i\epsilon^{ijk}\frac{k_j}{a}\left(4\mathcal{C}_{10}\beta_k\,\sigma_i + 4\mathcal{C}_{12}\,\sigma_i\,\dot{\beta}_k + \mathcal{C}_{15}\,\dot{\sigma}_i\,\beta_k\right)\Bigg], \tag{7.19}$$

The vector portions of Eq. (4.45) are solved to obtain equations for b_i and σ_i in terms of $\{\mathcal{Y}_i,\,\mathcal{Z}_i,\,h_i\}$. When these equations are substituted back into the action (7.16), the terms containing h_i cancel each other out such that the action is only expressed in terms of the gauge-invariant quantities $\{\mathcal{Y}_i,\,\mathcal{Z}_i\}$. The fully gauge-invariant action is given by

$$\delta^2\mathcal{S}_{\rm V} = \frac{1}{2\kappa^2}\int \mathrm{d}t\,\frac{\mathrm{d}^3k}{(2\pi)^{\frac{3}{2}}}\,a^3\Big[\frac{k^2}{a^2}\tilde{\mathcal{C}}_1\,\mathcal{Y}_i\,\mathcal{Y}^i - \frac{ik_j}{a}\tilde{\mathcal{C}}_2\,\mathcal{Y}_i\,\dot{\mathcal{Z}}^{ij} + \tilde{\mathcal{C}}_3\,\dot{\mathcal{Z}}_{ij}\,\dot{\mathcal{Z}}^{ij} + \frac{k^2}{a^2}\tilde{\mathcal{C}}_4\,\mathcal{Z}_{ij}\,\mathcal{Z}^{ij}$$
$$- \frac{ik_j}{a}\left(\tilde{\mathcal{C}}_5\,\beta_i\,\mathcal{Z}^{ij} + \tilde{\mathcal{C}}_7\,\beta_i\,\dot{\mathcal{Z}}^{ij}\right) + \frac{k^2}{a^2}\left(\tilde{\mathcal{C}}_6\,\beta_i\,\mathcal{Y}^i + \tilde{\mathcal{C}}_8\,\beta_i\,\beta^i\right) + \tilde{\mathcal{C}}_9\,\dot{\beta}_i\,\dot{\beta}^i\Big], \tag{7.20}$$

where $\tilde{\mathcal{C}}_i$ for $i \in [1,9]$ are detailed in Appendix C. $\mathcal{Y}_i$ the only non-dynamical variable. All coefficients are expressed in terms of a linear combination of functions from the BDLS action. Additionally, the imaginary contributions of i do not imply that the action is complex. It should be noted that the gauge-invariant $\mathcal{Z}_{ij}$ is imaginary, thus it always appears coupled with i such that the action is real. Taking a variation with respect to $\mathcal{Y}_i$ results in the constraint

$$0 = -2ik_j\tilde{\mathcal{C}}_1\mathcal{Y}_i + a\tilde{\mathcal{C}}_2\dot{\mathcal{Z}}_{ij} - ik_j\tilde{\mathcal{C}}_6\beta_i\,, \tag{7.21}$$

providing a solution for $\mathcal{Y}_i$ which is substituted back into the action in Eq. (7.20) to obtain the final form of the action

$$\delta^2\mathcal{S}_{\rm V} = \frac{1}{2\kappa^2}\int \mathrm{d}t\,\frac{\mathrm{d}^3k}{(2\pi)^{\frac{3}{2}}}\,a^3\Bigg[\left(\tilde{\mathcal{C}}_3 - \frac{\tilde{\mathcal{C}}_2^2}{4\tilde{\mathcal{C}}_1}\right)\dot{\mathcal{Z}}_{ij}\dot{\mathcal{Z}}^{ij} + \tilde{\mathcal{C}}_9\,\dot{\beta}_i\,\dot{\beta}^i + \frac{k^2}{a^2}\Bigg[\tilde{\mathcal{C}}_4\,\mathcal{Z}_{ij}\,\mathcal{Z}^{ij}$$
$$+ \left(\tilde{\mathcal{C}}_8 - \frac{\tilde{\mathcal{C}}_6^2}{4\tilde{\mathcal{C}}_1}\right)\beta_i\beta^i\Bigg] - \frac{ik_j}{a}\beta_i\left[\left(\tilde{\mathcal{C}}_7 - \frac{\tilde{\mathcal{C}}_2\tilde{\mathcal{C}}_6}{4\tilde{\mathcal{C}}_1}\right)\dot{\mathcal{Z}}^{ij} + \tilde{\mathcal{C}}_5\,\mathcal{Z}^{ij}\right]\Bigg], \tag{7.22}$$

such that the only quantities present are $\{\beta_i, \mathcal{Z}_{ij}\}$, and the coefficients are a product of the arbitrary functions of BDLS. The action holds provided $\tilde{\mathcal{C}}_1 \neq 0$. If $\tilde{\mathcal{C}}_1 = \mathcal{C}_1 = 0$, Eq. (7.20)

becomes

$$\delta^2\mathcal{S}_{\mathrm{V},\tilde{\mathcal{C}}_1=0} = \frac{1}{2\kappa^2}\int \mathrm{d}t\,\frac{\mathrm{d}^3k}{(2\pi)^{\frac{3}{2}}}\,a^3\Big[-\frac{ik_j}{a}\tilde{\mathcal{C}}_2\,\mathcal{Y}_i\,\dot{\mathcal{Z}}^{ij} + \tilde{\mathcal{C}}_3\,\dot{\mathcal{Z}}_{ij}\,\dot{\mathcal{Z}}^{ij} + \frac{k^2}{a^2}\tilde{\mathcal{C}}_4\,\mathcal{Z}_{ij}\,\mathcal{Z}^{ij} \\ - \frac{ik_j}{a}\left(\tilde{\mathcal{C}}_5\,\beta_i\,\mathcal{Z}^{ij} + \tilde{\mathcal{C}}_7\,\beta_i\,\dot{\mathcal{Z}}^{ij}\right) + \frac{k^2}{a^2}\left(\tilde{\mathcal{C}}_6\,\beta_i\,\mathcal{Y}^i + \tilde{\mathcal{C}}_8\,\beta_i\,\beta^i\right) + \tilde{\mathcal{C}}_9\,\dot{\beta}_i\,\dot{\beta}^i\Big]\,, \tag{7.23}$$

and $\mathcal{Y}_i$ is still the only non-dynamical quantity. Variation with respect to $\mathcal{Y}_i$ gives the relationship

$$0 = -ik^j a\tilde{\mathcal{C}}_2\dot{\mathcal{Z}}_{ij} + k^2\tilde{\mathcal{C}}_6\beta_i\,. \tag{7.24}$$

In order not to introduce higher order derivatives, Eq. (7.24) is solved for $\tilde{\mathcal{Z}}_{ij}$ and substituted back in Eq. (7.23) to obtain

$$\delta^2\mathcal{S}_{\mathrm{V},\tilde{\mathcal{C}}_1=0} = \frac{1}{2\kappa^2}\int \mathrm{d}t\,\frac{\mathrm{d}^3k}{(2\pi)^{\frac{3}{2}}}\,a^3\left[\frac{k^2}{a^2}\left(\left(\tilde{\mathcal{C}}_8 - \frac{\tilde{\mathcal{C}}_3\tilde{\mathcal{C}}_6^2}{\tilde{\mathcal{C}}_2^2} - \frac{\tilde{\mathcal{C}}_6\tilde{\mathcal{C}}_7}{\tilde{\mathcal{C}}_2}\right)\beta_i\beta^i + \tilde{\mathcal{C}}_4\,\mathcal{Z}_{ij}\,\mathcal{Z}^{ij} + 2\tilde{\mathcal{C}}_6\,\beta_i\,\mathcal{Y}^i\right) \\ - \frac{ik_j}{a}\tilde{\mathcal{C}}_5\,\beta_i\,\mathcal{Z}^{ij} + \tilde{\mathcal{C}}_9\,\dot{\beta}_i\,\dot{\beta}^i\right]\,, \tag{7.25}$$

where $\mathcal{Y}_i$ is still not eliminated and $\mathcal{Z}_{ij}$ is also non-dynamical. Hence, taking variations with respect to $\mathcal{Y}_i$ and $\mathcal{Z}_{ij}$ results in the constraints

$$0 = 2\tilde{\mathcal{C}}_6\beta_i\,, \tag{7.26}$$

$$0 = 2\frac{k^2}{a^2}\mathcal{Z}_{ij} - \frac{ik_j}{a}\tilde{\mathcal{C}}_5\beta_i\,. \tag{7.27}$$

The former constraint is solved by either setting $\beta_i = 0$ such that all modes are non-dynamical or $\tilde{\mathcal{C}}_6 = 0$. Hence, substituting Eq. (7.26) back into the action, gives

$$\delta^2\mathcal{S}_{\mathrm{V},\tilde{\mathcal{C}}_1=\tilde{\mathcal{C}}_6=0} = \frac{1}{2\kappa^2}\int \mathrm{d}t\,\frac{\mathrm{d}^3k}{(2\pi)^{\frac{3}{2}}}\,a^3\left[\frac{k^2}{a^2}\tilde{\mathcal{C}}_8\beta_i\beta^i - \frac{\tilde{\mathcal{C}}_4\tilde{\mathcal{C}}_5}{4}\beta_i\beta^i + \frac{\tilde{\mathcal{C}}_5^2}{2}\beta_i\beta^i + \tilde{\mathcal{C}}_9\,\dot{\beta}_i\,\dot{\beta}^i\right]\,. \tag{7.28}$$

with β_i being the only propagating mode. From Eq. (7.23) the case $\tilde{\mathcal{C}}_1 = \tilde{\mathcal{C}}_2 = 0$ crops up. Starting again from Eq. (7.20), the action becomes

$$\delta^2\mathcal{S}_{\mathrm{V},\tilde{\mathcal{C}}_1=\tilde{\mathcal{C}}_2=0} = \frac{1}{2\kappa^2}\int \mathrm{d}t\,\frac{\mathrm{d}^3k}{(2\pi)^{\frac{3}{2}}}\,a^3\Big[\tilde{\mathcal{C}}_3\,\dot{\mathcal{Z}}_{ij}\,\dot{\mathcal{Z}}^{ij} + \frac{k^2}{a^2}\tilde{\mathcal{C}}_4\,\mathcal{Z}_{ij}\,\mathcal{Z}^{ij} \\ - \frac{ik_j}{a}\left(\tilde{\mathcal{C}}_5\,\beta_i\,\mathcal{Z}^{ij} + \tilde{\mathcal{C}}_7\,\beta_i\,\dot{\mathcal{Z}}^{ij}\right) + \frac{k^2}{a^2}\left(\tilde{\mathcal{C}}_6\,\beta_i\,\mathcal{Y}^i + \tilde{\mathcal{C}}_8\,\beta_i\,\beta^i\right) + \tilde{\mathcal{C}}_9\,\dot{\beta}_i\,\dot{\beta}^i\Big]\,. \tag{7.29}$$

Varying with respect to $\mathcal{Y}_i$ gives two possible solutions: $\tilde{\mathcal{C}}_6 = 0$ or $\beta_i = 0$. If $\beta_i = 0$, then $\mathcal{Z}_{ij}$ is the only dynamical mode in the system, while if $\tilde{\mathcal{C}}_6 = 0$ the action has two propagating modes.

Moreover, if the ΛCDM case is considered, the coefficients $\{\tilde{\mathcal{C}}_2, \tilde{\mathcal{C}}_3, \tilde{\mathcal{C}}_4, \tilde{\mathcal{C}}_5, \tilde{\mathcal{C}}_7, \tilde{\mathcal{C}}_9\}$ are killed out and $2\tilde{\mathcal{C}}_1 = -\tilde{\mathcal{C}}_6 = 2\tilde{\mathcal{C}}_8 = 1$ such that Eq. (7.20) simplifies to

$$\delta^2 \mathcal{S}_{\mathrm{V},\Lambda\mathrm{CDM}} = \frac{1}{2\kappa^2} \int \mathrm{d}t \, \frac{\mathrm{d}^3 k}{(2\pi)^{\frac{3}{2}}} \, \frac{a^3}{2} \frac{k^2}{a^2} \left(\mathcal{Y}_i - \beta_i\right) \left(\mathcal{Y}^i - \beta^i\right) \,, \tag{7.30}$$

where all modes are non-dynamical, which when minimised by varying with respect to the auxiliary mode $\mathcal{Y}_i - \beta_i$ and substituted back into the action yields a trivial vector mode.

Tensor: Finally, the tensor sector constructed through the mode h_{ij}, as seen in Eq. (4.36), yields the gauge-invariant action of

$$\delta^2 S_{\mathrm{T}} = \frac{1}{2\kappa^2} \int \mathrm{d}t \, \frac{\mathrm{d}^3 k}{(2\pi)^{\frac{3}{2}}} \, \frac{a^3}{2} \left[\mathcal{D}_1 \, \dot{h}_{ij} \, \dot{h}^{ij} - \frac{k^2}{a^2} \mathcal{D}_2 \, h_{ij} \, h^{ij} \right] , \tag{7.31}$$

where

$$\begin{aligned} \mathcal{D}_1 &= G_4 - G_{\mathrm{Tele},T} + X\big(-2G_{4,X} + G_{5,\phi} - H\dot{\phi} G_{5,X} + 2G_{\mathrm{Tele},J_8} + \frac{1}{2} G_{\mathrm{Tele},J_5} \big) \,, \\ \mathcal{D}_2 &= G_4 - G_{\mathrm{Tele},T} - X(G_{5,\phi} + \ddot{\phi} G_{5,X}) \,. \end{aligned}$$

When taking the Horndeski limit $G_{\mathrm{Tele}} \to 0$, the result corresponds to that obtained in standard Horndeski in Ref. [112]. It is essential to require that $\mathcal{D}_1 \neq 0$, as a vanishing kinetic term could result in strong coupling of the graviton. In this case, graviton interactions would become non-linear, causing perturbation theory to break down. In Chapter 5 this condition was emphasised throughout the analysis to ensure that the tensor modes are always present in the theory. In the propagating DoFs analysis through GW this condition appeared as $G_4 - G_{\mathrm{Tele},T} \neq 0$ because the derivation was done in a Minkowski background and for a constant scalar field. In Sec. 7.2, the instability conditions will be calculated in detail. There, the excess speed of the tensor sector for BDLS can provide a better comparison with the Horndeski gravity results.

Eqs (7.12, 7.14, 7.22, 7.31) give the actions for all sectors expressed in terms of gauge-invariant quantities. To show how this formalism of BDLS can be easily adjustable to other theories, the next section explores different branches of BDLS which have been studied in literature with a particular gauge choice.

7.2 | Ghost and Laplacian Instabilities

The procedure to obtain the inequalities required to avoid ghost and Laplacian instabilities is presented here. First and foremost, it is required to have an action that has been perturbed

up to the second order. Any auxiliary / non-dynamical modes are identified and eliminated, by substituting the result upon varying with respect to the auxiliary mode. In general, the action is of the form

$$\delta^2\mathcal{S} = \frac{1}{2\kappa^2}\int \mathrm{d}t \frac{\mathrm{d}^3k}{(2\pi)^3}\, a^3 \left[\dot{\vec{\chi}}^{\intercal}\, \mathbf{K}(t,k)\, \dot{\vec{\chi}} + \vec{\chi}^{\intercal}\, \left(\frac{k^2}{a^2}\mathbf{G}(t,k) + \mathbf{M}(t,k)\right) \vec{\chi} + \vec{\chi}^{\intercal}\mathbf{Q}(t,k)\dot{\vec{\chi}}\right] , \quad (7.32)$$

where k is the co-vector obtained from spatial Fourier transformation, and matrices $\mathbf{K}$, $\mathbf{G}$, $\mathbf{M}$, $\mathbf{Q}$ correspond to coefficients to the dynamical modes in $\vec{\chi}$ [374, 375].

The kinetic matrix $\mathbf{K}$ here is a diagonalised matrix. It is not the case that the action obtained is of this form, hence extra steps are required. Consider a Lagrangian of the form

$$\mathcal{L} = \dot{\chi}'^{\intercal}\, \mathbf{K}'(t,k)\, \dot{\chi}' + \chi'^{\intercal}\, \mathbf{M}'(t,k)\chi' + \chi'^{\intercal}\mathbf{Q}'(t,k)\dot{\chi}' \,, \quad (7.33)$$

where the kinetic term $\mathbf{K}'$ is a non-diagonal matrix and χ' represents the dynamical modes to obtain a new Lagrangian of the form

$$\mathcal{L}_{\text{new}} = \dot{\chi}^{\intercal}\, \mathbf{K}(t,k)\, \dot{\chi} + \chi^{\intercal}\, \mathbf{M}(t,k)\chi' + \chi^{\intercal}\mathbf{Q}(t,k)\dot{\chi}' \,. \quad (7.34)$$

Additionally, matrix $\mathbf{K}'$ is a real symmetric matrix that can be diagonalised using orthogonal matrices. This would require obtaining the eigenvalues and eigenvectors of the matrix $\mathbf{K}'$ and extending the transformation to the rest of the matrices. This may give rise to complicated expressions upon diagonalisation, introducing square roots in the system. Since there are a large number of contributions in BDLS, as shown in the scalar and vector sectors in Sec. 7.1, an alternative method is applied. One of the simpler methods is to transform the modes in χ'. Assume $\mathbf{K}'$ is a (2×2) matrix and χ' is a vector with two modes of the form

$$\mathbf{K}' = \begin{pmatrix} K_{11} & K_{12} \\ K_{12} & K_{22} \end{pmatrix} , \qquad \chi' = \begin{pmatrix} X' \\ Y' \end{pmatrix} . \quad (7.35)$$

A transformation of the scalar fields is given by

$$X' = X \,, \qquad Y' = Y - \frac{K_{12}}{K_{22}} X \,. \quad (7.36)$$

where now $\chi^{\intercal} = \{X, Y\}$ are the new modes in the system. The modification stems from the triangulisation of a (2×2) matrix. In this work, the maximum number of dynamical modes is two, so the above expressions suffice. In the case of a larger matrix, these transformations would

need to be altered accordingly. The kinetic term transforms to

$$\dot{\chi}'^{\mathsf{T}}\mathbf{K}'\dot{\chi}' = \dot{\chi}^{\mathsf{T}}\overbrace{\begin{pmatrix} K_{11}-\frac{K_{12}^2}{K_{22}} & 0 \\ 0 & K_{22}\end{pmatrix}}^{\mathbf{K}}\dot{\chi} + \underbrace{\chi^{\mathsf{T}}\begin{pmatrix} K_{22}\left(\frac{\mathrm{d}}{\mathrm{d}t}\left(\frac{K_{12}}{K_{22}}\right)\right)^2 & 0 \\ 0 & 0\end{pmatrix}\chi}_{\text{portion contributing to }\mathbf{M}} + \underbrace{\chi^{\mathsf{T}}\begin{pmatrix} -2K_{22}\left(\frac{\mathrm{d}}{\mathrm{d}t}\left(\frac{K_{12}}{K_{22}}\right)\right)^2 & 0 \\ 0 & 0\end{pmatrix}\dot{\chi}}_{\text{portion contributing to }\mathbf{Q}}. \tag{7.37}$$

Extending transformations in Eq. (7.36) to the rest of the action gives

$$\chi'^{\mathsf{T}}\mathbf{Q}'\chi' = \dot{\chi}'^{\mathsf{T}}\begin{pmatrix} Q_{11} & Q_{12} \\ Q_{21} & Q_{22}\end{pmatrix}\dot{\chi}' = \chi^{\mathsf{T}}\overbrace{\begin{pmatrix} \left(-Q_{12}+\frac{Q_{21}}{K_{22}}\right)\frac{\mathrm{d}}{\mathrm{d}t}\left(\frac{K_{12}}{K_{22}}\right) & -\frac{Q_{22}}{2}\frac{\mathrm{d}}{\mathrm{d}t}\left(\frac{K_{12}}{K_{22}}\right) \\ -\frac{Q_{22}}{2}\frac{\mathrm{d}}{\mathrm{d}t}\left(\frac{K_{12}}{K_{22}}\right) & 0\end{pmatrix}}^{\text{portion contributing to }\mathbf{M}}\chi + \underbrace{\chi^{\mathsf{T}}\begin{pmatrix} Q_{11}-\frac{K_{12}}{K_{22}}\left(Q_{12}+Q_{21}-\frac{K_{12}}{K_{22}}Q_{22}\right) & Q_{12}-\frac{K_{12}}{K_{22}}Q_{22} \\ Q_{21}-\frac{K_{12}}{K_{22}}Q_{22} & Q_{22}\end{pmatrix}\dot{\chi}}_{\text{portion contributing to }\mathbf{Q}} \tag{7.38}$$

and

$$\chi'^{\mathsf{T}}\mathbf{M}'\chi' = \chi'^{\mathsf{T}}\begin{pmatrix} M_{11} & M_{12} \\ M_{12} & M_{22}\end{pmatrix}\chi' = \chi^{\mathsf{T}}\begin{pmatrix} M_{11}+\frac{K_{12}}{K_{22}}\left(-2M_{12}+\frac{K_{12}}{K_{22}}\right) & M_{12}-\frac{K_{12}}{K_{22}}M_{22} \\ M_{12}-\frac{K_{12}}{K_{22}}M_{22} & M_{22}\end{pmatrix}\chi, \tag{7.39}$$

resulting in the Lagrangian (7.34). Additionally, by performing a temporal Fourier transformation of the action in Eq. (7.32), the determinant of this system becomes

$$\det\left(-\omega^2\mathbf{K}+i\omega\mathbf{Q}+\frac{k^2}{a^2}\mathbf{G}+\mathbf{M}\right)=0, \tag{7.40}$$

which can be solved to obtain the Laplacian condition through c^2, since $\omega^2 = \frac{k^2}{a^2}c^2$. When considering stability conditions, the high-k limit is considered. At the small scales, where k has a large value and wavelengths are short, small instabilities could lead to the rapid growth of perturbations, resulting in non-viable structures. Hence, upon obtaining the determinant given by Eq. (7.40), only the leading order of k is kept by taking the limit $k \to \infty$, upon which some terms in Eq. (7.32) can be deemed negligible.

Scalar: Starting from Eq. (7.8), it was noted that in the kinetic portion of the action there is a mix of $\dot{\mathcal{X}}_1\dot{\mathcal{X}}_3$, which when expressed in terms of a matrix would result in a non-diagonal kinetic matrix. As detailed at the beginning of the section, the (2×2) kinetic matrix can be diagonalised by performing the transformation

$$\mathcal{X}_1 := \Psi_1\,, \qquad \mathcal{X}_3 := \Psi_2 - \frac{1}{2}\left(\frac{\hat{\mathcal{A}}_{10}}{\hat{\mathcal{A}}_6}\right)\Psi_1\,, \tag{7.41}$$

which remains gauge-invariant since Ψ_1 and Ψ_2 are constructed through a linear combination of gauge-invariant quantities $\mathcal{X}_1$ and $\mathcal{X}_3$. Performing a Taylor expansion at $k \to \infty$ up to order $\mathcal{O}\left(\frac{1}{k}\right)$ to obtain the kinetic term diagonalisation outlined in the beginning of this section. Hence, the action at high-k limit becomes[1]

$$\delta^2\mathcal{S}_{\rm S} = \frac{1}{2\kappa^2}\int \mathrm{d}t\,\frac{\mathrm{d}^3k}{(2\pi)^{\frac{3}{2}}}\,a^3\left[\breve{\mathcal{A}}_1\dot{\Psi}_1^2 + \breve{\mathcal{A}}_2\dot{\Psi}_2^2 + \frac{k^2}{a^2}\left(\breve{\mathcal{A}}_3\Psi_1^2 + \breve{\mathcal{A}}_4\Psi_2^2 + \breve{\mathcal{A}}_5\Psi_1\Psi_2\right)\right.$$
$$\left. + \breve{\mathcal{A}}_6\Psi_1^2 + \breve{\mathcal{A}}_7\Psi_2^2 + \breve{\mathcal{A}}_8\Psi_1\Psi_2 + \breve{\mathcal{A}}_9\Psi_1\dot{\Psi}_2\right]\,, \tag{7.42}$$

where $\breve{\mathcal{A}}_i$ for $i \in [1,5]$ can be found in Appendix C and the rest of the terms can be eliminated because they contribute at a lower k value when considering the leading order of k only. This is further clarified when calculating the determinant in Eq. (7.40). Provided $\omega \propto k$, the determinant becomes

$$0 = \omega^4 - \omega^2\frac{k^2}{a^2}\left(\frac{\breve{\mathcal{A}}_2\breve{\mathcal{A}}_3 + \breve{\mathcal{A}}_1\breve{\mathcal{A}}_4}{\breve{\mathcal{A}}_1\breve{\mathcal{A}}_2}\right) + \frac{k^4}{a^4}\left(\frac{\breve{\mathcal{A}}_3\breve{\mathcal{A}}_4 - \breve{\mathcal{A}}_5^2}{\breve{\mathcal{A}}_1\breve{\mathcal{A}}_2}\right)\,, \tag{7.43}$$

provided $\breve{\mathcal{A}}_1\breve{\mathcal{A}}_2 \neq 0$. This indicates that only terms arising from $\mathbf{Q}$ and $\mathbf{M}$ do not contribute at a high-k system and only $[\breve{\mathcal{A}}_1, \breve{\mathcal{A}}_5]$ are present. Taking variations with respect to Ψ_1 and Ψ_2, respectively, yields:

$$0 \approx \ddot{\Psi}_1 + \left(\frac{\breve{\mathcal{A}}_1'}{\breve{\mathcal{A}}_1}\right)\dot{\Psi}_1 - \frac{k^2}{a^2}\left(\frac{\breve{\mathcal{A}}_3}{\breve{\mathcal{A}}_1}\right)\Psi_1 - \frac{k^2}{a^2}\left(\frac{\breve{\mathcal{A}}_5}{2\breve{\mathcal{A}}_1}\right)\Psi_2\,, \tag{7.44}$$

$$0 \approx \ddot{\Psi}_2 + \left(\frac{\breve{\mathcal{A}}_2'}{\breve{\mathcal{A}}_2}\right)\dot{\Psi}_2 - \frac{k^2}{a^2}\left(\frac{\breve{\mathcal{A}}_4}{\breve{\mathcal{A}}_2}\right)\Psi_2 - \frac{k^2}{a^2}\left(\frac{\breve{\mathcal{A}}_5}{2\breve{\mathcal{A}}_2}\right)\Psi_1\,. \tag{7.45}$$

[1] Coefficients $\{\breve{\mathcal{A}}_6, \breve{\mathcal{A}}_7, \breve{\mathcal{A}}_8, \breve{\mathcal{A}}_9\}$ have been omitted due to their complexity and because the coefficients were not utilised for the remaining portion of the analysis as they correspond to lower orders of k.

The variations decouple Ψ_1 from Ψ_2 under the condition

$$\breve{\mathcal{A}}_5 = 0\,. \tag{7.46}$$

Under this condition, the propagating speed for each mode is given by

$$c^2_{\Psi_1} := -\frac{\breve{\mathcal{A}}_3}{\breve{\mathcal{A}}_1} > 0\,, \qquad c^2_{\Psi_2} := -\frac{\breve{\mathcal{A}}_4}{\breve{\mathcal{A}}_2} > 0\,. \tag{7.47}$$

Ghost stability is achieved when

$$\mathcal{M}_{\Psi_1} := \breve{\mathcal{A}}_1 > 0\,, \qquad \mathcal{M}_{\Psi_2} := \breve{\mathcal{A}}_2 > 0\,, \tag{7.48}$$

and Laplacian/gradient stability obtained when

$$\mathcal{N}_{\Psi_1} := -\breve{\mathcal{A}}_3 > 0\,, \qquad \mathcal{N}_{\Psi_2} := -\breve{\mathcal{A}}_4 > 0\,. \tag{7.49}$$

Any model considered in this system would need to satisfy the conditions Eq. (7.46), Eq. (7.48) and Eq. (7.49), which by definition would also satisfy Eq. (7.47).

Pseudoscalar: With no further modifications to the pseudoscalar action in Eq. (7.14), the ghost and Laplacian stability conditions can be determined, respectively given by:

$$\mathcal{M}_\sigma := k^2\mathcal{B}_1 > 0\,, \tag{7.50}$$

$$\mathcal{N}_\sigma = k^2\mathcal{B}_2 > 0\,, \tag{7.51}$$

such that the $c^2_{\rm PS}$ is given by

$$c^2_\sigma := \frac{\mathcal{N}_{\rm PS}}{\mathcal{M}_{\rm PS}} = \frac{4\left(G_{{\rm Tele},T_{\rm ax}} - 2XG_{{\rm Tele},J_1}\right)}{4G_{{\rm Tele},T_{\rm ax}} + 9XG_{{\rm Tele},J_5} - 12XG_{{\rm Tele},J_{10}}} > 0\,, \tag{7.52}$$

corresponding to the solution of the determinant of Eq. (7.40) where the dispersion equation is given by $\omega^2 = \frac{k^2}{a^2}c^2_\sigma$. Given that the pseudoscalar action is dependent on the teleparallel portion of BDLS gravity, in the cases of Horndeski [112], $f(\phi,T)$ [376], $f(T)$ [274], GBD [175], BD [61], $f(\mathring{R})$ [222] and GR, either the pseudoscalar reduces to a non-dynamical mode or is not present at first principle, resulting in σ being a non-propagating mode. These results are realised in the Minkowski background as well [373].

Vector: The gauge-invariant action in Eq. (7.20) contains two dynamical modes $\{\beta_i, \tilde{\mathcal{Z}}_{ij}\}$. The kinetic terms of each mode should impose ghost stability such that

$$\mathcal{M}_\beta = \tilde{\mathcal{C}}_9 > 0\,, \qquad\qquad \mathcal{M}_{\mathcal{Z}} = \tilde{\mathcal{C}}_3 - \frac{\tilde{\mathcal{C}}_2^2}{4\tilde{\mathcal{C}}_1} > 0\,, \tag{7.53}$$

which is easily attained as the kinetic modes are decoupled. To obtain the gradient stability condition, the determinant equation (7.40) is used. Thus, temporal Fourier transformation $\partial_0 \to i\omega$ is applied, and Eq. (7.20) is rewritten as follows, such that the Lagrangian density is of the form:

$$\delta^2\mathcal{L}_{\rm V} = \begin{pmatrix} \beta_i & \tilde{\mathcal{Z}}_{ij} \end{pmatrix} \begin{pmatrix} -\omega^2\tilde{\mathcal{C}}_9 + \frac{k^2}{a^2}\left(\tilde{\mathcal{C}}_8 - \frac{\tilde{\mathcal{C}}_6^2}{4\tilde{\mathcal{C}}_1}\right) & -\frac{ik_j}{2a}\left[i\omega\left(\tilde{\mathcal{C}}_7 - \frac{\tilde{\mathcal{C}}_6\tilde{\mathcal{C}}_2}{2\tilde{\mathcal{C}}_1}\right) + \tilde{\mathcal{C}}_5\right] \\ -\frac{ik^j}{2a}\left[i\omega\left(\tilde{\mathcal{C}}_7 - \frac{\tilde{\mathcal{C}}_6\tilde{\mathcal{C}}_2}{2\tilde{\mathcal{C}}_1}\right) + \tilde{\mathcal{C}}_5\right] & -\omega^2\left(\tilde{\mathcal{C}}_3 - \frac{\tilde{\mathcal{C}}_2^2}{4\tilde{\mathcal{C}}_1}\right) + \frac{k^2}{a^2}\tilde{\mathcal{C}}_4 \end{pmatrix} \begin{pmatrix} \beta^i \\ \tilde{\mathcal{Z}}^{ij} \end{pmatrix}, \tag{7.54}$$

whose determinant is given by

$$\begin{aligned} 0 = \omega^4 &+ \omega^2\frac{k^2}{a^2}\left(\frac{\tilde{\mathcal{C}}_2^2(\tilde{\mathcal{C}}_6^2 - 2\tilde{\mathcal{C}}_1\tilde{\mathcal{C}}_8) + 2\tilde{\mathcal{C}}_1(-\tilde{\mathcal{C}}_2\tilde{\mathcal{C}}_6\tilde{\mathcal{C}}_7 - \tilde{\mathcal{C}}_3\tilde{\mathcal{C}}_6^2 + \tilde{\mathcal{C}}_1(\tilde{\mathcal{C}}_7^2 + 4\tilde{\mathcal{C}}_3\tilde{\mathcal{C}}_8 + 4\tilde{\mathcal{C}}_4\tilde{\mathcal{C}}_9))}{2\tilde{\mathcal{C}}_1\tilde{\mathcal{C}}_9(\tilde{\mathcal{C}}_2^2 - 4\tilde{\mathcal{C}}_1\tilde{\mathcal{C}}_3)}\right) \\ &+ i\omega\frac{k^2}{a^2}\frac{\tilde{\mathcal{C}}_5(\tilde{\mathcal{C}}_2\tilde{\mathcal{C}}_6 - 2\tilde{\mathcal{C}}_1\tilde{\mathcal{C}}_7)}{\tilde{\mathcal{C}}_9(\tilde{\mathcal{C}}_2^2 - 4\tilde{\mathcal{C}}_1\tilde{\mathcal{C}}_3)} + \frac{k^4}{a^4}\frac{\tilde{\mathcal{C}}_4(\tilde{\mathcal{C}}_6^2 - 4\tilde{\mathcal{C}}_1\tilde{\mathcal{C}}_8)}{\tilde{\mathcal{C}}_9(\tilde{\mathcal{C}}_2^2 - 4\tilde{\mathcal{C}}_1\tilde{\mathcal{C}}_3)} - \frac{k^2}{a^2}\frac{\tilde{\mathcal{C}}_1\tilde{\mathcal{C}}_5^2}{\tilde{\mathcal{C}}_9(\tilde{\mathcal{C}}_2^2 - 4\tilde{\mathcal{C}}_1\tilde{\mathcal{C}}_3)}\,. \end{aligned} \tag{7.55}$$

Provided that $\omega \propto k$, the leading orders surviving when considering a high-k limit, the determinant reduces to

$$\begin{aligned} 0 = \omega^4 &+ \omega^2\frac{k^2}{a^2}\left(\frac{\tilde{\mathcal{C}}_2^2(\tilde{\mathcal{C}}_6^2 - 2\tilde{\mathcal{C}}_1\tilde{\mathcal{C}}_8) + 2\tilde{\mathcal{C}}_1(-\tilde{\mathcal{C}}_2\tilde{\mathcal{C}}_6\tilde{\mathcal{C}}_7 - \tilde{\mathcal{C}}_3\tilde{\mathcal{C}}_6^2 + \tilde{\mathcal{C}}_1(\tilde{\mathcal{C}}_7^2 + 4\tilde{\mathcal{C}}_3\tilde{\mathcal{C}}_8 + 4\tilde{\mathcal{C}}_4\tilde{\mathcal{C}}_9))}{2\tilde{\mathcal{C}}_1\tilde{\mathcal{C}}_9(\tilde{\mathcal{C}}_2^2 - 4\tilde{\mathcal{C}}_1\tilde{\mathcal{C}}_3)}\right) \\ &+ \frac{k^4}{a^4}\frac{\tilde{\mathcal{C}}_4(\tilde{\mathcal{C}}_6^2 - 4\tilde{\mathcal{C}}_1\tilde{\mathcal{C}}_8)}{\tilde{\mathcal{C}}_9(\tilde{\mathcal{C}}_2^2 - 4\tilde{\mathcal{C}}_1\tilde{\mathcal{C}}_3)}\,, \end{aligned} \tag{7.56}$$

which corresponds to matrices $\mathbf{K}$, $\mathbf{Q}$ and $\mathbf{G}$ when compared to the action (7.32). Hence, the Laplacian stability of all modes can be obtained directly from action (7.22):

$$\mathcal{N}_{\rm V}^{\beta} = -\tilde{\mathcal{C}}_8 + \frac{\tilde{\mathcal{C}}_6^2}{4\tilde{\mathcal{C}}_1} > 0\,, \qquad\qquad \mathcal{N}_{\rm V}^{\tilde{\mathcal{Z}}} = -\tilde{\mathcal{C}}_4 > 0\,. \tag{7.57}$$

Thus, the respective sound speed squared expression is given by

$$\left(c_{\rm V}^{\beta}\right)^2 = \frac{\tilde{\mathcal{C}}_6^2 - 4\tilde{\mathcal{C}}_1\tilde{\mathcal{C}}_8}{4\tilde{\mathcal{C}}_1\tilde{\mathcal{C}}_9} > 0\,, \qquad\qquad \left(c_{\rm V}^{\mathcal{Z}}\right)^2 = \frac{4\tilde{\mathcal{C}}_1\tilde{\mathcal{C}}_4}{\tilde{\mathcal{C}}_2^2 - 4\tilde{\mathcal{C}}_1\tilde{\mathcal{C}}_3} > 0\,. \tag{7.58}$$

When taking the Horndeski limit, the coefficients alter such that $\tilde{\mathcal{C}}_1 = \tilde{\mathcal{C}}_{18} = -2\tilde{\mathcal{C}}_6$ and $\tilde{\mathcal{C}}_2 = \tilde{\mathcal{C}}_3 = \tilde{\mathcal{C}}_4 = \tilde{\mathcal{C}}_9 \neq 0$, thus resulting in non-propagating vector modes. Vector analysis is commonly eliminated from Horndeski gravity studies and its subsets as vector modes do not propagate. Theories containing the teleparallel sector, especially J_i terms, realise stability conditions for the vector sector. While $f(T)$ and $f(\phi, T)$ do not provide stability within the vector sector, the case $f(T, T_{\rm ax}\, T_{\rm vec})$ does, given all terms are present at least at linear order and $9G_{{\rm Tele},T} + 2G_{{\rm Tele},T_{\rm ax}} = 0$.

To avoid repetition, the analyses for specific branches of the theory have been omitted. However, the following are some of the key results. The case $\tilde{\mathcal{C}}_1 = 0$ requires repeating the above analysis from the beginning; otherwise it leads to undefined regions. For the case $\tilde{\mathcal{C}}_1 = \tilde{\mathcal{C}}_6 = 0$ given by Eq. (7.28) the ghost stability condition is given by $\tilde{\mathcal{C}}_9 > 0$ and the Laplacian condition is $\tilde{\mathcal{C}}_8 > 0$, implying that only β_i is a dynamical mode. On the other hand, for $\tilde{\mathcal{C}}_1 = \tilde{\mathcal{C}}_2 = 0$ given by Eq. (7.29) two dynamical modes persist, thus conditions for both would need to be satisfied for the full extent of the subcase to give healthy branches. Conditions corresponding to β_i are still given by $\tilde{\mathcal{C}}_9 > 0$ and $\tilde{\mathcal{C}}_8 > 0$, and conditions for $\mathcal{Z}_{ij}$ are $\tilde{\mathcal{C}}_3 > 0$ and $\tilde{\mathcal{C}}_4 > 0$.

Tensor: The last modes considered are those of tensor nature. Eq. (7.31), naturally being gauge-invariant, results in a kinetic and gradient entry, respectively corresponding to the ghost and Laplacian condition for which stability is obtained if

$$\mathcal{M}_{\rm T} := \mathcal{D}_1 > 0\,, \tag{7.59}$$

$$\mathcal{N}_{\rm T} := \mathcal{D}_2 > 0\,, \tag{7.60}$$

such that the sound speed squared $c_{\rm T}^2$ is given by

$$\begin{aligned} c_{\rm T}^2 :&= \frac{\mathcal{N}_{\rm T}}{\mathcal{M}_{\rm T}} \\ &= \frac{G_4 - G_{{\rm Tele},T} - X(G_{5,\phi} + \ddot{\phi}G_{5,X})}{G_4 - G_{{\rm Tele},T} + X\big(-2G_{4,X} + G_{5,\phi} - H\dot{\phi}G_{5,X} + 2G_{{\rm Tele},J_8} + \frac{1}{2}G_{{\rm Tele},J_5}\big)} > 0\,. \end{aligned} \tag{7.61}$$

An interest in the deviation of light propagation has been shown following the results of GW signal GW170817 [80] and its electromagnetic counterpart labelled GRB170817A [81], as theories such as Horndeski have been ruled out due to being highly constrained to a minute graviton mass. The excess speed is given by

$$\alpha_{\rm T} = c_{\rm T}^2 - 1 = \frac{X(2G_{4,X} - 2G_{5,\phi} + (H\dot{\phi} - \ddot{\phi})G_{5,X} - 2G_{{\rm Tele},J_8} - \frac{1}{2}G_{{\rm Tele},J_5})}{G_4 - G_{{\rm Tele},T} + X\big(-2G_{4,X} + G_{5,\phi} - H\dot{\phi}G_{5,X} + 2G_{{\rm Tele},J_8} + \frac{1}{2}G_{{\rm Tele},J_5}\big)}\,, \tag{7.62}$$

corresponding to the result obtained in Ref. [78] when analysing GW propagation. The solution for $\ddot{\phi}$ can be obtained from the scalar field background equation (5.6), indicating there are, technically, dependencies on functions $\{G_2, G_3\}$ and scalars $\{T_{\rm vec}, I_2\}$. This solution is not substituted to avoid complicating the result in Eq. (7.62), but it further highlights the importance of ensuring that the background equations are always satisfied, as their solutions are used throughout the perturbation sectors.

7.3 | Actions in Branches of BDLS

The limits of BDLS theory can replicate results frequently studied in literature which would require a different approach rather than working with the gauge-invariant quantities. Oftentimes, gauge choices are implemented. In the case of the scalar sector, the unitary gauge in Eq. (7.5) is used where $\{\mathcal{A}_4, \mathcal{A}_5, \mathcal{A}_8, \mathcal{A}_9, \mathcal{A}_{16}, \mathcal{A}_{17}, \mathcal{A}_{18}, \mathcal{A}_{23}, \mathcal{A}_{24}, \mathcal{A}_{25}, \mathcal{A}_{26}, \mathcal{A}_{27}, \mathcal{A}_{28}\}$ coefficients from Eq. (7.3) do not appear. For the vector sector it would be more useful to implement $\sigma_i = 0$, **a** fix where $\{\mathcal{C}_{12}, \mathcal{C}_{15}\}$ are not present from Eq. (7.16). In the following subsections, the GR, Horndeski, $f(T)$, and $f(\phi, T)$ theories are explored.

7.3.1 | GR

The GR limit provides one of the simplest subcases of BDLS, and a crucial one at that, where $G_4 = 1$ and all other terms in BDLS vanish. Starting from the scalar action in unitary gauge (7.5), the coefficients $\{\mathcal{A}_1, \mathcal{A}_7, \mathcal{A}_{10}, \mathcal{A}_{11}, \mathcal{A}_{13}, \mathcal{A}_{19}\}$ vanish while other coefficients can be combined to result in the Lagrangian given in

$$\mathcal{L}^{\text{Unitary}}_{\text{S, GR}} = \frac{k^2}{a^2}\left[B\left(\mathcal{A}_6\varphi + \mathcal{A}_{12}\dot{\psi}\right) + \psi\left(-\mathcal{A}_{14}\varphi + \mathcal{A}_{21}\psi\right)\right] + \mathcal{A}_{22}\left(H^2\varphi^2 + \dot{\psi}^2\right) + \mathcal{A}_{15}\dot{\psi}\varphi\,. \tag{7.63}$$

The modes β and b always appear as a linear combination and are expressed as $B = -b + \beta$, as they appear in the metric (4.26). Here, the non-dynamical modes are B and φ. Taking variations with respect to both variables results in the following two conditions:

$$0 = \mathcal{A}_6\varphi + \mathcal{A}_{12}\dot{\psi}\,, \tag{7.64}$$

$$0 = \frac{k^2}{a^2}\left(\mathcal{A}_6 B - \mathcal{A}_{14}\psi\right) + 2H^2\mathcal{A}_{22}\varphi + \mathcal{A}_{15}\dot{\psi}\,, \tag{7.65}$$

where the former equation indicates that the dynamical mode of $\dot{\psi}$ can be expressed in terms of the non-dynamical mode of φ. Thus, solving and substituting back in Eq. (7.63) results in a trivial Lagrangian that has no propagating modes. The pseudoscalar sector given by Eq. (7.14) completely disappears in GR, correlating with the fact that the pseudoscalar mode does not appear in the symmetric metric (4.26) in the first place since the pseudoscalar only contributes due to the antisymmetric portion of the tetrad.

In the vector sector, starting from Eq. (7.17), $\{\mathcal{C}_1, \mathcal{C}_2, \mathcal{C}_6, \mathcal{C}_{10}\}$ no longer contribute and the action reduces to

$$\mathcal{L}^{\sigma_i=0}_{\text{V, GR}} = 2k^2\dot{h}^i\left(\dot{h}_i - \frac{1}{a}\,b_i\right) + \frac{k^2}{a^2}\left(\frac{1}{2}\,\beta_i\,\beta^i - b_i\,\beta^i - 2a\dot{\beta}_i\,h^i\right)\,. \tag{7.66}$$

b_i is a non-dynamical term that is eliminated from the action by varying with respect to b_i

$$0 = 2a\dot{h}_i + \beta_i \,, \tag{7.67}$$

and substituting back in Eq. (7.66), yielding

$$\mathcal{L}^{\sigma_i=0}_{\mathrm{V,\,GR}} = \frac{k^2}{a^2}\left(\beta_i\beta^i - 2a\dot{\beta}_i\, h^i\right) \,, \tag{7.68}$$

where once again, the action has a non-dynamical mode. Varying with respect to h_i results in $\dot{\beta}_i = 0$ such that the final vector action is trivially zero, implying that no vector modes propagate in GR.

As for the tensor sector, action (7.31) simplifies to

$$\mathcal{L}_{\mathrm{T,\,GR}} = \frac{1}{2}\left(\dot{h}_{ij}\,\dot{h}^{ij} - \frac{k^2}{a^2}h_{ij}\,h^{ij}\right) \,, \tag{7.69}$$

thus making the tensor modes the only modes propagating in GR, corresponding to the results obtained in Table 5.2.

7.3.2 | Horndeski Gravity

In Ref. [112], the Horndeski action was obtained within the ADM decomposition [377] of the metric. This result can be replicated by starting with the unitary gauge of the scalar action and setting $G_{\mathrm{Tele}} = 0$ such that

$$\mathcal{L}^{\mathrm{Unitary}}_{\mathrm{S,\,Horndeski}} = \frac{k^2}{a^2}\left(B\left(\mathcal{A}_2\varphi + \mathcal{A}_3\dot{\psi}\right) + \mathcal{A}_3\psi\left(\varphi + \psi\right)\right) + \mathcal{A}_{15}\dot{\psi}\varphi + \mathcal{A}_{20}\varphi^2 + \mathcal{A}_{22}\dot{\psi}^2 \,, \tag{7.70}$$

where once again β and b can be combined in B. Variations with respect to auxiliary modes B and φ provide the constraints

$$0 = \mathcal{A}_2\varphi + \mathcal{A}_3\dot{\psi} \,, \tag{7.71}$$

$$0 = \frac{k^2}{a^2}\left(\mathcal{A}_2 B + \mathcal{A}_3\psi\right) + \mathcal{A}_{15}\dot{\psi} + 2\mathcal{A}_{20}\varphi \,, \tag{7.72}$$

which when substituted back into Eq. (7.70) gives

$$\mathcal{L}^{\mathrm{Unitary}}_{\mathrm{S,\,Horndeski}} = \frac{k^2}{a^2}\left(\frac{\mathcal{A}_3^2}{\mathcal{A}_2} - \frac{1}{2a}\frac{\mathrm{d}}{\mathrm{d}t}\left(a\mathcal{A}_3\right)\right)\psi^2 + \left(\mathcal{A}_{22} - \frac{\mathcal{A}_3\mathcal{A}_{15}}{\mathcal{A}_2} + \frac{\mathcal{A}_3^2\mathcal{A}_{20}}{\mathcal{A}_2^2}\right)\dot{\psi}^2 \,, \tag{7.73}$$

such that only one scalar mode propagates. On the other hand, the pseudoscalar mode completely disappears, obtaining a trivial action for the Horndeski limit of Eq. (7.14).

Next, the vector modes are analysed. In the Horndeski limit, the coefficients of $\{\mathcal{C}_2, \mathcal{C}_5, \mathcal{C}_6, \mathcal{C}_{15}\}$ vanish. Fixing the gauge through $\sigma_i = 0$ yields

$$\mathcal{L}^{\sigma_i=0}_{\text{V, Horndeski}} = \frac{k^2}{a^2}\left[\mathcal{C}_1\left(b_i\, b^i + 4a^2\dot{h}^i\left(\dot{h}_i - \frac{1}{a}\, b_i\right) + \beta_i\, \beta^i - 2b_i\, \beta^i + 4a\beta_i\, \dot{h}^i\right) + \left(a\mathcal{C}_{10} + \frac{4}{a}\frac{\mathrm{d}}{\mathrm{d}t}\left(a^2\mathcal{C}_1\right)\right)\beta_i\, h^i\right]. \tag{7.74}$$

where h_i is dynamical upon performing integration by parts, but b and β are auxiliary modes. Varying with respect to b and β gives

$$0 = 2b_i - 4a^2\dot{h}_i - 2\beta_i\,, \tag{7.75}$$

$$0 = 2\mathcal{C}_1\left(-b_i + 2a\dot{h}_i + \beta_i\right) + a\mathcal{C}_{10}h_i + \frac{4}{a}\frac{\mathrm{d}}{\mathrm{d}t}\left(a^2\mathcal{C}_1\right)h_i \tag{7.76}$$

which when substituted back in the action gives a trivial solution with no dynamical modes, thus corresponding to the result in Ref. [112] where vector modes do not propagate in Horndeski gravity. As for the tensor modes, the form of Eq. (7.31) is not altered but the limits of $\mathcal{D}_1$ and $\mathcal{D}_2$ are modified to eliminate teleparallel contributions.

7.3.3 | $f(T)$ Gravity

$f(T)$ gravity has been widely studied in cosmology [206, 69, 215, 216, 217, 218, 219, 220, 221]. Standard Horndeski functions $\{G_2, G_3, G_4, G_5\}$ completely vanish and G_{Tele} is a function of torsion scalar T only. Applying $f(T)$ limits to Eq. (7.5), eliminates coefficients $\{\mathcal{A}_7, \mathcal{A}_{12}, \mathcal{A}_{13}\}$ and the Lagrangian becomes

$$\mathcal{L}^{\text{Unitary}}_{f(T)} = \frac{k^2}{a^2}\left(\frac{k^2}{a^2}\mathcal{A}_1 b^2 - b\left(\mathcal{A}_2\varphi + \mathcal{A}_3\dot{\psi}\right) - \beta\left(\mathcal{A}_6\varphi + \mathcal{A}_{10}\psi\right) - \mathcal{A}_{14}\psi\varphi + \mathcal{A}_{21}\psi^2\right) + \mathcal{A}_{15}\dot{\psi}\varphi + \mathcal{A}_{20}\varphi^2 + \mathcal{A}_{22}\dot{\psi}^2 - \frac{k^2}{a^2}\left(\mathcal{A}_{11}\beta\dot{\psi} + \frac{1}{a}\frac{\mathrm{d}}{\mathrm{d}t}\left(a\mathcal{A}_{11}\right)\beta\psi\right), \tag{7.77}$$

where an integration by parts has been performed when the Lagrangian is assumed to be in the action. φ, b and β are the auxiliary modes. Taking variation with respect to these quantities yields

$$0 = \frac{k^2}{a^2}\left(-\mathcal{A}_2 b - \mathcal{A}_6\beta - \mathcal{A}_{14}\psi\right) + \mathcal{A}_{15}\dot{\psi} + 2\mathcal{A}_{20}\varphi\,, \tag{7.78}$$

$$0 = 2\frac{k^2}{a^2}\mathcal{A}_1 b - \mathcal{A}_2\varphi - \mathcal{A}_3\dot{\psi}\,, \tag{7.79}$$

$$0 = \mathcal{A}_6\varphi + \mathcal{A}_{10}\psi + \mathcal{A}_{11}\dot{\psi} + \frac{1}{a}\frac{\mathrm{d}}{\mathrm{d}t}\left(a\mathcal{A}_{11}\right)\psi \tag{7.80}$$

and substituted back into the Lagrangian to retrieve

$$\mathcal{L}^{\text{Unitary}}_{f(T)} = 2\frac{\dot{H}}{H^2}\left(f_T + 12H^2 f_{TT}\right)\left[\dot{\psi}^2 - \frac{k^2}{a^2}\psi^2\right] + \mathcal{O}(k^0)\,, \tag{7.81}$$

where ψ is the only scalar dynamical mode. Note, the leading order of k is listed in Eq. (7.81) and $\dot{\psi}^2 \propto \omega^2\psi^2 \propto k^2\psi^2$. The ghost and Laplacian conditions boil down to $2\frac{\dot{H}}{H^2}(f_T + 12H^2 f_{TT}) > 0$, implying that the numerator needs to be positive since $H^2 > 0$. In the TEGR limit, $f(T) = -T$, and the condition becomes $2\frac{\dot{H}}{H^2} > 0$. Since the analysis is being performed in high-k limit, the system is within the matter-dominated era where $a \propto t^{\frac{2}{3}}$ such that $\dot{H} = -\frac{3}{2}H^2$. This implies that the condition $-3 \not> 0$, and the scalar mode ψ does not propagate. Hence, the TEGR result corresponds to the GR solutions evaluated in Sec. 7.3.1.

The pseudoscalar sector is trivial but the vector realm with the gauge choice of σ_i of Eq. (7.17) is given by

$$\begin{aligned}\mathcal{L}^{\sigma_i=0}_{\text{V},f(T)} = \frac{k^2}{a^2}\mathcal{C}_9\Bigg(&-\frac{1}{2}b_i\,b^i - 2a^2\dot{h}^i\left(\dot{h}_i - \frac{1}{a}\,b_i\right) - \frac{1}{2}\beta_i\,\beta^i + b_i\,\beta^i \\ &+ \left(4a - \frac{1}{a\mathcal{C}_9}\frac{\mathrm{d}}{\mathrm{d}t}\left(\frac{a^2}{2}\mathcal{C}_9\right)\right)\beta_i\,h^i - \frac{a}{2}\beta_i\,\dot{h}^i\Bigg)\,,\end{aligned} \tag{7.82}$$

where $\{\mathcal{C}_2, \mathcal{C}_5, \mathcal{C}_6\}$ are removed as they are zero for the theory, other coefficients were reduced in terms of $\mathcal{C}_9 = f_T$, and additional integration by parts is performed to obtained only h_i as the dynamical mode. Upon variation with respect to b and β

$$0 = -b_i + 2\dot{h}_i + \beta_i\,, \tag{7.83}$$

$$0 = b_i - \frac{a}{2}\dot{h}_i + 4ah_i - \beta_i - \frac{1}{a\mathcal{C}_9}\frac{\mathrm{d}}{\mathrm{d}t}\left(\frac{a^2}{2}\mathcal{C}_9\right)h_i\,, \tag{7.84}$$

which ultimately results in a trivial solution and no vector modes propagate. As for the tensor modes, Eq. (7.31) remains the same but $\mathcal{D}_1 = \mathcal{D}_2 = -f_T$, ensuring that tensor modes still propagate.

These results correspond to those obtained in Ref. [274], albeit the longitudinal gauge is used an additional assumption of $\beta = 0$ is added in the scalar sector. While the number of dynamical modes is not altered because β is non-dynamical, the result obtained in Eq. (7.81) would look different because now $\{\mathcal{A}_2, \mathcal{A}_3, \mathcal{A}_6, \mathcal{A}_{10}, \mathcal{A}_{21}, \mathcal{A}_{14}, \mathcal{A}_{11}\}$ would also not contribute. An overfixing situation has also been identified in Refs [218, 378, 379, 380]. Compared to the propagating DoFs analysis summarised in Table 5.1 in Minkowski background, $f(T)$ gravity falls under Case 7 where in the massive sector only one scalar mode propagates and in the massless sector has the tensor modes propagating.

7.3.4 | $f(\phi, T)$ Gravity

The interest in non-minimally coupled scalar-tensor theories such as $f(\phi, T)$ lies in its richer phenomenology, where the scalar field drives late time acceleration and has direct coupling with matter. $f(\phi, T)$ action can be obtained through the unitary gauge of Eq. (7.5) and additionally setting $\{\mathcal{A}_7, \mathcal{A}_{12}, \mathcal{A}_{13}\}$ to zero. The action and the variations with respect to non-dynamical terms are similar in form as those in the $f(T)$ case given by Eqs (7.77-7.80) with coefficients being slightly different, yielding to the Lagrangian

$$\mathcal{L}^{\text{Unitary}}_{\text{S},f(\phi,T)} = 2\frac{\dot{H}}{H^2}\left(f_T + 12H^2 f_{TT} + \frac{H}{\dot{H}}\dot{\phi} f_{\phi T}\right)\left[\dot{\psi}^2 - \frac{k^2}{a^2}\psi^2\right], \tag{7.85}$$

such that the stability conditions are dictated by the inequality $\dot{H}\left(f_T + 12H^2 f_{TT} + \frac{H}{\dot{H}}\dot{\phi} f_{\phi T}\right) > 0$. The results for the remaining sectors are identical to the $f(T)$ subclass evaluated in Sec. 7.3.3: pseudoscalar and vector modes do not propagate, and tensor modes propagate with a dependency on T only.

7.4 | Summary

The final area tackled in this work within BDLS theory is to determine the pathological branches within the gravitational theory. In the realm of vacuum, where matter is excluded, Ostrogradsky ghosts and Laplacian/gradient instabilities may arise [381]. While caution is taken in the construction of BDLS to avoid Ostrogradsky ghosts by ensuring that the theory does not result in higher order derivatives [78], further restrictions can be obtained through the analysis of the second order perturbation of the action. Additionally, to aid the study performed in Chapter 6, it is crucial to work with models that do not lead to Laplacian instabilities, as these would result in unphysical and non-viable rapid growths.

The perturbations introduced in Chapter 4 are used to extend the BDLS action (2.98) up to second order perturbations to result in Eq. (7.1). Performance of SVT decomposition allows the calculations to be broken down into sectors that do not interact with each other. These sectors are dictated by the behaviour of the gauge transformations listed in Eq. (4.42). Apart from the scalar-vector-tensor decomposition, the pseudoscalar also separates from the rest of the scalars as it is classified to be gauge-invariant. The same cannot be said for the pseudovector mode, which is a linear combination of other vector modes. For each sector, the action obtained is transformed in terms of the gauge-invariant quantities summarised in Eq. (4.45), whenever required. Integration by parts was performed throughout to yield the simplest form of the action. The auxiliary modes, referring to the non-dynamical terms in the action, are removed by first varying with respect to

the auxiliary quantity and substituting back the solution obtained. At this point, it is oftentimes more helpful to work within the spatial Fourier transformation. Especially in the scalar sector, it was noted that k dependencies appear in both the numerator and denominator along with a linear combination with terms that are not associated with derivatives. In cases where the kinetic portion of the action does not form a diagonal matrix, the diagonalisation process is performed. Despite dealing with symmetric matrices, the diagonalisation through orthogonal matrices yielded complicated systems. For this reason, a different approach was presented in this chapter, opting to introduce a transformation through a redefinition of gauge-invariant modes, as done in the scalar sector by Eq. (7.41). Expanding the action to obtain the high-k limit and selecting the leading order contributors of k, allows one to determine the constraints where ghost, Laplacian, and speed conditions are obtained.

Two scalar modes are noted to be propagating in Eq. (7.8) which upon diagonalisation and application of the high-k limit can attain the ghost stability constraint given in Eq. (7.48) and speed constraint Eq. (7.47) by imposing the condition (7.46) to ensure that the wave equations of modes Ψ_1 and Ψ_2 can decouple and propagate separately. The initial action obtained for the pseudoscalar, given by Eq. (7.14), did not require any further modifications. The ghost (7.50) and speed squared (7.52) stability conditions could easily be retrieved from the action since only kinetic and coefficients of k^2 are contributing. Additionally, since only one mode is present, no issues related to mode mixing occur. Constraints related to the pseudoscalar are dependent on the behaviour of the teleparallel sector, specifically invariant quantities constructed from the tetrad-scalar coupling. For the vector sector, a unique scenario is obtained. Typically, the vector sector is eliminated from the analysis as vector modes do not propagate. Due to the large number of invariants included within BDLS, two propagating gauge-invariant DoFs are attained for the full theory, as seen in Eq. (7.20). Ghost and Laplacian conditions are listed in Eq. (7.53) and Eq. (7.57), respectively. Then, the tensor modes were evaluated. Action (7.31) is slightly altered from the standard Horndeski result with the inclusion of additional teleparallel terms in the kinetic and Laplacian terms. Although the changes are minute, such a result has been able to reconsider previous Horndeski models which were eliminated due to the observation of GW170817 [80, 81]. This is because the excess speed in Eq. (7.62) allows for models which contain $G_{4,X}$ and G_5, as their behaviour can be balanced by teleparallel contributions without altering the graviton speed.

The convenience of setting up a general approach to a theory such as BDLS, without assuming a gauge choice, provides the structure to obtain the results of a large number of subclasses with the convention preferred. This is illustrated in Sec. 7.3 where the cases of GR, Horndeski gravity, $f(T)$, and $f(\phi, T)$ are evaluated through the results presented in Sec. 7.1. The theories were chosen due to the frequency with which they have been investigated, as well as their ability to draw a direct comparison with the outcomes presented in this chapter. This chapter not

only illustrates the intricacy that BDLS can reproduce, with several subclasses that have yet to be explored in further detail, but also provides restrictions to produce healthy branches of the theory.

8

Conclusion

This work explores the richness of the teleparallel analogue of Horndeski gravity, as the most general second-order theory of gravity under the torsionful formalism. This was done by introducing the construction of the theory, exploring its ability to revive previously discarded Horndeski models, tackling the CC problem, replicating the observed growth of structures, and deriving the necessary constraints applicable across all theories falling within the BDLS formalism. Throughout this work, the importance of presenting such a generalised formalism has been emphasised as it provides an avenue to facilitate theoretical calculations.

Chapter 1 introduced the topics tackled throughout this work and their motivation. Chapter 2 set up the assembly and technical details of BDLS. GR, which led to a paradigm shift in how to tackle problems in cosmology, by having geometric distortions in spacetime influencing the matter in the Universe. Given its success and passing the many classical and modern tests, it is difficult for researchers to consider a complete overhaul in the formalism to study gravity. For this reason, modified theories of gravity have become a natural alternative. One such approach is that of Horndeski gravity. While still relying on the curvature-based formalism and introducing an additional scalar field along with the metric tensors allows for relaxing Lovelock's theorem [74]. In recent years, Horndeski gravity has regained interest, especially in light of improved observational data, as it can encompass and explore multiple classes within it, such as Brans-Dicke [61], GBD [175], KGB [179], k-inflation [184], scalar-tensor form of $f(\mathring{R})$ [222] and GR, among others. The observation of GW170817 [80] and electromagnetic counterpart GRB170817A [81] have brought into question several subclasses of Horndeski gravity [83, 84]. The change in the geometric foundation, treating spacetime as torsionful rather than curvatureful, can replicate Horndeski gravity with additional terms arising from the fundamental dynamical object of the tetrad and its mixing with the scalar field. The teleparallel analog of Horndeski given by the action in Eq. (2.98) has been shown to revive the Horndeski model solely by considering the additional teleparallel term. Moreover, BDLS gravity can explore other well-studied subcases within the

teleparallel formalism such as $f(T)$ [69], $f(\phi, T)$ [298], NGR [70].

The previously disregarded Horndeski models had ruled out many models that could act as well-tempering models to screen out the vacuum energy, in an attempt to tackle the CC problem. Chapter 3 explored several models falling under the BDLS umbrella, in particular with a focus on the teleparallel sector, to construct viable well-tempering models. The methodology of well-tempering [44], inspired by self-tuning, allows breaking of Weinberg's no-go theorem [43] by imposing that the model has a dynamical scalar field, allowing a dynamical screening of the vacuum energy to account for the discrepancy between theoretical and observational CC value. What sets well-tempering out from self-tuning, is the ability to screen solely the vacuum energy while retaining radiation and matter epochs. By expressing the Hubble and scalar equations in the form given by Eqs (3.30-3.31), four functions are utilised to build the degeneracy equation (3.38) and consistency conditions (3.39), which need to be satisfied. Finally, provided the first Friedmann equation contains both the vacuum energy density and other time-dependent terms, then the model is classified as a viable well-tempering model. In this work, 6 models have been explored: 1) purely teleparallel arising from tetrad contribution in Sec. 3.2.1, 2) purely teleparallel sector with both tetrad and scalar field contributions in Sec. 3.2.2, 3) teleparallel function with scalar dependent quartic Horndeski function in Sec. 3.2.3, 4) teleparallel function with a quartic Horndeski function which had been eliminated within the standard Horndeski model in Sec. 3.2.4, 5) model containing all BDLS Lagrangians apart from the quintic in Sec. 3.2.5, and 6) explores a case without ϕ contribution in Sec. 3.2.6. Case 1 and Case 6 show models which do not well-temper, corresponding to models which do not contain a function of ϕ. The remaining models, all containing ϕ, provide a viable well-tempering model. Despite being able to well-temper, it does not necessarily imply that the model can attain the dynamics of a viable cosmology. With a focus on Case 5, chosen due to its consideration of several functions, the dynamical stability **was** investigated in Sec. 3.3. The main conclusion from these phase diagrams indicates that the systems are independent of the magnitude of the vacuum energy ρ_Λ and there is a link[1] between contribution from the teleparallel sector and the quartic function that is dependent on X. This further points towards the significance of the teleparallel sector whenever Horndeski models are revived. Finally, the behaviour of this model is evaluated during the matter-dominated era and while undergoing a phase transition, to ensure that the scalar field continues to propagate with time (Fig. 3.3b) and is not affected by phase transition (Fig. 3.5b), matter and dark energy density parameters add up to unity, and disturbances in the Hubble function only occurs during phase transition (Figs 3.3c-3.3d).

Given that at the background level BDLS has already been shown to produce a plethora of viable cosmologies, BDLS is extended to the perturbative level. Chapter 4 fleshed out per-

[1] In the particular model considered in Eq. (3.97) indicates a linear relationship

turbations up to second order for all components of BDLS. While background field equations are obtained in Sec. 3.1, the methodology restricts the possibility of obtaining the linearised field equations. An alternative method was presented in Sec. 4.2 by considering performing Euler-Lagrangian with respect to a generic tetrad and scalar field, under the assumption of the Weitzenböck gauge. This provides the equations of motion which can be perturbed to obtain linearised field equations for scalar, vector, and tensor modes upon applying an SVT decomposition. The SVT perturbations are applied without imposing a particular gauge choice. This is done to allow for any gauge choice to be obtained by taking appropriate limits. Additionally, the field equations are expressed in terms of gauge-invariant quantities.

With this system of equations, Chapter 5 uses the SVT decomposition of the field equations to obtain the propagating DoFs. This is done by deconstructing the field equations into a block matrix 5.16. The determinant of the block matrix corresponds to the principal polynomial equation, representing the propagating waves when set to vanish. Additionally, the determinant establishes a list of subcases within BDLS. The nullspace solutions are attained for the massless and massive sectors, whenever relevant, to determine which GW propagates. As summarised in Table 5.1, scenarios where both $\tilde{c}1 \neq 0$ (5.19a) and $\tilde{c}2 \neq 0$ (5.19b) hold always realise a massless and a massive sector. The other cases realise solely a massless cases unless further subcases are considered, as realised in Case 2.I.a and Case 4.I.a where $\tilde{c}_1 = \tilde{c}_2 = 0$, $\tilde{c}_3 \neq 0$ (5.49) and $\tilde{c}_4 \neq 0$ (5.50). The maximum number of propagating DoFs is 7 and the minimum is 2. While the modes may propagate, it does not necessarily provide the polarisation modes of GWs. For each subcase, the electric components of the Riemann tensor are evaluated to determine the polarisation mode and its nature: whether they are breathing, longitudinal, x-, y−, + and × modes. As summarised in Table. 5.2, all the massless scenarios give both + and × tensor modes, as expected, by imposing that $G_4 - G_{\text{Tele}} \neq 0$. Some cases give an additional breathing mode in the massless sector and give a total of 3 polarisation modes, but across all cases there are no vector polarisation modes. The branches explored can replicate the results of other theories of gravity such as GR through Case 8, Horndeski gravity in Case 7, NGR in Case 2.I.b, among others listed in Table. 5.3.

Chapter 6 investigated the behaviour of matter perturbation, with a focus on CDM as it dominates the matter-dominated epoch. This stage of the Universe dictates the growth of structures as matter accumulates, responsible for the formations observed today. In this work, the procedure for obtaining gravitational perturbations in terms of matter perturbations was outlined by using the linearised field equations and conservation of energy-momentum tensor is presented (6.23) without assuming the subhorizon limit. These expressions yield the Mészáros equation (6.43) with spatial dependencies still present. While typically k dependencies are eliminated through the assumption of $k \gg aH$ while deriving the Mészáros equation, theories such as $f(\mathring{R})$ gravity have been shown to result in inconsistencies [330, 222, 331]. Thus, for the the-

ories of $f(T)$ and $f(\phi, T)$, the significance of k-dependencies are explored through the growth parameters of the growth factor, growth index, $f\sigma_8$, and S_8. In the case of $f(T)$ in Sec. 6.4.1, the five models of Power Law (6.78), Linder (6.81), Exponential (6.84), Logarithmic (6.87) and Hyperbolic-Tangent (6.95), have shown that there are no discrepancies between k values within matter dominated scales and the subhorzion limit. But, as soon as a scalar field is introduced, discrepancies do arise. Sec. 6.4.2 investigates a particular subcase of $f(\phi, T)$, mimicking a modified GR model, with a quadratic (6.112), quartic (6.117) and exponential (6.123) scalar potentials, highly influenced by the initial conditions of ϕ and its derivative ϕ'.

Given the increase in possible viable cosmologies due to the vastness of BDLS theory, it becomes crucial to obtain the necessary constraints to narrow down and eliminate pathological branches. This is done by the expressions which result in ghost and Laplacian instabilities. The BDLS action is extended up to second order perturbation (7.1), and imposing that the kinetic and gradient terms of the theory are positive definite. If this is not the case, this would result in a theory that can produce negative energy and small perturbations result in rampant and unrealistic growths [381]. In this work, the constraints are explored separately for the scalar, pseudoscalar, vector, and tensor sectors in Sec. 7.2. Opting to express the action in terms of gauge-invariant quantities is appealing due to the easy adaptability of the system to adjust it to any gauge choice, especially given that theoretical and data analysis works tend to adopt different gauge conventions. Both the scalar and vector sectors give a maximum of two propagating DoFs, and an additional propagating mode for the pseudoscalar and tensor sectors, each. In comparison with the standard Horndeski gravity, additional scalar, pseudoscalar, and vector conditions are realised. While the pseudoscalar action (7.14) is dictated by purely teleparallel terms, the vector sector (7.22) does contain standard Horndeski terms which cancel out if teleparallel terms are removed. The tensor modes are always realised, as observed in Chapter 5. Subclasses of GR, Horndeski, $f(T)$ and $f(\phi, T)$ are also analysed in Sec. 7.3 to further drive the point that BDLS facilitates this analysis.

Chapters 3-7 provide a study of BDLS and its subclasses, tackling different issues within cosmology. From a theoretical point of view, BDLS allows obtaining a generalised formalism and constraints for a large number of subclasses of MTG theories. This provides easy access to different limits to carry out data analysis and comparison with observations. Due to the novelty of BDLS, these projects encompass some of the initial work done in BDLS. The following lists some of the future works to enhance the theoretical knowledge of BDLS.

Growth across Superhorizon and Subhorzion Scales: Chapter 6 explored the Mészáros equation and its solution within the epoch where subhorizon limit applies, with the assumption that CDM matter dominates and all matter contributions are boiled down to dust. As previously mentioned, the analysis disregards the minute contributions of post-decoupling baryons and mas-

sive neutrinos. It would be of interest to include these contributions within the subhorizon limit but alternatively, a full Boltzmann equation analysis spanning the superhorizon and subhorizon ranges. The Boltzmann equation governs the behaviour of matter and radiation through the statistical distribution of a collection of particles classified with common properties, taking into account collisions and interactions between particles, and accounting for the changes arising due to phase transitions such as the different treatment of neutrinos during the radiation and matter eras [88, 271]. In conjunction with gravitational contributions offered by Einstein equation, the complexity of these equations quickly arises, flagging the need of an Einstein-Boltzmann solver to provide a model-independent approach to gravitational theories through the evolution of cosmological perturbations in light of high precision surveys [2, 94, 345, 8, 106, 91, 95]. This led to the development of the publicly available Code for Anisotropies in the Microwave Background (CAMB) [382, 383]. Implementation of modified theories of gravity allows the testing of gravity on cosmological scales as done in the context of effective field theories [384]. Application of these modifications would require an array of theoretical considerations to be investigated: background equations, cosmological perturbations, gravitation and matter interactions, ghost, Laplacian, and tachyonic stabilities, among others.

Tachyonic Instabilities: In Chapter 7 only ghost and Laplacian instabilities were investigated. Due to the analysis being performed within a vacuum, these stability constraints sufficed. The introduction of matter fields gives a scenario where matter and scalar field mix, hence the mass of eigenvalues of the Hamiltonian of canonical fields could give rise to tachyonic instabilities [381]. Such cases imply that there is a tachyon particle that can move with a speed faster than light and its mass squared term is negative, resulting in rapid changes in the Universe's large structures [385]. A particular subcase of tachyonic instabilities is Jeans' instability, related to star formation. Interstellar gas clouds that experience gravitational collapse result in star formation [386]. Jeans studied the stability of self-gravitating bodies of homogeneous and spherical density within Newtonian formalism. His work resulted in a dependency on the mass and radius of the clouds, as functions of temperature and density [387]. Lifshitz adapted this work with the GR formalism [388] and took into account that inhomogeneities result in the growth of structures. This has also been adapted with modified theories of gravity, such as $f(\mathring{R})$ to investigate hydrostatic equilibrium [167]. This work would require the inclusion of the matter action, adopting the Schutz-Sorkin [389] to represent relativistic perfect fluids such that the equations of motion and the energy-momentum tensor can be retrieved from the action itself. The action perturbation would need to be calculated up to second order to obtain the form given by Eq. (7.32) to investigate the canonical mass of the propagating DoFs. This is done by normalising the fields and diagonalising the matrix associated with non-derivative terms i.e. coefficient of $\Psi_i\Psi_j$, where $\{\Psi_i, \Psi_i\}$ are perturbation modes. The inclusion of this extension to

the analysis performed in Chapter 7 provides a fuller stability analysis.

Vainshtein Screening: At the solar system level, local gravity tests are in agreement with GR [123]. Thus, scalar-tensor theories with propagating scalar field coupled with baryons should be limited at this scale. The Vainshtein mechanism suppresses the propagation of such modes when dealing with short distances [390]. The methodology was originally constructed because the quadratic Friez-Pauli theory suffers from the van DAM-Veltman-Zakharov (vDVZ) discontinuity [390]. The Friez-Pauli theory was constructed as a massive gravity theory to modify GR by implementing a graviton with mass that is nonzero wherein GWs would propagate with a non-relativistic speed. As mass $m \to 0$, GR is not recovered, dubbed as the vDVZ discontinuity [391, 392]. Vainshtein showed that within the limit of the Vainshtein radius, r_{V}, the linear regime is broken and the theory behaves as nonlinear, implying that at these small scales, nonlinear scalar modes contribute and recover GR. The mechanism has been adopted within scalar-tensor theories, initially applied in DGP [355], to recover GR at solar-system scales [393]. The work has been extended to Horndeski gravity [394, 395, 396]. Applying such a mechanism to BDLS ensures the subclasses of the gravitational model can recover GR and hold at the solar system level. This would require the inclusion of the matter action, again adopting the Schutz-Sorkin action [389] and taking the quasi-static approximation of the second-order perturbed action. While within large distances the linear regime can be recovered, the nonlinear regime is also obtained to implement the Vainshtein screening mechanism.

Multi-Scalar Field Theories: In both Horndeski gravity [66] and BDLS theory [78], weakening of Lovelock's theorem occurs through the introduction of a single scalar field in addition to the respective fundamental dynamical objects. This does not restrict the possibility of considering multiple scalar fields. The concept of double scalar field theories has cropped up to account for the initial inflation and late-time accelerated expansion that the Universe experiences. This is done by assigning one scalar field to behave as the inflaton [76] which dictates the initial inflationary epoch resulting from a period of rapid exponential expansion [76], while the other scalar is attributed to dark energy and drives the accelerated expansion of the Universe [153]. By dealing with separate scalar fields, it is possible to represent the different behaviours, provide distinct constraints on them, and explain their evolution as one scalar field is initially prominent, dies down and another scalar dominates at late times. Not necessarily independent of each other, the scalar fields could result in a coupling term. Construction of double scalar field Horndeski theory can be expressed as a linear combination of standard Horndeski theory per scalar field, and an additional term taking into account the interaction between the two fields, ensuring that the theory does not result in higher order derivatives.

In conclusion, this dissertation provides insight into the BDLS theory on the background and perturbative level, providing constraints for different viable cosmological models stemming from theoretical foundations and observational data. This research provides a critical step to understanding second-order theories within MTG and opens up doors to tackle cosmological issues through the lens of modified theories of gravity. Through continued investigation, such as those proposed previously, it becomes possible to compare with observational data as higher precision data from new surveys becomes available.

A

SVT Decomposition of Linearised Field Equations

The equations of motion given by the variation with respect to the tetrad (4.22a-4.22e) and to the scalar field (4.24a-4.24e) gives the general result for the fundamental dynamical objects for the Weitzenböck gauge (2.59). The SVT decomposition gives a system of equations for the scalar, vector, and tensor sector in terms of the quantities listed in Eq. (4.2) and Eq. (4.3). The gauge transformations given by Eq. (4.40-4.41) result in Eq. (4.42), verifying that the scalar, vector, and tensor sectors decouple from each other, and thus can be treated separately. The same can be said for the pseudoscalar. Due to the complexity of the field equations, they have not been written down explicitly, but rather listed as functions of gravitational perturbations: Eq. (4.29), Eq. (4.35), and Eq. (4.37). Snippets of the results obtained in `Mathematica` have been compiled here. It should be noted that only one component for each field equation is considered to illustrate the form of the result: $W_{0i} = W_{0x}$, $W_{0i} = W_{x0}$, and $W_{ij} = W_{yz}$. In general, all components would need to be considered. Prime ($'$) denotes time derivatives in the file.

In Chapter 5, BDLS field equations are on a Minkowski background and for a constant background scalar field. The results presented would require setting $\phi' = \phi'' = X = H = H' = 0$. In Chapter 6 the subcases of $f(T)$ and Modified GR are used. $f(T)$ limit can be obtained if $G_2 = G_3 = G_4 = G_5 = 0$ and $G_{\text{Tele}} = f(T)$. Modified GR can be obtained for $G_3 = G_5 = G_{\text{Tele}} = 0$, $G_2 = V(\phi) + P(\phi)X$ and $G_4 = 1$. Alternatively, Modified GR can be obtained through the teleparallel formalism by setting $G_2 = G_3 = G_4 = G_50$ and $G_{\text{Tele}} = -T + V(\phi) + P(\phi)X$. As for the standard Horndeski limit, the equations are obtained when $G_{\text{Tele}} = 0$, corresponding to those given in Ref. [112].

B

Fourier Transformation of a Perturbed Action

To obtain ghost and Laplacian instabilities, the actions are extended up to second-order perturbations. Following the complexity of the field equations in BDLS in Sec. 4.3, it is expected that the additional terms in BDLS would result in a more elaborate perturbed action in comparison with Horndeski. This is further confirmed in the GW analysis of Chapter 5, where a Minkowski background yields a total of 7 propagating DoFs. In preparation for Chapter 7, it would be ideal to introduce the Fourier transformation notation. While actions can be expressed in terms of spatial and temporal derivatives, the analysis would be simplified by employing spatial Fourier transformation while keeping time derivatives.

For the signature $(-,+,+,+)$, the complex exponential function is $e^{i\omega t - ik_j x^j}$ where k is the covector associated with the spatial component and ω is the angular frequency. A variable $X(t,x,y,z)$ can be expressed as a combination of two parts:

$$X(t,x^j) = \int \frac{d^3k}{(2\pi)^{3/2}} \left[X(t,k) e^{-ik_j x^j} + X^\dagger(t,k) e^{ik_j x^j} \right] , \tag{B.1}$$

where † denotes a Hermitian conjugate of the function.

Tensor perturbations h_{ij} are traceless, divergenceless, and symmetric. These conditions extend to transformation as follows:

$$k_j h^{ij} = 0 \,, \qquad k_j h^{\dagger\, ij} = 0 \,, \tag{B.2}$$

$$h_i{}^i = 0 \,, \qquad h^\dagger{}_i{}^i = 0 \,, \tag{B.3}$$

$$h_{ij} = h_{ji} \,, \qquad h^\dagger_{ij} = h^\dagger_{ji} \,. \tag{B.4}$$

Similarly, the divergenceless condition in a vector, say β_i, applies as

$$k_j \beta^j = 0 \,, \qquad k_j \beta^{\dagger\, j} = 0 \,. \tag{B.5}$$

As explained in Sec. 4.3.1, these properties account for shear-like deformations for the vector sector and shear deformation for the tensor sector. Hence, the sectors tackle separate issues to ensure that the tetrad does not result in unwanted behaviours and there is no overlapping between them.

Perturbations up to second-order yield actions with coupled variables, resulting in transformation containing two different k covectors. Consider functions $f(t, x^j)$ and $g(t, x^j)$ with covectors k and k', respectively. Multiplication of the two functions is given by

$$\begin{aligned} f(t,x^j)\, g(t,x'^j) &= \left(\int \frac{d^3k}{(2\pi)^{3/2}} \left[f(t,k) e^{-ik_j x^j} + f^\dagger(t,k) e^{ik_j x^j} \right] \right) \\ &\times \left(\int \frac{d^3k'}{(2\pi)^{3/2}} \left[g(t,k') e^{-ik'_j x^j} + g^\dagger(t,k') e^{ik'_j x^j} \right] \right) \\ &= \int \frac{d^3k}{(2\pi)^{3/2}} \int \frac{d^3k'}{(2\pi)^{3/2}} \Big[f\, g\, e^{-i(k_j+k'_j)x^j} + f\, g^\dagger\, e^{-i(k_j-k'_j)x^j} + f^\dagger\, g\, e^{i(k_j-k'_j)x^j} \\ &\quad + f^\dagger\, g^\dagger\, e^{i(k_j+k'_j)x^j} \Big] \,. \end{aligned} \tag{B.6}$$

Upon including an integration of these functions, the expression is altered. Before continuing with this derivation, it is important to introduce the notation for the Dirac delta function $\delta(x^\mu)$ where

$$\delta(x^\mu) = \Pi_{\mu=1}^3 \delta(x^\mu) = \delta(x^1)\delta(x^2)\delta(x^3)\,, \tag{B.7}$$

with the property of normalisation

$$\int_{\mathbb{R}^3} \mathrm{d}^3x\, \delta(x^\mu) = 1\,, \tag{B.8}$$

and symmetry

$$\delta(x^\mu) = \delta(-x^\mu) \tag{B.9}$$

When considering the condition of equality between two 3-vectors in Fourier space the expression becomes

$$\delta(x^\mu - x'^\mu) = \frac{1}{(2\pi)^{\frac{3}{2}}} \int_{\mathbb{R}^3} d^3k\, e^{i(x^\mu - x'^\mu)k_\mu}\,. \tag{B.10}$$

Applying the spatial integral to Eq. (B.6) and using Eq. (B.10), the action becomes

$$\int \mathrm{d}^3x \int \frac{d^3k}{(2\pi)^{3/2}} \int \frac{d^3k'}{(2\pi)^{3/2}} f(t,k_j)\, g(t,k'_j)\, e^{i(k_j+k'_j)x^j}$$
$$= \int \frac{d^3k}{(2\pi)^{3/2}} \int \frac{d^3k'}{(2\pi)^{3/2}} (2\pi)^{\frac{3}{2}} \delta(k_j+k'_j)\, f(t,k_j)\, g(t,k'_j) = \int \frac{d^3k}{(2\pi)^{3/2}} f(t,k_j)\, g(t,-k_j)\,, \quad \text{(B.11)}$$
$$\int \mathrm{d}^3x \int \frac{d^3k}{(2\pi)^{3/2}} \int \frac{d^3k'}{(2\pi)^{3/2}} f(t,k_j)\, g(t,k'_j)\, e^{i(k_j-k'_j)x^j}$$
$$= \int \frac{d^3k}{(2\pi)^{3/2}} \int \frac{d^3k'}{(2\pi)^{3/2}} (2\pi)^{\frac{3}{2}} \delta(k_j-k'_j)\, f(t,k_j)\, g(t,k'_j) = \int \frac{d^3k}{(2\pi)^{3/2}} f(t,k_j)\, g(t,k_j)\,. \quad \text{(B.12)}$$

Hence, Eq. (6.117) simplifies to

$$\int \mathrm{d}t\, \mathrm{d}^3x\, f(t,x^j)\, g(t,x^j) = \int \mathrm{d}t \frac{d^3k}{(2\pi)^{3/2}} \left[f\, g + f\, g^\dagger + f^\dagger\, g \, + f^\dagger\, g^\dagger \right]. \quad \text{(B.13)}$$

For the analysis in Sec. 7.2, it suffices to not include the Hermitian conjugate portion of the integral. Additionally, the following identities are used:

$$\int \mathrm{d}t\, \mathrm{d}^3x \partial_i f(t,x^j)\, \partial^i g(t,x'^j)$$
$$= \int \mathrm{d}t \frac{d^3k}{(2\pi)^{3/2}} \frac{d^3k'}{(2\pi)^{3/2}} (2\pi)^{\frac{3}{2}} \delta(k_j+k'_j) \left[-ik_i f(t,k_j)\right] \left[-ik'^i g(t,k'_j)\right]$$
$$= \int \mathrm{d}t \frac{d^3k}{(2\pi)^{3/2}} k_i k^i\, f\, g = \int \mathrm{d}t \frac{d^3k}{(2\pi)^{3/2}} k^2\, f\, g\,, \quad \text{(B.14)}$$
$$\int \mathrm{d}t\, \mathrm{d}^3x \partial_i \partial^i f(t,x^j)\, g(t,x'^j)$$
$$= \int \mathrm{d}t \frac{d^3k}{(2\pi)^{3/2}} \frac{d^3k'}{(2\pi)^{3/2}} (2\pi)^{\frac{3}{2}} \delta(k_j+k'_j) \left[(-ik_i)(-ik^i) f(t,k_j)\right] g(t,k'_j)$$
$$= \int \mathrm{d}t \frac{d^3k}{(2\pi)^{3/2}} (-k_i k^i)\, f\, g = \int \mathrm{d}t \frac{d^3k}{(2\pi)^{3/2}} (-k^2)\, f\, g\,, \quad \text{(B.15)}$$
$$\int \mathrm{d}t\, \mathrm{d}^3x \partial_i \partial^i f(t,x^j)\, \partial_m \partial^m g(t,x'^j)$$
$$= \int \mathrm{d}t \frac{d^3k}{(2\pi)^{3/2}} \frac{d^3k'}{(2\pi)^{3/2}} (2\pi)^{\frac{3}{2}} \delta(k_j+k'_j) \left[(-ik_i)(-ik^i) f(t,k_j)\right] \left[(-ik'_i)(-ik'^i) g(t,k'_j)\right]$$
$$= \int \mathrm{d}t \frac{d^3k}{(2\pi)^{3/2}} (k_i k^i)^2\, f\, g = \int \mathrm{d}t \frac{d^3k}{(2\pi)^{3/2}} k^4\, f\, g\,. \quad \text{(B.16)}$$

Here, it is clear that the spatial Fourier transformation takes into account the spatial integration by parts from the sign difference between Eq. (B.14) and Eq. (B.15). Upon attaining the action in its desired form, an additional transformation can be applied to express time derivatives into

the temporal Fourier variable of ω. The next sections would show only first-order time derivatives appear, and as such would transform as

$$\dot{X} \to i\omega X\,, \qquad\qquad \dot{X}^2 \to -\omega^2 X^2\,. \tag{B.17}$$

In Chapter 7, only spatial Fourier transformations are applied since ghost instabilities are tied to time derivatives which yield the kinetic term.

C

Coefficients of Second Order Perturbations

The expansion of the BDLS action (2.98) up to second-order perturbations is required to determine the ghost and Laplacian instabilities. The results obtained in Chapter 7 contain a large number of terms, particularly in the scalar and vector sectors. The following sections list all the details of the coefficients for these sectors and should be used as a supplement to Chapter 7.

C.1 | Scalar Sector

The initial scalar perturbation yields an action given by Eq. (7.3) where coefficients $\mathcal{A}_i$ are given by

$$
\begin{aligned}
\mathcal{A}_1 &= a^2\big(- G_{\text{Tele},T_{\text{vec}}} + 2H^2\left(9G_{\text{Tele},T_{\text{vec}}T_{\text{vec}}} - 12G_{\text{Tele},TT_{\text{vec}}} + 4G_{\text{Tele},TT}\right) + 2H\dot{\phi}\left(-3G_{\text{Tele},T_{\text{vec}}I_2}\right.\\
&\quad \left.+2G_{\text{Tele},TI_2}\right) + \frac{X}{3}\left(4G_{\text{Tele},J_8} + G_{\text{Tele},J_5} + 3G_{\text{Tele},I_2I_2}\right)\big)\,,\\
\mathcal{A}_2 &= -a\Big[-12H^3\left(9G_{\text{Tele},T_{\text{vec}}T_{\text{vec}}} + 4(-3G_{\text{Tele},TT_{\text{vec}}} + G_{\text{Tele},TT})\right) + \dot{\phi}\left(2G_{4,\phi} - G_{\text{Tele},I_2}\right.\\
&\quad -2X\left(G_{3,X} - 2G_{4,\phi X} + G_{\text{Tele},XI_2}\right)) - H^2\dot{\phi}\left(-54G_{\text{Tele},T_{\text{vec}}I_2} + 36G_{\text{Tele},TI_2} + 10XG_{5,X}\right.\\
&\quad \left.+4X^2G_{5,XX}\right) + 2H\left(2G_4 + 3G_{\text{Tele},T_{\text{vec}}} - 2G_{\text{Tele},T} + 2X(-4G_{4,X} - 2G_{\text{Tele},XT} + 3\left(G_{5,\phi}\right.\right.\\
&\quad \left.\left.-G_{\text{Tele},I_2I_2} + G_{\text{Tele},XT_{\text{vec}}}\right)) + 4X^2(-2G_{4,XX} + G_{5,\phi X})\right)\Big]\,,\\
\mathcal{A}_3 &= a\left[4G_4 + 6G_{\text{Tele},T_{\text{vec}}} - 4G_{\text{Tele},T} - 12H^2\left(9G_{\text{Tele},T_{\text{vec}}T_{\text{vec}}} - 12G_{\text{Tele},T\,T_{\text{vec}}} + 4G_{\text{Tele},TT}\right)\right.\\
&\quad \left.+2X\left(-4G_{4,X} + 2G_{5,\phi} - 3G_{\text{Tele},I_2I_2}\right) - 2H\dot{\phi}\left(-18G_{\text{Tele},T_{\text{vec}}\,I_2} + 12G_{\text{Tele},T\,I_2} + 2XG_{5,X}\right)\right]\,,\\
\mathcal{A}_4 &= a\left[H\left(-2G_{4,\phi} + 6XG_{3,X} - 20XG_{4,\phi X} + 4XG_{5,\phi\phi} + 3G_{\text{Tele},I_2} + 6G_{\text{Tele},\phi T_{\text{vec}}} - 4G_{\text{Tele},\phi T}\right)\right.\\
&\quad +H^2\dot{\phi}\left(6G_{4,X} - 6G_{5,\phi} + 12XG_{4,XX} - 8XG_{5,\phi X}\right) + H^3\left(6XG_{5,X} + 4X^2G_{5,XX}\right)\\
&\quad \left.+\dot{\phi}\left(G_{2,X} - 2G_{3,\phi} + 2G_{4,\phi\phi} + G_{\text{Tele},X} - G_{\text{Tele},\phi I_2}\right)\right]\,,
\end{aligned}
$$

$$
\begin{aligned}
\mathcal{A}_5 &= -a\Big[-2G_{4,\phi} + G_{\mathrm{Tele},I_2} + 2X(G_{3,X} - 2G_{4,\phi X} + G_{\mathrm{Tele},XI_2}) + H\dot{\phi}(4G_{4,X} - 4G_{5,\phi} \\
&\quad + 3G_{\mathrm{Tele},I_2I_2} - 6G_{\mathrm{Tele},XT_{\mathrm{vec}}} + 4G_{\mathrm{Tele},XT} + 4X(2G_{4,XX} - G_{5,\phi X})) \\
&\quad + H^2(-18G_{\mathrm{Tele},T_{\mathrm{vec}}I_2} + 12G_{\mathrm{Tele},TI_2} + 6XG_{5,X} + 4X^2G_{5,XX})\Big] , \\
\mathcal{A}_6 &= a\left[\dot{\phi}\left(2G_{4,\phi} - G_{\mathrm{Tele},I_2} - 2X(G_{3,X} - 2G_{4,\phi X})\right) + 2H\left(2G_4 + 3G_{\mathrm{Tele},T_{\mathrm{vec}}} - 2G_{\mathrm{Tele},T}\right.\right. \\
&\quad \left.\left. +2X(-4G_{4,X} + 3G_{5,\phi}) + 4X^2(-2G_{4,XX} + G_{5,\phi X})\right) - 2X\dot{\phi}H^2\left(5G_{5,X} + 2XG_{5,XX}\right)\right] , \\
\mathcal{A}_7 &= -\frac{2}{9}a\left[9G_{\mathrm{Tele},T_{\mathrm{vec}}} + 2X\left(-2G_{\mathrm{Tele},J_8} - 5G_{\mathrm{Tele},J_5} + 3G_{\mathrm{Tele},J_3} + 2XG_{\mathrm{Tele},J_6}\right)\right] , \\
\mathcal{A}_8 &= -a\Big[2XH^3(3G_{5,X} + 2XG_{5,XX}) + H^2\dot{\phi}[6G_{4,X} - 6G_{5,\phi} - 2G_{\mathrm{Tele},J_3} + 6\dot{H}(3G_{\mathrm{Tele},T_{\mathrm{vec}}J_3} \\
&\quad - 2G_{\mathrm{Tele},TJ_3}) + 4X(3G_{4,XX} - 2G_{5,\phi X}) - 3\ddot{\phi}G_{\mathrm{Tele},I_2J_3}] + \dot{\phi}[G_{2,X} - 2G_{3,\phi} + 2G_{4,\phi\phi} \\
&\quad + G_{\mathrm{Tele},X} - G_{\mathrm{Tele},\phi I_2} - \dot{H}(G_{\mathrm{Tele},J_3} + 3G_{\mathrm{Tele},I_2I_2}) - \ddot{\phi}G_{\mathrm{Tele},XI_2}] + H[-2G_{4,\phi} + G_{\mathrm{Tele},I_2} \\
&\quad + 18\dot{H}G_{\mathrm{Tele},T_{\mathrm{vec}}I_2} - 12\dot{H}G_{\mathrm{Tele},TI_2} + 2X(3G_{3,X} - 10G_{4,\phi X} + 2G_{5,\phi\phi} - G_{\mathrm{Tele},\phi J_3} \\
&\quad - 3\dot{H}G_{\mathrm{Tele},I_2J_3}) - \ddot{\phi}(G_{\mathrm{Tele},J_3} + 3G_{\mathrm{Tele},I_2I_2} + 2XG_{\mathrm{Tele},XJ_3})]\Big] , \\
\mathcal{A}_9 &= a\Big[-2G_{4,\phi} + 2X\left(G_{3,X} + H^2\left(3G_{5,X} + 2XG_{5,XX}\right) - 2G_{4,\phi X}\right) + G_{\mathrm{Tele},I_2} + H\dot{\phi}\left(4(G_{4,X}\right. \\
&\quad \left. +2XG_{4,XX} - G_{5,\phi} - XG_{5,\phi X}) + G_{\mathrm{Tele},J_3}\right)\Big] , \\
\mathcal{A}_{10} &= -2a\left[H\left(-6G_{\mathrm{Tele},T_{\mathrm{vec}}} + 4G_{\mathrm{Tele},T}\right) + \dot{\phi}G_{\mathrm{Tele},I_2}\right] , \\
\mathcal{A}_{11} &= -\frac{2}{9}a\left[18\left(G_{\mathrm{Tele},T_{\mathrm{vec}}} - G_{\mathrm{Tele},T}\right) + X\left(4G_{\mathrm{Tele},J_8} + 10G_{\mathrm{Tele},J_5} + 3G_{\mathrm{Tele},J_3} - 4XG_{\mathrm{Tele},J_6}\right)\right] , \\
\mathcal{A}_{12} &= 4a\left[-G_4 + X\left(2G_{4,X} - G_{5,\phi} + H\dot{\phi}G_{5,X}\right)\right] , \\
\mathcal{A}_{13} &= \frac{1}{9}a^2\Big[2X\left(-2G_{\mathrm{Tele},J_8} + 2XG_{\mathrm{Tele},J_6} - 5G_{\mathrm{Tele},J_5} + 3G_{\mathrm{Tele},J_3}\right) + 9G_{\mathrm{Tele},T_{\mathrm{vec}}}\Big] , \\
\mathcal{A}_{14} &= \frac{2}{9}\Big[-18\left(G_4 - G_{\mathrm{Tele},T} + G_{\mathrm{Tele},T_{\mathrm{vec}}}\right) + X\left(36G_{4,X} - 3G_{\mathrm{Tele},J_3} - 2(9G_{5,\phi} + 2G_{\mathrm{Tele},J_8}\right. \\
&\quad \left. +5G_{\mathrm{Tele},J_5})\right) + 18\dot{\phi}XHG_{5,X} + 4X^2G_{\mathrm{Tele},J_6}\Big] , \\
\mathcal{A}_{15} &= -3\Big[12H^3\left(9G_{\mathrm{Tele},T_{\mathrm{vec}}T_{\mathrm{vec}}} + 4(-3G_{\mathrm{Tele},TT_{\mathrm{vec}}} + G_{\mathrm{Tele},TT})\right) + \dot{\phi}\left(-2G_{4,\phi} + G_{\mathrm{Tele},I_2}\right. \\
&\quad +2X(G_{3,X} - 2G_{4,\phi X} + G_{\mathrm{Tele},XI_2})) + H^2\dot{\phi}\left(-54G_{\mathrm{Tele},T_{\mathrm{vec}}I_2} + 36G_{\mathrm{Tele},TI_2} + 10XG_{5,X}\right. \\
&\quad \left.\left. +4X^2G_{5,XX}\right) + 2H\left(-2G_4 - 3G_{\mathrm{Tele},T_{\mathrm{vec}}} + 2G_{\mathrm{Tele},T} + 2X(4G_{4,X} + 2G_{\mathrm{Tele},XT}\right.\right. \\
&\quad \left.\left. -3(G_{5,\phi} - G_{\mathrm{Tele},I_2I_2} + G_{\mathrm{Tele},XT_{\mathrm{vec}}})) + 4X^2(2G_{4,XX} - G_{5,\phi X})\right)\Big] , \\
\mathcal{A}_{16} &= G_{2,\phi} + G_{\mathrm{Tele},\phi} + 6H^2\left(G_{4,\phi} + 3G_{\mathrm{Tele},\phi T_{\mathrm{vec}}} - 2G_{\mathrm{Tele},\phi T} + X\left(-4G_{4,\phi X} - 4XG_{4,\phi XX}\right.\right. \\
&\quad \left.\left. +3G_{5,\phi\phi} + 2XG_{5,\phi\phi X})\right) - 2X(G_{2,\phi X} - G_{3,\phi\phi} + G_{\mathrm{Tele},\phi X}) - 2XH^3\dot{\phi}\left(5G_{5,\phi X}\right.\right. \\
&\quad \left.\left. +2XG_{5,\phi XX}\right) - 6H\dot{\phi}\left(XG_{3,\phi X} - G_{4,\phi\phi} - 2XG_{4,\phi\phi X} + G_{\mathrm{Tele},\phi I_2}\right) ,
\end{aligned}
$$

$$
\begin{aligned}
\mathcal{A}_{17} &= -2G_{4,\phi} + 2X\left(G_{3,X} - 2G_{4,\phi X} + H^2(3G_{5,X} + 2XG_{5,XX})\right) + G_{\mathrm{Tele},I_2} + H\dot{\phi}\,(4G_{4,X} \\
&\quad +8XG_{4,XX} - 4(G_{5,\phi} + XG_{5,\phi X}) + G_{\mathrm{Tele},J_3})\ , \\
\mathcal{A}_{18} &= -2H^3[15XG_{5,X} + 4X^2(5G_{5,XX} + XG_{5,XXX}) - 27G_{\mathrm{Tele},T_{\mathrm{vec}}I_2} + 18G_{\mathrm{Tele},TI_2}] \\
&\quad - 3H[-2G_{4,\phi} + G_{\mathrm{Tele},I_2} + 2X(3G_{3,X} + 2XG_{3,XX} - 8G_{4,\phi X} - 4XG_{4,\phi XX} \\
&\quad + 3G_{\mathrm{Tele},XI_2})] - 6H^2\dot{\phi}[3G_{4,X} + X(12G_{4,XX} + 4XG_{4,XXX} - 7G_{5,\phi X} - 2XG_{5,\phi XX}) \\
&\quad - 3(G_{5,\phi} - G_{\mathrm{Tele},I_2I_2} + G_{\mathrm{Tele},XT_{\mathrm{vec}}}) + 2G_{\mathrm{Tele},XT}] - \dot{\phi}[G_{2,X} - 2G_{3,\phi} + G_{\mathrm{Tele},X} \\
&\quad + 2X(G_{2,XX} - G_{3,\phi X} + G_{\mathrm{Tele},XX})]\,, \\
\mathcal{A}_{19} &= \frac{1}{9}\left[2X(-2G_{\mathrm{Tele},J_8} + 2XG_{\mathrm{Tele},J_6} - 5G_{\mathrm{Tele},J_5} + 3G_{\mathrm{Tele},J_3}) + 9G_{\mathrm{Tele},T_{\mathrm{vec}}}\right]\,, \\
\mathcal{A}_{20} &= 18H^4(9G_{\mathrm{Tele},T_{\mathrm{vec}}T_{\mathrm{vec}}} - 12G_{\mathrm{Tele},TT_{\mathrm{vec}}} + 4G_{\mathrm{Tele},TT}) + 3H^2[-2G_4 - 3G_{\mathrm{Tele},T_{\mathrm{vec}}} \\
&\quad + 2G_{\mathrm{Tele},T} + 2X(7G_{4,X} + X(16G_{4,XX} + 4XG_{4,XXX} - 9G_{5,\phi X} - 2XG_{5,\phi XX}) \\
&\quad - 6(G_{5,\phi} - G_{\mathrm{Tele},I_2I_2} + G_{\mathrm{Tele},XT_{\mathrm{vec}}}) + 4G_{\mathrm{Tele},XT})] + X[G_{2,X} - 2G_{3,\phi} + G_{\mathrm{Tele},X} \\
&\quad + 2X(G_{2,XX} - G_{3,\phi X} + G_{\mathrm{Tele},XX})] + 3H\dot{\phi}[-2G_{4,\phi} + G_{\mathrm{Tele},I_2} + 2X(2G_{3,X} + XG_{3,XX} \\
&\quad - 5G_{4,\phi X} - 2XG_{4,\phi XX} + 2G_{\mathrm{Tele},XI_2})] + 2H^3\dot{\phi}[15XG_{5,X} + 13X^2G_{5,XX} + 2X^3G_{5,XXX} \\
&\quad - 54G_{\mathrm{Tele},T_{\mathrm{vec}}I_2} + 36G_{\mathrm{Tele},TI_2}]\,, \\
\mathcal{A}_{21} &= \frac{2}{9}\left[9(G_4 + 2G_{\mathrm{Tele},T_{\mathrm{vec}}} - G_{\mathrm{Tele},T}) + X(-9G_{5,\phi} - 2G_{\mathrm{Tele},J_8} + 2XG_{\mathrm{Tele},J_6} - 5G_{\mathrm{Tele},J_5} \right. \\
&\quad \left. - 6G_{\mathrm{Tele},J_3} - 9\ddot{\phi}G_{5,X})\right]\,, \\
\mathcal{A}_{22} &= -6G_4 + 12XG_{4,X} - 6XG_{5,\phi} + 9XG_{\mathrm{Tele},I_2I_2} - 9G_{\mathrm{Tele},T_{\mathrm{vec}}} + 6G_{\mathrm{Tele},T} \\
&\quad + 18H^2[9G_{\mathrm{Tele},T_{\mathrm{vec}}T_{\mathrm{vec}}} - 12G_{\mathrm{Tele},TT_{\mathrm{vec}}} + 4G_{\mathrm{Tele},TT}] + 6H\dot{\phi}[XG_{5,X} - 9G_{\mathrm{Tele},T_{\mathrm{vec}}I_2} \\
&\quad + 6G_{\mathrm{Tele},TI_2}]\,, \\
\mathcal{A}_{23} &= \left[-4XH^2G_{5,X} + 4G_{4,\phi} - 2G_{\mathrm{Tele},I_2} + 4X(-2G_{4,\phi X} + G_{5,\phi\phi} - \dot{H}G_{5,X}) \right. \\
&\quad + 4\ddot{\phi}(-G_{4,X} - 2XG_{4,XX} + G_{5,\phi} + XG_{5,\phi X}) + H\dot{\phi}(-4G_{4,X} + 4G_{5,\phi} - 4XG_{5,\phi X} \\
&\quad \left. + G_{\mathrm{Tele},J_3} - 4\ddot{\phi}(G_{5,X} + XG_{5,XX}))\right]\,, \\
\mathcal{A}_{24} &= -3\left[2XH^3(3G_{5,X} + 2XG_{5,XX}) + H(6XG_{3,X} - 2G_{4,\phi} + 4X(-5G_{4,\phi X} + G_{5,\phi\phi}) \right. \\
&\quad + 3G_{\mathrm{Tele},I_2} + 6G_{\mathrm{Tele},\phi T_{\mathrm{vec}}} - 4G_{\mathrm{Tele},\phi T}) + 2H^2\dot{\phi}(3G_{4,X} + 6XG_{4,XX} - 3G_{5,\phi} - 4XG_{5,\phi X}) \\
&\quad \left. + \dot{\phi}(G_{2,X} - 2G_{3,\phi} + 2G_{4,\phi\phi} + G_{\mathrm{Tele},X} - G_{\mathrm{Tele},\phi I_2})\right]\,, \\
\mathcal{A}_{25} &= 3\left[2XG_{3,X} - 2G_{4,\phi} - 4XG_{4,\phi X} + G_{\mathrm{Tele},I_2} + 2H^2(3XG_{5,X} + 2X^2G_{5,XX} - 9G_{\mathrm{Tele},T_{\mathrm{vec}}I_2} \right. \\
&\quad + 6G_{\mathrm{Tele},TI_2}) + 2XG_{\mathrm{Tele},XI_2} + H\dot{\phi}(4G_{4,X} + 8XG_{4,XX} - 4G_{5,\phi} - 4XG_{5,\phi X} + 3G_{\mathrm{Tele},I_2I_2} \\
&\quad \left. - 6G_{\mathrm{Tele},XT_{\mathrm{vec}}} + 4G_{\mathrm{Tele},XT})\right]\,,
\end{aligned}
$$

$$
\begin{aligned}
\mathcal{A}_{26} = \frac{1}{2}\big[& - G_{2,X} + 2G_{3,\phi} - G_{\rm tele,X} - 4\dot{H}(G_{4,X} - G_{5,\phi}) - 2\ddot{\phi}(G_{3,X} - 3G_{4,\phi X}) - 4H^3\dot{\phi}(G_{5,X} \\
& + XG_{5,XX}) + H^2(-6G_{4,X} + 6G_{5,\phi} - 2\ddot{\phi}G_{5,X} + 10X(-2G_{4,XX} + G_{5,\phi X} - \ddot{\phi}G_{5,XX}) \\
& - 4X^2(G_{5,\phi XX} + \ddot{\phi}G_{5,XXX})) + H\dot{\phi}(-4G_{3,X} + 12G_{4,\phi X} - 4\dot{H}G_{5,X} - 12\ddot{\phi}G_{4,XX} \\
& + 8\ddot{\phi}G_{5,\phi X} + 4X(-2G_{4,\phi XX} + G_{5,\phi\phi X} - \dot{H}G_{5,XX} - 2\ddot{\phi}G_{4,XXX} + \ddot{\phi}G_{5,\phi XX})) \\
& + X(-2G_{3,\phi X} + 4G_{4,\phi\phi X} - 4\dot{H}(2G_{4,XX} - G_{5,\phi X}) - 2\ddot{\phi}(G_{3,XX} - 2G_{4,\phi XX}))\big] , \\
\mathcal{A}_{27} = \frac{1}{2}\big[& - 6H^4X(3G_{5,\phi X} + 2XG_{5,\phi XX}) + G_{2,\phi\phi} + G_{\rm Tele,\phi\phi} + 3\dot{H}(2G_{4,\phi\phi} - G_{{\rm Tele},\phi I_2}) \\
& - 3H\dot{\phi}\big(G_{2,\phi X} - 2G_{3,\phi\phi} + 2XG_{3,\phi\phi X} - 4XG_{4,\phi\phi\phi X} + G_{{\rm Tele},\phi X} + G_{{\rm Tele},\phi\phi I_2} + \dot{H}(4G_{4,\phi X} \\
& + 8XG_{4,\phi XX} - 4G_{5,\phi\phi} - 4XG_{5,\phi\phi X} + 3G_{{\rm Tele},\phi I_2 I_2} - 6G_{{\rm Tele},\phi X T_{\rm vec}} + 4G_{{\rm Tele},\phi XT})\big) \\
& - \ddot{\phi}(G_{2,\phi X} - 2G_{3,\phi\phi} + G_{{\rm Tele},\phi X}) - 6H\dot{\phi}\ddot{\phi}(G_{3,\phi X} - 3G_{4,\phi\phi X} + X(G_{3,\phi XX} - 2G_{4,\phi\phi XX}) \\
& + G_{{\rm Tele},\phi X I_2}) + 3H^2(4G_{4,\phi\phi} + 2X(-3G_{3,\phi X} + 6G_{4,\phi\phi X} + G_{5,\phi\phi\phi} + 2X(-2G_{4,\phi\phi XX} \\
& + G_{5,\phi\phi\phi X})) - 3G_{{\rm Tele},\phi I_2} - 2\dot{H}(3XG_{5,\phi X} + 2X^2G_{5,\phi XX} - 9G_{{\rm Tele},\phi T_{\rm vec} I_2} + 6G_{{\rm Tele},\phi T I_2}) \\
& - 2G_{4,\phi X}\ddot{\phi} + (2G_{5,\phi\phi} + 2X(-8G_{4,\phi XX} + 5G_{5,\phi\phi X} + 2X(-2G_{4,\phi XXX} + G_{5,\phi\phi XX})) \\
& - 3G_{{\rm Tele},\phi I_2 I_2})\ddot{\phi}) + 2X(-G_{2,\phi\phi X} + G_{3,\phi\phi\phi} - G_{{\rm Tele},\phi\phi X} - 3\dot{H}(G_{3,\phi X} - 2G_{4,\phi\phi X} \\
& + G_{{\rm Tele},\phi X I_2}) - \ddot{\phi}(G_{2,\phi XX} - G_{3,\phi\phi X} + G_{{\rm Tele},\phi XX})) - 2H^3\dot{\phi}(9G_{4,\phi X} - 9G_{5,\phi\phi} + 3\ddot{\phi}G_{5,\phi X} \\
& + X(18G_{4,\phi XX} - 7G_{5,\phi\phi X} + 2XG_{5,\phi\phi XX} + (7G_{5,\phi XX} + 2XG_{5,\phi XXX})\ddot{\phi}))\big] , \\
\mathcal{A}_{28} = \frac{1}{2}\big[& G_{2,X} - 2G_{3,\phi} + G_{{\rm Tele},X} + 2X(G_{2,XX} - G_{3,\phi X} + G_{{\rm Tele},XX}) + 6H\dot{\phi}(G_{3,X} - 3G_{4,\phi X} \\
& + X(G_{3,XX} - 2G_{4,\phi X}) + G_{{\rm Tele},XI_2}) + 2H^3\dot{\phi}(3G_{5,X} + 7XG_{5,XX} + 2X^2G_{5,XXX}) \\
& + 3H^2(2(G_{4,X} - G_{5,\phi}) + 2X(8G_{4,XX} - 5G_{5,\phi X}) + 4X^2(2G_{4,XXX} - G_{5,\phi XX}) \\
& + 3G_{{\rm Tele},I_2 I_2})\big] .
\end{aligned}
$$

Action (7.3) is rewritten in terms of gauge invariant quantities (4.45), yielding Eq. (7.8) where coefficients $\tilde{\mathcal{A}}_i$ are

$$
\begin{aligned}
\tilde{\mathcal{A}}_1 = & \, X\left(G_{2,X} - 2G_{3.\phi} + XG_{{\rm Tele},X}\right) + 2X^2\left(G_{2,XX} - G_{3,\phi X} + G_{{\rm Tele},XX}\right) - 9H^2G_{{\rm Tele},T_{\rm vec}} \\
& + 6XH\dot{\phi}\left(2G_{3,X} + XG_{3,XX} - 5G_{4,\phi X} - 2XG_{4,\phi XX} + 2G_{{\rm Tele},XI_2} + 5H^2G_{5,X}\right) \\
& + 6H^2\left(-G_4 + G_{{\rm Tele},T} + 7XG_{4,X} + 4XG_{{\rm Tele},XT} + 6X(-G_{5,\phi} + G_{{\rm Tele},I_2 I_2}\right. \\
& \left. -G_{{\rm Tele},XT_{\rm vec}})\right) + 6X^2H^2\left(4(4G_{4,XX} + XG_{4,XXX}) - 9G_{5,\phi X}\right) + 2H^3X^2\Big(13\dot{\phi}G_{5,XX} \\
& + 2X\dot{\phi}G_{5,XXX}\Big) + 3H\dot{\phi}\left(G_{{\rm Tele},I_2} - 2G_{4,\phi} - 6H^2(6G_{{\rm Tele},T_{\rm vec}I_2} - 4G_{{\rm Tele},TI_2})\right) \\
& + 18H^4\left(9G_{{\rm Tele},T_{\rm vec}T_{\rm vec}} - 12G_{{\rm Tele},TT_{\rm vec}} + 4G_{{\rm Tele},TT}\right) - 12X^3H^2G_{5,\phi XX} , \\
\tilde{\mathcal{A}}_2 = & \, \frac{1}{3}\left(3G_{{\rm Tele},T_{\rm vec}} + 2XG_{{\rm Tele},J_3} - \frac{10X}{3}G_{{\rm Tele},J_5} + \frac{4X}{3}(XG_{{\rm Tele},J_6} - G_{{\rm Tele},J_8})\right) ,
\end{aligned}
$$

$$
\begin{aligned}
\tilde{\mathcal{A}}_3 &= 2\left(G_4 - X(\ddot{\phi}G_{5,X} + G_{5,\phi}) + 2G_{\mathrm{Tele},T_{\mathrm{vec}}} - G_{\mathrm{Tele},T}\right) - \frac{10X}{9}G_{\mathrm{Tele},J_5} \\
&\quad + \frac{4X}{9}\left(XG_{\mathrm{Tele},J_6} - G_{\mathrm{Tele},J_8} - 3G_{\mathrm{Tele},J_3}\right) , \\
\tilde{\mathcal{A}}_4 &= 6\left(X(2G_{4,X} - G_{5,\phi}) - G_4 + G_{\mathrm{Tele},T}\right) + 6H\dot{\phi}\left(XG_{5,X} + 6G_{\mathrm{Tele},TI_2} - 9G_{\mathrm{Tele},T_{\mathrm{vec}}I_2}\right) \\
&\quad + 9\left(XG_{\mathrm{Tele},I_2I_2} - G_{\mathrm{Tele},T_{\mathrm{vec}}} + 2H^2(9G_{\mathrm{Tele},T_{\mathrm{vec}}T_{\mathrm{vec}}} - 12G_{\mathrm{Tele},TT_{\mathrm{vec}}} + 4G_{\mathrm{Tele},TT})\right) , \\
\tilde{\mathcal{A}}_5 &= H\dot{\phi}\left(-\frac{3}{2}G_{2,\phi X} - \frac{3}{2}G_{\mathrm{Tele},\phi X} - 3\ddot{\phi}(G_{3,\phi X} - 3G_{4,\phi\phi X} + G_{\mathrm{Tele},\phi XI_2}) - 3X\ddot{\phi}(G_{3,\phi XX}\right. \\
&\quad -2G_{4,\phi\phi XX}) + 6\dot{H}\left(G_{5,\phi\phi} - G_{4,\phi X} - \frac{3}{4}G_{\mathrm{Tele},\phi I_2I_2} + \frac{3}{2}G_{\mathrm{Tele},\phi XT_{\mathrm{vec}}} - G_{\mathrm{Tele},\phi XT}\right) \\
&\quad \left.+3X\left(2\dot{H}(G_{5,\phi\phi X} - 2G_{4,\phi XX}) - G_{3,\phi\phi X} - 6G_{4,\phi XX} + 2G_{4,\phi\phi\phi X}\right) + 3G_{3,\phi\phi}\right) + \frac{1}{2}G_{2,\phi\phi} \\
&\quad + \frac{1}{2}G_{\mathrm{Tele},\phi\phi} + \ddot{\phi}(G_{3,\phi\phi} - \frac{1}{2}G_{2,\phi X} - XG_{2,\phi XX} + XG_{3,\phi\phi X} - \frac{1}{2}G_{\mathrm{Tele},\phi X} - XG_{\mathrm{Tele},\phi XX}) \\
&\quad - X(G_{2,\phi\phi X} + G_{\mathrm{Tele},\phi\phi X}) + 9H^2X(2G_{4,\phi\phi X} - 3G_{3,\phi X} - H^2G_{5,\phi X}) + 3X\dot{H}(2G_{4,\phi\phi X} \\
&\quad - G_{3,\phi X} - 3H^2G_{5,\phi X} + G_{\mathrm{Tele},\phi XI_2}) + H^3\dot{\phi}\left(9(G_{5,\phi\phi} - G_{4,\phi X}) - 3\ddot{\phi}G_{5,\phi X} - 2X^2G_{5,\phi\phi XX}\right. \\
&\quad \left.+7X(G_{5,\phi\phi X} - \ddot{\phi}G_{5,\phi XX})\right) + 3H^2\ddot{\phi}\left(G_{5,\phi\phi} - G_{4,\phi X} + 5XG_{5,\phi\phi X} - 4X(2G_{4,\phi XX}\right. \\
&\quad \left.+XG_{4,\phi XXX}) - \frac{2}{3}HX^2\dot{\phi}G_{5,\phi XXX} + 2X^2G_{5,\phi\phi XX} - \frac{3}{2}G_{\mathrm{Tele},\phi I_2I_2}\right) + 6X^2H^2(G_{5,\phi\phi\phi X} \\
&\quad - 2G_{4,\phi\phi XX} - H^2G_{5,\phi XX} - \dot{H}G_{5,\phi XX}) + 3H^2\left(2G_{4,\phi\phi} + XG_{5,\phi\phi\phi} - \frac{3}{2}G_{\mathrm{Tele},\phi I_2}\right. \\
&\quad \left.+9\dot{H}G_{\mathrm{Tele},\phi T_{\mathrm{vec}}I_2} - 6\dot{H}G_{\mathrm{Tele},\phi TI_2}\right) + 3\dot{H}G_{4,\phi\phi} - \frac{3}{2}\dot{H}G_{\mathrm{Tele},\phi I_2} + XG_{3,\phi\phi\phi} - \frac{3}{2}H\dot{\phi}G_{\mathrm{Tele},\phi\phi I_2} , \\
\tilde{\mathcal{A}}_6 &= \frac{1}{2}\left(G_{2,X} - 2G_{3,\phi} + 2X(G_{\mathrm{Tele},XX} + G_{2,XX} - G_{3,\phi X}) + 6H\dot{\phi}(G_{3,X} + H^2G_{5,X} - 3G_{4,\phi X}\right. \\
&\quad -2XG_{4,\phi XX} + G_{\mathrm{Tele},XI_2}) + 2XH\dot{\phi}(2G_{3,XX} + 7H^2G_{5,XX}) + G_{\mathrm{Tele},X} + 6H^2\left(G_{4,X}\right. \\
&\quad \left.\left.+4X(2G_{4,XX} + XG_{4,XXX}) - G_{5,\phi} - 5XG_{5,\phi X} - 2X^2G_{5,\phi XX}\right) + 4X^2H^3\dot{\phi}G_{5,XXX}\right. \\
&\quad \left.+9H^2G_{\mathrm{Tele},I_2I_2}\right) , \\
\tilde{\mathcal{A}}_7 &= -\frac{1}{2}G_{2,X} - \frac{1}{2}G_{\mathrm{Tele},X} + G_{3,\phi} + \ddot{\phi}\left(2XG_{4,\phi XX} + 3G_{4,\phi X} - H^2G_{5,X} - G_{3,X} - XG_{3,XX}\right) \\
&\quad + 5XH^2(G_{5,\phi X} - \ddot{\phi}G_{5,XX} - 2G_{4,XX}) + 2XH\dot{\phi}(-\dot{H}G_{5,XX} - 2\ddot{\phi}G_{4,XXX} - 2G_{4,\phi XX} \\
&\quad + \ddot{\phi}G_{5,\phi XX} + G_{5,\phi\phi X}) - 2XH^2(H\dot{\phi}G_{5,XX} + X\ddot{\phi}G_{5,XXX} + XG_{5,\phi XX}) + 3H^2(G_{5,\phi} - G_{4,X}) \\
&\quad + 2\dot{H}(G_{5,\phi} - G_{4,X}) + 2X\dot{H}(G_{5,\phi X} - 2G_{4,XX}) + 2H\dot{\phi}(-G_{3,X} - H^2G_{5,X} - \dot{H}G_{5,X} \\
&\quad - 3\ddot{\phi}G_{4,XX} + 3G_{4,\phi X} + 2\ddot{\phi}G_{5,\phi X}) + X(2G_{4,\phi\phi X} - G_{3,\phi X}) , \\
\tilde{\mathcal{A}}_8 &= \frac{1}{3}a^2\left(X\left(4G_{\mathrm{Tele},J_8} + G_{\mathrm{Tele},J_5} + 3G_{\mathrm{Tele},I_2I_2}\right) - 3G_{\mathrm{Tele},T_{\mathrm{vec}}} + 6H\left(H(9G_{\mathrm{Tele},T_{\mathrm{vec}}T_{\mathrm{vec}}}\right.\right. \\
&\quad \left.\left.-12G_{\mathrm{Tele},TT_{\mathrm{vec}}} + 4G_{\mathrm{Tele},TT}) + \dot{\phi}(-3G_{\mathrm{Tele},T_{\mathrm{vec}}I_2} + 2G_{\mathrm{Tele},TI_2})\right)\right) ,
\end{aligned}
$$

$$
\begin{aligned}
\tilde{\mathcal{A}}_9 &= 3\big[-12H^3\left(9G_{\mathrm{Tele},T_{\mathrm{vec}}T_{\mathrm{vec}}}+4(-3G_{\mathrm{Tele},TT_{\mathrm{vec}}}+G_{\mathrm{Tele},TT})\right)+2H\left(2G_4+4X^2(-2G_{4,XX}\right.\\
&\quad +G_{5,\phi X})+3G_{\mathrm{Tele},T_{\mathrm{vec}}}-2G_{\mathrm{Tele},T}+2X(-4G_{4,X}+3G_{5,\phi}-3G_{\mathrm{Tele},I_2I_2}+3G_{\mathrm{Tele},XT_{\mathrm{vec}}}\\
&\quad -2G_{\mathrm{Tele},XT}))-2H^2\dot{\phi}(5XG_{5,X}+2X^2G_{5,XX}-27G_{\mathrm{Tele},T_{\mathrm{vec}}I_2}+18G_{\mathrm{Tele},TI_2})\\
&\quad \left.-\dot{\phi}\left(-2G_{4,\phi}+G_{\mathrm{Tele},I_2}+2X(G_{3,X}-2G_{4,\phi X}+G_{\mathrm{Tele},XI_2})\right)\right]\,,\\
\tilde{\mathcal{A}}_{10} &= \frac{2}{9}\big(18(G_4+G_{\mathrm{Tele},T_{\mathrm{vec}}}-G_{\mathrm{Tele},T})+X(-36G_{4,X}+18G_{5,\phi}+4G_{\mathrm{Tele},J_8}-4XG_{\mathrm{Tele},J_6}\\
&\quad +10G_{\mathrm{Tele},J_5}+3G_{\mathrm{Tele},J_3}-18H\dot{\phi}G_{5,X})\big)\,,\\
\tilde{\mathcal{A}}_{11} &= G_{2,\phi}+G_{\mathrm{Tele},\phi}+6H^2\left(G_{4,\phi}+X(-4G_{4,\phi X}+3G_{5,\phi\phi}-4XG_{4,\phi XX}+2XG_{5,\phi\phi X})\right.\\
&\quad \left.+3G_{\mathrm{Tele},\phi T_{\mathrm{vec}}}-2G_{\mathrm{Tele},\phi T}\right)-2X(G_{2,\phi X}-G_{3,\phi\phi}+G_{\mathrm{Tele},\phi X})-2H^3X\dot{\phi}(5G_{5,\phi X}\\
&\quad +2XG_{5,\phi XX})-6H\dot{\phi}\left(-G_{4,\phi\phi}+X(G_{3,\phi X}-2G_{4,\phi\phi X})+G_{\mathrm{Tele},\phi I_2}\right)\,,\\
\tilde{\mathcal{A}}_{12} &= -H^3\left(30XG_{5,X}+40X^2G_{5,XX}+8X^3G_{5,XXX}-54G_{\mathrm{Tele},T_{\mathrm{vec}}I_2}+36G_{\mathrm{Tele},TI_2}\right)\\
&\quad -3H\left(-2G_{4,\phi}+G_{\mathrm{Tele},I_2}+2X(3G_{3,X}-8G_{4,\phi X}+2X(G_{3,XX}-2G_{4,\phi XX})\right.\\
&\quad \left.+3G_{\mathrm{Tele},XI_2})\right)-6H^2\dot{\phi}\left(3G_{4,X}+X(12G_{4,XX}+4XG_{4,XXX}-7G_{5,\phi X}-2XG_{5,\phi XX})\right.\\
&\quad \left.-3(G_{5,\phi}-G_{\mathrm{Tele},I_2I_2}+G_{\mathrm{Tele},XT_{\mathrm{vec}}})+2G_{\mathrm{Tele},XT}\right)-\dot{\phi}\left(G_{2,X}-2G_{3,\phi}+G_{\mathrm{Tele},X}\right.\\
&\quad \left.+2X(G_{2,XX}-G_{3,\phi X}+G_{\mathrm{Tele},XX})\right)\,,\\
\tilde{\mathcal{A}}_{13} &= 2G_{4,\phi}-2X\left(G_{3,X}+H^2(3G_{5,X}+2XG_{5,XX})-2G_{4,\phi X}\right)-G_{\mathrm{Tele},I_2}-H\dot{\phi}\left(4(G_{4,X}\right.\\
&\quad \left.-G_{5,\phi}+X(2G_{4,XX}-G_{5,\phi X}))+G_{\mathrm{Tele},J_3}\right)\,,\\
\tilde{\mathcal{A}}_{14} &= -\frac{a\tilde{\mathcal{A}}_9}{3}\,,\\
\tilde{\mathcal{A}}_{15} &= 3\dot{\phi}\left(2G_{3,\phi}-G_{2,X}-G_{\mathrm{Tele},X}-2G_{4,\phi\phi}+G_{\mathrm{Tele},\phi I_2}\right)+6H^2\dot{\phi}\left(3(G_{5,\phi}-G_{4,X})\right.\\
&\quad \left.+2X(2G_{5,\phi X}-3G_{4,XX})\right)+3H\left(2G_{4,\phi}+4G_{\mathrm{Tele},\phi T}-6G_{\mathrm{Tele},\phi T_{\mathrm{vec}}}-3G_{\mathrm{Tele},I_2}\right)\\
&\quad +6XH\left(2(5G_{4,\phi X}-G_{5,\phi\phi})-3(G_{3,X}+H^2G_{5,X})\right)-12X^2H^3G_{5,XX}\,,\\
\tilde{\mathcal{A}}_{16} &= 3\left(2XG_{3,X}-2G_{4,\phi}+G_{\mathrm{Tele},I_2}\right)+6H\dot{\phi}\left(2G_{4,X}-2G_{5,\phi}-3G_{\mathrm{Tele},XT_{\mathrm{vec}}}+2G_{\mathrm{Tele},XT}\right)\\
&\quad +6X\left(G_{\mathrm{Tele},XI_2}-2G_{4,\phi X}\right)+9H\dot{\phi}G_{\mathrm{Tele},I_2I_2}+12XH\dot{\phi}\left(2G_{4,XX}-G_{5,\phi X}\right)\\
&\quad +6H^2\left(6G_{\mathrm{Tele},TI_2}-9G_{\mathrm{Tele},T_{\mathrm{vec}}I_2}+X(3G_{5,X}+2XG_{5,XX})\right)\,,\\
\tilde{\mathcal{A}}_{17} &= 4H\dot{\phi}\left(G_{5,\phi}-G_{4,X}-\ddot{\phi}G_{5,X}-X(\ddot{\phi}G_{5,XX}+G_{5,\phi X})\right)+4\ddot{\phi}\left(XG_{5,\phi X}+G_{5,\phi}-G_{4,X}\right.\\
&\quad \left.-2XG_{4,XX}\right)+4G_{4,\phi}-2G_{\mathrm{Tele},I_2}-4X\dot{H}G_{5,X}+4X\left(G_{5,\phi\phi}-2G_{4,\phi X}-H^2G_{5,X}\right)+H\dot{\phi}G_{\mathrm{Tele},J_3}\,,\\
\tilde{\mathcal{A}}_{18} &= a\big[4\left(G_4-G_{\mathrm{Tele},T}+X(G_{5,\phi}-2G_{4,X})\right)+4H\dot{\phi}\left(-XG_{5,X}+9G_{\mathrm{Tele},T_{\mathrm{vec}}I_2}-6G_{\mathrm{Tele},TI_2}\right)\\
&\quad +6\left(G_{\mathrm{Tele},T_{\mathrm{vec}}}-XG_{\mathrm{Tele},I_2I_2}\right)+12H^2\left(12G_{\mathrm{Tele},TT_{\mathrm{vec}}}-9G_{\mathrm{Tele},T_{\mathrm{vec}}T_{\mathrm{vec}}}-4G_{\mathrm{Tele},TT}\right)\big]\,,\\
\tilde{\mathcal{A}}_{19} &= a\Big[\dot{\phi}\left(G_{2,X}-2G_{3,\phi}+2G_{4,\phi\phi}+G_{\mathrm{Tele},X}-G_{\mathrm{Tele},\phi I_2}\right)+H\left(3G_{\mathrm{Tele},I_2}-2G_{4,\phi}\right.\\
&\quad \left.+6G_{\mathrm{Tele},\phi T_{\mathrm{vec}}}-4G_{\mathrm{Tele},\phi T}\right)+6H^2\dot{\phi}\left(G_{4,X}-G_{5,\phi}\right)+2XH\left(3G_{3,X}+6H\dot{\phi}G_{4,XX}\right.
\end{aligned}
$$

$$-10G_{4,\phi X}+2G_{5,\phi\phi})+2XH^2\left(3HG_{5,X}+2XHG_{5,XX}-4\dot{\phi}G_{5,\phi X}\right)\Big]\,,$$

$$\begin{aligned}\tilde{\mathcal{A}}_{20}=a\Big[&2X\left(2G_{4,\phi X}-G_{3,X}-G_{\mathrm{Tele},XI_2}\right)-G_{\mathrm{Tele},I_2}+2G_{4,\phi}+H\dot{\phi}\left(4(G_{5,\phi}-G_{4,X}\right.\\&-2XG_{4,XX}+XG_{5,\phi X}-G_{\mathrm{Tele},XT})+3(2G_{\mathrm{Tele},XT_{\mathrm{vec}}}-G_{\mathrm{Tele},I_2I_2}))\\&+H^2\left(6(3G_{\mathrm{Tele},T_{\mathrm{vec}}I_2}-2G_{\mathrm{Tele},TI_2}-XG_{5,X})-4X^2G_{5,XX}\right)\Big]\,,\end{aligned}$$

The elimination of auxiliary modes gives action (7.12), where

$$\begin{aligned}\tilde{a}\hat{\mathcal{A}}_1=&\,\tilde{\mathcal{A}}_{11}\tilde{\mathcal{A}}_{14}\tilde{\mathcal{A}}_{19}-\tilde{\mathcal{A}}_1\tilde{\mathcal{A}}_{19}^2-\tilde{\mathcal{A}}_5\tilde{\mathcal{A}}_{14}^2-\tilde{\mathcal{A}}_8\left(\tilde{\mathcal{A}}_{11}^2-4\tilde{\mathcal{A}}_1\tilde{\mathcal{A}}_5\right)+\frac{k^2}{a^2}\left(\tilde{\mathcal{A}}_{13}\tilde{\mathcal{A}}_{14}\tilde{\mathcal{A}}_{19}-\tilde{\mathcal{A}}_2\tilde{\mathcal{A}}_{19}^2\right.\\&\left.-\tilde{\mathcal{A}}_7\tilde{\mathcal{A}}_{14}^2+2\tilde{\mathcal{A}}_8\left(-\tilde{\mathcal{A}}_{11}\tilde{\mathcal{A}}_{13}+2\tilde{\mathcal{A}}_2\tilde{\mathcal{A}}_5+2\tilde{\mathcal{A}}_1\tilde{\mathcal{A}}_7\right)\right)-\frac{k^4}{a^4}\tilde{\mathcal{A}}_8\left(\tilde{\mathcal{A}}_{13}^2-4\tilde{\mathcal{A}}_2\tilde{\mathcal{A}}_7\right)\,,\\
\tilde{a}\hat{\mathcal{A}}_2=&\,\tilde{\mathcal{A}}_{20}\left(-\tilde{\mathcal{A}}_{11}\tilde{\mathcal{A}}_{14}+2\tilde{\mathcal{A}}_1\tilde{\mathcal{A}}_{19}\right)+\tilde{\mathcal{A}}_{12}\left(\tilde{\mathcal{A}}_{14}\tilde{\mathcal{A}}_{19}-2\tilde{\mathcal{A}}_8\tilde{\mathcal{A}}_{11}\right)+\frac{k^2}{a^2}\left(2\tilde{\mathcal{A}}_2\tilde{\mathcal{A}}_{19}\tilde{\mathcal{A}}_{20}\right.\\&\left.-\tilde{\mathcal{A}}_{13}\left(\tilde{\mathcal{A}}_{14}\tilde{\mathcal{A}}_{20}+2\tilde{\mathcal{A}}_8\tilde{\mathcal{A}}_{12}\right)\right)\,,\\
\tilde{a}\hat{\mathcal{A}}_3=&-\tilde{\mathcal{A}}_{12}\tilde{\mathcal{A}}_{14}\tilde{\mathcal{A}}_{20}-\tilde{\mathcal{A}}_1\tilde{\mathcal{A}}_{20}^2-\tilde{\mathcal{A}}_6\tilde{\mathcal{A}}_{14}^2-\tilde{\mathcal{A}}_8\left(\tilde{\mathcal{A}}_{12}^2-4\tilde{\mathcal{A}}_1\tilde{\mathcal{A}}_6\right)-\frac{k^2}{a^2}\tilde{\mathcal{A}}_2\left(\tilde{\mathcal{A}}_{20}^2-4\tilde{\mathcal{A}}_6\tilde{\mathcal{A}}_8\right)\,,\\
\tilde{a}\hat{\mathcal{A}}_4=&-\frac{k^2}{a^2}\tilde{\mathcal{A}}_3\left(\tilde{\mathcal{A}}_{14}^2-4\tilde{\mathcal{A}}_1\tilde{\mathcal{A}}_8\right)-\frac{k^4}{a^4}\tilde{\mathcal{A}}_8\left(\tilde{\mathcal{A}}_{10}^2-4\tilde{\mathcal{A}}_2\tilde{\mathcal{A}}_3\right)\,,\\
\tilde{a}\hat{\mathcal{A}}_5=&\,\frac{k^2}{a^2}\tilde{\mathcal{A}}_{10}\left(\tilde{\mathcal{A}}_{14}\tilde{\mathcal{A}}_{18}-2\tilde{\mathcal{A}}_8\tilde{\mathcal{A}}_9\right)\,,\\
\tilde{a}\hat{\mathcal{A}}_6=&-\tilde{\mathcal{A}}_4\tilde{\mathcal{A}}_{14}^2-\tilde{\mathcal{A}}_1\left(\tilde{\mathcal{A}}_{18}^2-4\tilde{\mathcal{A}}_4\tilde{\mathcal{A}}_8\right)+\tilde{\mathcal{A}}_9\left(\tilde{\mathcal{A}}_{14}\tilde{\mathcal{A}}_{18}-\tilde{\mathcal{A}}_8\tilde{\mathcal{A}}_9\right)-\frac{k^2}{a^2}\tilde{\mathcal{A}}_2\left(\tilde{\mathcal{A}}_{18}^2-4\tilde{\mathcal{A}}_4\tilde{\mathcal{A}}_8\right)\,,\\
\tilde{a}\hat{\mathcal{A}}_7=&\,\frac{k^2}{a^2}\left[-\tilde{\mathcal{A}}_{14}^2\tilde{\mathcal{A}}_{17}+\tilde{\mathcal{A}}_{10}\tilde{\mathcal{A}}_{14}\tilde{\mathcal{A}}_{19}-2\tilde{\mathcal{A}}_8\tilde{\mathcal{A}}_{10}\tilde{\mathcal{A}}_{11}+4\tilde{\mathcal{A}}_1\tilde{\mathcal{A}}_8\tilde{\mathcal{A}}_{17}\right]-2\frac{k^4}{a^4}\tilde{\mathcal{A}}_8\left(\tilde{\mathcal{A}}_{10}\tilde{\mathcal{A}}_{13}-2\tilde{\mathcal{A}}_2\tilde{\mathcal{A}}_{17}\right)\,,\\
\tilde{a}\hat{\mathcal{A}}_8=&-\frac{k^2}{a^2}\tilde{\mathcal{A}}_{10}\left(\tilde{\mathcal{A}}_{14}\tilde{\mathcal{A}}_{20}+2\tilde{\mathcal{A}}_8\tilde{\mathcal{A}}_{12}\right)\,,\\
\tilde{a}\hat{\mathcal{A}}_9=&-\tilde{\mathcal{A}}_{14}^2\tilde{\mathcal{A}}_{15}+\tilde{\mathcal{A}}_{11}\tilde{\mathcal{A}}_{14}\tilde{\mathcal{A}}_{18}-2\tilde{\mathcal{A}}_1\tilde{\mathcal{A}}_{18}\tilde{\mathcal{A}}_{19}+4\tilde{\mathcal{A}}_1\tilde{\mathcal{A}}_8\tilde{\mathcal{A}}_{15}+\tilde{\mathcal{A}}_9\tilde{\mathcal{A}}_{14}\tilde{\mathcal{A}}_{19}-2\tilde{\mathcal{A}}_8\tilde{\mathcal{A}}_9\tilde{\mathcal{A}}_{11}\\&+\frac{k^2}{a^2}\left(\tilde{\mathcal{A}}_{13}\tilde{\mathcal{A}}_{14}\tilde{\mathcal{A}}_{18}-2\tilde{\mathcal{A}}_2\tilde{\mathcal{A}}_{18}\tilde{\mathcal{A}}_{19}+4\tilde{\mathcal{A}}_2\tilde{\mathcal{A}}_8\tilde{\mathcal{A}}_{15}-2\tilde{\mathcal{A}}_8\tilde{\mathcal{A}}_9\tilde{\mathcal{A}}_{13}\right)\,,\\
\tilde{a}\hat{\mathcal{A}}_{10}=&-\tilde{\mathcal{A}}_{14}^2\tilde{\mathcal{A}}_{16}+\tilde{\mathcal{A}}_{12}\tilde{\mathcal{A}}_{14}\tilde{\mathcal{A}}_{18}+2\tilde{\mathcal{A}}_1\tilde{\mathcal{A}}_{18}\tilde{\mathcal{A}}_{20}+4\tilde{\mathcal{A}}_1\tilde{\mathcal{A}}_8\tilde{\mathcal{A}}_{16}-\tilde{\mathcal{A}}_9\left(\tilde{\mathcal{A}}_{14}\tilde{\mathcal{A}}_{20}+2\tilde{\mathcal{A}}_8\tilde{\mathcal{A}}_{12}\right)\\&+2\frac{k^2}{a^2}\tilde{\mathcal{A}}_2\left(\tilde{\mathcal{A}}_{18}\tilde{\mathcal{A}}_{20}+2\tilde{\mathcal{A}}_8\tilde{\mathcal{A}}_{16}\right)\,,\end{aligned}$$

and

$$\tilde{a}=-\tilde{\mathcal{A}}_{14}^2+4\tilde{\mathcal{A}}_8\left(\tilde{\mathcal{A}}_1+\frac{k^2}{a^2}\tilde{\mathcal{A}}_2\right)\,. \tag{C.3}$$

After diagonalisation of the kinetic matrix, the significant coefficients of Eq. (7.42) are given by

$$\breve{\mathcal{A}}_1=-\tilde{\mathcal{A}}_6-\frac{\tilde{\mathcal{A}}_{16}\tilde{\mathcal{A}}_{18}\tilde{\mathcal{A}}_{20}+\tilde{\mathcal{A}}_4\tilde{\mathcal{A}}_{20}^2+\tilde{\mathcal{A}}_8\tilde{\mathcal{A}}_{16}^2}{\tilde{\mathcal{A}}_{18}^2-4\tilde{\mathcal{A}}_4\tilde{\mathcal{A}}_8}\,,$$

$$
\begin{aligned}
\breve{\mathcal{A}}_2 &= \tilde{\mathcal{A}}_4 - \frac{\tilde{\mathcal{A}}_{18}^2}{4\tilde{\mathcal{A}}_8}\,,\\
\breve{\mathcal{A}}_3 &= \frac{1}{2}(\tilde{\mathcal{A}}_{10}\tilde{\mathcal{A}}_{13} - 2\tilde{\mathcal{A}}_2\tilde{\mathcal{A}}_{17})(\tilde{\mathcal{A}}_{18}\tilde{\mathcal{A}}_{20} + 2\tilde{\mathcal{A}}_8\tilde{\mathcal{A}}_{16}) + \frac{(\tilde{\mathcal{A}}_{10}^2 - 4\tilde{\mathcal{A}}_2\tilde{\mathcal{A}}_3)(\tilde{\mathcal{A}}_{18}\tilde{\mathcal{A}}_{20} + 2\tilde{\mathcal{A}}_8\tilde{\mathcal{A}}_{16})^2}{4(\tilde{\mathcal{A}}_{18}^2 - 4\tilde{\mathcal{A}}_4\tilde{\mathcal{A}}_8)}\\
&\quad + \frac{1}{4}(\tilde{\mathcal{A}}_{13}^2 - 4\tilde{\mathcal{A}}_2\tilde{\mathcal{A}}_7)(\tilde{\mathcal{A}}_{18}^2 - 4\tilde{\mathcal{A}}_4\tilde{\mathcal{A}}_8)\,,\\
\breve{\mathcal{A}}_4 &= \tilde{\mathcal{A}}_3 - \frac{\tilde{\mathcal{A}}_{10}^2}{4\tilde{\mathcal{A}}_2}\,,\\
\breve{\mathcal{A}}_5 &= \tilde{\mathcal{A}}_{17} - \frac{\tilde{\mathcal{A}}_{10}\tilde{\mathcal{A}}_{13}}{2\tilde{\mathcal{A}}_2} - \frac{(\tilde{\mathcal{A}}_{10}^2 - 4\tilde{\mathcal{A}}_2\tilde{\mathcal{A}}_3)(\tilde{\mathcal{A}}_{18}\tilde{\mathcal{A}}_{20} + 2\tilde{\mathcal{A}}_8\tilde{\mathcal{A}}_{16})}{2\tilde{\mathcal{A}}_2(\tilde{\mathcal{A}}_{18}^2 - 4\tilde{\mathcal{A}}_4\tilde{\mathcal{A}}_8)}\,.
\end{aligned}
$$

Coefficients $\breve{\mathcal{A}}_i$ for $i \in [6,9]$ vanish, which when considering a high-k limit, are seen to contribute at a lower k value than the rest of the coefficients.

C.2 | Vector Sector

The vector perturbations start off with the action (7.15) where $\mathcal{C}_i$ coefficients are given by

$$
\begin{aligned}
\mathcal{C}_1 &= \frac{1}{18}\big[2G_{\text{Tele},T_{\text{ax}}} + 3[3(G_4 - G_{\text{Tele},T}) + X(-6G_{4,X} + 3G_{5,\phi} + 2G_{\text{Tele},J_{10}} + 6G_{\text{Tele},J_8}\\
&\quad + 3G_{\text{Tele},J_5} - 3H\dot{\phi}G_{5,X})]\big]\,,\\
\mathcal{C}_2 &= G_{\text{Tele},T_{\text{vec}}} + \tfrac{X}{18}\left[-2G_{\text{Tele},J_8} - 5G_{\text{Tele},J_5} - 6G_{\text{Tele},J_3} + 2XG_{\text{Tele},J_6}\right]\,,\\
\mathcal{C}_3 &= 2(G_4 - G_{\text{Tele},T}) + X[-4G_{4,X} + 2G_{5,\phi} + 4G_{\text{Tele},J_8} + G_{\text{Tele},J_5} - 2H\dot{\phi}G_{5,X}]\,,\\
\mathcal{C}_4 &= \mathcal{C}_2\,,\\
\mathcal{C}_5 &= \frac{1}{9}\big[3X(4G_{\text{Tele},J_{10}} + 3G_{\text{Tele},J_5}) + 4G_{\text{Tele},T_{\text{ax}}}\big]\,,\\
\mathcal{C}_6 &= G_{\text{Tele},T_{\text{vec}}} + \frac{2X}{9}[-2G_{\text{Tele},J_8} - 5G_{\text{Tele},J_5} + 3G_{\text{Tele},J_3} + 2XG_{\text{Tele},J_6}]\,,\\
\mathcal{C}_7 &= \frac{1}{18}\big[2G_{\text{Tele},T_{\text{ax}}} + 9(G_4 - G_{\text{Tele},T}) - 3X(6G_{4,X} - 3G_{5,\phi} + 4G_{\text{Tele},J_{10}} - 6G_{\text{Tele},J_5}\\
&\quad + 3H\dot{\phi}G_{5,X})\big]\,,\\
\mathcal{C}_8 &= -\mathcal{C}_3\,,\\
\mathcal{C}_9 &= -\frac{1}{9}\big[9(G_4 - G_{\text{Tele},T}) - 2G_{\text{Tele},T_{\text{ax}}} + 3X(-6G_{4,X} + 3G_{5,\phi} - 3H\dot{\phi}G_{5,X} + G_{\text{Tele},J_{10}}\\
&\quad + 3G_{\text{Tele},J_5})\big]\,,\\
\mathcal{C}_{10} &= -\big[-4XH^2G_{5X}\dot{\phi} + H(4G_4 - 8XG_{4X} + 4XG_{5,\phi} - 4X^2G_{5\phi X} - 4G_{\text{Tele},T}\\
&\quad + 6G_{\text{Tele},T_{\text{vec}}} - 6XG_{5,X}\ddot{\phi} - 4X^2G_{5,XX}\ddot{\phi}) + \dot{\phi}(2XG_{5\phi\phi} + 2G_{4,\phi} - 4XG_{4,\phi X} - G_{\text{Tele},I_2}\\
&\quad - 2XG_{5,X}\dot{H} - 2G_{4,X}\ddot{\phi} - 4XG_{4,XX}\ddot{\phi} + 2G_{5,\phi}\ddot{\phi} + 2XG_{5,\phi X}\ddot{\phi})\big]\,,
\end{aligned}
$$

$$
\begin{aligned}
\mathcal{C}_{11} &= -\frac{1}{9}\big(18(G_4 - G_{\mathrm{Tele},T}) - X(36G_{4,X} - 18G_{5,\phi} - 3G_{\mathrm{Tele},J_3} - 10G_{\mathrm{Tele},J_5} + 4XG_{\mathrm{Tele},J_6} \\
&\quad - 4G_{\mathrm{Tele},J_8} - 18G_{\mathrm{Tele},T_{\mathrm{vec}}} + 18HG_{5,X}\dot{\phi})\,, \\
\mathcal{C}_{12} &= \mathcal{C}_5\,, \\
\mathcal{C}_{13} &= 4\mathcal{C}_{10}\,, \\
\mathcal{C}_{14} &= 4\mathcal{C}_{12}\,, \\
\mathcal{C}_{15} &= \frac{8}{9}\big[-3X(G_{\mathrm{Tele},J_{10}} + 3G_{\mathrm{Tele},J_5}) + 2G_{\mathrm{Tele},T_{\mathrm{ax}}} + 9G_{\mathrm{Tele},T}\big]\,, \\
\mathcal{C}_{16} &= 2\mathcal{C}_2\,.
\end{aligned}
$$

The fully gauge invariant action is given by Eq. (7.20) where the coefficients $\tilde{\mathcal{C}}_i$ are

$$
\begin{aligned}
\tilde{\mathcal{C}}_1 &= \frac{1}{18}\big[9(G_4 - G_{\mathrm{Tele},T}) + 2G_{\mathrm{Tele},T_{\mathrm{ax}}} + 3X(-6G_{4,X} + 3G_{5,\phi} + 2G_{\mathrm{Tele},J_{10}} + 6G_{\mathrm{Tele},J_8} \\
&\quad + 3G_{\mathrm{Tele},J_5} - 3H\dot{\phi}G_{5,X})\big]\,, \\
\tilde{\mathcal{C}}_2 &= -\frac{1}{9}\big[3X(4G_{\mathrm{Tele},J_{10}} + 3G_{\mathrm{Tele},J_5}) + 4G_{\mathrm{Tele},T_{\mathrm{ax}}}\big]\,, \\
\tilde{\mathcal{C}}_3 &= -\tilde{\mathcal{C}}_2\,, \\
\tilde{\mathcal{C}}_4 &= \frac{1}{18}\big[18G_{\mathrm{Tele},T_{\mathrm{vec}}} + X(-2G_{\mathrm{Tele},J_8} + 2XG_{\mathrm{Tele},J_6} - 5G_{\mathrm{Tele},J_5} - 6G_{\mathrm{Tele},J_3})\big]\,, \\
\tilde{\mathcal{C}}_5 &= \frac{2H}{9}\big(X(-4G_{\mathrm{Tele},J_8} + 4XG_{\mathrm{Tele},J_6} - 30G_{\mathrm{Tele},J_5} - 3G_{\mathrm{Tele},J_3}) + 9G_{\mathrm{Tele},T_{\mathrm{vec}}} + 9\dot{H}(X(4G_{\mathrm{Tele},T_{\mathrm{vec}}J_8} \\
&\quad - 4XG_{\mathrm{Tele},T_{\mathrm{vec}}J_6} + 10G_{\mathrm{Tele},T_{\mathrm{vec}}J_5} + 3G_{\mathrm{Tele},T_{\mathrm{vec}}J_3}) + 18G_{\mathrm{Tele},T_{\mathrm{vec}}T_{\mathrm{vec}}} + \frac{X}{3}(-8G_{\mathrm{Tele},TJ_8} \\
&\quad + 8XG_{\mathrm{Tele},TJ_6} - 20G_{\mathrm{Tele},TJ_5} - 6G_{\mathrm{Tele},TJ_3}) - 30G_{\mathrm{Tele},TT_{\mathrm{vec}}} + 12G_{\mathrm{Tele},TT})\big) + \dot{\phi}\big(-G_{\mathrm{Tele},I_2} \\
&\quad + \frac{X}{9}(-4G_{\mathrm{Tele},\phi J_8} + 4XG_{\mathrm{Tele},\phi J_6} - 10G_{\mathrm{Tele},\phi J_5} - 3G_{\mathrm{Tele},\phi J_3}) - 2G_{\mathrm{Tele},\phi T_{\mathrm{vec}}} + 2G_{\mathrm{Tele},\phi T} \\
&\quad + \frac{X\dot{H}}{3}(-4G_{\mathrm{Tele},I_2J_8} + 4XG_{\mathrm{Tele},I_2J_6} - 10G_{\mathrm{Tele},I_2J_5} - 3G_{\mathrm{Tele},I_2J_3}) - 6\dot{H}(G_{\mathrm{Tele},T_{\mathrm{vec}}I_2} - G_{\mathrm{Tele},TI_2})\big) \\
&\quad + H\ddot{\phi}\big(\frac{X}{3}(-4G_{\mathrm{Tele},I_2J_8} + 4XG_{\mathrm{Tele},I_2J_6} - 10G_{\mathrm{Tele},I_2J_5} - 3G_{\mathrm{Tele},I_2J_3}) - 6(G_{\mathrm{Tele},T_{\mathrm{vec}}I_2} \\
&\quad - G_{\mathrm{Tele},TI_2})\big) + \frac{1}{9}\dot{\phi}\ddot{\phi}\big(-4G_{\mathrm{Tele},J_8} + 8XG_{\mathrm{Tele},J_6} - 10G_{\mathrm{Tele},J_5} - 3G_{\mathrm{Tele},J_3} + X(-4G_{\mathrm{Tele},XJ_8} \\
&\quad + 4XG_{\mathrm{Tele},XJ_6} - 10G_{\mathrm{Tele},XJ_5} - 3G_{\mathrm{Tele},XJ_3}) - 18G_{\mathrm{Tele},XT_{\mathrm{vec}}} + 18G_{\mathrm{Tele},XT}\big)\,, \\
\tilde{\mathcal{C}}_6 &= -\frac{1}{9}\big[9(G_4 - G_{\mathrm{Tele},T}) - 2G_{\mathrm{Tele},T_{\mathrm{ax}}} + 3X(-6G_{4,X} + 3G_{5,\phi} + G_{\mathrm{Tele},J_{10}} + 3G_{\mathrm{Tele},J_5} - 3H\dot{\phi}G_{5,X})\big]\,, \\
\tilde{\mathcal{C}}_7 &= \frac{1}{9}\big[X(6G_{\mathrm{Tele},J_{10}} - 4G_{\mathrm{Tele},J_8} + 4XG_{\mathrm{Tele},J_6} + 8G_{\mathrm{Tele},J_5} - 3G_{\mathrm{Tele},J_3}) - 2(9G_{\mathrm{Tele},T_{\mathrm{vec}}} + 2G_{\mathrm{Tele},T_{\mathrm{ax}}})\big]\,, \\
\tilde{\mathcal{C}}_8 &= \frac{1}{18}\big[9(G_4 - G_{\mathrm{Tele},T}) + 2G_{\mathrm{Tele},T_{\mathrm{ax}}} - 3X(6G_{4,X} - 3G_{5,\phi} + 4G_{\mathrm{Tele},J_{10}} - 6G_{\mathrm{Tele},J_5} + 3H\dot{\phi}G_{5,X})\big]\,, \\
\tilde{\mathcal{C}}_9 &= \frac{1}{9}\big[9G_{\mathrm{Tele},T_{\mathrm{vec}}} + 2X(-2G_{\mathrm{Tele},J_8} + 2XG_{\mathrm{Tele},J_6} - 5G_{\mathrm{Tele},J_5} + 3G_{\mathrm{Tele},J_3})\big]\,,
\end{aligned}
$$

and no further steps are required since the system already has a diagionalised kinetic matrix.

References

[1] J. Beltrán Jiménez, L. Heisenberg, and T. S. Koivisto. The Geometrical Trinity of Gravity. *Universe*, 5(7):173, 2019.

[2] N. Aghanim et al. Planck 2018 results. VI. Cosmological parameters. *Astron. Astrophys.*, 641:A6, 2020. [Erratum: Astron.Astrophys. 652, C4 (2021)].

[3] C. M. Will. *Theory and Experiment in Gravitational Physics*. Cambridge University Press, 2018.

[4] A. Aghamousa et al. The DESI Experiment Part I: Science,Targeting, and Survey Design. 10 2016.

[5] A. Aghamousa et al. The DESI Experiment Part II: Instrument Design. 10 2016.

[6] E. Majerotto et al. Probing deviations from General Relativity with the Euclid spectroscopic survey. *Mon. Not. Roy. Astron. Soc.*, 424:1392–1408, 2012.

[7] C. Di Porto, L. Amendola, and E. Branchini. Simultaneous constraints on bias, normalization and growth index through power spectrum measurements. *Mon. Not. Roy. Astron. Soc.*, 423:L97–L101, 2012.

[8] Ž. Ivezić et al. LSST: from Science Drivers to Reference Design and Anticipated Data Products. *Astrophys. J.*, 873(2):111, 2019.

[9] C. W. Misner, K. S. Thorne, and J. A. Wheeler. *Gravitation*. Number pt. 3 in Gravitation. W. H. Freeman, San Francisco, 1973.

[10] R. S. Westfall. Hooke and the law of universal gravitation: A reappraisal af a reappraisal. *The British Journal for the History of Science*, 3(3):245–261, 1967.

[11] H. A. Lorentz. *Considerations on Gravitation*, pages 1038–1052. Springer Netherlands, Dordrecht, 2007.

[12] W. T. B. Kelvin. *Popular Lectures and Addresses: Constitution of matter*. Nature series. Macmillan, 1889.

[13] I. Newton, A. Motte, and J. Machin. *The Mathematical Principles of Natural Philosophy*. Number v. 1 in The Mathematical Principles of Natural Philosophy. B. Motte, 1729.

[14] F. Tisserand. Les travaux de Le Verrier. *Annales de l'Observatoire de Paris*, 15:23–43, January 1880.

[15] U. J. Le Verrier. Theorie du mouvement de Mercure. *Annales de l'Observatoire de Paris*, 5:1, January 1859.

[16] G. B. Airy. Account of some circumstances historically connected with the discovery of the planet exterior to Uranus. *MNRAS*, 7:121–144, November 1846.

[17] A. Bauch and S. Weyers. New experimental limit on the validity of local position invariance. *Phys. Rev. D*, 65:081101, 2002.

[18] I. I. Shapiro. Fourth Test of General Relativity. *Phys. Rev. Lett.*, 13:789–791, 1964.

[19] S. S. Shapiro, J. L. Davis, D. E. Lebach, and J. S. Gregory. Measurement of the Solar Gravitational Deflection of Radio Waves using Geodetic Very-Long-Baseline Interferometry Data, 1979-1999. *Phys. Rev. Lett.*, 92:121101, 2004.

[20] H. Thirring. Republication of: On the formal analogy between the basic electromagnetic equations and Einstein‘s gravity equations in first approximation. *Phys. Z.*, 19:204–205, 1918.

[21] J. Lense and H. Thirring. Ueber den Einfluss der Eigenrotation der Zentralkoerper auf die Bewegung der Planeten und Monde nach der Einsteinschen Gravitationstheorie. *Phys. Z.*, 19:156–163, 1918.

[22] R. Aldrovandi and J. G. Pereira. *Teleparallel Gravity: An Introduction*. Springer, 2013.

[23] R. Aldrovandi, P. B. Barros, and J. G. Pereira. Spin and anholonomy in general relativity. 2 2004.

[24] W. Heisenberg. Uber den anschaulichen Inhalt der quantentheoretischen Kinematik und Mechanik. *Z. Phys.*, 43:172–198, 1927.

[25] R. Penrose. Gravitational collapse and space-time singularities. *Phys. Rev. Lett.*, 14:57–59, 1965.

[26] S. W. Hawking and G. F. R. Ellis. *The Large Scale Structure of Space-Time*. Cambridge Monographs on Mathematical Physics. Cambridge University Press, 1975.

[27] J. M. M. Senovilla and D. Garfinkle. The 1965 Penrose singularity theorem. *Class. Quant. Grav.*, 32(12):124008, 2015.

[28] R. A. Carrigan and W. P. Trower. Magnetic Monopoles. *Nature*, 305:673–678, 1983.

[29] R. H. Dicke. *Gravitation and the Universe*. American Philosophical Society: Memoirs of the American Philosophical Society. American Philosophical Society, 1970.

[30] Y. B. Zeldovich and M. Y. Khlopov. On the Concentration of Relic Magnetic Monopoles in the Universe. *Phys. Lett. B*, 79:239–241, 1978.

[31] J. Preskill. Cosmological Production of Superheavy Magnetic Monopoles. *Phys. Rev. Lett.*, 43:1365, 1979.

[32] A. Einstein. Cosmological Considerations in the General Theory of Relativity. *Sitzungsber. Preuss. Akad. Wiss. Berlin (Math. Phys.)*, 1917:142–152, 1917.

[33] E. Hubble. A relation between distance and radial velocity among extra-galactic nebulae. *Proc. Nat. Acad. Sci.*, 15:168–173, 1929.

[34] A. G. Riess et al. Observational evidence from supernovae for an accelerating universe and a cosmological constant. *Astron. J.*, 116:1009–1038, 1998.

[35] L. Abbott. The Mystery of the Cosmological Constant. *Sci. Am.*, 258:106–113, 1988.

[36] D. J. Eisenstein and W. Hu. Baryonic features in the matter transfer function. *Astrophys. J.*, 496:605, 1998.

[37] C. Ma and E. Bertschinger. Cosmological perturbation theory in the synchronous and conformal Newtonian gauges. *Astrophys. J.*, 455:7–25, 1995.

[38] P. J. E. Peebles and J. T. Yu. Primeval adiabatic perturbation in an expanding universe. *Astrophys. J.*, 162:815–836, 1970.

[39] Y. B. Zeldovich. The Cosmological constant and the theory of elementary particles. *Sov. Phys. Usp.*, 11:381–393, 1968.

[40] S. Kalyana Rama. Can string theory avoid cosmological singularities? *Phys. Lett. B*, 408:91–97, 1997.

[41] A. Ashtekar and M. Bojowald. Quantum geometry and the Schwarzschild singularity. *Class. Quant. Grav.*, 23:391–411, 2006.

[42] G. Bertone, D. Hooper, and J. Silk. Particle dark matter: Evidence, candidates and constraints. *Phys. Rept.*, 405:279–390, 2005.

[43] S. Weinberg. The Cosmological Constant Problem. *Rev. Mod. Phys.*, 61:1–23, 1989.

[44] S. Appleby and E. V. Linder. The Well-Tempered Cosmological Constant. *JCAP*, 07:034, 2018.

[45] B. P. Abbott et al. Observation of Gravitational Waves from a Binary Black Hole Merger. *Phys. Rev. Lett.*, 116(6):061102, 2016.

[46] R. A. Hulse and J. H. Taylor. Discovery of a pulsar in a binary system. *Astrophys. J. Lett.*, 195:L51–L53, 1975.

[47] J. H. Taylor and J. M. Weisberg. A new test of general relativity: Gravitational radiation and the binary pulsar PS R 1913+16. *Astrophys. J.*, 253:908–920, 1982.

[48] B. P. Abbott et al. Sensitivity of the Advanced LIGO detectors at the beginning of gravitational wave astronomy. *Phys. Rev. D*, 93(11):112004, 2016. [Addendum: Phys.Rev.D 97, 059901 (2018)].

[49] M. Armano et al. The LISA Pathfinder Mission. *J. Phys. Conf. Ser.*, 610(1):012005, 2015.

[50] P. Auclair et al. Cosmology with the Laser Interferometer Space Antenna. *Living Rev. Rel.*, 26(1):5, 2023.

[51] A. Abramovici et al. LIGO: The Laser interferometer gravitational wave observatory. *Science*, 256:325–333, 1992.

[52] J. R. Smith. The Path to the enhanced and advanced LIGO gravitational-wave detectors. *Class. Quant. Grav.*, 26:114013, 2009.

[53] T. Accadia et al. Virgo: a laser interferometer to detect gravitational waves. *JINST*, 7:P03012, 2012.

[54] F. Acernese et al. Advanced Virgo: a second-generation interferometric gravitational wave detector. *Class. Quant. Grav.*, 32(2):024001, 2015.

[55] T. Akutsu et al. Overview of KAGRA: Detector design and construction history. *PTEP*, 2021(5):05A101, 2021.

[56] H. Luck. The GEO-600 project. *Class. Quant. Grav.*, 14:1471–1476, 1997.

[57] H. Lück et al. Status of the GEO600 detector. *Class. Quant. Grav.*, 23:S71–S78, 2006.

[58] A. Unzicker and T. Case. Translation of Einstein's attempt of a unified field theory with teleparallelism. 3 2005.

[59] E. Cartan. Sur les variétés à connexion affine et la théorie de la relativité généralisée. (première partie). *Annales Sci. Ecole Norm. Sup.*, 40:325–412, 1923.

[60] R. Weitzenböck. *Invariantentheorie*. P. Noordhoff, Groningen, 1923.

[61] C. Brans and R. H. Dicke. Mach's principle and a relativistic theory of gravitation. *Phys. Rev.*, 124:925–935, 1961.

[62] P. G. Bergmann. Comments on the scalar tensor theory. *Int. J. Theor. Phys.*, 1:25–36, 1968.

[63] H. A. Buchdahl. Non-Linear Lagrangians and Cosmological Theory. *Mon. Not. Roy. Astron. Soc.*, 150(1):1–8, 1970.

[64] J. D. Bekenstein. Relativistic gravitation theory for the MOND paradigm. *Phys. Rev. D*, 70:083509, 2004. [Erratum: Phys.Rev.D 71, 069901 (2005)].

[65] M. Bojowald. Absence of singularity in loop quantum cosmology. *Phys. Rev. Lett.*, 86:5227–5230, 2001.

[66] G. W. Horndeski. Second-order scalar-tensor field equations in a four-dimensional space. *Int. J. Theor. Phys.*, 10:363–384, 1974.

[67] S. Bahamonde and J. Levi Said. Teleparallel Gravity: Foundations and Observational Constraints—Editorial. *Universe*, 7(8):269, 2021.

[68] M. Krssak, R. J. van den Hoogen, J. G. Pereira, C. G. Böhmer, and A. A. Coley. Teleparallel theories of gravity: illuminating a fully invariant approach. *Class. Quant. Grav.*, 36(18):183001, 2019.

[69] R. Ferraro and F. Fiorini. Modified teleparallel gravity: Inflation without inflaton. *Phys. Rev. D*, 75:084031, 2007.

[70] K. Hayashi and T. Shirafuji. New general relativity. *Phys. Rev. D*, 19:3524–3553, 1979. [Addendum: Phys.Rev.D 24, 3312–3314 (1982)].

[71] S. Bahamonde, C. G. Böhmer, and M. Wright. Modified teleparallel theories of gravity. *Phys. Rev. D*, 92(10):104042, 2015.

[72] Z. Chen, Y. Wu, and H. Wei. Post-Newtonian Approximation of Teleparallel Gravity Coupled with a Scalar Field. *Nucl. Phys. B*, 894:422–438, 2015.

[73] C. Geng, C. Lee, E. N. Saridakis, and Y. Wu. "Teleparallel" dark energy. *Phys. Lett. B*, 704:384–387, 2011.

[74] D. Lovelock. The Einstein tensor and its generalizations. *J. Math. Phys.*, 12:498–501, 1971.

[75] A. A. Starobinsky. Spectrum of relict gravitational radiation and the early state of the universe. *JETP Lett.*, 30:682–685, 1979.

[76] A. H. Guth. The Inflationary Universe: A Possible Solution to the Horizon and Flatness Problems. *Phys. Rev. D*, 23:347–356, 1981.

[77] K. Sato. First Order Phase Transition of a Vacuum and Expansion of the Universe. *Mon. Not. Roy. Astron. Soc.*, 195:467–479, 1981.

[78] S. Bahamonde, K. F. Dialektopoulos, and J. Levi Said. Can Horndeski Theory be recast using Teleparallel Gravity? *Phys. Rev. D*, 100(6):064018, 2019.

[79] G. W. Horndeski and A. Silvestri. 50 Years of Horndeski Gravity: Past, Present and Future. *Int. J. Theor. Phys.*, 63(2):38, 2024.

[80] B. P. Abbott et al. GW170817: Observation of Gravitational Waves from a Binary Neutron Star Inspiral. *Phys. Rev. Lett.*, 119(16):161101, 2017.

[81] A. Goldstein et al. An Ordinary Short Gamma-Ray Burst with Extraordinary Implications: Fermi-GBM Detection of GRB 170817A. *Astrophys. J. Lett.*, 848(2):L14, 2017.

[82] P. Creminelli and F. Vernizzi. Dark Energy after GW170817 and GRB170817A. *Phys. Rev. Lett.*, 119(25):251302, 2017.

[83] Y. Gong, E. Papantonopoulos, and Z. Yi. Constraints on scalar–tensor theory of gravity by the recent observational results on gravitational waves. *Eur. Phys. J. C*, 78(9):738, 2018.

[84] C. D. Kreisch and E. Komatsu. Cosmological Constraints on Horndeski Gravity in Light of GW170817. *JCAP*, 12:030, 2018.

[85] E. A. Milne. *Relativity, Gravitation and World-structure.* International series of monographs on physics. Clarendon Press, 1935.

[86] P. J. E. Peebles and B. Ratra. The Cosmological Constant and Dark Energy. *Rev. Mod. Phys.*, 75:559–606, 2003.

[87] L. Baudis. Dark matter detection. *J. Phys. G*, 43(4):044001, 2016.

[88] S. Dodelson. *Modern Cosmology.* Academic Press, Amsterdam, 2003.

[89] P. A. R. Ade et al. Planck 2015 results. XIV. Dark energy and modified gravity. *Astron. Astrophys.*, 594:A14, 2016.

[90] S. Aiola et al. The Atacama Cosmology Telescope: DR4 Maps and Cosmological Parameters. *JCAP*, 12:047, 2020.

[91] F. Bianchini et al. Constraints on Cosmological Parameters from the 500 $\deg^2$ SPTpol Lensing Power Spectrum. *Astrophys. J.*, 888:119, 2020.

[92] S. H. Suyu et al. H0LiCOW – I. H0 Lenses in COSMOGRAIL's Wellspring: program overview. *Mon. Not. Roy. Astron. Soc.*, 468(3):2590–2604, 2017.

[93] D. Scolnic et al. The Pantheon+ Analysis: The Full Data Set and Light-curve Release. *Astrophys. J.*, 938(2):113, 2022.

[94] A. G. Adame et al. DESI 2024 VI: Cosmological Constraints from the Measurements of Baryon Acoustic Oscillations. 4 2024.

[95] R. Laureijs, J. Amiaux, S. Arduini, J. Augueres, J. Brinchmann, R. Cole, M. Cropper, C. Dabin, L. Duvet, A. Ealet, et al. Euclid definition study report. *arXiv preprint arXiv:1110.3193*, 2011.

[96] T. Clifton, P. G. Ferreira, A. Padilla, and C. Skordis. Modified Gravity and Cosmology. *Phys. Rept.*, 513:1–189, 2012.

[97] B. D. Fields. The primordial lithium problem. *Ann. Rev. Nucl. Part. Sci.*, 61:47–68, 2011.

[98] P. A. Zyla et al. Review of Particle Physics. *PTEP*, 2020(8):083C01, 2020.

[99] C. Pitrou, A. Coc, J. Uzan, and E. Vangioni. Precision big bang nucleosynthesis with improved Helium-4 predictions. *Phys. Rept.*, 754:1–66, 2018.

[100] P. Di Bari, S. F. King, and A. Merle. Dark Radiation or Warm Dark Matter from long lived particle decays in the light of Planck. *Phys. Lett. B*, 724:77–83, 2013.

[101] A. Rassat, J. L. Starck, P. Paykari, F. Sureau, and J. Bobin. Planck CMB Anomalies: Astrophysical and Cosmological Secondary Effects and the Curse of Masking. *JCAP*, 08:006, 2014.

[102] A. G. Riess, S. Casertano, W. Yuan, L. M. Macri, and D. Scolnic. Large Magellanic Cloud Cepheid Standards Provide a 1% Foundation for the Determination of the Hubble Constant and Stronger Evidence for Physics beyond ΛCDM. *Astrophys. J.*, 876(1):85, 2019.

[103] R. I. Anderson, N. W. Koblischke, and L. Eyer. Small-amplitude Red Giants Elucidate the Nature of the Tip of the Red Giant Branch as a Standard Candle. *Astrophys. J. Lett.*, 963(2):L43, 2024.

[104] K. C. Wong et al. H0LiCOW – XIII. A 2.4 per cent measurement of H0 from lensed quasars: 5.3σ tension between early- and late-Universe probes. *Mon. Not. Roy. Astron. Soc.*, 498(1):1420–1439, 2020.

[105] N. Schöneberg, L. Verde, H. Gil-Marín, and S. Brieden. BAO+BBN revisited — growing the Hubble tension with a 0.7 km/s/Mpc constraint. *JCAP*, 11:039, 2022.

[106] M. S. Madhavacheril et al. The Atacama Cosmology Telescope: DR6 Gravitational Lensing Map and Cosmological Parameters. *Astrophys. J.*, 962(2):113, 2024.

[107] V. Poulin, T. L. Smith, and T. Karwal. The Ups and Downs of Early Dark Energy solutions to the Hubble tension: A review of models, hints and constraints circa 2023. *Phys. Dark Univ.*, 42:101348, 2023.

[108] E. Di Valentino, C. Bøehm, E. Hivon, and F. R. Bouchet. Reducing the H_0 and σ_8 tensions with Dark Matter-neutrino interactions. *Phys. Rev. D*, 97(4):043513, 2018.

[109] K. Jedamzik, L. Pogosian, and G. Zhao. Why reducing the cosmic sound horizon alone can not fully resolve the Hubble tension. *Commun. in Phys.*, 4:123, 2021.

[110] M. Ostrogradsky. Mémoires sur les équations différentielles, relatives au problème des isopérimètres. *Mem. Acad. St. Petersbourg*, 6(4):385–517, 1850.

[111] R. P. Woodard. Ostrogradsky's theorem on Hamiltonian instability. *Scholarpedia*, 10(8):32243, 2015.

[112] T. Kobayashi. Horndeski theory and beyond: a review. *Rept. Prog. Phys.*, 82(8):086901, 2019.

[113] M. Hohmann, L. Järv, and U. Ualikhanova. Covariant formulation of scalar-torsion gravity. *Phys. Rev. D*, 97(10):104011, 2018.

[114] H. Abedi and M. Salti. Multiple field modified gravity and localized energy in teleparallel framework. *Gen. Rel. Grav.*, 47(8):93, 2015.

[115] L. Amendola. Cosmology with nonminimal derivative couplings. *Phys. Lett. B*, 301:175–182, 1993.

[116] C. Deffayet, Gilles Esposito-Farese, and A. Vikman. Covariant Galileon. *Phys. Rev. D*, 79:084003, 2009.

[117] A. Nicolis, R. Rattazzi, and E. Trincherini. The Galileon as a local modification of gravity. *Phys. Rev. D*, 79:064036, 2009.

[118] C. Charmousis, E. J. Copeland, A. Padilla, and P. M. Saffin. General second order scalar-tensor theory, self tuning, and the Fab Four. *Phys. Rev. Lett.*, 108:051101, 2012.

[119] G. Gubitosi and E. V. Linder. Purely Kinetic Coupled Gravity. *Phys. Lett. B*, 703:113–118, 2011.

[120] S. M. Carroll. *Spacetime and Geometry.* Cambridge University Press, 2019.

[121] A. Einstein. Approximative Integration of the Field Equations of Gravitation. *Sitzungsber. Preuss. Akad. Wiss. Berlin (Math. Phys.)*, 1916:688–696, 1916.

[122] A. Einstein. Über Gravitationswellen. *Sitzungsber. Preuss. Akad. Wiss. Berlin (Math. Phys.)*, 1918:154–167, 1918.

[123] C. M. Will. The Confrontation between General Relativity and Experiment. *Living Rev. Rel.*, 17:4, 2014.

[124] T. M. C. Abbott et al. Dark Energy Survey year 1 results: Cosmological constraints from galaxy clustering and weak lensing. *Phys. Rev. D*, 98(4):043526, 2018.

[125] G. Benevento, W. Hu, and M. Raveri. Can Late Dark Energy Transitions Raise the Hubble constant? *Phys. Rev. D*, 101(10):103517, 2020.

[126] S. Joudaki et al. KiDS-450 + 2dFLenS: Cosmological parameter constraints from weak gravitational lensing tomography and overlapping redshift-space galaxy clustering. *Mon. Not. Roy. Astron. Soc.*, 474(4):4894–4924, 2018.

[127] A. Einstein. On the electrodynamics of moving bodies. *Annalen Phys.*, 17:891–921, 1905.

[128] A. Einstein. The foundation of the general theory of relativity. *Annalen Phys.*, 49(7):769–822, 1916.

[129] Aldrovandi, R. and Pereira, J. G. *An Introduction To Geometrical Physics.* World Scientific Publishing Company, 1995.

[130] R. V. Eotvos, D. Pekar, and E. Fekete. Contributions to the Law of Proportionality of Inertia and Gravity. *Annalen Phys.*, 68:11–66, 1922.

[131] P. Touboul et al. MICROSCOPE Mission: First Results of a Space Test of the Equivalence Principle. *Phys. Rev. Lett.*, 119(23):231101, 2017.

[132] P. Touboul et al. MICROSCOPE Mission: Final Results of the Test of the Equivalence Principle. *Phys. Rev. Lett.*, 129(12):121102, 2022.

[133] Hermann Minkowski. *Raum und Zeit*, volume 10, page 104–111. 1909.

[134] D. Hilbert. Die Grundlagen der Physik. 1. *Gott. Nachr.*, 27:395–407, 1915.

[135] A. Einstein. Explanation of the Perihelion Motion of Mercury from the General Theory of Relativity. *Sitzungsber. Preuss. Akad. Wiss. Berlin (Math. Phys.)*, 1915:831–839, 1915.

[136] J. Soldner. Über die ablenkung eines lichtstrahls von seiner geradlinigen bewegung durch die attraktion eines weltkörpers, an welchem er nahe vorbeigeht. *Annalen der Physik*, 370(15):593–604, 1921.

[137] A. Einstein. On The influence of gravitation on the propagation of light. *Annalen Phys.*, 35:898–908, 1911.

[138] F. W. Dyson, A. S. Eddington, and C. Davidson. A Determination of the Deflection of Light by the Sun's Gravitational Field, from Observations Made at the Total Eclipse of May 29, 1919. *Phil. Trans. Roy. Soc. Lond. A*, 220:291–333, 1920.

[139] B. Bertotti, L. Iess, and P. Tortora. A test of general relativity using radio links with the Cassini spacecraft. *Nature*, 425:374–376, 2003.

[140] A Einstein. Prinzipielles zur allgemeinen relativitätstheorie. *Ann. Phys.*, 360(4):241–244, January 1918.

[141] I. Ciufolini and E. C. Pavlis. A confirmation of the general relativistic prediction of the Lense-Thirring effect. *Nature*, 431:958–960, 2004.

[142] C. W. F. Everitt et al. Gravity Probe B: Final Results of a Space Experiment to Test General Relativity. *Phys. Rev. Lett.*, 106:221101, 2011.

[143] I. Ciufolini, A. Paolozzi, E. Pavlis, J. Ries, V. Gurzadyan, R. Koenig, R. Matzner, R. Penrose, and G. Sindoni. Testing General Relativity and gravitational physics using the LARES satellite. *Eur. Phys. J. Plus*, 127:133, 2012.

[144] I. Ciufolini, A. Paolozzi, E. C. Pavlis, G. Sindoni, J. Ries, R. Matzner, R. Koenig, C. Paris, V. Gurzadyan, and R. Penrose. An Improved Test of the General Relativistic Effect of Frame-Dragging Using the LARES and LAGEOS Satellites. *Eur. Phys. J. C*, 79(10):872, 2019.

[145] I. Ciufolini et al. First results of the LARES 2 space experiment to test the general theory of relativity. *Eur. Phys. J. Plus*, 138(11):1054, 2023.

[146] J. M. Weisberg, D. J. Nice, and J. H. Taylor. Timing Measurements of the Relativistic Binary Pulsar PSR B1913+16. *Astrophys. J.*, 722:1030–1034, 2010.

[147] Joel M. Weisberg and Yuping Huang. Relativistic Measurements from Timing the Binary Pulsar PSR B1913+16. *Astrophys. J.*, 829(1):55, 2016.

[148] A. G. Lyne et al. A Double - pulsar system - A Rare laboratory for relativistic gravity and plasma physics. *Science*, 303:1153–1157, 2004.

[149] M. Kramer et al. Tests of general relativity from timing the double pulsar. *Science*, 314:97–102, 2006.

[150] Robert H. Brandenberger, Viatcheslav F. Mukhanov, and A. Sornborger. A Cosmological theory without singularities. *Phys. Rev. D*, 48:1629–1642, 1993.

[151] M. Novello and S. E. P. Bergliaffa. Bouncing Cosmologies. *Phys. Rept.*, 463:127–213, 2008.

[152] R. Brandenberger and P. Peter. Bouncing Cosmologies: Progress and Problems. *Found. Phys.*, 47(6):797–850, 2017.

[153] S. Perlmutter et al. Measurements of Ω and Λ from 42 High Redshift Supernovae. *Astrophys. J.*, 517:565–586, 1999.

[154] G. F. Smoot. COBE observations and results. *AIP Conf. Proc.*, 476(1):1–10, 1999.

[155] P. A. R. Ade et al. Planck 2015 results. XIII. Cosmological parameters. *Astron. Astrophys.*, 594:A13, 2016.

[156] E. Komatsu et al. Seven-Year Wilkinson Microwave Anisotropy Probe (WMAP) Observations: Cosmological Interpretation. *Astrophys. J. Suppl.*, 192:18, 2011.

[157] E. Di Valentino. A combined analysis of the H_0 late time direct measurements and the impact on the Dark Energy sector. *Mon. Not. Roy. Astron. Soc.*, 502(2):2065–2073, 2021.

[158] A. G. Riess et al. A Comprehensive Measurement of the Local Value of the Hubble Constant with 1 km s^{-1} Mpc^{-1} Uncertainty from the Hubble Space Telescope and the SH0ES Team. *Astrophys. J. Lett.*, 934(1):L7, 2022.

[159] A. Banerjee, E. Colgáin, M. Sasaki, M. M. Sheikh-Jabbari, and T. Yang. On problems with cosmography in cosmic dark ages. *Phys. Lett. B*, 818:136366, 2021.

[160] E. Lusso, E. Piedipalumbo, G. Risaliti, M. Paolillo, S. Bisogni, E. Nardini, and L. Amati. Tension with the flat ΛCDM model from a high-redshift Hubble diagram of supernovae, quasars, and gamma-ray bursts. *Astron. Astrophys.*, 628:L4, 2019.

[161] G. Risaliti and E. Lusso. Cosmological constraints from the Hubble diagram of quasars at high redshifts. *Nature Astron.*, 3(3):272–277, 2019.

[162] T. Abel, G. L. Bryan, and M. L. Norman. The formation of the first star in the Universe. *Science*, 295:93, 2002.

[163] L. Verde, P. Protopapas, and R. Jimenez. Planck and the local Universe: Quantifying the tension. *Phys. Dark Univ.*, 2:166–175, 2013.

[164] L. Perivolaropoulos and F. Skara. Challenges for ΛCDM: An update. *New Astron. Rev.*, 95:101659, 2022.

[165] Y. Akrami et al. *Modified Gravity and Cosmology: An Update by the CANTATA Network*. Springer, 2021.

[166] S. Capozziello. Curvature quintessence. *Int. J. Mod. Phys. D*, 11:483–492, 2002.

[167] S. Capozziello and M. De Laurentis. Extended Theories of Gravity. *Phys. Rept.*, 509:167–321, 2011.

[168] S. Nojiri and S. D. Odintsov. Unified cosmic history in modified gravity: from $f(R)$ theory to Lorentz non-invariant models. *Phys. Rept.*, 505:59–144, 2011.

[169] S. Nojiri, S. D. Odintsov, and V. K. Oikonomou. Modified Gravity Theories on a Nutshell: Inflation, Bounce and Late-time Evolution. *Phys. Rept.*, 692:1–104, 2017.

[170] A. Joyce, L. Lombriser, and F. Schmidt. Dark Energy Versus Modified Gravity. *Ann. Rev. Nucl. Part. Sci.*, 66:95–122, 2016.

[171] S. Capozziello and M. Francaviglia. Extended Theories of Gravity and their Cosmological and Astrophysical Applications. *Gen. Rel. Grav.*, 40:357–420, 2008.

[172] A. D. Linde. A New Inflationary Universe Scenario: A Possible Solution of the Horizon, Flatness, Homogeneity, Isotropy and Primordial Monopole Problems. *Phys. Lett. B*, 108:389–393, 1982.

[173] S. Bahamonde, K. F. Dialektopoulos, C. Escamilla-Rivera, G. Farrugia, V. Gakis, M. Hendry, M. Hohmann, J. Levi Said, J. Mifsud, and E. Di Valentino. Teleparallel gravity: from theory to cosmology. *Rept. Prog. Phys.*, 86(2):026901, 2023.

[174] V. Faraoni and S. Capozziello. *Beyond Einstein Gravity: A Survey of Gravitational Theories for Cosmology and Astrophysics*. Springer, Dordrecht, 2011.

[175] A. De Felice and S. Tsujikawa. Generalized Brans-Dicke theories. *JCAP*, 07:024, 2010.

[176] C. Deffayet, S. Deser, and G. Esposito-Farese. Generalized Galileons: All scalar models whose curved background extensions maintain second-order field equations and stress-tensors. *Phys. Rev. D*, 80:064015, 2009.

[177] C. Deffayet, X. Gao, D. A. Steer, and G. Zahariade. From k-essence to generalised Galileons. *Phys. Rev. D*, 84:064039, 2011.

[178] N. Chow and J. Khoury. Galileon Cosmology. *Phys. Rev. D*, 80:024037, 2009.

[179] C. Deffayet, O. Pujolas, I. Sawicki, and A. Vikman. Imperfect Dark Energy from Kinetic Gravity Braiding. *JCAP*, 10:026, 2010.

[180] C. Wetterich. Cosmology and the Fate of Dilatation Symmetry. *Nucl. Phys. B*, 302:668–696, 1988.

[181] B. Ratra and P. J. E. Peebles. Cosmological Consequences of a Rolling Homogeneous Scalar Field. *Phys. Rev. D*, 37:3406, 1988.

[182] S. D. Odintsov and V. K. Oikonomou. The reconstruction of $f(\phi)R$ and mimetic gravity from viable slow-roll inflation. *Nucl. Phys. B*, 929:79–112, 2018.

[183] C. Germani and A. Kehagias. New Model of Inflation with Non-minimal Derivative Coupling of Standard Model Higgs Boson to Gravity. *Phys. Rev. Lett.*, 105:011302, 2010.

[184] C. Armendariz-Picon, T. Damour, and V. F. Mukhanov. k-inflation. *Phys. Lett. B*, 458:209–218, 1999.

[185] T. Chiba, T. Okabe, and M. Yamaguchi. Kinetically driven quintessence. *Phys. Rev. D*, 62:023511, 2000.

[186] T. P. Sotiriou and V. Faraoni. $f(R)$ Theories Of Gravity. *Rev. Mod. Phys.*, 82:451–497, 2010.

[187] A. De Felice, S. Tsujikawa, J. Elliston, and R. Tavakol. Chaotic inflation in modified gravitational theories. *JCAP*, 08:021, 2011.

[188] S. A. Appleby, A. De Felice, and E. V. Linder. Fab 5: Noncanonical Kinetic Gravity, Self Tuning, and Cosmic Acceleration. *JCAP*, 10:060, 2012.

[189] T. Kobayashi, M. Yamaguchi, and J. Yokoyama. Generalized G-inflation: Inflation with the most general second-order field equations. *Prog. Theor. Phys.*, 126:511–529, 2011.

[190] J. Gleyzes, D. Langlois, F. Piazza, and F. Vernizzi. Essential Building Blocks of Dark Energy. *JCAP*, 08:025, 2013.

[191] K. Koyama. Cosmological Tests of Modified Gravity. *Rept. Prog. Phys.*, 79(4):046902, 2016.

[192] P. Martin-Moruno, N. J. Nunes, and F. S. N. Lobo. Horndeski theories self-tuning to a de Sitter vacuum. *Phys. Rev. D*, 91(8):084029, 2015.

[193] E. Babichev, C. Charmousis, and A. Lehébel. Black holes and stars in Horndeski theory. *Class. Quant. Grav.*, 33(15):154002, 2016.

[194] E. Babichev, C. Charmousis, and M. Hassaine. Charged Galileon black holes. *JCAP*, 05:031, 2015.

[195] E. Babichev, C. Charmousis, and A. Lehébel. Asymptotically flat black holes in Horndeski theory and beyond. *JCAP*, 04:027, 2017.

[196] A. Maselli, H. O. Silva, M. Minamitsuji, and E. Berti. Neutron stars in Horndeski gravity. *Phys. Rev. D*, 93(12):124056, 2016.

[197] A. Cisterna, T. Delsate, and M. Rinaldi. Neutron stars in general second order scalar-tensor theory: The case of nonminimal derivative coupling. *Phys. Rev. D*, 92(4):044050, 2015.

[198] H. Weyl. Gravitation and electricity. *Sitzungsber. Preuss. Akad. Wiss. Berlin (Math. Phys.)*, 1918:465, 1918.

[199] L. O'Raifeartaigh. *The dawning of gauge theory.* Princeton Univ. Press, Princeton, NJ, USA, 1997.

[200] L. O'Raifeartaigh and N. Straumann. Gauge theory: Historical origins and some modern developments. *Rev. Mod. Phys.*, 72:1–23, 2000.

[201] F. W. Hehl, J. D. McCrea, E. W. Mielke, and Y. Ne'eman. Metric affine gauge theory of gravity: Field equations, Noether identities, world spinors, and breaking of dilation invariance. *Phys. Rept.*, 258:1–171, 1995.

[202] S. Sternberg. *Lectures on Differential Geometry.* AMS Chelsea Publishing Series. American Mathematical Society, 1999.

[203] K. Hayashi and T. Nakano. Extended translation invariance and associated gauge fields. *Prog. Theor. Phys.*, 38:491–507, 1967.

[204] Tomas Ortin. *Gravity and strings.* Cambridge Monographs on Mathematical Physics. Cambridge Univ. Press, 3 2004.

[205] M. Krššák and E. N. Saridakis. The covariant formulation of $f(T)$ gravity. *Class. Quant. Grav.*, 33(11):115009, 2016.

[206] Y. Cai, S. Capozziello, M. De Laurentis, and E. N. Saridakis. $f(T)$ teleparallel gravity and cosmology. *Rept. Prog. Phys.*, 79(10):106901, 2016.

[207] G. M. Kremer, M. G. Richarte, and F. Teston. Jeans Instability in a Universe with Dissipation. *Phys. Rev. D*, 97(2):023515, 2018.

[208] V. C. de Andrade and J. G. Pereira. Gravitational Lorentz force and the description of the gravitational interaction. *Phys. Rev. D*, 56:4689–4695, 1997.

[209] F. W. Hehl, P. Von Der Heyde, G. D. Kerlick, and J. M. Nester. General Relativity with Spin and Torsion: Foundations and Prospects. *Rev. Mod. Phys.*, 48:393–416, 1976.

[210] K. S. Stelle. Classical Gravity with Higher Derivatives. *Gen. Rel. Grav.*, 9:353–371, 1978.

[211] S. Nojiri, S. D. Odintsov, and M. Sasaki. Gauss-Bonnet dark energy. *Phys. Rev. D*, 71:123509, 2005.

[212] T. Harko, F. S. N. Lobo, G. Otalora, and E. N. Saridakis. $f(T, \mathcal{T})$ gravity and cosmology. *JCAP*, 12:021, 2014.

[213] S. Bahamonde, K. F. Dialektopoulos, V. Gakis, and J. Levi Said. Reviving Horndeski theory using teleparallel gravity after GW170817. *Phys. Rev. D*, 101(8):084060, 2020.

[214] S. Bahamonde, C. G. Böhmer, and M. Krššák. New classes of modified teleparallel gravity models. *Phys. Lett. B*, 775:37–43, 2017.

[215] R. Ferraro and F. Fiorini. On Born-Infeld Gravity in Weitzenbock spacetime. *Phys. Rev. D*, 78:124019, 2008.

[216] G. R. Bengochea and R. Ferraro. Dark torsion as the cosmic speed-up. *Phys. Rev. D*, 79:124019, 2009.

[217] E. V. Linder. Einstein's Other Gravity and the Acceleration of the Universe. *Phys. Rev. D*, 81:127301, 2010. [Erratum: Phys.Rev.D 82, 109902 (2010)].

[218] S. Chen, J. B. Dent, S. Dutta, and E. N. Saridakis. Cosmological perturbations in $f(T)$ gravity. *Phys. Rev. D*, 83:023508, 2011.

[219] S. Basilakos, S. Capozziello, M. De Laurentis, A. Paliathanasis, and M. Tsamparlis. Noether symmetries and analytical solutions in f(T)-cosmology: A complete study. *Phys. Rev. D*, 88:103526, 2013.

[220] S. Bahamonde, K. Flathmann, and C. Pfeifer. Photon sphere and perihelion shift in weak $f(T)$ gravity. *Phys. Rev. D*, 100(8):084064, 2019.

[221] A. Paliathanasis, J. Levi Said, and J. D. Barrow. Stability of the Kasner Universe in $f(T)$ Gravity. *Phys. Rev. D*, 97(4):044008, 2018.

[222] A. De Felice and S. Tsujikawa. $f(R)$ theories. *Living Rev. Rel.*, 13:3, 2010.

[223] T. Damour. 1974: the discovery of the first binary pulsar. *Class. Quant. Grav.*, 32(12):124009, 2015.

[224] E. Abdalla et al. Cosmology intertwined: A review of the particle physics, astrophysics, and cosmology associated with the cosmological tensions and anomalies. *JHEAp*, 34:49–211, 2022.

[225] D. Benisty. Quantifying the S_8 tension with the Redshift Space Distortion data set. *Phys. Dark Univ.*, 31:100766, 2021.

[226] W. de Sitter. On the relativity of inertia. Remarks concerning Einstein's latest hypothesis. *Koninklijke Nederlandse Akademie van Wetenschappen Proceedings Series B Physical Sciences*, 19:1217–1225, March 1917.

[227] A. S. Eddington. *The Mathematical Theory of Relativity*. Cambridge University Press, 1930.

[228] S. M. Carroll. The Cosmological constant. *Living Rev. Rel.*, 4:1, 2001.

[229] E. L. Wright. Cosmology / COBE. In *23rd International Cosmic Ray Conference*, pages 0085–114, 7 1993.

[230] A. D. Lewis, E. Ellingson, S. L. Morris, and R. G. Carlberg. X-ray mass estimates at $Z \sim 0.3$ for the Canadian Network for Observational Cosmology Cluster Sample. *Astrophys. J.*, 517:587–608, 1999.

[231] B. Zumino. Supersymmetry and the Vacuum. *Nucl. Phys. B*, 89:535, 1975.

[232] R. Bousso, B. Freivogel, S. Leichenauer, and V. Rosenhaus. A geometric solution to the coincidence problem, and the size of the landscape as the origin of hierarchy. *Phys. Rev. Lett.*, 106:101301, 2011.

[233] R. Bousso. TASI Lectures on the Cosmological Constant. *Gen. Rel. Grav.*, 40:607–637, 2008.

[234] J. D. Barrow. *The Anthropic Cosmological Principle*. Oxford University Press, 1986.

[235] A. D. Dolgov. An Attempt to get rid of the Cosmological Constant. In *Nuffield Workshop on the Very Early Universe*, 1982.

[236] N. Kaloper and A. Padilla. Sequestering the Standard Model Vacuum Energy. *Phys. Rev. Lett.*, 112(9):091304, 2014.

[237] N. Kaloper and A. Padilla. Sequestration of Vacuum Energy and the End of the Universe. *Phys. Rev. Lett.*, 114(10):101302, 2015.

[238] P. Brax and P. Valageas. Cosmological cancellation of the vacuum energy density. *Phys. Rev. D*, 99(12):123506, 2019.

[239] D. Sobral Blanco and L. Lombriser. Local self-tuning mechanism for the cosmological constant. *Phys. Rev. D*, 102(4):043506, 2020.

[240] L. Lombriser. On the cosmological constant problem. *Phys. Lett. B*, 797:134804, 2019.

[241] N. Kaloper, A. Padilla, D. Stefanyszyn, and G. Zahariade. Manifestly Local Theory of Vacuum Energy Sequestering. *Phys. Rev. Lett.*, 116(5):051302, 2016.

[242] N. Arkani-Hamed, S. Dimopoulos, G. Dvali, and G. Gabadadze. Nonlocal modification of gravity and the cosmological constant problem. 9 2002.

[243] A. Amariti, C. Charmousis, D. Forcella, E. Kiritsis, and F. Nitti. Brane cosmology and the self-tuning of the cosmological constant. *JCAP*, 10:007, 2019.

[244] O. Evnin and K. Nguyen. Graceful exit for the cosmological constant damping scenario. *Phys. Rev. D*, 98(12):124031, 2018.

[245] C. Charmousis, E. J. Copeland, A. Padilla, and P. M. Saffin. Self-tuning and the derivation of a class of scalar-tensor theories. *Phys. Rev. D*, 85:104040, 2012.

[246] E. J. Copeland, A. Padilla, and P. M. Saffin. The cosmology of the Fab-Four. *JCAP*, 12:026, 2012.

[247] S. Appleby. Self Tuning Scalar Fields in Spherically Symmetric Spacetimes. *JCAP*, 05:009, 2015.

[248] S. Appleby and E. V. Linder. The Well-Tempered Cosmological Constant: The Horndeski Variations. *JCAP*, 12:036, 2020.

[249] S. Appleby and E. V. Linder. The well-tempered cosmological constant: fugue in $\mathrm{B}^\flat$. *JCAP*, 12:037, 2020.

[250] E. V. Linder. How Fabulous Is Fab 5 Cosmology? *JCAP*, 12:032, 2013.

[251] A. A. Starobinsky, S. V. Sushkov, and M. S. Volkov. The screening Horndeski cosmologies. *JCAP*, 06:007, 2016.

[252] D. I. Kazakov. Radiative Corrections, Divergences, Regularization, Renormalization, Renormalization Group and All That in Examples in Quantum Field Theory. 2008.

[253] Y. Nambu and G. Jona-Lasinio. Dynamical Model of Elementary Particles Based on an Analogy with Superconductivity. 1. *Phys. Rev.*, 122:345–358, 1961.

[254] R. C. Bernardo, J. Levi Said, M. Caruana, and S. Appleby. Well-tempered Minkowski solutions in teleparallel Horndeski theory. *Class. Quant. Grav.*, 39(1):015013, 2022.

[255] R. C. Bernardo, J. Levi Said, M. Caruana, and S. Appleby. Well-tempered teleparallel Horndeski cosmology: a teleparallel variation to the cosmological constant problem. *JCAP*, 10:078, 2021.

[256] M. Hohmann, L. Järv, M. Krššák, and C. Pfeifer. Modified teleparallel theories of gravity in symmetric spacetimes. *Phys. Rev. D*, 100(8):084002, 2019.

[257] C. Pfeifer. A quick guide to spacetime symmetry and symmetric solutions in teleparallel gravity. 1 2022.

[258] M. Hamermesh. *Group Theory and Its Application to Physical Problems*. Addison Wesley Series in Physics. Dover Publications, 1989.

[259] S. M. Carroll, M. Hoffman, and M. Trodden. Can the dark energy equation-of-state parameter w be less than -1? *Phys. Rev. D*, 68:023509, 2003.

[260] D. Bettoni and S. Liberati. Disformal invariance of second order scalar-tensor theories: Framing the Horndeski action. *Phys. Rev. D*, 88:084020, 2013.

[261] W. T. Emond, C. Li, P. M. Saffin, and S. Zhou. Well-Tempered Cosmology. *JCAP*, 05:038, 2019.

[262] S. Bahamonde, C. G. Böhmer, S. Carloni, E. J. Copeland, W. Fang, and N. Tamanini. Dynamical systems applied to cosmology: dark energy and modified gravity. *Phys. Rept.*, 775-777:1–122, 2018.

[263] S. Wiggins. *Introduction to Applied Nonlinear Dynamical Systems and Chaos*. Texts in Applied Mathematics. Springer New York, 2006.

[264] H. Bondi. *Cosmology*. Cambridge monographs on physics. Cambridge University Press, 1952.

[265] M. Hohmann. General cosmological perturbations in teleparallel gravity. *Eur. Phys. J. Plus*, 136(1):65, 2021.

[266] A. Golovnev and T. Koivisto. Cosmological perturbations in modified teleparallel gravity models. *JCAP*, 11:012, 2018.

[267] S. Capozziello, K. F. Dialektopoulos, and S. V. Sushkov. Classification of the Horndeski cosmologies via Noether Symmetries. *Eur. Phys. J. C*, 78(6):447, 2018.

[268] S. Bahamonde, K. F. Dialektopoulos, M. Hohmann, and J. Levi Said. Post-Newtonian limit of Teleparallel Horndeski gravity. *Class. Quant. Grav.*, 38(2):025006, 2020.

[269] L. Amendola and S. Tsujikawa. *Dark Energy: Theory and Observations*. Cambridge University Press, 2010.

[270] H. Kodama and M. Sasaki. Cosmological Perturbation Theory. *Prog. Theor. Phys. Suppl.*, 78:1–166, 1984.

[271] O. F. Piattella. *Lecture Notes in Cosmology*. UNITEXT for Physics. Springer, Cham, 2018.

[272] M. Bruni, S. Matarrese, S. Mollerach, and S. Sonego. Perturbations of space-time: Gauge transformations and gauge invariance at second order and beyond. *Class. Quant. Grav.*, 14:2585–2606, 1997.

[273] K. A. Malik and D. R. Matravers. A Concise Introduction to Perturbation Theory in Cosmology. *Class. Quant. Grav.*, 25:193001, 2008.

[274] K. Izumi and Y. C. Ong. Cosmological Perturbation in $f(T)$ Gravity Revisited. *JCAP*, 06:029, 2013.

[275] R. Zheng and Q. Huang. Growth factor in $f(T)$ gravity. *JCAP*, 03:002, 2011.

[276] R. Abbott et al. Tests of general relativity with binary black holes from the second LIGO-Virgo gravitational-wave transient catalog. *Phys. Rev. D*, 103(12):122002, 2021.

[277] P. Amaro-Seoane et al. Laser Interferometer Space Antenna. 2 2017.

[278] P. Campeti et al. LiteBIRD science goals and forecasts. A case study of the origin of primordial gravitational waves using large-scale CMB polarization. *JCAP*, 06:008, 2024.

[279] H. Bondi. Plane gravitational waves in general relativity. *Nature*, 179:1072–1073, 1957.

[280] H. Bondi, F. A. E. Pirani, and I. Robinson. Gravitational waves in general relativity. 3. Exact plane waves. *Proc. Roy. Soc. Lond. A*, 251:519–533, 1959.

[281] A. Einstein and N. Rosen. On Gravitational waves. *J. Franklin Inst.*, 223:43–54, 1937.

[282] B. S. Sathyaprakash and B. F. Schutz. Physics, Astrophysics and Cosmology with Gravitational Waves. *Living Rev. Rel.*, 12:2, 2009.

[283] A. A. Michelson and E. W. Morley. On the Relative Motion of the Earth and the Luminiferous Ether. *Am. J. Sci.*, 34:333–345, 1887.

[284] S. Babak, R. Balasubramanian, D. Churches, T. Cokelaer, and B. S. Sathyaprakash. A Template bank to search for gravitational waves from inspiralling compact binaries. I. Physical models. *Class. Quant. Grav.*, 23:5477–5504, 2006.

[285] T. Cokelaer. A Template bank to search for gravitational waves from inspiralling compact binaries. II. Phenomenological model. *Class. Quant. Grav.*, 24:6227–6242, 2007.

[286] S. Bahamonde, M. Caruana, K. F. Dialektopoulos, V. Gakis, M. Hohmann, J. Levi Said, E. N. Saridakis, and J. Sultana. Gravitational-wave propagation and polarizations in the teleparallel analog of Horndeski gravity. *Phys. Rev. D*, 104(8):084082, 2021.

[287] Y. Gong and S. Hou. The Polarizations of Gravitational Waves. *Universe*, 4(8):85, 2018.

[288] D. M. Eardley, D. L. Lee, A. P. Lightman, R. V. Wagoner, and C. M. Will. Gravitational-wave observations as a tool for testing relativistic gravity. *Phys. Rev. Lett.*, 30:884–886, 1973.

[289] R. Briffa, C. Escamilla-Rivera, J. Levi Said, J. Mifsud, and N. L. Pullicino. Impact of H_0 priors on $f(T)$ late time cosmology. *Eur. Phys. J. Plus*, 137(5):532, 2022.

[290] Andrew L. Miller. Recent results from continuous gravitational wave searches using data from LIGO/Virgo/KAGRA's third observing run. In *57th Rencontres de Moriond on Gravitation*, 5 2023.

[291] Michele Maggiore et al. Science Case for the Einstein Telescope. *JCAP*, 03:050, 2020.

[292] F. Badaracco. Einstein Telescope: Science and technology. *Nuovo Cim. C*, 47(3):66, 2024.

[293] M. Armano et al. In-depth analysis of LISA Pathfinder performance results: Time evolution, noise projection, physical models, and implications for LISA. *Phys. Rev. D*, 110(4):042004, 2024.

[294] S. Mastrogiovanni, D. Steer, and M. Barsuglia. Probing modified gravity theories and cosmology using gravitational-waves and associated electromagnetic counterparts. *Phys. Rev. D*, 102(4):044009, 2020.

[295] M. Hohmann, C. Pfeifer, J. Levi Said, and U. Ualikhanova. Propagation of gravitational waves in symmetric teleparallel gravity theories. *Phys. Rev. D*, 99(2):024009, 2019.

[296] L. Hörmander. *The Analysis of Linear Partial Differential Operators II: Differential Operators with Constant Coefficients*. Classics in Mathematics. Springer Berlin Heidelberg, 2004.

[297] L. Hörmander. *The Analysis of Linear Partial Differential Operators I: Distribution Theory and Fourier Analysis*. Grundlehren Der Mathematischen Wissenschaften. Springer Berlin Heidelberg, 2012.

[298] M. Hohmann, M. Krššák, C. Pfeifer, and U. Ualikhanova. Propagation of gravitational waves in teleparallel gravity theories. *Phys. Rev. D*, 98(12):124004, 2018.

[299] K. Hoffman and R.A. Kunze. *Linear Algebra*. Featured Titles for Linear Algebra (Advanced) Series. Prentice-Hall, 1971.

[300] S. Hou, Y. Gong, and Y. Liu. Polarizations of Gravitational Waves in Horndeski Theory. *Eur. Phys. J. C*, 78(5):378, 2018.

[301] E. Newman and R. Penrose. An Approach to gravitational radiation by a method of spin coefficients. *J. Math. Phys.*, 3:566–578, 1962.

[302] S. Chandrasekhar. *The Mathematical Theory of Black Holes*. International series of monographs on physics. Clarendon Press, 1998.

[303] J. M. Ezquiaga and M. Zumalacárregui. Dark Energy in light of Multi-Messenger Gravitational-Wave astronomy. *Front. Astron. Space Sci.*, 5:44, 2018.

[304] A. Nishizawa, A. Taruya, K. Hayama, S. Kawamura, and M. Sakagami. Probing non-tensorial polarizations of stochastic gravitational-wave backgrounds with ground-based laser interferometers. *Phys. Rev. D*, 79:082002, 2009.

[305] R. Abbott et al. Upper limits on the isotropic gravitational-wave background from Advanced LIGO and Advanced Virgo's third observing run. *Phys. Rev. D*, 104(2):022004, 2021.

[306] L. Amalberti, N. Bartolo, and A. Ricciardone. Sensitivity of third-generation interferometers to extra polarizations in the stochastic gravitational wave background. *Phys. Rev. D*, 105(6):064033, 2022.

[307] H. Omiya and N. Seto. Searching for anomalous polarization modes of the stochastic gravitational wave background with LISA and Taiji. *Phys. Rev. D*, 102(8):084053, 2020.

[308] D. Blixt, M. Hohmann, and C. Pfeifer. Hamiltonian and primary constraints of new general relativity. *Phys. Rev. D*, 99(8):084025, 2019.

[309] V. F. Mukhanov. *Physical Foundations of Cosmology*. Physical Foundations of Cosmology. Cambridge University Press, 2005.

[310] D. J. Eisenstein et al. Detection of the Baryon Acoustic Peak in the Large-Scale Correlation Function of SDSS Luminous Red Galaxies. *Astrophys. J.*, 633:560–574, 2005.

[311] J. Lesgourgues and S. Pastor. Massive neutrinos and cosmology. *Phys. Rept.*, 429:307–379, 2006.

[312] J. Lesgourgues and S. Pastor. Neutrino mass from Cosmology. *Adv. High Energy Phys.*, 2012:608515, 2012.

[313] E. V. Linder. Exploring the expansion history of the universe. *Phys. Rev. Lett.*, 90:091301, 2003.

[314] S. Capozziello, M. Caruana, G. Farrugia, J. Levi Said, and J. Sultana. Cosmic growth in $f(T)$ teleparallel gravity. *Gen. Rel. Grav.*, 56(2):27, 2024.

[315] M. Caruana, G. Farrugia, J. Levi Said, and J. Sultana. Spatial dependence of the growth factor in scalar-tensor cosmology. *JCAP*, 06:053, 2024.

[316] I. Smail, R. S. Ellis, M. J. Fitchett, and A. C. Edge. Gravitational lensing of distant field galaxies by rich clusters. 2. - cluster mass distributions. *Mon. Not. Roy. Astron. Soc.*, 273:277, 1995.

[317] C. Heymans et al. CFHTLenS tomographic weak lensing cosmological parameter constraints: Mitigating the impact of intrinsic galaxy alignments. *Mon. Not. Roy. Astron. Soc.*, 432:2433, 2013.

[318] H. Hildebrandt et al. KiDS-450: Cosmological parameter constraints from tomographic weak gravitational lensing. *Mon. Not. Roy. Astron. Soc.*, 465:1454, 2017.

[319] A. A. Penzias and R. W. Wilson. A Measurement of excess antenna temperature at 4080-Mc/s. *Astrophys. J.*, 142:419–421, 1965.

[320] F. Beutler, C. Blake, M. Colless, D. H. Jones, L. Staveley-Smith, L. Campbell, Q. Parker, W. Saunders, and F. Watson. The 6dF Galaxy Survey: Baryon Acoustic Oscillations and the Local Hubble Constant. *Mon. Not. Roy. Astron. Soc.*, 416:3017–3032, 2011.

[321] S. Alam et al. The clustering of galaxies in the completed SDSS-III Baryon Oscillation Spectroscopic Survey: cosmological analysis of the DR12 galaxy sample. *Mon. Not. Roy. Astron. Soc.*, 470(3):2617–2652, 2017.

[322] G. Farrugia and J. Levi Said. Growth factor in $f(T, \mathcal{T})$ gravity. *Phys. Rev. D*, 94(12):124004, 2016.

[323] A. Pouri, S. Basilakos, and M. Plionis. Precision growth index using the clustering of cosmic structures and growth data. *JCAP*, 08:042, 2014.

[324] D. Polarski and R. Gannouji. On the growth of linear perturbations. *Phys. Lett. B*, 660:439–443, 2008.

[325] J. Dossett, M. Ishak, J. Moldenhauer, Y. Gong, A. Wang, and Y. Gong. Constraints on growth index parameters from current and future observations. *JCAP*, 04:022, 2010.

[326] W. J. Percival. Cosmological structure formation in a homogeneous dark energy background. *Astron. Astrophys.*, 443:819, 2005.

[327] R. W. Pike and M. J. Hudson. Cosmological parameters from the comparison of the 2mass gravity field with peculiar velocity surveys. *Astrophys. J.*, 635:11–21, 2005.

[328] N. Kaiser. Clustering in real space and in redshift space. *Mon. Not. Roy. Astron. Soc.*, 227:1–27, 1987.

[329] K. Said et al. DESI Peculiar Velocity Survey – Fundamental Plane. 8 2024.

[330] S. Tsujikawa. Matter density perturbations and effective gravitational constant in modified gravity models of dark energy. *Phys. Rev. D*, 76:023514, 2007.

[331] A. de la Cruz-Dombriz, A. Dobado, and A. L. Maroto. On the evolution of density perturbations in $f(R)$ theories of gravity. *Phys. Rev. D*, 77:123515, 2008.

[332] R. Jimenez and A. Loeb. Constraining cosmological parameters based on relative galaxy ages. *Astrophys. J.*, 573:37–42, 2002.

[333] R. Jimenez, L. Verde, T. Treu, and D. Stern. Constraints on the equation of state of dark energy and the Hubble constant from stellar ages and the CMB. *Astrophys. J.*, 593:622–629, 2003.

[334] C. Zhang, H. Zhang, S. Yuan, T. Zhang, and Y. Sun. Four new observational $H(z)$ data from luminous red galaxies in the Sloan Digital Sky Survey data release seven. *Res. Astron. Astrophys.*, 14(10):1221–1233, 2014.

[335] M. Moresco, L. Pozzetti, A. Cimatti, R. Jimenez, C. Maraston, L. Verde, D. Thomas, A. Citro, R. Tojeiro, and D. Wilkinson. A 6% measurement of the Hubble parameter at $z \sim 0.45$: direct evidence of the epoch of cosmic re-acceleration. *JCAP*, 05:014, 2016.

[336] J. Simon, L. Verde, and R. Jimenez. Constraints on the redshift dependence of the dark energy potential. *Phys. Rev. D*, 71:123001, 2005.

[337] M. Moresco et al. Improved constraints on the expansion rate of the Universe up to z˜1.1 from the spectroscopic evolution of cosmic chronometers. *JCAP*, 08:006, 2012.

[338] D. Stern, R. Jimenez, L. Verde, M. Kamionkowski, and S. A. Stanford. Cosmic Chronometers: Constraining the Equation of State of Dark Energy. I: $H(z)$ Measurements. *JCAP*, 02:008, 2010.

[339] M. Moresco. Raising the bar: new constraints on the Hubble parameter with cosmic chronometers at $z \sim 2$. *Mon. Not. Roy. Astron. Soc.*, 450(1):L16–L20, 2015.

[340] A. J. Ross, L. Samushia, C. Howlett, W. J. Percival, A. Burden, and M. Manera. The clustering of the SDSS DR7 main Galaxy sample – I. A 4 per cent distance measure at $z = 0.15$. *Mon. Not. Roy. Astron. Soc.*, 449(1):835–847, 2015.

[341] H. du Mas des Bourboux et al. Baryon acoustic oscillations from the complete SDSS-III Lyα-quasar cross-correlation function at $z = 2.4$. *Astron. Astrophys.*, 608:A130, 2017.

[342] G. Zhao et al. The clustering of the SDSS-IV extended Baryon Oscillation Spectroscopic Survey DR14 quasar sample: a tomographic measurement of cosmic structure growth and expansion rate based on optimal redshift weights. *Mon. Not. Roy. Astron. Soc.*, 482(3):3497–3513, 2019.

[343] W. L. Freedman et al. The Carnegie-Chicago Hubble Program. VIII. An Independent Determination of the Hubble Constant Based on the Tip of the Red Giant Branch. *Astrophys. J.*, 882:34, 2019.

[344] A. Zitrin, A. Fabris, J. Merten, P. Melchior, M. Meneghetti, A. Koekemoer, D. Coe, M. Maturi, M. Bartelmann, M. Postman, K. Umetsu, G. Seidel, I. Sendra, T. Broadhurst, I. Balestra, A. Biviano, C. Grillo, A. Mercurio, M. Nonino, P. Rosati, L. Bradley, M. Carrasco, M. Donahue, H. Ford, B. L. Frye, and J. Moustakas. Hubble Space Telescope Combined Strong and Weak Lensing Analysis of the CLASH Sample: Mass and Magnification Models and Systematic Uncertainties. *APJ*, 801(1):44, March 2015.

[345] T. M. C. Abbott et al. Dark Energy Survey Year 3 results: Cosmological constraints from galaxy clustering and weak lensing. *Phys. Rev. D*, 105(2):023520, 2022.

[346] G. Efstathiou. Challenges to the Lambda CDM Cosmology. 6 2024.

[347] L. Amendola, D. Polarski, and S. Tsujikawa. Are $f(R)$ dark energy models cosmologically viable ? *Phys. Rev. Lett.*, 98:131302, 2007.

[348] G. Farrugia, J. Levi Said, and M. L. Ruggiero. Solar System tests in $f(T)$ gravity. *Phys. Rev. D*, 93(10):104034, 2016.

[349] L. Iorio and E. N. Saridakis. Solar system constraints on $f(T)$ gravity. *Mon. Not. Roy. Astron. Soc.*, 427:1555, 2012.

[350] M. L. Ruggiero and N. Radicella. Weak-Field Spherically Symmetric Solutions in $f(T)$ gravity. *Phys. Rev. D*, 91:104014, 2015.

[351] X. Deng. Probing $f(T)$ gravity with gravitational time advancement. *Class. Quant. Grav.*, 35(17):175013, 2018.

[352] A. Finch and J. Levi Said. Galactic Rotation Dynamics in $f(T)$ gravity. *Eur. Phys. J. C*, 78(7):560, 2018.

[353] S. Nesseris, S. Basilakos, E. N. Saridakis, and L. Perivolaropoulos. Viable $f(T)$ models are practically indistinguishable from ΛCDM. *Phys. Rev. D*, 88:103010, 2013.

[354] G. Farrugia and J. Levi Said. Stability of the flat FLRW metric in $f(T)$ gravity. *Phys. Rev. D*, 94(12):124054, 2016.

[355] G. R. Dvali, G. Gabadadze, and M. Porrati. 4-D gravity on a brane in 5-D Minkowski space. *Phys. Lett. B*, 485:208–214, 2000.

[356] K. Bamba, S. Capozziello, S. Nojiri, and S. D. Odintsov. Dark energy cosmology: the equivalent description via different theoretical models and cosmography tests. *Astrophys. Space Sci.*, 342:155–228, 2012.

[357] C. Deffayet. Cosmology on a brane in Minkowski bulk. *Phys. Lett. B*, 502:199–208, 2001.

[358] K. Bamba, C. Geng, C. Lee, and L. Luo. Equation of state for dark energy in $f(T)$ gravity. *JCAP*, 01:021, 2011.

[359] R. Gannouji, B. Moraes, and D. Polarski. The growth of matter perturbations in $f(R)$ models. In *12th Marcel Grossmann Meeting on General Relativity*, pages 1274–1276, 7 2009.

[360] S. Tsujikawa, R. Gannouji, B. Moraes, and D. Polarski. The dispersion of growth of matter perturbations in $f(R)$ gravity. *Phys. Rev. D*, 80:084044, 2009.

[361] S. Basilakos and J. Solà. Growth index of matter perturbations in running vacuum models. *Phys. Rev. D*, 92(12):123501, 2015.

[362] H. Wei. Growth Index of DGP Model and Current Growth Rate Data. *Phys. Lett. B*, 664:1–6, 2008.

[363] X. Fu, P. Wu, and H. Yu. The Growth of linear perturbations in the DGP model. *Phys. Lett. B*, 677:12–15, 2009.

[364] Y. Gong. The growth factor parameterization and modified gravity. *Phys. Rev. D*, 78:123010, 2008.

[365] E. V. Linder and R. N. Cahn. Parameterized Beyond-Einstein Growth. *Astropart. Phys.*, 28:481–488, 2007.

[366] S. Basilakos and P. Stavrinos. Cosmological equivalence between the Finsler-Randers space-time and the DGP gravity model. *Phys. Rev. D*, 87(4):043506, 2013.

[367] P. Wu and H. Yu. $f(T)$ models with phantom divide line crossing. *Eur. Phys. J. C*, 71:1552, 2011.

[368] A. D. Linde. Chaotic Inflation. *Phys. Lett. B*, 129:177–181, 1983.

[369] E. J. Copeland, A. R Liddle, and D. Wands. Exponential potentials and cosmological scaling solutions. *Phys. Rev. D*, 57:4686–4690, 1998.

[370] B. Flaugher and C. Bebek. The Dark Energy Spectroscopic Instrument (DESI). *Proc. SPIE Int. Soc. Opt. Eng.*, 9147:91470S, 2014.

[371] M. Martinelli et al. Euclid: Forecast constraints on the cosmic distance duality relation with complementary external probes. *Astron. Astrophys.*, 644:A80, 2020.

[372] J. Prat et al. The catalog-to-cosmology framework for weak lensing and galaxy clustering for LSST. 12 2022.

[373] S. Capozziello, M. Caruana, J. Levi Said, and J. Sultana. Ghost and Laplacian instabilities in teleparallel Horndeski gravity. *JCAP*, 03:060, 2023.

[374] N. Frusciante, G. Papadomanolakis, S. Peirone, and A. Silvestri. The role of the tachyonic instability in Horndeski gravity. *JCAP*, 02:029, 2019.

[375] A. De Felice, N. Frusciante, and G. Papadomanolakis. On the stability conditions for theories of modified gravity in the presence of matter fields. *JCAP*, 03:027, 2017.

[376] M. Gonzalez-Espinoza, G. Otalora, and J. Saavedra. Stability of scalar perturbations in scalar-torsion $f(T, \phi)$ gravity theories in the presence of a matter fluid. *JCAP*, 10:007, 2021.

[377] R. L. Arnowitt, S. Deser, and C. W. Misner. Dynamical Structure and Definition of Energy in General Relativity. *Phys. Rev.*, 116:1322–1330, 1959.

[378] J. B. Dent, S. Dutta, and E. N. Saridakis. $f(T)$ gravity mimicking dynamical dark energy. Background and perturbation analysis. *JCAP*, 01:009, 2011.

[379] Y. Cai, S. Chen, J. B. Dent, S. Dutta, and E. N. Saridakis. Matter Bounce Cosmology with the $f(T)$ Gravity. *Class. Quant. Grav.*, 28:215011, 2011.

[380] Y. Wu and C. Geng. Primordial Fluctuations within Teleparallelism. *Phys. Rev. D*, 86:104058, 2012.

[381] F. Sbisà. Classical and quantum ghosts. *Eur. J. Phys.*, 36:015009, 2015.

[382] A. Lewis, A. Challinor, and A. Lasenby. Efficient computation of CMB anisotropies in closed FRW models. *Astrophys. J.*, 538:473–476, 2000.

[383] A. Lewis and A. Challinor. Code for anisotropies in the microwave background.

[384] B. Hu, M. Raveri, N. Frusciante, and A. Silvestri. Effective Field Theory of Cosmic Acceleration: an implementation in CAMB. *Phys. Rev. D*, 89(10):103530, 2014.

[385] G. Feinberg. Possibility of Faster-Than-Light Particles. *Phys. Rev.*, 159:1089–1105, 1967.

[386] Stahler, S. W. and Palla, F. *The Formation of Stars*. Wiley, 2008.

[387] J. H. Jeans. The Stability of a Spherical Nebula. *Phil. Trans. A. Math. Phys. Eng. Sci.*, 199(312-320):1–53, 1902.

[388] E. Lifshitz. Republication of: On the gravitational stability of the expanding universe. *J. Phys. (USSR)*, 10(2):116, 1946.

[389] B. F. Schutz and R. Sorkin. Variational aspects of relativistic field theories, with application to perfect fluids. *Annals Phys.*, 107:1–43, 1977.

[390] A. I. Vainshtein. To the problem of nonvanishing gravitation mass. *Phys. Lett. B*, 39:393–394, 1972.

[391] H. van Dam and M. J. G. Veltman. Massive and massless Yang-Mills and gravitational fields. *Nucl. Phys. B*, 22:397–411, 1970.

[392] V. I. Zakharov. Linearized gravitation theory and the graviton mass. *JETP Lett.*, 12:312, 1970.

[393] E. Babichev and C. Deffayet. An introduction to the Vainshtein mechanism. *Class. Quant. Grav.*, 30:184001, 2013.

[394] A. De Felice, R. Kase, and S. Tsujikawa. Vainshtein mechanism in second-order scalar-tensor theories. *Phys. Rev. D*, 85:044059, 2012.

[395] R. Kimura, T. Kobayashi, and K. Yamamoto. Vainshtein screening in a cosmological background in the most general second-order scalar-tensor theory. *Phys. Rev. D*, 85:024023, 2012.

[396] R. Kase and S. Tsujikawa. Screening the fifth force in the Horndeski's most general scalar-tensor theories. *JCAP*, 08:054, 2013.